

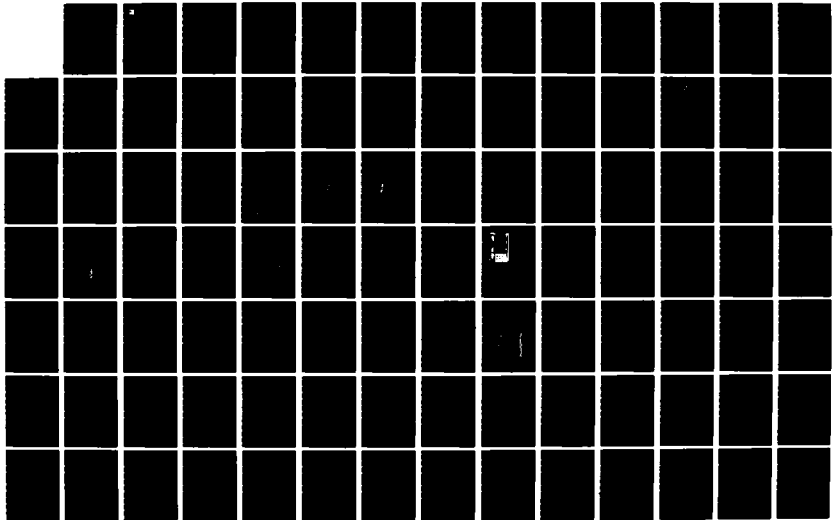
AD-A133 364

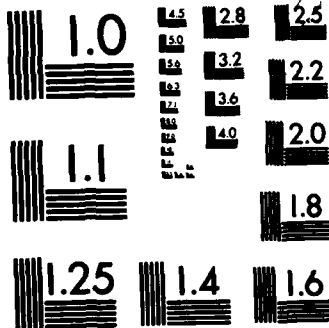
PROPELLANT NONLINEAR CONSTITUTIVE THEORY EXTENSION:
PRELIMINARY RESULTS. (U) UNITED TECHNOLOGIES CORP
SUNNYVALE CA CHEMICAL SYSTEMS DIV E C FRANCIS ET AL.
AUG 83 UTC/CSD-2742 AFRPL-TR-83-034

1/4

UNCLASSIFIED

F/G 21/9.2 NL





MICROCOPY RESOLUTION TEST CHART
 NATIONAL BUREAU OF STANDARDS-1963-A

10



AFRPL TR-83-034

AD:

A133364

A133364

Special Report
for the period
February 1981 to
September 31, 1982

Propellant Nonlinear Constitutive Theory Extension: Preliminary Results

August 1983

Authors:	Chemical Systems Division
E. C. Francis	1050 E. Arques Avenue
C. H. Carlton	Sunnyvale, CA 94086
R. Thompson	
W. M. Fisher	F04611-80-C-0052
D. Gutierrez-Lemini	UTC/CSD 2742

Approved for Public Release

Distribution unlimited. The AFRPL Technical Services Office has reviewed this report, and it is releasable to the National Technical Information Service, where it will be available to the general public, including foreign nationals.

DTIC
OCT 6 1983
A

DTIC FILE COPY

prepared for the: **Air Force
Rocket Propulsion
Laboratory**

Air Force Space Technology Center
Space Division, Air Force Systems Command
Edwards Air Force Base,
California 93523

3-8-24-1 A

83 10 04 119

NOTICES

When U.S. Government drawings, specifications, or other data are used for any purpose other than a definitely related Government procurement operation, the fact that the Government may have formulated, furnished, or in any way supplied the said drawings, specifications, or other data, is not to be regarded by implication or otherwise, or in any manner licensing the holder or any other person or corporation, or conveying any rights or permission to manufacture, use, or sell any patented invention that may be related thereto.

FOREWORD

This report was submitted by United Technologies Corporation/Chemical Systems Division, 1050 E. Arques Avenue, Sunnyvale CA 94086 under Contract F04611-80-C-0052, Job Order No. 2307MIEB with the Air Force Rocket Propulsion Laboratory, Edwards AFB CA 93523. This Special Technical Report is approved for release and publication in accordance with the distribution statement on the cover and in the DD Form 1473.

Durwood I. Thrasher
FOR DURWOOD I. THRASHER
Project Manager

R. John Moss
R. JOHN MOSS, Capt, USAF
Chief, Structural Integrity Section

FOR THE DIRECTOR

Thomas C. Meier
THOMAS C. MEIER, Lt Col, USAF
Director, Solid Rocket Division

Accession For	
NTIS GRA&I	<input checked="" type="checkbox"/>
DTIC TAB	<input type="checkbox"/>
Unannounced	<input type="checkbox"/>
Justification	
Distribution /	
Availability Codes	
Distribution for	
A	



Unclassified

SECURITY CLASSIFICATION OF THIS PAGE (When Data Entered)

REPORT DOCUMENTATION PAGE		READ INSTRUCTIONS BEFORE COMPLETING FORM	
1. REPORT NUMBER AFRPL-TR-83-034	2. GOVT ACCESSION NO. A133 364	3. RECIPIENT'S CATALOG NUMBER	
4. TITLE (and Subtitle) Solid Propellant Nonlinear Constitutive Theory Extension: Preliminary Results		5. TYPE OF REPORT & PERIOD COVERED Special Technical Report, Phases I, II, and III; Sept 80 - Sept 82	
		6. PERFORMING ORG. REPORT NUMBER CSD 2742	
7. AUTHOR(s) E. C. Francis, D. G. Lemini, C. Carlton, W. L. Hufferd, M. Gurtin, R. A. Schapery, M. Quinlan		8. CONTRACT OR GRANT NUMBER(s) F04611-80-C-0052	
9. PERFORMING ORGANIZATION NAME AND ADDRESS Chemical Systems Division 1050 E. Arques Avenue Sunnyvale, CA 94086		10. PROGRAM ELEMENT, PROJECT, TASK AREA & WORK UNIT NUMBERS	
11. CONTROLLING OFFICE NAME AND ADDRESS Air Force Rocket Propulsion Laboratory Edwards Air Force Base, CA 93523		12. REPORT DATE August 1983	
		13. NUMBER OF PAGES 322	
14. MONITORING AGENCY NAME & ADDRESS (if different from Controlling Office)		15. SECURITY CLASS. (of this report) Unclassified	
		15a. DECLASSIFICATION/DOWNGRADING SCHEDULE	
16. DISTRIBUTION STATEMENT (of this Report) APPROVED FOR PUBLIC RELEASE; DISTRIBUTION UNLIMITED The AFRPL Technical Services Office has reviewed this report, and it is releasable to the National Technical Information Service, where it will be available to the general public, including foreign nationals.			
17. DISTRIBUTION STATEMENT (of the abstract entered in Block 20, if different from Report)			
18. SUPPLEMENTARY NOTES			
19. KEY WORDS (Continue on reverse side if necessary and identify by block number)			
Strain	two-dimensional	straining-cooling	failure
Stress	three-dimensional	viscoelastic	time-dependent
Modulus	isothermal	nonlinear	elastic
Uniaxial	nonisothermal	linear	damage
Biaxial	constitutive	fracture	healing
20. ABSTRACT (Continue on reverse side if necessary and identify by block number)			
<p>→ This report details the technical effort put forth by CSD and its subcontractors during the first three phases of this program for propellant nonlinear constitutive theory extension. This includes the Phase I preliminary study in which the Quinlan theory was critiqued, alternate approaches were studied and detailed research planning accomplished. Also included are the detailed experimental evaluations of propellant during Phases II and III, the uniaxial/isothermal investigation and the two-dimensional variable temperature investigation. Detailed subcontractor theoretical development and predictions</p>			

DD FORM 1473
1 JAN 73

EDITION OF 1 NOV 68 IS OBSOLETE

Unclassified

are presented. ✓

This special technical report on Contract No. F04611-80-C-0052 consists of a summary of the Phase II and III laboratory propellant evaluation for UTP-3001 and UTP-19,360B propellants. The detailed experimental results were distributed in Data Packages A through G to all project personnel. Additional details are given in Section 1.0.

In performing the work required for the program, Chemical Systems Division (CSD) employed under subcontract the services of five scientists of national reputation: Drs. M. Quinlan, M. E. Gurtin, W. L. Hufferd, R. Wool, and R. A. Schapery. The program effort combined the comprehensive experience and specialized test capabilities of CSD in solid propellant mechanical properties with the theoretical expertise of these scientists. In addition, Dr. J. E. Fitzgerald was retained as a consultant to participate in the periodic technical reviews of the program status.

CONTENTS

Section		Page
1.0	PROGRAM OBJECTIVES AND OVERVIEW	1
2.0	TASK DESCRIPTION	5
2.1	Phase I - Preliminary Study	5
2.2	Phase II - Uniaxial/Isothermal Investigation	5
2.3	Phase III - Two-Dimensional and Variable Temperature Investigation	5
2.4	Phase IV - Three-Dimensional Investigation	5
3.0	LABORATORY TESTS, RESULTS, AND SUMMARY	6
3.1	Uniaxial/Isothermal Investigation	6
3.1.1	Constant Rate Test No. 1	11
3.1.2	Uniaxial Stress Endurance Test No. 2	13
3.1.3	Multirate Test No. 3	14
3.1.4	Stress Relaxation Modulus Test No. 4	14
3.1.5	Multiple Loading Test No. 5	21
3.1.6	Creep Test No. 6	25
3.1.7	Cyclic Loading Test No. 7	29
3.1.8	Relaxation Test No. 8	34
3.1.9	Predamaged-Relaxation Test No. 9	34
3.1.10	Complex Multiple Load Test No. 10	34
3.1.11	Quinlan Complex History Test No. 11	37
3.1.12	Similitude Test No. 12	76
3.1.13	Three-Step Relaxation Test No. 13	88
3.1.14	Propellant Aging Effects During Phase II Testing	103
3.2	Two-Dimensional and Variable Temperature Investigation	106
3.2.1	Biaxial Constant Rate Test No. 14	110
3.2.2	Biaxial Straining-Cooling Test No. 15	115
3.2.3	Biaxial Stress Relaxation Test No. 16	115
3.2.4	Shear Relaxation Test No. 17	116
3.2.5	Straining-Cooling Multiple Rates Test No. 18	117
3.2.6	Biaxial Quinlan Complex History Test No. 19	117
3.2.7	Cyclic Testing Test No. 20	119
3.2.8	Biaxial Ramp-Relax-Ramp Test No. 21	120
3.2.9	Propellant Aging Effects During Phase III Testing	121
4.0	THEORETICAL DEVELOPMENT	172
4.1	Introduction and Preliminary Study	172
4.1.1	Experimental Background	173
4.2	Selected Theories	179
4.2.1	Linear Viscoelastic Constitutive Equation	179
4.2.2	R. Farris' Nonlinear Theory for Solid Propellants	180
4.2.3	R. Schapery's Nonlinear Stress-Strain Law	203

CONTENTS (Cont'd)

Section		Page
	4.2.4 M. Gurtin's Theories for Nonlinear Viscoelastic Materials	219
	4.2.5 Russian Approach to Physically Nonlinear Viscoelastic Solids	248
	4.2.6 The Swanson Nonlinear Constitutive Law	267
	4.2.7 M. Quinlan's Theory of Materials with Variable Bonding	298
4.3	Conclusions	304
	REFERENCES	305
	APPENDIX A MULTISTATION AUTOMATED DATA REDUCTION	308
	SYMBOLS	316

ILLUSTRATIONS

Figure		Page
1	Program Logic	3
2	Uniaxial Isothermal Nondamaged Tests	7
3	Uniaxial/Isothermal Damaged Tests	8
4	Uniaxial/Isothermal Damaged Propellant Tests	9
5	Uniaxial Bar Specimen	10
6	Test No. 1 - Straining to Failure for UTP-3001 750/7768	11
7	Test No. 1 - Secant Modulus for UTP-3001 750/7768	13
8	Test No. 2 - Master Uniaxial Stress Endurance Curve for UTP-19,360B-400/1777	15
9	Test No. 2 - Uniaxial Stress Endurance Creep Behavior UTP-19,360B-400/1777 at 70°F	17
10	Test No. 2 - Uniaxial Stress Endurance Creep Secant Modulus Behavior for UTP-19,350B-400/1777 at 70°F	18
11	Test No. 3 - High-Low Constant Rate Tests of UTP-19,360B-400/1777 at 70°F	21
12	Test No. 3 - Low-High Constant Rate Tests of UTP-19,360B-400/1777 at 70°F	22
13	Master Modulus Data for UTP-3001-750/7768 with Experimental Shift	25
14	Constant Rate Master Modulus Data for UTP-3001-750/7768 JANNAF Specimens	27
15	Test No. 5 - Stress While Cycling for UTP-19,360B-400/1777	30
16	Test No. 6 - Creep Test with 6-in. Bar Specimens	34
17	Procedure for Loading and Incrementally Unloading Creep Samples	35
18	Test No. 6 - Strain-Time Data for Creep Test of UTP-19,360B-400/1777 at 71°F	36
19	Stress-Time Data for Creep Test of UTP-19,360B-400/1777 at 71°F	36

ILLUSTRATIONS (Cont'd)

Figure		Page
20	Corrected Stress-Time Data for Creep Test of UTP-19,360B-400/1777 at 71°F	37
21	Secant Modulus Data for Creep Test of UTP-19,360B-400/1777 at 71°F	38
22	Test No. 7 - Stress While Cycling for UTP-19,360B-400/1777	48
23	Test No. 8 - Stress While Step Straining for UTP-19,360B-400/1777	56
24	Test No. 9 - Stress While Step Straining for UTP-19,360B-400/1777	58
25	Test No. 10 - Stress While Complex Straining for UTP-19,360B-400/1777	61
26	Test No. 11, Part 1 - Stress While Cycling for UTP-3001-750/7768	89
27	Test No. 11, Part 1 - Stress While Cycling for UTP-3001-750/7768	90
28	Test No. 11, Part 1 - Stress While Cycling for UTP-3001-750/7768	91
29	Test No. 11, Part 1 - Stress While Cycling for UTP-3001-750/7768	92
30	Test No. 11, Part 2 - Stress While Cycling for UTP-3001-750/7768	93
31	Test No. 11, Part 2 - Stress While Cycling for UTP-3001-750/7768	94
32	Test No. 11, Part 2 - Stress While Cycling for UTP-3001-750/7768	95
33	Test No. 12 - Stress While Step Straining for UTP-19,360B-400/1777	96
34	Test No. 13 - Stress While Step Straining for UTP-3001-750/7768	99
35	Initial Ramp for UTP-3001-750/7768 39°F Tests Compared to the 6-in. Bar Constant Rate Data	106

ILLUSTRATIONS (Cont'd)

Figure		Page
36	Initial Ramp for UTP-3001-750/7768 75°F Tests Compared to the 6-in. Bar Constant Rate Data	107
37	Initial Ramp for UTP-3001-750/7768 124°F Tests Compared to the 6-in. Bar Constant Rate Data	107
38	Initial Ramp for UTP-19,360B-400/1777 40°F Tests Compared to the 6-in. Bar Constant Rate Data	108
39	Initial Ramp for UTP-19,360B-400/1777 70°F Tests Compared to the 6-in. Bar Constant Rate Data	109
40	Initial Ramp for UTP-19,360B-400/1777 123°F Tests Compared to the 6-in. Bar Constant Rate Data	110
41	1/2-in. Bar Stress Relaxation Data at 3% Nominal Strain	115
42	Biaxial and Nonisothermal Phase III Testing	116
43	Finished Biaxial Specimen	117
44	Principal Stress and Strain Ratios at the Center of Biaxial Strips for Varying Height-to-Width Ratios for a Poisson's Ratio of 1/2	118
45	Normalized Axial and Lateral Strains along the Midplane Biaxial Strip Specimen	119
46	Strain Variations Along Midline of Strip Specimen (N = 0) for Poisson's Ratio of 1/2	120
47	Stress Variations Along Midline of Strip Specimen (N = 0) for Poisson's Ratio of 1/2	121
48	Shear Sample and Test Attachment	122
49	Biaxial Test Setup and Instrumentation	123
50	Test No. 14 - Stress for UTP-19,360B-400/1777	124
51	Test No. 14 - Stress for UTP-19,360B-400/1777	125
52	Stress While Straining and Cooling for UTP-3001-750/7768	127
53	Test No. 16 - Stress While Step Straining for UTP-19,360B-400/1777	129

ILLUSTRATIONS (Cont'd)

Figure		Page
54	Test No. 17 - Stress While Step Straining for UTP-3001-750/7768	131
55	Test No. 18 - Stress While Straining and Cooling for UTP-3001-750/7768	134
56	Test No. 19, Part 1 - Stress for UTP-3001-750/7768	136
57	Test No. 19, Part 2 - Stress for UTP-3001-750/7768	137
58	Test No. 19, Part 3 - Stress for UTP-3001-750/7768	138
59	Test No. 20 - Stress While Cycling for UTP-19,360B-400/1777 for Complete Test	145
60	Test No. 21 - Stress While Complex Straining and Cooling for UTP-3001-750/7768	161
61	Biaxial Constant Rate Data for UTP-3001	166
62	Test No. 14 - Biaxial Constant Rate Data for UTP-3001	167
63	Biaxial Constant Rate Data for UTP-19,360B	169
64	Test No. 14 - Biaxial Constant Rate Data for UTP-19,360B	170
65	Relaxation after Damage	175
66	Relaxation after Damage	177
67	Stress-Strain Curve for Rubber	179
68	Linear Viscoelastic Stress Predictions for UTP-19,360B-400/1777 Constant Rate Test History (Code No. 1)	181
69	Linear Viscoelastic Stress Predictions for UTP-19,360B-400/1777 Constant Rate Test History (Code No. 1)	182
70	Linear Viscoelastic Stress Predictions for UTP-19,360B-400/1777 Two Rate Test History (Code No. 3)	183
71	Linear Viscoelastic Stress Predictions for UTP-19,360B-400/1777 Two Rate Test History (Code No. 3)	184
72	Linear Viscoelastic Stress Predictions for UTP-19,360B-400/1777 Multiple Loading Test History (Code No. 5)	185

ILLUSTRATIONS (Cont'd)

Figure		Page
73	Linear Viscoelastic Stress Predictions for UTP-19,360B-400/ 1777 Similitude Test History (Code No. 12)	186
74	Linear Viscoelastic Stress Predictions for UTP-19,360B-400/ 1777 Similitude Test History (Code No. 12)	187
75	Linear Viscoelastic Stress Predictions for UTP-19,360B-400/ 1777 Three Step Relaxation Test History (Code No. 13)	188
76	Linear Viscoelastic Stress Predictions for UTP-19,360B-400/ 1777 Constant Rate Test History (Code No. 1)	189
77	Linear Viscoelastic Stress Predictions for UTP-19,360B-400/ 1777 Constant Rate Test History (Code No. 1)	190
78	Linear Viscoelastic Stress Predictions for UTP-19,360B-400/ 1777 Constant Rate Test History (Code No. 1)	191
79	Linear Viscoelastic Stress Predictions for UTP-3001-750/7768 Constant Rate Test History (Code No. 1)	192
80	Linear Viscoelastic Stress Predictions for UTP-3001-750/7768 Constant Rate Test History (Code No. 1)	193
81	Linear Viscoelastic Stress Predictions for UTP-3001-750/7768 Multiple Loading Test History (Code No. 5)	194
82	Linear Viscoelastic Stress Predictions for UTP-3001-750/7768 Similitude Test History (Code No. 12)	195
83	Linear Viscoelastic Stress Predictions for UTP-3001-750/7768 Similitude Test History (Code No. 12)	196
84	Linear Viscoelastic Stress Predictions for UTP-3001-750/7768 Constant Rate Test History (Code No. 1)	197
85	Linear Viscoelastic Stress Predictions for UTP-3001-750/7768 Constant Rate Test History (Code No. 1)	198
86	Linear Viscoelastic Stress Predictions for UTP-3001-750/7768 Constant Rate Test History (Code No. 1)	199
87	Dr. Schapery's Nonlinear Viscoelastic Stress Predictions for UTP-19,360B 400/1777 Constant Rate Test Data (Code No. 1)	208
88	Dr. Schapery's Nonlinear Viscoelastic Stress Predictions for UTP-19,360B 400/1777 Constant Rate Test Data (Code No. 1)	209

ILLUSTRATIONS (Cont'd)

Figure		Page
89	Dr. Schapery's Nonlinear Viscoelastic Stress Predictions for UTP-19,360B 400/1777 Multiple Loading Test Data (Code No. 5)	210
90	Dr. Schapery's Nonlinear Viscoelastic Stress Predictions for UTP-19,360B 400/1777 Two Rate Test Data (Code No. 3)	211
91	Dr. Schapery's Nonlinear Viscoelastic Stress Predictions for UTP-19,360B 400/1777 Two Rate Test Data (Code No. 3)	212
92	Dr. Schapery's Nonlinear Viscoelastic Stress Predictions for UTP-19,360B 400/1777 Similitude Test History Data (Code No. 12)	213
93	Dr. Schapery's Nonlinear Viscoelastic Stress Predictions for UTP-19,360B 400/1777 Similitude Test History (Code No. 12)	214
94	Dr. Schapery's Nonlinear Viscoelastic Stress Predictions for UTP-19,360B 400/1777 Three Step Relaxation Test History (Code No. 13)	215
95	Strain History Used To Characterize the Damage Function	226
96	Damage Function for Unloading (TP-H1011)	228
97	Damage Function for Reloading (TP-H1011)	229
98	Two-Rate Loading (1 in./min. to 0.1 in./min.) of UTP-19,360B-400/1777	234
99	Relaxation-Unload-Reload of 6-in. Bar of UTP-19,360B-400/1777	235
100	Relaxation-Unload-Reload of 6-in. Bar of UTP-19,360B-400/1777	236
101	Relaxation-Unload-Reload of 6-in. Bar of UTP-19,360B-400/1777	237
102	Three-Step Relaxation of 6-in. Bar of UTP-19,360B-400/1777	238
103	Three-Step Relaxation of 6-in. Bar of UTP-19,360B-400/1777	239
104	Three-Step Relaxation of 6-in. Bar of UTP-19,360B-400/1777	240
105	Nonlinear Viscoelastic Stress Predictions for UTP-19,360B-400/1777 at 0.001 in./min. and 74 F (M. Gurtin's Theory)	244
106	Nonlinear Viscoelastic Stress Predictions for UTP-19,360B-400/1777 at 70 F (M. Gurtin's Theory)	245

ILLUSTRATIONS (Cont'd)

Figure		Page
107	Nonlinear Viscoelastic Stress Predictions for UTP-19,360B-400/1777 at 123 F (M. Gurtin's Theory)	246
108	Nonlinear Viscoelastic Stress Predictions for UTP-19,360B-400/1777 at 40 F (M. Gurtin's Theory)	247
109	Solution for m as a Function of Strain Rate	256
110	Nonlinear Viscoelastic Stress Predictions for UTP-19,360B-400/1777	258
111	Nonlinear Viscoelastic Stress Predictions for UTP-19,360B-400/1777	259
112	Nonlinear Viscoelastic Stress Predictions for Two-Rate Test (UTP-19,360B-400/1777)	260
113	Nonlinear Viscoelastic Stress Predictions for Two-Rate Test (UTP-19,360B-400/1777)	261
114	Nonlinear Viscoelastic Stress Predictions for Short Similitude Test (UTP-19,360B-400/1777) (W. L. Hufferd's Theory)	262
115	Constant Rate Test (0.001 in./min.)	263
116	Constant Rate Test (0.01 in./min.)	264
117	Constant Rate Test (10 in./min.)	265
118	Softening Function During Relaxation	266
119	Softening Function During Unloading	266
120	Effect of Deformation and Pressure on the Strain Softening Function	272
121	Nonlinear Viscoelastic Stress Predictions for Constant-Rate Test (UTP-19,360B-400/1777)	275
122	Nonlinear Viscoelastic Stress Predictions for Constant-Rate Test (UTP-19,360B-400/1777)	276
123	Nonlinear Viscoelastic Stress Predictions for Saw-Tooth Test (UTP-19,360B-400/1777)	277
124	Nonlinear Viscoelastic Stress Predictions for Two-Rate Test (UTP-19,360B-400/1777)	278

ILLUSTRATIONS (Cont'd)

Figure		Page
125	Nonlinear Viscoelastic Stress Predictions for Two-Rate Test (UTP-19,360B-400/1777)	279
126	Nonlinear Viscoelastic Stress Predictions for Long Similitude Test (UTP-19,360B-400/1777)	280
127	Nonlinear Viscoelastic Stress Predictions for 3-Step Relaxation (UTP-19,360B-400/1777)	281
128	Nonlinear Viscoelastic Stress Predictions for Short Similitude Test (UTP-19,360B-400/1777)	282
129	Nonlinear Viscoelastic Stress Predictions for UTP-19,360B-400/1777 at 123 F	283
130	Nonlinear Viscoelastic Stress Predictions for UTP-19,360B-400/1777 at 40 F	284
131	Nonlinear Viscoelastic Stress Predictions for UTP-19,360B-400/1777 (Biaxial Sample) Hercules Theory	292
132	Nonlinear Viscoelastic Stress Predictions for UTP-19,360B-400/1777 (Biaxial Sample) Hercules Theory	293
133	Nonlinear Viscoelastic Stress Predictions for UTP-19,360B-400/1777 (Biaxial Sample) Hercules Theory	294
134	Nonlinear Viscoelastic Stress Predictions for UTP-19,360B-400/1777 (Biaxial Sample) Hercules Theory	295
135	Nonlinear Viscoelastic Stress Predictions for UTP-19,360B-400/1777 (Biaxial Sample) Hercules Theory	296
136	Nonlinear Viscoelastic Stress Predictions for UTP-19,360B-400/1777 (Biaxial Sample) Hercules Theory	297

TABLES

Table		Page
1	1/2-in. Bar Straining to Failure	12
2	Test No. 2 - UTP-19,360B 400/1777 Constant Endurance Test	16
3	Test No. 2 - Uniaxial Stress Endurance Creep Behavior for UTP-19,360B-400/1777 at 70°F	19
4	Test No. 3 - High-Low Constant Rate Tests of UTP-19,360B-400/1777 at 70°F with 1/2 x 1/2 x 6-in. Bar Samples	23
5	Test No. 3 - Low-High Constant Rate Tests of UTP-19,360B-400/1777 at 70°F with 1/2 x 1/2 x 6-in. Bar Samples	24
6	Test No. 4 - 1/2-in. Bar Stress Relaxation Data Reduction	26
7	Master Modulus Curves for UTP-3001 Stress Relaxation and Constant Rate Tests	28
8	Test No. 5 - 1/2-in. Bar Stress While Cycling	31
9	Test No. 6 - 1/2-in. Bar Stress While Cycling (Full Stress Creep)	39
10	Full Stress Creep Test For UTP-19,360B-400/1777 at 71°F	47
11	Test No. 7 - 1/2-in. Bar Stress While Cycling	49
12	Test No. 8 - 1/2-in. Bar Stress While Step Straining	57
13	Test No. 9 - 1/2-in. Bar Stress While Step Straining	59
14	Test No. 10 - 1/2-in. Bar Stress While Complex Straining	62
15	Test No. 11, Part 1 - Quinlan Complex History for UTP-3001	64
16	Test No. 11, Part 1 - 1/2-in. Bar Stress While Cycling	65
17	Test No. 11, Part 2 - Quinlan Complex History for UTP-3001	76
18	Test No. 11, Part 2 - 1/2-in. Bar Stress While Cycling	77
19	Test No. 11, Part 3 - UTP-3001-750/7768 1/2-in. Bar Stress While Cycling	87
20	Test No. 12 - 1/2-in. Bar Stress While Step Straining	97
21	Test No. 13 - 1/2-in. Bar Stress While Step Straining	100

TABLES (Cont'd)

Table		Page
22	Stress-Strain Comparison for UTP-3001 Tests	111
23	Stress-Strain for UTP-19,360B Tests	113
24	Minibiaxial Stress While Straining and Cooling	126
25	Minibiaxial Stress While Straining and Cooling	128
26	Minibiaxial Stress While Step Straining	130
27	Shear Stress While Step Straining	132
28	1/2-in. Bar Stress While Straining and Cooling	135
29	Test No. 19 - Minibiaxial Stress, Sample	139
30	1/2-in. Bar Stress While Cycling	146
31	Minibiaxial Stress While Complex Straining and Cooling	162
32	Stress-Strain Comparison for UTP-3001 Tests Phase III	164
33	Stress-Strain Comparison for UTP-19,360B Tests Phase III	165
34	Comparison of Uniaxial, Biaxial, and Shear Test Data from Phase III	171

1.0 PROGRAM OBJECTIVES AND OVERVIEW

The objective of the Propellant Nonlinear Constitutive Theory Extension Program is to develop and demonstrate an accurate and usable nonlinear thermal-mechanical constitutive law for solid rocket propellants. The program has been conducted through three phases of a four phase project. These four phases are summarized below:

Phase I - Preliminary Study

A variety of nonlinear theories were considered and five methods were selected for further study.

- Modified Swanson Theory
- Russian - (Hufferd) Theory
- Schapery Theory
- Gurtin Theory
- Quinlan Theory.

Dr. Richard Wool presented a review of available micro-mechanics theories which could be considered for inclusion within the nonlinear constitutive theories.

Phase II - Uniaxial Isothermal Investigation

A series of uniaxial tests were conducted with two materials - a PBAN and an HTPB propellant. The data was fit to each of the nonlinear theories. Then the material constants derived for each analytic method were used in a predictive calculation of a complex laboratory test history which included some typical long time rocket motor mechanical bonding sequences. A review of the analytic methods and predictive results showed that all of the theories could be adapted to give better correlations with realistic motor loading conditions. Other test histories were also suggested that would permit more direct evaluation of the pertinent nonlinear material behavior required for each theory. Numerical difficulties were encountered with some theories and refinements were determined

that would hopefully eliminate these problems. All five theories were considered acceptable and were to be further developed in the next phase.

Phase III - Two-Dimensional and Variable Temperature Investigation

The analytic and numerical improvements were made with each theory. These refined methods were then evaluated with the test data from phase II plus the additional recommended tests from the phase II review meetings. Most of the analytic methods looked very good with the final refinements. This effort, using the latest data, used most of the scheduled time for this phase. In addition to the suggested uniaxial mechanical tests, a variety of shear, biaxial and uniaxial (some with simultaneous thermal and mechanical loading) tests were conducted with some very complex load histories. This latest test data was only considered in a preliminary way since the theory modifications were very extensive.

Phase IV - Three Dimensional Investigation (Not started)

The additional laboratory data developed in phase III plus some instrumented structural test vehicle data will be used with the various nonlinear constitutive theories. One or more selected theories will be determined and the computer codes will be installed and checked out on the Air Force Rocket Propulsion Laboratory's computer.

The program logic chart relating each of the phases and their respective tasks is presented in Figure 1.

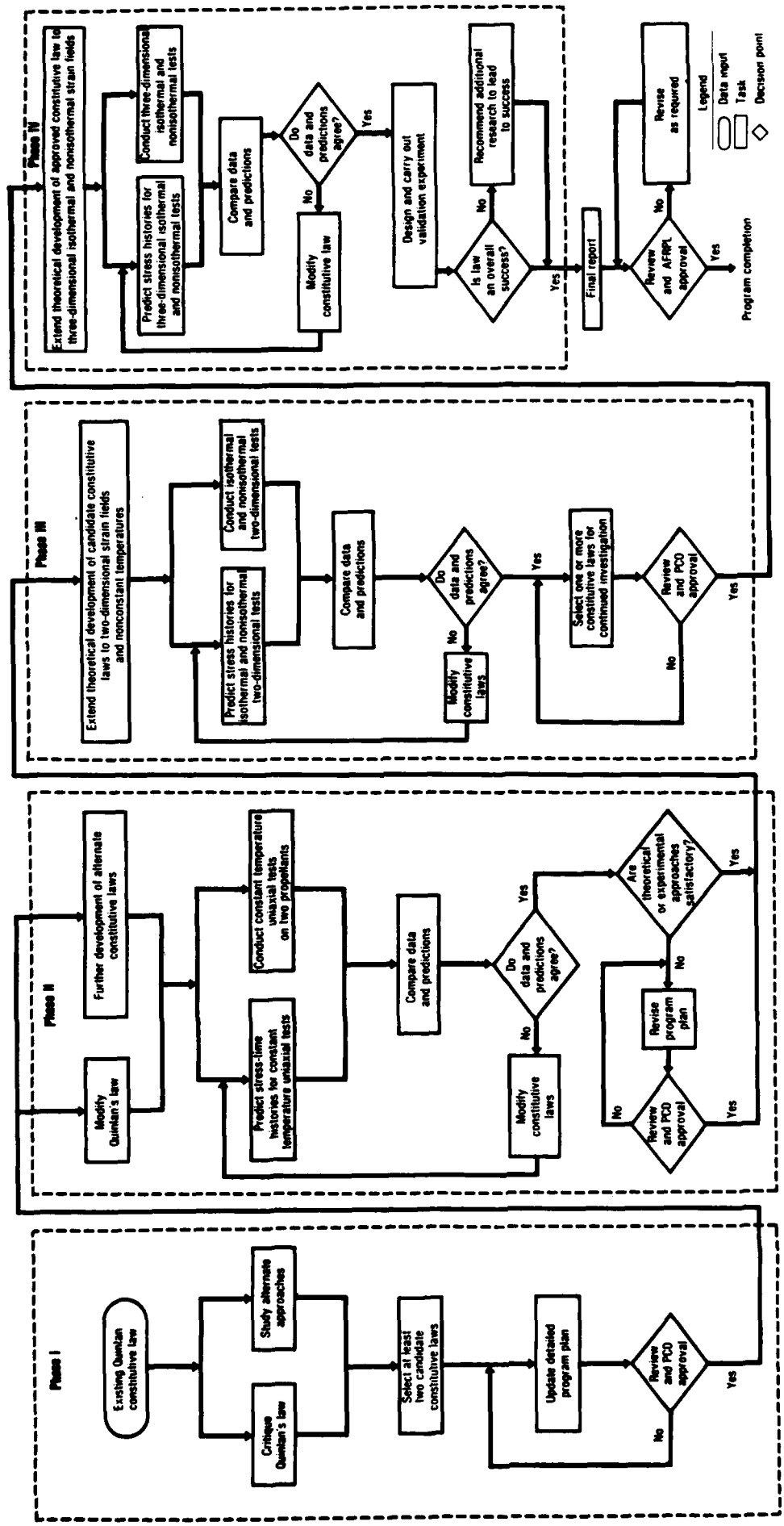


Figure 1. Program Logic

2.0 TASK DESCRIPTION

2.1 PHASE I - PRELIMINARY STUDY

The objective of phase I was to critique the Quinlan theory, propose at least one alternate approach to the constitutive law solution, and make detailed research plans for evaluating and modifying the candidate constitutive law approaches.

2.2 PHASE II - UNIAXIAL/ISOTHERMAL INVESTIGATION

The objective of phase II was to carry out modifications to Quinlan's law and to do theoretical development of the other candidate constitutive laws. These laws were used to make stress-time predictions for uniaxial/isothermal tests. Concurrently, actual uniaxial/isothermal tests were conducted in the laboratory. A comparison of the predictions and actual data was then made, and the theoretical and experimental approaches were evaluated.

2.3 PHASE III - TWO-DIMENSIONAL AND VARIABLE TEMPERATURE INVESTIGATION

The objective of phase III was to extend the theoretical development of the candidate constitutive laws to two-dimensional and variable temperature tests. Stress-time predictions were made concurrently with actual testing in the laboratory. A comparison of predictions and actual data was made and two constitutive law candidates were selected for further investigation from those results.

2.4 PHASE IV - THREE-DIMENSIONAL INVESTIGATION

The objective of the final phase is to extend the theoretical development of the candidate constitutive laws to three-dimensional and variable temperature history tests. Concurrently, three-dimensional, variable temperature laboratory tests are to be conducted. Data and predictions will be compared and any final modifications to the constitutive law made. A validation experiment is to be conducted, and stress-time predictions made with the finalized version of the nonlinear constitutive law. A final assessment of the overall success of the new law will be made and recommendations will be presented for further avenues of research. Recommendations for utilizing the new law in existing solid rocket motor structural analysis techniques will also be made.

3.0 LABORATORY TESTS, RESULTS, AND SUMMARY

The laboratory testing was divided into the categories of uniaxial/isothermal, two-dimensional and variable temperature, and three-dimensional investigations.

The two propellants selected for the program were (1) a PBAN currently being used in the first stage of the Titan missile system (UTP-3001-750/7768) and (2) a HTPB propellant developed for the IUS motor (UTP-19,360B-400/1777). The first numbers are the propellant designation, the next the mixer size, and the last a batch number.

In each of the uniaxial or biaxial groups, a specific test of each type was selected to show the test details in graphic and tabular form. While tests were run on both propellants, only one is shown. The details of test temperatures and rates are discussed with each test type.

3.1 UNIAXIAL/ISOTHERMAL INVESTIGATION

Testing uniaxial specimens of UTP-3001 and UTP-19,360B propellants, in phase II of the contract, was done for the nondamaged material as indicated in Figure 2 and for damaged material per Figures 3 and 4. Most of the tests were run with 1/2 x 1/2 x 6-in. bars with redwood end tabs. The exceptions were stress endurance (test 2) and constant rate (comparison to test No. 4) data were obtained with JANNAF Class B specimens.⁽¹⁾ The details of the individual test types are discussed in subsections below.

The uniaxial bars were machined from redwood boxes of propellant. The redwood was sealed then lined in the same manner as a rocket motor. After a partial cure of the liner, propellant was cast in the box and the system cured to provide a good bond to the redwood end tabs. The redwood box assembly and finished specimen are shown in Figure 5. After the specimen is mill finished,

Reference 1 - Solid Propellant Mechanical Behavior Manual, CPIA Publication No. 21, Section 4.3.2

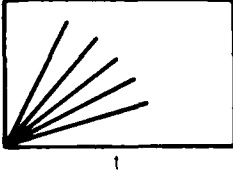
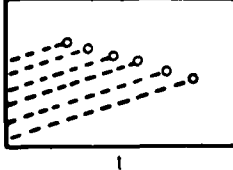
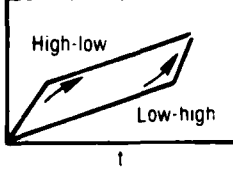
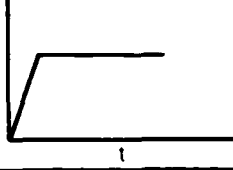
Test No.	Test Description	Temperature, °F	Pressure, psig	Rate, in./min	Strain, %	Experimental Effects	Strain History
1	Constant rate	70 120 40	0 0 0	0.001 " 10	To failure	Time and rate temperature sample type	
2	Stress endurance	70 120 40	0 0 0	— —	To failure	Time and temperature	
3	Multirate	70	0	0.1-1 1.0 - 0.1	12 12	Rate change	
4	Stress relaxation	70 120 40 23	0 0 0 0	1 1 1 1	3 3 3 3	Temperature	
Note: Nominal tests were run with three samples per set							Legend: ε = strain t = time

Figure 2. Uniaxial Isothermal Nondamaged Tests

24406R1

a 1/8 in. hole is drilled on the center line of each end tab for attachment purposes. (Attachment fixtures are shown in Figure 16).

Due to the enormous test load compared to the available time, both calendar and contract wise, the decision was made to run all tests on six-channel testers. Both the Chemical Systems Division (CSD) manufactured six-channel tester and a modified Instron were used in conjunction with a Hewlett-Packard computer to collect digitized data for the tests. (See Appendix A details on the automated data reduction system). While the CSD tester was equipped with an oscillograph as backup for relatively short duration tests, the modified Instron had no backup. In instances where a power surge occurred, the data were lost and the test had to be rerun.

Test No.	Test Description	Damage Cycle				Remarks	Test				Strain Cycle
		Temperature, °F	Pressure, psi	Rate, in./min	Strain, %		Temperature, °F	Pressure, psi	Rate, in./min	Strain, %	
5	Multiple loading with rest periods: step cycle	70	0	0.1, 1, 10	3	30-min hold between cycles	70	0	0.1, 1, 10	3 to 12	
6	Creep	70, 120, 40	0	1	1/4, 1/2, ~maximum	3-hr creep periods: first step only for 120 and 40°F	70	0	1	1/4, 1/2, ~maximum	
7	Cyclic loading	70	0	1	4, 8, 12	20 cycles: return to zero stress and monitor E recovery	70	0	1	4, 8, 12	
8	24-hr relaxation	70	0	20	4, 8, 12	Monitor the unload	70	0	1	4, 8, 12	
9	Predamage relaxation (1 hr)	70	0	0.1	6, 12	30-min hold between loading: monitor unload	70	0	20, 1	3, 4, 8	
10	Complex multiple load	70	0	0.1, 1, 5	12, 8, 4	High strain followed by low strain: return to zero stress and monitor strain	70	0	0.1, 1, 5	12, 8, 4	

Note: Nominal tests were run with three samples per set

Legend
 ϵ = strain
 1 = time

Figure 3. Uniaxial/Isothermal Damaged Tests

24407R1

Test	Test Description	Damage Cycle	Test	Strain Cycle
11	Quinlan complex history	Single samples clamped in rigid Instron jaws were run on UTP-3001 and UTP-19,360B. In returning to zero strain the samples were put into compression. Data are reported in "Data Package F".		
12	Similitude	Similitude tests were run with 6-in. bar samples of UTP-3001 and UTP-19,360B. Data are reported in "Data Package E" and the September meeting handout.		
13	Three step relaxation	Short and long time tests were run with 6-in. bar samples of UTP-3001 and UTP-19,360B. Data are reported in "Data Package E" and the September meeting handout.		
<p>Note: Nominal tests were run with three samples per set</p> <p>Legend: ϵ = strain t = time</p>				

Figure 4. Uniaxial/Isothermal Damaged Propellant Tests

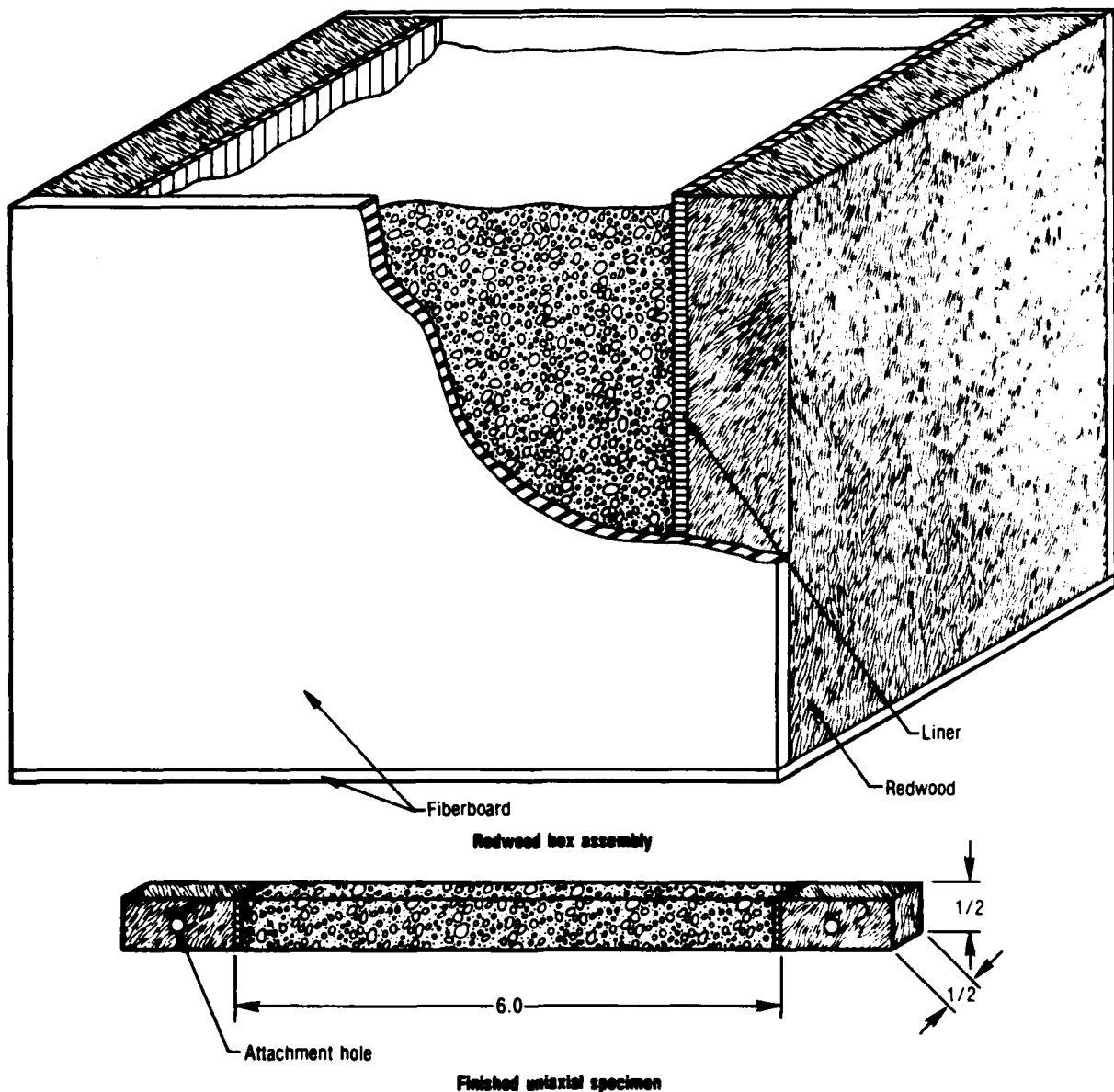


Figure 5. Uniaxial Bar Specimen

28804

The attachment linkages on both testers were such that the specimens could not be put into compression when the crosshead was returned to an equivalent zero strain position. The strain measurement was done with a linear potentiometer attached to the crosshead; consequently, the data had to be modified to reflect the propellant strain relaxation behavior after the stress had returned to zero (free hanging specimen).

Strain relaxation was measured on samples in some of the tests during the final unload cycle. Cathetometer measurements were made periodically and strain versus time data were plotted. These data were used to estimate the relaxation behavior on cyclic tests where there was insufficient time for measurements.

A data modification was made to estimate the peak or minimum stress and strain points, which were not recorded by the digitized data acquisition system. The sampling rate limited the crosshead rate that could be used and still obtain enough points to adequately define a ramp. The available computer memory also influenced the sampling rate in some of the long tests.

3.1.1 Constant Rate Test No. 1

Uniaxial constant rate tests to failure were run on 6-in. bars of UTP-3001 and UTP-19,360B. The 70°F tests were at crosshead rates of 10, 1, 0.1, 0.01, and 0.001 in./min. while 40 and 120°F tests were at 10, 1, and 0.1 in./min. A typical load-time curve is shown in Figure 6 for the UTP-3001 at 75°F and 10 in./min., and tabular data are given in Table 1. Because of the computer

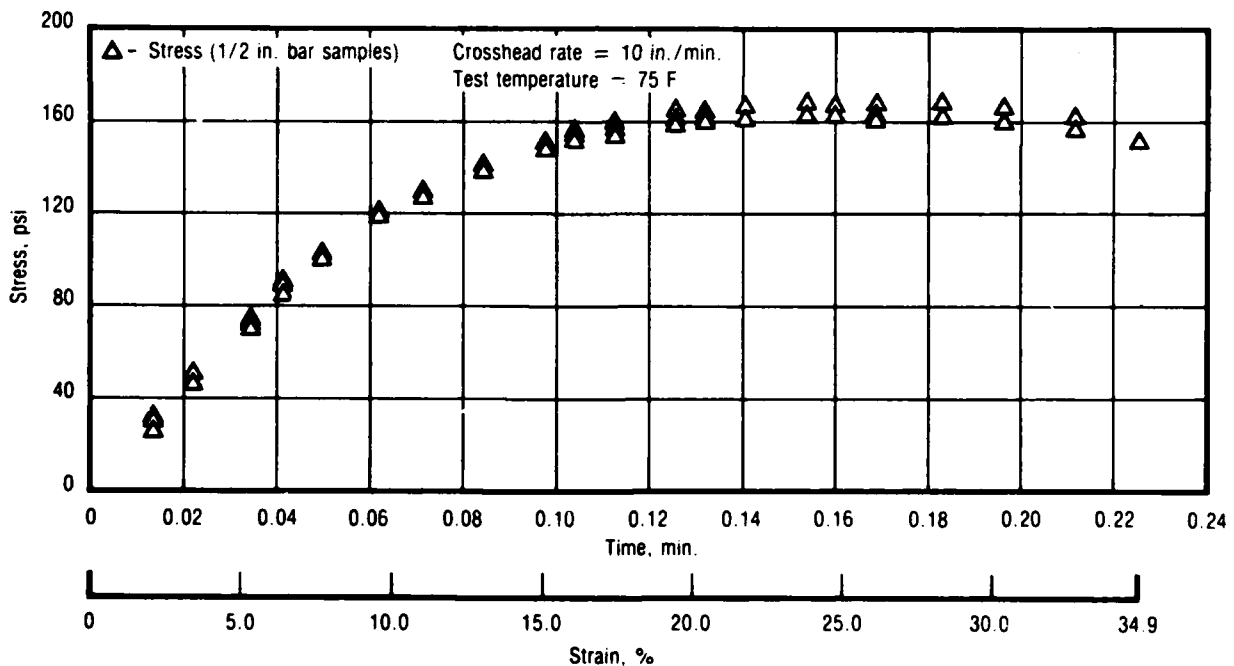


Figure 6. Test No. 1 - Straining to Failure for UTP-3001 750/7768

28387

TABLE 1. 1/2-IN. BAR STRAINING TO FAILURE

PROPELLANT: UTP 3001 750/7768
 REQUESTOR: Carlton
 WDR:

DATE: 4/21/81
 OPERATOR: JMB

DEFINITIONS:

- T = Time From Start of Test (min)
- σ = Stress (Psi)
- ε = Strain (%)
- E = Secant Modulus (psi)
- T (air) = Test Air Temperature (F)
- T (prop) = Test Propellant Temperature (F)

RELATIONSHIPS:

- σ = Force/Area
- ε = Sample Extension/Length

NOMINAL VALUES:
 Test Temp = 75 F
 Gage Length = 6.10 in
 XHB Rate = 10 in/min

CALIBRATION DATA:

	1	2	3	4
Cal Wt = 10.0 lbs				
Load Cal (lbs/volts)	-4.24	-3.11	-3.33	-2.70
Offset (volts)	-0.04	-0.05	-0.06	
Ret Cal (in/volts) =	1.33			
Temp (F)	73.9			

SAMPLE

	1	2	3	4
Cal Wt = 10.0 lbs				
Load Cal (lbs/volts)	-4.24	-3.11	-3.33	-2.70
Offset (volts)	-0.04	-0.05	-0.06	

AREAS (sq in):

	0.252	0.250	0.249	0.250
Area 1	1520.92	1788.15	1893.57	1826.01
Area 2	1604.31	1768.68	1793.69	1732.62
Area 3	1902.81	1939.29	1988.39	1953.68
Area 4	1442.01	1537.49	1508.44	1520.54
Area 5	1409.10	1458.85	1421.10	1450.73
Area 6	1349.83	1322.48	1349.12	1357.11
Area 7	1287.58	1297.13	1269.25	1285.44
Area 8	1220.62	1224.03	1199.75	1215.00
Area 9	1124.75	1147.70	1126.31	1142.55
Area 10	1073.24	1107.11	1094.29	1108.72
Area 11	1005.20	1022.32	1039.79	1055.37
Area 12	969.81	980.02	972.63	986.01
Area 13	949.64	949.64	949.64	954.02
Area 14	899.50	899.50	899.50	916.42
Area 15	876.72	851.44	849.93	859.17
Area 16	852.16	827.64	823.34	834.36
Area 17	814.05	788.76	779.84	794.22
Area 18	769.02	733.02		746.52
Area 19	711.01	683.14		692.08
Area 20	653.60	631.85		642.73
Area 21	582.66	582.66		

SECANT MODULUS

Time	T(prop)	T(air)	Strain	Area	Avg	St Dev
1.3508E-02			1.72	1520.92	1757.76	94.351
2.1967E-02			2.09	1604.31	1721.65	45.672
3.4541E-02			3.04	1902.81	1903.28	23.789
4.1517E-02			6.24	1442.01	1502.12	24.137
4.9858E-02			7.65	1409.10	1434.94	13.665
6.2217E-02			9.66	1349.83	1357.11	8.682
7.1442E-02			11.13	1287.58	1284.85	6.882
8.4617E-02			13.05	1220.62	1215.00	6.202
9.7823E-02			15.04	1124.75	1142.55	10.163
1.0396E-01			16.03	1073.24	1108.72	10.014
1.1265E-01			17.43	1005.20	1055.37	12.210
1.2480E-01			19.44	969.81	986.01	12.030
1.3177E-01			20.33	949.64	954.02	9.977
1.4066E-01			21.69	899.50	916.42	10.626
1.5389E-01			23.59	876.72	859.17	10.643
1.5971E-01			24.39	852.16	834.36	10.945
1.6873E-01			25.84	814.05	794.22	12.546
1.8228E-01			28.19	769.02	746.52	16.093
2.1155E-01			30.30	711.01	692.08	19.709
2.2044E-01			32.71	653.60	642.73	15.379
2.2044E-01			34.94	582.66		

data sampling rate, the 10-in./min. tests were run one propellant at a time. Sample 4 (Table 1) shows the load cell reached the limit of its adjustment so did not record the specimen failure. The 6-in. bar specimens always fail below what would be obtained from JANNAF specimens. Since response properties are what is of interest, particularly in the small strain region, the uniform cross sectional area specimen does what it is supposed to do. The continual changing effective gage length of the JANNAF dogbone is avoided.

These data were also reduced to secant modulus ($\lambda\sigma/\epsilon$) as shown in Figure 7. The data are compared to the stress relaxation modulus from test No. 4 later.

3.1.2 Uniaxial Stress Endurance Test No. 2

Stress endurance tests were run on the two propellants using JANNAF Class B dogbones. The ultimate failure properties were of importance in this test rather than small strain response hence the dogbones. This is a constant load test with plastic extensometer to monitor the strain increase with time (also known as a creep test). They were run at 23, 70, and 120°F. The data shifted

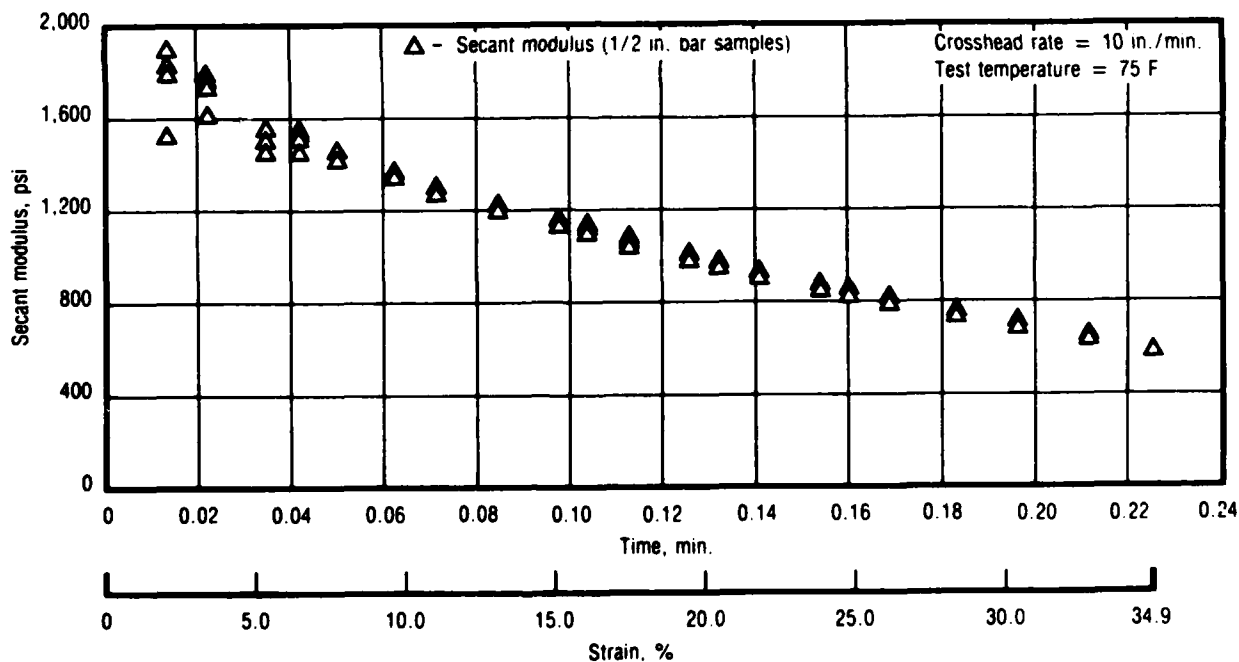


Figure 7. Test No. 1 - Secant Modulus for UTP-3001 750/7768

28751

to a master endurance curve as shown in Figure 8 for UTP-19,360B with typical 70°F data given in Table 2. The strain creep effect on stress is shown in Figure 9 where the engineering stress (F/A_0) is multiplied by the extension ratio ($1+\epsilon$) to account for the sample's necking down. The secant modulus ($\lambda\sigma/\epsilon$) for the 70°F data are shown in Figure 10 and data are given in Table 3. This same type of data were generated for UTP-3001.

3.1.3 Multirate Test No. 3

Constant rate tests were run on the two propellants and the rate was changed in the middle of the test. Because of the different response for the high-low compared to the low-high, an example of both is given. The test was included with the nondamaged tests because there was no rest or reversal in the crosshead direction. The first leg of the test could be considered the damage. The 1.0 to 0.1 in./min. rate change is shown in Figure 11 for UTP-19,360B and the 0.1 to 1.0 in./min. is shown in Figure 12. The corresponding data for the first sample of each group are given in Table 4 and 5, respectively.

3.1.4 Stress Relaxation Modulus Test No. 4

The stress relaxation modulus tests were run at a nominal 3% strain using 1/2 x 1/2 x 6-in. samples of propellant bonded to redwood end tabs for both propellants. The samples were loaded to 3% strain at a crosshead rate of 1 in./min. for temperatures of 20, 43, 73, and 122°F. The load was monitored with time. Strain was determined by cathetometer measurements on the samples. The relaxation modulus (E_R) was then calculated at specific time intervals by the following equation:

$$E_R = \frac{F}{A_0} \frac{\lambda}{\epsilon}$$

where F = force as measured by the load cell

A_0 = initial area

$\lambda = 1 + \epsilon$

ϵ = strain

The master stress relaxation modulus data for UTP-3001 are presented in Figure 13 and typical data at 73°F are given in Table 6.

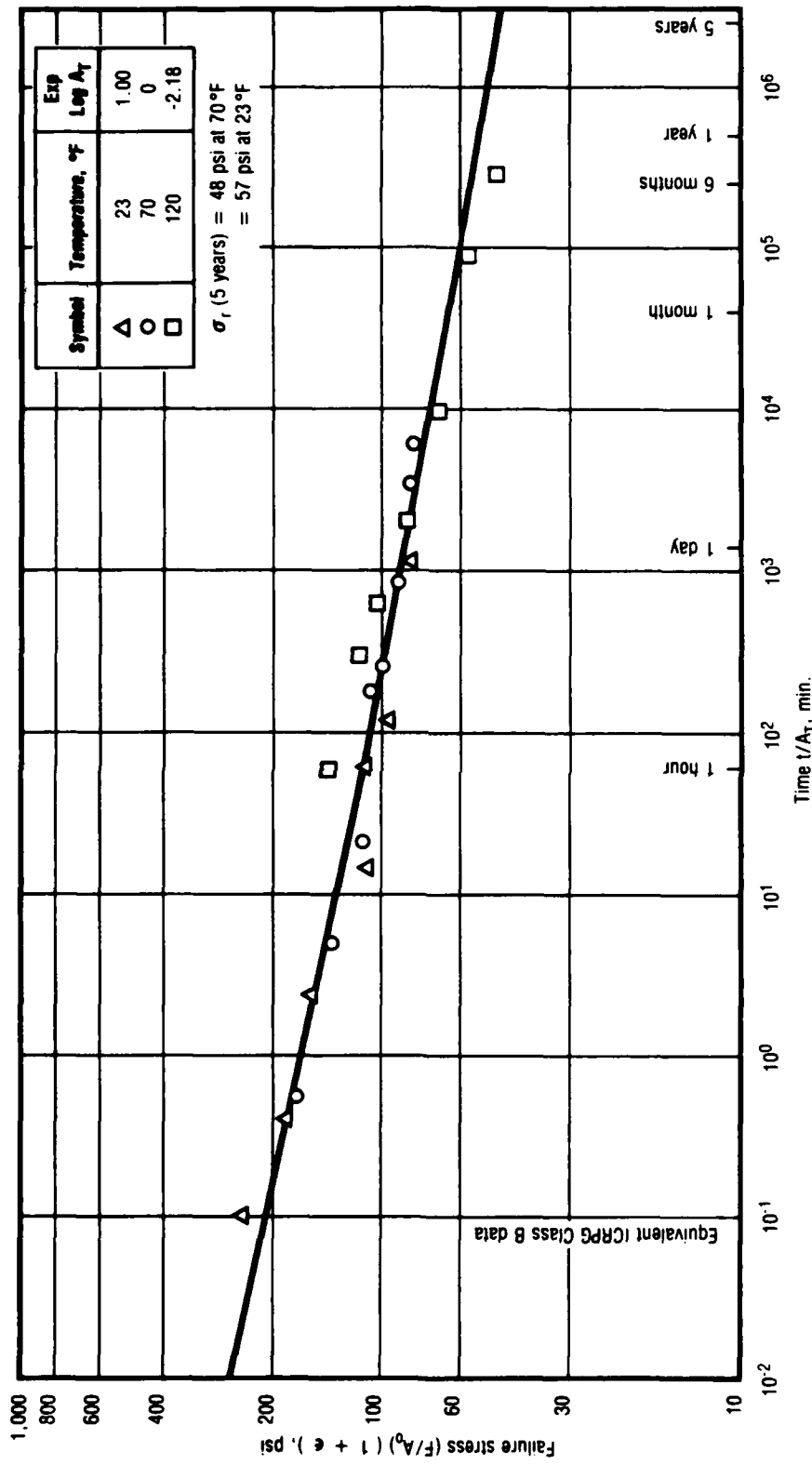


Figure 8. Test No. 2 - Master Uniaxial Stress Endurance Curve for UTP-19, 360B-400/1777 28388

TABLE 2. TEST NO. 2 - UTP-19, 360B 400/1777 CONSTANT ENDURANCE TEST

CONTRACTOR: Corliss, Franets
 TEST DATE: 3-23-61
 TEST YEAR: 251-9501
 TEST YEAR: 2 1/2

THE DATA REDUCTION CONSISTS OF 2 LEAST SQUARE FITS: In(t) vs In(e) and In(t) vs In(e)

NOTE: THE DATA REDUCTION IS BASED ON THE FOLLOWING ASSUMPTIONS:
 - FAILURE TIME CURVE STRAIGHTENED EXPERIMENTALLY DETERMINED
 - LEAST SQUARE FAILURE VALUES AS THE EXPERIMENTAL FAILURE TIME
 - LEAST SQUARE MINUS LEAST SQUARE VALUES
 - STANDARD DEVIATION OF LEAST SQUARES
 - STANDARD ERROR OF ESTIMATE, SLOPE AND INTERCEPT
 - LEAST SQUARE FAILURE VALUES OF THESE FAILURE TIMES

AREA (ins)	t (min)	s (psi)	Ls (psi)	VE (psi)	e (%)	Lsc (Z)	ae (Z)
0.185	5.88	137.63	136.63	1.01	61.00	57.21	1.77
0.194	3.88	121.62	121.62	-1.02	59.00	58.77	0.23
0.172	21.88	118.82	121.79	-1.95	58.00	58.81	0.81
0.188	684.00	88.57	77.34	3.23	47.00	48.86	1.86
0.172	833.00	88.64	88.64	0.00	50.00	50.99	0.99
0.183	176.68	106.52	107.69	3.83	57.00	53.33	3.67

e1	A1	S(E)	S(A1)	S(Ae)	1 year	5 year
5.0462	-0.0801	0.0543	0.0076	0.8365	86.80	47.56
4.1285	-0.0294	0.0720	0.0043	0.483	66.41	42.17

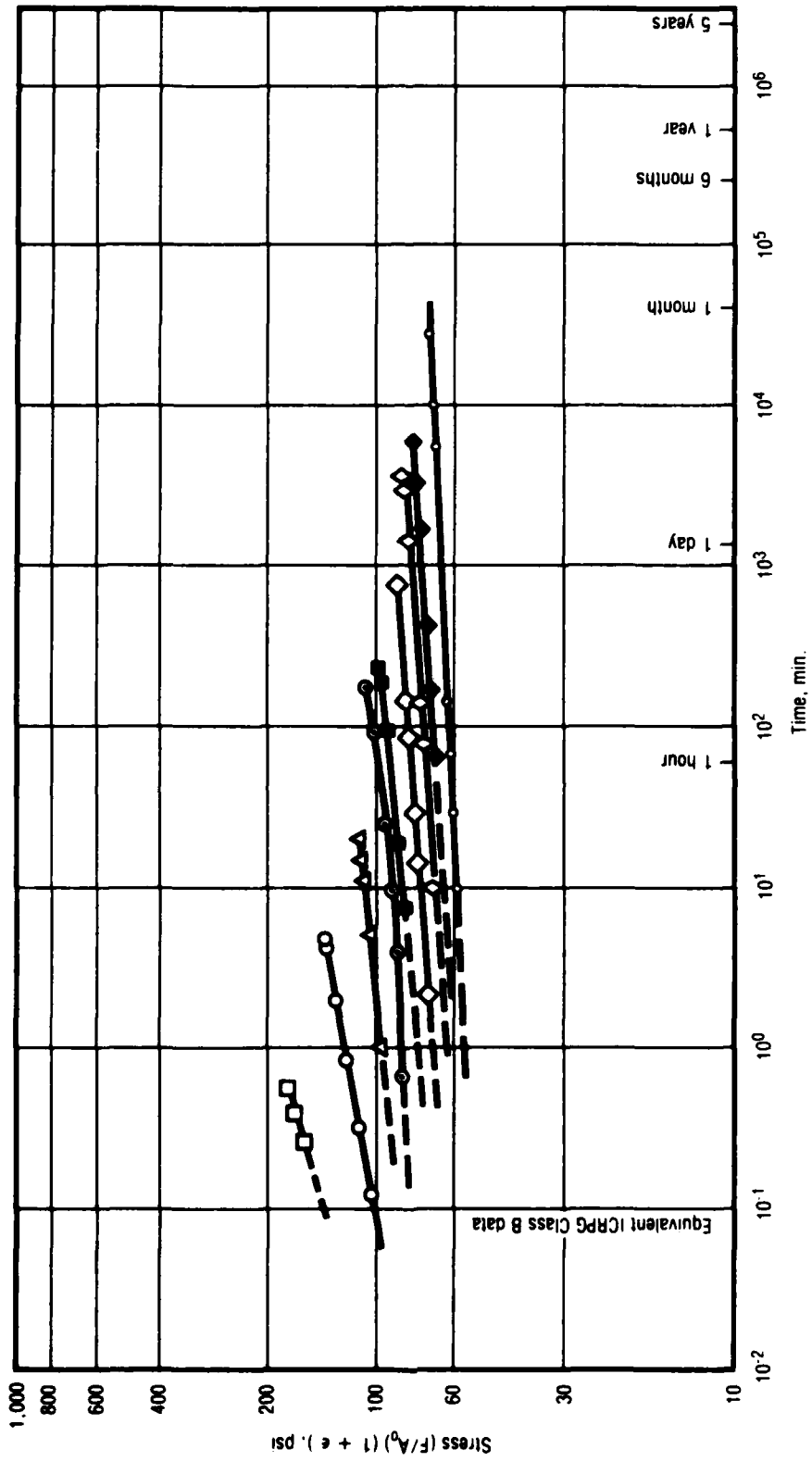


Figure 9. Test No. 2 - Uniaxial Stress Endurance Creep Behavior UTP-19,360B-400/1777 at 70°F 28389

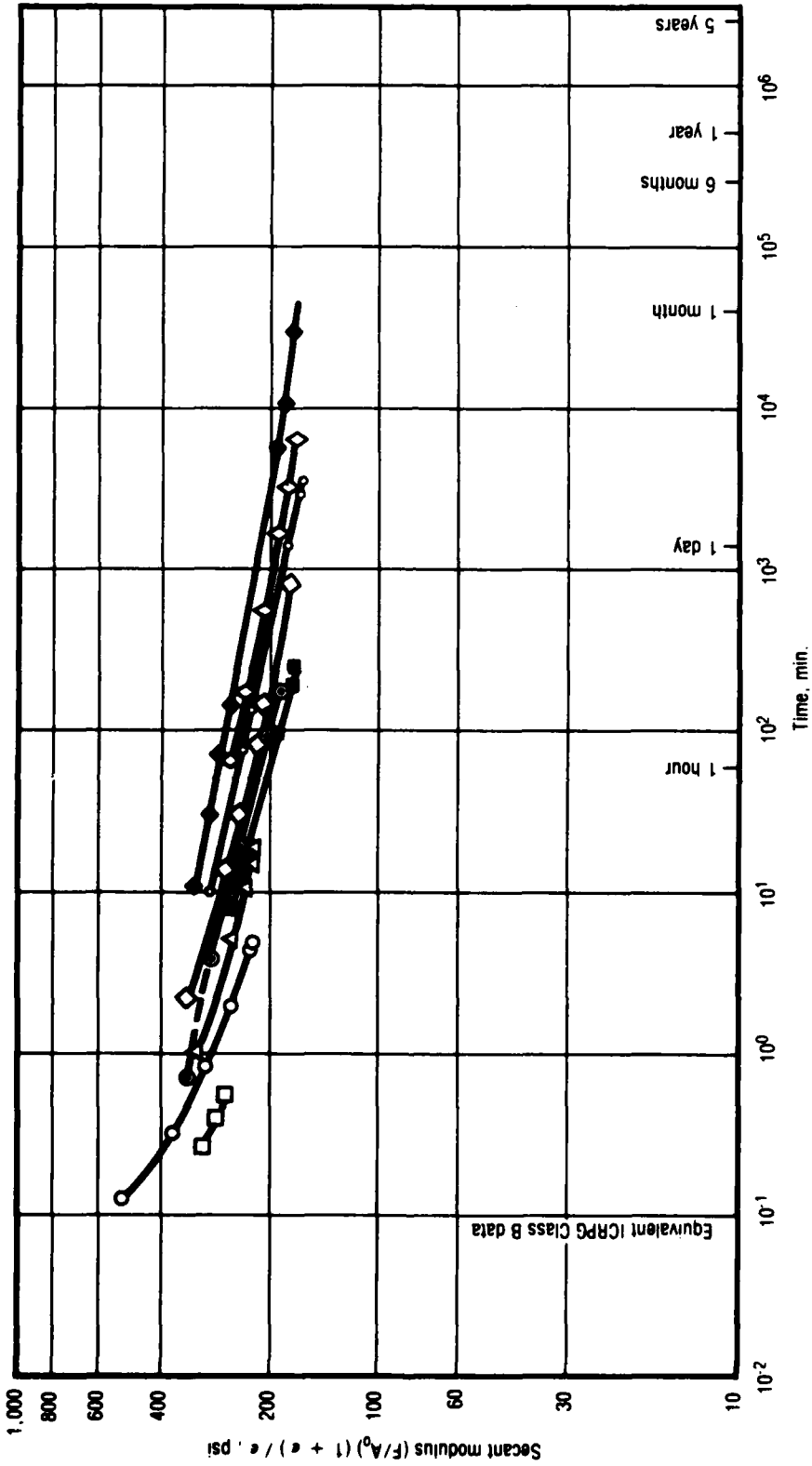


Figure 10. Test No. 2 - Uniaxial Stress Endurance Creep Secant Modulus Behavior for UTP-19, 360B-400/1777 at 70°F

28390

TABLE 3. TEST NO. 2 - UNIAXIAL STRESS ENDURANCE CREEP BEHAVIOR FOR
UTP-19,360B-400/1777 at 70°F

(SHEET 1 OF 2)

T8706

Temperature, F	Sample	Time, min.	Strain, %	Load, g	Area, in. ²	Stress (F/A), psi	$\lambda\sigma$, psi	Secant Modulus ($\lambda\sigma/\epsilon$), psi
70	1	0.13	20	7,180	0.185	85.5	102.6	513
		0.33	30				111.2	370
		0.87	40				119.7	299
		2.0	50				128.3	257
		4.4	60				136.8	228
		5.0	61				137.7	226
70	2	0.27	50	8,720	0.184	104.4	156.6	313
		0.41	60				167.1	279
		0.55	64				171.2	268
70	3	1.0	30	6,000	0.179	73.8	95.9	320
		5.3	40				103.3	258
		11.0	46				107.7	234
		14.9	50				110.7	221
		21.0	50				110.7	221
70	4	7.5	33	5,200	0.182	62.9	83.6	253
		18.0	38				86.8	228
		95.0	49				93.7	191
		196.0	56				98.1	175
		247.0	56				98.1	175
70	5	65.0	27	4,480	0.180	54.8	69.6	258
		190.0	30				71.2	237
		440.0	35				73.9	211
		1,640.0	40				76.7	192
		3,325.0	45				79.5	177
		6,086.0	47				80.6	172
70	6	2.2	21	4,750	0.177	59.1	71.5	340
		14.0	29				76.2	263
		30.0	32				78.0	244
		84.0	37				80.9	219
		150.0	38				81.6	214
		833.0	50				88.7	177

TABLE 3. TEST NO. 2 - UNIAXIAL STRESS ENDURANCE CREEP BEHAVIOR FOR
UTP-19,360B-400/1777 at 70°F

(SHEET 2 OF 2)

T8706

Temperature, F	Sample	Time, min.	Strain, %	Load, g	Area, in. ²	Stress (F/A), psi	$\lambda\sigma$, psi	Secant Modulus ($\lambda\sigma/\epsilon$), psi
70	7	0.7	25	5,630	0.183	67.8	84.8	339
		4.0	30				88.1	294
		10.0	35				91.5	261
		26.0	42				96.3	229
		92.0	51				102.4	200
		177.0	57				106.5	187
70	8	10.0	24	4,660	0.184	55.8	69.2	288
		77.0	30				72.5	242
		140.0	32				73.7	230
		1,418.0	44				80.4	182
		2,900.0	49				83.1	169
		3,500.0	49				83.1	169
70	9	10.0	19	4,030	0.178	49.9	59.4	312
		30.0	20				59.9	299
		70.0	22				60.9	277
		140.0	24				61.9	258
		5,496.0	35				67.4	193
		10,040	37				68.4	185
		Unbroken 28,600	≈ 41				70.4	172

3.1.4.1 Constant Rate Modulus

Constant rate modulus tests were run on the 6-in. bar samples described above and on JANNAF Class B specimens. The 6-in. bar samples use the wood-to-wood distance as the effective gage length while the JANNAF's were analyzed using 2.70-in. effective gage length through the test even though it is varying. Strain was determined by the crosshead travel. The constant rate modulus ($F(t)$) is calculated from the following equation at specific strain levels through the tests.

$$F(t) = \frac{F}{A_0} \frac{\lambda}{\epsilon(t)}$$

where: $\epsilon(t)$ = strain at time t

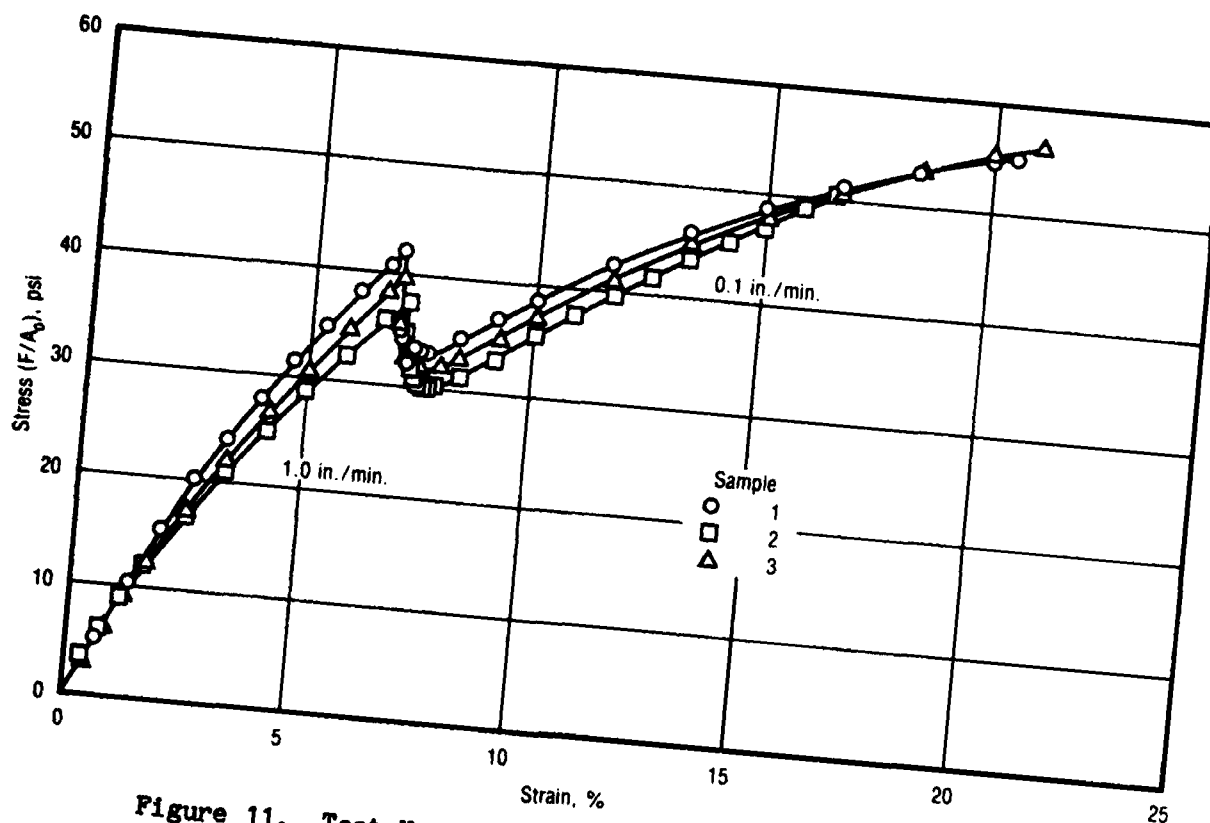


Figure 11. Test No. 3 - High-Low Constant Rate Tests of UTP-19,360B-400/1777 at 70°F

28391

Constant rate modulus data for UTP-3001, with the curve drawn through the small strain portion of the results, are compared to the relaxation modulus in Figure 14. Tabular data for the relaxation and constant rate moduli for 6-in. bars and JANNAF's are given in Table 7.

3.1.5 Multiple Loading Test No. 5

The multiple loading tests on 6-in. bars of UTP-3001 and UTP-19,360B were run five cycles with increasing strain levels for each cycle and with a rest period between cycles. All tests were at 70°F and at crosshead rates of 5, 1, and 0.1 in./min. An attempt was made with UTP-3001 to run at 10 in./min. (i.e., planned rate instead of five) but the data sampling rate did not provide sufficient data points to clearly define the load-time curve, particularly on the first low strain cycle. As previously mentioned, this data had to be reworked.

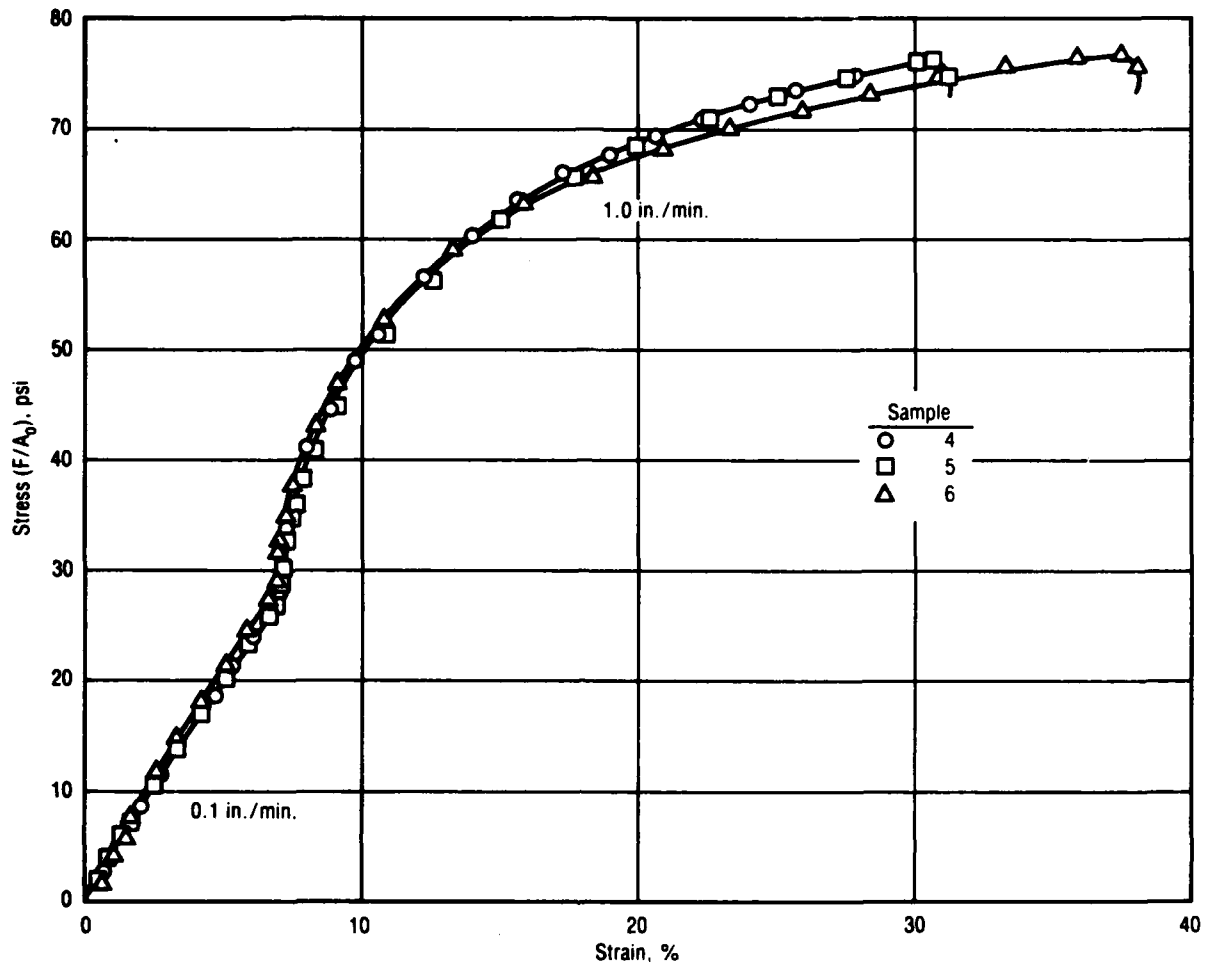


Figure 12. Test No. 3 - Low-High Constant Rate Tests of UTP-19,360B-400/1777 at 70°F

28392

The rework of the data consisted of estimating maximum and minimum stress and strain points that were not picked up by the digitized data acquisition system. The data reduction system computed strain from crosshead travel. This was satisfactory except at and below zero stress. The sample linkage attachment was such that specimens would not be put into compression with the exception of test No. 11, which was run in an Instron with rigid clamp jaws. The actual propellant strain decay was estimated from other tests where strain recovery was monitored by cathetometer measurements for the part of the tests at zero stress (i.e., no load on the samples). The 5-in./min. crosshead test for UTP-19,360B was selected as typical and shown in Figure 15. While the load-unload ramps

TABLE 4. TEST NO. 3 - HIGH-LOW CONSTANT RATE TESTS OF UTP-19,360B-400/1777
AT 70°F WITH 1/2 x 1/2 x 6-IN. BAR SAMPLES

T8707

Sample No. 1
 Crosshead speed, in./min. 1.0 and 0.1
 Chart speed, in./min. 10 and 1
 Load scale 5 lb/in.
 Area, in. 0.500 x 0.501
 Gage length, in. 6.00

Chart Distance, in.	Load Signal, in.	Strain, %	Stress (F/A ₀), psi
0	0	0	0
0.4	0.26	0.667	5.190
0.8	0.52	1.333	10.379
1.2	0.77	2.00	15.369
1.6	1.00	2.667	19.960
2.0	1.20	3.333	23.952
2.4	1.39	4.00	27.745
2.8	1.57	4.667	31.337
3.2	1.74	5.333	34.731
3.6	1.90	6.00	37.924
4.0	2.04	6.667	40.719
4.15	2.10	6.917	41.916
Change to 0.1 in./min.			
4.20	1.74	7.00	34.731
4.25	1.70	7.083	33.932
4.30	1.68	7.167	33.533
4.40	1.66	7.333	33.134
4.50	1.65	7.50	32.934
4.60	1.65	7.667	32.934
5.0	1.73	8.33	34.531
5.5	1.83	9.167	36.527
6.0	1.93	10.00	38.523
7.0	2.12	11.667	42.315
8.0	2.29	13.333	45.709
9.0	2.43	15.00	48.503
10.0	2.55	16.667	50.898
11.0	2.66	18.33	53.094
12.0	2.74	20.00	54.691
12.3	2.76	20.50	55.090

TABLE 5. TEST NO. 3 - LOW-HIGH CONSTANT RATE TESTS OF UTP-19,360B-400/1777
AT 70°F WITH 1/2 x 1/2 x 6-IN. BAR SAMPLES

T8708

Sample No. 4
 Crosshead speed, in./min. 0.1 and 1.0
 Chart speed, in./min. 1.0 and 1.0

Load scale 5 lb/in.
 Area, in. 0.502 x 0.500
 Gage length 6.00

Chart Distance, in.	Load Signal, in.	Strain, %	Stress (F/A ₀), psi
0	0	0	0
0.4	0.14	0.667	2.789
0.8	0.28	1.333	5.578
1.2	0.43	2.00	8.566
1.6	0.57	2.667	11.355
2.0	0.69	3.333	13.745
2.4	0.83	4.00	16.534
2.8	0.94	4.667	18.725
3.2	1.07	5.333	21.315
3.6	1.19	6.00	23.705
4.0	1.30	6.667	25.896
4.18	1.36	6.967	27.092
Change to 1 in./min.			
4.2	1.68	7.300	33.466
4.25	2.05	8.134	40.837
4.3	2.23	8.967	44.422
4.35	2.45	9.800	48.805
4.4	2.57	10.634	51.195
4.5	2.82	12.300	56.175
4.6	3.03	13.967	60.359
4.7	3.18	15.634	63.347
4.8	3.30	17.300	65.737
4.9	3.39	18.967	67.530
5.0	3.48	20.634	69.323
5.1	3.55	22.300	70.717
5.2	3.62	23.967	72.112
5.3	3.68	25.634	73.307
5.43	3.75	27.80	74.701

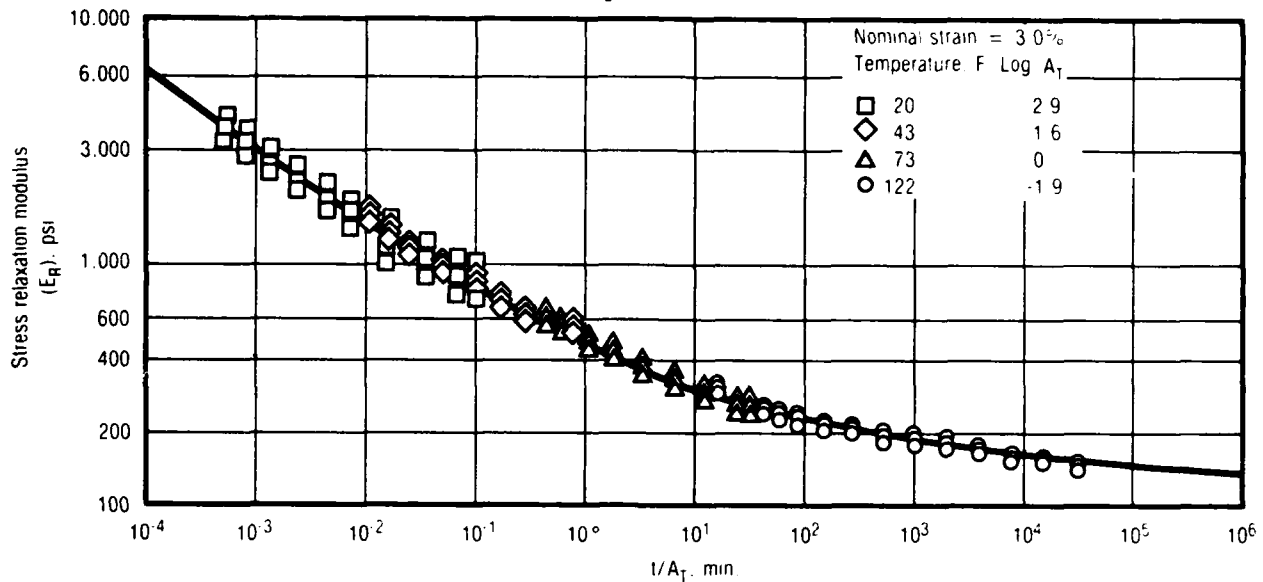


Figure 13. Master Modulus Data for UTP-3001-750/7768 with Experimental Shift

28393

are not clearly shown in the figure because of the scale necessary to show the total test duration, the detailed data are given in Table 8.

3.1.6 Creep Test No. 6

Creep tests were run on 6-in. bars of UTP-3001 and UTP-19,360B by hanging weights on the samples and allowing them to deform under load. The loading was done by setting the weight on the Instron crosshead and then lowering the crosshead away from them as shown in Figure 16. Proper spacing of the segmented weight provided a means of incrementally unloading the samples. The two propellants were run separately to allow access for spacer insertion without disturbing the samples. The procedure for unloading part of the load and still maintaining the balance as a constant load creep test is shown in Figures 17. Tests were run at the maximum load the sample would be sure to survive, then at half and quarter loads. Tests were repeated for 70, 120, and 40° F. The full stress creep test for UTP-19,360B at 71°F is shown as typical. The strain time curve from crosshead and cathetometer measurements is shown in Figure 18 with engineering stress, corrected stress, and secant modulus shown in Figures 19, 20, and 21, respectively. The test data are given in Table 9 and summarized in Table 10 with cathetometer and secant modulus data.

(Text continued on page 29.)

TABLE 6. TEST NO. 4 - 1/2-IN. BAR STRESS RELAXATION DATA REDUCTION

PROPELLANT: UTP 3001 750/7768
 REQUESTOR: Carlton
 WOR:

DATE: 5/5/81
 OPERATOR: JWD

DEFINITIONS:
 Time = Time From Start of Test (min)
 Stress (psi) = Force/Area
 Strain (%) = Sample Extension/Length
 E (air) = Modulus (psi)
 T (air) = Test Air Temperature (F)
 T (prop) = Test Propellant Temperature (F)

RELATIONSHIPS:
 = Force/Area
 E = (Sample Extension)/Length

NOMINAL TEST CONDITIONS:
 Strain = 1%
 Temperature = 73 F
 Gage Length = 6.1 in

CALIBRATION DATA:
 Pretest: Cal Wt = 5 lbs
 Diffusion (lbs/volt)
 Zero Offset (volt), SAMPLE 3
 -1.016
 -0.149

CATHODEMETER STRAIN DATA:
 Initial Upper 89265
 Initial Lower 73525
 Final Upper 88255
 Final Lower 73060
 Strain (%) 3.05

AREAS (sq in) 0.2505 0.2495 0.2495

LOAD DISPLACEMENT DATA: (volt)
 TIME Initial Upper
 4.14E-01 12
 4.14E-01 5.11
 1.02E 00 4.76
 3.82E 00 4.21
 6.62E 00 3.74
 1.30E 01 3.34
 3.58E 01 3.07
 5.03E 01 2.72

MODULUS DATA (psi):
 TIME T(prop) T(air)
 4.14E-01 70.1 68.4
 4.14E-01 70.1 68.4
 1.02E 00 70.1 68.4
 3.82E 00 70.1 68.4
 6.62E 00 70.2 68.7
 1.30E 01 70.4 69.2
 3.58E 01 70.4 69.5
 5.03E 01 70.5 69.5

AVG 92 624
 550.928
 485.524
 375.18
 300.41
 270.65
 250.928
 215.924
 112.421
 11.124
 10.746

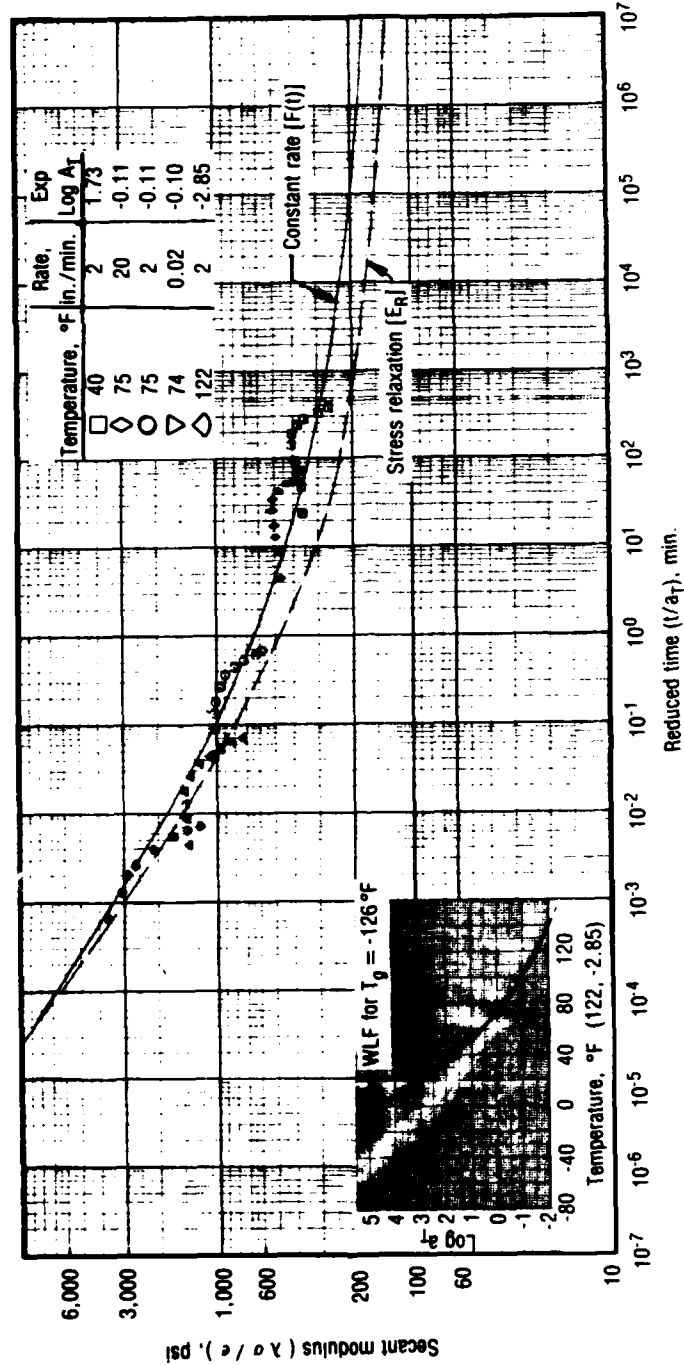


Figure 14. Constant Rate Master Modulus Data for UTP-3001-750/7768 JANNAF Specimens

28394

TABLE 7. MASTER MODULUS CURVES FOR UTP-3001 STRESS RELAXATION AND
CONSTANT RATE TESTS

(SHEET 1 OF 2)

T8709

Reduced Time, t/A_T , min.	6-in. Bar, E_R , psi	6-in. Bar, $F(t)$, psi	JANNAF, $F(t)$, psi
1 x 10 ⁻⁵	-	-	-
2 x 10 ⁻⁵	-	-	-
4 x 10 ⁻⁵	8,750*	10,000*	8,750*
6 x 10 ⁻⁵	7,600*	8,900*	7,800*
8 x 10 ⁻⁵	6,850*	8,200*	7,150*
1 x 10 ⁻⁴	6,350*	7,700*	6,700*
2 x 10 ⁻⁴	5,000*	6,300*	5,400*
4 x 10 ⁻⁴	4,000*	5,200*	4,450*
6 x 10 ⁻⁴	3,500	4,650*	3,950*
8 x 10 ⁻⁴	3,170	4,300	3,630*
1 x 10 ⁻³	3,000	4,070	3,400
2 x 10 ⁻³	2,400	3,350	2,760
4 x 10 ⁻³	1,930	2,760	2,300
6 x 10 ⁻³	1,720	2,520	2,070
8 x 10 ⁻³	1,570	2,320	1,920
1 x 10 ⁻²	1,470	2,180	1,800
2 x 10 ⁻²	1,220	1,830	1,500
4 x 10 ⁻²	1,020	1,550	1,260
6 x 10 ⁻²	910	1,400	1,130
8 x 10 ⁻²	840	1,300	1,070
1 x 10 ⁻¹	800	1,240	1,020
2 x 10 ⁻¹	675	1,060	870
4 x 10 ⁻¹	580	905	765
6 x 10 ⁻¹	520	835	705
8 x 10 ⁻¹	490	790	665
1 x 10 ⁰	470	755	640
2 x 10 ⁰	412	660	570
4 x 10 ⁰	362	580	510
6 x 10 ⁰	340	540	475
8 x 10 ⁰	320	510	460
1 x 10 ¹	308	490	440
2 x 10 ¹	278	445	400
4 x 10 ¹	256	403	370
6 x 10 ¹	243	380	352
8 x 10 ¹	235	365	340

TABLE 7. MASTER MODULUS CURVES FOR UTP-3001 STRESS RELAXATION AND
CONSTANT RATE TESTS

(SHEET 2 OF 2)

T8709

Reduced Time, t/A_T , min.	6-in. Bar, E_R , psi	6-in. Bar, $F(t)$, psi	JANNAF, $F(t)$, psi
1×10^2	230	353	332
2×10^2	218	326	310
4×10^2	207	300	290*
6×10^2	201	290	280*
8×10^2	198	280	273*
1×10^3	193	275	268*
2×10^3	185	258*	255*
4×10^3	182	245*	242*
6×10^3	179	236*	235*
8×10^3	172	232*	230*
1×10^4	169	228*	227*
2×10^4	163	219*	218*
4×10^4	157*	210*	210*
6×10^4	154*	205*	205*
8×10^4	152*	203*	202*
1×10^5	151*	200*	200*
2×10^5	147*	193*	194*
4×10^5	143*	188*	188*
6×10^5	141*	184*	185*
8×10^5	140*	182*	183*
1×10^6	139*	181*	182*
2×10^6	136*	177*	178*
4×10^6	133*	174*	174*
6×10^6	131*	171*	172*
8×10^6	130*	169*	170*

* Extrapolated data

3.1.7 Cyclic Loading Test No. 7

Cyclic loading tests were run on 6-in. bars of UTP-3001 and UTP-19,360B propellants at ambient temperature. The cycling was for 20 cycles at nominal strain levels of 4, 8, and 12% for UTP-19,360B with UTP-3001 limited to 12%. At the end of the test (after unloading to zero stress) the strain was monitored on the samples with a cathetometer. The test at a nominal 12% strain is shown in Figure 22 for UTP-19,360B. These data were modified to insert the estimated maximum stress points and the propellant strain decay while at zero stress. Data for the test are given in Table 11. (Text continued on page 34.)

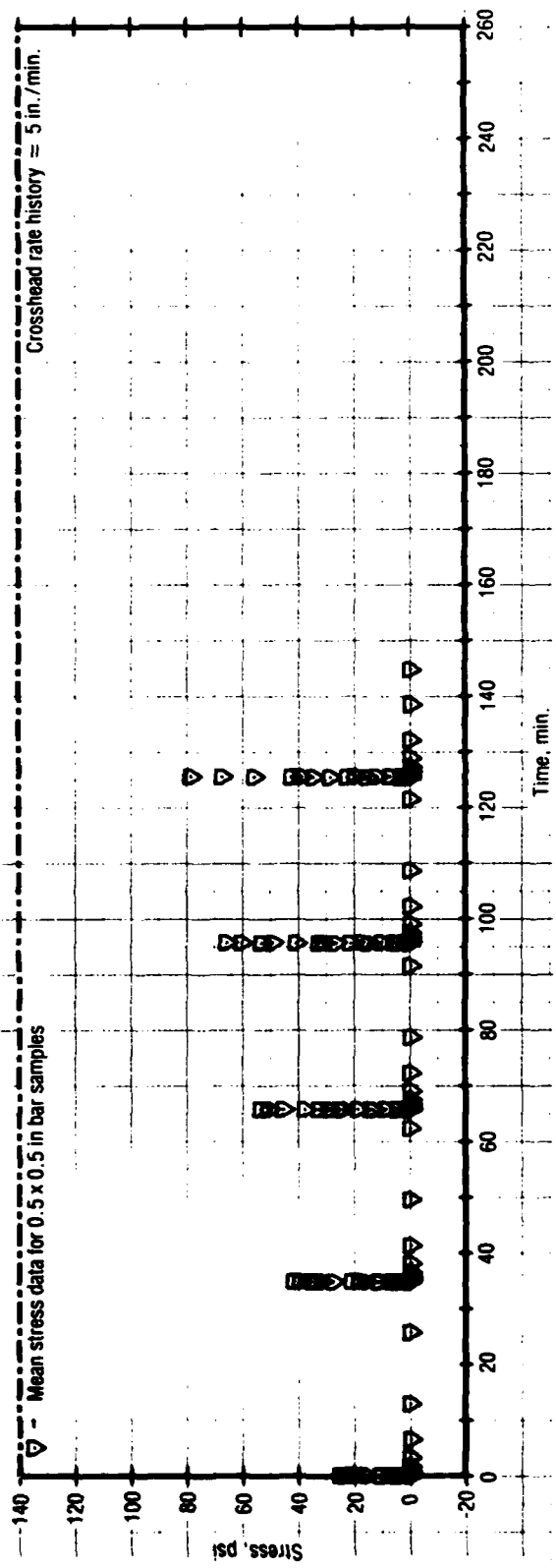
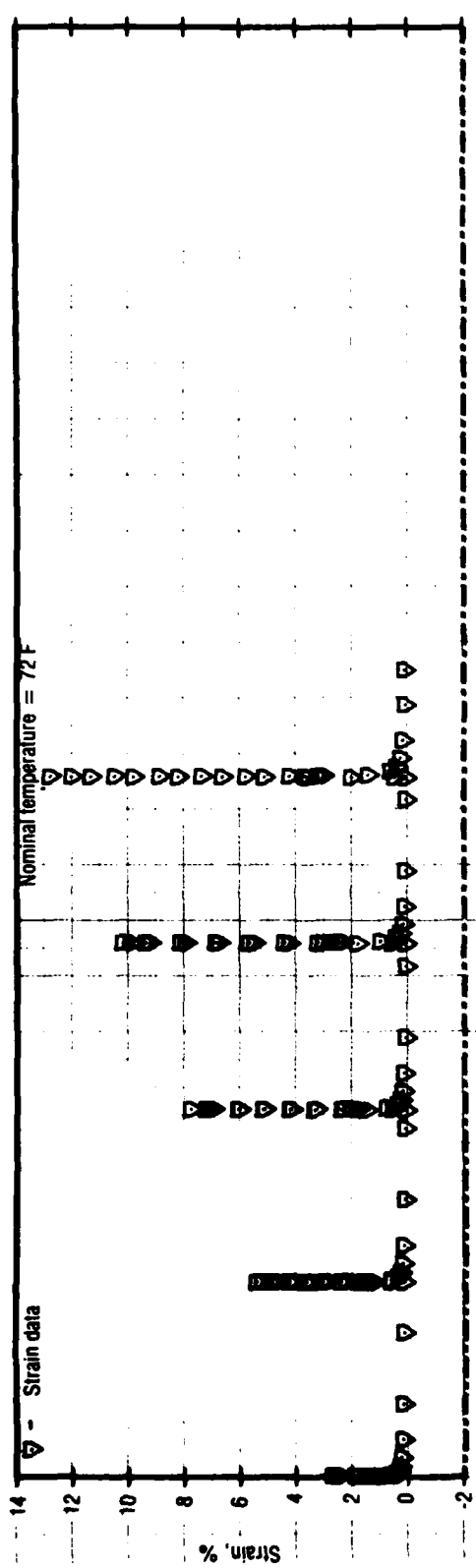


Figure 15. Test No. 5 - Stress While Cycling for UTP-19, 360B-400/1777

TABLE 8. TEST NO. 5 - 1/2-IN. BAR STRESS WHILE CYCLING
(SHEET 1 of 3)

PROPELLANT: UTP 19360B 400/1777
REQUESTOR: Carlton
WOR:

DATE: 5/6/81
(OPERATOR: JWD)

DEFINITIONS:
Time = Time From Start of Test (min)
σ = Stress (psi)
ε = Strain (%)
T(air) = Test Air Temperature (F)
T(prop) = Test Propellant Temperature (F)

RELATIONSHIPS:
σ = Force/Area
ε = Sample Extension/Length

NOMINAL VALUES:
Test Temp = 72 F
Gage Length = 5.95 in
Nom. Strain = 2.5, 5, 7.5, 10, 12.5 %
XHD Rate = 5 in/min

CALIBRATION DATA:
Cal Wt = 5.0 lbs
Lead Cal (lbs/velts)
Offset (velts)
Pot Cal (in/velts) =
Temp (F)

SAMPLE 1
5.850
0.049
-0.388
-73.2

SAMPLE 2
6.098
0.045

SAMPLE 3
6.118
0.093

AREAS (sq in):

0.251

0.253

0.255

STRESS DATA (psi) Time
1 0.06607
2 0.01226
3 0.01861
4 0.02409
5 0.03044
6 0.03595
7 0.04156
8 0.04798
9 0.05238
10 0.05678
11 0.06118
12 0.06559
13 0.07045
14 0.07941
15 0.08798
16 0.09653
17 0.10511
18 0.11366
19 0.12218
20 0.13071

T(prop) T(air)

73.4 74.2
73.2 74.4
73.4 74.2
73.5 74.1
73.4 74.0
73.1 73.8

STRAIN

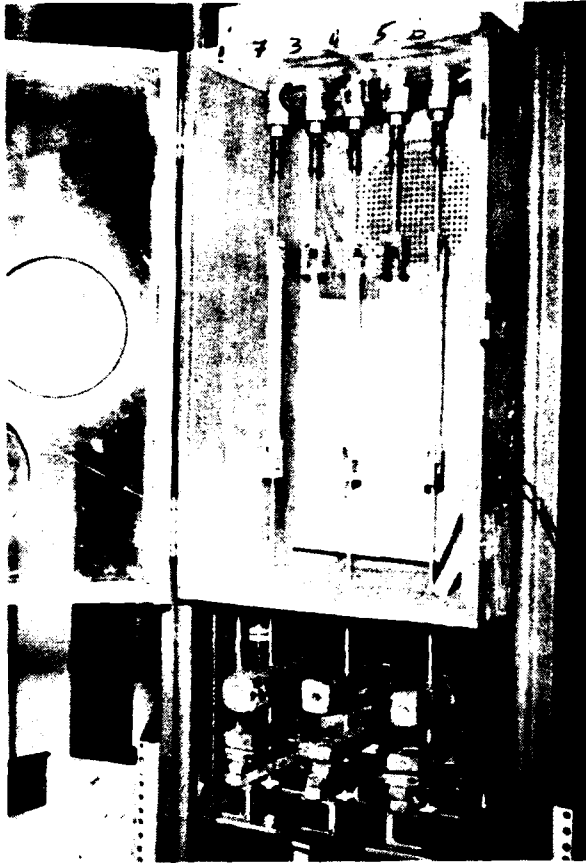
0.90
1.42
1.88
2.35
2.82
3.29
3.76
4.23
4.70
5.17
5.64
6.11
6.58
7.05
7.52
7.99
8.46
8.93
9.40
9.87

SAMPLE 1
3.58
9.89
14.65
18.58
22.75
27.03
31.35
35.70
40.00
44.35
48.70
53.00
57.35
61.70
66.00
70.35
74.70
79.00
83.35
87.70
92.00
96.35
100.70

3
15.87
11.64
16.40
21.16
25.92
30.68
35.44
40.20
44.96
49.72
54.48
59.24
64.00
68.76
73.52
78.28
83.04
87.80
92.56
97.32
102.08
106.84

AVG
4.53
10.63
15.47
23.58
31.76
39.92
48.08
56.24
64.40
72.56
80.72
88.88
97.04
105.20
113.36
121.52
129.68
137.84
146.00
154.16
162.32
170.48
178.64

ST. Dev
0.666
0.632
0.601
0.580
0.560
0.540
0.520
0.500
0.480
0.460
0.440
0.420
0.400
0.380
0.360
0.340
0.320
0.300
0.280
0.260
0.240
0.220
0.200



13845-1

Figure 16. Test No. 6 - Creep
Test with 6-in. Bar Specimens

28747

allowed to rest, then reloaded to 8 or 4% strain at 20 in./min. After relaxing 1 hr the samples were unloaded at 1.0 in./min. and strain was monitored after unloading. These tests were repeated for a 6% predamage strain followed by a reload to 4 or 2% as above. The 12% predamage followed by 8% stress relaxation for UTP-19,360B is shown in Figure 24, and tabular data are given in Table 13. Comparison data for UTP-3001 was limited to 6% predamage followed by 3% relaxation. These data were modified to obtain the peak stress and strain relaxation after the samples were unloaded. Strain was monitored with a cathetometer after the relaxation part of the test.

3.1.10 Complex Multiple Load Test No. 10

The complex multiple load tests were run with 6-in. bars on UTP-3001 and UTP-19,360B propellants. Tests were run at crosshead rates of 5, 1, and

3.1.8 Relaxation Test No. 8

Stress relaxation tests were run on 6-in. bars of UTP-3001 and UTP-19,360B propellant for a 24-hr period and then monitored for strain decay after they were unloaded. The tests at ambient temperature were repeated for 4, 8, and 12% nominal strain levels for UTP-19,360B but limited to 4% for UTP-3001. They were loaded at a crosshead rate of 20 in./min. and unloaded at 1 in./min. after the 24-hr relaxation. A plot for the UTP-19,360B at 4% nominal strain is shown as typical in Figure 23, and data are given in Table 12.

3.1.9 Predamaged-Relaxation Test No. 9

The predamage-relaxation tests were run with 6-in. bars on UTP-19,360B propellant at ambient temperature. They were preloaded to 12% and unloaded at a crosshead rate of 0.1 in./min.,

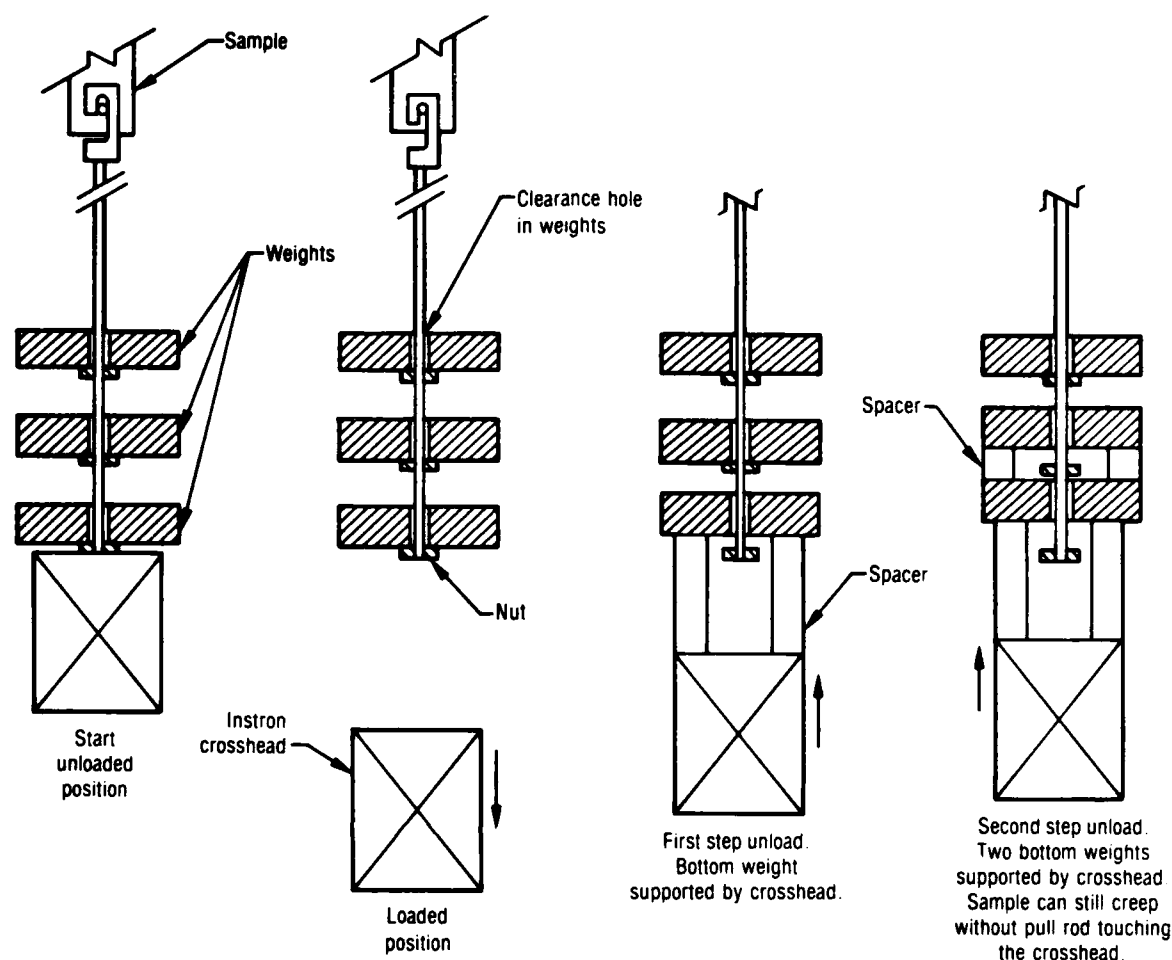


Figure 17. Procedure for Loading and Incrementally Unloading Creep Samples 28805

0.1 in./min. The test sequence was 12 to 8 to 12 to 4% strain, then unload, reload to 4% strain, and unload (four cycles) with cathetometer monitoring of strain decay. The same type of sequence was repeated with maximum strains of 8 and then 4% where the 4% maximum strain was shortened by one cycle. The 5 in./min., 12% maximum strain test on UTP-19,360B as typical is shown in Figure 25, and tabular data are given in Table 14. The data were reworked to insert maximum and minimum stress values as well as strain decay for unloaded specimens. The cathetometer strain after the final unload was incorporated into the data. The 5 in./min 12% strain test for UTP-3001 was deleted because the modulus was outside the range of the remainder of the data (i.e. carton to carton difference).

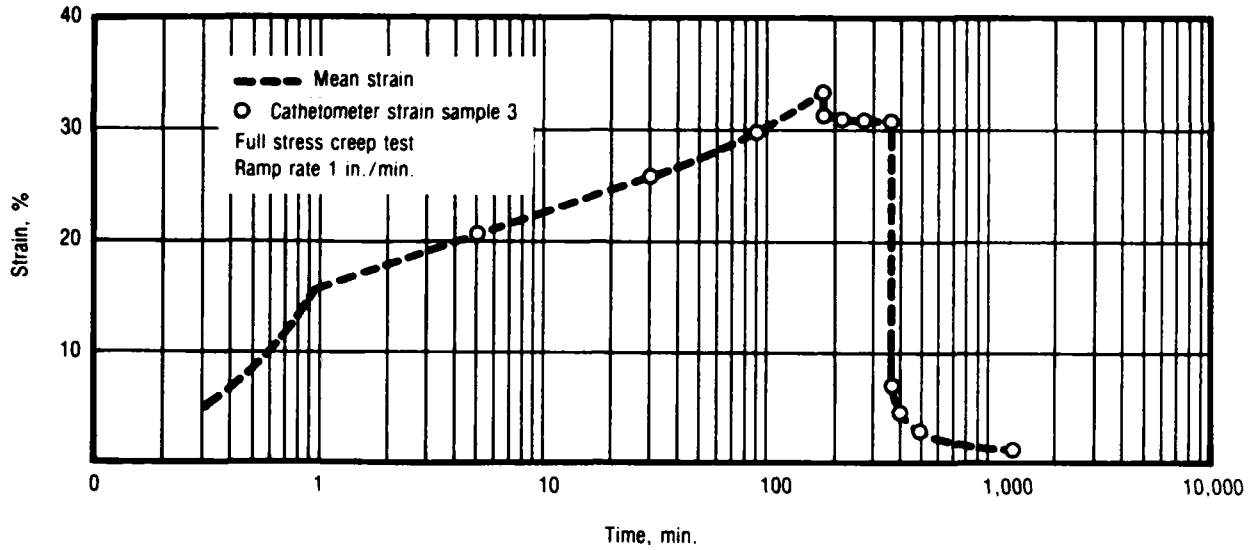


Figure 18. Test No. 6 - Strain-Time Data for Creep Test of UTP-19,360B-400/1777 at 71°F

28748

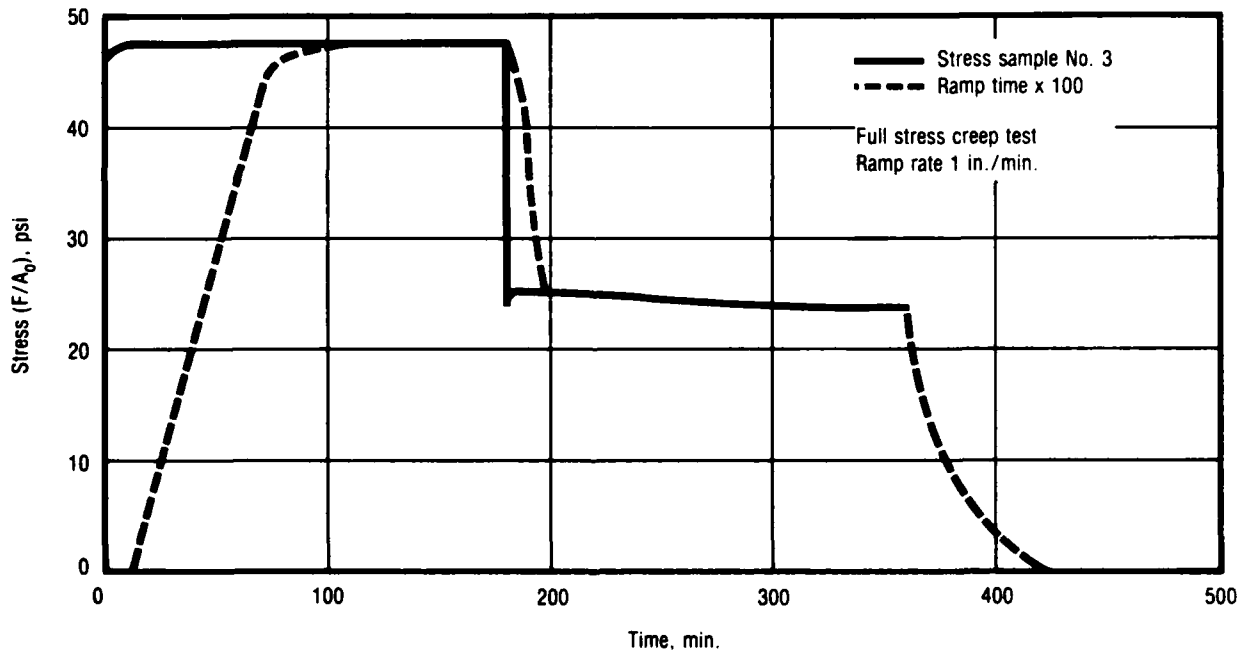


Figure 19. Stress-Time Data for Creep Test of UTP-19,360B-400/1777 at 71°F

28749

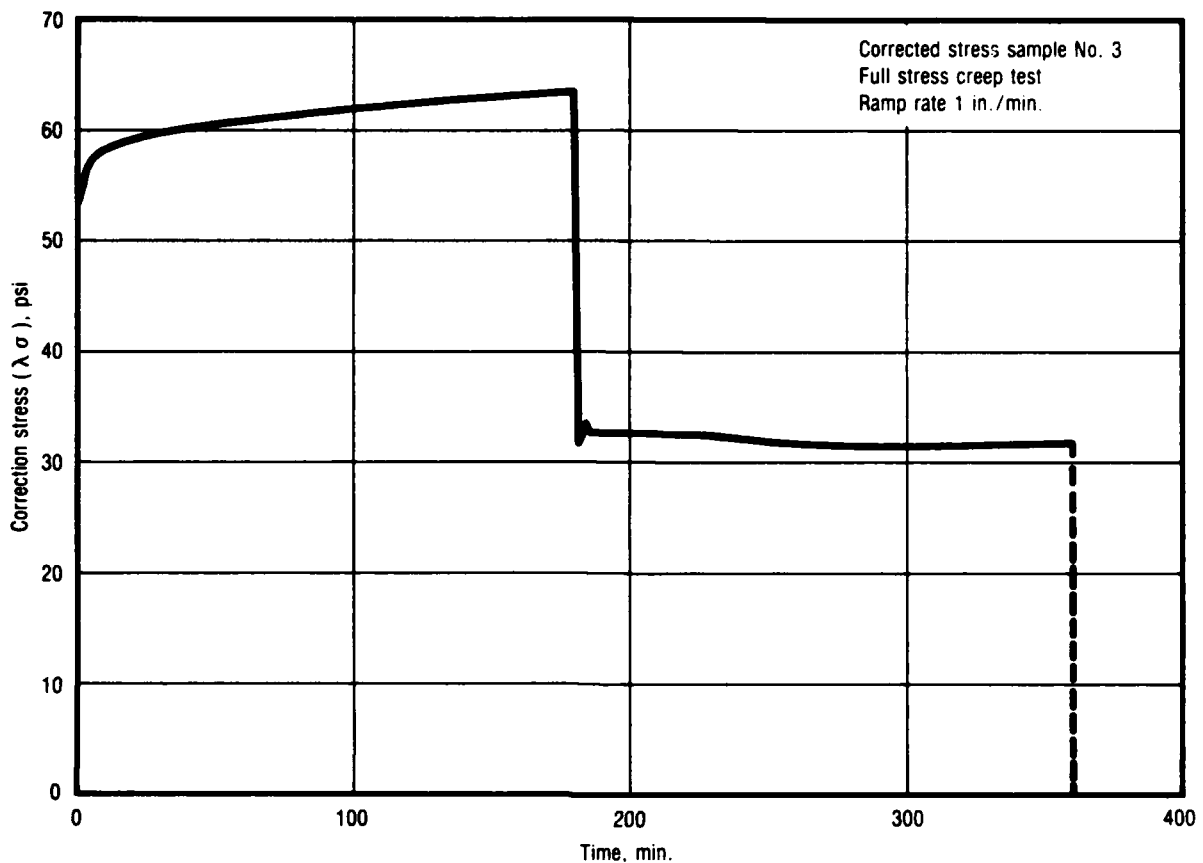


Figure 20. Corrected Stress-Time Data for Creep Test of UTP-19,360B-400/1777 at 71 F

28750

3.1.11 Quinlan Complex History Test No. 11A

This particular test is very complex and required 2 full months to complete. It was run with single samples (one at a time) in an Instron using 6-in. bar specimens of UTP-3001 and UTP-19,360B propellant. The samples were pinned through the redwood end tabs and clamped onto pins to avoid crushing the redwood (because that would generate a compression load on the sample) during attachment. All coupling joints were heavy and tightly pinned so that the sample would be put into compression when returned to the zero strain position.

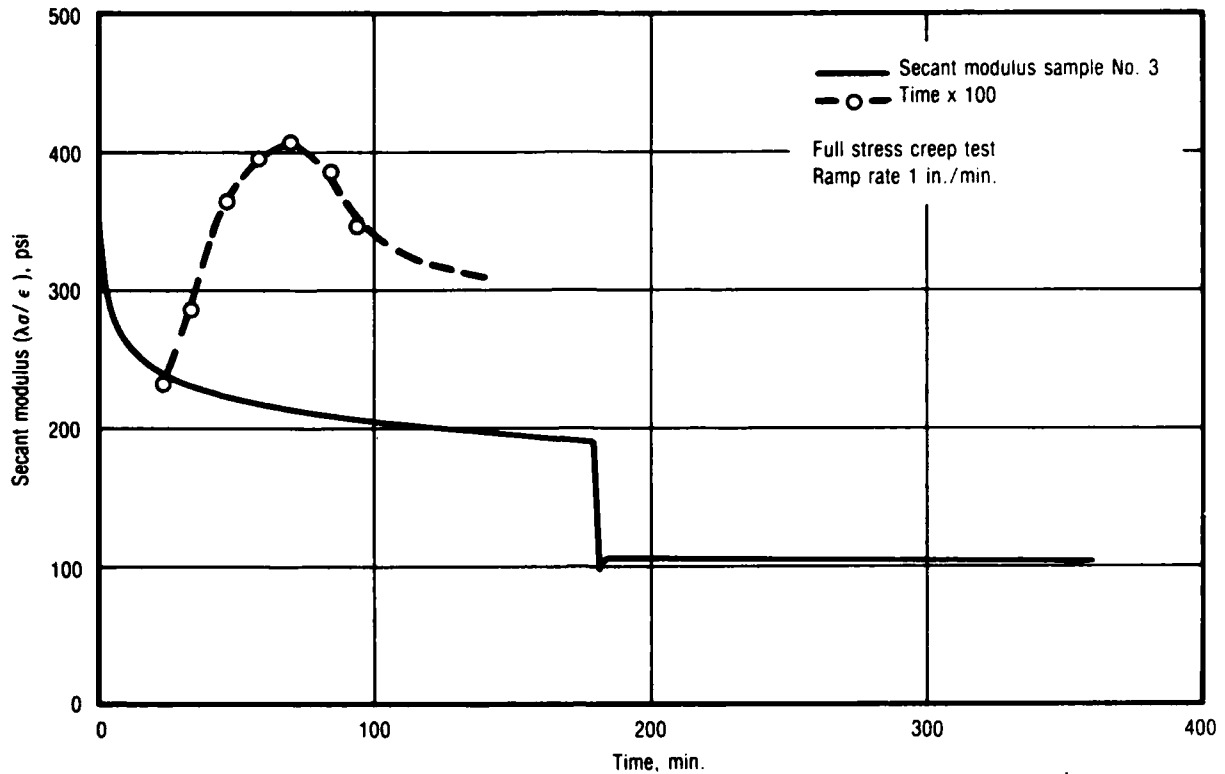


Figure 21. Secant Modulus Data for Creep Test of UTP-19,360B-400/1777 at 71°F

28752

The test on UTP-3001 is presented but the test is so complex that it has been divided into three parts. Part 1 is described in Table 15 with data given in Table 16. Since an actual Instron trace of the load-time curve was obtained, the peaks and minimum (compression) stresses were selected data reduction points. Part 1 of the test is expanded in time scale to show some detail of the process (Figures 26 through 29). Part 2 is described in Table 17 with data given in Table 18. Test sequence for Part 2 is shown in Figures 30, 31, and 32. Part 3 (selected cycle maximum and minimum) are given in Table 19. The last figure of this part (Figure 32) is some of the cyclic loading at the end of the test. The chart speed was set such that good definition of the cycles could be recorded.

(Text continued on page 64.)

TABLE 9. TEST NO. 6 - 1/2-IN. BAR STRESS WHILE CYCLING (FULL STRESS CREEP)
(SHEET 1 OF 8)

PROPELLANT: UTP 19360B 400/1777
REQUESTOR: Carlton
WOR:

DATE: 5/7/81
OPERATOR: JWD

DEFINITIONS:
Time = Time From Start of Test (min)
Stress (psi) = Force/Area
Strain (%) = Sample Extension/Length
T(air) = Test Air Temperature (F)
T(prop) = Test Propellant Temperature (F)

RELATIONSHIPS:
= Force/Area
= Sample Extension/Length

NOMINAL VALUES: = 71 F
Test Temp = 6.00 in
Gage Length = 3 %
Nom. Strain = 1 in/min
XHD Rate = 1 in/min

CALIBRATION DATA:
Cal Wt = 5.0 lbs
Lead Cal (lbs/volts) = 5.85
Offset (volts) = 0.03
Pot Cal (in/volts) = -0.38
Temp (F) = 72.5

SAMPLE 1 2 3
6.03 6.12 0.07
0.03

AREAS (sq in): 0.252 0.250 0.251

TIME	T(prop)	T(air)	Strain	SAMPLE	3	Avg	St Dev
6.5768E-03			0.11	1	0.01	-0.00	0.010
1.3369E-02			0.34	2	-0.01	-0.00	0.004
2.6935E-02			0.45	3	-0.01	-0.01	0.005
3.3710E-02			0.56	1	0.01	0.00	0.006
4.0485E-02			0.68	2	0.00	0.00	0.003
5.4019E-02			0.90	3	0.01	-0.00	0.001
6.0802E-02			1.01	1	-0.01	-0.01	0.009
7.7569E-02			1.25	2	0.00	0.00	0.006
8.4344E-02			1.37	3	0.00	0.00	0.016
9.7885E-02			1.46	1	-0.01	0.00	0.052
1.0147E-01			1.50	2	0.01	0.00	0.085
1.0827E-01			1.70	3	0.00	0.00	0.542
1.1504E-01			1.81	1	-0.01	0.00	0.738
1.2184E-01			1.91	2	0.00	0.00	0.920
1.2862E-01			2.01	3	-0.01	0.00	1.144
1.3542E-01			2.23	1	0.00	0.00	1.369
1.4220E-01			2.36	2	0.02	1.07	1.649
1.4900E-01			2.45	3	0.04	1.07	1.826
1.5580E-01			2.56	1	0.04	1.07	2.182

TABLE 9. TEST NO. 6 - 1/2-IN. BAR STRESS WHILE CYCLING (FULL STRESS CREEP)
(SHEET 8 OF 8)

6276E	02222	27.8	-0.49	1.90	0.38	0.934
6277E	00000	0.267	-0.510	1.813	0.328	0.902
6278E	00000	0.229	-0.511	1.602	0.224	0.814
6279E	02222	0.228	-0.511	1.525	0.218	0.788
6280E	00000	0.269	-0.511	1.452	0.114	0.753
6281E	02222	0.267	-0.510	1.323	0.10	0.669
6282E	00000	0.229	-0.510	1.107	0.06	0.604
6283E	02222	0.267	-0.510	0.925	0.043	0.552
6284E	00000	0.267	-0.500	0.85	0.033	0.510
6285E	02222	0.277	-0.501	0.70	0.025	0.448
6286E	00000	0.267	-0.510	0.61	0.06	0.414
6287E	02222	0.277	-0.510	0.50	0.10	0.413
6288E	00000	0.267	-0.510	0.438	0.125	0.373
6289E	02222	0.267	-0.509	0.288	0.119	0.335
6290E	00000	0.267	-0.49	0.187	0.123	0.282
6291E	02222	0.27	-0.5	0.107	-0.123	0.24

TABLE 10. FULL STRESS CREEP TEST FOR UTP-19, 360B-400/1777 at 710F

T8710

Time, min.	Cathetometer Strain, %			Stress F(A ₀), psi			λσ, psi	Secant Modulus, psi	
	No. 1	No. 2	No. 3	Average	No. 1	No. 2			No. 3
0.0066				0.01	0	0	0	0	-
0.1218				2.03	0	2.80	0	0	-
0.2377				3.96	6.21	11.41	8.95	8.95	235
0.3338				5.56	12.46	16.66	15.18	15.18	288
0.4643				7.74	22.43	26.24	26.32	26.32	366
0.5810				9.68	30.33	33.87	34.84	34.84	395
0.6979				11.63	37.42	40.52	42.61	42.61	409
0.8146				13.58	43.53	45.80	46.30	46.30	387
0.9261				15.44				46.34	346
5	Broke	Broke	20.43	20.43				47.50	280
18.557				24.20			47.53	47.52	244
30			25.64	25.64				47.42	232
56.958				27.80			47.32	47.32	218
90			29.81	29.81				47.39	206
108.16				30.70			47.46	47.40	202
150				32.40				47.46	194
180			33.64	32.64				47.46	189
181.78				32.78				23.85	96.6
183.16				32.12			23.85	25.15	103.4
185			31.23	31.25				25.00	105.1
215			31.00	31.00				24.90	105.2
233.56				30.90				24.75	104.8
275			30.76	30.76				24.00	102.0
284.76				30.78			24.23	24.23	102.9
360			30.83	30.83			24.23	24.23	102.8
363.26				12.00				-	
363.32				10.00				-	
365			7.96	7.96			0	0	
390			4.61	4.61			0	0	
480			2.91	2.91			0	0	
1290			1.15	1.15			0	0	

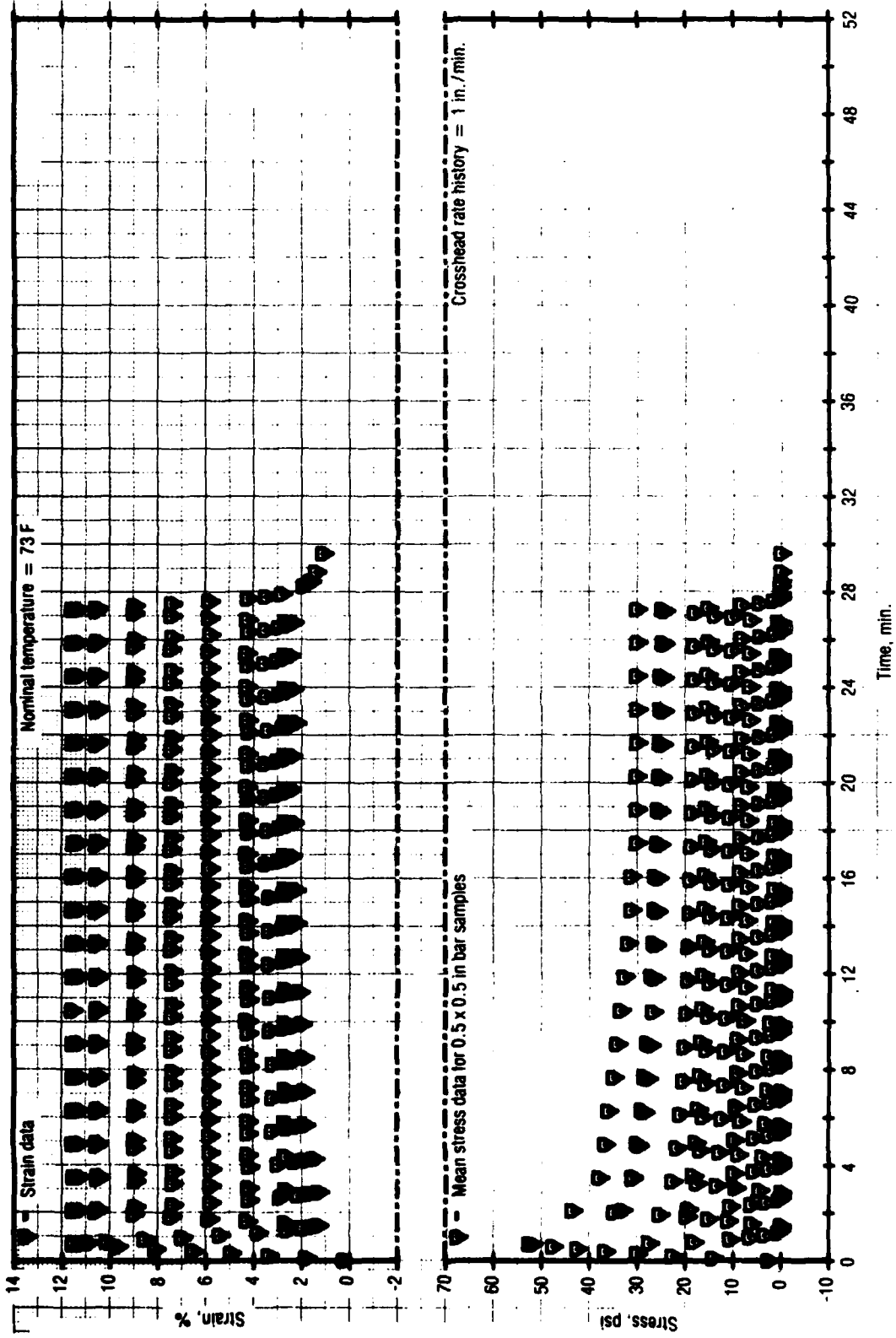


Figure 22. Test No. 7 - Stress While Cycling for UTP-19, 360B-400/1777

TABLE 11. TEST NO. 7 - 1/2-IN. BAR STRESS WHILE CYCLING
(SHEET 1 OF 7)

PROPELLANT: UTP 19360B 400/1777
REQUESTOR: Carlton

DATE: 6/4/81
OPERATOR: JWD

DEFINITIONS:
Time = Time From Start of Test (min)
Stress (psi)
Strain (%)
T(air) = Test Air Temperature (F)
T(prop) = Test Propellant Temperature (F)

RELATIONSHIPS:
= Force/Area
= Sample Extension/Length

NOMINAL VALUES:
Test Temp = 73 F
Gage Length = 6.00 in
Nom. Strain = 12%
XHD Rate = 1 in/min

CALIBRATION DATA:
Cal Wt = 5.0 lbs
Lead Cal (lbs/volts)
Offset (volts)
Pot Cal (in/volts) =
Temp (F)

SAMPLE 3
2 1.03
-0.024

1.855
0.022
-0.389

AREAS (sq in):

0.249 0.250 0.250

STRESS DATA (psi):

SE1	1	2	3	4	5	6	7	8	9	10	11	12	13	14	15	16	17	18	19	20	21	22	23	24	25	26	
	1990	1045	2062	3018	3981	4901	5860	6761	7751	8841	9801	1075	1174	1267	1364	1474	1550	1631	1716	1801	1891	1974	2061	2141	2221	2301	2377

T(prop)	75.1	74.9	74.7	74.9	74.5	74.5	74.5	74.8	74.9	74.7	74.5	74.9	74.7	74.7	74.7	74.8	74.8	74.8	74.8	74.8	74.8	74.8	74.8	74.8	74.8	74.8	74.8
T(air)	74.9	74.7	74.7	74.9	74.5	74.5	74.5	74.8	74.9	74.7	74.5	74.9	74.7	74.7	74.7	74.8	74.8	74.8	74.8	74.8	74.8	74.8	74.8	74.8	74.8	74.8	74.8
STRAIN	0.281	1.339	4.654	6.810	9.128	11.524	14.559	18.265	21.695	1.602	1.719	2.266	2.419	2.865	2.919	3.221	3.334	3.419	3.419	3.419	3.419	3.419	3.419	3.419	3.419	3.419	3.419

SAMPLE	2	22	22	34	35	72	95	64	82	88	98	00	00	00	00	00	00	00	00	00	00	00	00	00	00	00	00
	120	227	330	383	477	554	627	682	727	769	828	871	917	960	1000	1000	1000	1000	1000	1000	1000	1000	1000	1000	1000	1000	1000
AVG	14.18	20.64	36.68	42.58	51.84	52.75	54.42	56.69	59.27	60.44	60.30	60.00	60.00	60.00	60.00	60.00	60.00	60.00	60.00	60.00	60.00	60.00	60.00	60.00	60.00	60.00	60.00
ST	1.0	1.2	2.2	2.2	2.2	2.2	2.2	2.2	2.2	2.2	2.2	2.2	2.2	2.2	2.2	2.2	2.2	2.2	2.2	2.2	2.2	2.2	2.2	2.2	2.2	2.2	2.2

TABLE 11. TEST NO. 7 - 1/2-IN. BAR STRESS WHILE CYCLING
(SHEET 6 OF 7)

266	10.714	11.75	10.14	9.720	11.597	10.48	10.839
267	11.75	12.96	11.75	13.118	12.96	11.48	11.839
268	12.96	14.39	12.96	14.099	14.39	12.48	12.839
269	14.39	15.39	14.39	14.493	15.39	13.33	13.839
270	15.39	16.02	15.39	14.705	16.02	14.48	15.282
271	16.02	17.34	16.02	15.030	17.34	15.58	16.645
272	17.34	18.00	17.34	15.000	18.00	16.00	17.320
273	18.00	18.00	18.00	15.000	18.00	16.00	17.320
274	18.00	18.00	18.00	15.000	18.00	16.00	17.320
275	18.00	18.00	18.00	15.000	18.00	16.00	17.320
276	18.00	18.00	18.00	15.000	18.00	16.00	17.320
277	18.00	18.00	18.00	15.000	18.00	16.00	17.320
278	18.00	18.00	18.00	15.000	18.00	16.00	17.320
279	18.00	18.00	18.00	15.000	18.00	16.00	17.320
280	18.00	18.00	18.00	15.000	18.00	16.00	17.320
281	18.00	18.00	18.00	15.000	18.00	16.00	17.320
282	18.00	18.00	18.00	15.000	18.00	16.00	17.320
283	18.00	18.00	18.00	15.000	18.00	16.00	17.320
284	18.00	18.00	18.00	15.000	18.00	16.00	17.320
285	18.00	18.00	18.00	15.000	18.00	16.00	17.320
286	18.00	18.00	18.00	15.000	18.00	16.00	17.320
287	18.00	18.00	18.00	15.000	18.00	16.00	17.320
288	18.00	18.00	18.00	15.000	18.00	16.00	17.320
289	18.00	18.00	18.00	15.000	18.00	16.00	17.320
290	18.00	18.00	18.00	15.000	18.00	16.00	17.320
291	18.00	18.00	18.00	15.000	18.00	16.00	17.320
292	18.00	18.00	18.00	15.000	18.00	16.00	17.320
293	18.00	18.00	18.00	15.000	18.00	16.00	17.320
294	18.00	18.00	18.00	15.000	18.00	16.00	17.320
295	18.00	18.00	18.00	15.000	18.00	16.00	17.320
296	18.00	18.00	18.00	15.000	18.00	16.00	17.320
297	18.00	18.00	18.00	15.000	18.00	16.00	17.320
298	18.00	18.00	18.00	15.000	18.00	16.00	17.320
299	18.00	18.00	18.00	15.000	18.00	16.00	17.320
300	18.00	18.00	18.00	15.000	18.00	16.00	17.320
301	18.00	18.00	18.00	15.000	18.00	16.00	17.320
302	18.00	18.00	18.00	15.000	18.00	16.00	17.320
303	18.00	18.00	18.00	15.000	18.00	16.00	17.320
304	18.00	18.00	18.00	15.000	18.00	16.00	17.320
305	18.00	18.00	18.00	15.000	18.00	16.00	17.320
306	18.00	18.00	18.00	15.000	18.00	16.00	17.320
307	18.00	18.00	18.00	15.000	18.00	16.00	17.320
308	18.00	18.00	18.00	15.000	18.00	16.00	17.320
309	18.00	18.00	18.00	15.000	18.00	16.00	17.320
310	18.00	18.00	18.00	15.000	18.00	16.00	17.320
311	18.00	18.00	18.00	15.000	18.00	16.00	17.320
312	18.00	18.00	18.00	15.000	18.00	16.00	17.320
313	18.00	18.00	18.00	15.000	18.00	16.00	17.320
314	18.00	18.00	18.00	15.000	18.00	16.00	17.320
315	18.00	18.00	18.00	15.000	18.00	16.00	17.320
316	18.00	18.00	18.00	15.000	18.00	16.00	17.320
317	18.00	18.00	18.00	15.000	18.00	16.00	17.320
318	18.00	18.00	18.00	15.000	18.00	16.00	17.320
319	18.00	18.00	18.00	15.000	18.00	16.00	17.320
320	18.00	18.00	18.00	15.000	18.00	16.00	17.320

TABLE 11. TEST NO. 7 - 1/2-IN. BAR STRESS WHILE CYCLING
(SHEET 7 OF 7)

3190	26.0	75.0	76.1	7.6	7.3	9.5	2.0	8.4	0.0	6.4
3210	26.0	75.0	76.1	7.6	7.3	9.5	2.0	8.4	0.0	6.4
3225	26.0	75.0	76.1	7.6	7.3	9.5	2.0	8.4	0.0	6.4
3235	26.0	75.0	76.1	7.6	7.3	9.5	2.0	8.4	0.0	6.4
3245	26.0	75.0	76.1	7.6	7.3	9.5	2.0	8.4	0.0	6.4
3255	26.0	75.0	76.1	7.6	7.3	9.5	2.0	8.4	0.0	6.4
3267	26.0	75.0	76.1	7.6	7.3	9.5	2.0	8.4	0.0	6.4
3289	26.0	75.0	76.1	7.6	7.3	9.5	2.0	8.4	0.0	6.4
3301	26.0	75.0	76.1	7.6	7.3	9.5	2.0	8.4	0.0	6.4
3311	26.0	75.0	76.1	7.6	7.3	9.5	2.0	8.4	0.0	6.4
3323	26.0	75.0	76.1	7.6	7.3	9.5	2.0	8.4	0.0	6.4
3334	26.0	75.0	76.1	7.6	7.3	9.5	2.0	8.4	0.0	6.4
3345	26.0	75.0	76.1	7.6	7.3	9.5	2.0	8.4	0.0	6.4
3357	26.0	75.0	76.1	7.6	7.3	9.5	2.0	8.4	0.0	6.4
3367	26.0	75.0	76.1	7.6	7.3	9.5	2.0	8.4	0.0	6.4
3378	26.0	75.0	76.1	7.6	7.3	9.5	2.0	8.4	0.0	6.4
3389	26.0	75.0	76.1	7.6	7.3	9.5	2.0	8.4	0.0	6.4
3399	26.0	75.0	76.1	7.6	7.3	9.5	2.0	8.4	0.0	6.4
3410	26.0	75.0	76.1	7.6	7.3	9.5	2.0	8.4	0.0	6.4
3423	26.0	75.0	76.1	7.6	7.3	9.5	2.0	8.4	0.0	6.4
3433	26.0	75.0	76.1	7.6	7.3	9.5	2.0	8.4	0.0	6.4

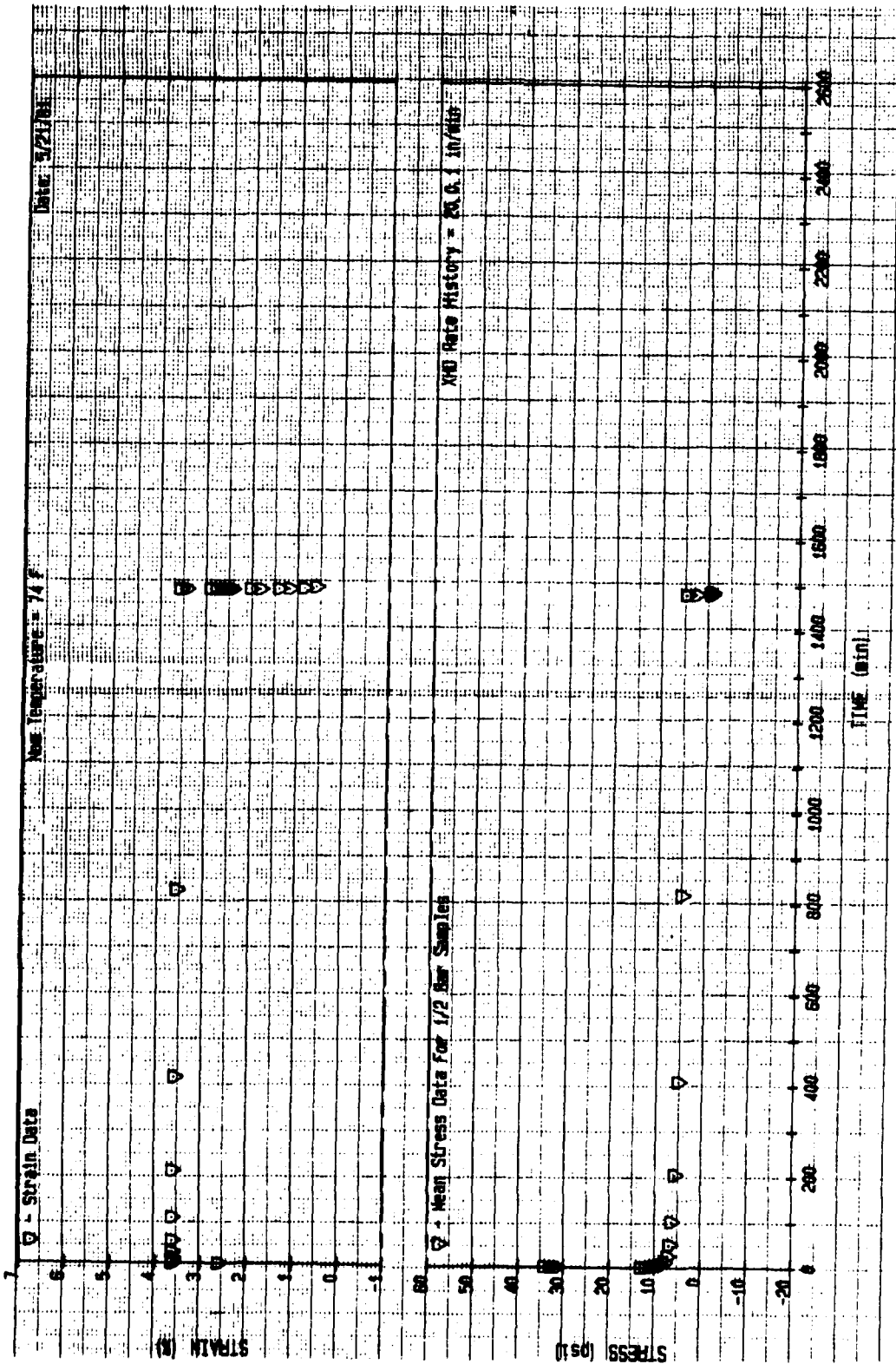


Figure 23. Test No. 8 - Stress While Step Straining for UTP-19, 360B-400/1777

TABLE 12. TEST NO. 8 - 1/2-IN. BAR STRESS WHILE STEP STRAINING

PROPELLANT: VTP 19360R 400/1777
 REQUESTOR: Carlton

DATE: 5/21/81
 OPERATOR: JWD

DEFINITIONS:
 Time = Time From Start of Test (min)
 Stress (psi)
 Strain (%)
 T(air) = Test Air Temperature (F)
 T(prop) = Test Propellant Temperature (F)

RELATIONSHIPS:
 = Force/Area
 = Sample Extension/Length

NOMINAL VALUES:
 Test Temp = 74 F
 Gage Length = 6.00 in
 Nom. Strain = 4%
 XHD Rate = 20.0.1 in/min

SAMPLE 2
 6.098
 0.022

1
 5.850
 0.059
 -0.75.1

CATHARTOMETER STRAIN DATA:
 Initial Upper (5 digits)
 Initial Lower (5 digits)
 Final Upper (5 digits)
 Final Lower (5 digits)
 Strain at 0.02 min

82710
 68030
 82730
 87520
 3.61

82925
 68360
 82945
 87835
 3.74

0.250
 SAMPLE

0.254

STRESS DATA (psi):

STRESS	Time	T(prop)	T(air)	Strain
1	0.01770			2.60
2	0.02100			3.61
3	0.02450			3.63
4	0.03541	75.9	76.3	3.63
5	0.05544	75.5	76.5	3.63
6	0.09546	75.6	76.5	3.63
7	1.75558	75.4	76.5	3.63
8	3.35594	75.8	76.3	3.63
9	6.95704	75.8	76.1	3.63
10	12.75741	75.6	76.7	3.62
11	25.35796	74.9	76.6	3.60
12	51.35806	74.4	76.5	3.58
13	102.95716	75.4	76.7	3.58
14	209.75945	76.1	76.1	3.58
15	409.35983	75.5	76.2	3.58
16	819.67000			3.58
17	1478.97000			3.58
18	1478.97676			3.58
19	1479.09712			3.58
20	1479.06729			3.58
21	1479.09680			3.58
22	1479.12785			3.58
23	1479.39548			3.58
24	1479.59606			3.58
25	1480.31144			3.58
26	1482.11454			3.58
27	1485.91523			3.58
28		76.1	76.2	3.58
29		76.1	76.1	3.58
30		76.0	76.3	3.58
31		75.7	76.2	3.58

Avg 4

STRESS	Time	T(prop)	T(air)	Strain	Avg 4	Day
1	0.01770			2.60	31.42	829
2	0.02100			3.61	34.88	0.728
3	0.02450			3.63	32.52	0.705
4	0.03541	75.9	76.3	3.63	12.92	0.170
5	0.05544	75.5	76.5	3.63	11.96	0.143
6	0.09546	75.6	76.5	3.63	10.94	0.135
7	1.75558	75.4	76.5	3.63	10.00	0.118
8	3.35594	75.8	76.3	3.63	9.31	0.102
9	6.95704	75.8	76.1	3.63	9.40	0.099
10	12.75741	75.6	76.7	3.62	7.23	0.093
11	25.35796	74.9	76.6	3.60	6.76	0.089
12	51.35806	74.4	76.5	3.58	6.50	0.083
13	102.95716	75.4	76.7	3.58	5.55	0.066
14	209.75945	76.1	76.1	3.58	5.27	0.065
15	409.35983	75.5	76.2	3.58	4.62	0.065
16	819.67000			3.58	4.48	0.065
17	1478.97000			3.58	4.60	0.065
18	1478.97676			3.58	4.62	0.065
19	1479.09712			3.58	4.50	0.065
20	1479.06729			3.58	4.25	0.065
21	1479.09680			3.58	4.27	0.065
22	1479.12785			3.58	4.64	0.065
23	1479.39548			3.58	4.74	0.065
24	1479.59606			3.58	4.53	0.065
25	1480.31144			3.58	4.55	0.065
26	1482.11454			3.58	4.72	0.065
27	1485.91523			3.58	4.69	0.065
28		76.1	76.2	3.58	4.70	0.065
29		76.1	76.1	3.58	4.70	0.065
30		76.0	76.3	3.58	4.71	0.065
31		75.7	76.2	3.58	4.71	0.065

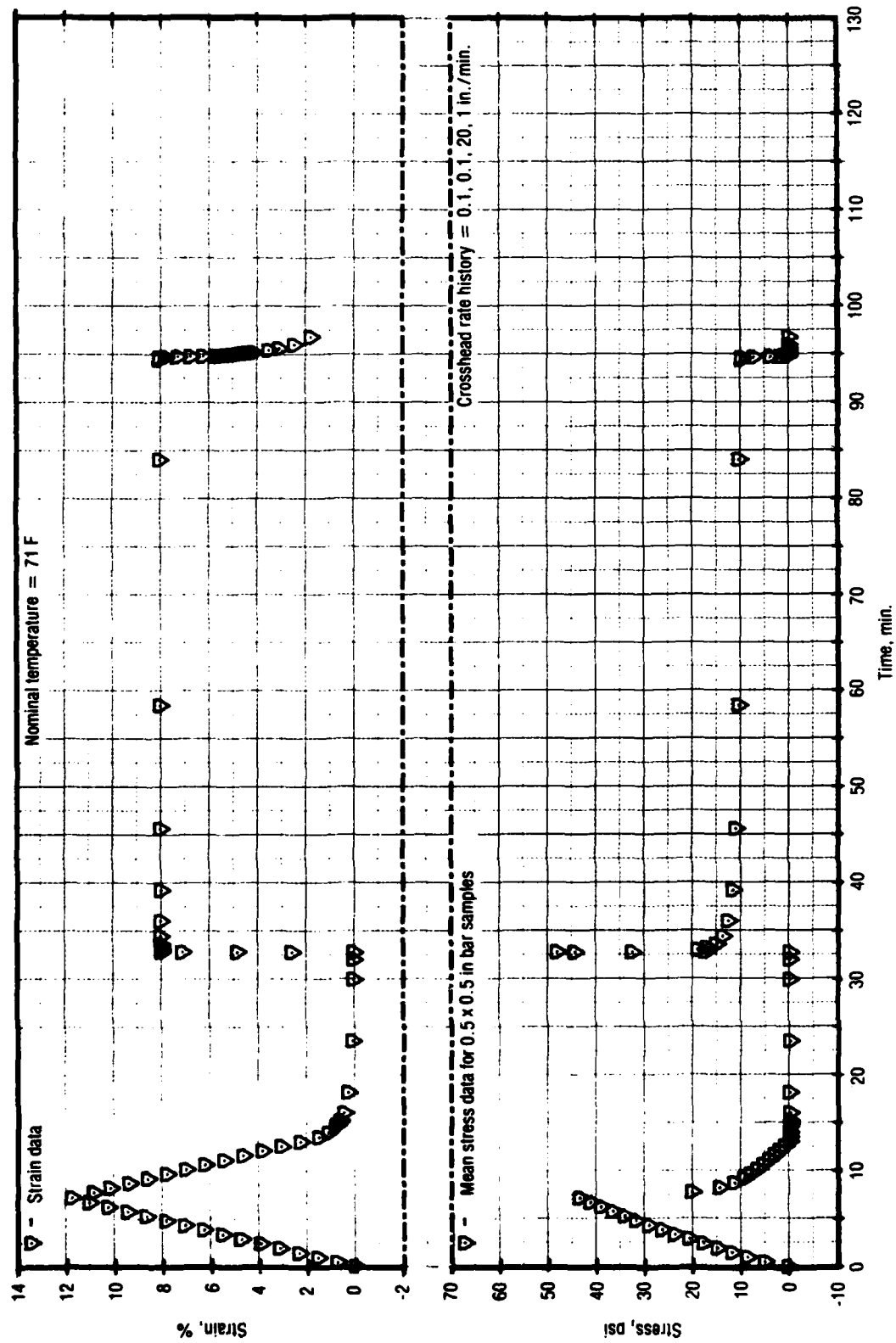


Figure 24. Test No. 9 - Stress While Step Straining for UTP-19,360B-400/1777

28753

TABLE 13. TEST NO. 9 - 1/2-IN. BAR STRESS WHILE STEP STRAINING
(SHEET 1 OF 2)

PROPELLANT: UTP 193608 400/1777
REQUESTOR: CARLTON
DATE: 5/28/81
OPERATOR: WRP

DEFINITIONS:
Time = Time From Start of Test (min)
 σ = Stress (psi)
 ϵ = Strain (%)
T (air) = Test Air Temperature (F)
T (prop) = Test Propellant Temperature (F)

RELATIONSHIPS:
 σ = Force/Area
 ϵ = Sample Extension/Length

NOMINAL VALUES:
Test Temp = 71 F
Gage Length = 6.00 in
Nom. Strain = 12.12, 8.8, 2.0, 1.0 in/min
XHD Rate = 0.1, 0.1, 2.0, 1.0 in/min

CALIBRATION DATA:
Cal Wt = 5.0 lbs
Lead Cal (lbs/volts)
Offset (volts)
Pot Cal (in/volts) =
Temp (F)

59

AREAS (sq In):

STRESS SET	Time	T (prop)	T (air)	Strain	SAMPLE	Avg	Dev
1	0.00567	75.5	76.4	0.29	1	0.58	0.154
2	0.48623	75.5	76.4	0.79	2	1.87	0.149
3	0.96630	75.5	76.4	1.29	3	3.03	0.286
4	1.44610	75.5	76.4	1.78	4	4.18	0.307
5	1.92573	75.5	76.4	2.28	5	5.34	0.418
6	2.40500	75.5	76.4	2.77	6	6.49	0.584
7	2.88388	75.5	76.4	3.27	7	7.64	0.677
8	3.36303	75.5	76.4	3.77	8	8.79	0.747
9	3.84243	75.5	76.4	4.27	9	9.94	0.814
10	4.32199	75.5	76.4	4.77	10	11.09	0.949
11	4.80177	75.5	76.4	5.27	11	12.24	1.124
12	5.28167	75.5	76.4	5.77	12	13.39	1.301
13	5.76177	75.5	76.4	6.27	13	14.54	1.479
14	6.24200	75.5	76.4	6.77	14	15.69	1.657
15	6.72243	75.5	76.4	7.27	15	16.84	1.836
16	7.20299	75.5	76.4	7.77	16	17.99	2.014
17	7.68366	75.5	76.4	8.27	17	19.14	2.192
18	8.16433	75.5	76.4	8.77	18	20.29	2.371
19	8.64500	75.5	76.4	9.27	19	21.44	2.549
20	9.12577	75.5	76.4	9.77	20	22.59	2.728
21	9.60667	75.5	76.4	10.27	21	23.74	2.906
22	10.08760	75.5	76.4	10.77	22	24.89	3.084
23	10.56856	75.5	76.4	11.27	23	26.04	3.263
24	11.04953	75.5	76.4	11.77	24	27.19	3.441
25	11.53050	75.5	76.4	12.27	25	28.34	3.620

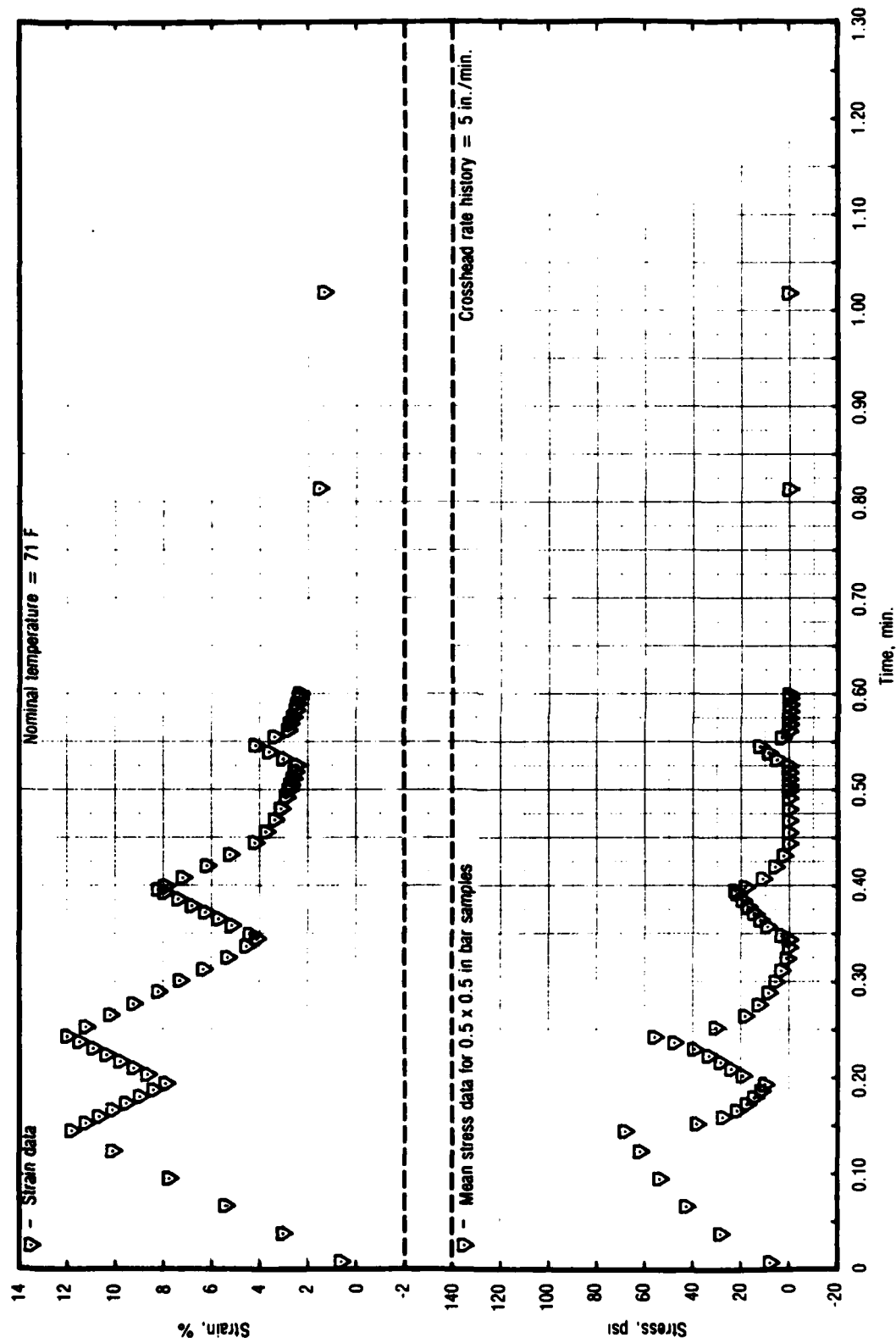


Figure 25. Test No. 10 - Stress While Complex Straining for UTP-19, 360B-400/1777

28799

TABLE 14. TEST NO. 10 - 1/2-IN. BAR STRESS WHILE COMPLEX STRAINING
(SHEET 1 OF 2)

PROPELLANT: UTP 19360B 400/1777
REQUESTOR: Carlton
MOR:

DATE: 5/15/81
OPERATOR: JMD

DEFINITIONS:
Time = Time From Start of Test (min)
 σ = Stress (psi)
 ϵ = Strain (%)
T (air) = Test Air Temperature (F)
T (prop) = Test Propellant Temperature (F)

RELATIONSHIPS:
 σ = Force/Area
 ϵ = Sample Extension/Length

NOMINAL VALUES: = 71 F
Test Temp = 6.00 in
Gage Length = 12.8, 12, 4, 8, 0, 4, 0 %
Nom. Strain = 5 in/min
XHD Rate =

CALIBRATION DATA:
Cal Wt = 5.0 lbs
Load Cal = (lbs/volts)
Offset = (volts)
Pot Cal = (in/volts) =
Temp = (F)

SAMPLE
2.078
0.013

3
6.119
0.092

AREAS (sq in):

0.252

0.251

0.249

STRESS DATA (psi):
Time
1 0.0744
2 0.03682
3 0.06548
4 0.09408
5 0.12268
6 0.14379
7 0.15167
8 0.15857
9 0.16544
10 0.17232
11 0.17920
12 0.18607
13 0.19293
14 0.20089
15 0.20885
16 0.21671
17 0.22464
18 0.23256
19 0.24048
20 0.24840
21 0.25637
22 0.26431
23 0.27224
24 0.28017
25 0.28811
26 0.29604
27 0.30397
28 0.31190

T (prop) T (air) Strain
0.61 0.78
3.02 3.24
7.75 7.97
10.81 11.03
11.22 11.44
10.66 10.88
9.11 9.33
8.97 9.19
8.41 8.63
8.90 9.12
8.66 8.88
9.79 10.01
9.75 9.97
10.98 11.20
11.11 11.33
11.11 11.33
10.98 11.20
8.73 8.95
7.30 7.52
6.53 6.75

SAMPLE
7.08
29.324
55.74
64.56
70.56
33.26
22.13
15.03
11.39
10.84
12.9
34.95
40.95
33.4
49.4
53.1
18.8
5.9
1.1

3.78
8.78
24.70
53.18
66.04
35.26
25.05
16.24
13.40
10.93
18.99
22.85
32.87
39.7
49.15
55.7
16.65
11.40
7.4
4.27

AVG
7.43
28.59
53.64
61.97
68.31
38.41
27.49
21.44
14.42
11.91
19.16
23.23
33.08
40.25
33.4
57.7
57.1
18.5
5.1
0.1

Dev
0.848
0.991
1.207
1.354
1.584
1.447
1.231
1.031
1.052
0.758
0.695
0.437
0.545
0.713
0.773
1.167
1.671
0.696
0.583
0.444
0.347

TABLE 15. TEST NO. 11, PART 1 - QUINLAN COMPLEX HISTORY FOR UTP-3001

T7859

Cycle		Rate, in./min.	Remarks
1-7	Load	2	Approximately 15 min. rest after cycle
	Unload	2	Approximately 15 min. rest after cycle
8	Load	1	Approximately 15 min. rest after cycle
	Unload	1	
9	Load	5	Approximately 15 min. rest after cycle
	Unload	5	
10	Load	0.5	Approximately 15 min. rest after cycle
	Unload	0.5	
11	Load	10	Approximately 15 min. rest after cycle
	Unload	10	
12	Load	0.2	Approximately 15 min. rest after cycle
	Unload	0.2	
13	Load	2	Approximately 30 min. rest after cycle
	Relax	1/2 hr	
	Unload	2	
14	Load	2	4 day rest after cycle
	Relax	1 hr	
	Unload	2	
15	Load	2	7 day rest after cycle
	Relax	1 hr	
	Unload	2	

The later part of the cycling is represented only by the maximum and minimum stress-strain points. Part 3 of this test, the balance of cycling to failure, is recorded in Table 19 as maxima and minima for selected cycles sufficiently close to describe the upper and lower bounds. A plot of the data would be similar to Figure 32. The strain values in Table 19 are stable, while the maximum stress shows a continual decay, and compressive (negative values) stresses become less compressive.

(Text continued on page 76)

TABLE 16. TEST NO. 11, PART 1 - 1/2-IN. BAR STRESS WHILE CYCLING
(SHEET 1 OF 11)

PROPELLANT: UTP 3001 750/7768
 REQUESTOR: Carlton
 DATE: 1/4/82
 OPERATOR: JMD

DEFINITIONS:
 Time = Time From Start of Test (min)
 σ = Stress (psi)
 ϵ = Strain (%)
 T (air) = Test Air Temperature (F)
 T (prop) = Test Propellant Temperature (F)

RELATIONSHIPS:
 σ = Force/Area
 ϵ = Sample Extension/Length

NOMINAL VALUES:
 Test Temp = 70 F
 Gage Length = 6.00 in
 Nom. Strain = 3.6, 8 %
 XHD Rate = 2 in/min

CALIBRATION DATA:
 Cal Wt = 50 lbs
 Load Cal (lbs/in)
 Offset (in) =
 Temp (F) = 70.0

AREAS (sq in): 0.251

STRESS SET	Time	T(prop)	T(air)	Strain	SAMPLE	Avg	St Dev
1	0.00500			0.17	3.43	3.43	0.000
2	0.01000			0.33	6.29	6.29	0.000
3	0.01500			0.50	9.32	9.32	0.000
4	0.02000	0.0	0.0	0.67	11.87	11.87	0.000
5	0.02500			0.83	14.34	14.34	0.000
6	0.03000			1.00	16.57	16.57	0.000
7	0.03500			1.17	18.96	18.96	0.000
8	0.05000			1.67	25.34	25.34	0.000
9	0.06500			2.17	31.39	31.39	0.000
10	0.08000			2.67	37.21	37.21	0.000
11	0.09250			3.08	41.83	41.83	0.000
12	0.09350			3.08	41.83	41.83	0.000
13	0.09500			3.08	37.45	37.45	0.000
14	0.09750			3.08	33.86	33.86	0.000
15	0.10000			3.08	27.89	27.89	0.000
16	0.10500			2.85	23.11	23.11	0.000
17	0.11000			2.67	17.05	17.05	0.000
18	0.11500			2.33	12.91	12.91	0.000
19	0.12000			2.17	9.96	9.96	0.000
20	0.12500			2.00	7.81	7.81	0.000
21	0.13500			1.67	5.82	5.82	0.000
22	0.14500			1.33	3.03	3.03	0.000
23	0.16000			0.83	0.64	0.64	0.000
					-2.47	-2.47	0.000

TABLE 16. TEST NO. 11, PART 1 - 1/2-IN. BAR STRESS WHILE CYCLING
(SHEET 2 OF 11)

24	0.18000	0.17	-7.17	7.17	0.000
25	0.20000	0.17	-4.30	4.30	0.000
26	0.22000	0.17	-3.19	3.19	0.000
27	0.24000	0.17	-2.07	2.07	0.000
28	0.26000	0.17	-1.55	1.55	0.000
29	0.28000	0.17	-1.59	1.59	0.000
30	0.30000	0.17	-1.35	1.35	0.000
31	0.32000	0.17	-1.20	1.20	0.000
32	0.34000	0.17	-0.88	0.88	0.000
33	0.36000	0.17	-0.56	0.56	0.000
34	0.38000	0.17	-0.40	0.40	0.000
35	0.40000	0.17	-0.32	0.32	0.000
36	0.42000	0.17	-0.32	0.32	0.000
37	0.44000	0.17	-0.32	0.32	0.000
38	0.46000	0.33	-0.55	0.55	0.000
39	0.48000	0.50	-0.57	0.57	0.000
40	0.50000	0.67	7.63	7.63	0.000
41	0.52000	1.00	15.22	15.22	0.000
42	0.54000	1.33	18.51	18.51	0.000
43	0.56000	1.67	22.74	22.74	0.000
44	0.58000	2.00	27.41	27.41	0.000
45	0.60000	2.33	31.87	31.87	0.000
46	0.62000	2.67	37.07	37.07	0.000
47	0.64000	3.00	42.41	42.41	0.000
48	0.66000	3.33	47.11	47.11	0.000
49	0.68000	3.67	52.17	52.17	0.000
50	0.70000	4.00	56.77	56.77	0.000
51	0.72000	4.33	61.30	61.30	0.000
52	0.74000	4.67	65.72	65.72	0.000
53	0.76000	5.00	70.71	70.71	0.000
54	0.78000	5.33	75.01	75.01	0.000
55	0.80000	5.67	79.74	79.74	0.000
56	0.82000	6.00	84.11	84.11	0.000
57	0.84000	6.33	88.56	88.56	0.000
58	0.86000	6.67	93.11	93.11	0.000
59	0.88000	7.00	97.89	97.89	0.000
60	0.90000	7.33	102.87	102.87	0.000
61	0.92000	7.67	108.11	108.11	0.000
62	0.94000	8.00	113.56	113.56	0.000
63	0.96000	8.33	119.11	119.11	0.000
64	0.98000	8.67	124.79	124.79	0.000
65	1.00000	9.00	130.67	130.67	0.000
66	1.02000	9.33	136.81	136.81	0.000
67	1.04000	9.67	143.11	143.11	0.000
68	1.06000	10.00	149.56	149.56	0.000
69	1.08000	10.33	156.11	156.11	0.000
70	1.10000	10.67	162.79	162.79	0.000
71	1.12000	11.00	169.67	169.67	0.000
72	1.14000	11.33	176.81	176.81	0.000
73	1.16000	11.67	184.11	184.11	0.000
74	1.18000	12.00	191.56	191.56	0.000
75	1.20000	12.33	199.11	199.11	0.000

TABLE 16. TEST NO. 11, PART 1 - 1/2-IN. BAR STRESS WHILE CYCLING
(SHEET 3 OF 11)

76	16.24000	0.30	-0.22	-0.72	0.000
77	16.84000	0.30	-0.56	-0.56	0.000
78	19.64000	0.30	-0.40	-0.40	0.000
79	23.64000	0.30	-0.32	-0.32	0.000
80	29.84000	0.47	-0.79	-0.79	0.000
81	29.85000	0.63	5.34	7.41	0.000
82	29.85500	0.63	7.41	7.41	0.000
83	29.85500	0.63	7.41	7.41	0.000
84	29.86500	1.13	11.08	13.08	0.000
85	29.86500	1.13	13.08	13.08	0.000
86	29.89500	2.63	20.70	24.70	0.000
87	29.91000	3.13	24.70	24.70	0.000
88	29.92500	3.13	29.86	32.86	0.000
89	29.94000	4.17	33.86	34.06	0.000
90	29.95500	4.17	34.06	34.06	0.000
91	29.96500	4.17	34.06	34.06	0.000
92	29.97500	4.80	35.92	39.92	0.000
93	29.98500	5.33	39.92	39.92	0.000
94	29.99100	5.33	39.92	39.92	0.000
95	29.99300	5.33	39.92	39.92	0.000
96	29.99500	5.33	39.92	39.92	0.000
97	29.99800	5.33	39.92	39.92	0.000
98	30.00000	5.33	39.92	39.92	0.000
99	30.00250	5.33	39.92	39.92	0.000
100	30.00500	4.87	30.22	30.22	0.000
101	30.01000	4.70	22.71	22.71	0.000
102	30.02000	4.33	12.19	12.19	0.000
103	30.03000	4.33	7.81	7.81	0.000
104	30.04500	5.33	3.67	3.67	0.000
105	30.06500	2.87	0.63	0.63	0.000
106	30.10500	1.03	-2.89	-2.89	0.000
107	30.12000	1.03	-5.13	-5.13	0.000
108	30.88000	1.03	-3.03	-3.03	0.000
109	30.92000	1.03	-2.07	-2.07	0.000
110	30.98000	1.03	-1.51	-1.51	0.000
111	30.98000	1.03	-1.43	-1.43	0.000
112	30.98000	1.03	-1.20	-1.20	0.000
113	30.98000	1.03	-1.04	-1.04	0.000
114	31.02000	1.03	-0.72	-0.72	0.000
115	31.06000	1.03	0.40	0.40	0.000
116	31.12000	1.03	0.32	0.32	0.000
117	31.32000	1.03	0.32	0.32	0.000
118	31.72000	1.03	0.32	0.32	0.000
119	31.72000	1.03	0.32	0.32	0.000
120	34.72000	1.03	0.32	0.32	0.000
121	38.72000	1.03	0.32	0.32	0.000
122	46.96000	1.03	0.32	0.32	0.000
123	46.96400	1.03	0.32	0.32	0.000
124	46.96900	1.03	0.32	0.32	0.000
125	46.97400	1.03	0.32	0.32	0.000
126	46.98400	1.03	0.32	0.32	0.000
127	46.99400	1.03	0.32	0.32	0.000
128	47.00400	1.03	0.32	0.32	0.000
129		12.50	13.94	13.94	0.000

TABLE 16. TEST NO. 11, PART 1 - 1/2-IN. BAR STRESS WHILE CYCLING
(SHEET 4 OF 11)

130	47.02400	3.17	21.31	0.000
131	47.04400	3.83	26.49	0.000
132	47.06400	4.50	32.47	0.000
133	47.08400	5.17	40.24	0.000
134	47.10400	5.83	51.59	0.000
135	47.12400	6.50	64.14	0.000
136	47.14050	7.05	72.11	0.000
137	47.14250	7.98	76.33	0.000
138	47.14400	6.93	60.76	0.000
139	47.14650	6.87	60.99	0.000
140	47.14900	6.77	52.42	0.000
141	47.15400	6.60	45.42	0.000
142	47.15900	6.43	35.86	0.000
143	47.16650	6.48	22.71	0.000
144	47.17400	5.73	19.53	0.000
145	47.18400	5.60	14.34	0.000
146	47.19900	5.10	10.36	0.000
147	47.21900	4.43	5.98	0.000
148	47.23900	3.77	1.39	0.000
149	47.26400	2.93	0.00	0.000
150	47.28900	2.10	0.00	0.000
151	47.31950	1.08	0.00	0.000
152	47.33950	1.08	0.00	0.000
153	47.35950	1.08	0.00	0.000
154	47.39950	1.08	0.00	0.000
155	47.43950	1.08	0.00	0.000
156	47.49950	1.08	0.00	0.000
157	47.59950	1.08	0.00	0.000
158	47.69950	1.08	0.00	0.000
159	47.89950	1.08	0.00	0.000
160	48.09950	1.08	0.00	0.000
161	48.69950	1.08	0.00	0.000
162	52.69950	1.08	0.00	0.000
163	60.79950	1.08	0.00	0.000
164	60.78250	1.35	0.40	0.000
165	60.79250	1.52	4.18	0.000
166	60.79750	1.60	6.37	0.000
167	60.80750	2.02	8.17	0.000
168	60.82250	2.18	11.16	0.000
169	60.84250	3.18	15.14	0.000
170	60.86250	3.85	19.72	0.000
171	60.88750	4.68	24.50	0.000
172	60.91250	5.52	30.88	0.000
173	60.93750	6.37	38.65	0.000
174	60.96250	7.18	50.20	0.000
175	60.98950	8.08	66.14	0.000
176	60.99250	7.98	78.49	0.000
177	60.99500	7.90	66.73	0.000
178	60.99750	7.82	57.77	0.000
179	61.00250	7.65	50.80	0.000
180	61.00750	7.48	40.64	0.000
181	61.01250	7.32	33.86	0.000
182	61.02250	6.98	28.69	0.000
183	61.03250	6.66	22.11	0.000
			17.73	0.000

TABLE 16. TEST NO. 11, PART 1 - 1/2-IN. BAR STRESS WHILE CYCLING
(Sheet 5 of 11)

184	61.04250	6.32	14.34	0.000
185	61.05750	5.82	10.56	0.000
186	61.10250	4.12	16.97	0.000
187	61.12750	3.48	2.79	0.000
188	61.15250	2.65	-0.20	0.000
189	61.17750	1.82	-3.78	0.000
190	61.19700	1.17	-5.57	0.000
191	61.21700	1.17	-5.98	0.000
192	61.23700	1.17	-4.78	0.000
193	61.25700	1.17	-3.98	0.000
194	61.31700	1.17	-2.39	0.000
195	61.41700	1.17	-1.99	0.000
196	61.61700	1.17	-1.39	0.000
197	62.01700	1.17	-1.00	0.000
198	62.41700	1.17	-0.80	0.000
199	65.41700	1.17	-0.60	0.000
200	65.55700	1.17	-0.40	0.000
201	75.56350	1.59	3.19	0.000
202	75.56850	1.55	5.58	0.000
203	75.57350	1.52	7.37	0.000
204	75.57850	1.88	9.65	0.000
205	75.58350	2.55	11.73	0.000
206	75.61350	3.40	17.30	0.000
207	75.64350	5.25	27.87	0.000
208	75.67350	6.73	42.18	0.000
209	75.70350	8.05	56.19	0.000
210	75.73350	8.82	79.16	0.000
211	75.76350	7.77	47.82	0.000
212	75.79350	7.38	37.25	0.000
213	75.82350	7.05	26.89	0.000
214	75.85350	6.77	16.93	0.000
215	75.88350	6.52	12.37	0.000
216	75.91350	6.27	8.38	0.000
217	75.94350	6.02	4.38	0.000
218	75.97350	5.77	0.38	0.000
219	75.81350	6.23	1.99	0.000
220	75.82350	6.52	1.78	0.000
221	75.83350	6.77	1.58	0.000
222	75.84350	7.02	1.38	0.000
223	75.85350	7.27	1.18	0.000
224	75.86350	7.52	0.98	0.000
225	77.14850	2.05	3.99	0.000
226	77.16850	2.22	5.99	0.000
227	77.18850	2.39	7.99	0.000
228	77.20850	2.56	9.99	0.000
229	77.24850	2.73	11.99	0.000
230	77.28850	2.90	13.99	0.000
231	77.32850	3.07	15.99	0.000
232	77.36850	3.24	17.99	0.000
233	82.23650	2.88	19.99	0.000
234	82.24650	2.88	21.99	0.000
235	92.24650	2.88	23.99	0.000
236	92.24650	2.88	25.99	0.000
237	92.24650	2.88	27.99	0.000

TABLE 16. TEST NO. 11, PART 1 - 1/2-IN. BAR STRESS WHILE CYCLING
(SHEET 6 OF '11)

238	92.25150	98	8.96	8.96	0.000
239	92.27650	3	15.14	15.14	0.000
240	92.30150	4	20.52	20.52	0.000
241	92.32650	5	25.50	25.50	0.000
242	92.35150	6	31.08	31.08	0.000
243	92.37650	7	37.25	37.25	0.000
244	92.40150	7	46.21	46.21	0.000
245	92.42650	8	56.37	56.37	0.000
246	92.45150	8	60.76	60.76	0.000
247	92.47650	7	67.81	67.81	0.000
248	92.50150	7	78.84	78.84	0.000
249	92.52650	7	82.27	82.27	0.000
250	92.55150	7	84.30	84.30	0.000
251	92.57650	6	85.54	85.54	0.000
252	92.60150	5	85.16	85.16	0.000
253	92.62650	4	85.18	85.18	0.000
254	92.65150	3	85.79	85.79	0.000
255	92.67650	2	85.79	85.79	0.000
256	92.70150	2	85.37	85.37	0.000
257	92.72650	1	85.98	85.98	0.000
258	92.75150	1	85.98	85.98	0.000
259	92.77650	1	85.38	85.38	0.000
260	92.80150	1	85.39	85.39	0.000
261	92.82650	1	85.59	85.59	0.000
262	93.02700	1	85.19	85.19	0.000
263	93.62700	1	85.50	85.50	0.000
264	94.62700	1	85.00	85.00	0.000
265	98.82700	1	80.60	80.60	0.000
270	108.02700	1	60.60	60.60	0.000
271	108.03700	1	60.60	60.60	0.000
272	108.04700	1	60.60	60.60	0.000
273	108.06700	1	60.60	60.60	0.000
274	108.08700	1	60.60	60.60	0.000
275	108.12700	2	60.60	60.60	0.000
276	108.16700	3	60.60	60.60	0.000
277	108.18700	3	60.60	60.60	0.000
278	108.23700	4	60.60	60.60	0.000
279	108.28700	5	60.60	60.60	0.000
280	108.33700	6	60.60	60.60	0.000
281	108.38200	7	60.60	60.60	0.000
282	108.41700	7	60.60	60.60	0.000
283	108.45200	8	60.60	60.60	0.000
284	108.45700	8	60.60	60.60	0.000
285	108.46700	7	60.60	60.60	0.000
286	108.48200	7	60.60	60.60	0.000
287	108.50700	7	60.60	60.60	0.000
288	108.53700	6	60.60	60.60	0.000
289	108.56700	6	60.60	60.60	0.000
290	108.60200	6	60.60	60.60	0.000
291	108.63700	5	60.60	60.60	0.000
292	108.69700	4	60.60	60.60	0.000

TABLE 16. TEST NO. 11, PART 1 - 1/2-IN. BAR STRESS WHILE CYCLING
(SHEET 7 OF 11)

293	108.75700	3.13	-0.60	-0.80	0.000
294	108.81200	3.227	-3.59	-5.57	0.000
295	108.86900	1.127	-5.57	-5.38	0.000
296	108.88900	1.27	-4.38	-4.38	0.000
297	108.90900	1.27	-3.78	-2.99	0.000
298	108.92900	1.27	-2.99	-2.59	0.000
299	108.96900	1.27	-2.59	-1.39	0.000
300	109.02900	1.27	-1.39	-1.00	0.000
301	109.12900	1.27	-1.00	-0.80	0.000
302	109.42900	1.27	-0.80	-0.60	0.000
303	109.82900	1.27	-0.60	-0.40	0.000
304	110.82900	1.27	-0.40	-0.40	0.000
305	114.82900	1.27	-0.40	-0.40	0.000
306	123.18900	1.27	-0.40	-0.40	0.000
307	123.19340	1.63	-4.98	-9.56	0.000
308	123.19740	1.97	-9.56	-12.95	0.000
309	123.20140	2.30	-12.95	-16.14	0.000
310	123.20540	2.67	-16.14	-19.12	0.000
311	123.20940	3.07	-19.12	-25.10	0.000
312	123.22040	3.88	-25.10	-30.68	0.000
313	123.22740	4.47	-30.68	-37.85	0.000
314	123.23840	5.82	-37.85	-45.02	0.000
315	123.24940	6.22	-45.02	-54.18	0.000
316	123.25840	7.05	-54.18	-64.74	0.000
317	123.26640	7.72	-64.74	-70.92	0.000
318	123.27040	8.05	-70.92	-78.09	0.000
319	123.27460	8.40	-78.09	-73.70	0.000
320	123.27540	8.33	-73.70	-62.15	0.000
321	123.27740	8.17	-62.15	-51.82	0.000
322	123.27940	8.03	-51.82	-43.27	0.000
323	123.28140	7.85	-43.27	-34.50	0.000
324	123.28340	7.71	-34.50	-24.74	0.000
325	123.28940	7.45	-24.74	-14.57	0.000
326	123.29840	6.33	-14.57	-6.80	0.000
327	123.31140	4.17	-6.80	-4.38	0.000
328	123.32540	2.83	-4.38	-9.56	0.000
329	123.334140	1.83	-9.56	-6.57	0.000
330	123.33740	1.50	-6.57	-4.78	0.000
331	123.33940	1.50	-4.78	-3.39	0.000
332	123.34140	1.50	-3.39	-1.79	0.000
333	123.45740	1.50	-1.79	-1.39	0.000
334	123.55740	1.50	-1.39	-1.00	0.000
335	123.65740	1.50	-1.00	-0.60	0.000
336	123.95740	1.50	-0.60	-0.40	0.000
337	130.13740	1.50	-0.40	-0.40	0.000
338	137.45740	1.50	-0.40	-0.40	0.000
339	137.48740	1.75	-0.40	-2.59	0.000
340	137.48740	2.08	-2.59	-4.78	0.000
341	137.52740	3.33	-4.78	-8.37	0.000
342	137.57740	4.17	-8.37	-11.16	0.000
343	137.67740	4.83	-11.16	-14.74	0.000
344	137.77740	4.17	-14.74	-17.33	0.000
345	137.85740	4.83	-17.33	-21.12	0.000
346	137.95740	5.67	-21.12	-21.12	0.000

TABLE 16. TEST NO. 11, PART 1 - 1/2-IN. BAR STRESS WHILE CYCLING
(SHEET 8 OF 11)

347	138.05740	6.50	25.10	25.10	0.000
348	138.14740	7.83	30.28	30.28	0.000
349	138.21740	8.75	36.06	36.06	0.000
350	138.29740	9.75	46.02	46.02	0.000
351	138.30740	8.18	36.45	36.45	0.000
352	138.32740	7.93	29.28	29.28	0.000
353	138.35740	7.68	23.31	23.31	0.000
354	138.38740	7.68	19.92	19.92	0.000
355	138.44740	6.35	14.94	14.94	0.000
356	138.54740	5.98	9.96	9.96	0.000
357	138.66740	4.68	5.98	5.98	0.000
358	138.74740	3.77	3.59	3.59	0.000
359	138.85740	3.22	1.00	1.00	0.000
360	138.95740	1.53	-1.39	-1.39	0.000
361	139.12740	1.53	-5.18	-5.18	0.000
362	139.16740	1.53	-3.98	-3.98	0.000
363	139.20740	1.53	-2.99	-2.99	0.000
364	139.24740	1.53	-2.79	-2.79	0.000
365	139.32740	1.53	-2.39	-2.39	0.000
366	139.52740	1.53	-1.79	-1.79	0.000
367	139.92740	1.53	-1.39	-1.39	0.000
368	140.52740	1.53	-1.00	-1.00	0.000
369	141.12740	1.53	-0.80	-0.80	0.000
370	147.12740	1.53	-0.60	-0.60	0.000
371	152.94740	1.87	-0.60	-0.60	0.000
372	152.94930	1.87	-5.18	-5.18	0.000
373	152.95130	2.17	10.56	10.56	0.000
374	152.95480	2.75	17.53	17.53	0.000
375	152.95980	3.53	26.47	26.47	0.000
376	152.96430	4.53	33.47	33.47	0.000
377	152.97030	5.13	42.23	42.23	0.000
378	152.97510	6.13	49.40	49.40	0.000
379	152.97930	6.83	57.77	57.77	0.000
380	152.98230	7.33	63.15	63.15	0.000
381	152.98480	7.75	69.92	69.92	0.000
382	152.98830	8.33	82.07	82.07	0.000
383	152.99130	8.93	94.02	94.02	0.000
384	152.99420	9.23	104.18	104.18	0.000
385	152.99480	9.23	107.01	107.01	0.000
386	152.99580	9.03	87.65	87.65	0.000
387	152.99630	8.80	81.08	81.08	0.000
388	152.99730	8.80	69.92	69.92	0.000
389	152.99830	8.80	60.16	60.16	0.000
390	152.99980	8.38	48.80	48.80	0.000
391	153.00130	8.38	40.04	40.04	0.000
392	153.00330	8.07	31.27	31.27	0.000
393	153.00630	7.40	22.11	22.11	0.000
394	153.01130	6.57	16.57	16.57	0.000
395	153.01580	4.88	1.99	1.99	0.000
396	153.02580	4.05	-1.99	-1.99	0.000
397	153.03580	4.05	-5.38	-5.38	0.000
398	153.03890	4.05	-11.16	-11.16	0.000
399	153.05890	4.05	-15.98	-15.98	0.000
400		4.05			0.000

TABLE 16. TEST NO. 11, PART 1 - 1/2-IN. BAR STRESS WHILE CYCLING
(SHEET 9 OF 11)

401	153.07890	1.87	-3.78	0.000
402	153.07890	1.87	-2.39	0.000
403	153.11890	1.87	-1.59	0.000
404	153.21890	1.87	-1.00	0.000
405	153.31890	1.87	-0.80	0.000
406	153.81890	1.87	-0.60	0.000
407	160.91890	1.87	-0.40	0.000
408	167.85890	1.87	-0.40	0.000
409	167.87040	1.91	-2.39	0.000
410	167.88540	1.96	4.58	0.000
411	167.91040	2.04	8.17	0.000
412	167.93540	2.12	10.56	0.000
413	167.96290	2.23	14.34	0.000
414	167.99540	2.33	17.33	0.000
415	168.02790	2.43	21.91	0.000
416	168.05290	2.51	26.89	0.000
417	168.06790	2.56	31.27	0.000
418	168.07040	2.61	34.90	0.000
419	168.07540	2.66	38.51	0.000
420	168.08040	2.72	42.52	0.000
421	168.08540	2.77	46.13	0.000
422	168.09540	2.84	49.94	0.000
423	168.10540	2.91	53.76	0.000
424	168.12540	3.02	61.57	0.000
425	168.15040	3.19	70.78	0.000
426	168.18040	3.49	81.00	0.000
427	168.21040	3.98	91.59	0.000
428	168.24290	4.08	101.18	0.000
429	168.27590	4.27	110.59	0.000
430	168.31590	4.44	120.39	0.000
431	168.35590	4.61	130.19	0.000
432	168.45590	4.85	140.59	0.000
433	168.52590	5.09	150.99	0.000
434	168.62590	5.39	161.39	0.000
435	172.62590	6.59	171.79	0.000
436	179.17590	8.23	181.19	0.000
437	179.18290	8.37	190.58	0.000
438	179.19290	8.57	199.97	0.000
439	179.20290	8.73	209.36	0.000
440	179.21290	8.90	218.74	0.000
441	179.23790	9.07	228.14	0.000
442	179.26790	9.27	237.54	0.000
443	179.29790	9.47	246.90	0.000
444	179.32790	9.67	256.27	0.000
445	179.34790	9.73	265.45	0.000
446	179.36790	9.80	274.63	0.000
447	179.38790	9.87	283.81	0.000
448	179.40290	9.93	292.99	0.000
449	179.41690	9.98	302.17	0.000
450	179.43690	10.03	311.35	0.000
451	179.65690	10.03	320.53	0.000
452	180.05690	10.03	329.71	0.000
453	180.82690	10.03	338.89	0.000
454	182.45690	10.03	348.07	0.000

TABLE 16. TEST NO. 11, PART 1 - 1/2-IN. BAR STRESS WHILE CYCLING
(SHEET 10 OF 11)

455	185.65690	8.03	24.10	24.10	0.000
456	192.05690	8.03	22.11	22.11	0.000
457	204.85690	8.03	20.12	20.12	0.000
458	211.25290	7.53	19.16	19.16	0.000
460	211.23290	7.00	4.00	4.00	0.000
461	211.24790	6.17	0.00	0.00	0.000
462	211.29790	6.14	-3.98	-3.98	0.000
463	211.32790	6.07	-5.98	-5.98	0.000
464	211.35790	6.05	-8.98	-8.98	0.000
465	211.37790	6.03	-5.98	-5.98	0.000
466	211.40290	6.02	-3.99	-3.99	0.000
467	211.42790	6.00	-2.99	-2.99	0.000
468	211.45690	5.98	-1.20	-1.20	0.000
469	211.48690	5.70	0.00	0.00	0.000
470	211.89690	4.63	0.00	0.00	0.000
471	219.89690	0.00	0.00	0.00	0.000
472	241.63690	1.39	6.37	6.37	0.000
473	241.66840	1.39	14.32	14.32	0.000
474	241.70840	1.39	20.49	20.49	0.000
475	241.74340	1.39	26.87	26.87	0.000
476	241.77840	1.39	31.65	31.65	0.000
477	241.80540	1.39	37.83	37.83	0.000
478	241.82840	1.39	42.60	42.60	0.000
479	241.84340	1.39	49.60	49.60	0.000
480	241.85840	1.39	56.75	56.75	0.000
481	241.86890	1.39	64.06	64.06	0.000
482	241.94890	1.39	72.48	72.48	0.000
483	242.04890	1.39	80.91	80.91	0.000
484	242.24890	1.39	89.31	89.31	0.000
485	242.44890	1.39	97.69	97.69	0.000
486	242.64890	1.39	106.08	106.08	0.000
487	243.04890	1.39	114.48	114.48	0.000
488	245.04890	1.39	122.89	122.89	0.000
489	248.24890	1.39	131.31	131.31	0.000
490	254.64890	1.39	139.72	139.72	0.000
491	265.44890	1.39	148.12	148.12	0.000
492	269.66890	1.39	156.54	156.54	0.000
493	269.67340	1.39	164.96	164.96	0.000
494	269.68340	1.39	173.38	173.38	0.000
495	269.69340	1.39	181.80	181.80	0.000
496	269.70840	1.39	190.22	190.22	0.000
497	269.73340	1.39	198.64	198.64	0.000
498	269.75840	1.39	207.06	207.06	0.000
499	269.79340	1.39	215.48	215.48	0.000
500	269.82340	1.39	223.90	223.90	0.000
501	269.84840	1.39	232.32	232.32	0.000
502	269.87840	1.39	240.74	240.74	0.000
503	269.90840	1.39	249.16	249.16	0.000
504	271.06940	1.39	257.58	257.58	0.000
505	271.46940	1.39	266.00	266.00	0.000
506	273.46940	1.39	274.42	274.42	0.000
507	283.46940	1.39	282.84	282.84	0.000
508	7288.46940	0.00	0.00	0.00	0.000

TABLE 16. TEST NO. 11, PART 1 - 1/2-IN. BAR STRESS WHILE CYCLING
(SHEET 11 OF 11)

509	7288.48640	0.00	0.00	0.00	0.00	0.00	0.00
510	7288.49440	0.27	5.58	5.58	0.00	0.00	0.00
511	7288.50440	0.60	10.76	10.76	0.00	0.00	0.00
512	7288.51440	0.94	15.14	15.14	0.00	0.00	0.00
513	7288.52940	1.44	20.72	20.72	0.00	0.00	0.00
514	7288.54440	1.94	25.30	25.30	0.00	0.00	0.00
515	7288.56940	2.77	32.87	32.87	0.00	0.00	0.00
516	7288.59440	3.60	39.84	39.84	0.00	0.00	0.00
517	7288.61940	4.44	47.01	47.01	0.00	0.00	0.00
518	7288.64440	5.27	54.58	54.58	0.00	0.00	0.00
519	7288.66940	6.10	62.55	62.55	0.00	0.00	0.00
520	7288.67940	6.44	65.94	65.94	0.00	0.00	0.00
521	7288.69440	6.74	72.71	72.71	0.00	0.00	0.00
522	7288.70940	7.44	81.67	81.67	0.00	0.00	0.00
523	7288.72640	8.00	93.23	93.23	0.00	0.00	0.00
524	7289.02640	8.00	44.22	44.22	0.00	0.00	0.00
525	7289.52640	8.00	37.45	37.45	0.00	0.00	0.00
526	7290.52640	8.00	32.87	32.87	0.00	0.00	0.00
527	7292.52640	8.00	32.48	32.48	0.00	0.00	0.00
528	7304.52640	8.00	26.49	26.49	0.00	0.00	0.00
529	7352.52640	8.00	24.10	24.10	0.00	0.00	0.00
530	7352.52640	8.00	21.91	21.91	0.00	0.00	0.00
531	7352.53140	8.00	20.12	20.12	0.00	0.00	0.00
532	7352.53640	7.67	15.54	15.54	0.00	0.00	0.00
533	7352.54140	7.50	12.15	12.15	0.00	0.00	0.00
534	7352.54640	7.34	9.56	9.56	0.00	0.00	0.00
535	7352.55140	7.00	7.57	7.57	0.00	0.00	0.00
536	7352.55640	7.00	4.58	4.58	0.00	0.00	0.00
537	7352.56640	6.67	2.39	2.39	0.00	0.00	0.00
538	7352.58140	6.67	0.20	0.20	0.00	0.00	0.00
539	7352.60640	6.46	-0.40	-0.40	0.00	0.00	0.00
540	7352.63140	6.31	-7.37	-7.37	0.00	0.00	0.00
541	7352.65640	6.20	-9.96	-9.96	0.00	0.00	0.00
542	7352.68140	6.10	-12.55	-12.55	0.00	0.00	0.00
543	7352.69440	6.05	-13.74	-13.74	0.00	0.00	0.00
544	7352.70140	6.02	-19.96	-19.96	0.00	0.00	0.00
545	7352.71140	5.97	-5.98	-5.98	0.00	0.00	0.00
546	7352.71640	5.97	-4.98	-4.98	0.00	0.00	0.00
547	7352.72640	5.93	-3.98	-3.98	0.00	0.00	0.00
548	7352.74140	5.89	-3.39	-3.39	0.00	0.00	0.00
549	7352.76640	5.80	-2.99	-2.99	0.00	0.00	0.00
550	7352.77140	5.78	-1.79	-1.79	0.00	0.00	0.00
551	7352.80140	5.70	-1.00	-1.00	0.00	0.00	0.00
552	7352.88140	5.50	-0.60	-0.60	0.00	0.00	0.00
553	7362.56640	0.00	0.00	0.00	0.00	0.00	0.00

TABLE 17. TEST NO. 11, PART 2 - QUINLAN COMPLEX HISTORY FOR UTP-3001
T8714

Cycle	Rate, in./min.	Remarks	
16	Load unload	0.02 0.02	Approximately 30 min. rest after cycle
17	Load unload	0.02 0.02	Approximately 30 min. rest after cycle
18	Load relax unload	0.05 3 hr 0.05	2 weeks rest after cycle
19	Load unload	0.02 0.02	Approximately 30 min. rest after cycle
20	Load unload	0.02 0.02	Approximately 30 min. rest after cycle
21	Load relax unload	0.05 3 hr 0.05	1 month rest after cycle
22-42	Cycling	5	Several cycles monitored followed by several with only maximum and minimum recorded.

Note: Part 3 of this test was continuing cycling to failure. The maximum and minimum values at larger intervals have been tabulated but not incorporated into the disk files.

3.1.12 Similitude Test No. 12

This similitude test and the one following it were run with the intent that only the strain-time history would be supplied to the subcontractors, who would then predict the stress-time histories from their respective predictive theories for the program review meeting held at the end of the phase II testing in September 1982.

This similitude test on the 6-in. bar specimens of UTP-3001 and UTP-19,360B propellants was: (1) a 0.01 in./min. ramp to 10% strain followed by relaxation; (2) a 1 in./min. unload to 5% strain and relaxation; and (3) 0.1 in./min. ramp to failure. The same test was repeated for ramp rates of 0.001, 0.1, and 0.01 in./min. The data as reported at the September meeting are shown for UTP-19,360B in Figure 33. The ramp rates were 0.01, 1, and 0.1 in./min. Tabular data for the test are given in Table 20.

TABLE 18. TEST NO. 11, PART 2 - 1/2-IN. BAR STRESS WHILE CYCLING
(SHEET 2 OF 10)

16	18825	53140	3.96	13.71	0.000
17	18825	53140	3.91	12.97	0.000
18	18825	53140	3.88	12.27	0.000
19	18826	53140	3.85	10.76	0.000
20	18826	53140	3.81	9.56	0.000
21	18827	53140	3.76	9.11	0.000
22	18828	53140	3.71	8.93	0.000
23	18829	53140	3.67	8.98	0.000
24	18829	53140	3.61	8.02	0.000
25	18831	53140	3.59	5.52	0.000
26	18831	53140	3.53	3.23	0.000
27	18833	53140	3.48	2.96	0.000
28	18834	53140	3.42	0.24	0.000
29	18835	53140	3.37	1.27	0.000
30	18837	53140	3.31	1.39	0.000
31	18837	53140	3.25	1.91	0.000
32	18837	53140	3.19	1.59	0.000
33	18838	53140	3.13	1.43	0.000
34	18839	53140	3.07	1.27	0.000
35	18840	53140	3.01	1.12	0.000
36	18842	53140	2.95	1.76	0.000
37	18845	53140	2.89	0.80	0.000
38	18850	53140	2.83	0.56	0.000
39	18858	53140	2.77	0.40	0.000
40	18868	53140	2.71	0.40	0.000
41	18868	53140	2.65	0.40	0.000
42	18869	53140	2.59	0.56	0.000
43	18871	53140	2.53	2.40	0.000
44	18877	53140	2.47	4.06	0.000
45	18877	53140	2.41	6.84	0.000
46	18880	53140	2.35	10.54	0.000
47	18884	53140	2.29	15.24	0.000
48	18884	53140	2.23	20.40	0.000
49	18888	53140	2.17	24.14	0.000
50	18890	53140	2.11	27.89	0.000
51	18891	53140	2.05	31.55	0.000
52	18893	53140	1.99	36.06	0.000
53	18895	53140	1.93	46.62	0.000
54	18895	53140	1.87	53.42	0.000
55	18896	53140	1.81	37.07	0.000
56	18897	53140	1.75	31.87	0.000
57	18897	53140	1.69	28.47	0.000
58	18898	53140	1.63	23.67	0.000
59	18899	53140	1.57	20.32	0.000
60	18900	53140	1.51	16.89	0.000
61	18902	53140	1.45	14.50	0.000
62	18904	53140	1.39	11.79	0.000
63	18907	53140	1.33	8.61	0.000
64	18911	53140	1.27	5.10	0.000
65	18916	53140	1.21	1.20	0.000
66	18922	53140	1.15	1.43	0.000
67	18923	53140	1.09	3.19	0.000
68	18925	53140	1.03	3.87	0.000
69	18925	53140	0.97	2.47	0.000

TABLE 18. TEST NO. 11, PART 2 - 1/2-IN. BAR STRESS WHILE CYCLING
(SHEET 3 OF 10)

70	18924	81640	0.28	-2.23	0.000
71	18926	81640	0.28	-1.91	0.000
72	18930	81640	0.28	-1.59	0.000
73	18936	81640	0.28	-1.27	0.000
74	18946	81640	0.28	-1.04	0.000
75	18955	81640	0.28	-0.96	0.000
76	18955	21640	0.41	0.32	0.000
77	18955	61640	0.74	1.83	0.000
78	18956	21640	1.24	3.82	0.000
79	18957	21640	2.08	6.85	0.000
80	18958	61640	3.24	10.76	0.000
81	18959	81640	4.58	14.02	0.000
82	18960	81640	5.91	16.89	0.000
83	18961	81640	6.74	20.16	0.000
84	18962	81640	7.58	24.14	0.000
85	18963	81640	8.24	29.48	0.000
86	18964	81640	8.24	35.78	0.000
87	18964	81640	8.24	33.47	0.000
88	18965	21640	8.24	31.71	0.000
89	18966	01640	8.24	29.96	0.000
90	18967	61640	8.24	28.29	0.000
91	18970	81640	8.24	26.85	0.000
92	18977	21640	8.24	25.26	0.000
93	18990	01640	8.24	23.27	0.000
94	19015	81640	8.24	21.83	0.000
95	19066	81640	8.24	20.56	0.000
96	19144	45640	8.24	19.76	0.000
97	19144	61640	8.24	17.21	0.000
98	19144	81640	8.24	15.30	0.000
99	19145	21640	7.7	12.83	0.000
100	19145	81640	7.7	10.96	0.000
101	19146	41640	6.6	8.37	0.000
102	19147	81640	6.6	6.94	0.000
103	19147	81640	6.6	4.94	0.000
104	19148	81640	4.94	2.87	0.000
105	19150	81640	4.94	0.80	0.000
106	19152	81640	1.28	-4.38	0.000
107	19154	01640	0.28	-6.61	0.000
108	19154	21640	0.28	-5.66	0.000
109	19154	61640	0.28	-4.62	0.000
110	19155	21640	0.28	-4.62	0.000
111	19156	01640	0.28	-4.22	0.000
112	19157	01640	0.28	-3.75	0.000
113	19158	81640	0.28	-3.43	0.000
114	19160	81640	0.28	-3.13	0.000
115	19164	81640	0.28	-2.69	0.000
116	19168	81640	0.28	-2.23	0.000
117	32622	81640	0.00	0.00	0.000
118	32623	81640	0.16	1.99	0.000
119	32624	31640	0.50	3.98	0.000
120	32625	31640	0.83	5.90	0.000
121	32625	31640	1.33	8.95	0.000
122	32628	81640	1.30	11.95	0.000

TABLE 18. TEST NO. 11, PART 2 - 1/2-IN. BAR STRESS WHILE CYCLING
(SHEET 4 OF 10)

124	32630	81640	2.66	14.90	14.90	0.000
125	32632	81640	3.33	17.85	17.85	0.000
126	32634	46640	3.98	20.16	20.16	0.000
127	32634	81640	3.76	15.94	15.94	0.000
128	32635	31640	3.60	13.47	13.47	0.000
129	32635	81640	3.43	11.71	11.71	0.000
130	32636	81640	3.10	9.24	9.24	0.000
131	32637	81640	2.76	7.49	7.49	0.000
132	32640	31640	1.93	3.90	3.90	0.000
133	32642	81640	1.10	0.80	0.80	0.000
134	32645	96640	0.05	-2.55	-2.55	0.000
135	32646	06640	0.05	-2.23	-2.23	0.000
136	32646	56640	0.05	-1.83	-1.83	0.000
137	32647	06640	0.05	-1.59	-1.59	0.000
138	32647	56640	0.05	-1.43	-1.43	0.000
139	32648	56640	0.05	-1.27	-1.27	0.000
140	32656	56640	0.05	-0.96	-0.96	0.000
141	32653	56640	0.05	-0.80	-0.80	0.000
142	32659	56640	0.05	-0.48	-0.48	0.000
143	32665	56640	0.05	-0.32	-0.32	0.000
144	32676	16640	0.05	-0.24	-0.24	0.000
145	32676	36640	0.11	0.48	0.48	0.000
146	32676	86640	0.28	1.59	1.59	0.000
147	32677	86640	0.61	3.27	3.27	0.000
148	32680	36640	1.45	6.53	6.53	0.000
149	32682	86640	2.28	9.96	9.96	0.000
150	32685	36640	3.11	13.55	13.55	0.000
151	32687	86640	3.95	17.37	17.37	0.000
152	32690	36640	4.78	21.27	21.27	0.000
153	32692	86640	5.61	25.58	25.58	0.000
154	32695	36640	6.45	30.84	30.84	0.000
155	32697	86640	7.28	38.01	38.01	0.000
156	32700	36640	8.11	49.08	49.08	0.000
157	32701	86640	8.61	57.37	57.37	0.000
158	32702	81640	8.93	62.15	62.15	0.000
159	32703	11640	8.83	49.00	49.00	0.000
160	32703	36640	8.73	43.82	43.82	0.000
161	32703	86640	8.58	37.21	37.21	0.000
162	32704	36640	8.41	32.67	32.67	0.000
163	32705	36640	8.08	26.93	26.93	0.000
164	32706	36640	7.75	23.11	23.11	0.000
165	32709	86640	7.25	18.96	18.96	0.000
166	32710	86640	6.25	16.63	16.63	0.000
167	32712	86640	5.58	11.08	11.08	0.000
168	32715	86640	4.75	8.29	8.29	0.000
169	32717	86640	3.91	5.98	5.98	0.000
170	32722	86640	2.25	1.67	1.67	0.000
171	32727	86640	0.58	-2.39	-2.39	0.000
172	32729	31640	0.10	-3.90	-3.90	0.000
173	32729	41640	0.10	-3.59	-3.59	0.000
174	32729	91640	0.10	-3.19	-3.19	0.000
175	32729	91640	0.10	-2.95	-2.95	0.000
176	32730	41640	0.10	-2.63	-2.63	0.000
177	32731	41640	0.10	-2.63	-2.63	0.000

TABLE 18. TEST NO. 11, PART 2 - 1/2-IN. BAR STRESS WHILE CYCLING
(SHEET 5 OF 10)

178	32732	41640	0.10	-2.39	-2.39	0.000
179	32734	41640	0.10	-2.15	-2.15	0.000
180	32747	41640	0.10	-1.91	-1.91	0.000
181	32741	41640	0.10	-1.67	-1.67	0.000
182	32746	41640	0.10	-1.51	-1.51	0.000
183	32751	41640	0.10	-1.35	-1.35	0.000
184	32758	41640	0.10	-1.20	-1.20	0.000
185	32758	61640	0.26	0.20	0.20	0.000
186	32759	01640	0.60	2.19	2.19	0.000
187	32760	01640	1.43	5.78	5.78	0.000
188	32761	01640	2.26	9.46	9.46	0.000
189	32762	01640	3.10	12.55	12.55	0.000
190	32763	01640	3.93	15.74	15.74	0.000
191	32764	01640	4.76	18.73	18.73	0.000
192	32765	01640	5.60	22.71	22.71	0.000
193	32766	01640	6.43	27.49	27.49	0.000
194	32767	01640	7.26	34.26	34.26	0.000
195	32767	83640	7.95	42.23	42.23	0.000
196	32768	23640	7.95	38.25	38.25	0.000
197	32768	73640	7.95	35.86	35.86	0.000
198	32770	73640	7.95	32.07	32.07	0.000
199	32774	73640	7.95	29.04	29.04	0.000
200	32782	73640	7.95	26.49	26.49	0.000
201	32798	73640	7.95	24.70	24.70	0.000
202	32830	73640	7.95	22.91	22.91	0.000
203	32894	73640	7.95	22.31	22.31	0.000
204	32947	73640	7.95	20.52	20.52	0.000
205	32947	93640	7.78	16.93	16.93	0.000
206	32948	13640	7.61	15.14	15.14	0.000
207	32948	53640	7.28	12.55	12.55	0.000
208	32948	93640	6.95	10.36	10.36	0.000
209	32949	53640	6.45	8.37	8.37	0.000
210	32950	36640	6.11	6.97	6.97	0.000
211	32951	36640	5.75	5.98	5.98	0.000
212	32951	13640	5.45	5.98	5.98	0.000
213	32952	93640	4.45	3.99	3.99	0.000
214	32952	93640	3.61	1.00	1.00	0.000
215	32953	93640	3.78	-1.99	-1.99	0.000
216	32955	93640	1.95	-3.78	-3.78	0.000
217	32955	93640	1.11	-5.78	-5.78	0.000
218	32957	13640	0.11	-8.17	-8.17	0.000
219	32957	33640	0.11	-6.57	-6.57	0.000
220	32957	53640	0.11	-6.18	-6.18	0.000
221	32958	13640	0.11	-5.98	-5.98	0.000
222	32958	63640	0.11	-5.58	-5.58	0.000
223	32959	13640	0.11	-5.38	-5.38	0.000
224	32960	13640	0.11	-4.78	-4.78	0.000
225	32961	13640	0.11	-4.58	-4.58	0.000
226	32963	13640	0.11	-3.98	-3.98	0.000
227	32966	13640	0.11	-3.78	-3.78	0.000
228	32971	13640	0.11	-3.19	-3.19	0.000
229	32976	13640	0.11	-2.79	-2.79	0.000
230	32983	13640	0.11	-2.79	-2.79	0.000

AD-A133 364

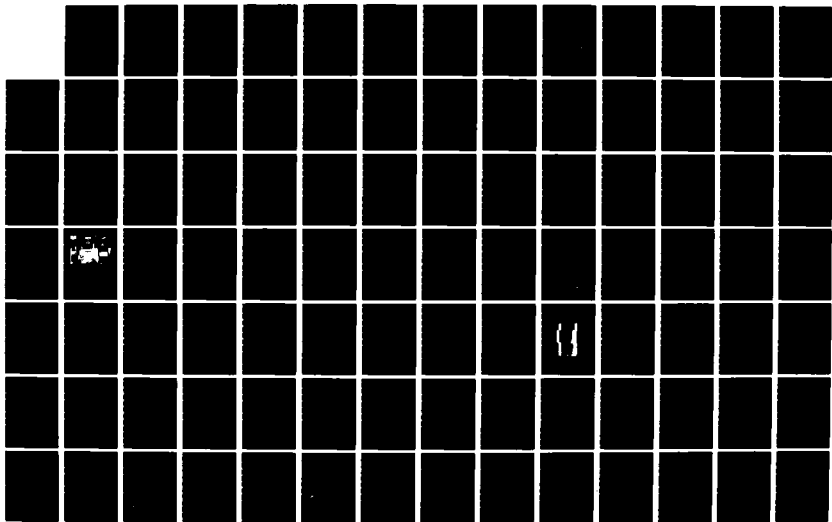
PROPELLANT NONLINEAR CONSTITUTIVE THEORY EXTENSION:
PRELIMINARY RESULTS. (U) UNITED TECHNOLOGIES CORP
SUNNYVALE CA CHEMICAL SYSTEMS DIV E C FRANCIS ET AL

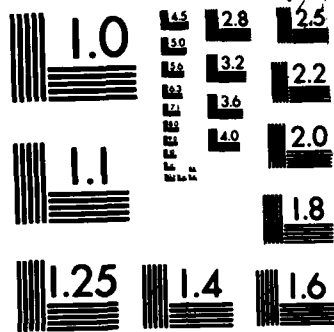
2/4

UNCLASSIFIED

AUG 83 UTC/CSD-2742 AFRPL-TR-83-034

F/G 21/9.2 NL





MICROCOPY RESOLUTION TEST CHART
NATIONAL BUREAU OF STANDARDS-1963-A

TABLE 18. TEST NO. 11, PART 2 - 1/2-IN. BAR STRESS WHILE CYCLING
(SHEET 6 OF 10)

232	74383	13640	0.00	0.00	0.00	0.00
233	74383	15140	0.00	0.00	0.00	0.00
234	74383	15640	0.84	12.71	0.00	0.00
235	74383	16140	1.25	31.08	0.00	0.00
236	74383	16640	2.09	45.42	0.00	0.00
237	74383	19140	3.59	62.95	0.00	0.00
238	74383	20640	4.84	82.47	0.00	0.00
240	74383	22140	7.09	102.79	0.00	0.00
241	74383	23640	8.34	126.64	0.00	0.00
242	74383	25140	9.59	154.18	0.00	0.00
243	74383	26640	10.84	175.30	0.00	0.00
244	74383	28140	12.17	190.04	0.00	0.00
245	74383	29640	12.17	200.80	0.00	0.00
246	74383	29890	11.84	157.37	0.00	0.00
247	74383	30140	11.42	113.94	0.00	0.00
248	74383	30640	11.00	81.67	0.00	0.00
249	74383	31140	9.75	63.74	0.00	0.00
250	74383	31640	9.00	51.39	0.00	0.00
251	74383	32640	8.00	36.25	0.00	0.00
252	74383	33640	7.00	26.69	0.00	0.00
253	74383	35140	5.70	17.13	0.00	0.00
254	74383	37640	3.85	5.98	0.00	0.00
255	74383	42990	0.60	-12.79	0.00	0.00
256	74383	43940	0.60	-12.79	0.00	0.00
257	74383	44940	0.60	-4.38	0.00	0.00
258	74383	46440	0.60	16.33	0.00	0.00
259	74383	48440	0.60	28.62	0.00	0.00
260	74383	48440	0.60	39.84	0.00	0.00
261	74383	50440	0.60	50.60	0.00	0.00
262	74383	51940	0.60	64.54	0.00	0.00
263	74383	53440	0.60	77.29	0.00	0.00
264	74383	54440	0.60	94.82	0.00	0.00
265	74383	55440	1.30	119.52	0.00	0.00
266	74383	56440	1.80	135.06	0.00	0.00
267	74383	57640	1.17	156.57	0.00	0.00
268	74383	57640	1.80	100.00	0.00	0.00
269	74383	57940	1.80	171.71	0.00	0.00
270	74383	58440	1.80	56.18	0.00	0.00
271	74383	58940	1.80	46.61	0.00	0.00
272	74383	59440	1.80	32.90	0.00	0.00
273	74383	60440	1.80	17.53	0.00	0.00
274	74383	61440	1.80	17.53	0.00	0.00
275	74383	62440	1.80	17.53	0.00	0.00
276	74383	64440	1.40	-2.39	0.00	0.00
277	74383	67440	1.20	-9.56	0.00	0.00
278	74383	69940	1.20	-2.79	0.00	0.00
279	74383	70740	1.20	8.37	0.00	0.00
280	74383	72240	1.20	18.73	0.00	0.00
281	74383	73740	1.20	29.48	0.00	0.00
282	74383	75740	1.20	40.64	0.00	0.00
283	74383	77740	1.20	51.39	0.00	0.00
284	74383	79240	1.20	66.53	0.00	0.00
285	74383	80740	1.20	81.53	0.00	0.00

TABLE 18. TEST NO. 11, PART 2 - 1/2-IN. BAR STRESS WHILE CYCLING
(SHEET 7 OF 10)

286	74383.81740	10.30	80.08	0.000
287	74383.82740	11.10	100.40	0.000
288	74383.83240	11.40	114.74	0.000
289	74383.83990	12.17	140.24	0.000
290	74383.84240	11.80	199.60	0.000
291	74383.84740	11.20	69.72	0.000
292	74383.85240	11.10	54.58	0.000
293	74383.86240	10.20	37.05	0.000
294	74383.87240	8.00	17.13	0.000
295	74383.88740	5.70	5.98	0.000
296	74383.91240	3.60	-2.39	0.000
298	74383.93740	1.50	-8.76	0.000
299	74383.95990	2.80	-2.39	0.000
300	74383.98990	3.70	12.91	0.000
301	74384.00490	5.10	35.06	0.000
302	74384.02990	6.80	43.82	0.000
303	74384.04490	8.00	55.78	0.000
304	74384.05990	9.80	66.53	0.000
305	74384.06990	10.50	81.67	0.000
306	74384.07990	11.35	103.59	0.000
308	74384.08990	11.70	121.51	0.000
309	74384.09490	12.17	130.68	0.000
310	74384.09990	12.00	132.39	0.000
311	74384.10490	11.60	170.12	0.000
312	74384.10990	11.20	53.78	0.000
313	74384.11990	10.50	36.65	0.000
314	74384.12990	9.50	26.69	0.000
315	74384.13990	8.60	19.52	0.000
316	74384.15990	6.70	9.96	0.000
318	74384.18490	4.20	0.80	0.000
319	74384.21190	1.70	-7.97	0.000
320	74384.22190	2.90	0.00	0.000
321	74384.23190	4.20	6.77	0.000
322	74384.24690	5.90	16.70	0.000
323	74384.26190	6.90	35.06	0.000
324	74384.28190	8.10	44.22	0.000
325	74384.29690	9.00	52.59	0.000
326	74384.30690	9.75	61.75	0.000
327	74384.32690	10.50	75.70	0.000
328	74384.33690	11.30	95.62	0.000
329	74384.34190	11.90	109.56	0.000
330	74384.34640	12.17	124.70	0.000
331	74384.34940	11.80	87.65	0.000
332	74384.35190	11.60	73.70	0.000
333	74384.35690	11.25	56.18	0.000
334	74384.36160	10.70	45.82	0.000
335	74384.36690	10.40	37.45	0.000
336	74384.37190	10.00	31.47	0.000
337	74384.38190	9.00	22.71	0.000
338	74384.39190	8.30	16.73	0.000
339	74384.41190	6.50	17.97	0.000

TABLE 18. TEST NO. 11, PART 2 - 1/2-IN. BAR STRESS WHILE CYCLING
(SHEET 8 OF 10)

340	74384.43690	4.20	-0.80	-0.80	0.000
341	74384.45990	1.80	-7.97	-7.97	0.000
342	74384.46890	2.30	-1.20	-1.20	0.000
343	74384.48390	3.60	8.76	8.76	0.000
344	74384.49890	4.50	19.12	19.12	0.000
345	74384.51390	5.70	27.09	27.09	0.000
346	74384.52890	8.30	34.26	34.26	0.000
347	74384.54390	8.90	42.23	42.23	0.000
348	74384.55390	9.90	49.80	49.80	0.000
349	74384.56390	10.50	58.96	58.96	0.000
350	74384.57390	11.30	71.51	71.51	0.000
351	74384.58390	11.80	90.04	90.04	0.000
352	74384.58890	12.17	102.79	102.79	0.000
353	74384.59490	11.60	121.12	121.12	0.000
354	74384.59890	11.20	176.89	176.89	0.000
355	74384.60390	10.90	57.77	57.77	0.000
356	74384.60890	10.50	45.82	45.82	0.000
357	74384.61390	19.50	37.85	37.85	0.000
358	74384.62390	19.50	27.49	27.49	0.000
359	74384.63390	8.90	19.92	19.92	0.000
360	74384.64890	5.60	12.35	12.35	0.000
361	74384.67390	3.90	4.38	4.38	0.000
362	74384.69390	2.20	-2.97	-2.97	0.000
363	74384.71390	3.00	-3.59	-3.59	0.000
364	74384.71890	3.70	4.38	4.38	0.000
365	74384.72890	4.50	11.16	11.16	0.000
366	74384.73890	5.90	17.53	17.53	0.000
367	74384.74890	6.90	25.90	25.90	0.000
368	74384.76390	8.10	32.67	32.67	0.000
369	74384.77890	9.30	41.83	41.83	0.000
370	74384.79390	9.80	48.21	48.21	0.000
371	74384.80390	10.80	56.57	56.57	0.000
372	74384.81390	11.60	68.53	68.53	0.000
373	74384.82390	11.90	83.66	83.66	0.000
374	74384.83390	12.17	98.80	98.80	0.000
375	74384.84540	11.60	117.13	117.13	0.000
376	74384.84890	11.10	178.09	178.09	0.000
377	74384.85390	10.60	57.37	57.37	0.000
378	74384.85890	9.70	45.42	45.42	0.000
379	74384.85890	7.60	31.87	31.87	0.000
380	74384.86890	7.60	23.51	23.51	0.000
381	74384.87890	5.80	14.74	14.74	0.000
382	74384.89390	4.00	-6.40	-6.40	0.000
383	74384.91390	2.00	-7.17	-7.17	0.000
384	74384.93390	3.40	0.40	0.40	0.000
385	74384.95640	3.40	6.77	6.77	0.000
386	74384.96640	4.20	13.94	13.94	0.000
387	74384.97640	6.60	19.52	19.52	0.000
388	74384.98640	6.60	34.66	34.66	0.000
389	74384.99640	7.80	42.63	42.63	0.000
390	74385.01140	8.70	50.60	50.60	0.000
391	74385.02640				
392	74385.04140				
393	74385.05140				

TABLE 18. TEST NO. 11, PART 2 - 1/2-IN. BAR STRESS WHILE CYCLING
(SHEET 9 OF 10)

394	74385.06140	9.40	60.16	60.16	0.000
395	74385.07140	10.25	73.31	73.31	0.000
396	74385.08140	11.10	93.63	93.63	0.000
397	74385.08640	11.60	108.37	108.37	0.000
398	74385.08890	12.17	115.54	115.54	0.000
399	74385.09390	11.80	72.51	72.51	0.000
400	74385.10390	11.20	43.82	43.82	0.000
401	74385.11390	10.60	30.64	30.64	0.000
402	74385.12390	10.60	22.31	22.31	0.000
403	74385.13390	7.90	11.95	11.95	0.000
404	74385.14390	5.40	10.40	10.40	0.000
405	74385.20090	2.10	7.17	7.17	0.000
406	74385.21390	3.90	17.13	17.13	0.000
407	74385.23390	5.50	28.29	28.29	0.000
408	74385.25390	7.20	37.85	37.85	0.000
409	74385.27390	8.80	51.00	51.00	0.000
410	74385.29390	10.00	59.76	59.76	0.000
411	74385.30390	10.00	74.50	74.50	0.000
412	74385.31390	10.60	95.63	95.63	0.000
413	74385.32390	11.70	112.74	112.74	0.000
414	74385.32890	12.17	63.74	63.74	0.000
415	74385.33390	11.80	48.64	48.64	0.000
416	74385.34390	10.20	29.08	29.08	0.000
417	74385.35390	10.20	21.51	21.51	0.000
418	74385.36390	10.10	15.14	15.14	0.000
419	74385.37390	8.30	5.59	5.59	0.000
420	74385.40390	3.30	3.98	3.98	0.000
421	74385.43690	3.30	16.73	16.73	0.000
422	74385.45690	4.70	32.27	32.27	0.000
423	74385.47690	7.00	43.82	43.82	0.000
424	74385.50690	8.50	61.75	61.75	0.000
425	74385.52690	10.00	75.70	75.70	0.000
426	74385.54690	10.90	110.36	110.36	0.000
427	74385.56990	12.17	77.28	77.28	0.000
428	74385.57190	11.80	55.45	55.45	0.000
430	74385.58690	11.60	37.45	37.45	0.000
431	74385.58690	10.80	26.69	26.69	0.000
432	74385.59690	9.80	15.14	15.14	0.000
433	74385.61690	8.30	7.17	7.17	0.000
434	74385.64690	5.20	4.48	4.48	0.000
435	74385.67790	3.40	17.09	17.09	0.000
436	74385.69390	4.70	38.65	38.65	0.000
437	74385.71590	6.30	52.95	52.95	0.000
438	74385.73590	7.80	62.68	62.68	0.000
439	74385.75590	9.30	79.68	79.68	0.000
440	74385.78590	10.30	108.37	108.37	0.000
441	74385.79590	10.90	70.42	70.42	0.000
442	74385.80690	12.17	49.80	49.80	0.000
443	74385.81090	11.70	33.86	33.86	0.000
444	74385.81590	11.00	23.90	23.90	0.000
445	74385.82590	10.20	9.50	9.50	0.000
446	74385.83590	9.50			0.000
447	74385.83590				0.000

TABLE 18. TEST NO. 11, PART 2 - 1/2-IN. BAR STRESS WHILE CYCLING
(SHEET 10 OF 10)

448	74385.85590	9.10	13.15	13.15	0.000
449	74385.88590	5.00	1.20	-1.20	0.000
450	74385.91590	3.26	-7.17	-7.17	0.000
451	74386.04490	12.17	108.37	108.37	0.000
452	74386.15390	12.17	-6.77	-6.77	0.000
453	74386.28290	12.17	107.17	107.17	0.000
454	74386.39190	12.17	-6.77	-6.77	0.000
455	74386.52090	12.17	105.58	105.58	0.000
456	74386.62890	12.40	-6.77	-6.77	0.000
457	74386.75690	12.17	104.78	104.78	0.000
458	74386.86390	12.40	-6.77	-6.77	0.000
459	74386.98990	12.17	103.59	103.59	0.000
460	74387.09690	12.40	-6.77	-6.77	0.000
461	74387.22390	12.17	102.39	102.39	0.000
462	74387.32990	12.40	-6.77	-6.77	0.000
463	74387.45790	12.17	101.19	101.19	0.000
464	74387.56390	12.40	-6.77	-6.77	0.000
465	74387.68990	12.17	100.40	100.40	0.000
466	74387.81590	12.40	-6.37	-6.37	0.000
467	74387.94190	12.17	99.60	99.60	0.000
468	74388.04790	12.40	-6.37	-6.37	0.000

TABLE 19. TEST NO. 11, PART 3 - UTP-3001-750/7768 1/2-IN.
BAR STRESS WHILE CYCLING

(SHEET 1 OF 2)

T8715

Time	Strain	Stress	Remarks
74388.0479	2.40	-6.37	End of cycle 20
74390.3479	12.17	93.23	Peak of cycle 30
74390.4539	2.40	-5.98	End of cycle 30
74391.3819	12.17	92.03	Peak of cycle 34
74391.4239	2.40	-5.58	End of cycle 34
74391.9432	12.17	91.24	Peak of cycle 40
74391.9859	2.40	-5.58	End of cycle 40
74392.0799	12.17	89.64	Peak of cycle 50
74392.1219	2.40	-5.18	End of cycle 50
74393.0099	12.17	88.45	Peak of cycle 60
74393.0519	2.40	-5.18	End of cycle 60
74394.7799	12.17	84.86	Peak of cycle 80
74394.8219	2.40	-4.78	End of cycle 80
74395.7279	12.17	80.10	Peak of cycle 102
74395.7479	2.40	-4.78	End of cycle 102
74418.3479	12.17	76.49	Peak of cycle 164
74418.3979	2.40	-4.78	End of cycle 164
74451.5979	12.17	71.71	Peak of cycle 330
74451.8779	2.40	-4.38	End of cycle 330
74474.2779	12.17	68.92	Peak of cycle 442
74474.3179	2.40	-3.98	End of cycle 442
74698.0179	12.17	62.95	Peak of cycle 980
	2.40	-3.59	End of cycle 980
74928.0179	12.17	60.16	Peak of cycle 1980
	2.40	-3.59	End of cycle 1980
75158.0179	12.17	56.97	Peak of cycle 2980
	2.40	-3.59	End of cycle 2980
75388.0179	12.17	56.18	Peak of cycle 3980
	2.40	-3.59	End of cycle 3980

TABLE 19. TEST NO. 11, PART 3 - UTP-3001-750/7768 1/2-IN.
 BAR STRESS WHILE CYCLING
 (SHEET 2 OF 2)

T8715

Time	Strain	Stress	Remarks
75618.0179	12.17 2.40	53.39 -3.59	Peak of cycle 4980 End of cycle 4980
75695.5179	12.17 2.40	51.39 -3.59	Peak of cycle 5317 End of cycle 5317
		SAMPLE BROKE	

3.1.13 Three-Step Relaxation Test No. 13

The three-step relaxation tests were run as similitude tests in which the strain-time data were reported to the subcontractors and they were to predict the stress-time histories. The test consisted of loading 6-in. bar specimens at 0.05 in./min. crosshead rate to 10%, relaxing 1 hr, unloading at the same rate to 7% strain, relaxing 1 hr, and repeating the process at 3% strain, then unload. The tests were then repeated with nominal 24 hr relaxation periods for both UTP-3001 and UTP-19,360B propellants.

These data were reworked to make sure that peak and minimum stress points were included in the data. Relaxation was monitored after the sample was unloaded to zero stress. Data for UTP-3001 is shown in Figure 34 with the 1 hr relaxation periods. Tabular data are given in Table 21.

(Text continued on page 103.)

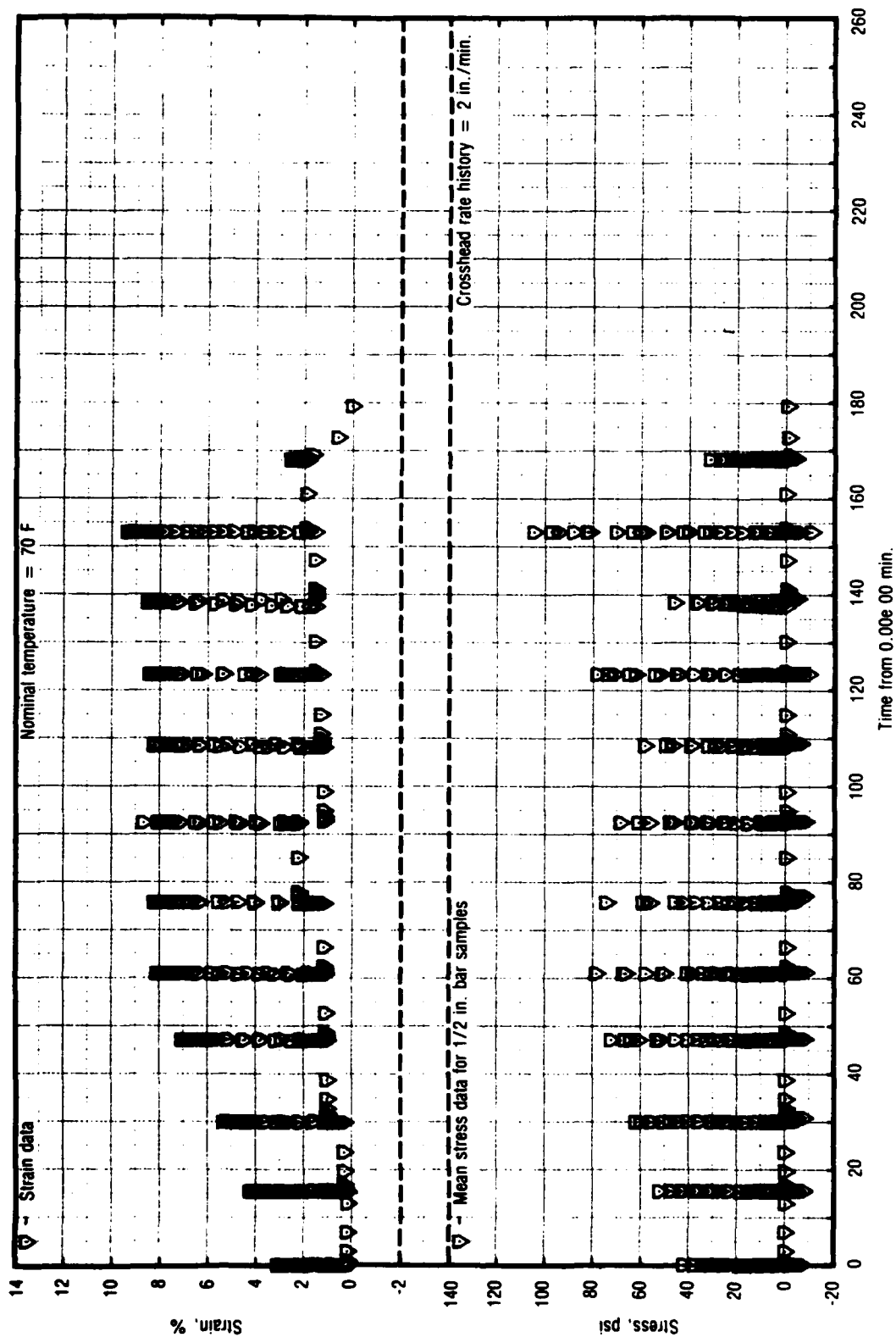


Figure 26. Test No. 11, Part 1 - Stress While Cycling for UTP-3001-750/7768

28757

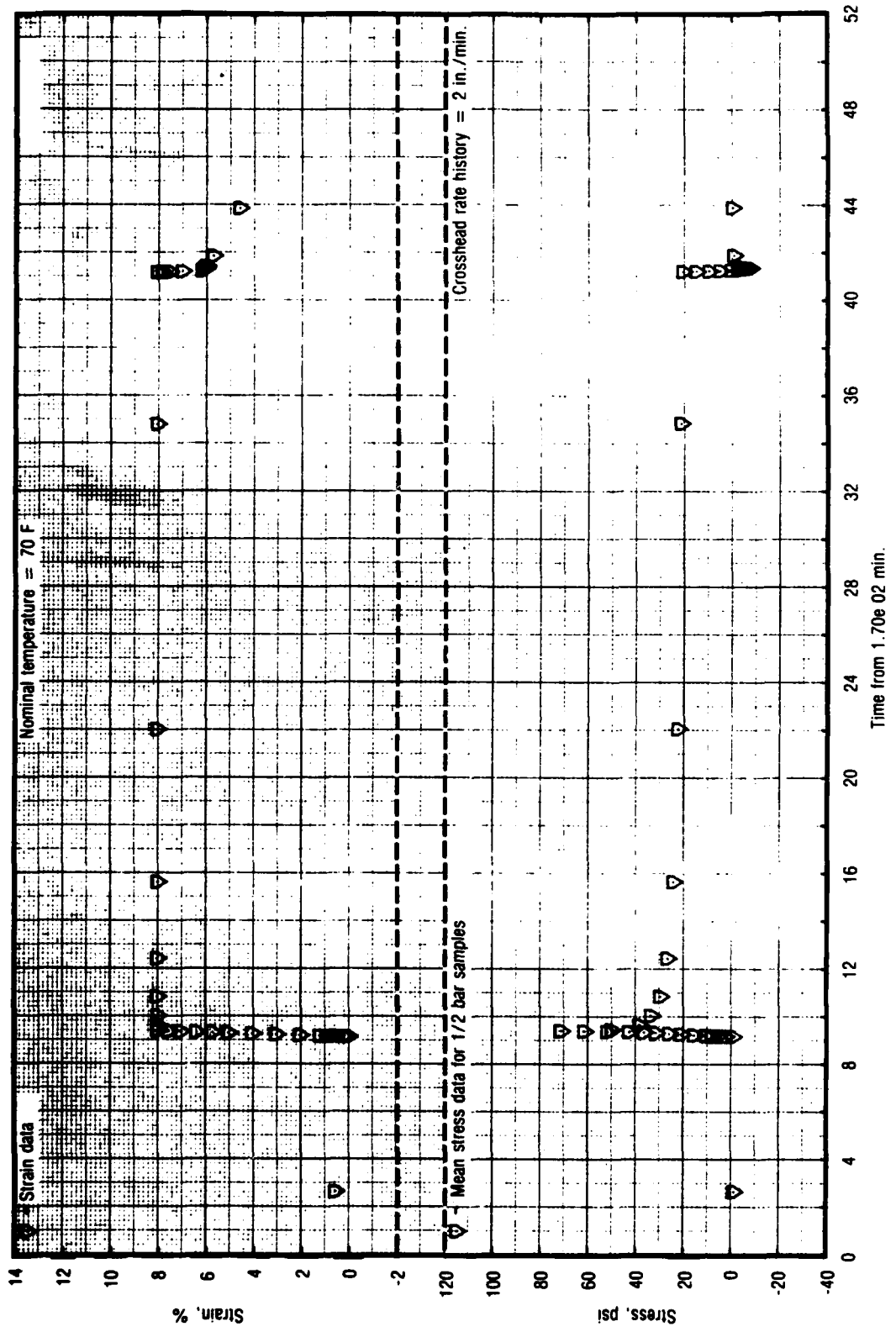


Figure 27. Test No. 11, Part 1 - Stress While Cycling for UTP-3001-750/7768 28758

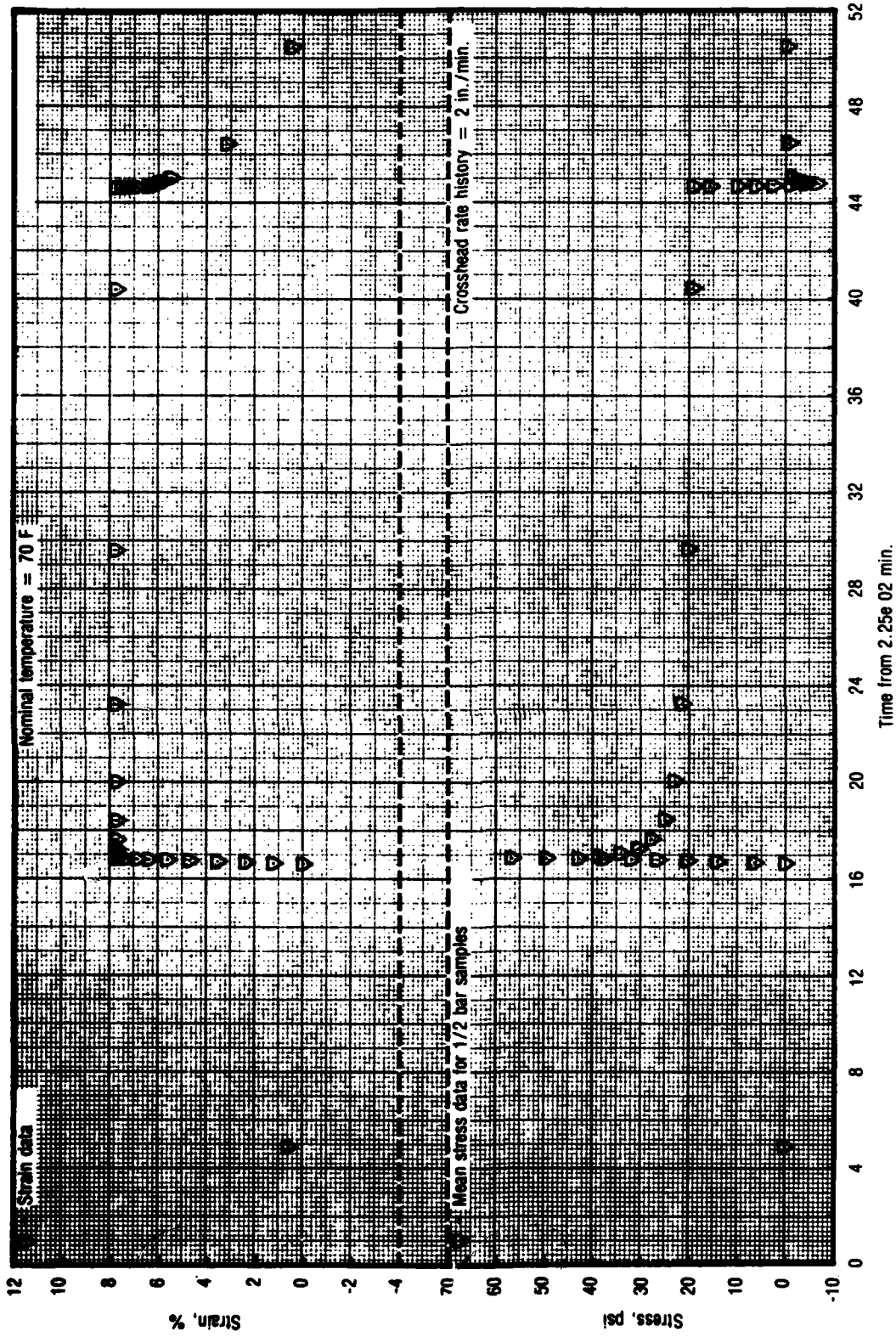


Figure 28. Test No. 11, Part 1 - Stress While Cycling for UTP-3001-750/7768

28797

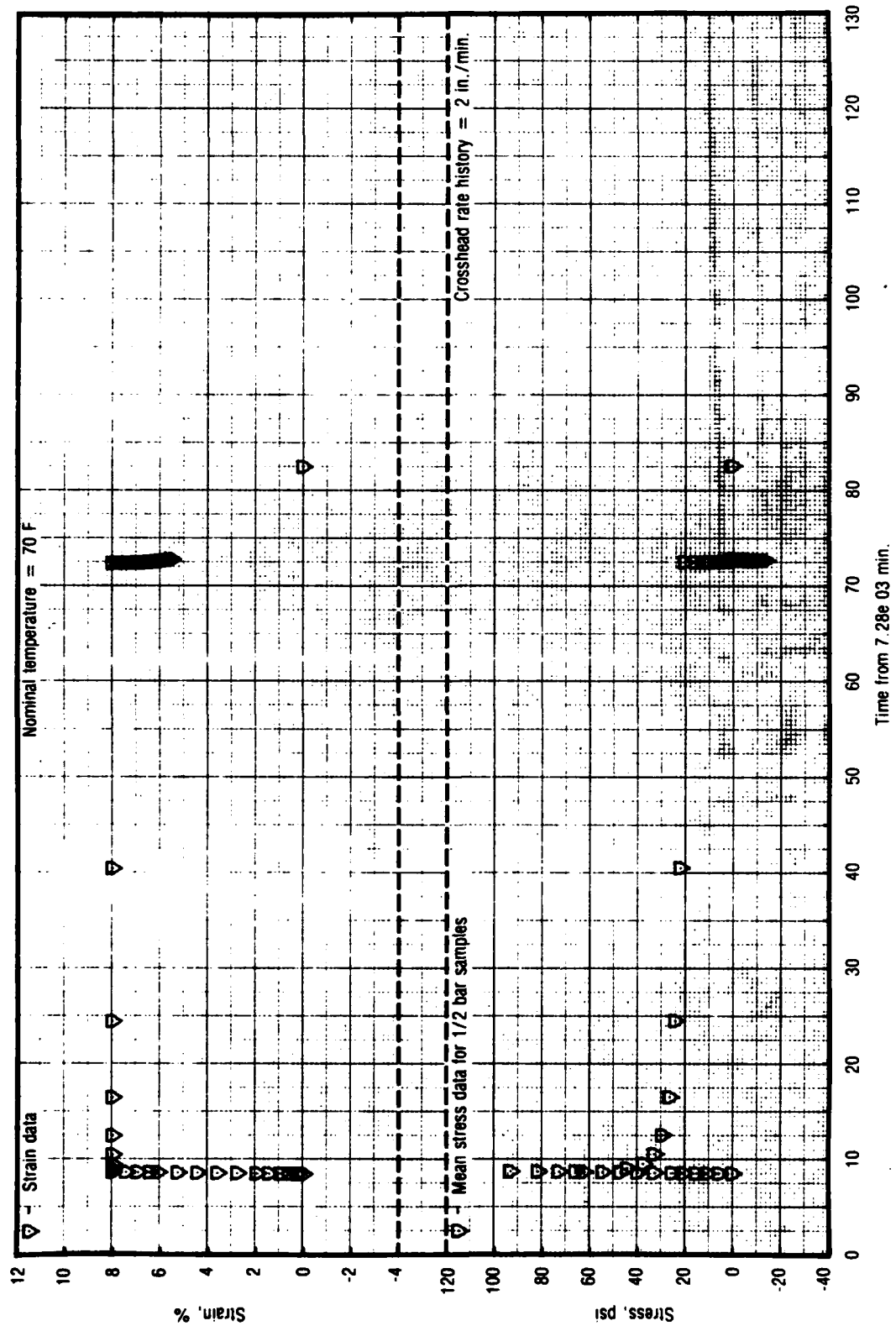


Figure 29. Test No. 11, Part 1 - Stress While Cycling for UTP-3001-750/7768

28798

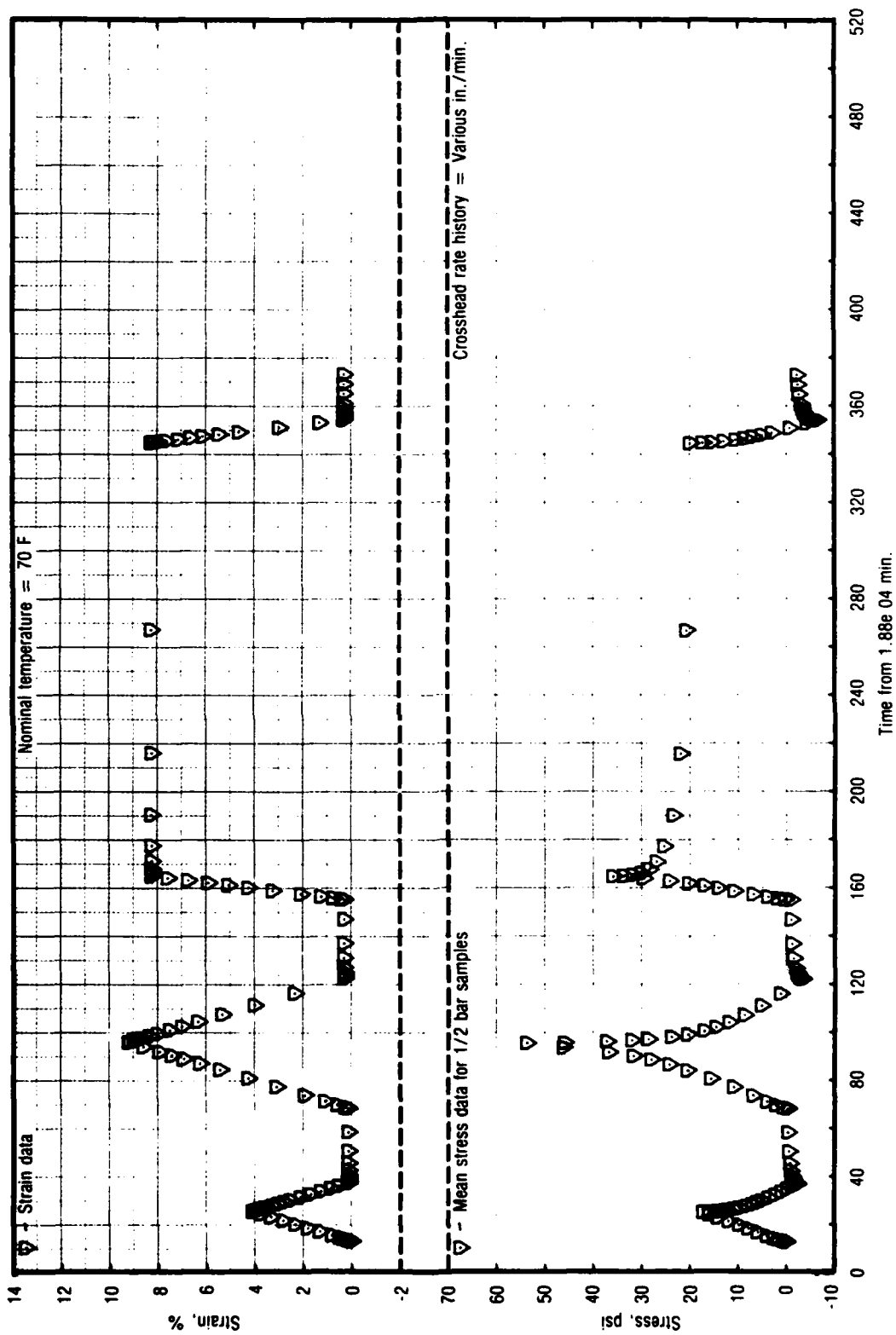


Figure 30. Test No. 11, Part 2 - Stress While Cycling for UTP-3001-750/7768

28759

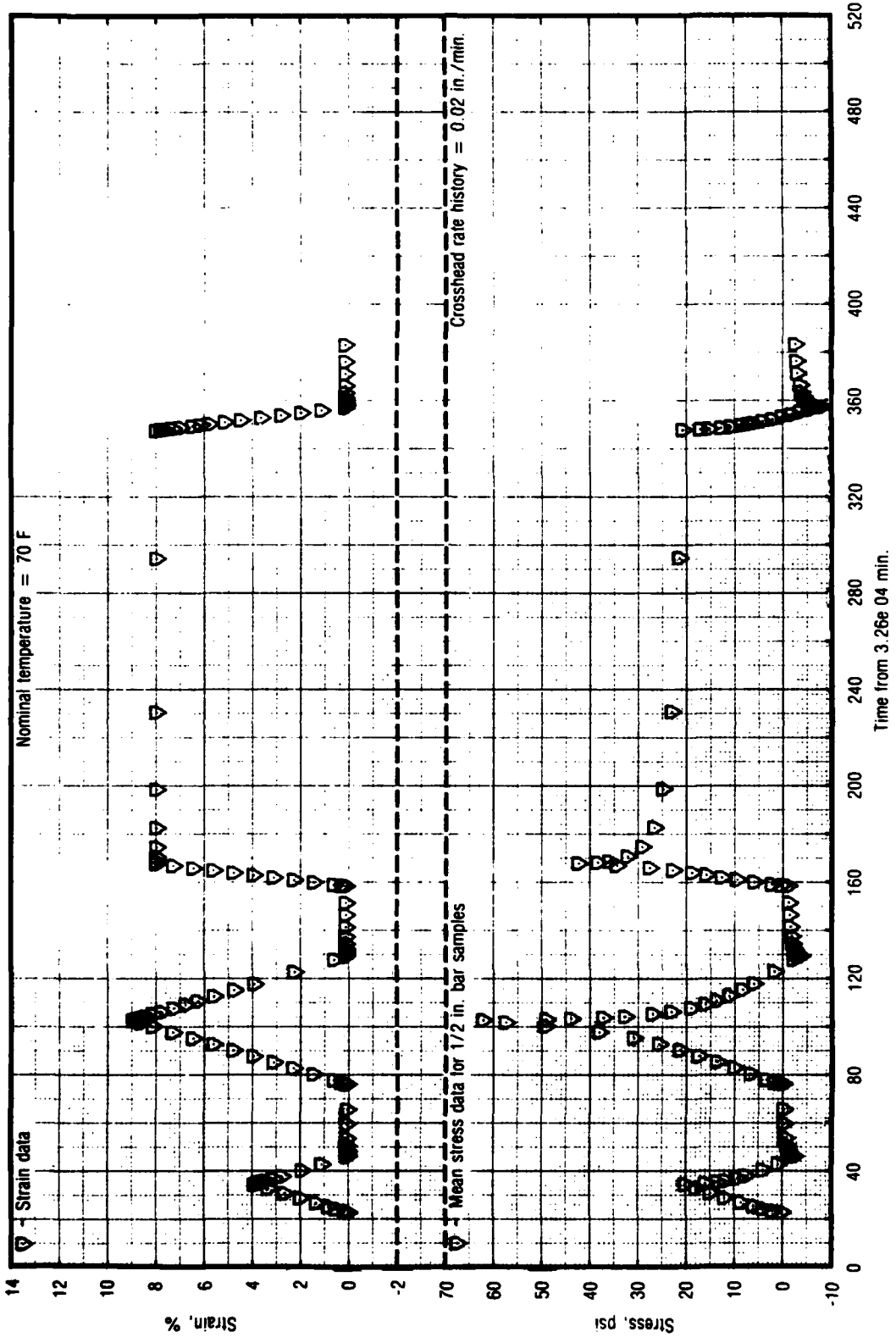


Figure 31. Test No. 11, Part 2 - Stress While Cycling for UTP-3001-750/7768

28760

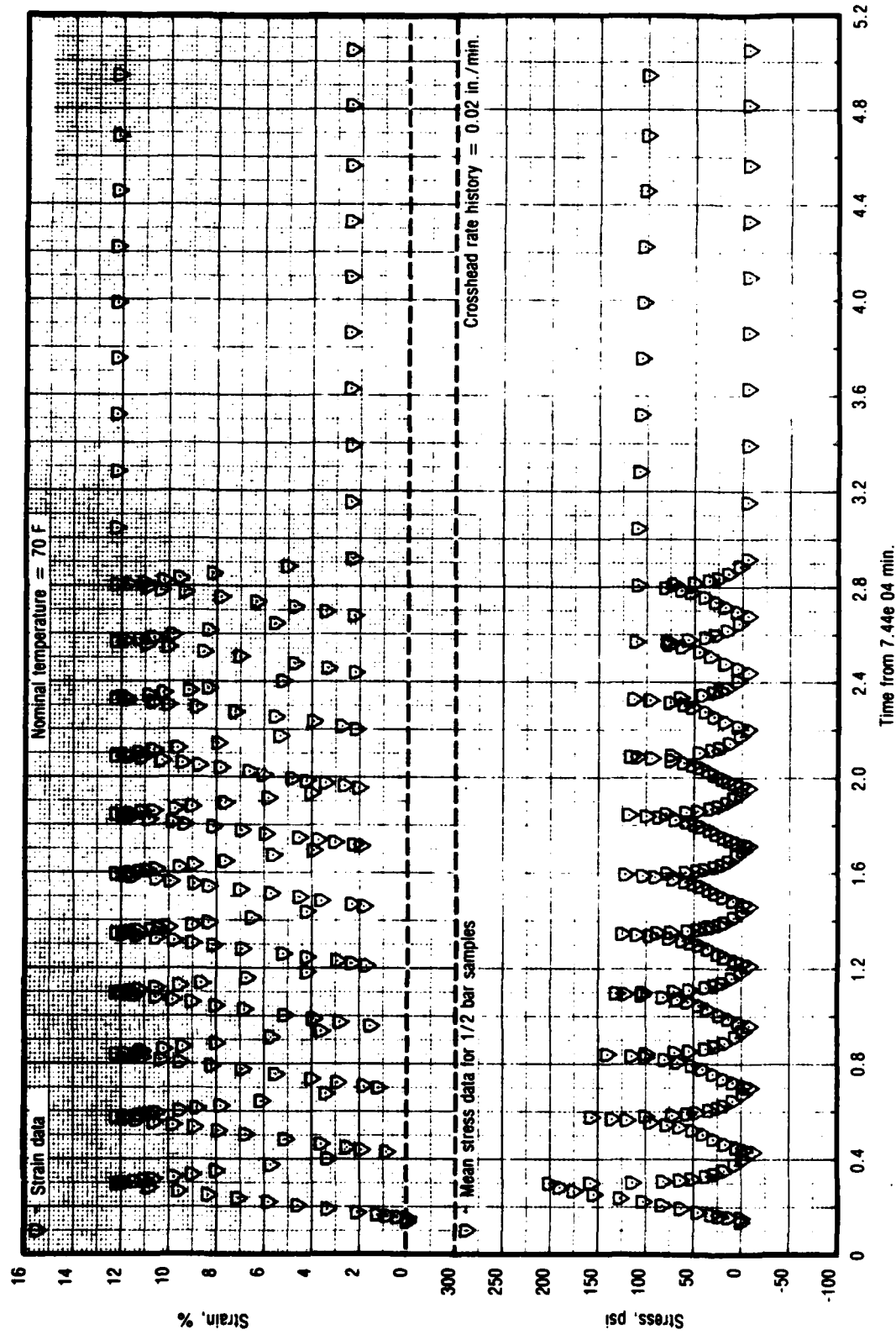


Figure 32. Test No. 11, Part 2 - Stress While Cycling for UTP-3001-750/7768
28761

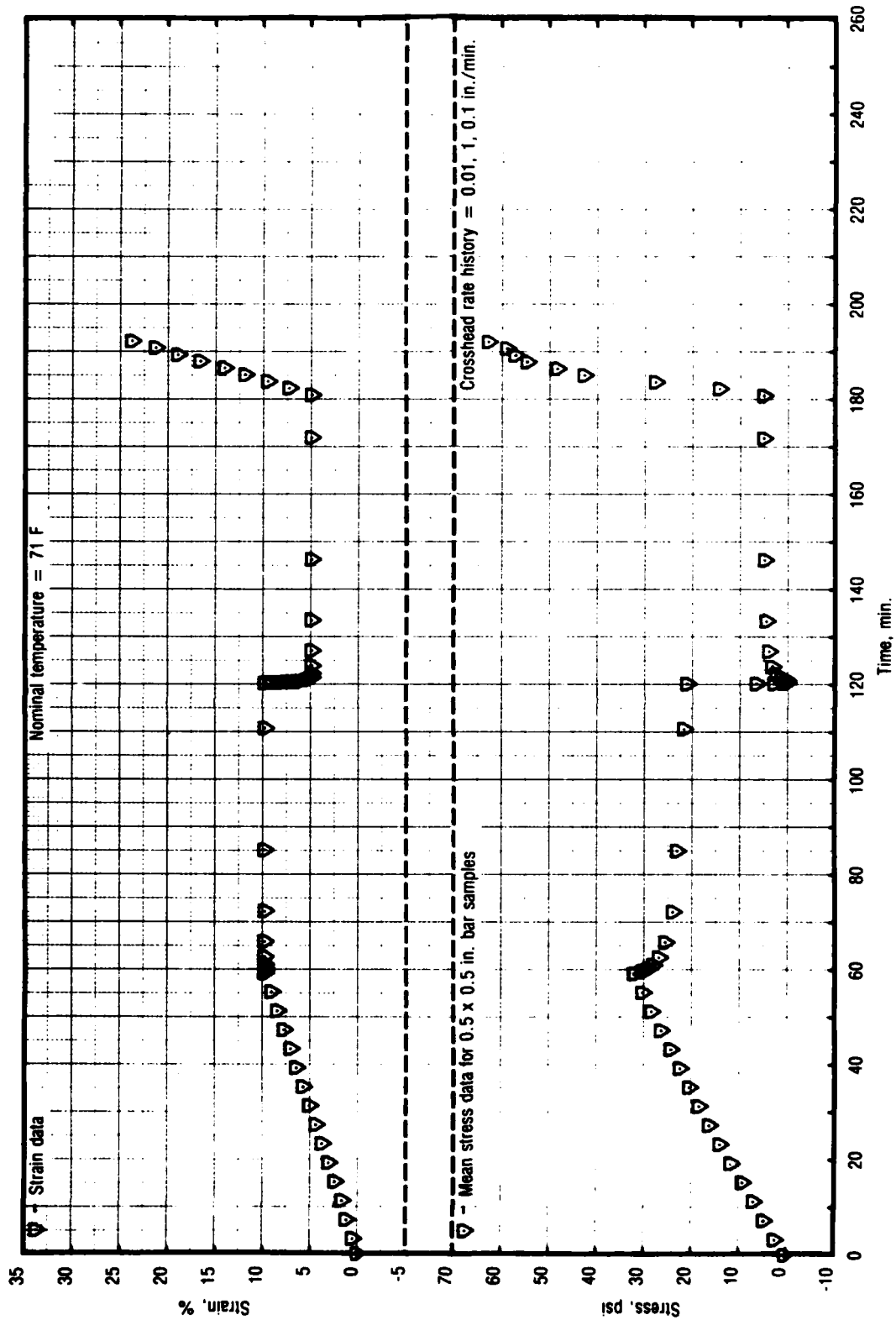


Figure 33. Test No. 12 - Stress While Step Straining for UTP-19,360B-400/1777

28762

TABLE 20. TEST NO. 12 - 1/2-IN. BAR STRESS WHILE STEP STRAINING
(SHEET 1 OF 2)

PROPELLANT: UTP 19360B 400/1777
REQUESTOR: Carlton

DATE: 6/16/81
OPERATOR: JWD

DEFINITIONS:
Time = Time From Start of Test (min)
 σ = Stress (psi)
 ϵ = Strain (%)
T(air) = Test Air Temperature (F)
T(prop) = Test Propellant Temperature (F)

RELATIONSHIPS:
 σ = Force/Area
 ϵ = Sample Extension/Length
NOMINAL VALUES: = 71 F
Gage Length = 6.00 in
Nom. Strain = 10.5% Failure %
XHD Rate = .01, .1, .1 in/min

CALIBRATION DATA:
Cal Wt = 5.0 lbs
Load Cal (lbs/volts)
Offset (volts)
Pot Cal (in/volts) =
Temp (F)

SAMPLE 3
6.120
-0.075

1.856
0.029
-0.386
-71.0

AREAS (sq in):

0.250 0.249 0.249

STRESS DATA (psi):

SET	Time
1	0.0000
2	0.22987
3	0.23012
4	11.233028
5	19.2329925
6	27.233060
7	35.233004
8	43.233019
9	51.233033
10	59.153388
11	59.61435
12	59.81462
13	60.21553
14	61.61616
15	62.81652
16	62.21747
17	85.01775
18	110.61869

T(prop)	T(air)	Strain
73.6	72.6	0.00
73.6	72.6	0.50
73.1	73.1	1.18
73.9	73.8	2.40
75.1	74.0	3.06
72.7	72.4	3.73
74.6	73.0	4.62
75.2	73.9	5.06
73.8	73.3	6.42
72.6	72.1	7.09
73.5	72.0	8.02
73.7	72.0	9.70
72.9	72.4	9.71
73.0	73.1	9.69
72.5	72.7	9.70
73.1	72.9	9.70
73.4	73.0	9.72
74.8	73.1	9.71
73.0	72.5	9.73
73.1	72.4	9.73

SAMPLE	St Dev	Avg	3
1	0.011	0.241	0.23
2	0.178	4.41	2.19
3	0.425	4.71	4.15
4	0.958	6.92	6.89
5	0.239	9.25	7.80
6	1.511	11.61	9.70
7	1.770	13.15	11.35
8	0.010	16.15	16.61
9	0.222	18.31	18.70
10	0.421	22.43	22.78
11	0.575	22.43	22.80
12	0.725	26.30	26.90
13	0.844	28.31	29.03
14	0.939	30.10	32.57
15	0.031	32.10	32.57
16	0.836	32.10	32.57
17	0.778	31.19	27.16
18	0.683	30.90	25.47
19	0.588	28.08	24.80
20	0.472	27.77	24.02
21	0.365	26.53	23.89
22	0.216	25.39	23.10
23	0.160	23.97	20.58
24	0.041	21.53	19.72

TABLE 20. TEST NO. 12 - 1/2-IN. BAR STRESS WHILE STEP STRAINING
(SHEET 2 OF 2)

7	72.9	72.7	9.70	54	92	21.15	20.87	995
2			9.705	50	17.91	5.69	6.26	1.761
3			9.81	42	5.25	2.06	6.45	0.565
4			7.88	1.04	0.00	0.00	0.00	0.000
5			7.29	0.00	0.00	0.00	0.00	0.000
6			6.58	0.00	0.00	0.00	0.00	0.000
7			6.52	0.00	0.00	0.00	0.00	0.000
8			6.14	0.00	0.00	0.00	0.00	0.000
9			5.33	0.00	0.00	0.00	0.00	0.000
10			5.09	0.00	0.00	0.00	0.00	0.000
11		73.19	5.09	0.09	0.71	0.77	0.03	0.255
12		73.66	4.82	1.65	1.23	1.98	1.17	0.390
13		73.60	4.81	3.79	3.57	3.59	3.73	0.421
14		73.23	4.81	4.96	4.40	4.50	4.28	0.441
15		73.6	4.81	5.36	4.47	4.71	4.61	0.429
16		73.3	4.80	5.50	4.4	4.82	4.82	0.445
17		73.10	4.80	5.50	4.4	4.71	4.82	0.445
18		73.00	4.79	5.1	4.13	4.13	4.13	1.375
19		73.3	13.98	10.69	12.39	12.39	12.39	3.542
20		72.9	16.86	12.89	14.9	14.9	14.9	5.539
21		72.8	18.18	16.28	19.10	19.10	19.10	7.161
22		72.8	23.1	20.59	25.49	25.49	25.49	10.0

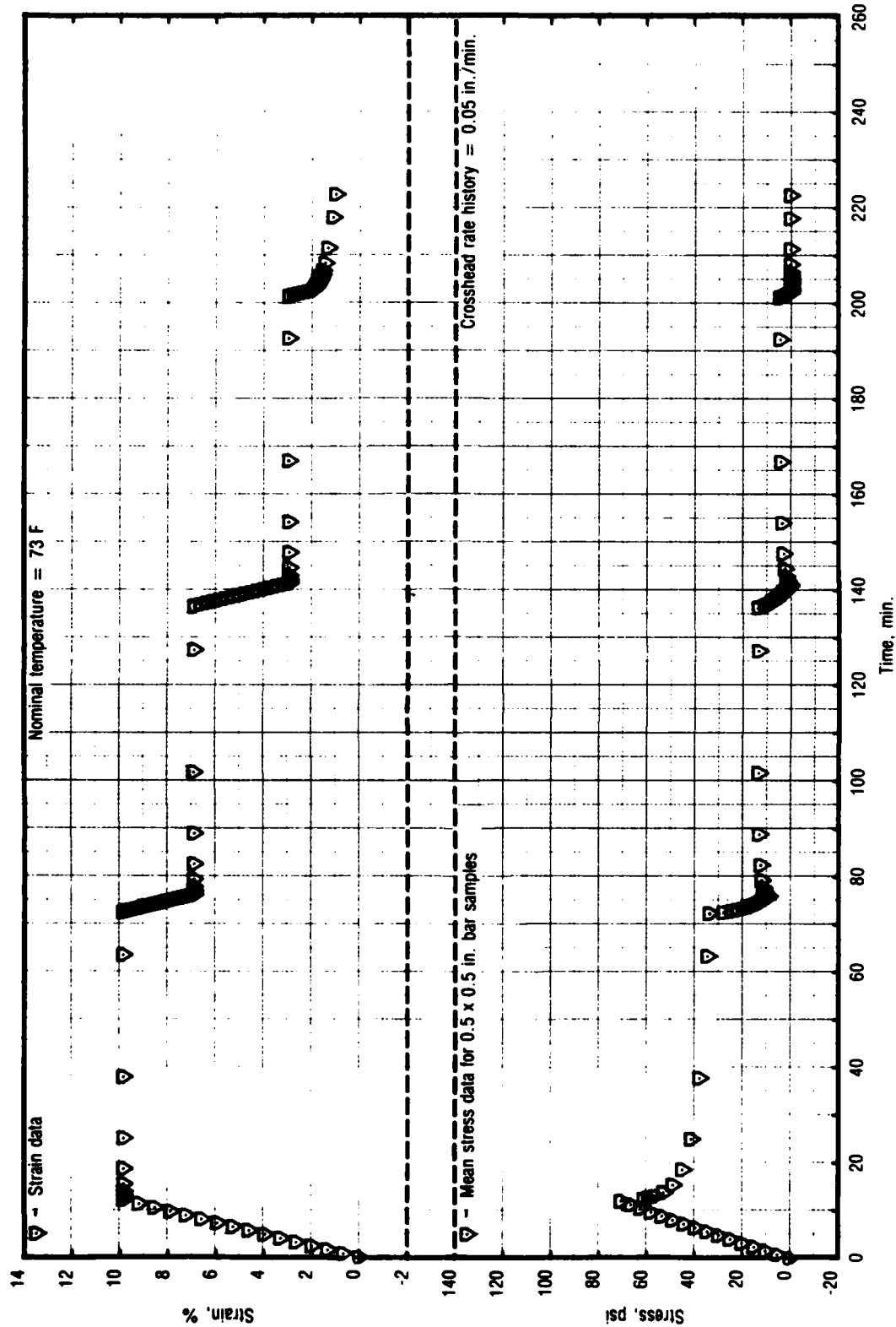


Figure 34. Test No. 13 - Stress While Step Straining for UTP-3001-750/7768

28763

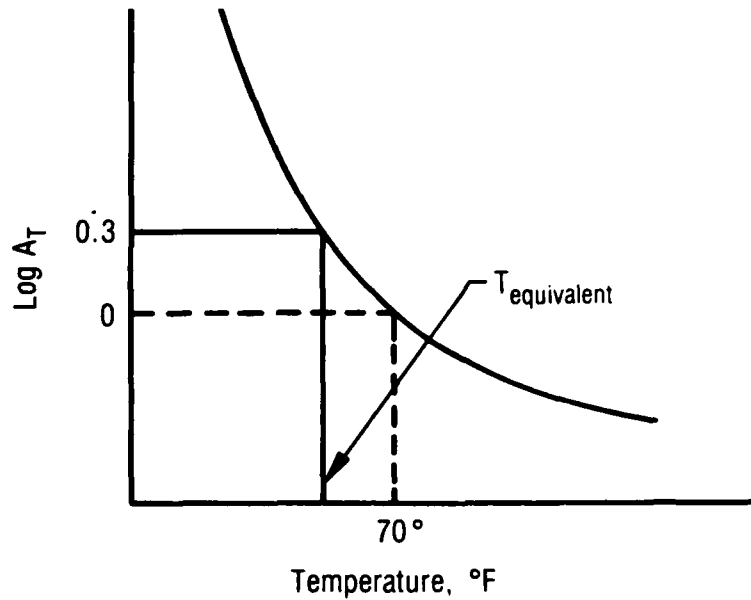
TABLE 21. TEST NO. 13 - 1/2-IN. BAR STRESS WHILE STEP STRAINING
(SHEET 3 OF 3)

85	75.0	75.4	2.14	0.24	0.00	0.28	0.18	0.109
86	75.5	75.5	1.91	0.00	0.00	0.00	0.00	0.000
87	74.8	75.7	1.87	0.00	0.00	0.00	0.00	0.000
88	75.2	75.9	1.83	0.00	0.00	0.00	0.00	0.000
89	75.0	75.2	1.77	0.00	0.00	0.00	0.00	0.000
90	75.5	75.0	1.75	0.00	0.00	0.00	0.00	0.000
91	74.3	75.9	1.70	0.00	0.00	0.00	0.00	0.000
92	75.1	75.9	1.68	0.00	0.00	0.00	0.00	0.000
93	76.1	75.9	1.65	0.00	0.00	0.00	0.00	0.000
94	75.4	75.9	1.61	0.00	0.00	0.00	0.00	0.000
95	75.5	77.4	1.56	0.00	0.00	0.00	0.00	0.000
96	75.2	76.4	1.53	0.00	0.00	0.00	0.00	0.000
97	75.5	76.4	1.43	0.00	0.00	0.00	0.00	0.000
98	75.8	75.2	1.10	0.00	0.00	0.00	0.00	0.000
99	75.5	75.9	0.98	0.100	0.00	0.00	0.00	0.000
100								
101								
102								
103								
104								

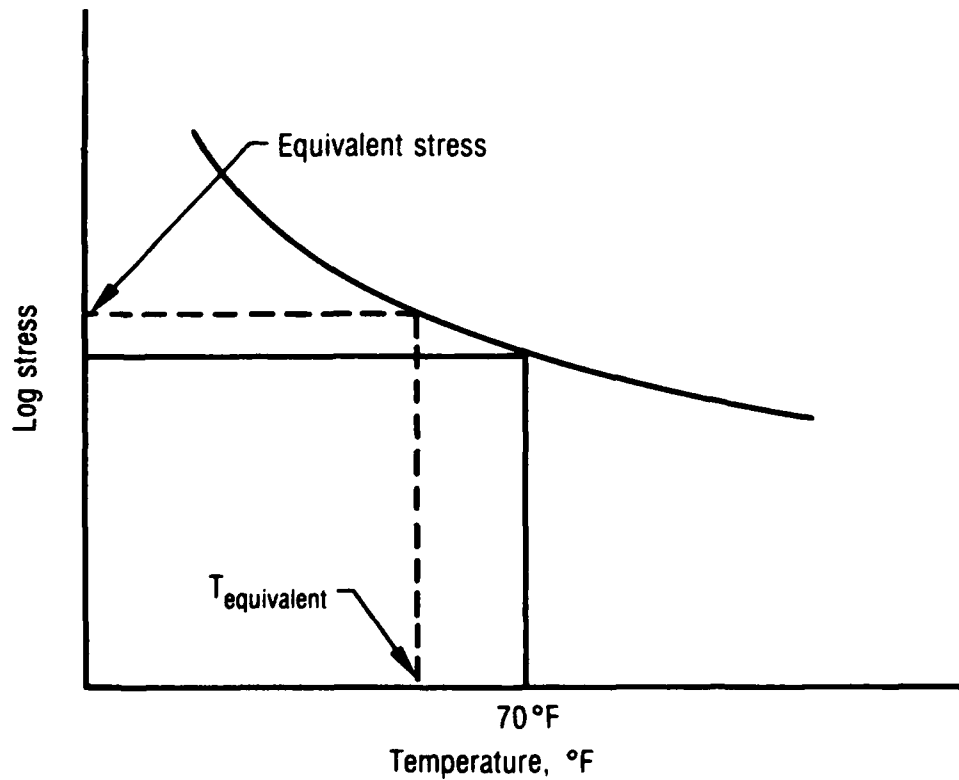
3.1.14 Propellant Aging Effects During Phase II Testing

The numerous and complex tests involved in the uniaxial-isothermal evaluation of the two propellants (UTP-3001 and UTP-19,360B) covered an approximate 3-month time period. Since the 6-in. bar specimens at constant rate (test No. 1) were run first, they were used as the standard to compare the balance of the data.

Stress-strain plots of UTP-3001, test No. 1 are shown in Figures 35, 36, and 37 for 41, 75, and 124°F tests, respectively. Crosshead rates of 10, 1, and 0.1 in./min. are shown for each temperature with the ambient tests down to 0.001 in./min. The same data are shown in Figures 38, 39, and 40 for UTP-19,360B. Comparison of the other tests was based on the initial ramp loading or undamaged state. Test No. 6 was a full, one-half and one-quarter load creep test with crosshead loading rate of 1 in./min. The peak stress-strain points, when the crosshead stopped, were compared to the constant rate plots as shown in Figure 35, etc. All the data are given in Tables 22 and 23 for UTP-3001 and UTP-19,360B, respectively. When crosshead rates did not match, a time-temperature equivalent stress value was selected for comparison purposes. These data were considered approximate. Stress values that were considered reliable (i.e., very close) were marked in the tables with a single approximate sign (~) while those that left some doubt due to the shift were marked with a double approximate (\approx). Some tests were run at 5 in./min. rather than the 10 in./min. comparison data. The 10 in./min. equivalent of the 5 in./min. data can be determined from the rate shift (i.e., $\log A_T = \log 10/5 = 0.30$). The WLF curve (in text figure) is used to pick off the equivalent temperature. The high rate stress value being sought is equivalent to a lower temperature at the lower rate (5 in./min.).



The equivalent temperature is then used to obtain the equivalent stress value from a stress-temperature plot (in text Figure).



The stress-temperature plot can also be used to obtain equivalent stress values when the temperatures do not match at the same rate.

After the initial ramp loading, the propellant was considered damaged. In most instances the tests were of short enough duration to neglect any aging effect during test. Since bulk storage at controlled ambient conditions has not shown a significant aging effect over 3 months, this was also neglected. Rather it was lumped into the between carton difference. The sample handling procedure established was to machine one carton at a time, hold all samples overnight in a nitrogen flushed dry box ($\leq 10\%$ RH) before testing, and then test all samples from the dry box before machining additional specimens. The data in Table 22 for UTP-3001 indicate little difference between boxes 1 and 2 but a one-third higher average stress in box 3. The other significant change was within a box due to the amount of storage time in the dry box. During the 13 days the residual of box 2 was in the dry box, the stress changed from 30% below the mean to 10% above the mean. The UTP-3001 tests from box 3 have been replaced with another carton which was sample tested before doing the program tests. This provided a reasonable assurance that the results would be of the same family as the original constant rate data (test No. 1). The data from UTP-19,360B in Table 23 do not show as much effect for dry box storage or between box differences compared to the UTP-3001 propellant.

Both propellants have indicated that dry box storage will increase the stress capability. This is assumed to be due to loss of moisture and it is reversible as is shown in Figure 41 for UTP-3001. In this example, specimens held in the dry box for 4 months were exposed to 58 and 85% relative humidity for 1 week. All six samples were tested simultaneously in a CSD multistation tester.

The one test which may need some special treatment is the Quinlan complex history No. 11 (see section 3.1.11). After 12 cycles and 2 relaxation periods, the samples were removed for 4 days storage in a dry box. They were then followed by (1) relaxation - 7 days in a dry box, (2) two cycles - a relaxation period - 2 weeks in a dry box, (3) two cycles - a relaxation period - 1 month in a dry box, and (4) cycling to failure. At this point it is not clear just how to separate the stress increase due to rehealing from the dehydration effect of

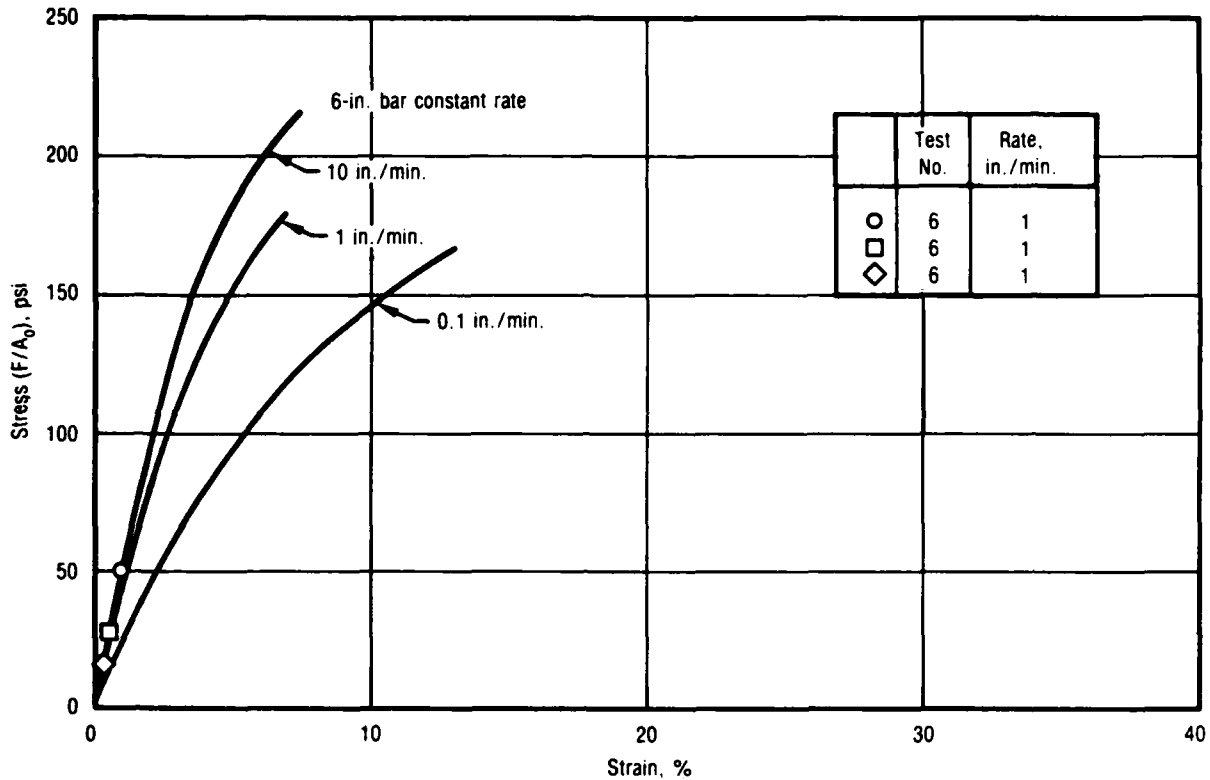


Figure 35. Initial Ramp for UTP-3001-750/7768 39°F Tests Compared to the 6-in. Bar Constant Rate Data

28769

the dry box particularly for the 1 month storage period. The test times at approximately 50% RH were too short to have any significant effect on propellant stress capability. Both propellants showed reasonable correspondence of the initial ramp to the reference constant rate data.

3.2 TWO-DIMENSIONAL AND VARIABLE TEMPERATURE INVESTIGATION

The biaxial and nonisothermal testing was conducted on specimens of UTP-3001 and UTP-19,360B propellants as detailed in Figure 42. The biaxial samples were cast into prelined redwood boxes with a 1.25-in. gage length by 6-in. wide and machined flat to a 0.25-in. thickness. The response properties rather than failure properties were of interest so the discontinuity at the redwood interface did not affect the desired behavior. The 1/2 x 1/2 x 6-in. specimens were used for straining-cooling and cyclic strain tests. Shear relaxation tests

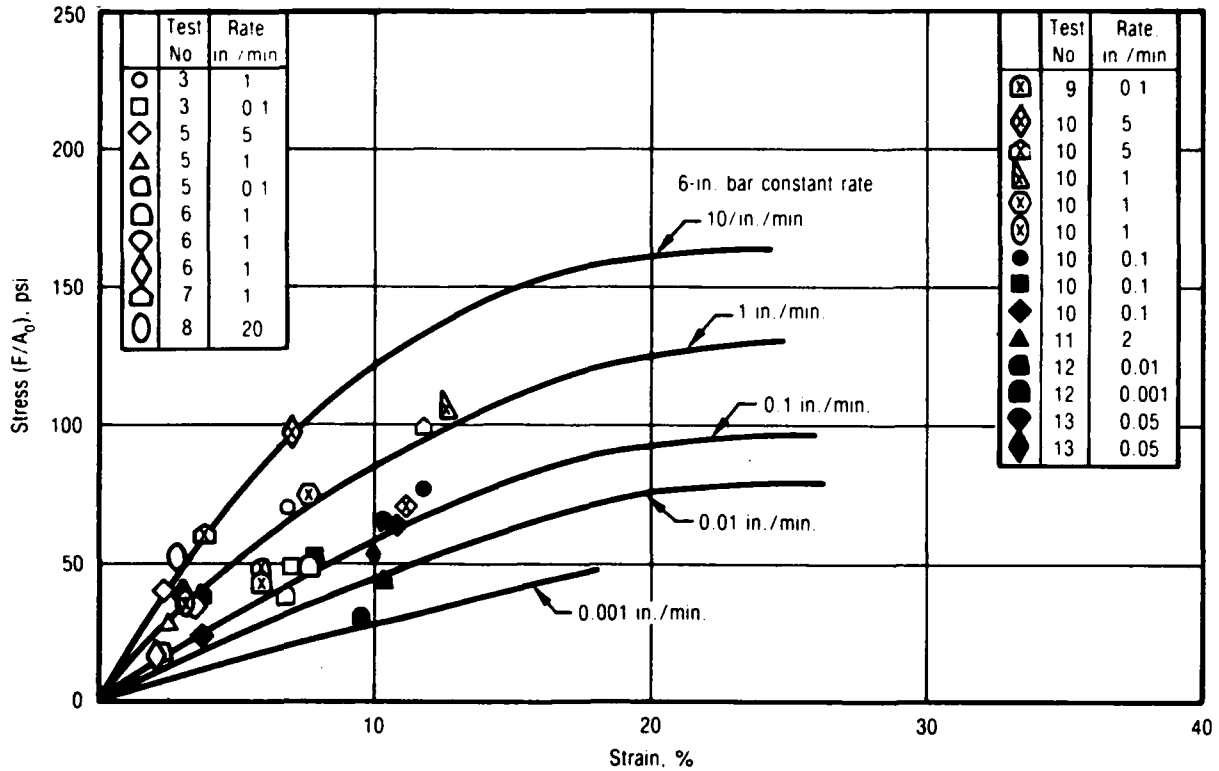


Figure 36. Initial Ramp for UTP-3001-750/7768 75°F Tests Compared to the 6-in. Bar Constant Rate Data

28766

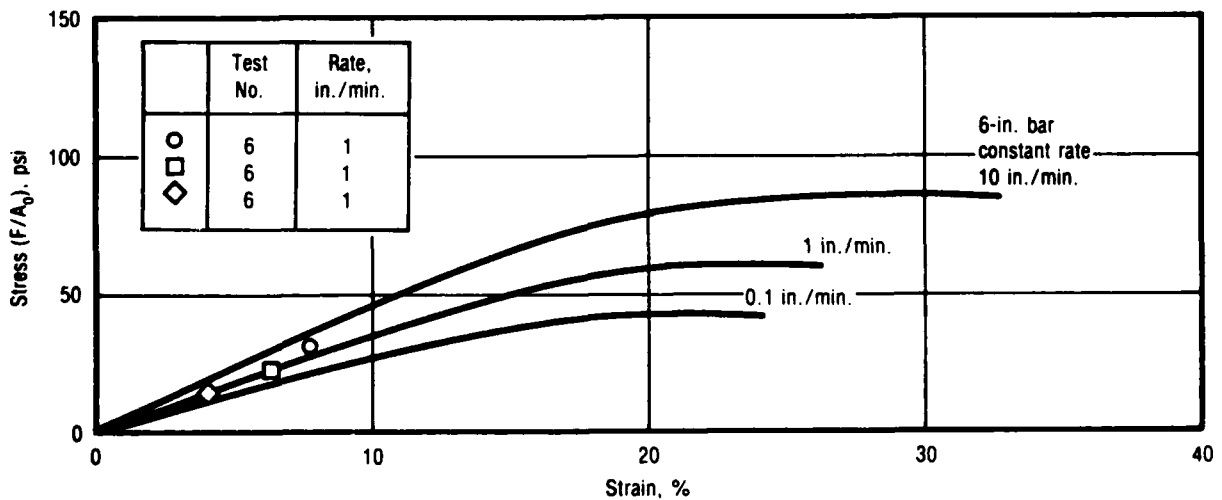


Figure 37. Initial Ramp for UTP-3001-750/7768 124°F Tests Compared to the 6-in. Bar Constant Rate Data

28768

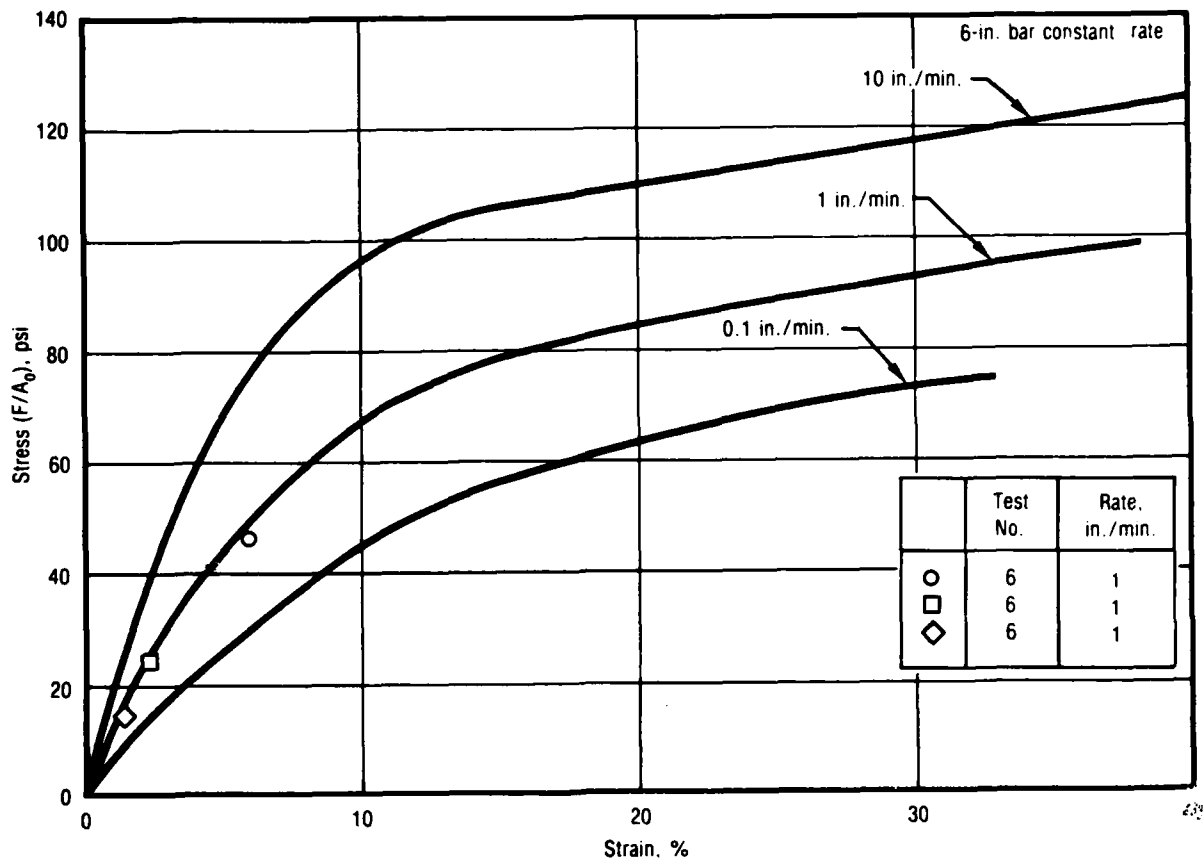


Figure 38. Initial Ramp for UTP-19,360B-40C/1777 40°F Tests Compared to the 6-in. Bar Constant Rate Data

28770

were run with 1 x 1 x 3-in. specimens bonded directly to steel anvils. Details are given in later sections. The equipment discussed in section 3.1 was utilized for this testing; however, only three biaxial specimens could be tested at once because of space limitations in the oven.

The biaxial specimens used in this part of the program were cast into redwood boxes similar to that shown in Figure 5. The space between redwood blocks was 1.25-in. instead of the 6-in. for the uniaxial bars. A mill finished specimen is shown in Figure 43. The propellant was left flat rather than necking it down as with standard JANNAF biaxial specimens. The gage length was designated at the wood to wood distance for strain evaluation. Response properties rather than failure properties were of interest so the boundary

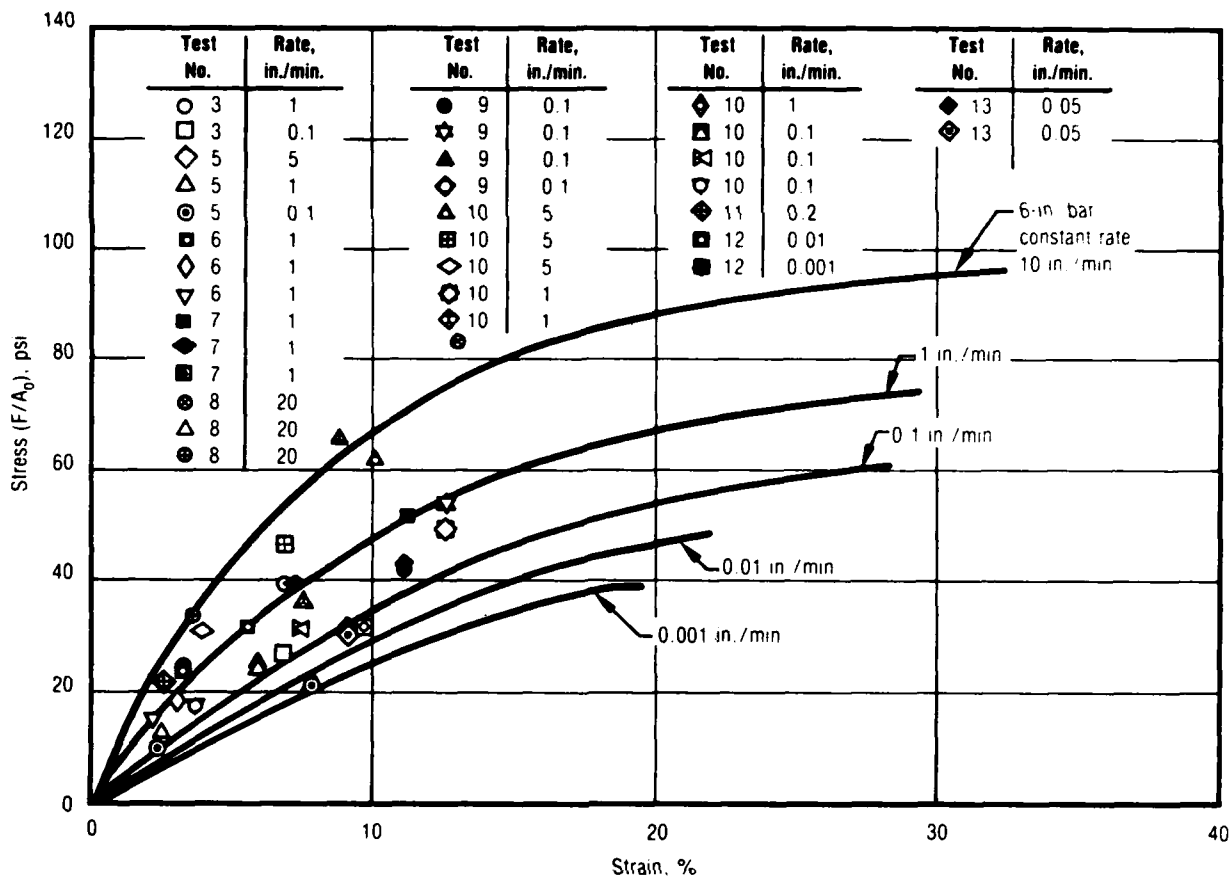


Figure 39. Initial Ramp for UTP-19,360B-400/1777 70°F Tests Compared to the 6-in. Bar Constant Rate Data

28771

perturbation was neglected. Some data taken from the literature⁽²⁾ have been reproduced for evaluation of the stress-strain behavior across the biaxial field (see Figures 44 through 47).

The shear samples (Test No. 17) were 1 x 1 x 3-in. blocks of propellant that were bonded to the test fixture (shown in Figure 48) after being machined. The pull rods were attached to the offset plates so that the load was transmitted through the center of the sample as shown. Since strain was limited to 5% for the shear relaxation test, the sample was assumed to be in simple shear. The shear strain (γ) was calculated as the tangent of

Reference 2 - Jones, J., "Solid Propellant Structural Integrity Investigations: Dynamic Response and Failure Mechanisms in Solid Propellants," RPL-TDR-64-32, Vol. I, Lockheed Propulsion Co., February 1964.

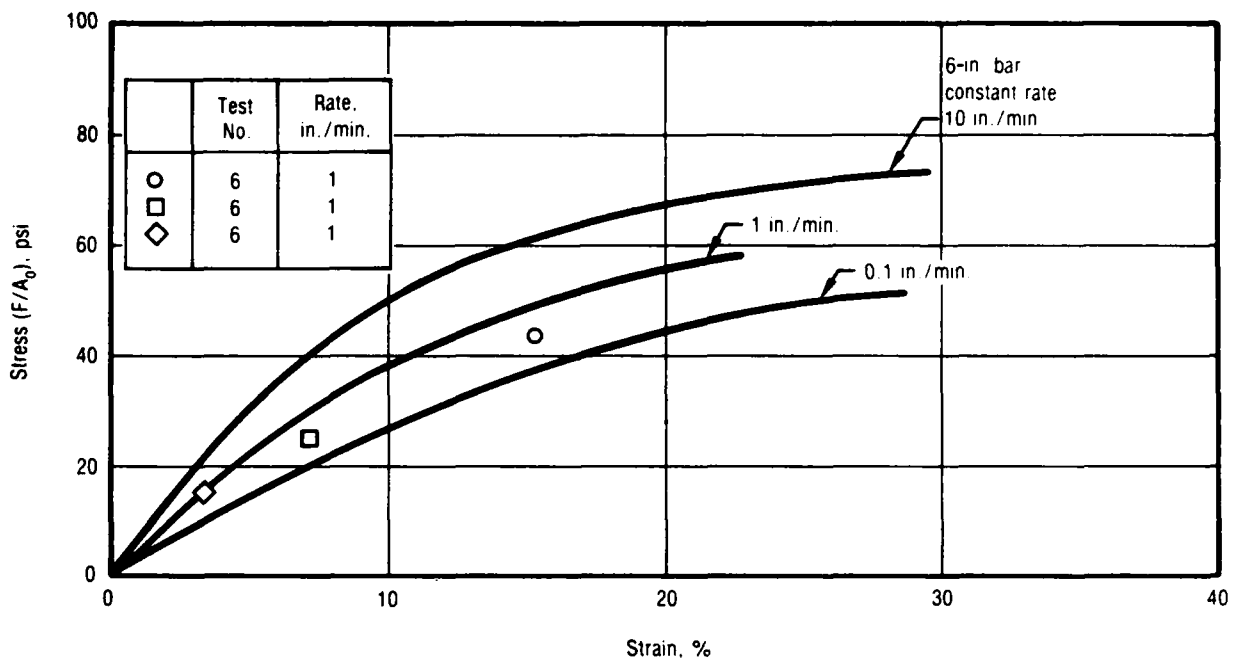


Figure 40. Initial Ramp for UTP-19,360B-400/1777 123°F Tests Compared to the 6-in. Bar Constant Rate Data

28772

the displacement angle or $\Delta L/G.L.$ The shear stress (τ) was calculated as force/area (area = 3 sq. in.).

The data modification to insert peak and minimum stress points previously discussed were utilized for the biaxial and nonisothermal tests.

3.2.1 Biaxial Constant Rate Test No. 14

The biaxial constant rate tests to failure were run with the 1/4 x 1-1/4 x 6-in. specimens of UTP-3001 and UTP-19,360B. The 40, 70, and 120°F tests were run at crosshead rates of 2, 0.2, and 0.2 in./min. The test equipment, with specimens in place, is shown in Figure 49. A typical load-time curve is shown in Figure 50 for UTP-19,360B at 71°F and 2 in./min. crosshead rate. Because of the fixtures and more difficulty in adjusting linkage than with the 6-in. bar specimens, the three samples did not start loading simultaneously. Sample 2 was adjusted to an effective zero and is shown in Figure 51. Tabular data are given in Table 24.

TABLE 22. STRESS-STRAIN COMPARISON FOR UTP-3001 TESTS
(SHEET 1 OF 2)

T8718

Test No.	Temp-erature, F	Rate, in./min.	Strain, %	Stress, psi	Stress, Test No. 1, psi	Differ-ence, %	Box No.	Days After Machin-ing	Remarks
5	Ambient	5	2.40	40.66	~36	13	1	11	Mean +4.2%
	Ambient	1	2.47	27.28	27.5	-1	1	15	
	Ambient	0.1	2.36	16.70	16.5	1	1	15	
6	Ambient	1	5.94	47.8	57	-16	2	1	Box 2
	Ambient	1	3.54	33.62	37	-9	2	2	Box 2
	Ambient	1	1.55	17.17	18	-5	2	5	Mean +1.1%
	120	1	6.29	22.40	22.5	-0.4	2	6	over box 1
	120	1	4.02	15.3	15	2	2	6	
	120	1	7.71	30.1	27	11	2	7	
	40	1	1.00	50.0	50	0	2	7	
	40	1	0.48	25.8	24	8	2	8	
	40	1	0.35	15.2	15	1	2	8	
10	Ambient	5	6.94	96.1	~87	10	2	9	
		5	3.78	59.8	~55	9	2	9	
		1	12.55	106	98	8	2	9	
		1	7.53	76.3	68.5	11	2	9	
		1	3.29	36.7	35	5	2	12	
		0.1	11.78	76.7	66.5	15	2	12	
		0.1	7.83	52.0	47	11	2	12	
		0.1	3.72	23.6	24	-2	2	12	
	Ambient								
3	Ambient	1	6.91	69.74	64	9	3	1	
	Ambient	0.1	6.93	47.73	42.5	12	3	1	
8	Ambient	20	3.05	56.7	~58	-22	4	2	

TABLE 22. STRESS-STRAIN COMPARISON FOR UTP-3001 TESTS
(SHEET 2 OF 2)

T8718

Test No.	Temp- erature, R	Rate in./min.	Strain %	Stress, psi	Stress, psi Test No. 1	Differ- ence, %	Box No.	Days After Machin- ing	Remarks
9	Ambient	0.1	6.63	41.8	41	1.9	4	2	
7	Ambient	1	12.08	98.9	96	3	4	2	
13	Ambient	.05	10.81	64.3	~56	14.7	4	4	
	Ambient	.05	10.08	56.2	~53	5.9	4	4	
12	Ambient	0.01	10.40	40.5	46	-12	4	3	
	Ambient	0.001	9.82	29.9	27	10.7	4	3	
11	Ambient	2	3.08	41.8	~36	-14	1	3	

Notes: 1. Box 1 used up 16 days after machining; test 5 mean = 4.2% over constant rates tests.
2. Box 2 used up in 13 days after machining; box 2 mean = 1.1% over box 1 constant rate but it changed from -30 to +10% during the 13 days.

TABLE 23. STRESS-STRAIN FOR UTP-19, 360B TESTS
(SHEET 1 OF 2)

T8719

Test No.	Temp- erature, F	Rate, in./min.	Strain, %	Stress, psi	Stress, psi Test No. 1	Differ- ence, %	Box No.	Days After Machin- ing	Remarks
5	Ambient	5	2.49	21.8	~24	-9	1	11	Mean
	Ambient	1	2.47	12.89	17.5	-26	1	15	-8.0% below
	Ambient	0.1	2.36	10.54	9.5	11	1	15	test 1
6	Ambient	1	5.50	32.0	31.5	2	2	1	Box 2
	Ambient	1	3.08	18.05	20.5	-12	↓	2	mean
	Ambient	1	2.24	14.76	16	-8	↓	5	-2.7%
	120	1	15.29	43.57	49	-11	↓	6	below box 1
	120	1	7.10	25.0	29.6	-16	↓	6	
	40	1	3.48	14.35	15.5	-7	↓	7	
	40	1	5.95	46.13	50	-8	↓	7	
10	Ambient	1	2.22	24.26	24.5	-1	↓	8	
	Ambient	1	1.35	14.0	16	-12	2	8	
	Ambient	5	6.94	46.5	~50	-7	2	9	
	Ambient	5	3.78	30.8	~33	-7	↓	9	
3	Ambient	1	12.55	49.7	54.5	-9	↓	9	
	Ambient	1	7.53	36.7	39	-6	↓	9	
	Ambient	1	3.29	24.1	21.6	12	↓	12	
	Ambient	0.1	11.06	41.8	38	10	↓	12	
	Ambient	0.1	7.38	31.2	27	16	↓	12	
	Ambient	0.1	3.72	17.2	15	15	↓	12	
	Ambient	5	10.11	62.0	~62	0	2	12	
	Ambient	1	7.00	39.57	37.5	6	3	1	Box 3
	Ambient	0.1	6.89	27.2	25.5	7	3	1	mean
	Ambient	↓	↓	↓	↓	↓	↓	↓	+7.6% above box 1
8	Ambient	20	13.04	85.1	~85	0	3	1	
	Ambient	20	8.46	66.7	~68	-2	3	2	
	Ambient	20	3.61	32.9	~40	-18	3	3	

TABLE 23. STRESS-STRAIN FOR UTP-19, 360B TESTS
(SHEET 2 OF 2)

T8719

Test No.	Temp- erature, F	Rate, in./min.	Strain, %	Stress, psi	Stress, psi Test No. 1	Differ- ence, %	Box No.	Days After Machin- ing	Remarks
9	Ambient	0.1	11.07	41.4	37.7	10	3	10	
		0.1	12.53	43.3	41.2	5		13	
		0.1	5.95	24.8	22	13		14	
	Ambient	0.1	5.95	24.2	22	10	3	14	
7	Ambient	1	11.28	51.8	51.5	0	3	15	
	Ambient	1	7.09	38.5	37.5	3	3	15	
	Ambient	1	3.27	23.6	21.5	10	3	16	
13	Ambient	0.05	9.21	32.1	~31	4	3	16	
	Ambient	0.05	9.16	30.9	~30.5	1	3	20	
12	Ambient	0.01	9.68	31.8	28.5	12	3	26	
	Ambient	0.001	7.86	21.9	20	10	3	41	
11	Ambient	2	3.03	23.2	~21	10	1	3	

Note: All of these data appear to be the same family with a few exceptions. While the percentages are high the absolute differences are not that great. There is an indication of drift from low to high during testing with box 2.

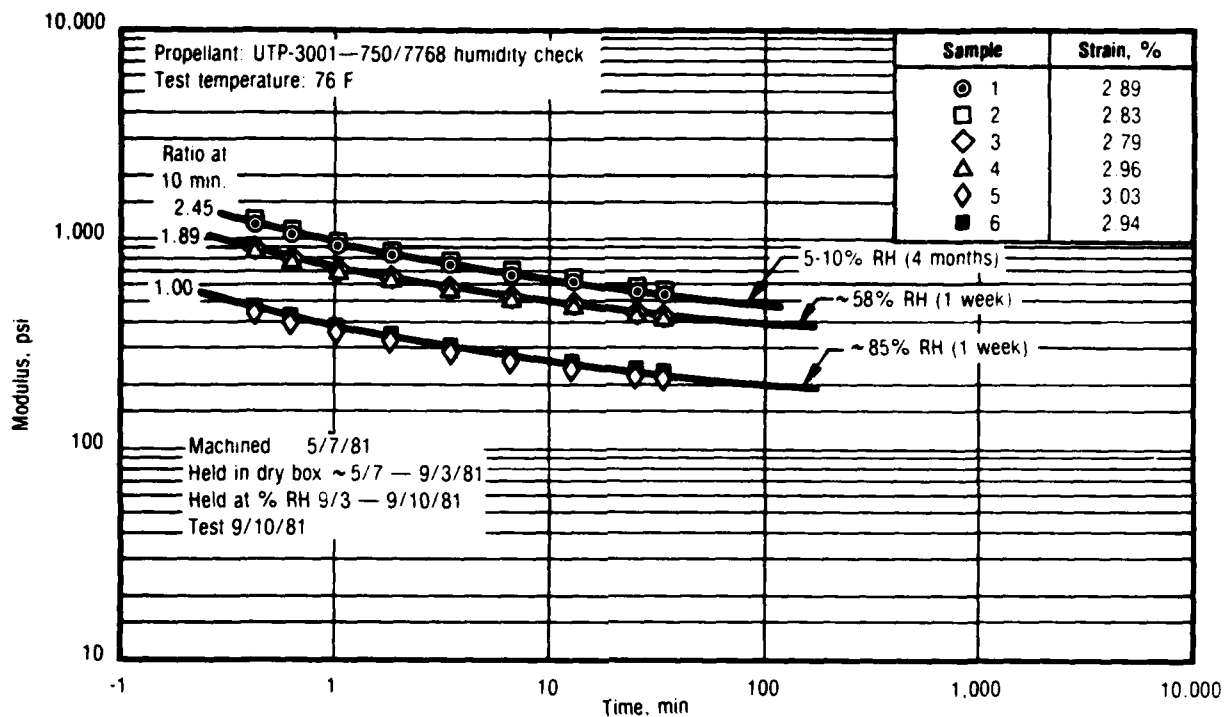


Figure 41. 1/2-in. Bar Stress Relaxation Data at 3% Nominal Strain

28773

3.2.2 Biaxial Straining-Cooling Test No. 15

Biaxial specimens of UTP-3001 and UTP-19,360B propellants were simultaneously strained and cooled from 115 to 40°F at a crosshead rate of approximately 3×10^{-5} in./min. over a 40-hr period. The results for UTP-3001 are shown in Figure 52. The stress-time traces for all three samples appear to start together but spread out as the test progresses. The tabular data are given in Table 25.

3.2.3 Biaxial Stress Relaxation Test No. 16

Biaxial stress relaxation tests were run with the 1/4 x 1-1/4 x 6-in. specimens of UTP-3001 and UTP-19,360B propellants at a nominal 3% strain and temperatures of 40, 70, and 120 F. The 40°F data for UTP-19,360B are shown in Figure 53 as typical with good reproducibility. The loading ramp rate was 0.2 in./min. Data are given in Table 26.

Test	Test Description	Damage Cycle/Test	Strain Cycle
14	Biaxial constant rate	Biaxial samples of UTP-3001 and UTP-19.360B were ramp loaded to failure at rates of 2, 0.2, and 0.02 in./min. at temperatures of 41, 70, and 120°F.	
15	Biaxial straining-cooling	Biaxial samples of UTP-3001 and UTP-19.360B were simultaneously strain and cooled from 120 to 40°F over a 40 hr. period.	
16	Biaxial relaxation	Biaxial samples of UTP-3001 and UTP-19.360B were run in stress relaxation tests at 40, 70, and 120°F.	
17	Shear relaxation	Shear samples of UTP-3001 and UTP-19.360B were run in stress relaxation tests at 70°F.	See above
18	6-in. bar straining-cooling	6-in. bars of UTP-3001 and UTP-19.360B were simultaneously strain and cooled from 120 to 40°F at three slow rates.	
19	Biaxial Quinlan complex history	Biaxial samples of UTP-3001 and UTP-19.360B were cycled for the Quinlan complex history test at 70°F.	
20	6-in. bar cyclic test	6-in. bars of UTP-3001 and UTP-19.360B were run in cyclic strain tests at 0.1 in./min. and 70°F.	
21	Biaxial thermal similitude	Biaxial samples of UTP-3001 and UTP-19.360B were run in ramp-relaxation-ramp tests with simultaneous cooling or heating (i.e., for reverse ramp)	See above plus last half thermal cycled
Note: Nominally three samples were run for each test and condition.			Legend: T = temperature t = time epsilon = strain

Figure 42. Biaxial and Nonisothermal Phase III Testing

28774

3.2.4 Shear Relaxation Test No. 17

Shear relaxation tests were run on 1 x 1 x 3-in. samples of UTP-3001 and UTP-19,360B propellants. The samples were post bonded to steel plates and run one at a time by loading them at 0.2 in./min and ambient temperature with offset fixtures so the load was transmitted through the center line of the sample. The 3 samples for each propellant were hand reduced and digitized for computer storage and printout. A typical example is shown for UTP-3001 in Figure 54 with data given in Table 27. Peak stresses and strain were very close as was the 1 hour relaxation stress on each propellant even though the samples were run separately.

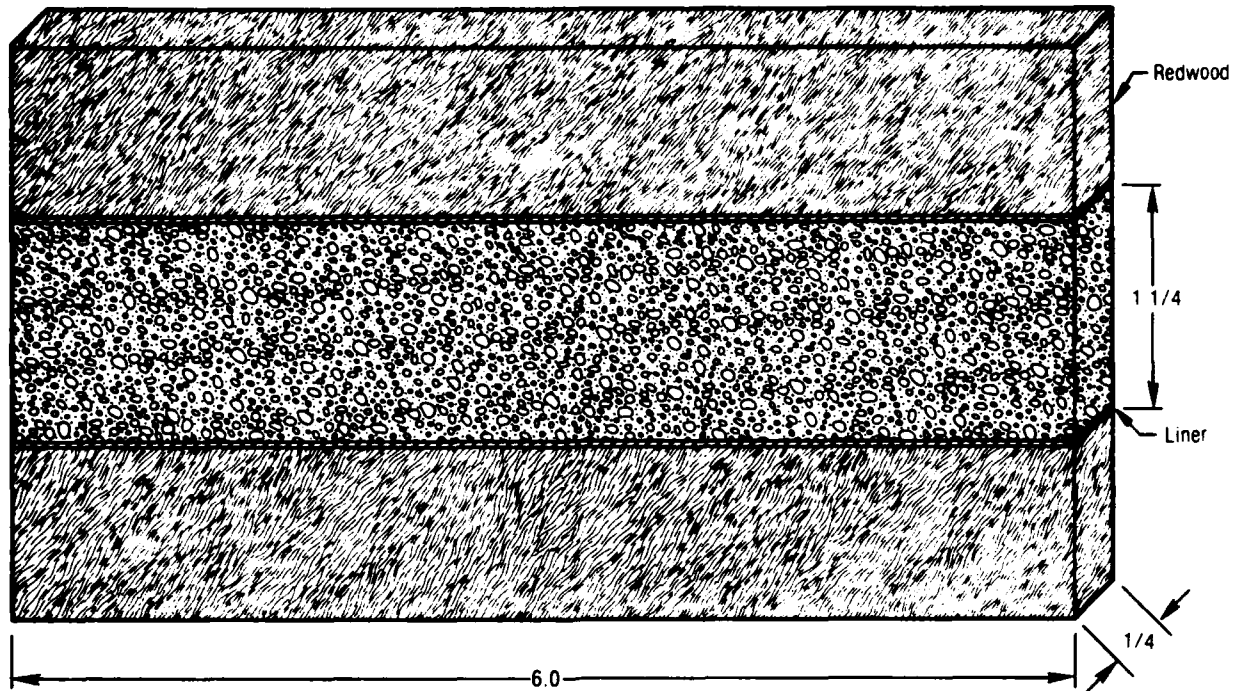


Figure 43. Finished Biaxial Specimen

28806

3.2.5 Straining-Cooling Multiple Rates Test No. 18

The rate effect on the straining-cooling response was determined on UTP-3001 and UTP-19,360B propellants. The 1/2 x 1/2 x 6-in. bar sample was used so that testing could be completed in the shortest time possible. The rate effect for the uniaxial specimens was then applied to the biaxial test No. 15. Cooling was from 110°F to 40°F at the crosshead rates of 0.002, 0.0002, and 0.0004 in./min. Typical data are shown for the 0.002 in./min. rate for UTP-3001 in Figure 55. Good reproducibility is shown within the set of 3 samples. Data are given in Table 28.

3.2.6 Biaxial Quinlan Complex History Test No. 19

The 1/4 x 1-1/4 x 6-in. biaxial samples of UTP-3001 and UTP-19,360B were subjected to the complex cycling and relaxation history indicated in Figure 42. When the tests were run the linkage, misalignment, etc. was such that the samples were not loaded an equivalent amount. The first sample to be loaded had the correct strain determined but strain on the other samples had to be adjusted to the time the stress ramp started on each. Each sample was reduced separately

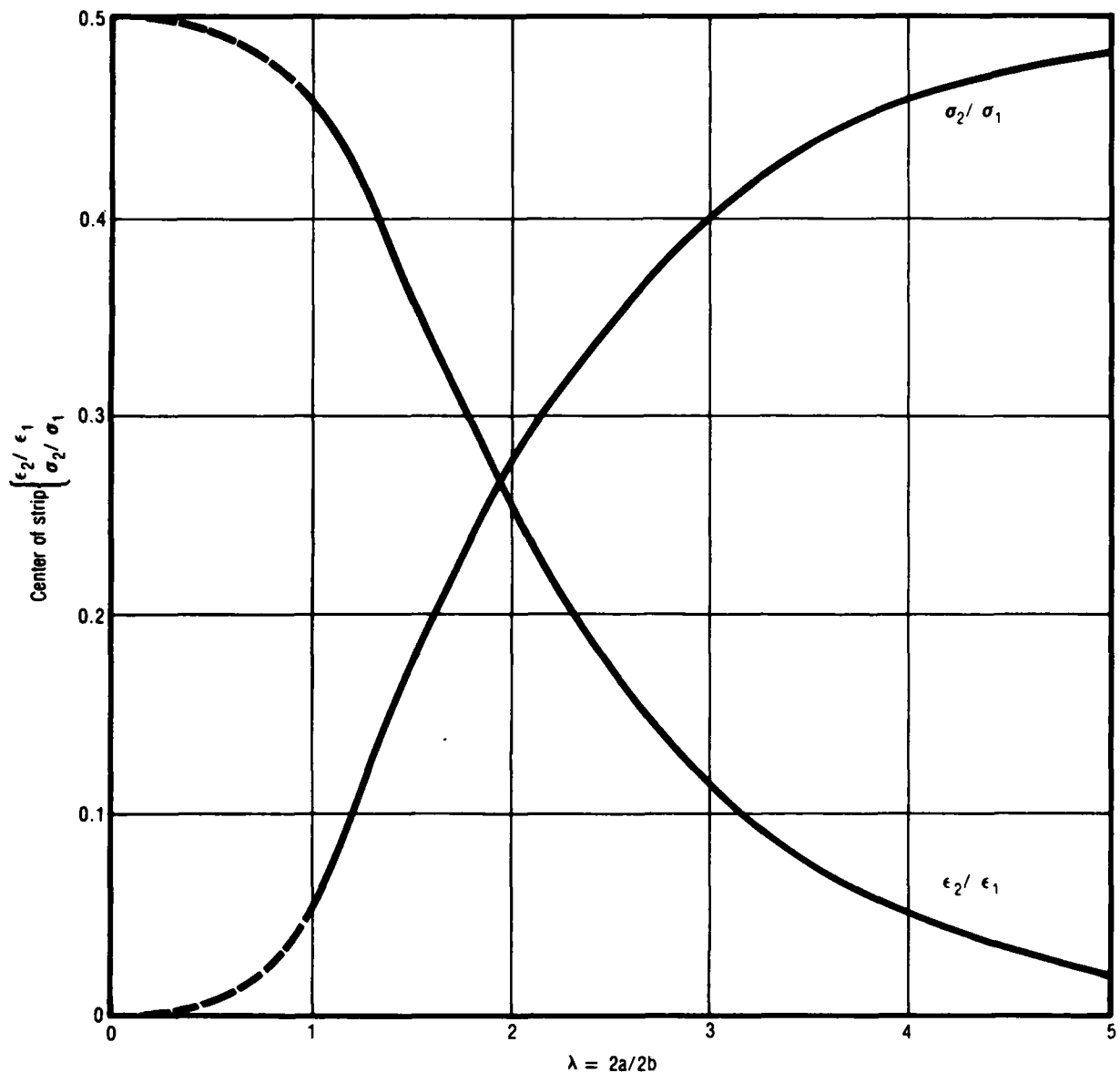


Figure 44. Principal Stress and Strain Ratios at the Center of Biaxial Strips for Varying Height-to-Width Ratios for a Poisson's Ratio of 1/2 28807

and data were modified to pick up the peak and minimum stress points. Sample 1 for UTP-3001 is shown in Figures 56 through 58 where the complex test has been divided into segments on an expanded time scale to show test details. The first cycle in Figure 56 showed no load and the second cycle showed very little. By contrast sample 3 (not included here) had a first peak stress-strain of 37 psi, 2.26% and second peak of 76 psi, 4.97%. During the unload part of the cycle

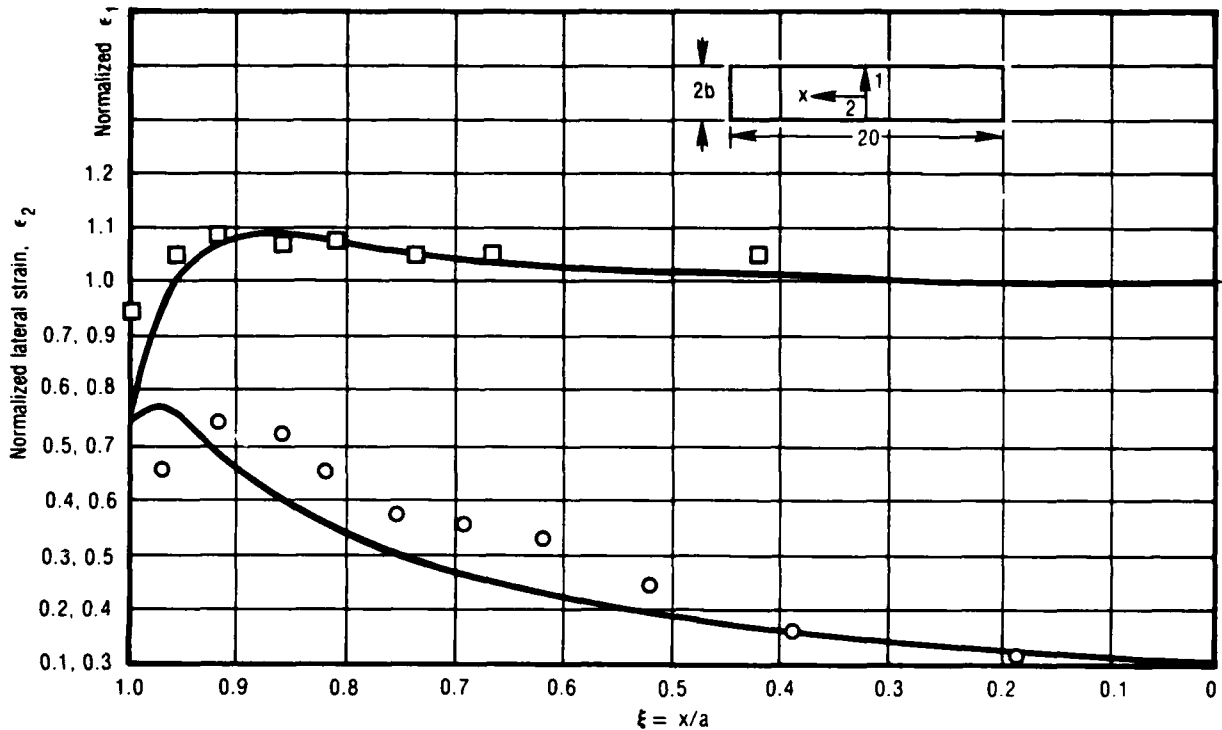


Figure 45. Normalized Axial and Lateral Strains Along the Midplane Biaxial Strip Specimen

28808

after stress reached zero, strain decay was estimated from other tests where strain was measured by cathetometer. Data are given in Table 29.

3.2.7 Cyclic Testing Test No. 20

The complex cyclic testing of UTP-3001 and UTP-19360B propellants was done with the 1/2 x 1/2 x 6-in. bar samples. These tests were run at 70% with cycling from 8 to 4% then 12 to 8% followed by 8 to 4% strain at a crosshead rate of 0.1 in./min. The strain levels were set so that the sample would not reach zero stress on the unload cycles. By doing that a correct evaluation of strain was obtained during the tests. Data for the UTP-19,360B propellant are shown as typical in Figure 59 with digitized results given in Table 30. This propellant broke without completing the nominal 30 cycles but UTP-3001 went all the way through the test. The nominal 10 cycles per segment was dependent upon when the time scale matched available personnel. It was 11 cycles for the first 2 segments for UTP-19360B as shown in Figure 59.

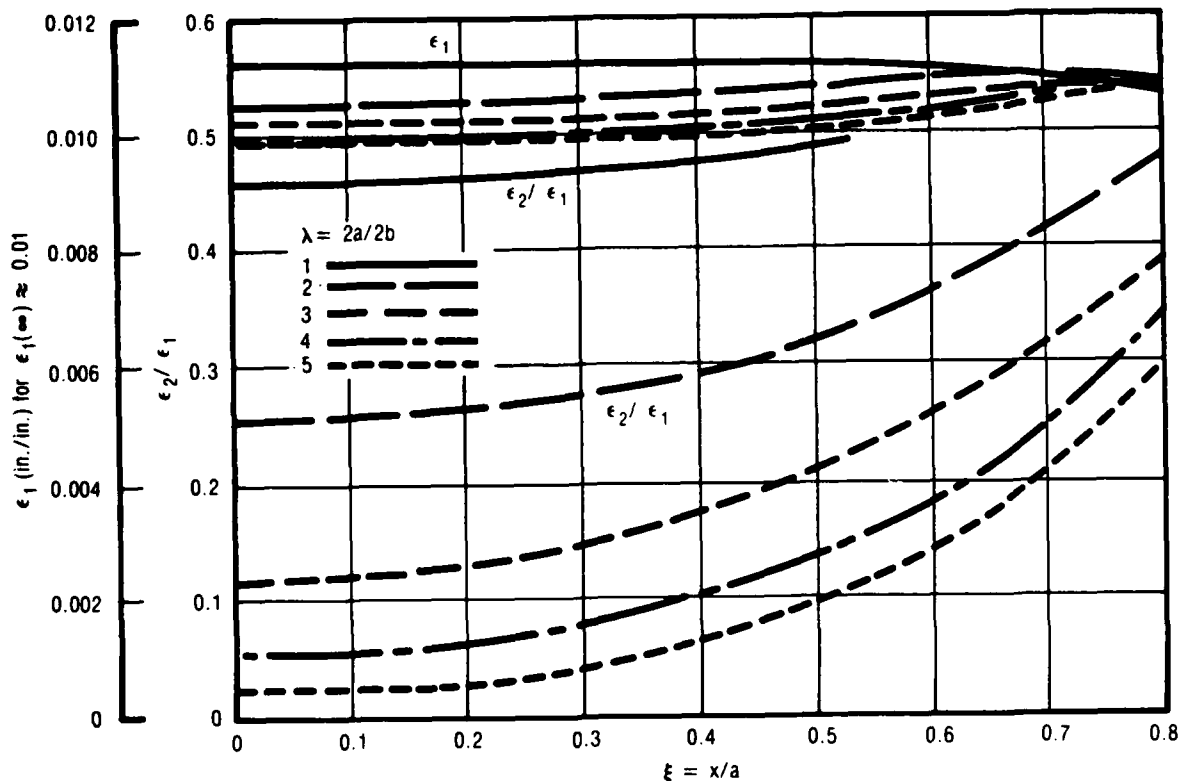


Figure 46. Strain Variations Along Midline of Strip Specimen
($N = 0$) for Poisson's Ratio of $1/2$

28809

3.2.8 Biaxial Ramp-Relax-Ramp Test No. 21

The ramp-relax-ramp tests were run on UTP-3001 and UTP-19,360B propellants with the $1/4 \times 1-1/4 \times 6$ -in. biaxial specimens. The first test was ramped at 0.0005 in./min. to 6% strain and simultaneously cooled from 120 to 70°F. It was held at 6% strain nearly 23 hours then ramp to failure while cooling towards 40°F. The data for UTP-3001 are shown in Figure 60 with data points given in Table 31 as shown in Figure 60. The cooling cycle did not end at the peak strain consequently the relaxation of stress was not the normal type behavior. The continued cooling increased the propellant stress capability so that the normal relaxation behavior did not start until the propellant temperature stabilized.

This test was repeated starting at 110°F and taken to 6% strain with a peak stress of 70 psi compared to 30 psi for the above test. The longer ramp time

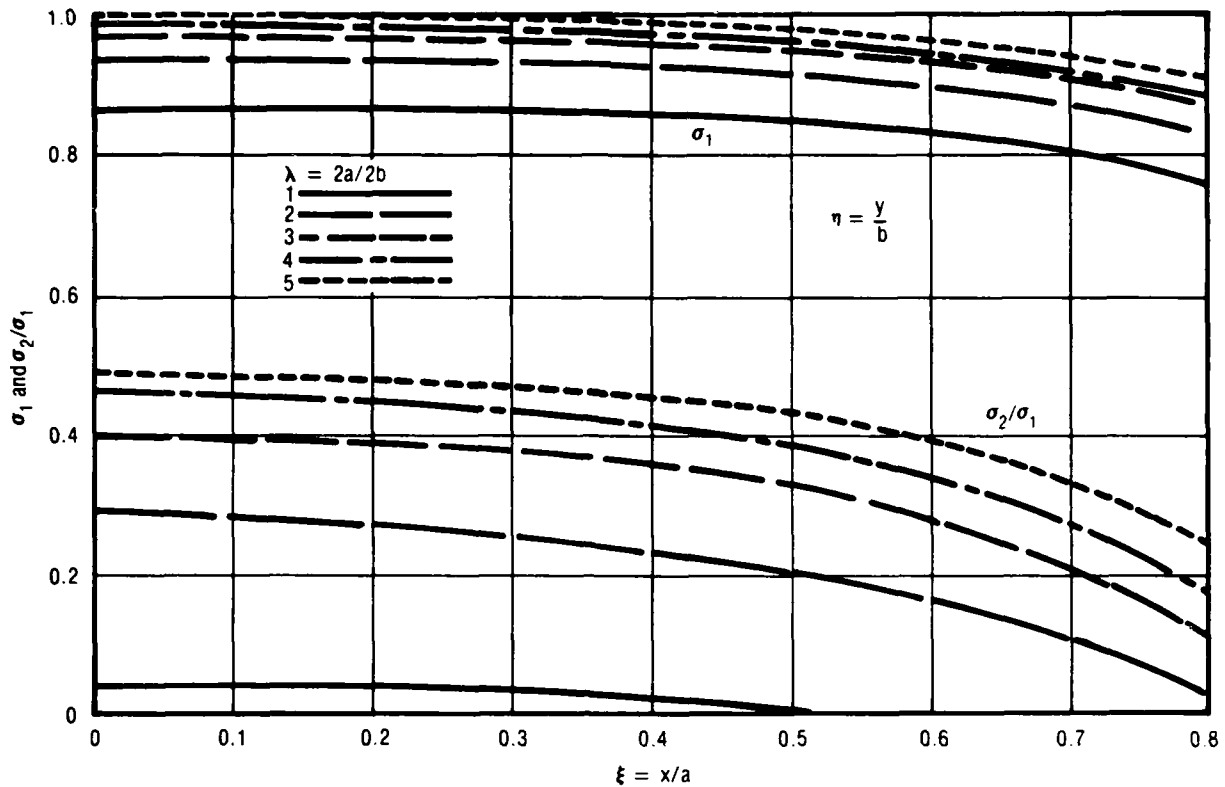


Figure 47. Stress Variations Along Midline of Strip Specimen
($N = 0$) for Poisson's Ratio of 1/2

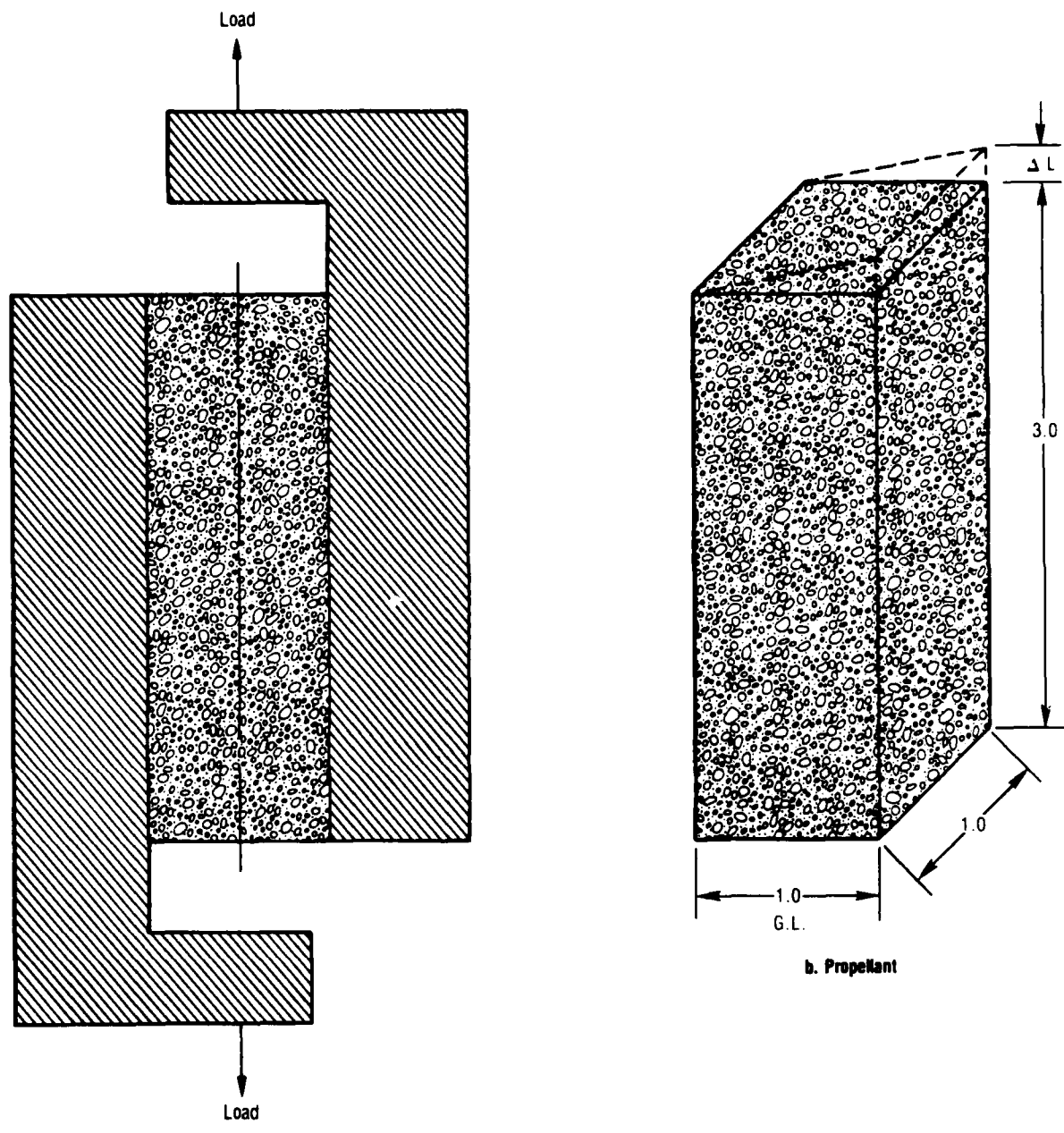
28810

allowed the cooling to reach 40°F at the peak stress. The samples were allowed to relax overnight and then unloaded to 3% while warming the samples to room temperature. Figure 60 was considered to be sufficient to represent the test.

3.2.9 Propellant Aging Effects During Phase III Testing

The biaxial testing in Phase III was scheduled to minimize the dry box storage time after sample machining. The purpose was to reduce the within carton or box variability encountered during the uniaxial testing in Phase II. The majority of the testing was accomplished within 1 week of machining the samples. Those that went over a week did not seem to be influenced excessively.

The data obtained for initial ramp loadings (i.e., undamaged behavior) on the tests run are given in Table 32 for UTP-3001 and Table 33 for UTP-19,360B. The biaxial constant rate data for UTP-3001 are plotted in Figure 61. These

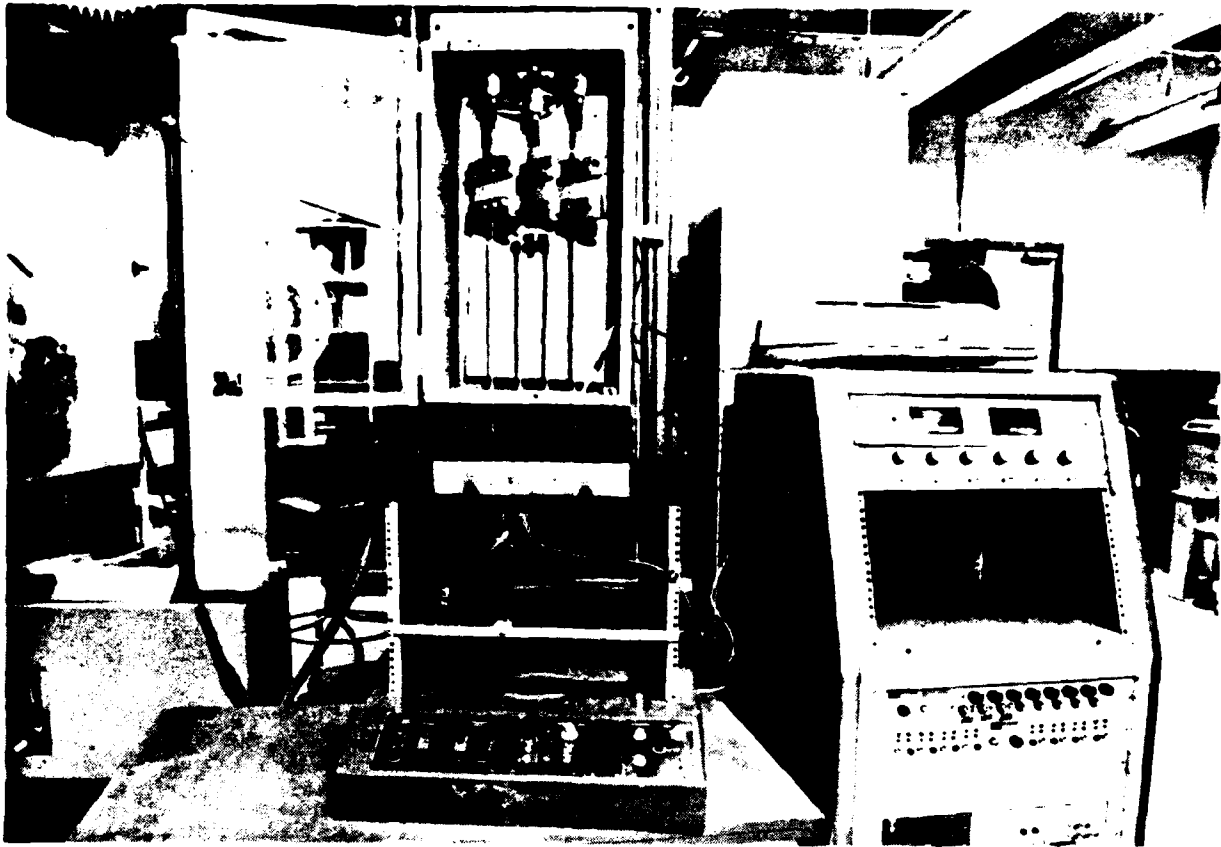


a. Propellant and Loading Fixture

b. Propellant

Figure 48. Shear Sample and Test Attachment

28811



14262-4

Figure 49. Biaxial Test Setup and Instrumentation

28385

results were used to obtain comparison data for other tests at different strain levels in Table 32. The stress at 8% strain versus temperature is shown in Figure 62 for UTP-3001. The tests at different temperatures were taken from different redwood boxes of propellant and there appears to be some between box and sample differences. The data shifted for rate effects to the 0.2 in./min. in the lower plot indicates that extrapolation of the temperature stress plot would be unreliable. This eliminated any reasonable direct comparison with the slower rate straining - cooling tests as noted in Table 32. The comparisons did show reasonable agreement with some samples from each of the redwood boxes used. The straining-cooling data are expected to be of the same general family.

(Text continued on page 168.)

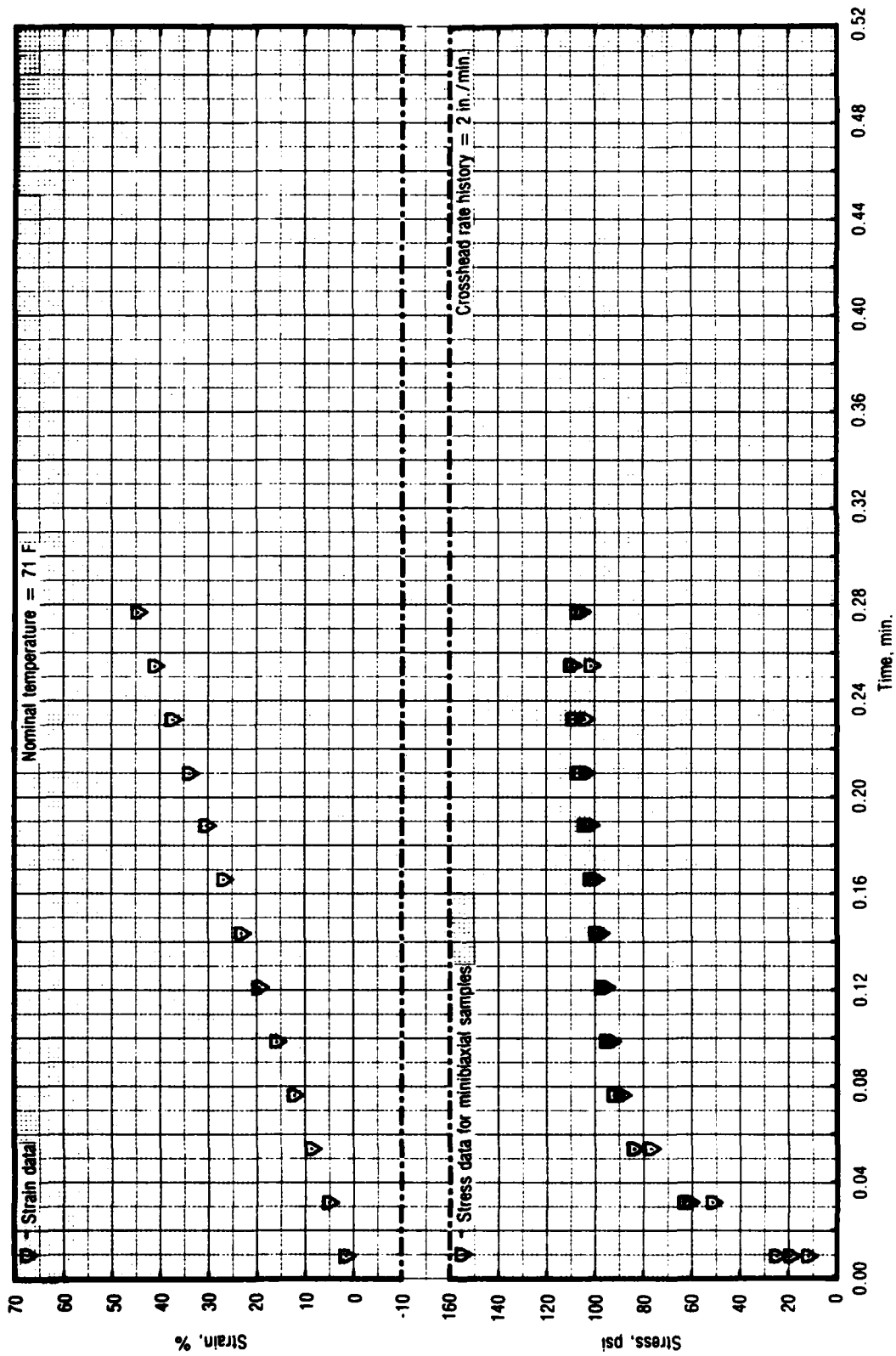


Figure 50. Test No. 14 - Stress for UTP-19, 360B-400/1777

28812

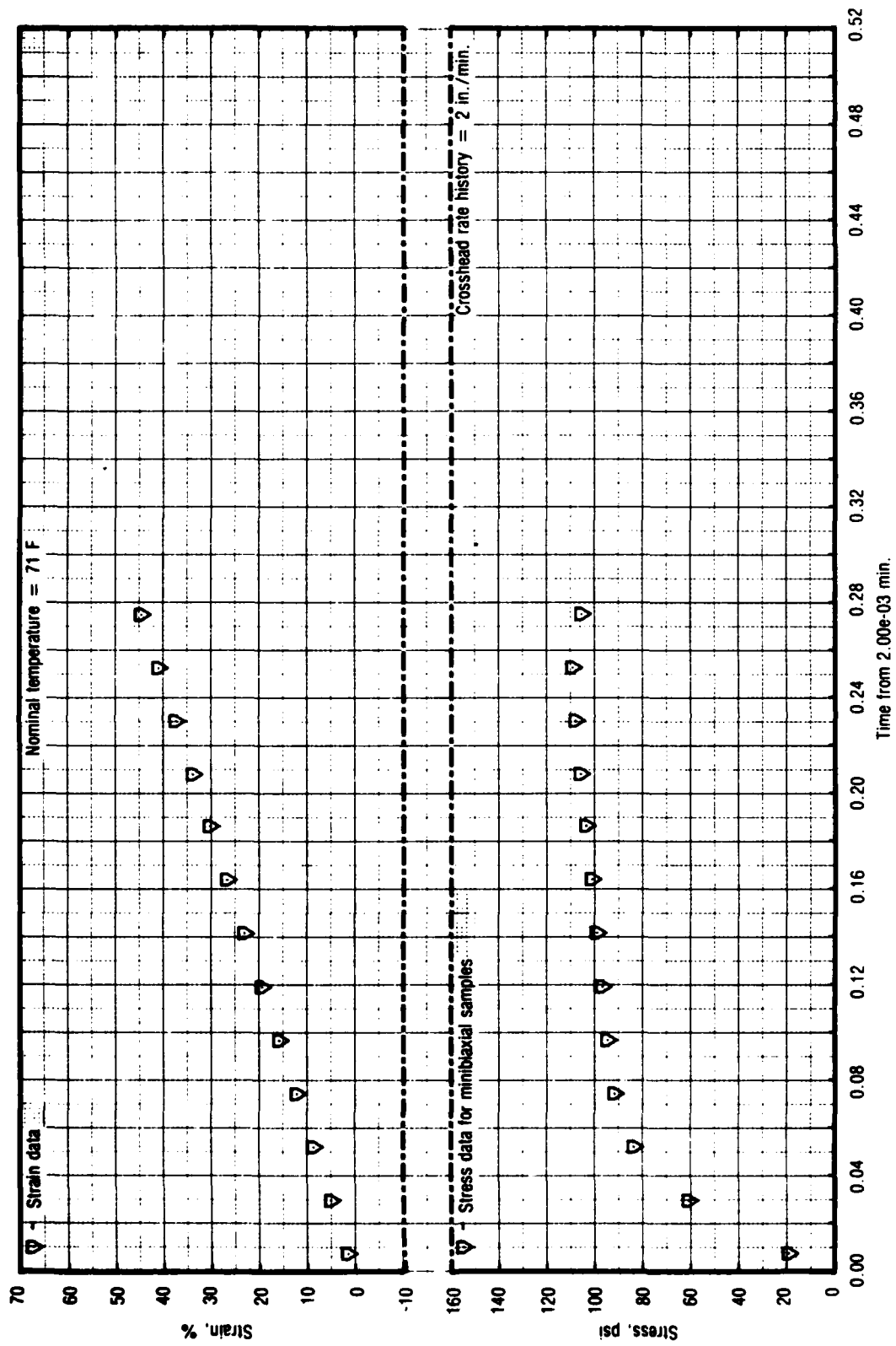


Figure 51. Test No. 14 - Stress for UTP-19, 360B-400/1777

28813

TABLE 24. MINIBIAXIAL STRESS WHILE STRAINING AND COOLING

PROPELLANT: UTP 19368B 400/1777
 REQUESTOR: Carlton Francis
 WOR: 2742-400-0000

DATE: 12/10/81
 OPERATOR: JMD

DEFINITIONS:

Time = Time From Start of Test (min)
 Stress (psi) = Force/Area
 Strain (%) = Sample Extension/Length
 T(air) = Test Air Temperature (F)
 T(prop) = Test Propellant Temperature (F)

RELATIONSHIPS:
 = Force/Area
 = Sample Extension/Length

NOMINAL VALUES:
 Test Temp = 71 F
 Gage Length = 1.25 in
 Nom. Strain = 50 %
 XHD Rate = 2 in/min

CALIBRATION DATA:
 Cal Wt = 10.0 lbs
 Lead Cal (lbs/volts)
 Offset (volts)
 Pot Cal (in/volts) =
 Temp (F)

SAMPLE 1
 19.991
 0.101
 -0.193
 -0.222

SAMPLE 2
 19.980
 0.170

AREAS (sq in):

1.537 1.494 1.512

STRESS DATA (psi):

TIME
 1 0.03159
 2 0.05402
 3 0.07682
 4 0.12120
 5 0.14361
 6 0.16858
 7 0.18811
 8 0.21821
 9 0.25480
 10 0.27716

T(prop)
 74.10
 74.02
 73.99
 74.10
 74.23
 74.38
 74.10
 74.11
 74.10

T(air)
 74.23
 73.99
 73.94
 73.92
 74.11
 74.19
 73.99
 74.10

Strain
 1.08
 0.63
 0.28
 0.42
 0.68
 0.79
 0.73
 0.55

SAMPLE 1
 11.43
 11.28
 11.68
 11.77
 11.50
 11.54
 11.67
 11.74
 11.84
 11.26

SAMPLE 2
 18.92
 18.76
 18.54
 18.74
 18.69
 18.87
 19.11
 19.45
 19.89
 19.12

SAMPLE 3
 24.52
 22.96
 23.09
 23.17
 23.44
 23.68
 24.11
 24.48
 25.58
 27.27

AVG
 18.26
 18.14
 18.94
 19.52
 19.60
 19.80
 20.10
 20.55
 20.72
 21.33

DEV
 1.67
 1.77
 1.84
 1.54
 1.39
 1.37
 1.64
 1.82
 1.32
 1.32

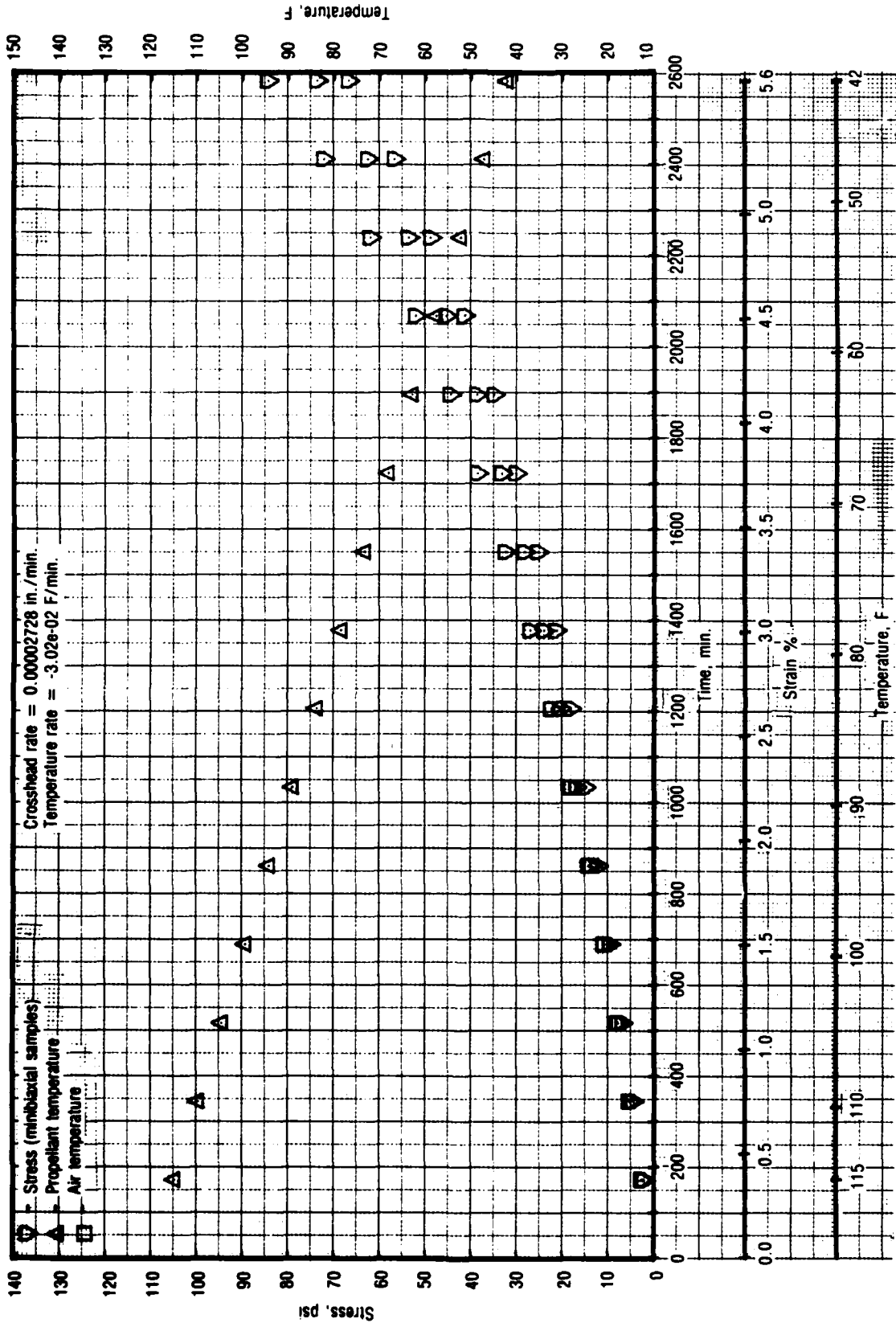


Figure 52. Stress While Straining and Cooling for UTP-3001-750/7768 28814

TABLE 25. MINIBIAXIAL STRESS WHILE STRAINING AND COOLING

PROPELLANT: UTP 3001 750/7768
 REQUESTOR: Carlito Francisco
 DOR: 242-400-0000

DATE: 12/22/81
 OPERATOR: JMD

DEFINITIONS: Time = Time From Start of Test (min)
 σ = Stress (Psi)
 ϵ = Strain (%)
 T (air) = Test Air Temperature (F)
 T (prop) = Test Propellant Temperature (F)

RELATIONSHIPS:
 $\sigma = \text{Force}/\text{Area}$
 $\epsilon = \text{Sample Extension}/\text{Length}$

NOMINAL VALUES:
 Test Temp = 120 to 40 F
 Gage Length = 1.25 in
 Nom Strain = 10 %
 XHD Rate = .00002728 in/min

CALIBRATION DATA:
 Pretest: Cal Wt = 0.0 lbs
 Load Cal (lbs/in) = 6.73
 Offset (in) = 1.25
 Temp (F) = 120.0

Post Test: Cal Wt = 10.0 lbs
 Load Cal (lbs/in) = 6.85
 Offset (in) = 0.32
 Temp (F) = 38.0

AREAS (sq in):

STRESS SET	CALIBRATION DATA		TEMPERATURE		STRAIN		AREAS		SAMPLE	Avg	St Dev
	Time	Stress	T (prop)	T (air)	1	2	1	2			
1	172.3000	114.8	109.6	104.4	0.38	2.05	2.63	2.74	2	2.74	0.286
2	344.5000	109.6	104.4	104.4	0.75	4.41	5.20	4.91	3	4.91	0.307
3	516.8000	104.4	104.4	104.4	1.13	6.77	7.94	7.48	3	7.48	0.341
4	689.1000	94.0	94.0	94.0	1.50	9.44	10.92	10.35	3	10.35	0.361
5	861.3000	88.8	88.8	88.8	1.88	12.05	14.07	13.20	3	13.20	0.377
6	1033.6000	83.6	83.6	83.6	2.25	14.81	17.27	16.18	3	16.18	0.397
7	1205.9000	78.4	78.4	78.4	2.63	18.04	22.02	20.10	3	20.10	0.434
8	1378.1000	73.2	73.2	73.2	3.01	21.21	27.02	24.91	3	24.91	0.471
9	1550.4000	68.0	68.0	68.0	3.38	25.07	32.54	28.95	3	28.95	0.506
10	1722.7000	62.8	62.8	62.8	3.76	30.07	38.95	33.93	3	33.93	0.541
11	1894.9000	57.6	57.6	57.6	4.14	34.87	44.46	39.30	3	39.30	0.573
12	2067.2000	52.4	52.4	52.4	4.51	41.37	52.13	46.30	3	46.30	0.603
13	2239.4000	47.2	47.2	47.2	4.89	48.82	62.10	54.92	3	54.92	0.633
14	2411.7000	42.0	42.0	42.0	5.26	56.82	72.29	63.92	3	63.92	0.659
15	2584.0000	42.0	42.0	42.0	5.64	66.85	84.49	75.03	3	75.03	0.689

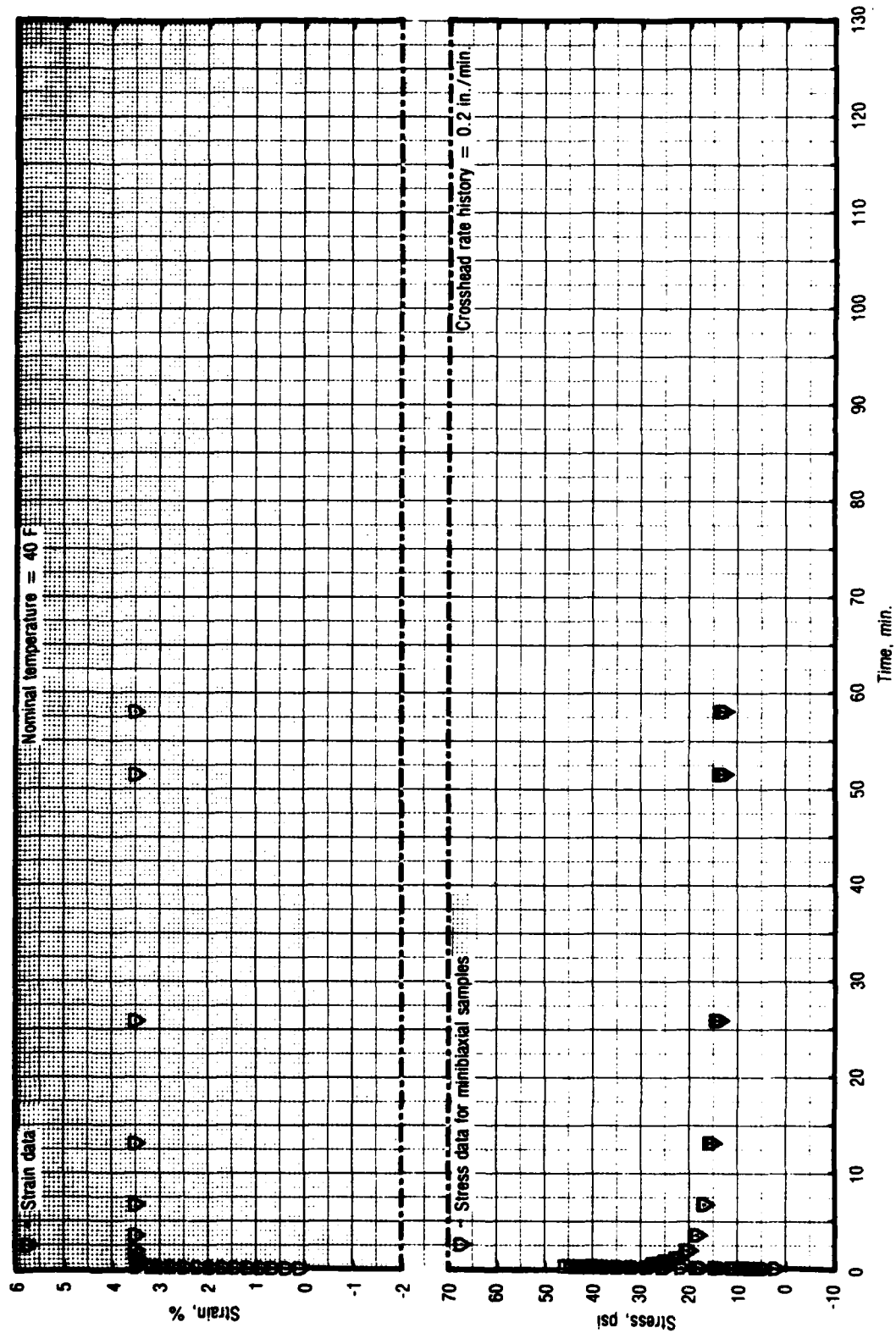


Figure 53. Test No. 16 - Stress While Step Straining for UTP-19, 360B-400/177

28815

TABLE 26. MINIBIAXIAL STRESS WHILE STEP STRAINING

PROPELLANT: UTP 193608 400/1777
 REQUESTOR: Carliton
 NDR: 2742-400-0000

DATE: 12-28-81
 OPERATOR: BC

DEFINITIONS:
 Time = Time From Start of Test (min)
 σ = Stress (Psi)
 ϵ = Strain (%)
 $T(air)$ = Test Air Temperature (F)
 $T(prop)$ = Test Propellant Temperature (F)

KFLATIONSHIPS:
 $\sigma = E \cdot \epsilon$
 $\epsilon = \text{Sample Extension} / \text{Length}$

NOMINAL VALUES:
 Test Temp = 40 F
 Gage Length = 1.25 in
 Nom. Strain = 3%
 XHD Rate = .2 in/min

CALIBRATION DATA:
 Cal Wt = 10.0 lbs
 Load Cal (lbs/volts) = 29.816
 Offset (volts) = 0.058
 Pot Cal (in/volts) = -0.385
 Temp (F) = 42.1

SAMPLE
 2
 29.773
 0.251

1
 29.816
 0.058
 -0.385
 42.1

AREAS (sq in): 1.478 1.478 1.478

SET	Time	T(prop)	T(air)	Strain	SAMPLE	Avg	St
1	0.0023	42.1	42.0	0.17	2.04	2.10	0.047
2	0.02523	42.1	42.0	0.34	4.58	5.34	0.709
3	0.04242	42.0	41.9	0.67	7.79	9.39	0.989
4	0.05957	42.0	41.7	1.01	11.22	13.05	1.163
5	0.07672	42.0	41.4	1.33	14.75	16.84	1.293
6	0.09397	42.0	41.5	1.63	18.15	20.49	1.431
7	0.11116	42.0	41.2	1.93	21.68	24.15	1.514
8	0.12759	42.0	41.3	2.25	24.98	27.48	1.535
9	0.14468	42.0	41.3	2.50	28.51	30.78	1.535
10	0.16188	42.0	41.1	2.76	31.84	33.78	1.477
11	0.17917	42.0	41.3	3.00	34.39	36.44	1.277
12	0.19632	42.0	41.0	3.20	37.40	39.09	1.198
13	0.20809	42.0	41.5	3.40	39.45	40.90	1.222
14	0.22900	42.0	42.0	3.50	42.65	44.00	1.188
15	0.23369	42.0	41.5	3.50	44.64	42.80	1.144
16	0.25096	42.0	41.1	3.50	47.51	46.64	0.444
17	0.27097	42.0	41.8	3.50	50.23	52.69	0.351
18	1.11024	42.7	41.1	3.50	22.09	22.47	0.289
19	3.51132	42.4	41.0	3.50	20.58	22.03	0.189
20	6.511208	42.4	41.4	3.50	18.91	18.53	0.135
21	13.511242	42.6	40.8	3.50	15.53	15.53	0.116
22	20.511287	42.0	40.9	3.50	13.34	13.34	0.089
23	27.51364	42.0	40.8	3.50	11.44	11.44	0.061
24	34.515404	42.4	40.5	3.50	10.75	10.75	0.039

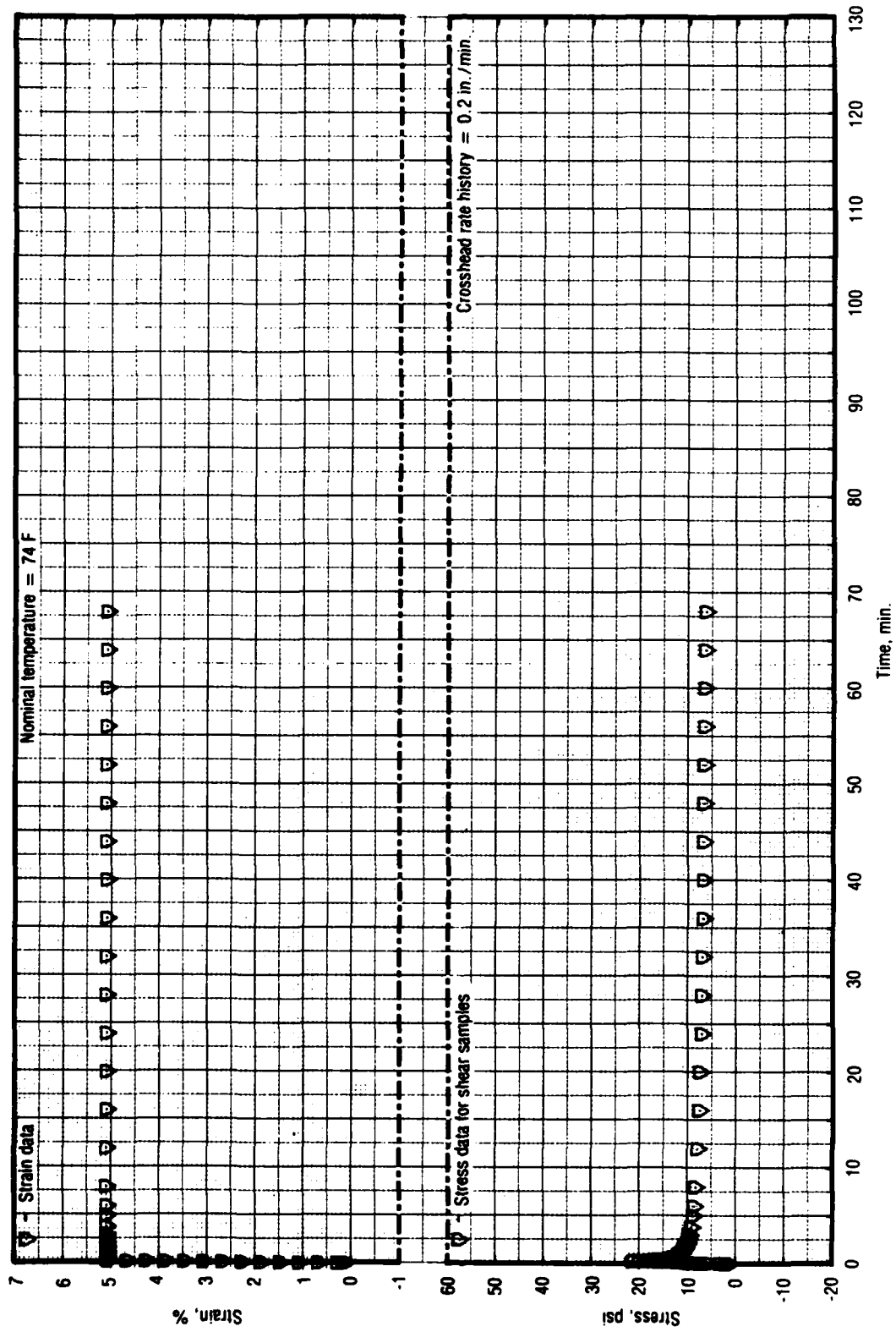


Figure 54. Test No. 17 - Stress While Step Straining for UTP-3001-750/7768

28816

TABLE 27. SHEAR STRESS WHILE STEP STRAINING
(SHEET 1 OF 2)

PROPELLANT: UTP 3001 750/7268
REQUESTOR: CAPT. FRANCIS
WOK: 2742-400-0000

DATE: 12/81
OPERATOR: JWD/EG

DEFINITIONS:
Time = Time From Start of Test (Min)
= Stress (Psi)
= Strain (%)
T(air) = Test Air Temperature (F)
T(prop) = Test Propellant Temperature (F)

RELATIONSHIPS:
= Force/Area
= Sample Extension/Length

NOMINAL VALUES:
Test Temp = 74 F
Gage Length = 1.01 in
Nom. Strain = 6 %
XHD Rate = .2 in/min

CALIBRATION DATA:
Cal Wt = 10.0 lbs
Load Cal (lbs/in)
Offset (in)
Temp (F)

SAMPLE
1
20.000
0.000
74.0

AREAS (sq in):

3.004

STRESS SET	Time	T(prop)	T(air)	Strain	SAMPLE	Avg	Dev
1	0.00600			0.128	1	12.00	0.000
2	0.01400			0.268	2	13.13	0.000
3	0.02400			1.077	3	15.57	0.000
4	0.03400			1.447	4	16.66	0.000
5	0.04400			1.827	5	17.45	0.000
6	0.05400			2.226	6	17.98	0.000
7	0.06400			2.646	7	18.44	0.000
8	0.07400			3.086	8	18.97	0.000
9	0.08400			3.546	9	19.30	0.000
10	0.09400			4.025	10	19.64	0.000
11	0.10400			4.525	11	19.97	0.000
12	0.11400			5.044	12	20.24	0.000
13	0.12400			5.584	13	20.55	0.000
14	0.13400			6.144	14	20.84	0.000
15	0.14400			6.724	15	21.10	0.000
16	0.15400			7.324	16	21.35	0.000
17	0.16400			7.944	17	21.58	0.000
18	0.17400			8.584	18	21.80	0.000
19	0.18400			9.244	19	22.00	0.000
20	0.19400			9.924	20	22.18	0.000
21	0.20400			10.624	21	22.35	0.000
22	0.21400			11.344	22	22.50	0.000
23	0.22400			12.084	23	22.64	0.000
24	0.23400			12.844	24	22.78	0.000
25	0.24400			13.624	25	22.90	0.000
26	0.25400			14.424	26	23.01	0.000
27	0.26400			15.244	27	23.10	0.000
28	0.27400			16.084	28	23.18	0.000
29	0.28400			16.944	29	23.25	0.000

TABLE 27. SHEAR STRESS WHILE STEP STRAINING
(SHEET 2 OF 2)

30	23600	5.08	9.72	9.72	0.000
31	3600	5.08	9.45	9.45	0.000
32	3600	5.08	9.19	9.19	0.000
33	3600	5.08	8.79	8.79	0.000
34	3600	5.08	8.59	8.59	0.000
35	3600	5.08	8.26	8.26	0.000
36	3600	5.08	7.86	7.86	0.000
37	3600	5.08	7.52	7.52	0.000
38	3600	5.08	7.39	7.39	0.000
39	3600	5.08	7.23	7.23	0.000
40	3600	5.08	6.99	6.99	0.000
41	3600	5.08	6.86	6.86	0.000
42	3600	5.08	6.79	6.79	0.000
43	3600	5.08	6.72	6.72	0.000
44	3600	5.08	6.66	6.66	0.000
45	3600	5.08	6.59	6.59	0.000
46	3600	5.08	6.52	6.52	0.000
47	3600	5.08	6.46	6.46	0.000
48	3600	5.08	6.42	6.42	0.000
49	3600	5.08	6.39	6.39	0.000
50	3600	5.08	6.32	6.32	0.000
51	3600	5.08	6.32	6.32	0.000

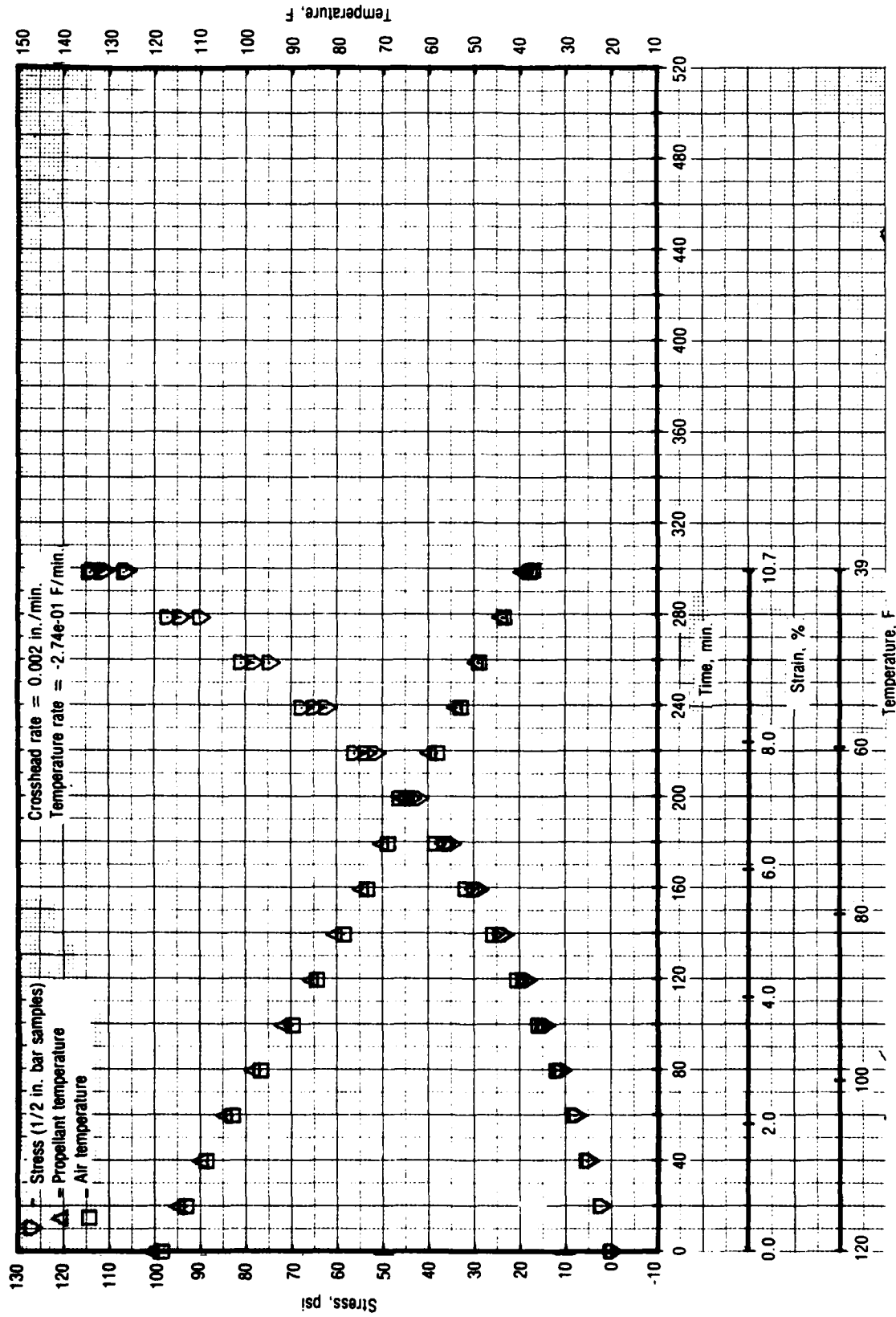


Figure 55. Test No. 18 - Stress While Straining and Cooling for UTP-3001-750/7768

28817

TABLE 28. 1/2-IN. BAR STRESS WHILE STRAINING AND COOLING

PROPELLANT: UTP 3001 750/7768
 REQUESTOR: 2942-400-0000
 WORK:

DATE: 12/2/81
 OPERATOR: JMD

DEFINITIONS:
 Time = Time From Start of Test (Min)
 Stress (Psi) = Force/Area
 Strain (%) = Sample Extension/Length
 T(air) = Test Air Temperature (F)
 T(prop) = Test Propellant Temperature (F)

RELATIONSHIPS:
 = Force/Area
 = Sample Extension/Length

NOMINAL VALUES:
 Test Temp = 120 to 40 F
 Gage Length = 5.97 in
 Nom. Strain = 10 %
 XHD Rate = .002 in/min

CALIBRATION DATA:
 Pretest: Cal Wt = 10.0 lbs
 Load Cal (lbs/volts) = 1.03
 Offset (volts) = -4.43
 Pot Cal (in/volts) = -0.00
 Temp (F) = 120.6
 Post Test: Cal Wt = 10.0 lbs
 Load Cal (lbs/volts) = -4.07
 Offset (volts) = -0.56
 Pot Cal (in/volts) = -39.1
 Temp (F) =

SAMPLE 2
 -4.43
 -0.00

SAMPLE 3
 -4.13
 -0.02

-4.17
 -0.16

AREAS (sq in):

0.228

0.228

0.230

STRESS DATA (psi):
 Time 00 120.00
 0.99E 01 114.75
 1.98E 01 109.54
 2.97E 01 98.25
 3.96E 01 85.44
 4.95E 02 74.19
 5.94E 02 65.55
 6.93E 02 59.57
 7.92E 02 53.49
 8.91E 02 49.93
 9.90E 02 43.38

T(air) 119.5
 113.7
 103.5
 96.7
 84.5
 73.9
 64.9
 59.1
 53.0
 49.0
 43.7

Strain 0.00
 0.35
 1.35
 2.35
 3.35
 4.35
 5.35
 6.35
 7.35
 8.35
 9.35
 10.69

SAMPLE 1
 0.44
 2.58
 11.96
 12.83
 23.81
 25.67
 38.81
 44.28
 51.19
 57.78
 64.76

-0.22
 2.47
 10.18
 11.39
 23.52
 25.15
 35.42
 44.28
 51.19
 57.78
 106.32

AVG 5
 0.37
 5.19
 11.42
 15.37
 26.40
 36.44
 45.25
 52.05
 58.12
 68.92
 110.42

ST 0.22
 0.08
 0.16
 0.32
 0.57
 0.83
 1.08
 1.33
 1.58
 1.83
 2.08
 2.33

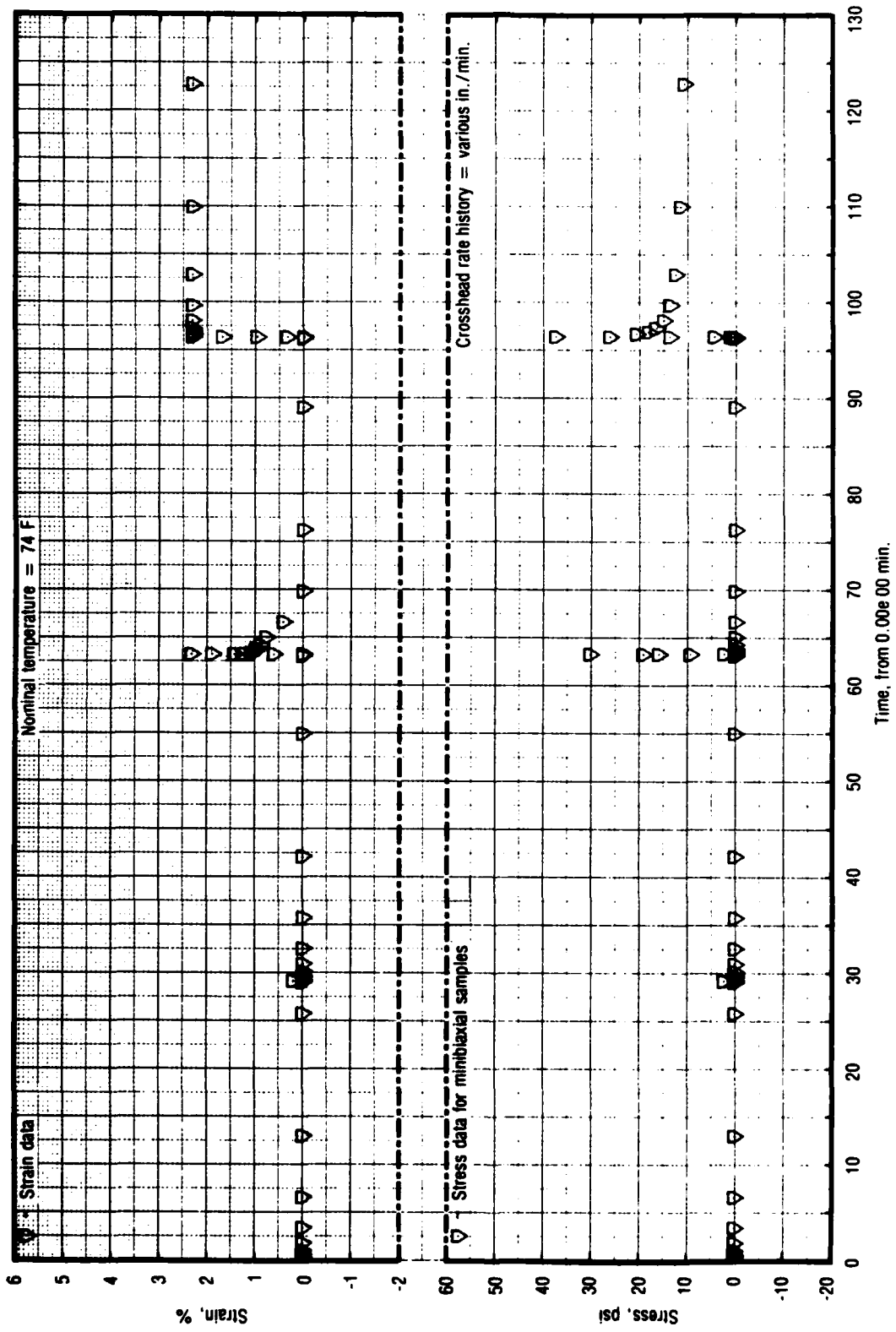


Figure 56. Test No. 19, Part 1 - Stress for UTP-3001-750/7768

28818

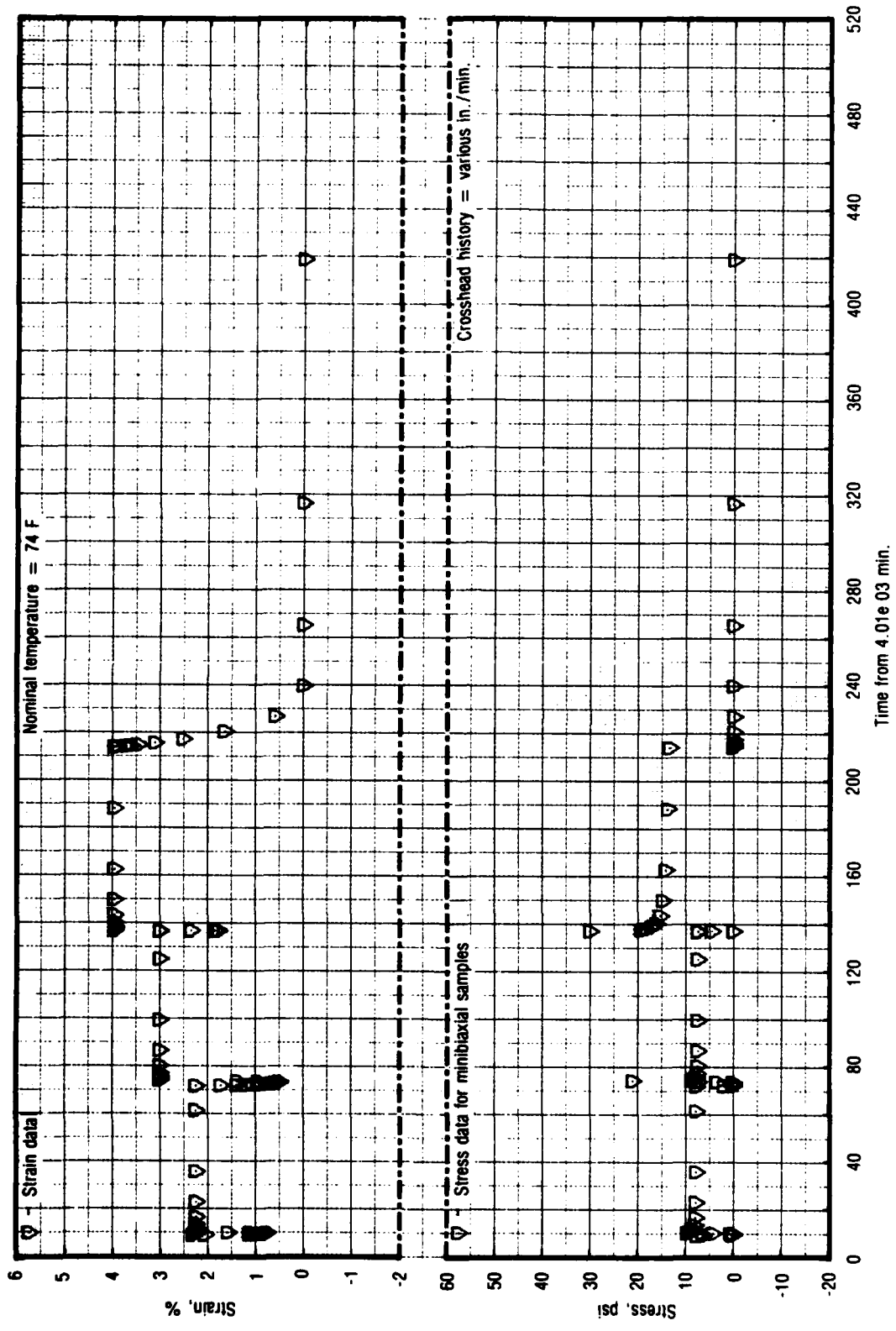


Figure 57. Test No. 19, Part 2 - Stress for UTP-3001-750/7768

28819

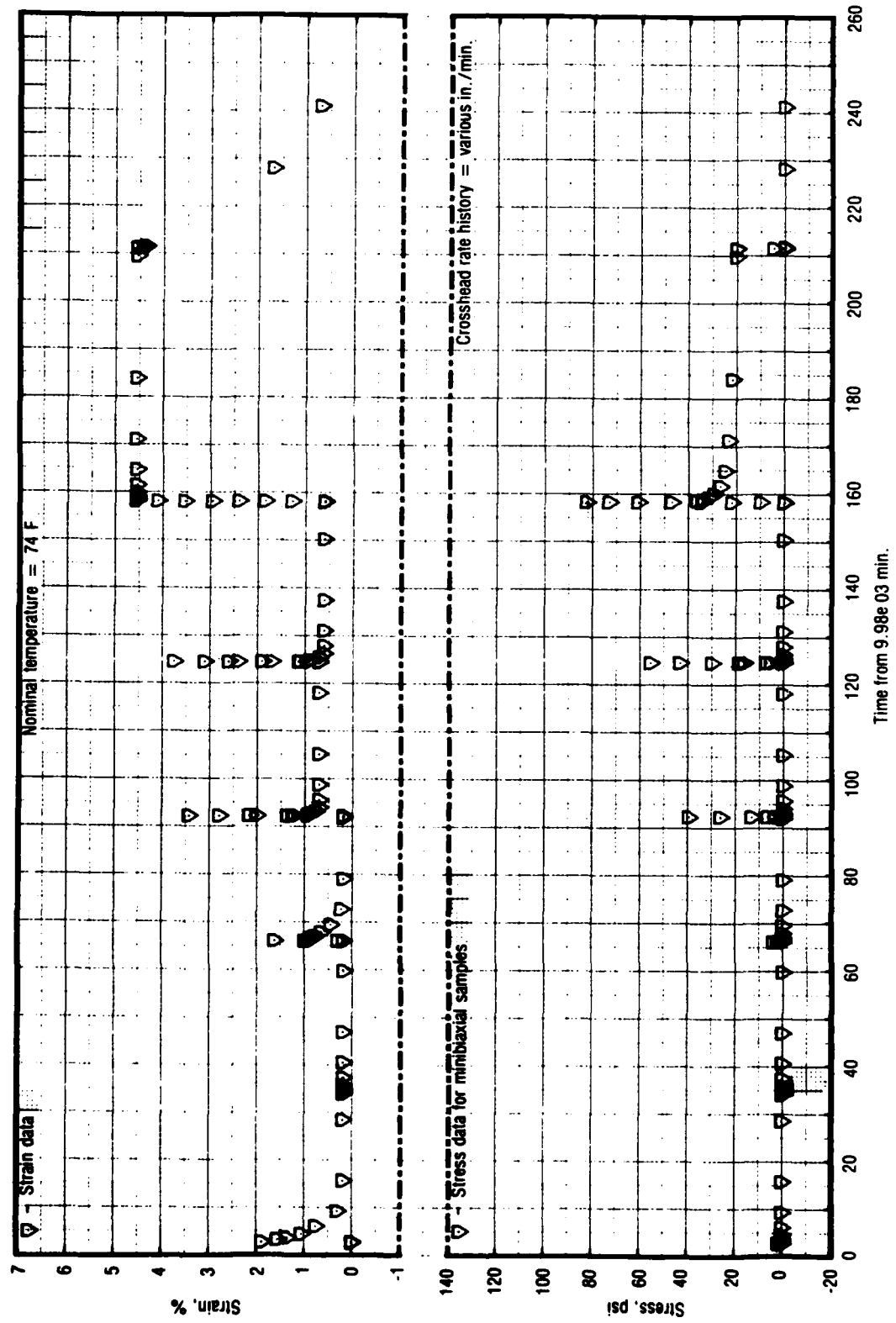


Figure 58. Test No. 19, Part 3 - Stress for UTP-3001-750/7768

28820

TABLE 29. TEST NO. 19 - MINIBIAXIAL STRESS, SAMPLE
(SHEET 1 OF 6)

PROPELLANT: UTP 3001 750/7768
 REQUESTOR: CALTON FRANCIS
 WOR: 2742-400-0000

DATE: 1/18/82 S1
 OPERATOR: JMD

DEFINITIONS:
 Time = Time From Start of Test (min)
 σ = Stress (psi)
 ϵ = Strain (%)
 T(air) = Test Air Temperature (t)
 T(prop) = Test Propellant Temperature (F)

RELATIONSHIPS:
 $\sigma = \text{Force/Area}$
 $\epsilon = \text{Sample Extension/Length}$

NOMINAL VALUES:
 Test Temp = 74 F
 Gage Length = 1.25 in
 Nom. Strain = Various %
 XRD Rate = Various in/min

CALIBRATION DATA

Cal Wt = 10.0 lbs	SAMPLE
Load Cal (lbs/volts)	24.768
Offset (volts)	0.083
Pot Cal (in/volts) =	-0.396
Temp (F)	77.1

AREAS (sq in): 1.477

STRESS DATA (psi)	Time	T(prop)	T(air)	Strain	SAMPLE	Avg	St Dev
1	0.01882			0.00	0.00	0.00	0.000
2	0.01450			0.00	0.00	0.00	0.000
3	0.02154			0.00	0.00	0.00	0.000
4	0.02793			0.00	0.00	0.00	0.000
5	0.03523			0.00	0.00	0.00	0.000
6	0.04142			0.00	0.00	0.00	0.000
7	0.04766	80.4	79.4	0.00	0.00	0.00	0.000
8	0.05506	80.0	79.4	0.00	0.00	0.00	0.000
9	0.05560	80.2	79.1	0.00	0.00	0.00	0.000
10	0.05656	80.0	79.3	0.00	0.00	0.00	0.000
11	1.75691	80.0	79.0	0.00	0.00	0.00	0.000
12	3.35766	80.0	77.1	0.00	0.00	0.00	0.000
13	6.55836	77.4	75.9	0.00	0.00	0.00	0.000
14	12.65954	77.2	76.5	0.00	0.00	0.00	0.000
15	20.01546	78.0	76.9	0.00	0.00	0.00	0.000
16	29.11960			0.00	0.00	0.00	0.000
17	29.11966			0.00	0.00	0.00	0.000
18	29.12845			0.00	0.00	0.00	0.000
19	29.12845			0.00	0.00	0.00	0.000
20	29.13286			0.00	0.00	0.00	0.000
21	29.13729			0.00	0.00	0.00	0.000
22	29.14171			0.00	0.00	0.00	0.000
23	29.14613			0.00	0.00	0.00	0.000
24	29.15056			0.00	0.00	0.00	0.000
25	29.15499			0.00	0.00	0.00	0.000
26	29.15937			0.00	0.00	0.00	0.000
27	29.16379			0.00	0.00	0.00	0.000
28	29.16821			0.00	0.00	0.00	0.000
29	29.17266			0.00	0.00	0.00	0.000
30	29.17707			0.00	0.00	0.00	0.000
31	29.17948			0.00	0.00	0.00	0.000

TABLE 29. TEST NO. 19 - MINIBIAXIAL STRESS, SAMPLE
(SHEET 3 OF 6)

89	97	27119	77.2	76.4	2.32	16.58	0.000
90	98	07191	77.7	76.1	2.32	14.98	0.000
91	99	47222	77.2	77.1	2.32	13.57	0.000
92	100	87297	78.0	76.8	2.32	12.49	0.000
93	101	95481	77.9	76.9	2.32	11.51	0.000
94	102	75506	77.0	76.9	2.32	10.75	0.000
95	103	35598	77.9	75.9	2.32	9.41	0.000
96	104	55619	76.2	76.4	2.32	8.29	0.000
97	105	75647	76.0	75.7	2.32	8.23	0.000
98	106	95673	75.0	75.1	2.32	8.10	0.000
99	107	1735	76.9	74.5	2.32	7.90	0.000
100	108	35786	73.0	73.4	2.32	7.60	0.000
101	109	55836	72.8	73.0	2.32	7.50	0.000
102	110	75852	72.8	72.7	2.32	7.50	0.000
103	111	95300	72.9	72.7	2.32	7.50	0.000
104	112	10492	72.8	72.7	2.32	6.17	0.000
105	113	16003	72.1	72.6	2.32	6.17	0.000
106	114	21589	72.7	72.6	2.32	6.17	0.000
107	115	27155	72.9	72.6	2.32	6.17	0.000
108	116	32726	72.9	72.6	2.32	6.17	0.000
109	117	38217	72.9	72.6	2.32	6.17	0.000
110	118	43774	72.9	72.6	2.32	6.17	0.000
111	119	51315	72.9	72.6	2.32	6.17	0.000
112	120	56893	72.9	72.6	2.32	6.17	0.000
113	121	62442	72.9	72.6	2.32	6.17	0.000
114	122	69200	72.9	72.6	2.32	6.17	0.000
115	123	73594	72.9	72.6	2.32	6.17	0.000
116	124	80500	72.9	72.6	2.32	6.17	0.000
117	125	84646	72.9	72.6	2.32	6.17	0.000
118	126	90266	72.9	72.6	2.32	6.17	0.000
119	127	98000	72.9	72.6	2.32	6.17	0.000
120	128	10073	72.9	72.6	2.32	6.17	0.000
121	129	50095	72.9	72.6	2.32	6.17	0.000
122	130	70133	72.9	72.6	2.32	6.17	0.000
123	131	70165	72.9	72.6	2.32	6.17	0.000
124	132	30195	72.9	72.6	2.32	6.17	0.000
125	133	30221	72.9	72.6	2.32	6.17	0.000
126	134	90275	72.9	72.6	2.32	6.17	0.000
127	135	70319	72.9	72.6	2.32	6.17	0.000
128	136	30357	72.9	72.6	2.32	6.17	0.000
129	137	4081	72.9	72.6	2.32	6.17	0.000
130	138	66658	72.9	72.6	2.32	6.17	0.000
131	139	73385	72.9	72.6	2.32	6.17	0.000
132	140	74000	72.9	72.6	2.32	6.17	0.000
133	141	85459	72.9	72.6	2.32	6.17	0.000
134	142	96775	72.9	72.6	2.32	6.17	0.000
135	143	07901	72.9	72.6	2.32	6.17	0.000
136	144	19011	72.9	72.6	2.32	6.17	0.000
137	145	30063	72.9	72.6	2.32	6.17	0.000
138	146	47000	72.9	72.6	2.32	6.17	0.000
139	147	52342	72.9	72.6	2.32	6.17	0.000
140	148	63396	72.9	72.6	2.32	6.17	0.000
141	149	74528	72.9	72.6	2.32	6.17	0.000
142	150	88589	72.9	72.6	2.32	6.17	0.000
143	151	99699	72.9	72.6	2.32	6.17	0.000
144	152	00810	72.9	72.6	2.32	6.17	0.000
145	153	11976	72.9	72.6	2.32	6.17	0.000
146	154	23042	72.9	72.6	2.32	6.17	0.000
147	155	34181	72.9	72.6	2.32	6.17	0.000
148	156	46000	72.9	72.6	2.32	6.17	0.000
149	157	56427	72.9	72.6	2.32	6.17	0.000

TABLE 29. TEST NO. 19 - MINIBIAXIAL STRESS, SAMPLE
(SHEET 4 OF 6)

150	4083.67483	73.2	73.0	1.38	7.26	7.26	0.000
151	4084.12792	73.2	72.9	3.01	21.00	21.00	0.000
152	4084.32878	73.5	72.8	3.01	8.40	8.40	0.000
153	4084.72931	73.1	73.3	3.01	8.02	8.02	0.000
154	4085.52965	74.4	73.8	3.01	7.72	7.72	0.000
155	4090.33106	74.2	73.5	3.01	7.47	7.47	0.000
156	4096.33148	73.8	73.4	3.01	7.37	7.37	0.000
157	4109.53174	72.9	73.1	3.01	7.34	7.34	0.000
159	4135.13241	73.3	73.0	3.01	7.34	7.34	0.000
160	4146.69191	73.3	73.1	3.01	7.33	7.33	0.000
161	4146.92433			3.01	7.33	7.33	0.000
162	4146.93106			1.85	0.00	0.00	0.000
163	4146.93548			1.80	0.00	0.00	0.000
164	4146.94226			1.78	0.00	0.00	0.000
165	4146.94667			3.43	4.43	4.43	0.000
166	4146.96000			3.96	30.00	30.00	0.000
167	4147.45818	9	73.1	3.96	19.24	19.24	0.000
168	4147.85867	23.2	73.0	3.96	18.16	18.16	0.000
169	4148.65890	73.4	73.3	3.96	17.16	17.16	0.000
170	4150.25924	73.6	73.3	3.96	16.08	16.08	0.000
171	4159.86051	73.8	73.5	3.96	15.29	15.29	0.000
172	4172.66086	73.9	73.4	3.96	14.64	14.64	0.000
173	4198.26115	73.4	73.3	3.96	14.12	14.12	0.000
174	4223.96353	73.6	73.3	3.96	13.63	13.63	0.000
175	4224.04053			3.95	13.30	13.30	0.000
177	4224.04726			3.94	0.00	0.00	0.000
178	4224.05169			3.93	0.00	0.00	0.000
179	4224.05610			3.92	0.00	0.00	0.000
180	4224.06049			3.92	0.00	0.00	0.000
181	4224.34755			3.73	0.00	0.00	0.000
182	4224.54796	3	73.1	3.62	0.00	0.00	0.000
183	4224.94817	73.6	73.5	3.46	0.00	0.00	0.000
184	4235.74866	73.3	73.3	3.22	0.00	0.00	0.000
185	4237.34919	73.6	73.3	3.52	0.00	0.00	0.000
186	4238.54950	74.2	73.3	1.63	0.00	0.00	0.000
187	4249.94982	73.6	73.6	0.59	0.00	0.00	0.000
188	4250.75073	73.4	73.6	0.00	0.00	0.00	0.000
189	4275.35104	74.1	73.3	0.00	0.00	0.00	0.000
190	4358.55171	74.9	74.0	0.00	0.00	0.00	0.000
191	4428.95216	75.8	75.2	0.00	0.00	0.00	0.000
192	4633.75293	74.7	73.7	0.00	0.00	0.00	0.000
193	5043.35376	72.9	73.1	0.00	0.00	0.00	0.000
194	5862.55471	75.7	75.5	0.00	0.00	0.00	0.000
195	7550.58566	76.2	75.7	0.00	0.00	0.00	0.000
196	7982.58566			0.00	0.00	0.00	0.000
197	7982.70146			0.00	0.00	0.00	0.000
198	7982.71234			0.00	0.00	0.00	0.000
199	7982.71866			0.00	0.00	0.00	0.000
200	7982.72501			1.88	0.00	0.00	0.000
201	7982.73200	0	75.8	1.88	1.41	1.41	0.000
202	7983.23743	6	75.8	1.55	0.97	0.97	0.000
203	7983.65837	75.9	75.6	1.35	0.00	0.00	0.000
204	7984.45893	75.9	75.7	1.05	0.00	0.00	0.000
205	7984.45893	75.6	75.5	0.77	0.00	0.00	0.000
206	7989.26041	76.1	75.3	0.30	0.00	0.00	0.000
207	7995.66106	77.1	75.9	0.18	0.00	0.00	0.000
209	10008.46150		76.7	0.18	0.00	0.00	0.000

TABLE 29. TEST NO. 19 - MINIBIAXIAL STRESS, SAMPLE
(SHEET 5 OF 6)

210	10013.95679	76.7	76.9	0.18	0.00	0.00	0.00
211	10014.02590			0.18	0.00	0.00	0.00
212	10014.02937			0.18	0.00	0.00	0.00
213	10014.03456			0.18	0.00	0.00	0.00
214	10014.04814			0.18	0.00	0.00	0.00
215	10014.13224			0.18	0.00	0.00	0.00
216	10014.23267	76.8	77.1	0.18	0.00	0.00	0.00
217	10014.23353	76.6	77.1	0.18	0.00	0.00	0.00
218	10015.33354	77.5	77.5	0.18	0.00	0.00	0.00
219	10015.33388	77.7	77.8	0.18	0.00	0.00	0.00
220	10020.51420	78.3	77.8	0.18	0.00	0.00	0.00
221	10026.87473	77.6	77.4	0.18	0.00	0.00	0.00
222	10039.73775	78.1	77.6	0.18	0.00	0.00	0.00
223	10045.77967	78.5	77.4	0.18	0.00	0.00	0.00
224	10046.16500			0.18	0.00	0.00	0.00
225	10046.06581			0.18	0.00	0.00	0.00
226	10046.07122			0.30	0.00	0.00	0.00
227	10046.07562			0.30	0.50	0.50	0.00
228	10046.08073			0.30	3.82	3.82	0.00
229	10046.08476			1.62	0.00	0.00	0.00
230	10046.08800			0.92	0.00	0.00	0.00
231	10046.09127			0.92	0.00	0.00	0.00
232	10046.09346			0.91	0.00	0.00	0.00
233	10046.09546			0.91	0.00	0.00	0.00
234	10046.10375			0.86	0.00	0.00	0.00
235	10046.12716			0.86	0.00	0.00	0.00
236	10046.22736	78.0	76.9	0.86	0.00	0.00	0.00
237	10047.02811	77.9	76.9	0.82	0.00	0.00	0.00
238	10047.82983	77.6	76.5	0.76	0.00	0.00	0.00
239	10047.82969	77.4	76.6	0.74	0.00	0.00	0.00
240	10052.63057	76.5	75.5	0.73	0.00	0.00	0.00
241	10057.03137	78.4	78.3	0.18	0.00	0.00	0.00
242	10071.83166	77.5	77.5	0.18	0.00	0.00	0.00
243	10072.15161			0.18	0.00	0.00	0.00
244	10072.23891			0.18	0.00	0.00	0.00
245	10072.24882			0.18	0.00	0.00	0.00
246	10072.24924			0.18	0.00	0.00	0.00
247	10072.25600			0.93	0.51	0.51	0.00
248	10072.25807			1.35	3.13	3.13	0.00
249	10072.26249			2.00	12.98	12.98	0.00
250	10072.26693			2.78	36.12	36.12	0.00
251	10072.27136			2.78	39.26	39.26	0.00
252	10072.27820			2.12	6.43	6.43	0.00
253	10072.28300			1.24	0.00	0.00	0.00
254	10072.28705			1.24	0.00	0.00	0.00
255	10072.29145			1.23	0.00	0.00	0.00
256	10072.29582			1.23	0.00	0.00	0.00
257	10072.30021			1.22	0.00	0.00	0.00
258	10072.30461			0.85	0.00	0.00	0.00
259	10072.30900	77.3	77.6	0.76	0.00	0.00	0.00
260	10073.17346	77.9	77.7	0.70	0.00	0.00	0.00
261	10073.17405	78.9	78.1	0.70	0.00	0.00	0.00
262	10075.57456	78.2	77.8	0.70	0.00	0.00	0.00
263	10078.77486	78.1	77.7	0.70	0.00	0.00	0.00
264	10085.17571	78.1	77.7	0.70	0.00	0.00	0.00
265	10097.97634	76.6	75.5	0.70	0.00	0.00	0.00
266	10104.41636			0.70	0.00	0.00	0.00
267	10104.49450			0.70	0.00	0.00	0.00
268	10104.49732			0.70	0.00	0.00	0.00
269	10104.50174			0.70	0.00	0.00	0.00

TABLE 29. TEST NO. 19 - MINIBIAL STRESS, SAMPLE
(SHEET 6 OF 6)

270	10104.50900			0.70	0.00	0.00	0.00	0.00
271	10104.51057			0.95	5.24	5.24	0.00	0.00
272	10104.51501			1.70	16.42	16.42	0.00	0.00
273	10104.51946			3.40	29.90	29.90	0.00	0.00
274	10104.52391			3.10	43.24	43.24	0.00	0.00
275	10104.52800			3.74	55.50	55.50	0.00	0.00
276	10104.53517			2.90	18.73	18.73	0.00	0.00
277	10104.53959			1.90	7.04	7.04	0.00	0.00
278	10104.54399			1.13	0.61	0.61	0.00	0.00
279	10104.54840			1.13	0.00	0.00	0.00	0.00
280	10104.55281			1.12	0.00	0.00	0.00	0.00
281	10104.55723			1.11	0.00	0.00	0.00	0.00
282	10104.56161			1.11	0.00	0.00	0.00	0.00
283	10104.56601			1.11	0.00	0.00	0.00	0.00
284	10104.56312	77.0	76.7	0.90	0.00	0.00	0.00	0.00
285	10105.46336	77.0	77.0	0.60	0.00	0.00	0.00	0.00
286	10106.26492	77.3	76.9	0.60	0.00	0.00	0.00	0.00
287	10107.86525	78.1	77.4	0.60	0.00	0.00	0.00	0.00
288	10111.06546	77.5	77.2	0.60	0.00	0.00	0.00	0.00
289	10117.46576	77.2	77.4	0.60	0.00	0.00	0.00	0.00
290	10130.26605	78.2	78.4	0.60	0.00	0.00	0.00	0.00
291	10137.99869	78.8	78.6	0.60	0.00	0.00	0.00	0.00
292	10138.18300			0.60	0.00	0.00	0.00	0.00
293	10138.18910			0.60	0.00	0.00	0.00	0.00
294	10138.19351			0.60	0.00	0.00	0.00	0.00
295	10138.19700			0.60	0.00	0.00	0.00	0.00
296	10138.20234			1.85	9.84	9.84	0.00	0.00
297	10138.20674			2.96	21.96	21.96	0.00	0.00
298	10138.21116			2.40	34.42	34.42	0.00	0.00
299	10138.21559			2.95	47.10	47.10	0.00	0.00
300	10138.22001			3.53	60.96	60.96	0.00	0.00
301	10138.22443			4.10	73.07	73.07	0.00	0.00
302	10138.22880			4.54	82.50	82.50	0.00	0.00
303	10138.27723	78.2	76.4	4.54	36.47	36.47	0.00	0.00
304	10138.27746	77.9	76.0	4.54	34.09	34.09	0.00	0.00
305	10139.17268	77.7	75.8	4.54	31.60	31.60	0.00	0.00
306	10139.27295	77.6	75.8	4.54	29.19	29.19	0.00	0.00
307	10141.37841	77.2	75.8	4.54	26.75	26.75	0.00	0.00
308	10144.77931	76.1	76.1	4.54	24.69	24.69	0.00	0.00
309	10151.18012	76.1	77.1	4.54	22.94	22.94	0.00	0.00
310	10163.98056	77.0	77.2	4.54	21.64	21.64	0.00	0.00
311	10189.58086	76.4	76.0	4.54	20.54	20.54	0.00	0.00
312	10191.26333	76.3	76.4	4.54	20.26	20.26	0.00	0.00
313	10191.32941			4.43	4.77	4.77	0.00	0.00
314	10191.33616			4.42	0.00	0.00	0.00	0.00
315	10191.34059			4.41	0.00	0.00	0.00	0.00
316	10191.34499			4.41	0.00	0.00	0.00	0.00
317	10191.34940			4.40	0.00	0.00	0.00	0.00
318	10191.35378			4.40	0.00	0.00	0.00	0.00
319	10191.35817			4.40	0.00	0.00	0.00	0.00
320	10191.36256			4.39	0.00	0.00	0.00	0.00
321	10191.36696			4.39	0.00	0.00	0.00	0.00
322	10191.37136			4.39	0.00	0.00	0.00	0.00
323	10191.37577			4.36	0.00	0.00	0.00	0.00
324	10191.62483	76.5	76.4	4.36	0.00	0.00	0.00	0.00
325	10208.00000			1.70	0.00	0.00	0.00	0.00
326	10221.00000			0.70	0.00	0.00	0.00	0.00

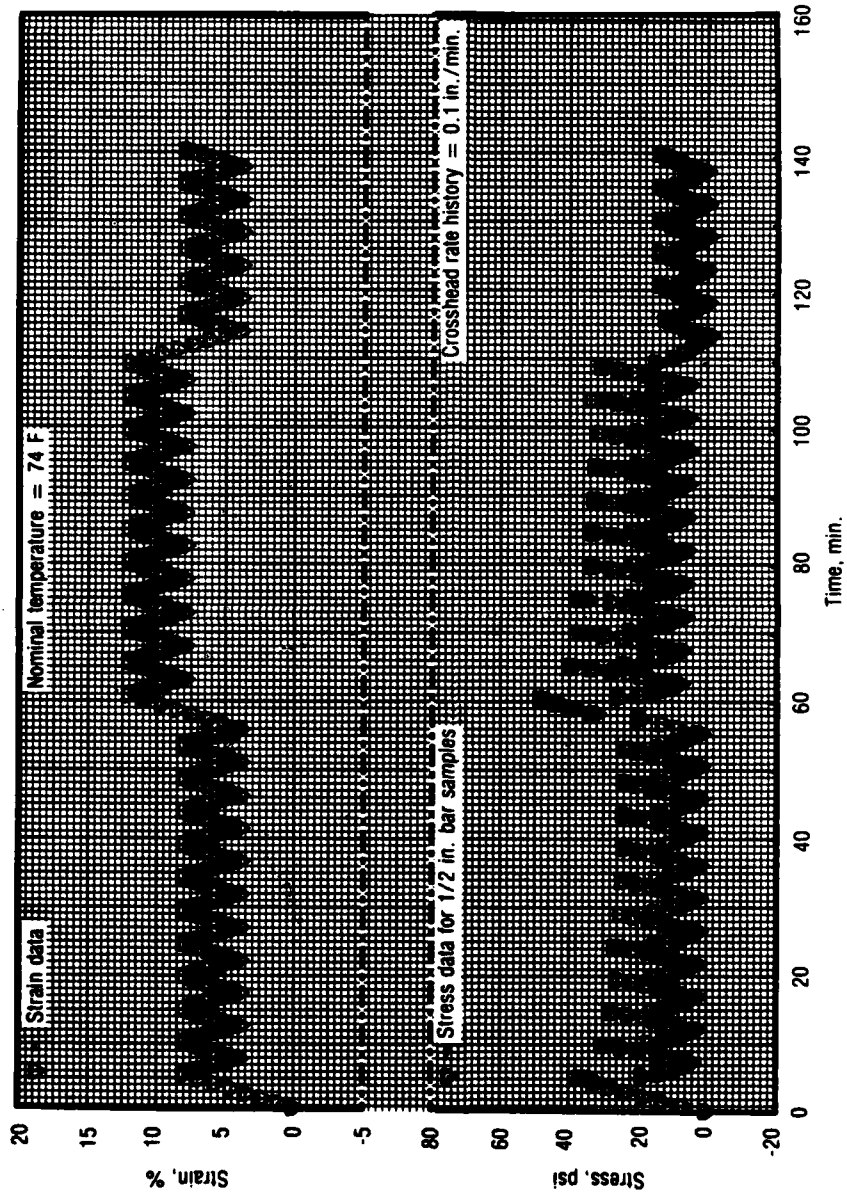


Figure 59. Test No. 20 - Stress While Cycling for UTP-19,360B-400/1777 for Complete Test

28821

TABLE 30. 1/2-IN. BAR STRESS WHILE CYCLING
(SHEET 1 OF 15)

PROPELLANT: UTP 19360B 400/1777
 REQUESTOR: Carlton Francis
 MOR: 2742-400-0000

DATE: 1/14/81
 INSTRATOR: JWD

DEFINITIONS: t = Time From Start of Test (min)
 σ = Stress (psi)
 ϵ = Strain (%)
 T (air) = Test Air Temperature (F)
 T (prop) = Test Propellant Temperature (F)

RELATIONSHIPS:
 $c = \frac{\text{Force}}{\text{Area}}$
 $\epsilon = \frac{\text{Sample Extension}}{\text{Length}}$

NOMINAL VALUES:
 Test Temp = 74 F
 Gage Length = 6.00 in
 Nom. Strain = 8.4, 12.8, 4, 8, 0 %
 XHD Rate = .1 in/Min

CALIBRATION DATA:
 Cal Wt = 10.0 lbs
 Load Cal (lbs/volts)
 Offset (volts)
 Pot Cal (in/volts) =
 Temp (F)

	SAMPLE 1	SAMPLE 2	3
Cal Wt	29.776	29.679	29.966
Load Cal	0.080	-0.012	0.036
Offset	-0.393		
Pot Cal	77.2		

AREAS (sq-in): 0.253 0.252 0.252

LOAD DIFFLECTION DATA (volts):

Line	Pat	Disp
0	0.0500	-0.001
1	0.69073	-0.176
2	1.37645	-0.351
3	2.06217	-0.525
4	2.74789	-0.700
5	3.43361	-0.875
6	4.11933	-1.050
7	4.80505	-1.225
8	5.49077	-1.400
9	6.17649	-1.575
10	6.86221	-1.750
11	7.54793	-1.925
12	8.23365	-2.100
13	8.91937	-2.275
14	9.60509	-2.450
15	10.29081	-2.625
16	10.97653	-2.800
17	11.66225	-2.975
18	12.34797	-3.150
19	13.03369	-3.325
20	13.71941	-3.500
21	14.40513	-3.675
22	15.09085	-3.850
23	15.77657	-4.025
24	16.46229	-4.200
25	17.14801	-4.375
26	17.83373	-4.550
27	18.51945	-4.725
28	19.20517	-4.900
29	19.89089	-5.075
30	20.57661	-5.250

TABLE 30. 1/2-IN. BAR STRESS WHILE CYCLING
(SHEET 2 OF 15)

31	11.69215	-0.690	0.122	0.025	0.075
32	12.05490	-0.598	0.109	0.010	0.062
33	12.39773	-0.591	0.147	0.054	0.100
34	12.74051	-0.779	0.168	0.074	0.121
35	13.08376	-0.1867	0.188	0.092	0.142
36	13.42624	-0.934	0.209	0.114	0.164
37	13.76949	-1.041	0.236	0.141	0.191
38	14.11250	-1.128	0.310	0.215	0.269
39	14.47511	-1.124	0.121	0.085	0.170
40	14.81803	-1.034	0.160	0.094	0.134
41	15.16114	-0.951	0.142	0.044	0.112
42	15.50364	-0.863	0.129	0.056	0.096
43	15.84717	-0.776	0.118	0.024	0.082
44	16.19245	-0.688	0.106	0.012	0.071
45	16.53945	-0.595	0.142	0.048	0.059
46	17.03753	-0.687	0.163	0.072	0.095
47	17.53038	-0.775	0.181	0.090	0.116
48	17.92369	-0.863	0.203	0.108	0.136
49	18.36606	-0.950	0.227	0.133	0.157
50	18.60919	-1.037	0.263	0.148	0.183
51	18.95166	-1.124	0.300	0.207	0.212
52	19.31323	-1.216	0.209	0.116	0.274
53	19.65618	-1.117	0.175	0.082	0.163
54	19.99925	-0.943	0.154	0.062	0.129
55	20.34244	-0.856	0.139	0.048	0.108
56	20.68484	-0.769	0.114	0.032	0.075
57	21.02751	-0.681	0.104	0.010	0.069
58	21.37077	-0.600	0.107	0.017	0.061
59	21.69569	-0.602	0.138	0.046	0.093
60	22.03863	-0.688	0.159	0.067	0.114
61	22.32164	-0.776	0.178	0.086	0.134
62	22.62419	-0.863	0.199	0.109	0.150
63	22.96710	-1.038	0.224	0.131	0.180
64	23.41033	-1.125	0.257	0.162	0.215
65	23.75287	-1.209	0.290	0.192	0.248
66	24.09591	-1.207	0.307	0.210	0.264
67	24.43905	-1.121	0.208	0.114	0.164
68	24.78195	-1.035	0.174	0.083	0.129
69	25.12460	-0.948	0.153	0.057	0.108
70	25.46800	-0.861	0.137	0.043	0.092
71	25.81034	-0.773	0.125	0.033	0.079
72	26.15294	-0.686	0.113	0.022	0.067
73	26.51768	-0.593	0.101	0.012	0.053
74	26.85828	-0.690	0.137	0.045	0.092
75	27.20153	-0.777	0.158	0.066	0.113
76	27.54412	-0.865	0.177	0.087	0.132
77	27.88735	-0.953	0.197	0.109	0.153
78	28.22959	-1.040	0.221	0.127	0.178
79	28.57258	-1.127	0.256	0.163	0.212
80	28.93549	-1.219	0.291	0.200	0.249
81	29.27824	-1.128	0.208	0.115	0.164
82	29.62146	-1.041	0.174	0.081	0.129
83	30.30720	-0.954	0.153	0.060	0.107
84	30.64994	-0.867	0.137	0.045	0.092
85	30.99282	-0.780	0.114	0.029	0.079
86	31.33500	-0.600	0.101	0.019	0.067
87					
88					
89					
90					

TABLE 30. 1/2-IN. BAR STRESS WHILE CYCLING
(SHEET 3 OF 15)

91	31.69814	-0.691	0.135	0.043	0.090
92	32.04118	-0.728	0.135	0.041	0.111
93	32.38296	-0.866	0.195	0.081	0.130
94	33.72879	-0.954	0.195	0.101	0.151
95	35.06544	-1.040	0.219	0.125	0.175
96	33.41208	-1.128	0.250	0.157	0.202
97	33.77510	-1.220	0.286	0.191	0.245
98	34.11826	-1.317	0.206	0.178	0.161
99	34.46080	-1.410	0.151	0.127	0.127
100	34.80374	-1.503	0.151	0.059	0.106
101	35.14670	-0.866	0.136	0.043	0.090
102	35.48994	-0.779	0.123	0.039	0.077
103	35.83240	-0.691	0.111	0.019	0.066
104	36.17523	-0.598	0.109	0.008	0.054
105	36.51865	-0.692	0.134	0.041	0.089
106	36.86115	-0.779	0.154	0.063	0.110
107	37.20373	-0.867	0.174	0.079	0.129
108	37.54681	-0.954	0.194	0.098	0.149
109	37.89055	-1.041	0.217	0.124	0.174
110	38.23521	-1.128	0.250	0.155	0.207
111	38.57927	-1.220	0.204	0.188	0.242
112	38.92327	-1.317	0.204	0.109	0.160
113	39.26725	-1.410	0.150	0.078	0.126
114	39.61125	-0.954	0.150	0.058	0.105
115	39.95460	-0.867	0.135	0.040	0.090
116	40.29804	-0.779	0.132	0.030	0.077
117	40.64166	-0.692	0.111	0.019	0.065
118	41.03509	-0.599	0.099	0.008	0.053
119	41.37791	-0.693	0.134	0.040	0.089
120	41.72090	-0.781	0.154	0.060	0.109
121	42.06418	-0.869	0.173	0.077	0.129
122	42.40658	-0.956	0.194	0.099	0.149
123	42.74937	-1.043	0.218	0.125	0.174
123A	43.09250	-1.130	0.250	0.154	0.202
125	43.43380	-1.222	0.284	0.184	0.243
126	43.79670	-1.313	0.202	0.105	0.157
127	44.13952	-1.407	0.170	0.074	0.124
128	44.48292	-0.949	0.149	0.055	0.104
129	44.82580	-0.862	0.134	0.040	0.088
130	45.16797	-0.775	0.121	0.029	0.075
131	45.51093	-0.687	0.110	0.017	0.065
132	45.84334	-0.602	0.109	0.006	0.052

TABLE 30. 1/2-IN. BAR STRESS WHILE CYCLING
(SHEET 4 OF 15)

133	45.85361	-0.603	0.191	0.010	0.056
134	46.19653	-0.690	0.133	0.040	0.087
135	46.53977	-0.777	0.153	0.056	0.108
136	46.88214	-0.865	0.172	0.077	0.127
137	47.22508	-0.952	0.192	0.097	0.147
138	47.56827	-1.040	0.216	0.121	0.172
139	47.91093	-1.127	0.248	0.152	0.204
140	48.27385	-1.214	0.282	0.185	0.238
141	48.61673	-1.301	0.303	0.167	0.158
142	48.95995	-1.387	0.170	0.076	0.125
143	49.30255	-0.953	0.149	0.057	0.104
144	49.64514	-0.866	0.134	0.039	0.088
145	49.98835	-0.778	0.121	0.026	0.075
146	50.33095	-0.691	0.109	0.015	0.063
147	50.69400	-0.598	0.097	0.004	0.051
148	51.03687	-0.490	0.132	0.016	0.087
149	51.37976	-0.777	0.153	0.038	0.107
150	51.72266	-0.865	0.172	0.075	0.126
151	52.06615	-0.953	0.191	0.096	0.146
152	52.40829	-1.040	0.215	0.119	0.170
153	52.75131	-1.127	0.247	0.149	0.203
154	53.11390	-1.214	0.280	0.180	0.237
155	53.45673	-1.301	0.202	0.105	0.157
156	53.80002	-1.040	0.169	0.071	0.124
157	54.14286	-0.953	0.149	0.053	0.103
158	54.48586	-0.866	0.133	0.037	0.087
159	54.82875	-0.778	0.120	0.024	0.074
160	55.17092	-0.691	0.108	0.015	0.063
161	55.51443	-0.603	0.097	0.009	0.052
162	55.85833	-0.607	0.103	0.009	0.058
163	56.20100	-0.781	0.152	0.027	0.107
164	56.54367	-0.957	0.191	0.036	0.142
165	57.02599	-1.131	0.246	0.150	0.202
166	58.28189	-1.304	0.358	0.262	0.318
167	58.98386	-1.479	0.413	0.314	0.373
168	59.68594	-1.657	0.450	0.349	0.409
169	60.37566	-1.841	0.487	0.385	0.446
170	60.71865	-1.748	0.301	0.204	0.257
171	61.06170	-1.659	0.247	0.151	0.202
172	61.40450	-1.570	0.216	0.120	0.170
173	61.74770	-1.482	0.193	0.098	0.148
174	62.09027	-1.394	0.177	0.080	0.138
175	62.43270	-1.307	0.163	0.067	0.118
176	62.77583	-1.219	0.150	0.054	0.103
177	62.81698	-1.220	0.158	0.060	0.113
178	63.16006	-1.307	0.192	0.077	0.148
179	63.50262	-1.394	0.218	0.125	0.173
180	63.84548	-1.482	0.244	0.149	0.199
181	64.18884	-1.570	0.273	0.179	0.229
182	64.53186	-1.660	0.311	0.213	0.267
183	64.87410	-1.749	0.363	0.264	0.326
184	65.23684	-1.842	0.418	0.317	0.376
185	65.58808	-1.750	0.283	0.193	0.239
186	65.92330	-1.662	0.234	0.137	0.189
187	66.26555	-1.573	0.204	0.109	0.159
188	66.60820	-1.485	0.185	0.089	0.139
189	66.95145	-1.397	0.170	0.070	0.122
190	67.29437	-1.309	0.157	0.062	0.110
191	67.63680	-1.221	0.145	0.051	0.099
192	67.67079	-1.212	0.144	0.049	0.097

TABLE 30. 1/2-IN. BAR STRESS WHILE CYCLING
(SHEET 5 OF 15)

193	67.68110	1.214	0.146	0.087	0.190
194	68.02414	1.302	0.207	0.110	0.136
195	68.36718	1.389	0.231	0.115	0.164
196	68.70974	1.476	0.257	0.161	0.214
197	69.05241	1.564	0.290	0.237	0.290
198	69.39534	1.654	0.335	0.281	0.337
199	69.73815	1.743	0.380	0.293	0.349
200	70.08162	1.835	0.426	0.275	0.327
201	70.42405	1.926	0.472	0.130	0.180
202	70.76712	2.019	0.519	0.103	0.152
203	71.11010	2.114	0.567	0.084	0.133
204	71.45257	2.207	0.614	0.070	0.118
205	71.79507	2.303	0.662	0.058	0.105
206	72.13819	2.400	0.710	0.046	0.094
207	72.48119	2.497	0.758	0.046	0.092
208	72.82423	2.594	0.806	0.079	0.130
209	73.16727	2.691	0.854	0.106	0.154
210	73.51027	2.788	0.902	0.127	0.177
211	73.85325	2.885	0.950	0.149	0.202
212	74.19620	2.982	1.000	0.174	0.233
213	74.53914	3.079	1.048	0.200	0.275
214	74.88206	3.176	1.096	0.224	0.317
215	75.22496	3.273	1.144	0.249	0.359
216	75.56782	3.370	1.192	0.271	0.392
217	75.91072	3.467	1.240	0.286	0.425
218	76.25362	3.564	1.288	0.311	0.467
219	76.59652	3.661	1.336	0.336	0.509
220	76.93942	3.758	1.384	0.361	0.551
221	77.28232	3.855	1.432	0.386	0.593
222	77.62522	3.952	1.480	0.411	0.635
223	77.96812	4.049	1.528	0.436	0.677
224	78.31102	4.146	1.576	0.461	0.719
225	78.65392	4.243	1.624	0.486	0.761
226	78.99682	4.340	1.672	0.511	0.803
227	79.33972	4.437	1.720	0.536	0.845
228	79.68262	4.534	1.768	0.561	0.887
229	80.02552	4.631	1.816	0.586	0.929
230	80.36842	4.728	1.864	0.611	0.971
231	80.71132	4.825	1.912	0.636	1.013
232	81.05422	4.922	1.960	0.661	1.055
233	81.39712	5.019	2.008	0.686	1.097
234	81.74002	5.116	2.056	0.711	1.139
235	82.08292	5.213	2.104	0.736	1.181
236	82.42582	5.310	2.152	0.761	1.223
237	82.76872	5.407	2.200	0.786	1.265
238	83.11162	5.504	2.248	0.811	1.307
239	83.45452	5.601	2.296	0.836	1.349
240	83.79742	5.698	2.344	0.861	1.391
241	84.14032	5.795	2.392	0.886	1.433
242	84.48322	5.892	2.440	0.911	1.475
243	84.82612	5.989	2.488	0.936	1.517
244	85.16902	6.086	2.536	0.961	1.559
245	85.51192	6.183	2.584	0.986	1.601
246	85.85482	6.280	2.632	1.011	1.643
247	86.19772	6.377	2.680	1.036	1.685
248	86.54062	6.474	2.728	1.061	1.727
249	86.88352	6.571	2.776	1.086	1.769
250	87.22642	6.668	2.824	1.111	1.811
251	87.56932	6.765	2.872	1.136	1.853
252	87.91222	6.862	2.920	1.161	1.895
253	88.25512	6.959	2.968	1.186	1.937

TABLE 30. 1/2-IN. BAR STRESS WHILE CYCLING
(SHEET 6 OF 15)

254	86.48366	-1.396	0.159	0.063	0.112
255	86.82636	-1.308	0.147	0.051	0.099
256	87.16879	-1.221	0.134	0.048	0.087
257	87.51110	-1.223	0.141	0.046	0.095
258	87.85424	-1.310	0.173	0.075	0.126
259	87.89750	-1.398	0.196	0.098	0.149
260	88.24031	-1.486	0.219	0.121	0.172
261	88.58294	-1.574	0.243	0.143	0.197
262	88.92570	-1.662	0.274	0.174	0.228
263	89.26830	-1.751	0.316	0.213	0.271
264	89.41104	-1.844	0.361	0.253	0.314
265	89.97389	-1.749	0.260	0.160	0.214
266	90.31715	-1.660	0.217	0.119	0.171
267	90.65963	-1.571	0.192	0.088	0.144
268	91.00313	-1.483	0.173	0.073	0.126
269	91.14572	-1.395	0.145	0.060	0.110
270	91.48815	-1.308	0.145	0.048	0.098
271	92.03160	-1.220	0.132	0.035	0.086
272	92.41599	-1.217	0.138	0.039	0.091
273	92.75875	-1.304	0.171	0.071	0.124
274	93.10115	-1.479	0.215	0.115	0.146
275	93.44418	-1.569	0.240	0.119	0.162
276	93.78690	-1.656	0.269	0.168	0.193
277	94.13026	-1.745	0.309	0.208	0.223
278	94.47266	-1.834	0.349	0.248	0.264
279	94.51115	-1.832	0.359	0.254	0.304
280	94.85648	-1.744	0.276	0.176	0.213
281	95.19885	-1.655	0.219	0.119	0.209
282	95.54230	-1.566	0.189	0.092	0.168
283	95.88524	-1.478	0.171	0.071	0.142
284	96.22789	-1.391	0.156	0.057	0.109
285	96.57071	-1.309	0.144	0.044	0.097
286	96.91355	-1.209	0.130	0.031	0.084
287	97.25667	-1.304	0.169	0.072	0.123
288	97.61854	-1.392	0.192	0.091	0.145
289	97.96165	-1.479	0.214	0.116	0.167
290	98.30405	-1.568	0.237	0.139	0.191
291	98.64723	-1.656	0.266	0.148	0.221
292	98.98996	-1.745	0.306	0.208	0.261
293	99.35204	-1.839	0.348	0.250	0.304
294	99.69545	-1.747	0.266	0.155	0.209
295	100.03721	-1.658	0.215	0.114	0.168
296	100.38059	-1.569	0.189	0.087	0.142
297	100.72343	-1.481	0.170	0.076	0.123
298	101.06668	-1.393	0.156	0.059	0.109
299	101.40969	-1.305	0.143	0.049	0.096
300	101.75201	-1.217	0.130	0.039	0.084
301	101.79533	-1.214	0.135	0.040	0.089
302	102.13879	-1.302	0.168	0.071	0.121
303	102.47835	-1.389	0.190	0.095	0.141
304	102.82107	-1.477	0.212	0.117	0.165
305	103.16400	-1.566	0.235	0.137	0.189
306	103.50675	-1.654	0.264	0.166	0.217
307	103.84983	-1.742	0.302	0.203	0.257
308	104.19229	-1.831	0.340	0.240	0.297
309	104.53299	-1.838	0.366	0.264	0.321
310	104.87618	-1.750	0.256	0.158	0.209
311	104.91883	-1.662	0.214	0.118	0.167
312	105.26146	-1.573	0.184	0.092	0.142

TABLE 30. 1/2-IN. BAR STRESS WHILE CYCLING
(SHEET 7 OF 15)

314	105.60444	-1.485	0.170	0.073	0.123
315	105.94774	-1.397	0.156	0.061	0.108
316	106.29054	-1.309	0.143	0.046	0.093
317	106.63323	-1.221	0.134	0.035	0.088
318	107.01948	-1.134	0.121	0.020	0.142
319	107.36178	-1.047	0.115	0.015	0.164
320	107.70476	-0.960	0.111	0.013	0.188
321	108.04770	-0.873	0.106	0.011	0.217
322	108.39058	-0.786	0.101	0.009	0.256
323	108.73310	-0.700	0.093	0.007	0.299
324	109.07600	-0.613	0.080	0.005	0.344
325	109.41885	-0.527	0.074	0.004	0.391
326	109.80496	-0.441	0.068	0.003	0.440
327	110.19023	-0.355	0.064	0.002	0.491
328	110.57603	-0.270	0.060	0.002	0.544
329	111.16238	-0.184	0.057	0.001	0.599
330	111.86238	-0.098	0.054	0.001	0.656
331	112.54743	0.000	0.051	0.000	0.714
332	113.23370	0.086	0.048	0.000	0.773
333	113.90282	0.171	0.045	0.000	0.833
334	114.59879	0.256	0.042	0.000	0.894
335	114.94216	0.341	0.040	0.000	0.956
336	115.28495	0.426	0.038	0.000	1.019
337	115.62779	0.511	0.036	0.000	1.083
338	115.97046	0.596	0.034	0.000	1.148
339	116.31235	0.681	0.032	0.000	1.214
340	116.65557	0.766	0.030	0.000	1.281
341	116.99854	0.851	0.028	0.000	1.349
342	117.34157	0.936	0.026	0.000	1.417
343	117.68433	1.021	0.024	0.000	1.486
344	118.02685	1.106	0.022	0.000	1.556
345	118.36969	1.191	0.020	0.000	1.627
346	118.71300	1.276	0.018	0.000	1.699
347	119.05659	1.361	0.016	0.000	1.773
348	119.40001	1.446	0.014	0.000	1.848
349	119.74239	1.531	0.012	0.000	1.924
350	120.08500	1.616	0.010	0.000	2.001
351	120.42846	1.701	0.008	0.000	2.079
352	120.77066	1.786	0.006	0.000	2.158
353	121.11370	1.871	0.004	0.000	2.238
354	121.47650	1.956	0.002	0.000	2.319
355	121.81948	2.041	0.001	0.000	2.401
356	122.16266	2.126	0.000	0.000	2.484
357	122.50503	2.211	0.000	0.000	2.568
358	122.84802	2.296	0.000	0.000	2.653
359	123.19144	2.381	0.000	0.000	2.739
360	123.51307	2.466	0.000	0.000	2.826
361	123.82342	2.551	0.000	0.000	2.914
362	124.13342	2.636	0.000	0.000	3.003
363	124.20911	2.721	0.000	0.000	3.093
364	124.55249	2.806	0.000	0.000	3.184
365	124.89486	2.891	0.000	0.000	3.276
366	125.23819	2.976	0.000	0.000	3.369
367	125.58055	3.061	0.000	0.000	3.463
368	125.94280	3.146	0.000	0.000	3.558
369	126.28570	3.231	0.000	0.000	3.654
370					
371					
372					
373					

TABLE 30. 1/2-IN. BAR STRESS WHILE CYCLING
(SHEET 8 OF 15)

374	126.62850	-1.038	0.140	0.042	0.092
375	126.97140	-0.951	0.126	0.028	0.079
376	127.31448	-0.863	0.115	0.019	0.062
377	127.65706	-0.775	0.105	0.007	0.056
378	128.00000	-0.688	0.095	-0.004	0.038
379	128.34300	-0.595	0.085	-0.016	0.038
380	128.68626	-0.502	0.116	0.018	0.069
381	129.02909	-0.410	0.133	0.033	0.086
382	129.37209	-0.318	0.147	0.049	0.100
383	129.71432	-0.226	0.160	0.058	0.114
384	130.05760	-0.134	0.173	0.071	0.127
385	130.40069	-0.042	0.187	0.087	0.140
386	130.74319	0.050	0.200	0.099	0.153
387	130.76350	0.142	0.198	0.095	0.151
388	131.10642	0.234	0.159	0.059	0.113
389	131.44955	0.326	0.141	0.040	0.094
390	131.79233	0.418	0.127	0.030	0.080
391	132.13514	0.510	0.115	0.018	0.068
392	132.47798	0.602	0.105	0.010	0.059
393	132.82093	0.694	0.096	-0.001	0.049
394	133.16310	0.786	0.087	-0.012	0.039
395	133.50340	0.878	0.089	-0.009	0.042
396	133.84667	0.970	0.115	0.019	0.069
397	134.18950	1.062	0.132	0.034	0.086
398	134.53217	1.154	0.147	0.049	0.101
399	134.87468	1.246	0.159	0.063	0.114
400	135.21799	1.338	0.174	0.077	0.127
401	135.56112	1.430	0.188	0.088	0.141
402	135.90444	1.522	0.201	0.099	0.154
403	135.90052	1.614	0.199	0.099	0.152
404	136.24318	1.706	0.160	0.062	0.113
405	136.58615	1.798	0.141	0.046	0.095
406	136.92950	1.890	0.127	0.031	0.080
407	137.27200	1.982	0.115	0.019	0.069
408	137.61480	2.074	0.105	0.010	0.058
409	137.95777	2.166	0.096	0.009	0.049
410	138.30040	2.258	0.086	-0.009	0.039
411	138.64273	2.350	0.088	-0.007	0.042
412	138.98513	2.442	0.115	0.020	0.069
413	139.02861	2.534	0.132	0.031	0.085
414	139.37078	2.626	0.146	0.045	0.100
415	139.71382	2.718	0.160	0.055	0.113
416	140.05702	2.810	0.172	0.071	0.127
417	140.39932	2.902	0.186	0.084	0.140
418	140.74162	3.000	0.201	0.097	0.155

TABLE 30. 1/2-IN. BAR STRESS WHILE CYCLING
(SHEET 9 OF 15)

STRESS SET	T (psi)	T (prop)	T (air)	Strain	SAMPLE 1	SAMPLE 2	SAMPLE 3	Avg	St Dev
1	0.00500	77.2	76.3	0.015	-0.14	-0.19	-0.11	-0.15	0.028
2	0.49071	76.9	76.0	1.30	6.62	6.32	7.02	6.89	0.142
3	1.37645	76.5	76.1	2.34	12.67	12.85	13.01	12.82	0.174
4	2.06274	76.6	76.1	3.49	23.01	22.92	23.63	23.19	0.294
5	2.74785	76.3	75.8	4.54	27.24	27.65	28.45	27.98	0.458
6	3.43359	76.6	76.0	5.88	32.51	31.44	32.20	32.38	0.628
7	4.11977	76.2	76.0	7.97	36.85	35.75	35.18	34.59	0.804
8	4.79166	76.3	75.9	7.41	38.87	38.06	38.72	38.54	0.926
9	5.47779	76.2	76.0	6.27	41.06	40.47	41.71	41.76	1.044
10	6.16369	76.3	75.9	5.71	43.03	42.47	43.61	43.76	1.162
11	6.84910	76.2	76.0	4.95	45.53	44.95	46.11	45.71	1.280
12	7.53447	76.3	76.0	3.97	48.12	47.52	48.68	48.36	1.398
13	8.21987	76.2	76.0	3.54	50.82	49.82	51.00	50.59	1.516
14	8.90522	76.3	76.0	3.11	53.54	52.54	53.72	53.31	1.634
15	9.59055	76.4	76.1	2.63	56.27	55.27	56.45	56.04	1.752
16	10.27588	76.3	76.1	2.19	59.02	57.73	58.90	58.50	1.870
17	10.96121	76.4	76.0	1.74	61.78	60.23	61.40	61.00	1.988
18	11.64654	76.3	76.0	1.29	64.55	62.95	64.12	63.72	2.106
19	12.33187	76.2	76.0	0.84	67.32	65.65	66.82	66.42	2.224
20	13.01720	76.4	76.1	0.39	70.09	68.35	69.52	69.12	2.342
21	13.70253	76.3	76.0	0.00	72.86	71.05	72.22	71.82	2.460
22	14.38786	76.4	76.1	0.45	75.63	73.75	74.92	74.52	2.578
23	15.07319	76.2	76.0	0.90	78.40	76.46	77.63	77.23	2.696
24	15.75852	76.4	76.1	1.35	81.17	79.17	80.34	79.94	2.814
25	16.44385	76.3	76.0	1.80	83.94	81.88	83.05	82.65	2.932
26	17.12918	76.4	76.1	2.25	86.71	84.59	85.76	85.36	3.050
27	17.81451	76.2	76.0	2.70	89.48	87.30	88.47	88.07	3.168
28	18.50000	76.3	76.0	3.15	92.25	90.01	91.18	90.78	3.286
29	19.18549	76.4	76.1	3.60	95.02	92.72	93.89	93.49	3.404
30	19.87098	76.2	76.0	4.05	97.79	95.43	96.60	96.20	3.522
31	20.55647	76.4	76.1	4.50	100.56	98.14	99.31	98.91	3.640
32	21.24196	76.3	76.0	4.95	103.33	100.85	102.02	101.62	3.758
33	21.92745	76.4	76.1	5.40	106.10	103.56	104.73	104.33	3.876
34	22.61294	76.2	76.0	5.85	108.87	106.27	107.44	107.04	3.994
35	23.29843	76.4	76.1	6.30	111.64	108.98	110.15	109.75	4.112
36	23.98392	76.3	76.0	6.75	114.41	111.69	112.82	112.42	4.230
37	24.66941	76.4	76.1	7.20	117.18	114.40	115.49	115.09	4.348
38	25.35490	76.2	76.0	7.65	119.95	117.11	118.16	117.76	4.466
39	26.04039	76.4	76.1	8.10	122.72	119.82	120.87	120.47	4.584
40	26.72588	76.3	76.0	8.55	125.49	122.53	123.58	123.18	4.702
41	27.41137	76.4	76.1	9.00	128.26	125.24	126.29	125.89	4.820
42	28.09686	76.2	76.0	9.45	131.03	127.95	128.84	128.44	4.938
43	28.78235	76.4	76.1	9.90	133.80	130.66	131.39	130.99	5.056
44	29.46784	76.3	76.0	10.35	136.57	133.37	134.42	134.02	5.174
45	30.15333	76.4	76.1	10.80	139.34	136.08	137.13	136.73	5.292
46	30.83882	76.2	76.0	11.25	142.11	138.79	139.84	139.44	5.410
47	31.52431	76.4	76.1	11.70	144.88	141.50	142.59	142.19	5.528
48	32.20980	76.3	76.0	12.15	147.65	144.21	145.30	144.90	5.646
49	32.89529	76.4	76.1	12.60	150.42	146.92	148.01	147.61	5.764
50	33.58078	76.2	76.0	13.05	153.19	149.63	150.72	150.32	5.882
51	34.26627	76.4	76.1	13.50	155.96	152.34	153.43	153.03	6.000
52	34.95176	76.3	76.0	13.95	158.73	155.05	156.14	155.74	6.118
53	35.63725	76.4	76.1	14.40	161.50	157.76	158.85	158.45	6.236
54	36.32274	76.2	76.0	14.85	164.27	160.47	161.56	161.16	6.354
55	37.00823	76.4	76.1	15.30	167.04	163.18	164.27	163.87	6.472
56	37.69372	76.3	76.0	15.75	169.81	165.89	166.98	166.58	6.590
57	38.37921	76.4	76.1	16.20	172.58	168.60	169.69	169.29	6.708
58	39.06470	76.2	76.0	16.65	175.35	171.31	172.36	171.96	6.826
59	39.75019	76.4	76.1	17.10	178.12	174.02	175.07	174.67	6.944

TABLE 30. 1/2-IN. BAR STRESS WHILE CYCLING
(SHEET 10 OF 15)

60	21.68537	76.6	76.1	3.93	2.82	2.66	2.48	2.66	0.121
61	21.69569	77.1	76.2	3.51	3.13	3.39	2.97	3.16	0.121
62	22.13863	76.5	76.2	4.08	4.83	4.80	4.26	4.30	0.087
63	22.72419	76.5	76.0	5.08	9.33	9.36	9.21	9.36	0.007
64	23.06710	76.5	76.2	6.23	11.56	11.57	11.05	11.56	0.101
65	23.41033	76.4	76.2	6.40	14.94	14.84	14.05	14.94	0.074
66	23.75287	76.7	76.4	7.92	20.89	20.46	17.05	16.94	0.249
67	24.09591	76.3	76.3	7.91	24.78	23.97	21.15	20.84	0.421
68	24.43905	76.8	76.3	7.35	26.78	26.15	27.02	26.65	0.319
69	24.78195	76.3	76.3	6.78	15.11	14.80	15.14	15.02	0.132
70	25.12460	76.7	76.3	6.21	11.09	11.17	11.03	11.10	0.048
71	25.46800	76.9	76.3	6.60	8.60	8.18	8.50	8.43	0.155
72	25.81034	76.1	76.1	6.25	6.74	6.54	6.50	6.54	0.094
73	26.15294	76.1	76.1	5.07	5.25	4.79	5.04	5.19	0.149
74	26.51526	76.1	76.1	4.89	3.46	4.07	3.65	3.87	0.214
75	26.85828	76.4	76.4	4.52	2.46	2.74	2.19	2.48	0.041
76	27.20133	76.4	76.4	5.09	6.18	6.22	6.9	6.72	0.064
77	27.54412	76.8	76.2	5.67	11.40	11.63	11.38	11.47	0.097
78	27.88735	76.8	76.2	6.24	13.80	14.13	13.86	13.93	0.124
79	28.22959	76.9	76.4	7.18	16.65	16.39	16.84	16.62	0.158
80	28.57255	76.9	76.4	7.38	20.61	20.34	20.89	20.69	0.125
81	28.91549	76.8	76.4	7.99	24.83	24.98	25.19	25.00	0.126
82	29.25822	76.8	76.4	7.32	15.11	14.97	15.07	15.07	0.067
83	29.60114	77.1	76.4	6.82	11.12	10.94	11.00	11.02	0.065
84	29.94412	77.1	76.4	6.25	8.58	8.54	8.43	8.43	0.059
85	30.28720	77.0	76.3	5.11	6.20	6.71	6.57	6.65	0.118
86	30.63028	77.1	76.5	4.34	3.52	3.69	3.19	3.29	0.097
87	30.97344	77.2	76.5	4.53	6.44	6.45	6.83	6.77	0.122
88	31.31652	77.2	76.4	5.67	11.19	11.23	11.08	11.08	0.083
89	31.65968	77.3	76.4	6.82	13.33	13.23	13.48	13.46	0.103
90	32.00282	77.1	76.4	7.99	16.21	16.19	16.48	16.39	0.114
91	32.34594	77.1	76.4	7.38	20.21	20.18	20.42	20.30	0.119
92	32.68914	77.1	76.5	7.38	24.18	24.14	24.48	24.38	0.151
93	33.03230	77.1	76.5	7.38	14.80	14.43	14.88	14.74	0.117
94	33.37550	77.1	76.5	10.89	10.89	10.56	10.78	10.74	0.149
95	33.71874	77.1	76.5	6.83	6.83	6.32	6.27	6.33	0.083
96	34.06194	77.1	76.5	5.68	6.60	6.45	6.36	6.47	0.088
97	34.40514	77.2	76.5	5.10	5.08	4.86	4.92	4.92	0.098
98	34.74834	77.3	76.5	4.53	3.23	3.63	3.05	3.20	0.100
99	35.09154	77.3	76.6	4.53	2.42	2.55	2.88	2.89	0.062
100	35.43474	77.5	76.6	5.10	8.78	8.78	8.69	8.75	0.039
101	35.77794	77.5	76.6	11.06	11.06	10.77	10.97	10.93	0.104
102	36.12114	77.1	76.6	16.21	16.21	16.01	16.24	16.17	0.102
103	36.46434	77.0	76.6	20.06	20.06	19.64	19.98	19.98	0.212
104	36.80754	77.0	76.6	24.15	24.15	23.49	24.43	24.42	0.170
105	37.15074	77.0	76.6	18.28	18.28	18.28	18.65	18.65	0.065
106	37.49394	77.0	76.6	18.28	18.28	18.28	18.65	18.65	0.043
107	37.83714	77.0	76.6	6.45	6.45	6.14	6.30	6.30	0.110
108	38.18034	76.8	76.6	4.53	4.53	4.4	4.58	4.58	0.062
109	38.52354	76.8	76.6	4.53	4.53	4.4	4.58	4.58	0.039
110	38.86674	76.8	76.6	4.53	4.53	4.4	4.58	4.58	0.039
111	39.20994	76.8	76.6	4.53	4.53	4.4	4.58	4.58	0.039
112	39.55314	76.8	76.6	4.53	4.53	4.4	4.58	4.58	0.039
113	39.89634	76.8	76.6	4.53	4.53	4.4	4.58	4.58	0.039
114	40.23954	76.8	76.6	4.53	4.53	4.4	4.58	4.58	0.039
115	40.58274	76.8	76.6	4.53	4.53	4.4	4.58	4.58	0.039
116	40.92594	76.8	76.6	4.53	4.53	4.4	4.58	4.58	0.039
117	41.26914	76.8	76.6	4.53	4.53	4.4	4.58	4.58	0.039
118	41.61234	76.8	76.6	4.53	4.53	4.4	4.58	4.58	0.039
119	41.95554	76.8	76.6	4.53	4.53	4.4	4.58	4.58	0.039
120	42.29874	76.8	76.6	4.53	4.53	4.4	4.58	4.58	0.039

TABLE 30. 1/2-IN. BAR STRESS WHILE CYCLING
(SHEET 11 OF 15)

121	42.06418	76.4	76.2	5.62	10.94	10.94	10.94	10.79	0.185
122	42.40659	76.1	76.1	6.84	13.41	13.41	13.41	13.30	0.117
123	43.09250	76.1	75.9	6.74	16.27	16.27	16.27	16.23	0.091
124	43.45380	76.1	75.8	8.01	20.08	20.08	20.08	19.97	0.206
125	44.22670	75.8	75.9	7.36	14.56	14.56	14.56	14.41	0.211
126	44.13952	76.0	75.6	6.22	10.19	10.19	10.19	10.36	0.093
127	44.48292	76.0	75.8	5.08	6.85	6.85	6.85	6.47	0.088
128	45.16797	75.7	75.6	5.49	3.21	3.21	3.21	3.40	0.118
129	45.84334	75.7	75.5	3.94	2.52	2.52	2.52	2.08	0.109
130	45.85361	75.8	75.5	3.95	2.53	2.53	2.53	2.49	0.125
131	46.53977	75.2	75.6	5.52	6.08	6.08	6.08	6.37	0.172
132	46.88214	75.8	75.9	5.67	6.62	6.62	6.62	8.37	0.204
133	47.22507	75.7	75.6	6.24	10.90	10.90	10.90	10.73	0.129
134	47.56827	75.8	75.7	6.81	13.25	13.25	13.25	13.08	0.137
135	47.91093	75.6	75.8	7.38	16.83	16.83	16.83	17.67	0.180
136	48.27385	75.7	75.7	7.38	16.83	16.83	16.83	17.67	0.180
137	48.61673	75.6	75.7	8.81	24.53	24.53	24.53	24.35	0.288
138	48.95925	75.6	75.6	6.25	10.65	10.65	10.65	14.35	0.178
139	49.30219	75.6	75.6	6.67	11.16	11.16	11.16	10.50	0.103
140	49.68835	75.6	75.6	5.13	6.34	6.34	6.34	8.05	0.097
141	50.39400	75.9	75.8	5.53	4.85	4.85	4.85	6.15	0.131
142	51.10087	75.8	75.9	3.44	2.00	2.00	2.00	4.64	0.104
143	51.37978	75.8	75.8	3.09	1.56	1.56	1.56	4.30	0.074
144	52.24015	75.8	76.0	6.24	18.83	18.83	18.83	1.88	0.074
145	52.40829	75.9	76.0	6.81	19.63	19.63	19.63	1.88	0.186
146	52.75130	75.9	75.9	7.38	23.79	23.79	23.79	8.39	0.110
147	53.11190	75.9	75.9	7.99	27.99	27.99	27.99	8.39	0.190
148	53.48066	75.9	75.9	6.24	18.83	18.83	18.83	10.57	0.172
149	53.84886	75.9	75.9	6.81	19.63	19.63	19.63	15.73	0.188
150	54.17072	75.9	75.9	7.38	23.79	23.79	23.79	19.42	0.230
151	54.51443	76.2	75.7	7.99	27.99	27.99	27.99	23.79	0.283
152	54.85866	76.2	75.8	6.24	18.83	18.83	18.83	19.42	0.283
153	55.17072	76.2	75.8	6.81	19.63	19.63	19.63	23.79	0.283
154	55.55532	76.2	75.9	7.38	23.79	23.79	23.79	23.79	0.300
155	55.92974	76.2	75.9	7.99	27.99	27.99	27.99	23.79	0.300
156	56.30386	76.2	75.9	8.56	32.10	32.10	32.10	23.79	0.300
157	56.66994	76.2	76.2	9.06	36.21	36.21	36.21	23.79	0.300
158	57.03866	76.2	76.2	11.45	44.47	44.47	44.47	23.79	0.300
159	57.40994	76.2	76.2	10.87	42.68	42.68	42.68	23.79	0.300
160	57.78386	76.2	76.2	11.45	44.47	44.47	44.47	23.79	0.300
161	58.16070	76.2	76.2	10.87	42.68	42.68	42.68	23.79	0.300
162	58.54050	76.2	76.2	10.87	42.68	42.68	42.68	23.79	0.300
163	58.92320	76.2	76.2	10.87	42.68	42.68	42.68	23.79	0.300
164	59.30870	76.2	76.2	10.87	42.68	42.68	42.68	23.79	0.300
165	59.69690	76.2	76.2	10.87	42.68	42.68	42.68	23.79	0.300
166	60.08860	76.2	76.2	10.87	42.68	42.68	42.68	23.79	0.300
167	60.48380	76.2	76.2	10.87	42.68	42.68	42.68	23.79	0.300
168	60.88240	76.2	76.2	10.87	42.68	42.68	42.68	23.79	0.300
169	61.28440	76.2	76.2	10.87	42.68	42.68	42.68	23.79	0.300
170	61.68980	76.2	76.2	10.87	42.68	42.68	42.68	23.79	0.300
171	62.09860	76.2	76.2	10.87	42.68	42.68	42.68	23.79	0.300
172	62.51080	76.2	76.2	10.87	42.68	42.68	42.68	23.79	0.300
173	62.92640	76.2	76.2	10.87	42.68	42.68	42.68	23.79	0.300
174	63.34540	76.2	76.2	10.87	42.68	42.68	42.68	23.79	0.300
175	63.76780	76.2	76.2	10.87	42.68	42.68	42.68	23.79	0.300
176	64.19360	76.2	76.2	10.87	42.68	42.68	42.68	23.79	0.300
177	64.62280	76.2	76.2	10.87	42.68	42.68	42.68	23.79	0.300
178	65.05540	76.2	76.2	10.87	42.68	42.68	42.68	23.79	0.300
179	65.49140	76.2	76.2	10.87	42.68	42.68	42.68	23.79	0.300
180	65.93080	76.2	76.2	10.87	42.68	42.68	42.68	23.79	0.300

TABLE 30. 1/2-IN. BAR STRESS WHILE CYCLING
(SHEET 12 OF 15)

181	64.18884	76.4	76.4	10.29	22.77	22.44	22.82	0.160
182	64.87410	76.4	76.4	10.46	22.76	22.44	22.77	0.146
183	65.23684	76.4	76.4	11.07	22.86	22.44	22.77	0.146
184	65.58008	76.4	76.4	11.47	22.86	22.44	22.77	0.146
185	65.92320	76.4	76.4	11.89	22.86	22.44	22.77	0.146
186	66.26555	76.4	76.4	12.30	22.86	22.44	22.77	0.146
187	66.60820	76.4	76.4	12.73	22.86	22.44	22.77	0.146
188	66.95145	76.4	76.4	13.15	22.86	22.44	22.77	0.146
189	67.29457	76.4	76.4	13.58	22.86	22.44	22.77	0.146
190	67.63680	76.4	76.4	14.00	22.86	22.44	22.77	0.146
191	67.97879	76.4	76.4	14.42	22.86	22.44	22.77	0.146
192	68.32079	76.4	76.4	14.85	22.86	22.44	22.77	0.146
193	68.66279	76.4	76.4	15.27	22.86	22.44	22.77	0.146
194	69.00479	76.4	76.4	15.70	22.86	22.44	22.77	0.146
195	69.34679	76.4	76.4	16.12	22.86	22.44	22.77	0.146
196	69.68879	76.4	76.4	16.55	22.86	22.44	22.77	0.146
197	70.03079	76.4	76.4	16.97	22.86	22.44	22.77	0.146
198	70.37279	76.4	76.4	17.40	22.86	22.44	22.77	0.146
199	70.71479	76.4	76.4	17.82	22.86	22.44	22.77	0.146
200	71.05679	76.4	76.4	18.25	22.86	22.44	22.77	0.146
201	71.39879	76.4	76.4	18.67	22.86	22.44	22.77	0.146
202	71.74079	76.4	76.4	19.10	22.86	22.44	22.77	0.146
203	72.08279	76.4	76.4	19.52	22.86	22.44	22.77	0.146
204	72.42479	76.4	76.4	19.95	22.86	22.44	22.77	0.146
205	72.76679	76.4	76.4	20.37	22.86	22.44	22.77	0.146
206	73.10879	76.4	76.4	20.80	22.86	22.44	22.77	0.146
207	73.45079	76.4	76.4	21.22	22.86	22.44	22.77	0.146
208	73.79279	76.4	76.4	21.65	22.86	22.44	22.77	0.146
209	74.13479	76.4	76.4	22.07	22.86	22.44	22.77	0.146
210	74.47679	76.4	76.4	22.50	22.86	22.44	22.77	0.146
211	74.81879	76.4	76.4	22.92	22.86	22.44	22.77	0.146
212	75.16079	76.4	76.4	23.35	22.86	22.44	22.77	0.146
213	75.50279	76.4	76.4	23.77	22.86	22.44	22.77	0.146
214	75.84479	76.4	76.4	24.20	22.86	22.44	22.77	0.146
215	76.18679	76.4	76.4	24.62	22.86	22.44	22.77	0.146
216	76.52879	76.4	76.4	25.05	22.86	22.44	22.77	0.146
217	76.87079	76.4	76.4	25.47	22.86	22.44	22.77	0.146
218	77.21279	76.4	76.4	25.90	22.86	22.44	22.77	0.146
219	77.55479	76.4	76.4	26.32	22.86	22.44	22.77	0.146
220	77.89679	76.4	76.4	26.75	22.86	22.44	22.77	0.146
221	78.23879	76.4	76.4	27.17	22.86	22.44	22.77	0.146
222	78.58079	76.4	76.4	27.60	22.86	22.44	22.77	0.146
223	78.92279	76.4	76.4	28.02	22.86	22.44	22.77	0.146
224	79.26479	76.4	76.4	28.45	22.86	22.44	22.77	0.146
225	79.60679	76.4	76.4	28.87	22.86	22.44	22.77	0.146
226	79.94879	76.4	76.4	29.30	22.86	22.44	22.77	0.146
227	80.29079	76.4	76.4	29.72	22.86	22.44	22.77	0.146
228	80.63279	76.4	76.4	30.15	22.86	22.44	22.77	0.146
229	80.97479	76.4	76.4	30.57	22.86	22.44	22.77	0.146
230	81.31679	76.4	76.4	31.00	22.86	22.44	22.77	0.146
231	81.65879	76.4	76.4	31.42	22.86	22.44	22.77	0.146
232	82.00079	76.4	76.4	31.85	22.86	22.44	22.77	0.146
233	82.34279	76.4	76.4	32.27	22.86	22.44	22.77	0.146
234	82.68479	76.4	76.4	32.70	22.86	22.44	22.77	0.146
235	83.02679	76.4	76.4	33.12	22.86	22.44	22.77	0.146
236	83.36879	76.4	76.4	33.55	22.86	22.44	22.77	0.146
237	83.71079	76.4	76.4	33.97	22.86	22.44	22.77	0.146
238	84.05279	76.4	76.4	34.40	22.86	22.44	22.77	0.146
239	84.39479	76.4	76.4	34.82	22.86	22.44	22.77	0.146
240	84.73679	76.4	76.4	35.25	22.86	22.44	22.77	0.146
241	85.07879	76.4	76.4	35.67	22.86	22.44	22.77	0.146

TABLE 30. 1/2-IN. BAR STRESS WHILE CYCLING
(SHEET 13 OF 15)

243	82	34858	75.9	76.3	7.92	4.14	5.89	6.02	6.09	0.164
244	82	62210	75.9	76.4	8.57	11.12	10.72	10.63	10.91	0.135
245	83	03434	75.9	76.2	9.14	13.86	13.80	13.68	13.56	0.218
246	83	72000	75.7	76.3	9.72	16.51	16.28	16.28	16.19	0.257
247	84	06339	75.6	76.3	10.88	19.49	19.21	19.30	19.27	0.166
248	84	40370	75.6	76.2	10.88	23.13	23.01	23.01	22.78	0.357
249	84	76873	75.6	76.2	11.46	28.02	28.90	28.20	27.71	0.507
250	85	11190	75.6	76.2	12.07	33.21	31.87	33.42	32.93	0.674
251	85	45476	75.7	76.2	10.88	16.53	20.51	16.42	16.19	0.421
252	85	79725	75.7	76.2	10.88	16.53	13.56	13.02	13.09	0.344
253	86	14009	75.8	76.2	9.73	11.13	10.23	10.78	10.71	0.316
254	86	48366	75.6	76.2	9.15	7.85	9.79	9.93	9.90	0.177
255	86	82636	75.6	76.2	8.00	7.42	7.95	7.47	7.56	0.185
256	87	16879	75.6	76.4	8.01	6.22	6.80	6.90	6.97	0.156
257	87	21110	75.7	76.4	8.58	7.98	8.26	10.61	10.62	0.254
258	87	87750	75.7	76.4	9.19	13.67	13.92	13.41	13.33	0.268
259	88	24031	75.8	76.4	9.73	16.23	15.26	16.09	16.04	0.228
260	88	58294	75.7	76.3	10.32	19.23	18.85	19.04	18.86	0.372
261	88	92570	75.7	76.3	10.89	22.81	21.85	22.76	22.48	0.386
262	89	26830	75.8	76.1	11.47	27.85	26.47	27.82	27.38	0.556
263	89	63106	75.7	76.4	12.08	33.16	31.36	33.97	32.59	0.756
264	89	97389	75.8	76.4	11.46	21.26	20.21	21.07	20.86	0.393
265	90	65963	75.9	76.3	10.88	16.21	15.41	16.96	16.60	0.389
266	90	31715	75.9	76.5	9.72	13.91	11.76	12.83	12.60	0.320
267	91	00313	75.9	76.3	9.72	13.91	10.52	10.79	10.60	0.323
268	91	34572	75.9	76.4	9.14	9.26	9.74	9.85	9.85	0.264
269	91	68815	75.9	76.4	8.57	7.14	7.46	7.44	7.37	0.227
270	92	03160	75.7	76.5	7.99	6.14	6.00	5.89	5.84	0.191
271	92	07254	75.7	76.4	7.98	6.14	6.00	5.89	5.84	0.197
272	92	41599	75.9	76.4	8.55	7.39	8.00	7.38	7.29	0.219
273	92	75975	75.9	76.4	9.12	13.79	12.41	13.09	12.95	0.353
274	93	10115	76.1	76.3	9.98	15.91	14.93	15.72	15.52	0.359
275	93	44418	75.8	76.4	10.85	18.28	17.73	18.65	18.41	0.441
276	93	78690	75.8	76.6	10.85	20.72	21.14	20.55	20.41	0.441
277	94	13026	75.9	76.4	11.44	27.01	25.85	26.99	26.62	0.464
278	94	47266	75.9	76.4	12.00	32.22	30.51	32.81	32.32	0.498
279	94	51315	76.0	76.5	12.00	32.22	31.74	32.48	32.31	0.498
280	94	85646	76.0	76.4	11.43	20.87	19.76	20.48	20.31	0.358
281	95	19885	76.0	76.3	10.26	12.84	12.28	12.56	12.56	0.198
282	95	54230	76.0	76.2	10.26	12.84	12.76	12.56	12.56	0.198
283	95	88524	76.1	76.5	9.11	8.97	8.08	8.71	8.55	0.300
284	96	22789	76.0	76.5	8.53	7.49	6.64	7.10	7.10	0.303
285	96	52071	76.0	76.5	8.53	7.49	6.64	7.10	7.10	0.303
286	96	93266	76.4	76.5	7.92	5.93	5.61	5.61	5.64	0.285
287	97	27567	76.2	76.5	8.55	13.16	12.95	13.24	13.24	0.198
288	97	61854	76.1	76.5	9.16	15.78	15.07	16.24	16.46	0.392
289	97	96145	76.0	76.4	9.16	15.78	15.07	16.24	16.46	0.392
290	98	30405	76.0	76.4	10.27	18.55	17.78	18.35	18.23	0.385
291	98	64725	76.1	76.6	11.43	21.97	20.84	21.65	21.66	0.303
292	98	98996	76.1	76.6	11.43	21.97	20.84	21.65	21.66	0.303
293	99	35204	76.4	76.4	11.45	20.78	19.51	20.55	20.48	0.472
294	99	69545	76.4	76.4	11.45	20.78	19.51	20.55	20.48	0.472
295	100	03771	76.2	76.4	10.87	12.86	11.69	12.54	12.44	0.272
296	100	38059	76.4	76.4	10.28	12.86	11.69	12.54	12.44	0.420
297	100	72345	76.3	76.7	9.73	12.86	11.69	12.54	12.44	0.130
298	101	06668	76.3	76.4	9.73	12.86	11.69	12.54	12.44	0.130
299	101	40969	76.3	76.7	8.97	10.97	10.36	10.87	10.84	0.226
300	101	75201	76.3	76.7	8.97	10.97	10.36	10.87	10.84	0.157
301	101	79251	76.4	76.4	7.95	7.95	6.10	5.61	5.61	0.150

TABLE 30. 1/2-IN. BAR STRESS WHILE CYCLING
(SHEET 14 OF 15)

303	102.13579	76.4	8.53	10.33	9.74	10.07	10.78	0.210
304	102.47835	76.6	9.10	13.03	12.66	12.78	12.78	0.149
305	102.82107	76.3	9.67	15.50	15.27	15.27	15.34	0.131
306	103.16400	76.9	10.26	18.30	17.56	18.00	18.00	0.273
307	103.50673	76.7	10.83	21.67	20.93	21.49	21.36	0.525
308	103.84985	76.7	11.42	26.13	25.70	26.90	26.41	0.352
309	104.19245	76.5	12.00	30.63	29.70	30.41	30.41	0.446
310	104.53299	76.3	12.47	33.78	33.37	33.82	33.37	0.528
311	104.87618	76.6	13.04	37.22	36.98	37.49	37.49	0.267
312	104.91885	76.5	13.47	40.81	40.53	40.99	40.54	0.186
313	105.26146	76.6	13.99	44.78	44.26	45.26	45.26	0.184
314	105.60444	76.6	14.51	48.64	48.05	48.33	48.33	0.211
315	105.94774	76.7	15.08	52.81	51.53	52.52	52.52	0.214
316	106.29054	76.9	15.60	57.22	55.82	57.10	57.10	0.147
317	106.63322	76.8	16.12	61.88	60.09	61.52	61.52	0.298
318	106.97594	76.8	16.64	66.42	64.56	65.82	65.82	0.302
319	107.01948	76.9	17.16	70.22	68.22	69.98	69.98	0.214
320	107.36178	76.9	17.68	74.46	72.08	73.58	73.58	0.283
321	107.70476	76.7	18.19	78.21	75.99	77.21	77.21	0.170
322	108.04728	76.8	18.70	82.11	79.47	80.98	80.98	0.245
323	108.39058	76.8	19.21	86.22	83.44	85.19	85.19	0.374
324	108.73310	76.8	19.72	90.52	87.62	89.19	89.19	0.314
325	109.07600	76.8	20.23	94.91	91.51	93.71	93.71	0.492
326	109.11885	76.9	20.74	99.40	95.44	97.14	97.14	0.633
327	109.80495	77.0	21.25	104.00	100.00	101.00	101.00	0.327
328	110.49023	77.1	21.76	108.80	104.44	106.04	106.04	0.245
329	111.17603	77.1	22.27	113.80	109.22	111.04	111.04	0.161
330	111.86238	77.2	22.78	118.80	114.48	116.84	116.84	0.149
331	112.54743	77.1	23.29	124.00	119.62	122.08	122.08	0.162
332	113.23370	77.3	23.80	129.20	124.70	127.04	127.04	0.242
333	113.92027	77.5	24.31	134.60	129.80	132.00	132.00	0.000
334	113.91317	77.5	24.82	140.00	135.00	137.00	137.00	0.000
335	114.25626	77.4	25.33	145.40	140.20	142.40	142.40	0.184
336	114.59879	77.7	25.84	150.80	145.50	148.00	148.00	0.184
337	114.94216	77.2	26.35	156.40	150.80	153.60	153.60	0.185
338	115.28495	77.3	26.86	162.00	156.10	159.20	159.20	0.387
339	115.62779	77.4	27.37	167.80	161.40	164.80	164.80	0.350
340	115.97046	77.2	27.88	173.60	166.70	170.40	170.40	0.413
341	116.30202	77.2	28.39	179.60	172.00	176.20	176.20	0.247
342	116.65557	77.1	28.90	185.60	177.30	182.00	182.00	0.287
343	116.99854	77.1	29.41	191.80	182.60	187.40	187.40	0.251
344	117.34157	77.2	29.92	198.00	188.00	192.80	192.80	0.155
345	117.68433	77.1	30.43	204.40	193.40	198.20	198.20	0.155
346	118.02685	77.1	30.94	210.80	198.80	203.60	203.60	0.178
347	118.36969	77.1	31.45	217.40	204.20	209.00	209.00	0.196
348	118.70330	77.1	31.96	224.00	209.80	214.40	214.40	0.224
349	118.71368	77.0	32.47	230.80	215.40	220.00	220.00	0.244
350	119.05659	76.8	32.98	237.60	221.00	225.60	225.60	0.244
351	119.40001	76.8	33.49	244.60	226.60	231.20	231.20	0.246
352	119.74239	76.5	34.00	251.60	232.20	236.80	236.80	0.198
353	120.08506	76.6	34.51	258.80	237.80	242.40	242.40	0.198
354	120.42846	76.5	35.02	266.00	243.40	248.00	248.00	0.132
355	120.77066	76.5	35.53	273.40	249.00	253.60	253.60	0.132
356	121.11370	76.7	36.04	280.80	254.60	259.20	259.20	0.337
357	121.45650	76.5	36.55	288.40	260.20	264.80	264.80	0.337
358	121.81948	76.0	37.06	296.00	265.80	270.40	270.40	0.455
359	122.16266	76.9	37.57	303.80	271.40	276.00	276.00	0.385
360	122.50503	76.4	38.08	311.60	277.00	281.60	281.60	0.385
361	122.84802	75.9	38.59	319.60	282.60	287.20	287.20	0.172
362	123.19144	76.4	39.10	327.60	288.60	292.80	292.80	0.172
363	123.51307	76.0	39.61	335.80	294.60	298.40	298.40	0.163
364	123.82342	76.7	40.12	344.00	300.60	304.00	304.00	0.209
365	124.13368	76.5	40.63	352.40	306.60	309.60	309.60	0.209
366	124.44388	76.5	41.14	360.80	312.60	315.20	315.20	0.352
367	124.80911	76.4	41.65	369.40	318.60	320.80	320.80	0.352
368	124.55249	76.5	42.16	378.00	324.60	326.40	326.40	0.350

TABLE 30. 1/2-IN. BAR STRESS WHILE CYCLING
(SHEET 15 OF 15)

369	124	89486	75.8	76.5	6.26	9.29	8.53	9.01	8.95	0.271
370	125	23016	75.5	76.3	7.40	10.41	10.93	10.58	10.50	0.196
371	125	54280	75.6	76.4	7.13	12.41	13.97	13.18	12.19	0.281
372	126	28550	75.9	76.5	7.30	9.20	9.41	9.79	9.68	0.249
373	126	7148	75.7	76.2	6.66	5.41	4.71	5.03	5.05	0.178
374	127	31786	75.7	76.5	5.41	2.1	2.26	2.48	2.41	0.235
375	128	68000	75.7	76.5	3.90	0.54	0.65	0.74	0.71	0.232
380	128	76320	75.7	76.5	3.54	4.20	4.35	4.68	4.69	0.245
381	129	70626	75.6	76.5	5.19	6.15	5.77	6.64	6.52	0.308
382	129	4861	75.7	76.5	6.26	9.46	8.54	9.16	8.95	0.440
383	129	7772	75.7	76.2	7.26	12.59	11.61	12.34	12.18	0.384
384	130	42069	75.8	76.4	7.40	12.18	11.13	11.87	11.72	0.370
385	130	52319	75.5	76.4	7.94	13.32	12.40	13.03	12.86	0.485
386	131	76350	75.8	76.5	7.38	9.18	8.60	9.04	8.92	0.335
388	131	10642	75.8	76.5	6.34	7.13	6.91	7.22	7.22	0.226
389	131	44957	75.9	76.4	6.97	12.15	11.33	11.94	11.82	0.226
390	132	17748	75.9	76.5	4.52	1.87	1.81	1.91	1.87	0.144
391	132	8293	75.9	76.5	3.88	1.87	1.81	1.91	1.87	0.207
392	132	11812	76.0	76.6	3.88	1.87	1.81	1.91	1.87	0.207
393	133	16970	75.8	76.6	3.24	1.17	0.71	0.92	0.88	0.335
396	133	80340	75.8	76.4	5.12	6.16	5.71	6.52	6.44	0.167
397	133	84667	76.0	76.7	5.69	6.88	6.24	7.11	6.94	0.267
398	134	18950	76.0	76.7	6.23	9.36	8.89	9.61	9.57	0.228
400	134	53217	76.5	76.7	7.41	11.22	10.48	10.81	10.80	0.226
401	134	87468	76.9	76.6	7.94	12.26	11.12	12.44	12.33	0.322
402	135	34712	75.8	76.6	7.94	14.03	13.01	13.99	13.79	0.422
403	135	5744	75.8	76.5	7.38	19.40	18.73	19.71	19.08	0.369
404	135	90052	75.9	76.5	6.81	7.33	6.86	7.11	7.08	0.173
405	136	24318	76.1	76.7	6.24	7.33	6.93	6.93	7.23	0.145
406	136	58615	76.4	76.7	5.67	4.16	3.54	3.88	3.90	0.184
407	137	27200	76.2	76.8	4.52	1.87	1.47	1.61	1.72	0.151
408	137	61480	76.2	76.8	4.52	1.87	1.47	1.61	1.60	0.152
409	137	61480	76.2	76.8	4.52	1.87	1.47	1.61	1.60	0.151
410	137	95777	76.2	76.7	3.92	0.73	0.58	0.70	0.69	0.151
411	137	9948	76.1	76.6	4.49	0.92	0.73	0.70	0.73	0.182
412	138	34275	76.0	76.6	5.06	6.07	5.07	5.88	5.73	0.122
413	138	68513	76.1	76.6	6.4	7.81	6.67	7.51	7.33	0.368
414	139	42841	76.2	76.6	6.24	9.43	8.47	9.14	8.92	0.419
415	139	37078	76.2	76.7	6.24	9.43	8.47	9.14	8.92	0.576
416	139	71382	76.0	76.7	6.24	10.89	9.76	10.74	10.46	0.430
417	140	95702	76.0	76.7	7.35	12.26	11.24	12.34	12.04	0.483
418	140	35932	76.2	76.6	7.92	14.26	12.84	14.10	13.74	0.549

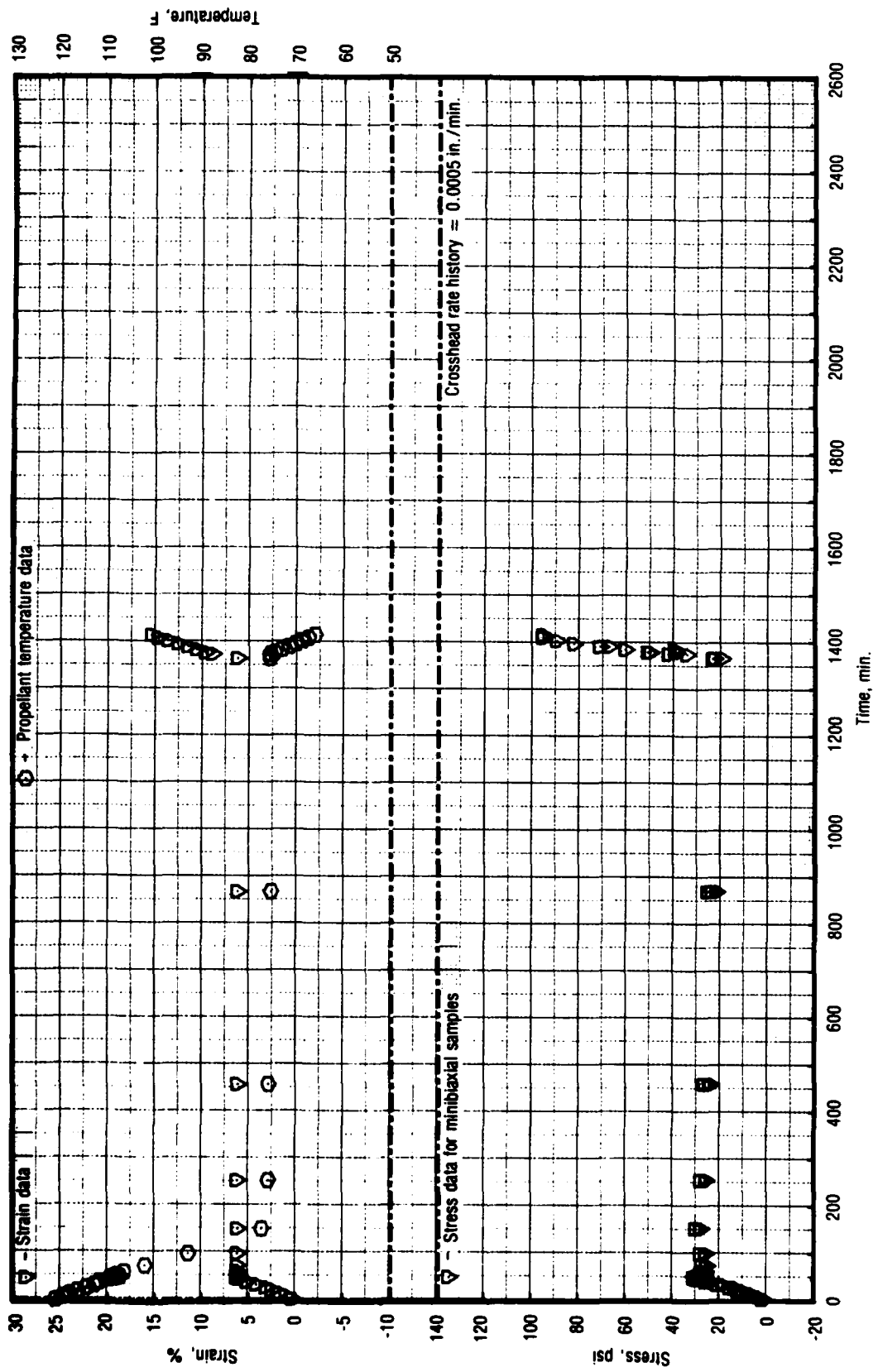


Figure 60. Test No. 21 - Stress While Complex Straining and Cooling for UTP-3001-750/7768

28827

TABLE 31. MINIBIAXIAL STRESS WHILE COMPLEX STRAINING AND COOLING
(SHEET 1 OF 2)

PROPELLANT: OYP 3001 750/7768
REQUESTOR: Capleton Francis
WOR: 2742-400-0000

DATE: 1/5/82
OPERATOR: JWD

DEFINITIONS: Time = Time From Start of Test (min)
σ = Stress (psi)
ε = Strain (%)
T (air) = Test Air Temperature (F)
T (prop) = Test Propellant Temperature (F)

RFLATIONSHIPS:
σ = Force/Area
ε = Sample Extension/Length

NOMINAL VALUES:
Test Temp = 120.70 hold, 40F F
Gage Length = 1.25 in
Nom. Strain = 0.6610 %
XHD Rate = .0005 in/min

CALIBRATION DATA: Cal Wt = 10.0 lbs

Pretest:	1	2	3
Cal (lbs/volts)	29.713	29.633	29.910
Load Cal (volts)	0.051	0.116	0.105
Offset			
Pot Cal (in/volts) =			
Temp (F)	119.8		

Post Test: Cal Wt = 10.0 lbs

Load Cal (lbs/volts)	29.756	29.505	29.874
Offset (volts)	0.199	0.099	0.135
Pot Cal (in/volts) =	-0.192		
Temp (F)	65.4		

AREAS (sq in): 1.480 1.453 1.480

SET	STRESS DATA (psi):		T (prop)	T (air)	Strain	SAMPLE			St Dev
	Time	Stress				1	2	3	
1	-2.87174	121.1	121.3	121.3	0.00	0.06	0.01	0.05	0.018
2	3.37825	121.3	121.3	121.3	0.37	0.75	1.52	1.63	0.338
3	9.62879	119.6	121.4	121.4	1.00	3.36	4.45	4.58	0.426
4	15.87840	118.1	117.9	115.2	1.71	6.38	7.89	7.99	0.637
5	22.12876	116.4	114.6	111.2	3.14	10.11	11.84	11.89	0.718
6	28.37846	114.6	111.2	108.3	4.18	13.23	15.21	15.23	0.809
7	34.62882	112.8	108.3	108.3	5.20	18.25	20.53	20.43	0.910
8	40.87880	109.7	108.3	108.3	6.27	23.17	25.53	25.44	0.943
9	47.12866	109.0	108.3	108.3	7.27	28.03	30.61	30.32	1.014
10	49.48019	109.1	110.0	110.0	8.27	30.61	30.61	30.33	0.993
11	49.54240	108.7	108.3	108.3	9.27	30.61	30.61	30.34	0.973
12	49.75356	108.6	108.3	108.3	10.27	27.74	30.24	30.00	0.973
13	49.95449	108.0	105.3	105.3	11.27	27.66	29.75	29.79	0.954
14	50.35535	108.0	107.5	107.5	12.27	27.07	29.12	29.52	0.937
15	51.15616	107.4	107.5	107.5	13.27	26.52	28.57	28.63	0.889
16	52.75655	108.0	106.7	106.7	14.27	26.52	26.52	27.96	0.777
17	55.95708	106.6	106.3	106.3	15.27	25.96	26.53	27.49	0.717
18	59.35736	102.1	99.3	99.3	16.27	25.34	25.34	26.20	0.791
19	63.75802	99.9	90.9	90.9	17.27	25.34	25.34	26.90	0.843
20	75.15874	77.3	73.8	73.8	18.27	25.34	25.34	26.41	0.897
21	103.49094	75.9	69.3	69.3	19.27	25.34	25.34	26.50	0.921
22	153.49094	75.9	69.3	69.3	20.27	25.34	25.34	26.50	0.897
23	255.89124	75.9	69.3	69.3	21.27	25.34	25.34	26.50	0.897

TABLE 31. MINIBIAXIAL STRESS WHILE COMPLEX STRAINING AND COOLING
(SHEET 2 OF 2)

24	460.69174	75.9	75.1	6.23	24.29	23.67	26.34	24.77	0.287
25	870.29243	75.4	75.1	6.23	23.36	21.39	24.90	23.22	1.243
26	1365.87154	75.5	77.4	6.23	22.17	19.17	22.96	21.50	1.443
27	1776.04224			6.23	22.34	19.06	22.85	21.42	1.454
29	1374.70000	75.6	77.5	8.90	41.50	34.00	42.00	39.17	3.169
30	1384.54646	74.6	73.6	9.65	49.65	38.56	50.62	46.28	4.738
31	1391.79651	73.1	73.1	10.58	60.16	39.00	60.28	53.14	8.662
32	1397.39661	71.5	72.9	12.56	70.88		67.04	68.96	8.713
33	1403.54688	68.7	68.9	13.59	81.90			89.00	0.000
34	1407.79659	67.3	68.2	14.66	89.00			94.86	0.000
35	1407.79659	67.3	68.2	14.66	94.86			94.86	0.000
36	1416.04644	65.9	66.6	15.33	94.92			94.92	0.000

TABLE 32. STRESS-STRAIN COMPARISON FOR UTP-3001 TESTS PHASE III

T8613

Test No.	Temperature, F	Rate, in./min.	Strain, %	Stress, psi	Stress Test No. 15	Difference, %	Box No.	Days After Machining	Remarks
14	41	2	6.85	290			2	3	Average Sample No. 3
	41	2	9.65	352			2	3	
	41	0.2	10.26	239			2	3	
	41	0.02	5.29	123			2	3	Average No. 3
	41	0.02	10.10	209			2	3	
	70	2	10.14	203			1	5	
	71	0.2	9.84	147			1	5	
	71	0.02	9.86	115			1	5	
	116	2	10.38	97.0			2	2	
	118	0.2	5.03	28.0			2	2	Average No. 1
	118	0.2	10.09	64.3			2	2	No. 3
14 (1)	118	0.02	10.17	48.6			2	2	Straining-cooling
15	99.2	0.000027	1.50	10.4			3	4	
16	40	0.2	3.13	107	95	12.6	3	10	
16	73	0.2	3.22	50.8	53	-4.2	3	4	
16	117	0.2	3.30	20.5	21	-2.4	3	5	
17 (2)	74	0.2	5.08	21.3	≈ 23.2	-8.2	-	11	No. 1 shear
17	74	0.2	5.87	23.6	≈ 26.5	-14.2	-	11	No. 2 shear
17	74	0.2	6.52	25.0	≈ 29.2	-14.4	-	11	No. 3 shear
18 (1)	95.2	0.0002	2.53	9.57			1	7	Straining-cooling
18	97.6	0.0004	2.29	10.4			1	3	" "
18	190.4	0.002	1.95	7.97			1	5	" "
19	74	1	2.26	37.0	~ 42	-11.9	4	18	No. 3
21 (1)	118.1	0.0005	1.71	7.42			4	5	Straining-cooling

Notes: (1) Insufficient data to extrapolate to an equivalent temperature for stress adjustment.
 (2) Comparison of shear to biaxial data is only approximate.

TABLE 33. STRESS-STRAIN COMPARISON FOR UTP-19,360B TESTS PHASE III

T8612

Test No.	Temperature, F	Rate, in./min.	Strain, %	Stress, psi	Stress Test #15	Difference, %	Box No.	Days After Machining	Remarks
14	41	2	10.01	112			2	8	Average Sample #2
	41	2	10.01	111			2	8	
	41	0.2	10.22	80.6			2	8	
	41	0.02	10.15	63.0			2	8	
	71	2	8.63	81.4			1	2	
	70	0.2	10.20	65.6			1	3	Average #2 and 3
	71	0.02	10.03	50.4			1	7	
	120	2	10.13	63.9			2	6	
	119	0.2	10.24	50.4			2	7	Average #1
	119	0.2	9.87	49.4			2	7	Average #2
	118	0.02	10.02	40.0			2	7	Straining-cooling
	118	0.02	10.14	40.3			2	7	
15 (1)	99.5	0.00004	2.13	5.09	~ 4.50	13.1	3	2	
16	40	0.2	3.50	44.0	40.0	10.0	3	12	
16	70	0.2	3.18	30.0	28.8	4.2	3	6	
16	117	0.2	3.09	19.6	16.7	17.4	3	7	
17	70	0.2	5.33	13.8	~ 13.0	6.2	-	13	#1 Shear
17	70	0.2	5.73	14.5	~ 13.7	5.8	-	13	#2 Shear
17	70	0.2	5.79	14.6	~ 13.8	5.8	-	13	#3 Shear
18 (1)	95.2	0.0002	2.53	6.39	~ 6.20	3.1	1	9	Straining-cooling
18	97.6	0.0004	2.29	6.91	~ 6.10	13.3	1	4	" "
18	98.2	0.002	2.59	8.07	~ 8.60	-6.2	1	7	" "
19	70	1	1.91	29.0	23.4	23.9	4	7	Average #2 and 3
21 (1)	118.3	0.0005	1.83	6.34	~ 4.70	34.9	4	4	Straining-cooling

Notes: (1) Straining-cooling tests were compared as small strain and accompanying temperature to avoid the strain-thermal shift complication.

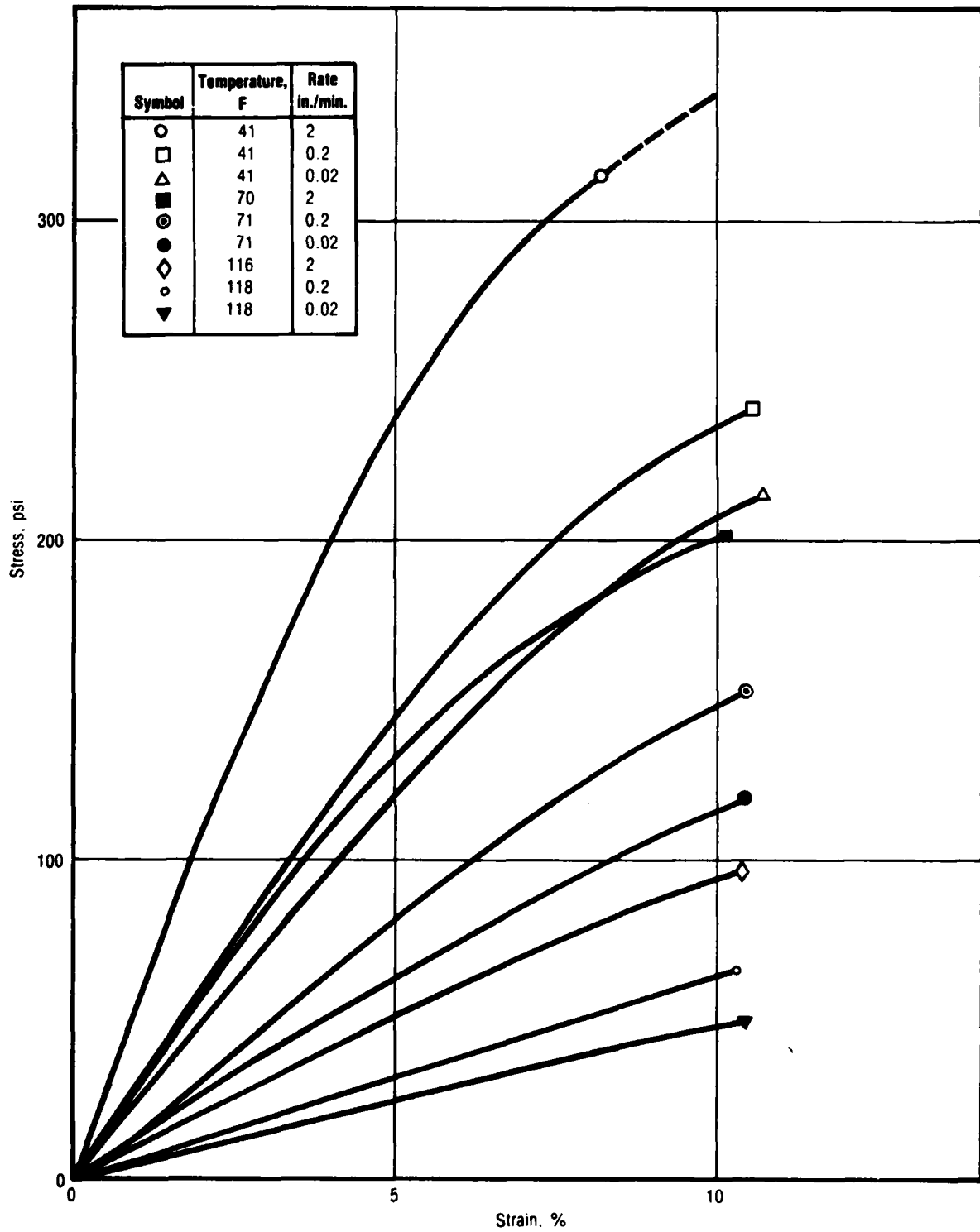


Figure 61. Biaxial Constant Rate Data for UTP-3001

28828

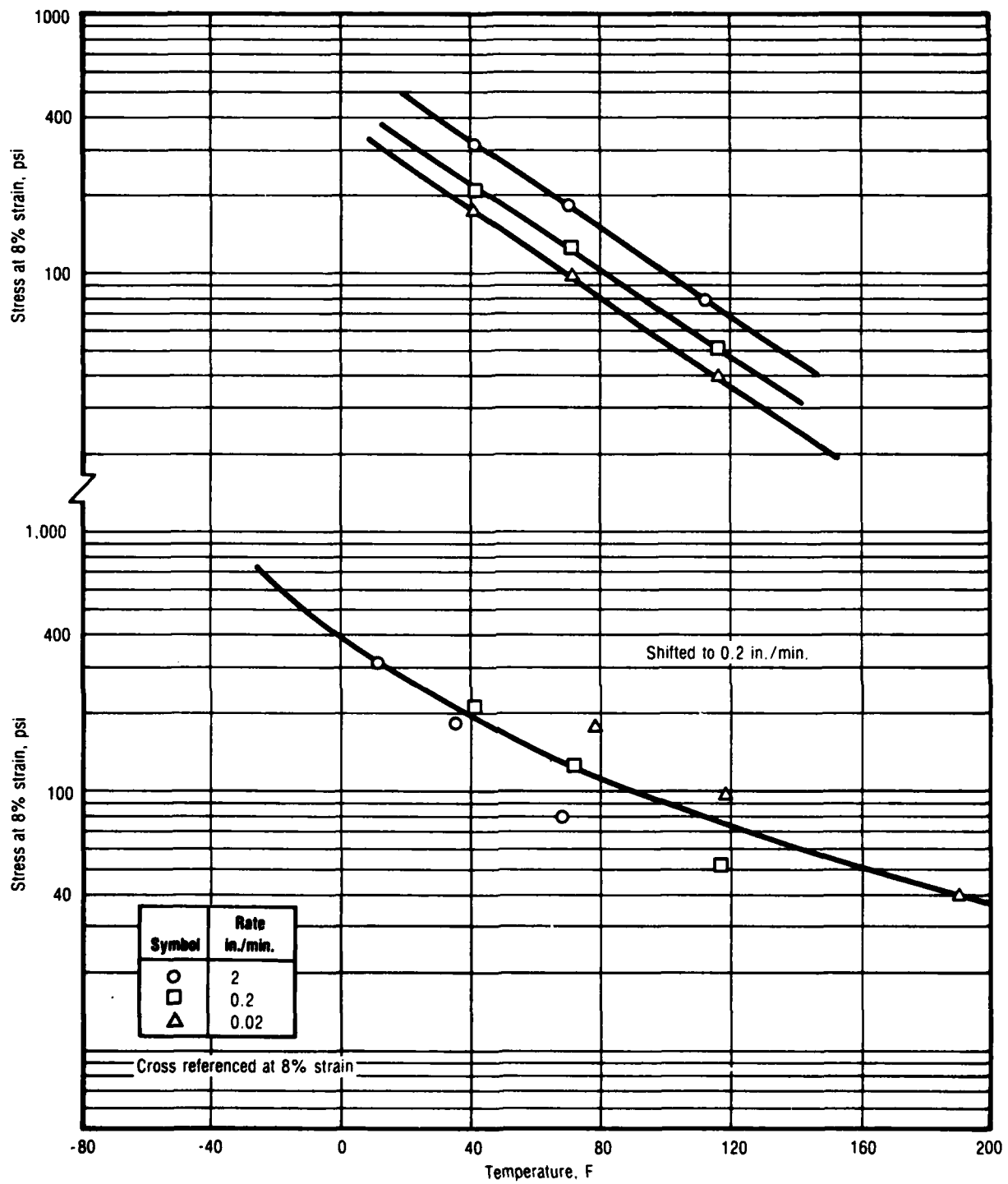


Figure 62. Test No. 14 - Biaxial Constant Rate Data for UTP-3001

28829

The UTP-19,360B biaxial constant rate data plotted in Figure 63 were used to obtain the stress comparison data (Table 33) at different strain levels. The stress-temperature plot in Figure 64 gave a good temperature extrapolation which was used to obtain comparison stress values for the slower rate straining-cooling tests. The stress values selected for comparison were early in the test at an elevated temperature and small strain. This was chosen to specifically avoid the complication of evaluating the combined thermal-mechanical interaction shift factor (A_T). While one of the straining-cooling tests showed a difference of 35%, the absolute delta stress was small.

Uniaxial, Biaxial and Shear Comparison

Comparisons of the different samples were made in order to show that the propellant, used in each of the tests, was of the same family. This was done at ambient temperature for selected rates and was limited to strain rates that were close to each other. This minimized the time-temperature equivalence shifts to small changes for neglectable data input errors. The adjustments made for strain levels are given in Table 34.

The comparisons between uniaxial and biaxial in the table are close to the theoretical ratio of 75 to 80%. The shear to uniaxial ratios of 0.28 and 0.39 bracket the nominal theoretical value of 1/3. For the comparisons made in Table 34, the UTP-3001 and UTP-19,360B propellants have to be considered part of the same family. Any minor differences can be attributed to a between carton effect.

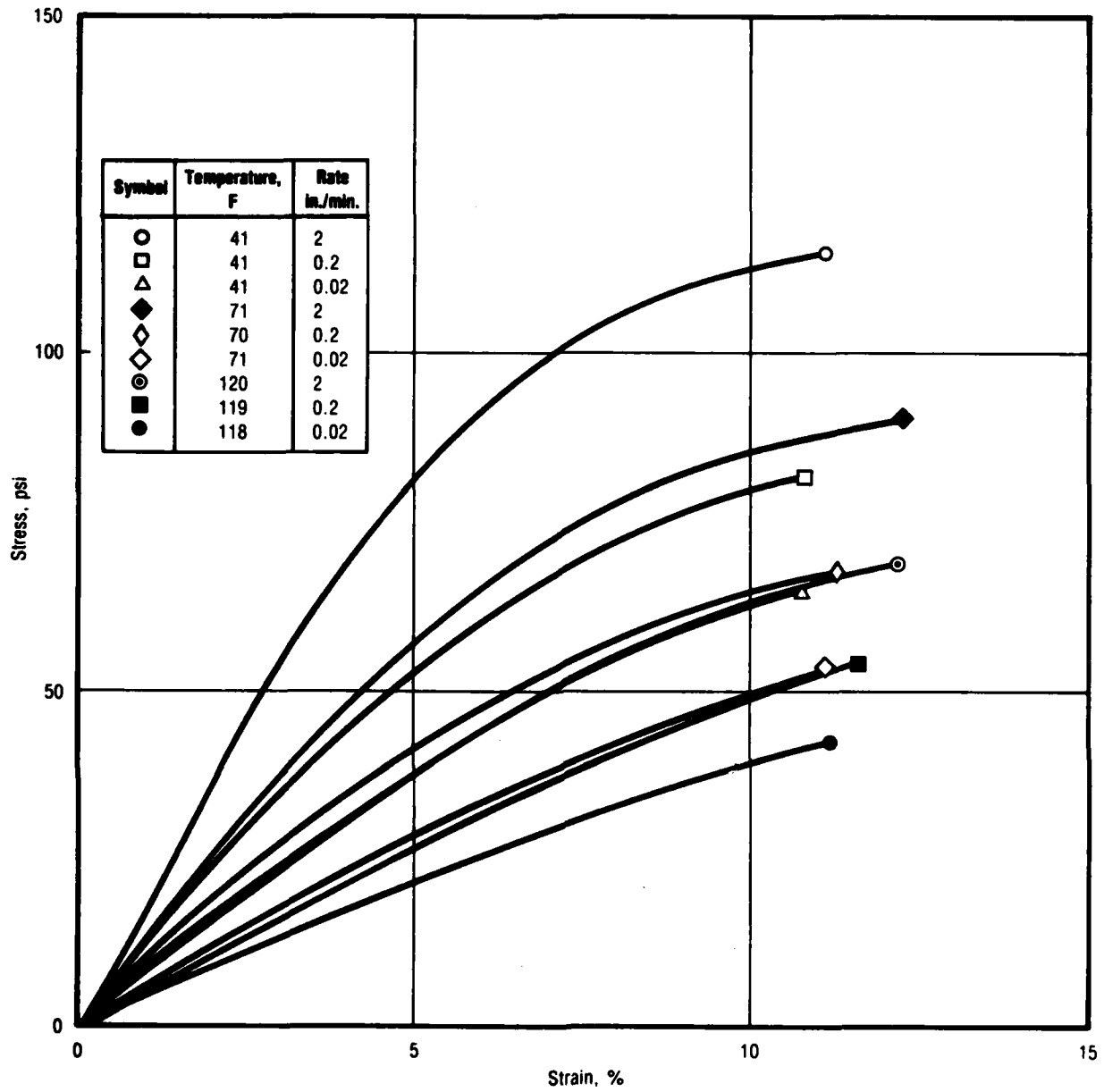


Figure 63. Biaxial Constant Rate Data for UTP-19,360B

28831

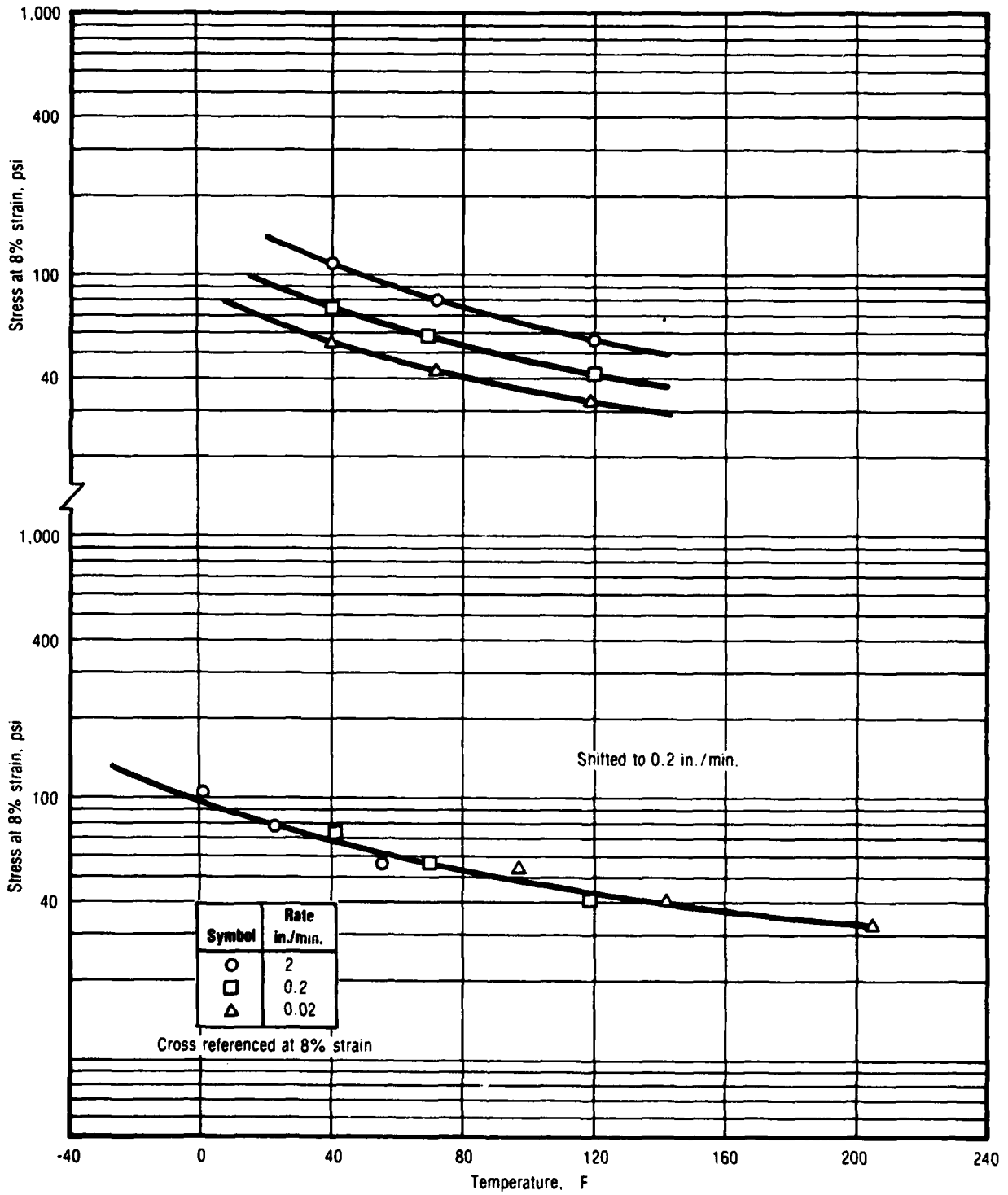


Figure 64. Test No. 14 - Biaxial Constant Rate Data for UTP-19,360B

28832

TABLE 34. COMPARISON OF UNIAXIAL, BIAxIAL, AND SHEAR TEST DATA FROM PHASE III

T8611

Sample	Temperature, F	Rate, in./min.	Strain Rate, in./in./min.	UTP-3001		UTP-19,360B	
				Strain, %	Stress, psi	Strain, %	Stress, psi
Uniaxial Adjusted to	70	1	0.1667	10.0	128	10.0	57.7
				5.8	86.8	5.6	38.9
Biaxial	70	0.2	0.160	10.0	148	10.0	65.0
Shear Adjusted to	70	0.2	0.160	5.8	23.3	5.6	14.3
					24.0		15.0
Stress Ratios for:				<u>UTP 3001</u>		<u>UTP 19360B</u>	
Uniaxial/biaxial				128/148 = 0.86		57.7/65.0 = 0.89	
Shear/uniaxial				24.0/86.8 = 0.28		15.0/38.9 = 0.39	

4.0 THEORETICAL DEVELOPMENT

4.1 INTRODUCTION AND PRELIMINARY STUDY

Generally speaking, solid propellants may be considered as lightly cross-linked long-chain polymers, highly filled with coarse solid particles. They respond viscoelastically to the action of external stimuli, but certain aspects of their behavior cannot be reproduced by the classical linear or nonlinear theories of fading-memory materials. Thus, in recent years, much work has been concerned with the development of appropriate models to predict the mechanical response of solid propellants. A current trend is to express the observed response in terms of some measure of "damage" at the continuum level where damage is described as the difference between the observed response and that predicted by a fading-memory theory, like Linear Viscoelasticity. There is now sufficient experimental evidence to show that damage (References 13, 17, 20, 24, and 28) per se is a microscopic phenomenon associated with the initiation and growth of flaws, debonding between matrix and solid filler particles, and molecular chain scission. Although it is largely irreversible, damage is partially recoverable shortly after removal of the loading system. This recovery from damage is termed healing. It is clear that, depending on the propellant and service requirements, it may also have to be accounted for in a constitutive theory for solid propellants.

In the present program, two approaches to characterizing damage have been followed. In the first one, damage is treated as the algebraic difference between the measured stress and that predicted by Linear Viscoelasticity, so that:

$$\sigma_c(t) = \sigma(t) - \sigma_q(t) \quad (1)$$

in which σ_q and σ_c are the linear-viscoelastic and correction terms, respectively, with σ , the measured stress. In the second approach, the difference between measured and fading-memory type stresses is handled through a stress-correction function in the following form.

$$\sigma(t) = C(\epsilon_{\max}, \dots) \sigma_f(t) \quad (2)$$

The softening function (C) is made to depend on the past maximum strain or stress and $\sigma_f(t)$ represents an appropriate function of the fading-memory type stresses.

Broadly speaking, the current versions of models by M. Gurtin and M. Quinlan are of the type presented in equation (1) above, while those of R. Schapery, W. Hufferd and Swanson are of the form given by equation (2).

The following presents some experimental evidence on the type of nonlinearities exhibited by solid propellants, and briefly discusses the pioneering work of Mullins and Tobin in treating the large hysteresis observed in tire rubbers. Next, the theory of Linear Viscoelasticity is applied to predict the response of UTP-19,360B and UTP-3001 under various strain histories. The ensuing results are meant as a basis for comparing the propellant response as predicted by each of the candidate constitutive laws. This comparison should be most meaningful because each of the theories considered evolved from a set of modifications to Linear Viscoelasticity. Subsequently, the nonlinear theory of Farris (Reference 5) is presented. This theory was employed during the first phase of the program to predict the response of TP-H1011 and to compare the results with those of the other five constitutive laws. Finally, a detailed description is given of each of these five stress-strain relations. This includes the original concept of the models, their current versions, comparisons of predicted and measured stresses for a variety of strain histories, and some pertinent guidelines for characterizing solid propellant according to each theory.

4.1.1 Experimental Background

The complex behavior of solid propellants, as well as some attempts at developing usable stress-strain laws for these materials, are well documented in References 3 through 31. It is shown there that a given deformation process causes a change in the response properties of solid propellants, for instance a drop in the relaxation modulus. As stated before, this deviation from some

expected response is what has been called damage. It is evidenced as phenomenological macroscopic changes that are caused by undefined, but real, irreversible or partially reversible microscopic changes. Polymer bond breakage, vacuole formation in the polymer matrix, dewetting between the polymer matrix and solid filler particles, microcracking, etc., are among the possible microscopic causes of observed permanent-memory effects in propellants.

Studies on uniaxial solid propellant samples have indicated that these materials exhibit large hysteresis even at small strains. These studies have also revealed that the state of damage in solid propellants is determined primarily by the maximum strain or stress undergone during the loading histories.

The typical nonlinear hysteresis and permanent-memory effects exhibited by solid propellants are illustrated in Figure 65. A series of finite-duration, variable-strain-level ramp pulses were used to obtain the propellant response subsequent to a given damage history (References 12 and 13). All ramps had the same initial moderate rise rate, with two exceptions to be noted later, and all ramps had the same very slow decline rate.

Observations of the load on the specimen after returning to its original length (zero strain) showed that it took approximately 30 min for the stress to relax to zero.

A series of tests were run on a 1/4 x 1/4 x 4-in. tab-end sample. The virgin specimen was initially strained to a level of 7.04% and allowed to relax to achieve a rest-state condition. The first part of the testing is shown in the lower half of Figure 65 (curves A-H) and the last part in the upper half (curves H-M).

Curve A shows the load response to this first pulse. The specimen was then subjected to four successive ramp strain pulses ranging from $\epsilon^0 = 3.82\%$ to $\epsilon^0 = 6.34\%$. There was a rest period allowed between each pulse. The results are shown in Figure 65 as curves B through E.

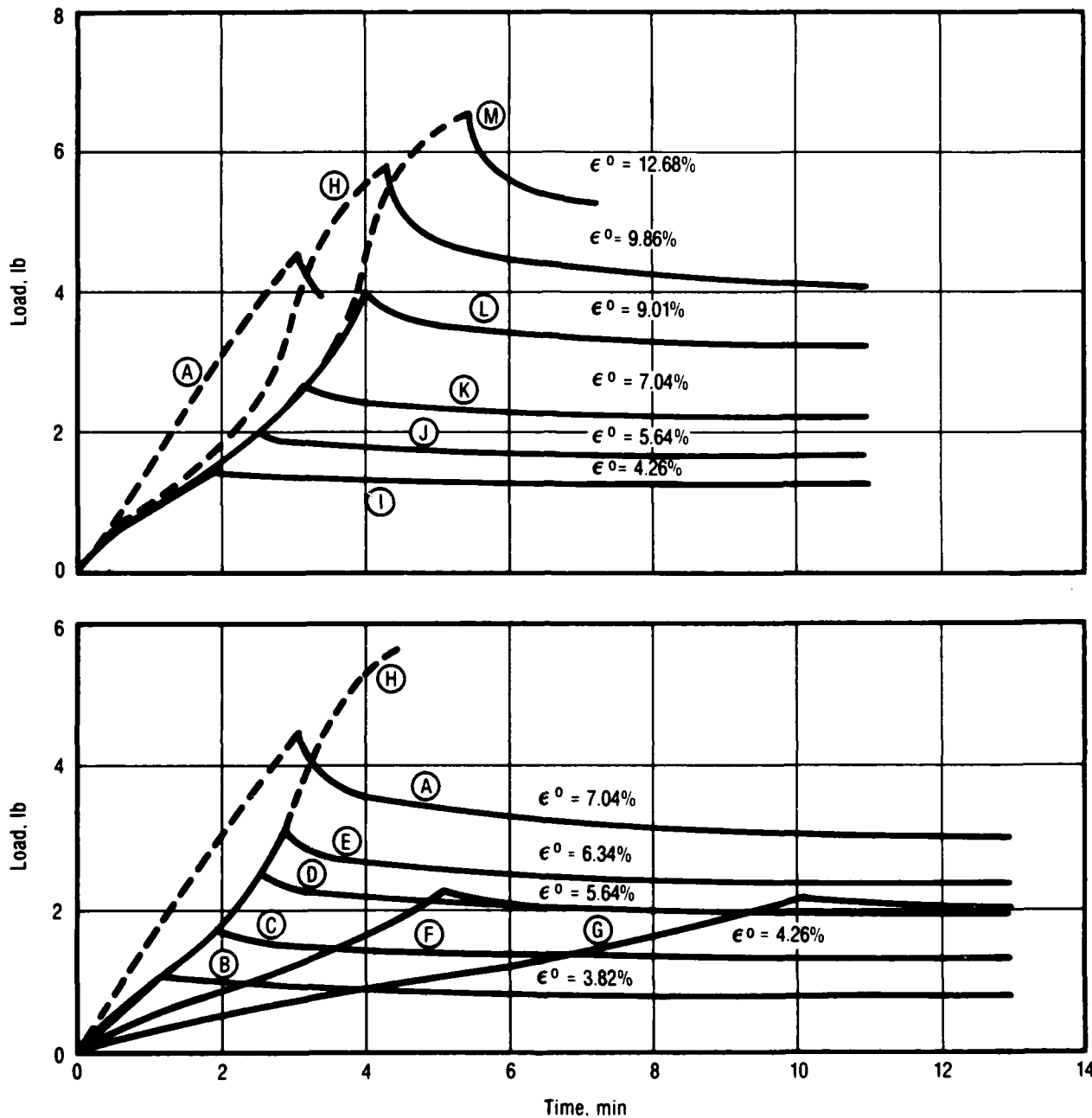


Figure 65. Relaxation after Damage

22019

Two aspects of the propellant's behavior are worth noting. First, during the constant strain rate portion of the ramp, each successive load-time curve is essentially identical. This indicates that the "new material" has the same nonlinear rate-dependency under repeated strain conditions as long as the strain

levels are below the previous maximum strain of $\epsilon^0 = 7.04\%$. Second, the relaxation portions of the curves are essentially homologous, indicating that a viscoelastic relaxation process is taking place.

Curves F and G present the results of two additional tests at two successively lower strain rates where the sample was loaded to 5.64% strain each time. A strong rate dependency is observed during the rise portion of the ramp; however, curves F and G rapidly rejoin curve D indicating that the material is behaving in a viscoelastic fading-memory fashion.

The specimen was next subjected to a ramp strain pulse reaching a higher strain level ($\epsilon^0 = 9.86\%$) than the maximum 7.04% previously experienced (Figure 65, curve H). The first part of curve H repeats the loading ramp portion of curves B-E to indicate the same "new material" rest-state. Note that the load-time curve returns to the initial or virgin constant strain rate curve once the previous maximum strain (7.04%) has been passed.

Subsequently, the specimen was strained with the ramp pulse to four different strain levels less than 9.86% ($\epsilon^0 = 4.26\%$, 5.64%, 7.04%, and 9.01%), as shown in curves I through L. The results show that a new rate-dependency has developed (compare the rising portions of I through L with the rising portion of H). Thus, another "new-material" rest-state has been produced as a result of the second maximum strain level of 9.86%. Lastly, the specimen was strained to another new maximum of $\epsilon^0 = 12.68\%$ as shown in curve M. It again appears that it returned to the virgin undamaged curve once the 9.86% strain level was exceeded.

The above experimental evidence suggests that the form of the constitutive equation should remain unchanged with respect to the material's current rest-state. This condition should remain as long as the damage is unchanged (i.e., the ϵ_{\max} is unchanged during its subsequent strain histories).

Figure 66 shows a replot (curves N and O) of some of the results just discussed. After an initial maximum strain (7.04%) the specimen was allowed to

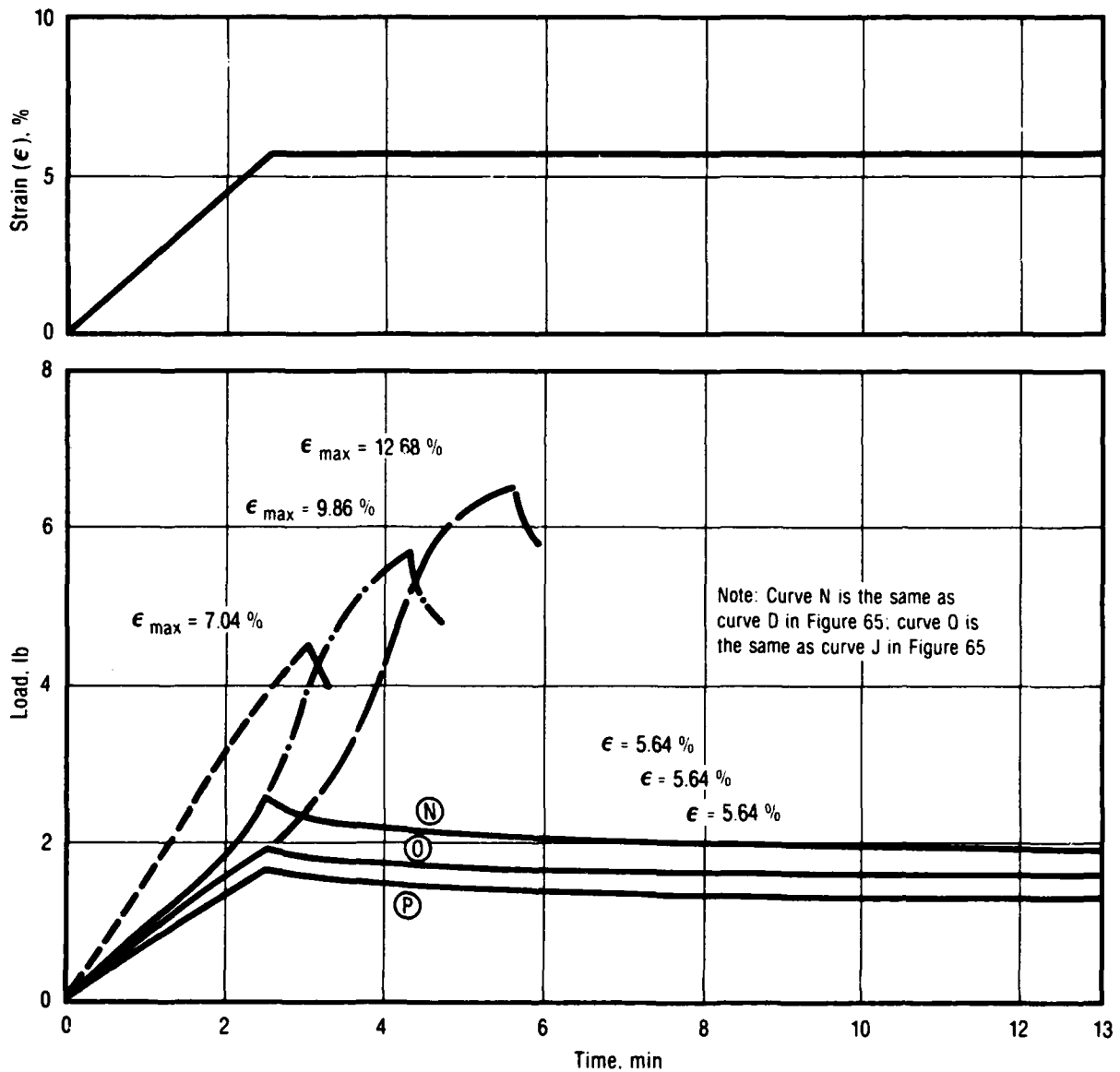


Figure 66. Relaxation after Damage

22020

return to a rest-state and then strained to a value of $\epsilon^0 = 5.64\%$, with the result shown as curve P. These three identical strain history tests of three different material states indicate that the higher the state of damage (primarily ϵ_{max}), the softer the material response upon subsequent testing.

In addition, other experimental studies have pointed out the importance of healing effects, load duration, and initial strain rate (References 12, 13, 14,

AD-A133 364

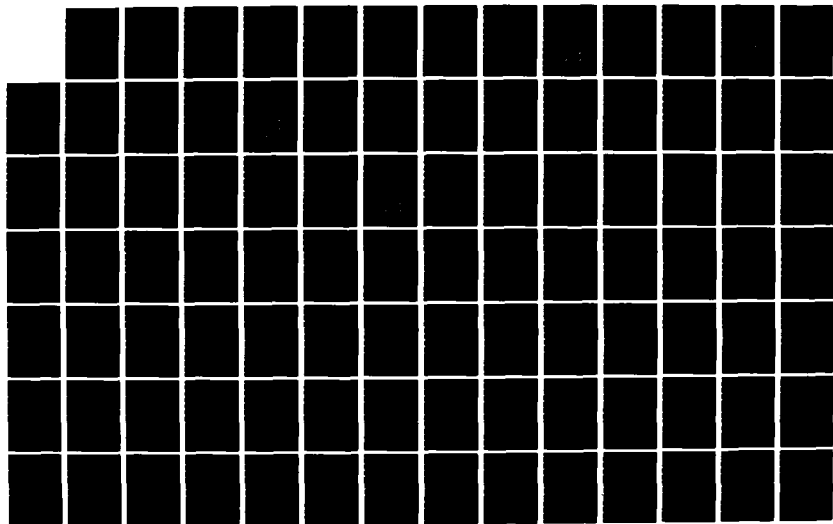
PROPELLANT NONLINEAR CONSTITUTIVE THEORY EXTENSION:
PRELIMINARY RESULTS. (U) UNITED TECHNOLOGIES CORP
SUNNYVALE CA CHEMICAL SYSTEMS DIV E C FRANCIS ET AL.
AUG 83 UTC/CSD-2742 AFRPL-TR-83-034

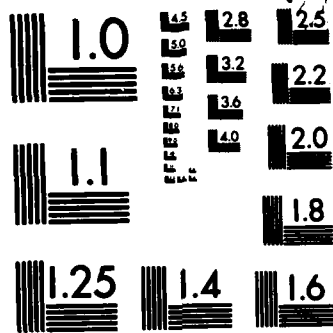
3/4

UNCLASSIFIED

F/G 21/9. 2

NL





MICROCOPY RESOLUTION TEST CHART
 NATIONAL BUREAU OF STANDARDS-1963-A

and 15). Finally, it is important to note that the behavior of solid propellant, depicted in Figures 65 and 66, is similar to that exhibited by rubber. The nonlinear uniaxial stress response of rubber, with and without carbon black filler and in the absence of time effects, was characterized quite well by Mullins and Tobin (Reference 27) with equation (3).

$$\epsilon = \epsilon_u F \quad (3)$$

where:

ϵ = engineering strain. The Mullins-Tobin model is not limited to small strains.

$\epsilon_u = \epsilon_u(\sigma)$ = strain as a function of engineering stress for the polymer without filler and without damage. The characteristic shape of this function is shown in Figure 67.

$F = F(\sigma_{\max}, N)$ = damage or softening function which depends on the maximum stress experienced by the rubber and the number N of loading and unloading cycles. F is not very sensitive to N , but depends strongly on any hard filler particles that may be present.

A large amount of rubber data can be predicted by means of this equation when the samples are not allowed to rest between cycles. Recovery or healing occurs as a function of the rest time. Therefore, healing would have to be considered in an accurate characterization of rubber.

Introducing the inverse of $\epsilon_u = \epsilon_u(\sigma)$, equation (3) may be put in the form:

$$\epsilon = f(\epsilon/F) \quad (4)$$

which shows that F (where $F \leq 1$) is a strain-magnification factor. The ratio ϵ/F is interpreted by Mullins and Tobin to be the average strain in the rubber phase of a hard particle-filled rubber. Without damage in a highly-filled rubber, $F \ll 1$. As the rubber is cycled between the strains $\epsilon = 0$ and $\epsilon = \epsilon_{\max}$, the ratio ϵ/F at any strain decreases, and therefore the stress decreases. The shape of the

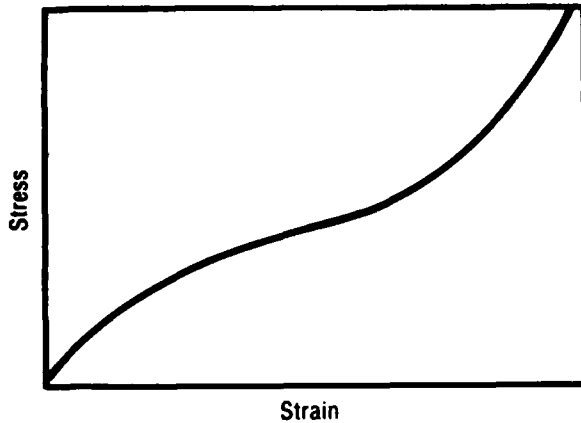


Figure 67. Stress-Strain Curve for Rubber

stress-strain curve is still as shown in Figure 67. It is similar to that for solid propellant after first-time loading. This fact and the ability of the model presented in equation (3) to reproduce a large amount of rubber data explains the great influence of the Mullins-Tobin approach on the development of nonlinear constitutive theories for solid propellants.

4.2 SELECTED THEORIES 22074

4.2.1 Linear Viscoelastic Constitutive Equation

4.2.1.1 Linear Viscoelastic Model

The one-dimensional stress-strain law for a thermorheologically simple linear viscoelastic solid may be expressed as:

$$\sigma(t) = \int_0^t E(S_t - S_\tau) \frac{d\xi}{d\tau}(\tau) d\tau \quad (5)$$

where:

σ = stress

ϵ = strain

$E(t)$ = relaxation modulus (PRONY series representation using a matrix solution for curve fitting data; CSD Data Analysis Procedure No. 7.3)

$S_t - S_\tau$ = temperature-shifted time, given by:

$$S_t - S_\tau = \int_\tau^t \frac{d\tau}{a_T [T(\tau)]} \quad (6)$$

and

a_T = time-temperature shift function, taken in the form:

$$A_T = \left(\frac{T_R - T_a}{T - T_a} \right)^m \quad (7)$$

in which T_R is the shift reference temperature, and both T_a and m are material parameters. The material parameters were obtained using CSD Data Analysis Procedure No. 7.4, which is a curve fit routine using Powell's algorithm.

The linear viscoelastic model was used to predict the response of UTP-19,360B and UTP-3001 under several strain histories. The corresponding results are included here as a basis against which to compare the stress predictions obtained using the nonlinear stress-strain laws considered in the program.

4.2.1.2 Stress Predictions

The measured response is compared against that predicted by linear viscoelasticity for UTP-19,260B in the following order (Figures 68 through 78).

The results for the lowest and highest constant-rate tests (Test No. 1) appear in Figures 68 and 69. Those for the dual-rate tests (high-to-low and low-to-high, Test No. 3) are shown in Figures 70 and 71. Figure 72 contains the comparisons for a saw-tooth strain history (Test No. 5) with increasing strain peaks and rest periods between cycles. The results corresponding to short- and long-duration similitude tests are presented in Figures 73 and 74. The predicted and measured responses for the three-step relaxation test (Test No. 13) are included in Figure 75. In addition, the time-temperature superposition principle is put to use with constant rate tests (Test No. 1) at 70, 40 and 123°F, as shown in Figures 76 to 78, respectively. Stress predictions for some of the same tests on UTP-3001 are shown in Figures 79 through 86.

4.2.2 R. Farris Nonlinear Theory for Solid Propellants

The work of R. Farris (Reference 5) was a major attempt at predicting the nonlinear response of solid propellants in rocket motor analyses.

Experience with Farris' stress-strain law at Chemical Systems showed that this theory could not predict the response of solid propellants under strain

(Text continued on page 200.)

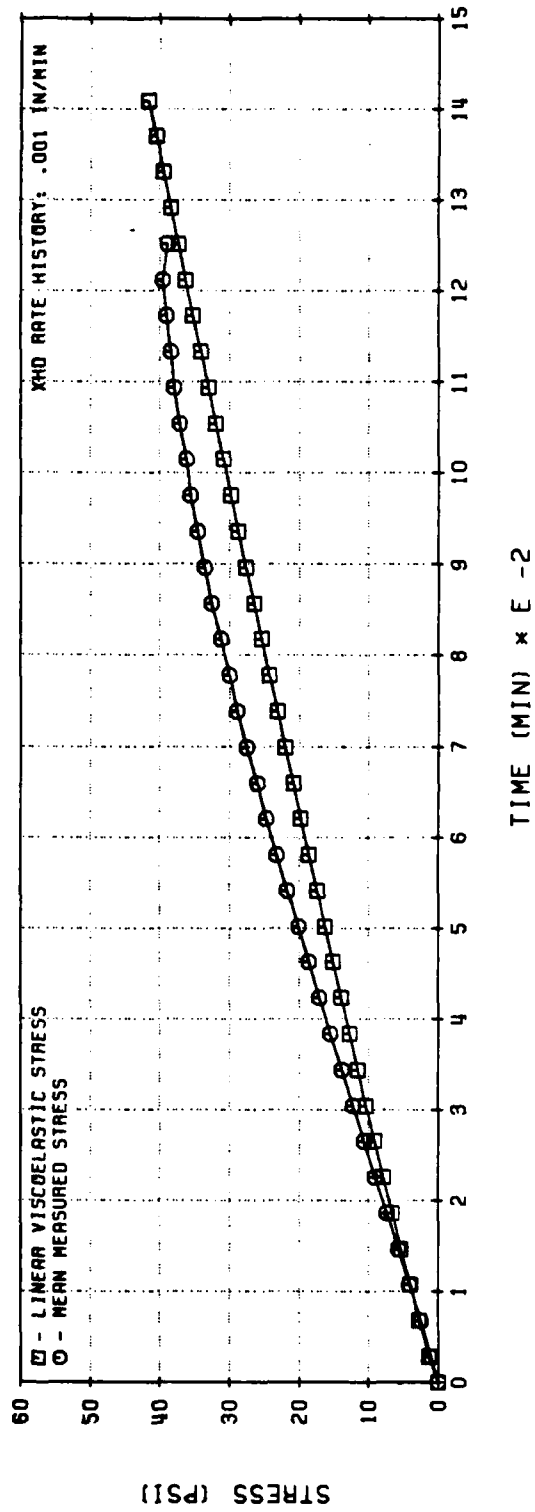
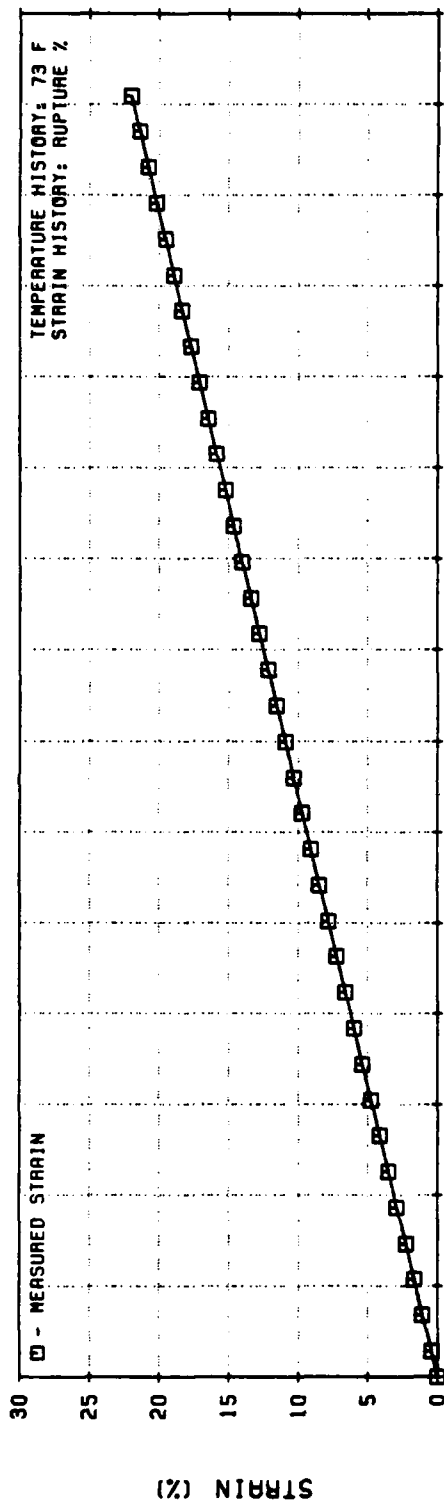


Figure 68. Linear Viscoelastic Stress Predictions for UTP-19,360B-400/1777
Constant Rate Test History (Code No. 1)

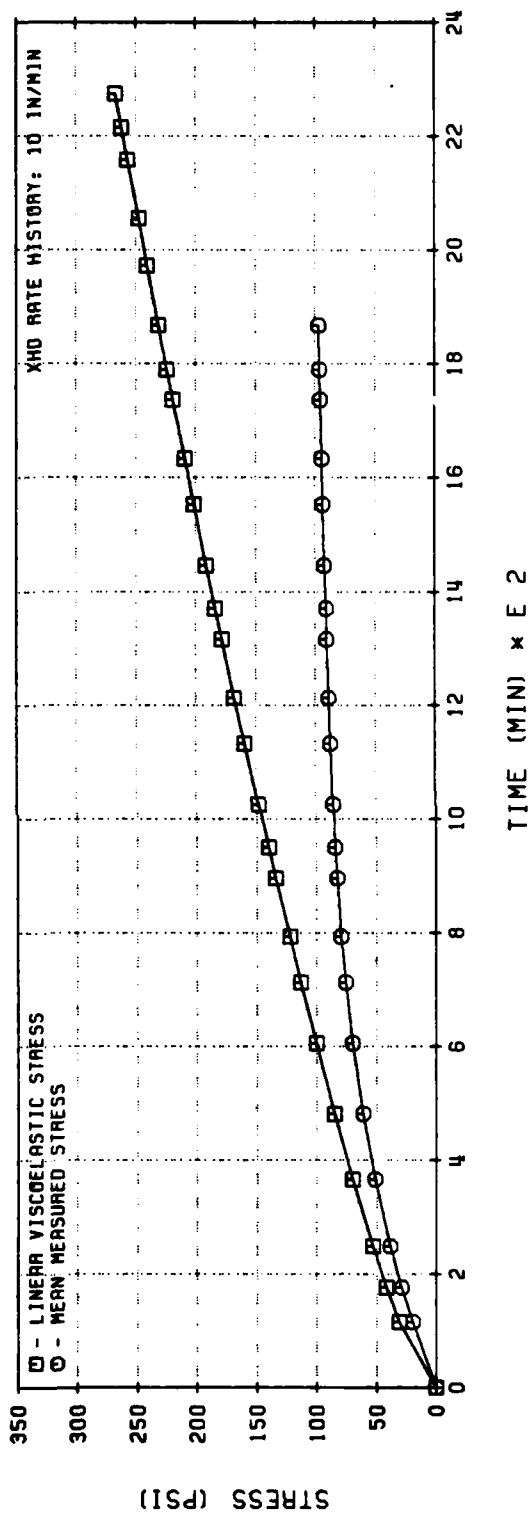
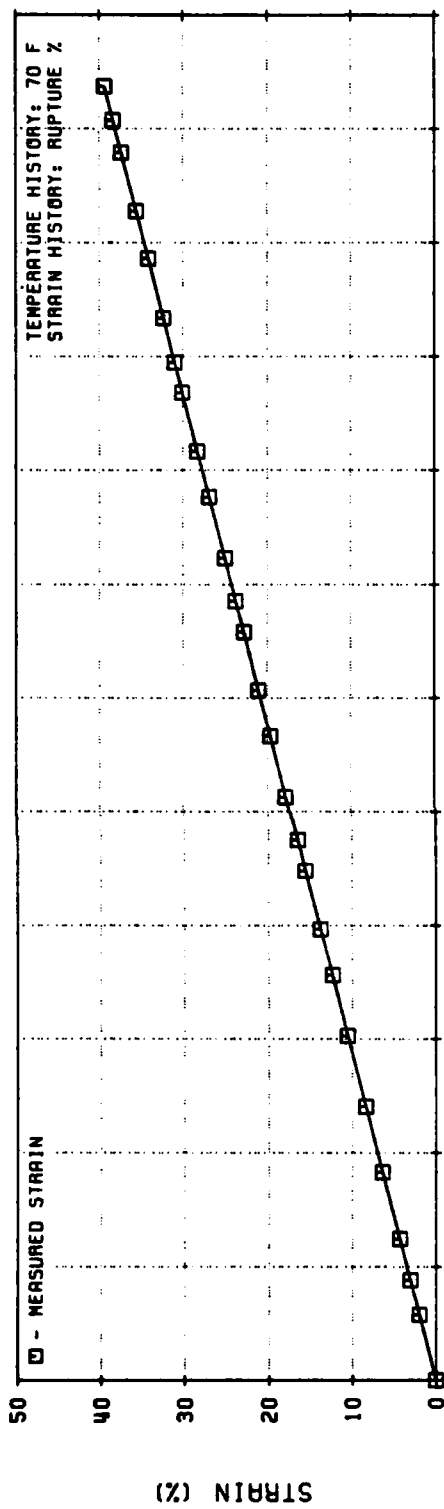


Figure 69. Linear Viscoelastic Stress Predictions for UTP-19, 360B-400/1777
Constant Rate Test History (Code No. 1)

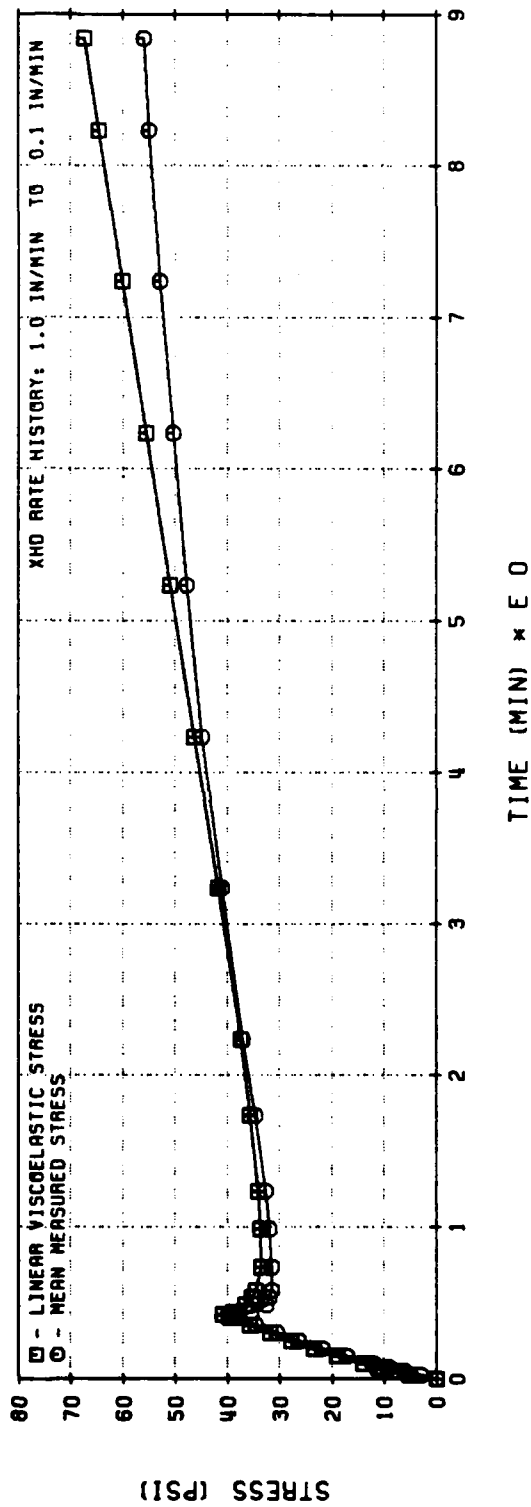
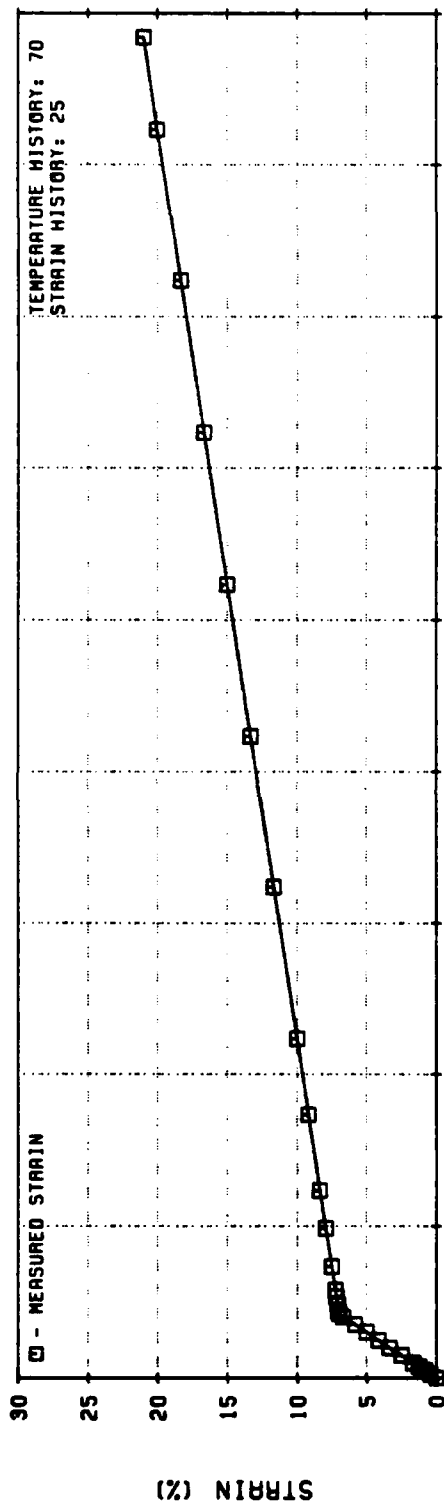


Figure 70. Linear Viscoelastic Stress Predictions for UTP-19, 360B-400/1777
Two Rate Test History (Code No. 3)

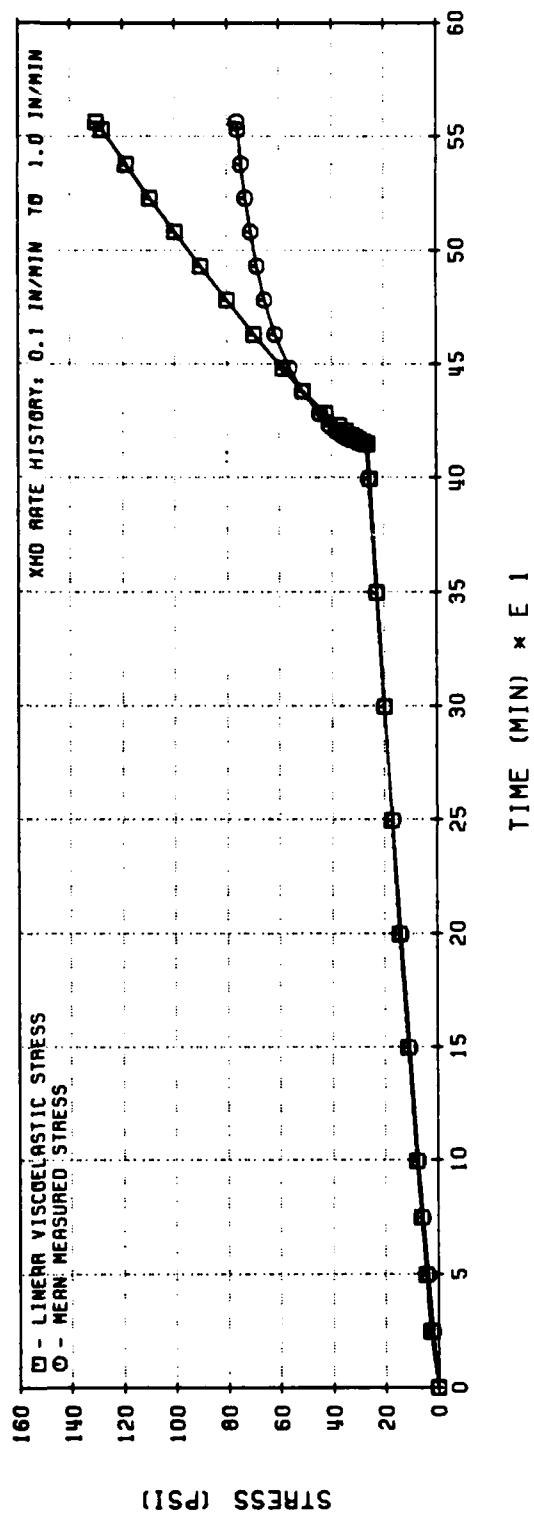
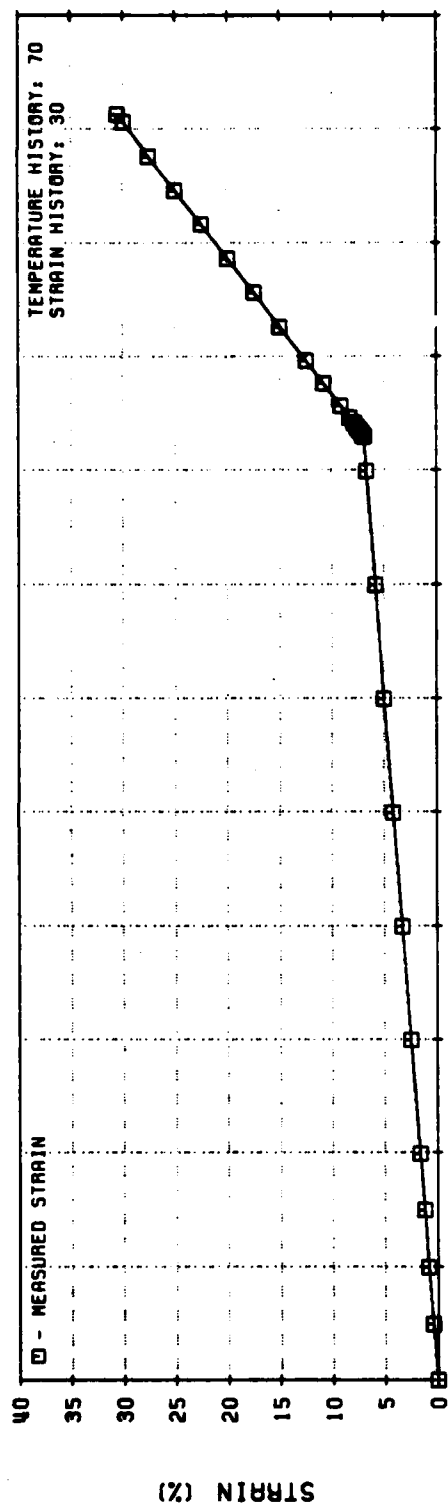


Figure 71. Linear Viscoelastic Stress Predictions for UTP-19,360B-400/1777
Two Rate Test History (Code No. 3)

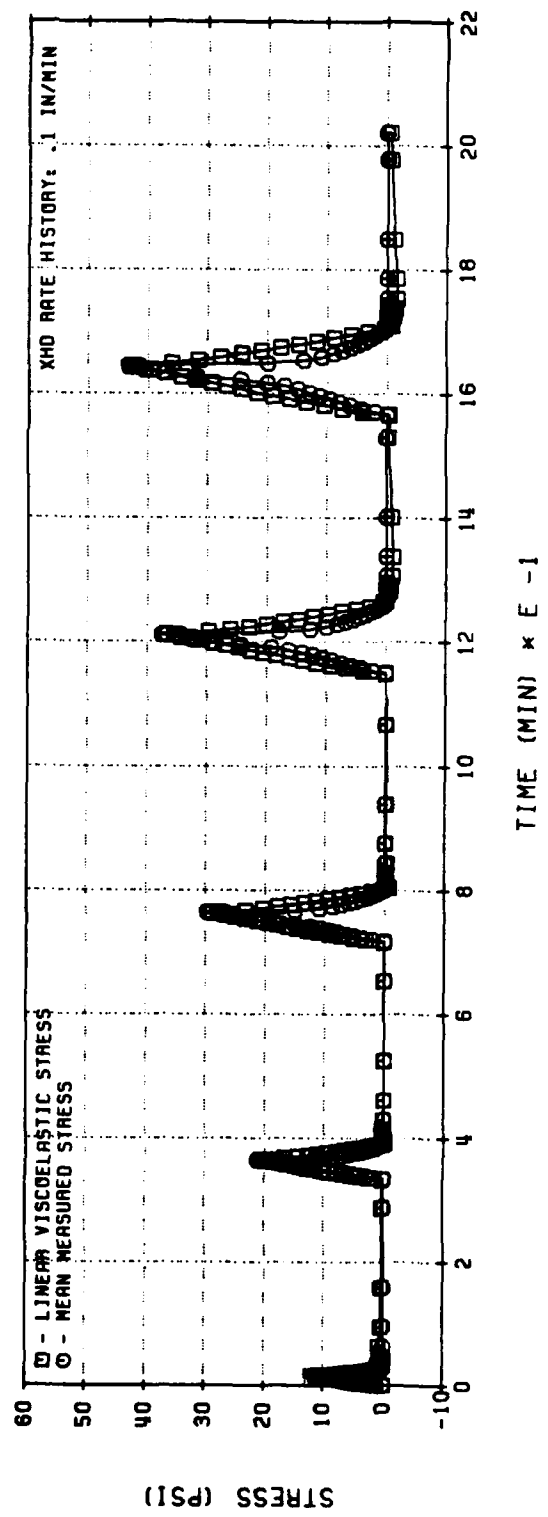
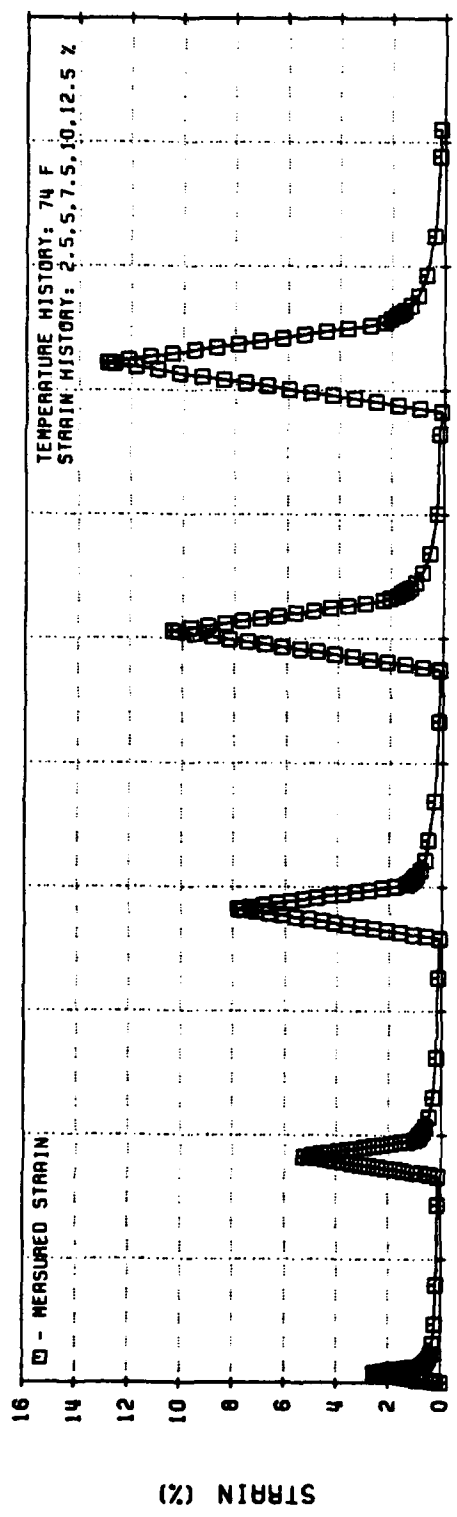


Figure 72. Linear Viscoelastic Stress Predictions for UTP-19,360B-400/1777
 Multiple Loading Test History (Code No. 5)

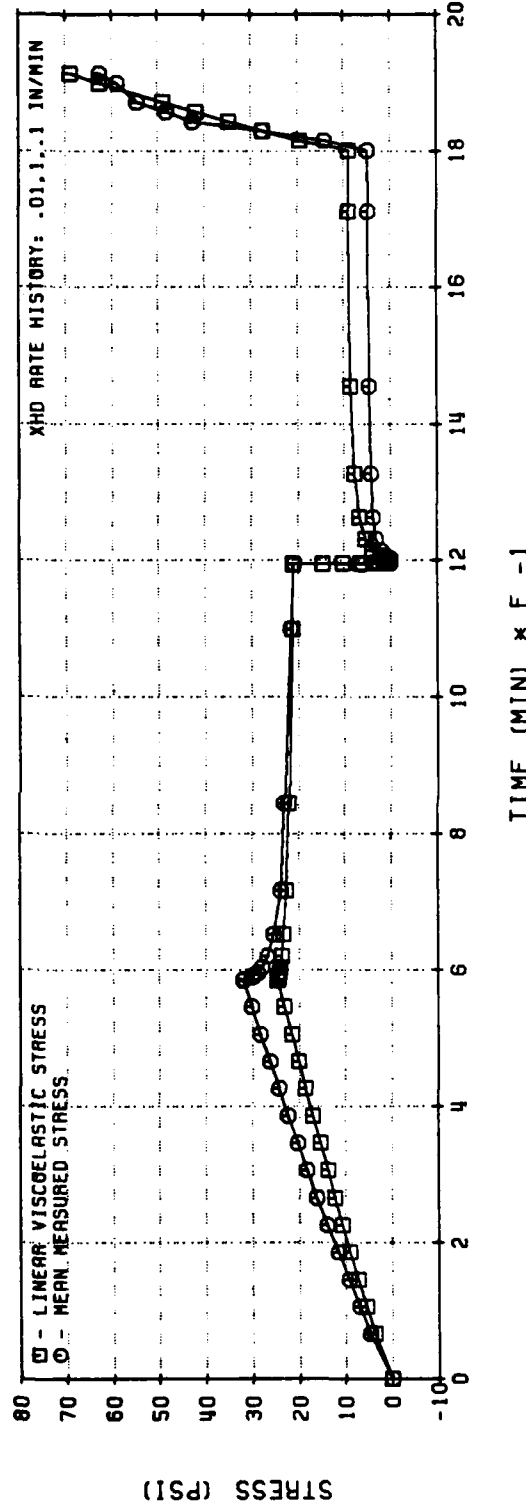
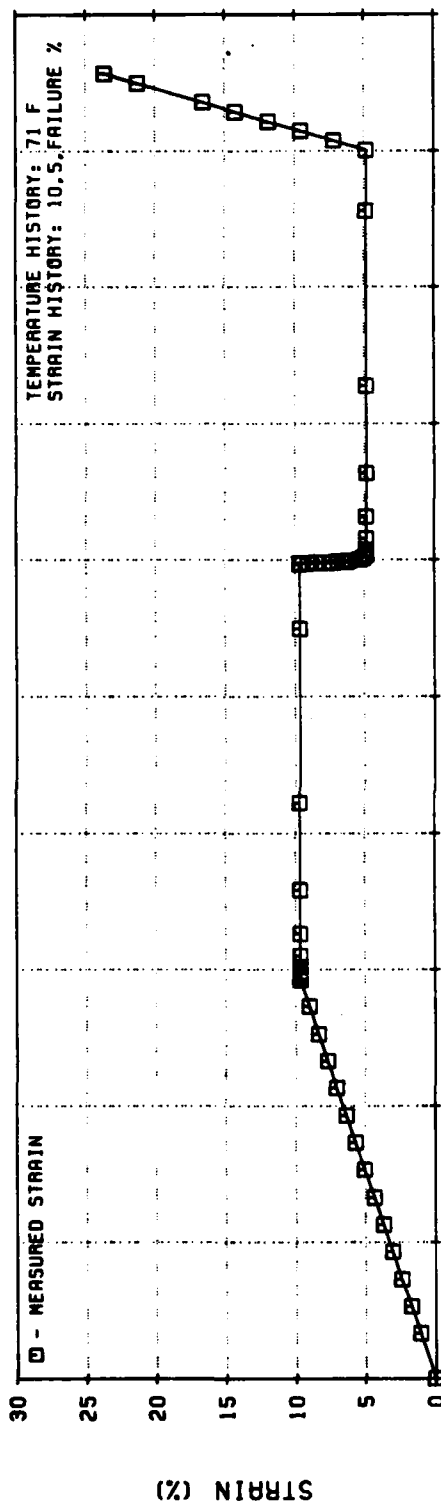


Figure 73. Linear Viscoelastic Stress Predictions for UTP-19,360B-400/1777
Similitude Test History (Code No. 12)

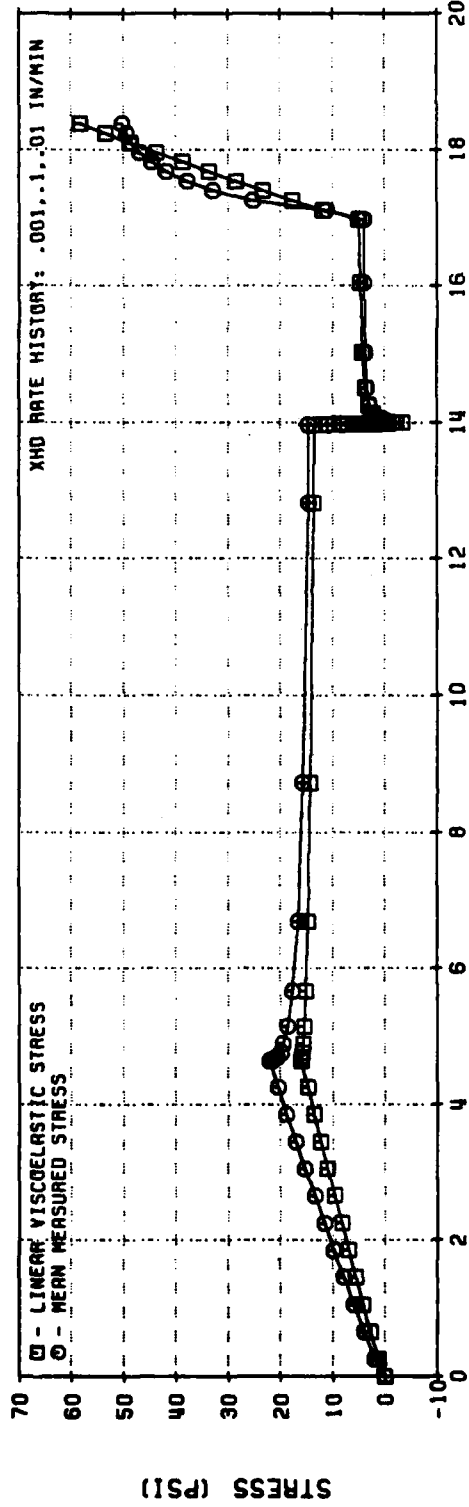
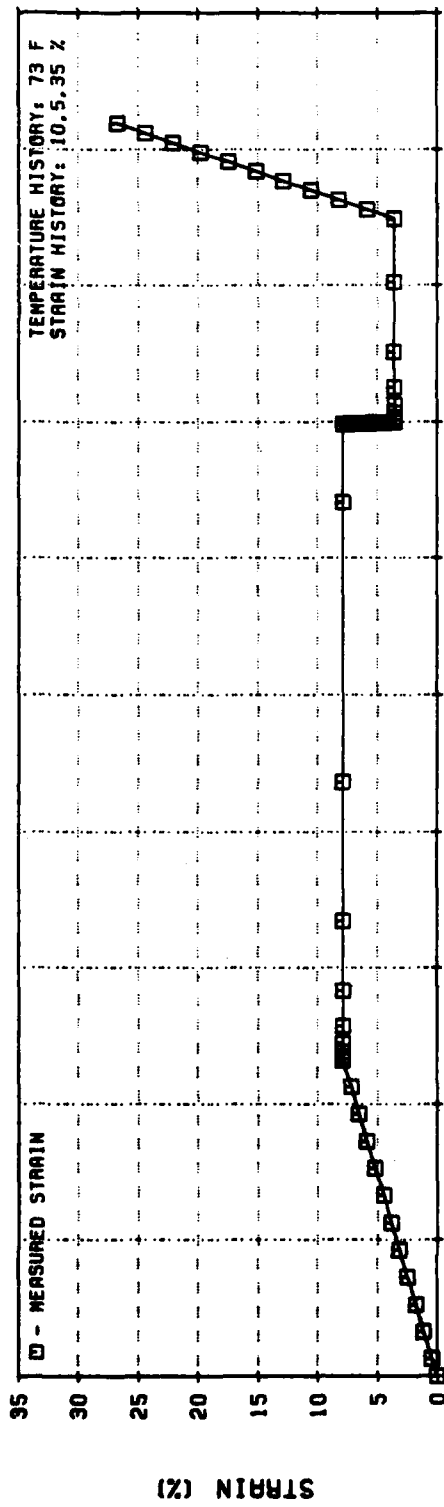


Figure 74. Linear Viscoelastic Stress Predictions for UTP-19,360B-400/1777 Similitude Test History (Code No. 12)

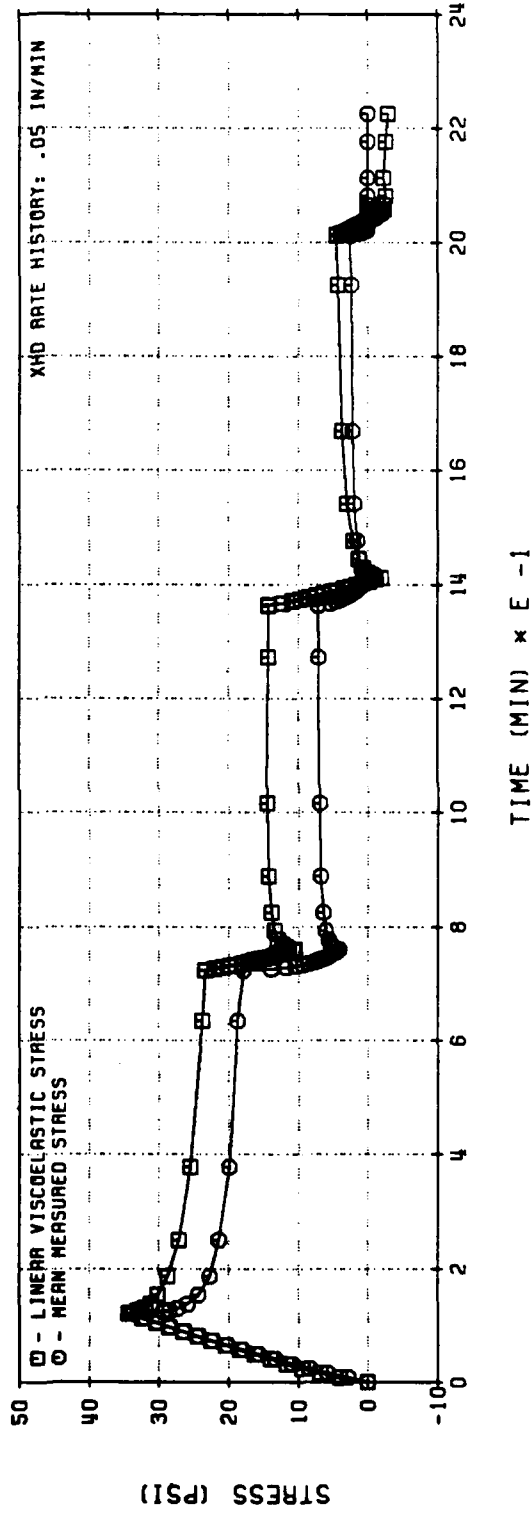
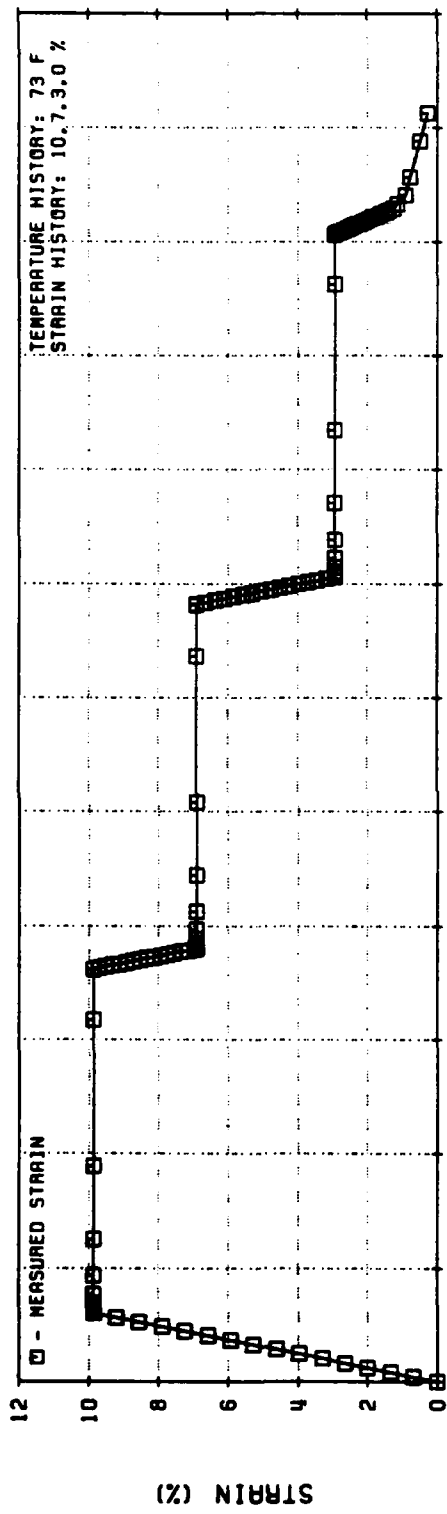


Figure 75. Linear Viscoelastic Stress Predictions for UTP-19,360B-400/1777
Three Step Relaxation Test History (Code No. 13)

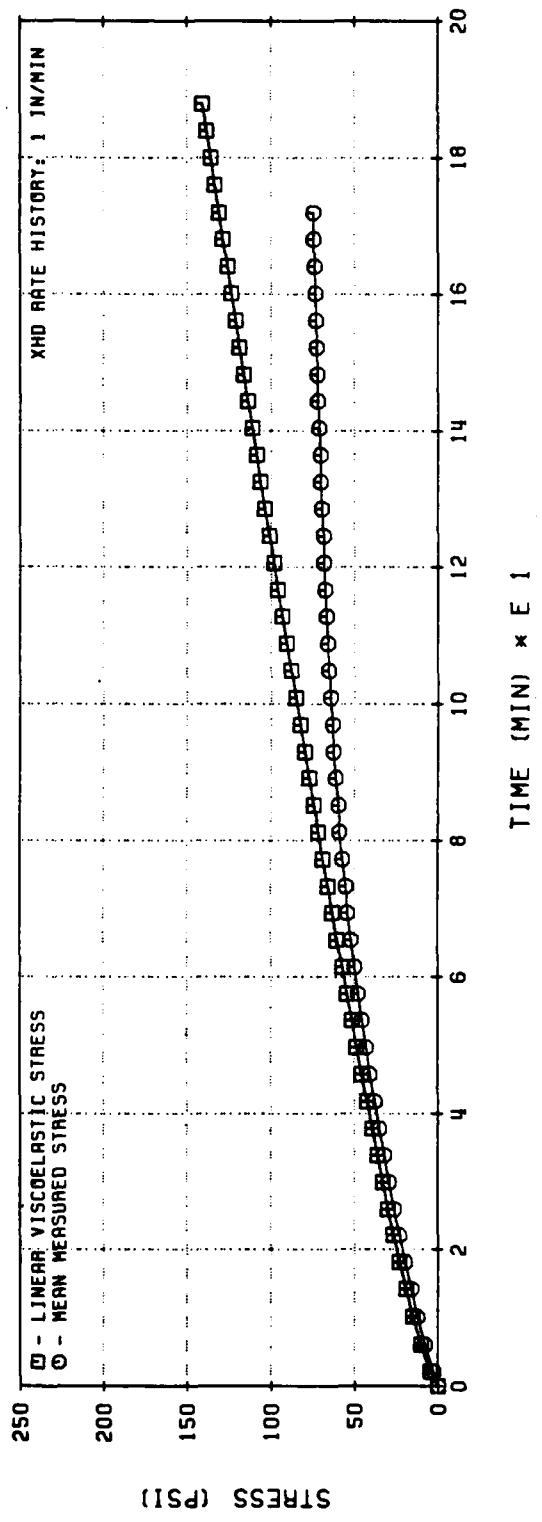
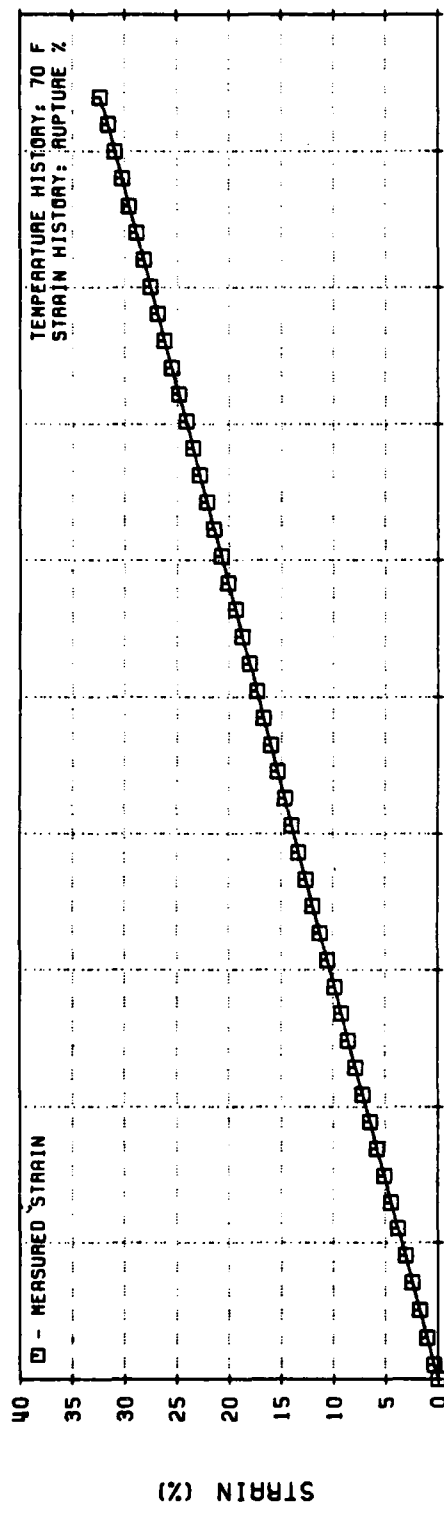


Figure 76. Linear Viscoelastic Stress Predictions for UTP-19, 360B-400/1777
Constant Rate Test History (Code No. 1)

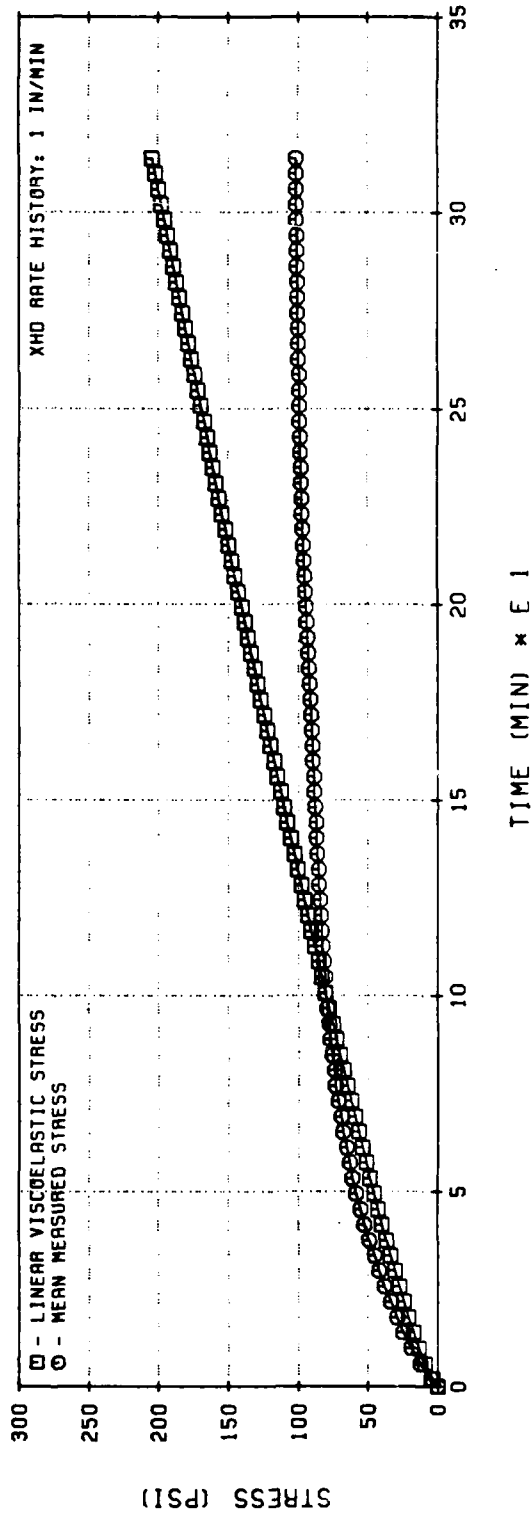
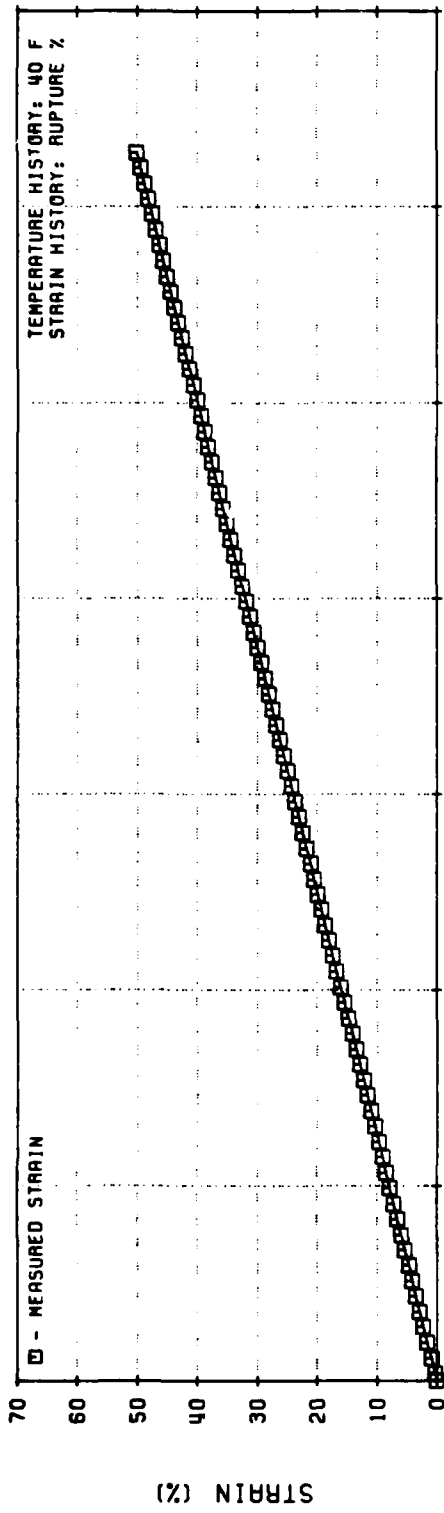


Figure 77. Linear Viscoelastic Stress Predictions for UTP-19, 360B-400/1777
Constant Rate Test History (Code No. 1)

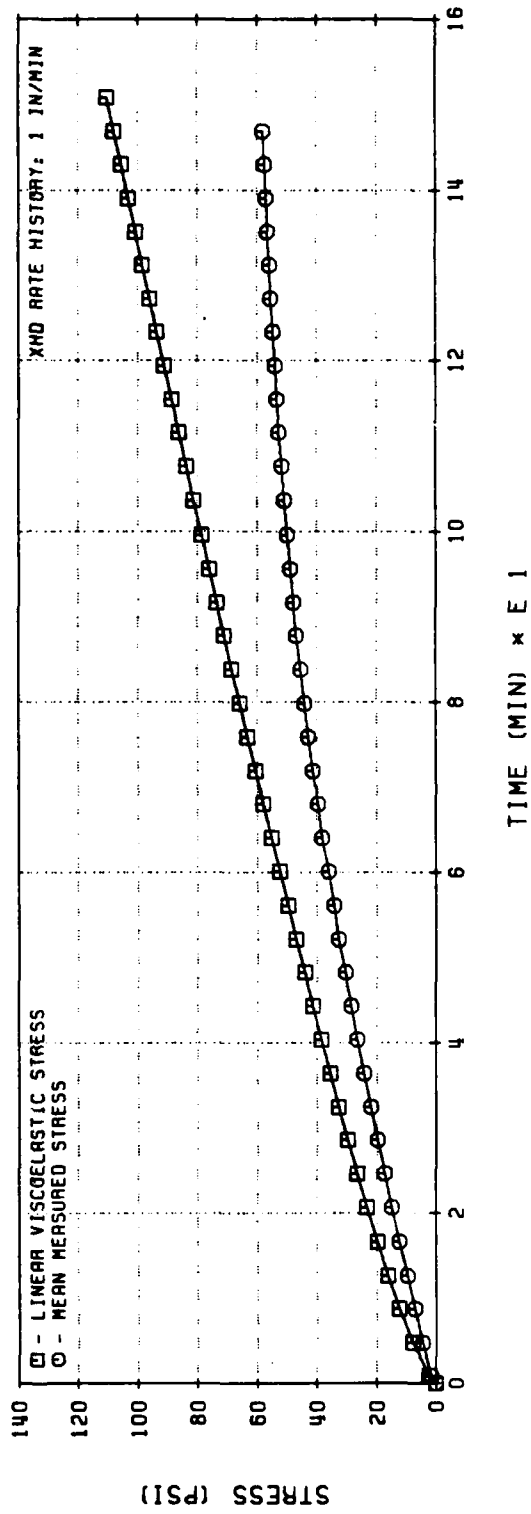
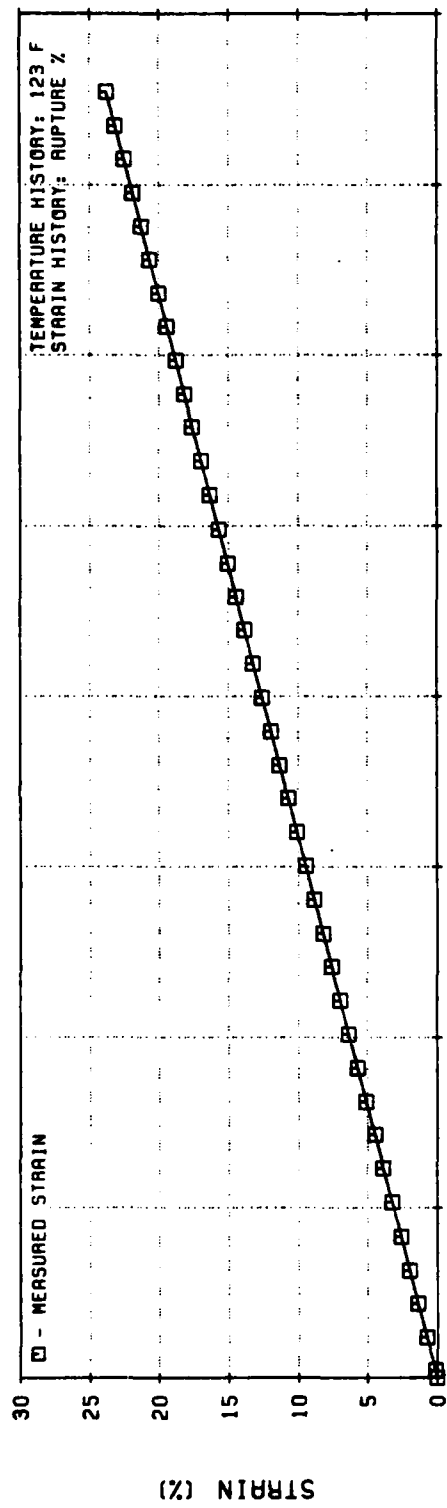


Figure 78. Linear Viscoelastic Stress Predictions for UTP-19, 360B-400/1777
Constant Rate Test History (Code No. 1)

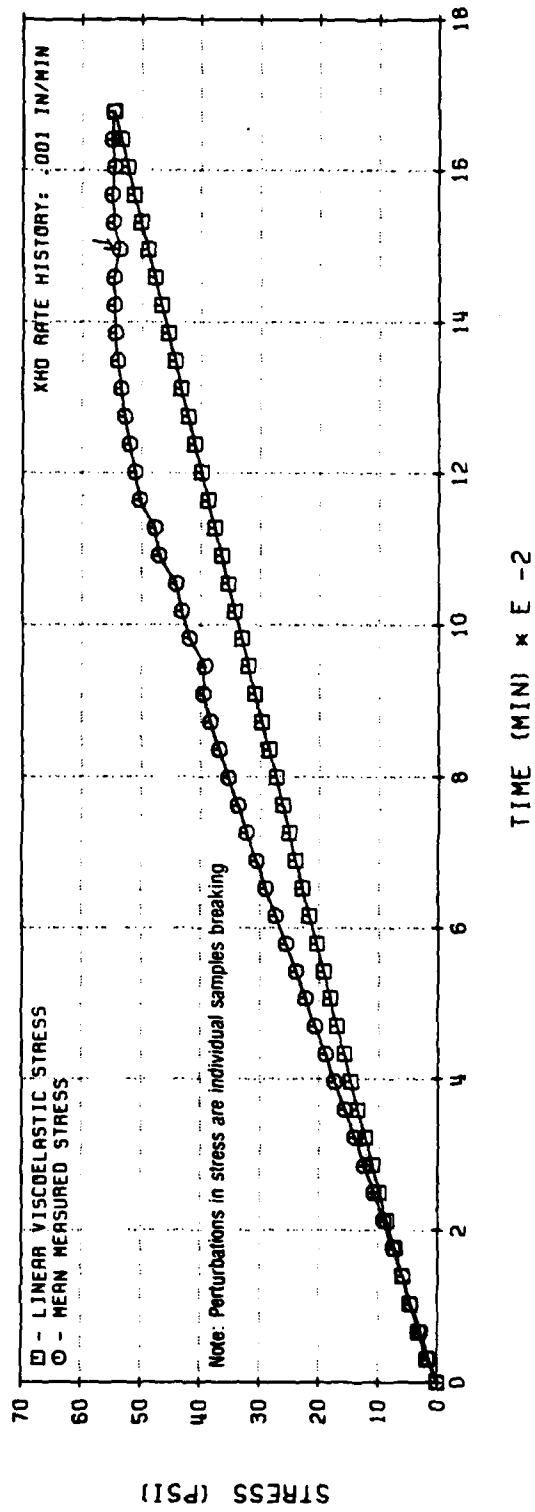
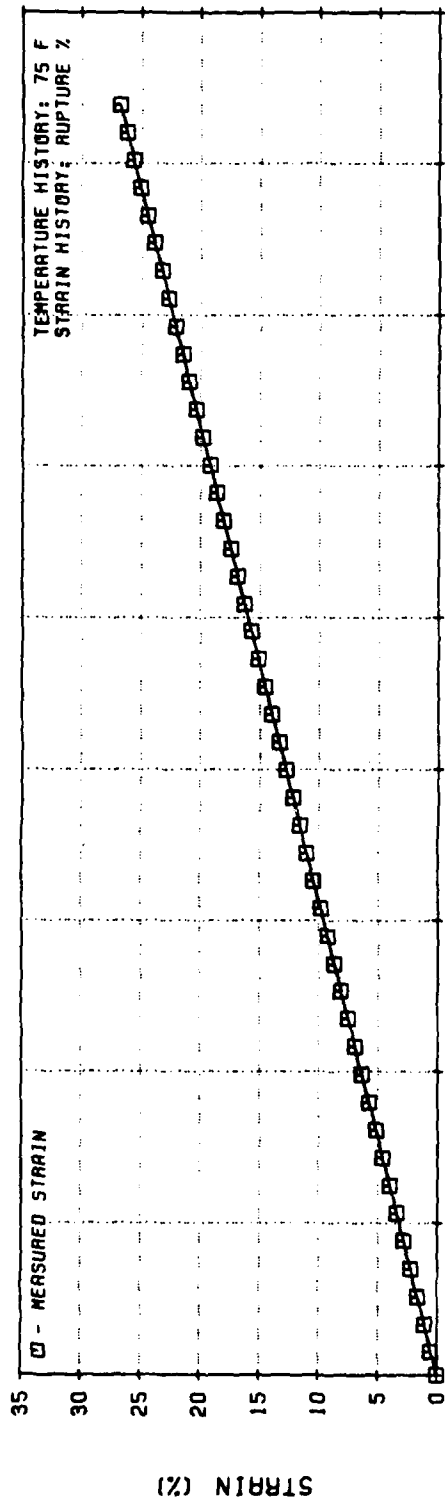


Figure 79. Linear Viscoelastic Stress Predictions for UTP-3001-750/7768
Constant Rate Test History (Code No. 1)

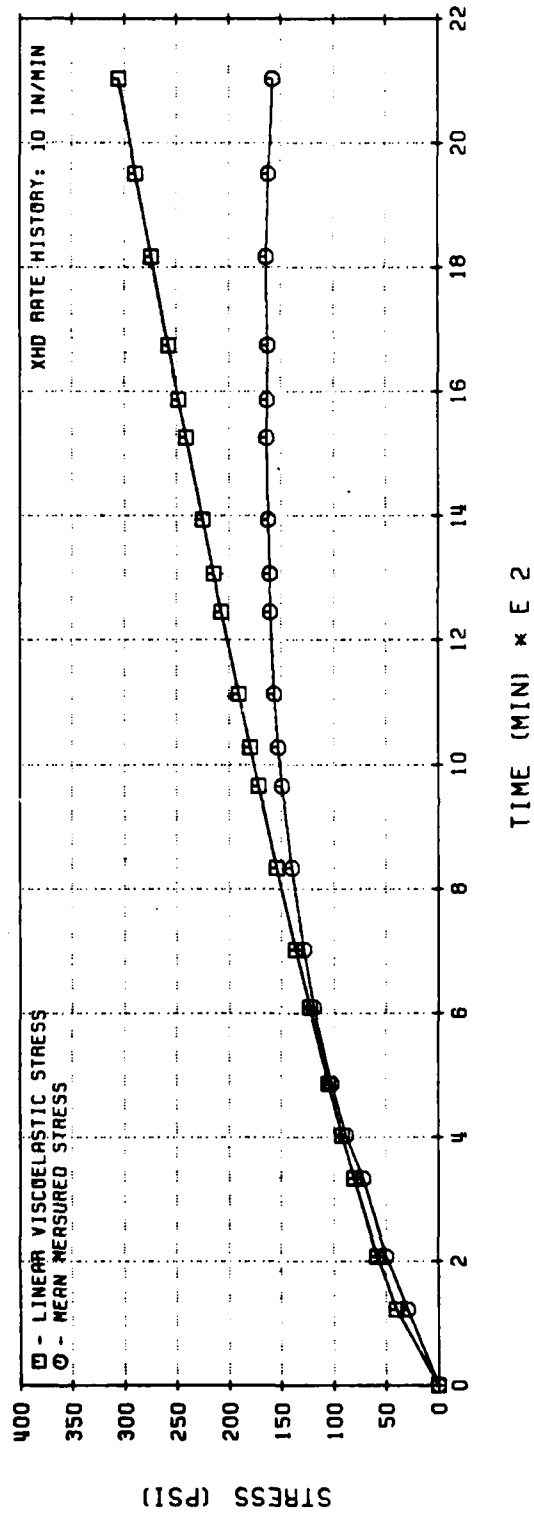
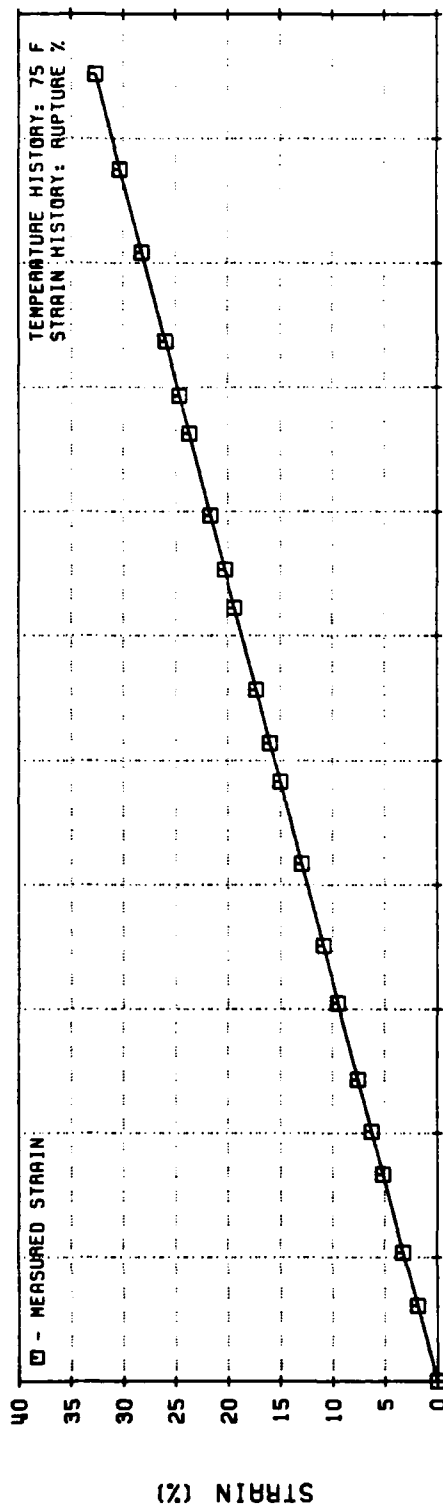


Figure 80. Linear Viscoelastic Stress Predictions for UTP-3001-750/7768
Constant Rate Test History (Code No. 1)

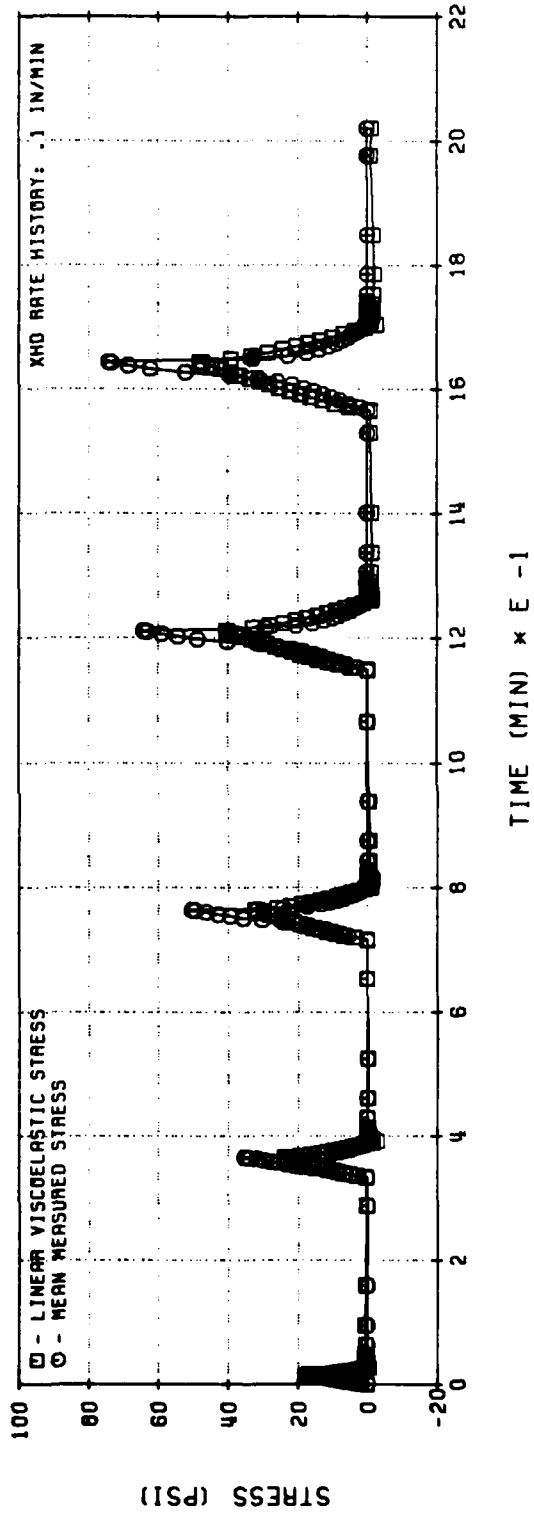
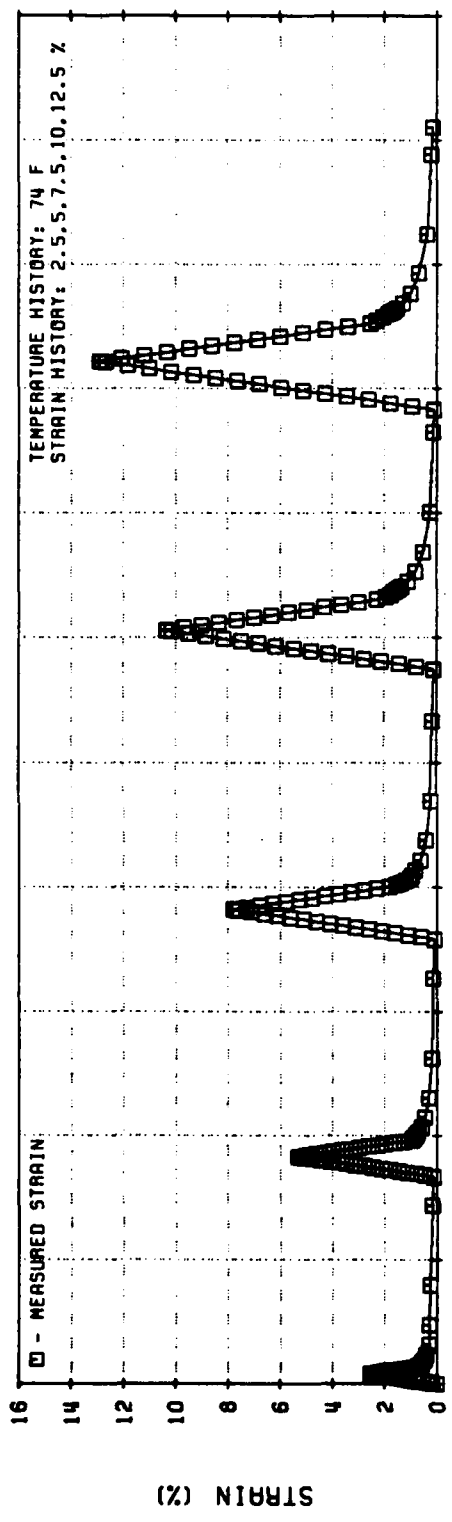


Figure 81. Linear Viscoelastic Stress Predictions for UTP-3001-750/7768
Multiple Loading Test History (Code No. 5)

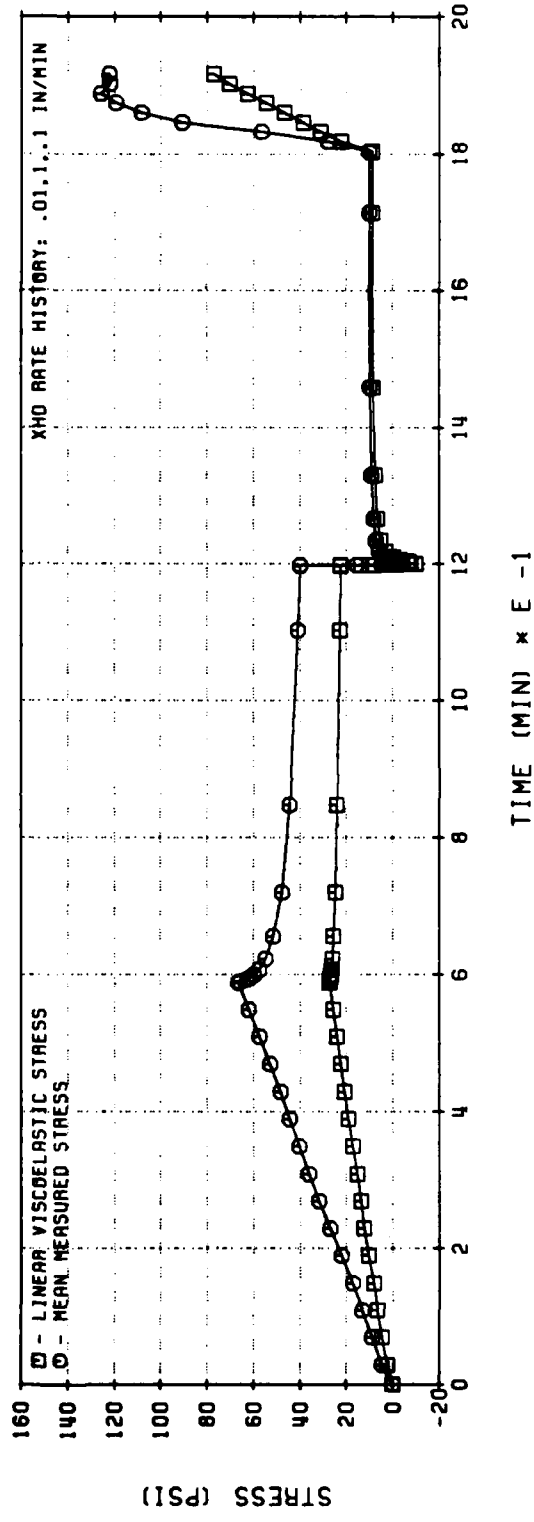
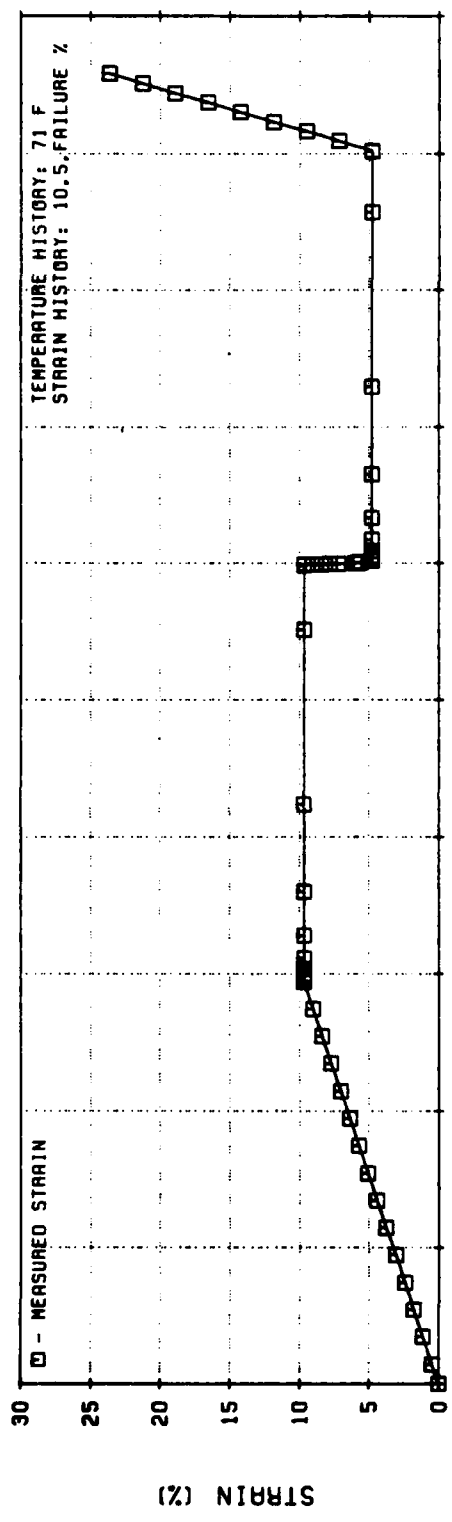


Figure 82. Linear Viscoelastic Stress Predictions for UTP-3001-750/7768
Similitude Test History (Code No. 12)

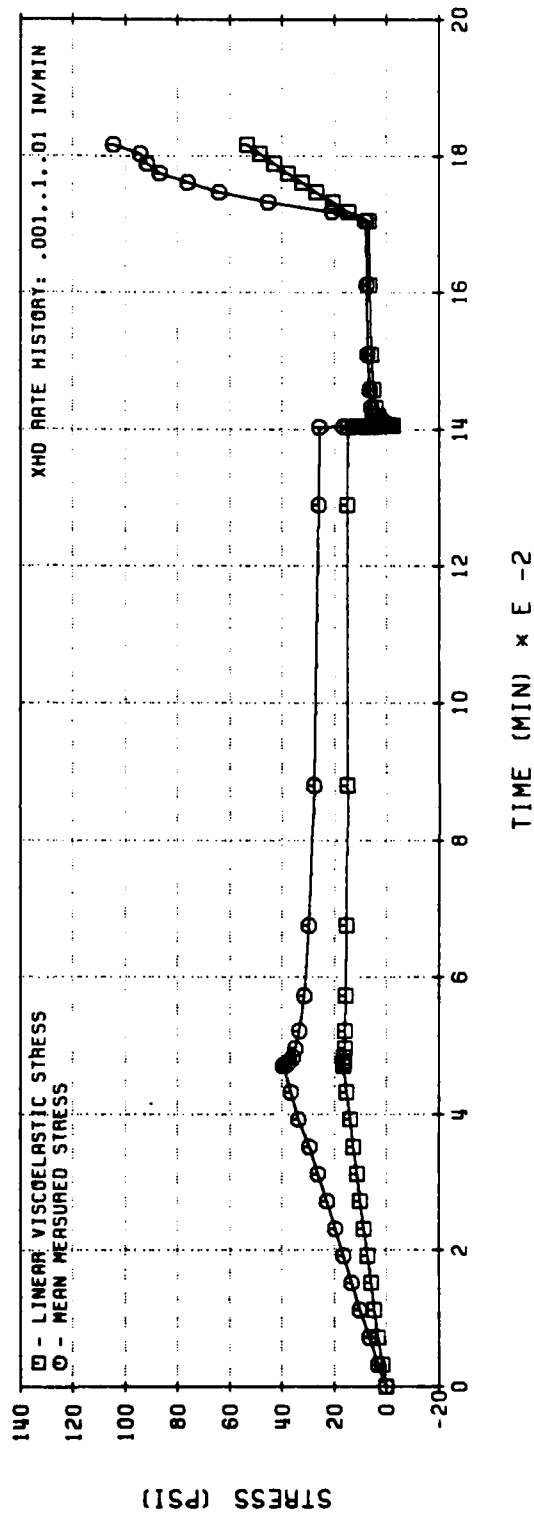
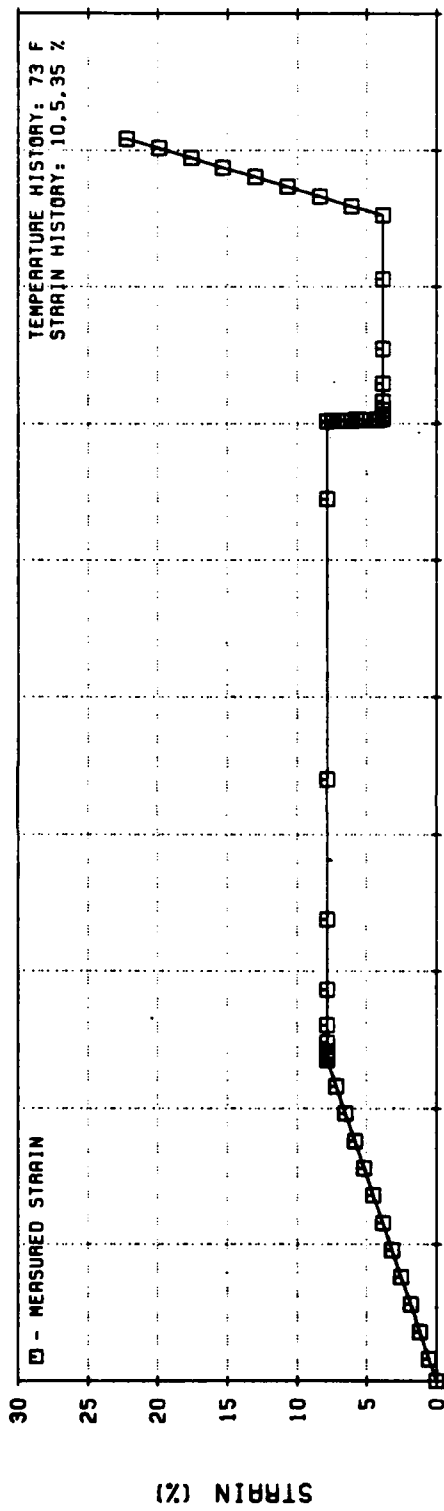


Figure 83. Linear Viscoelastic Stress Predictions for UTP-3001-750/7768
Similitude Test History (Code No. 12)

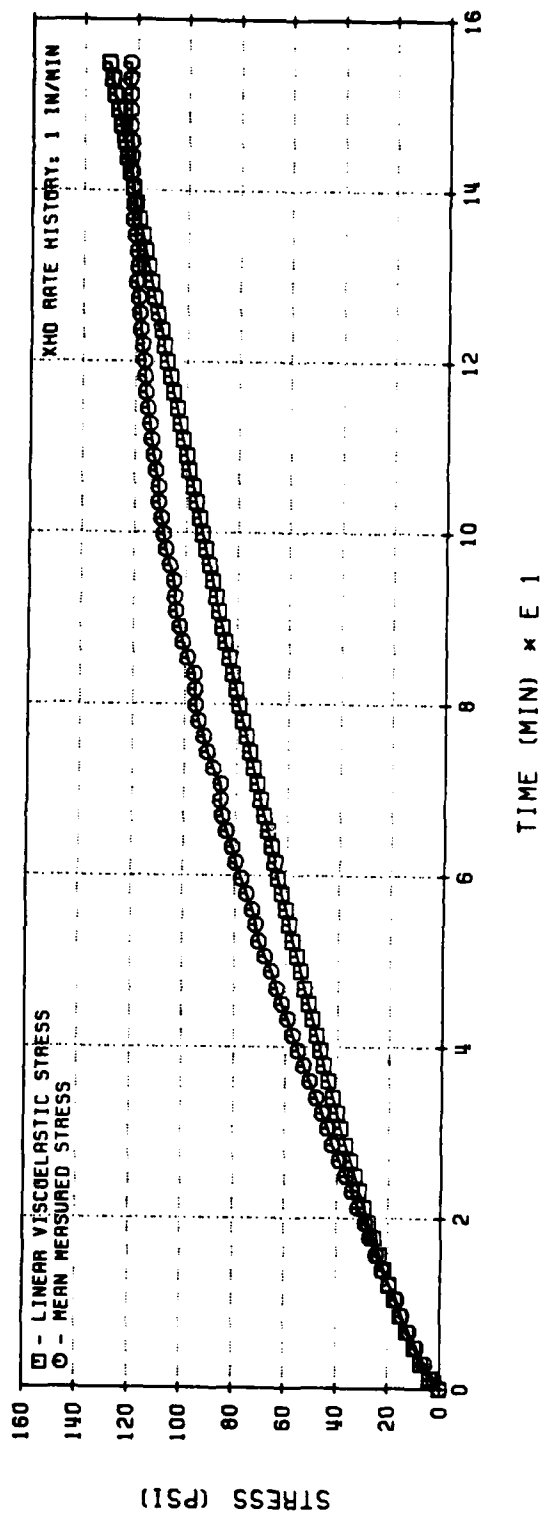
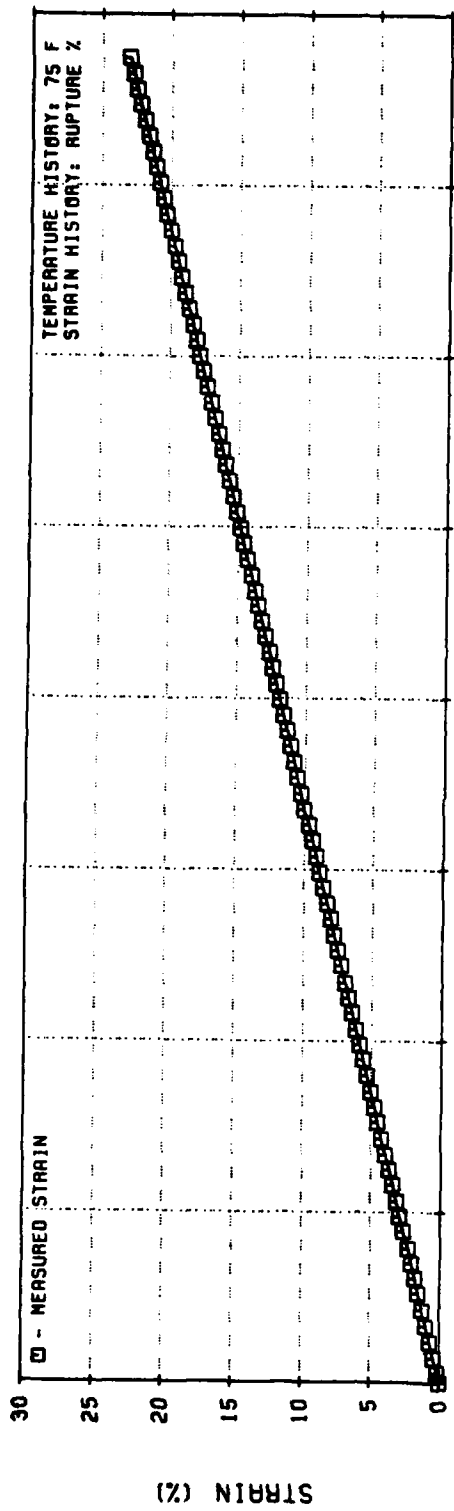


Figure 84. Linear Viscoelastic Stress Predictions for UTP-3001-750/7768
Constant Rate Test History (Code No. 1)

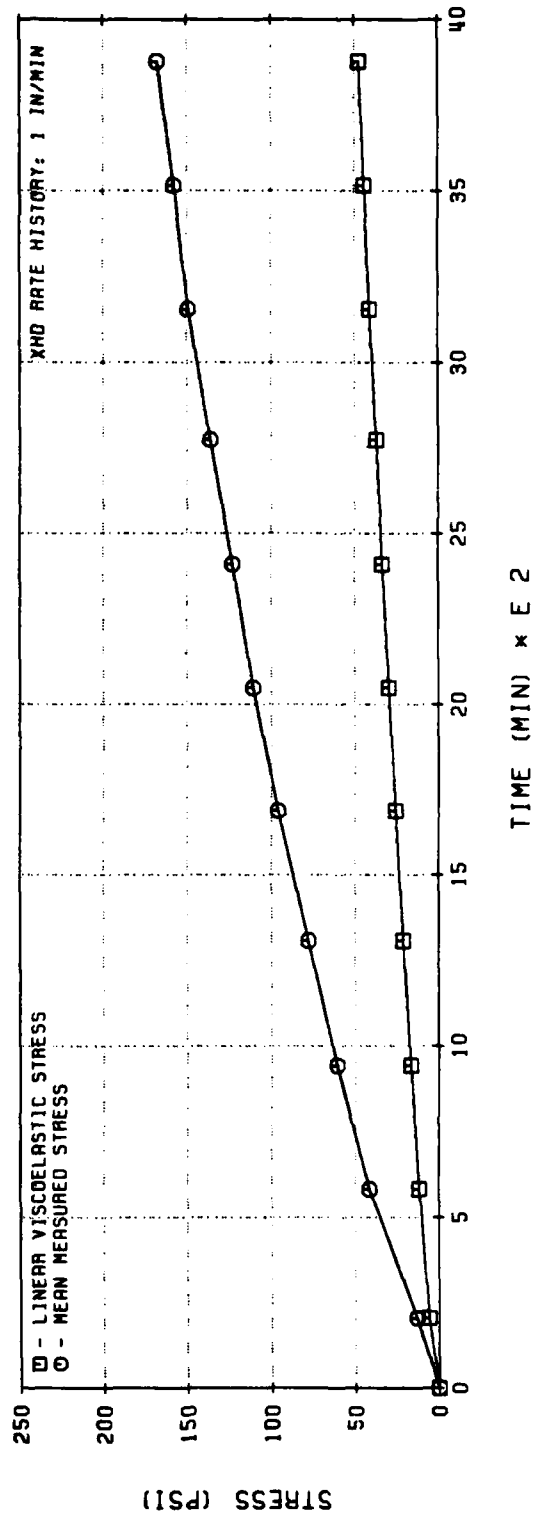
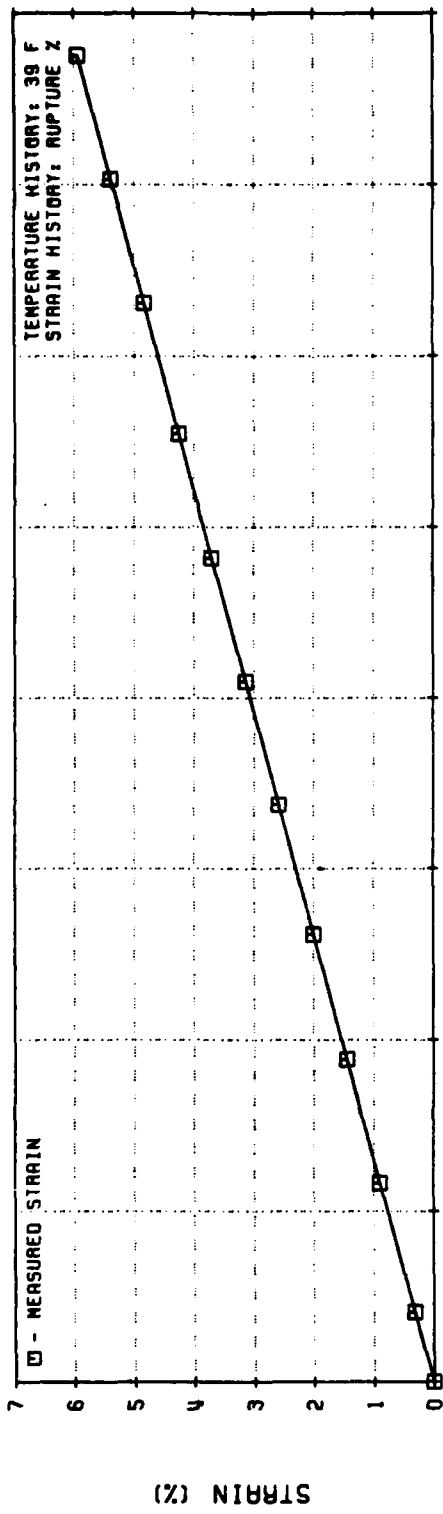


Figure 85. Linear Viscoelastic Stress Predictions for UTP-3001-750/7768
Constant Rate Test History (Code No. 1)

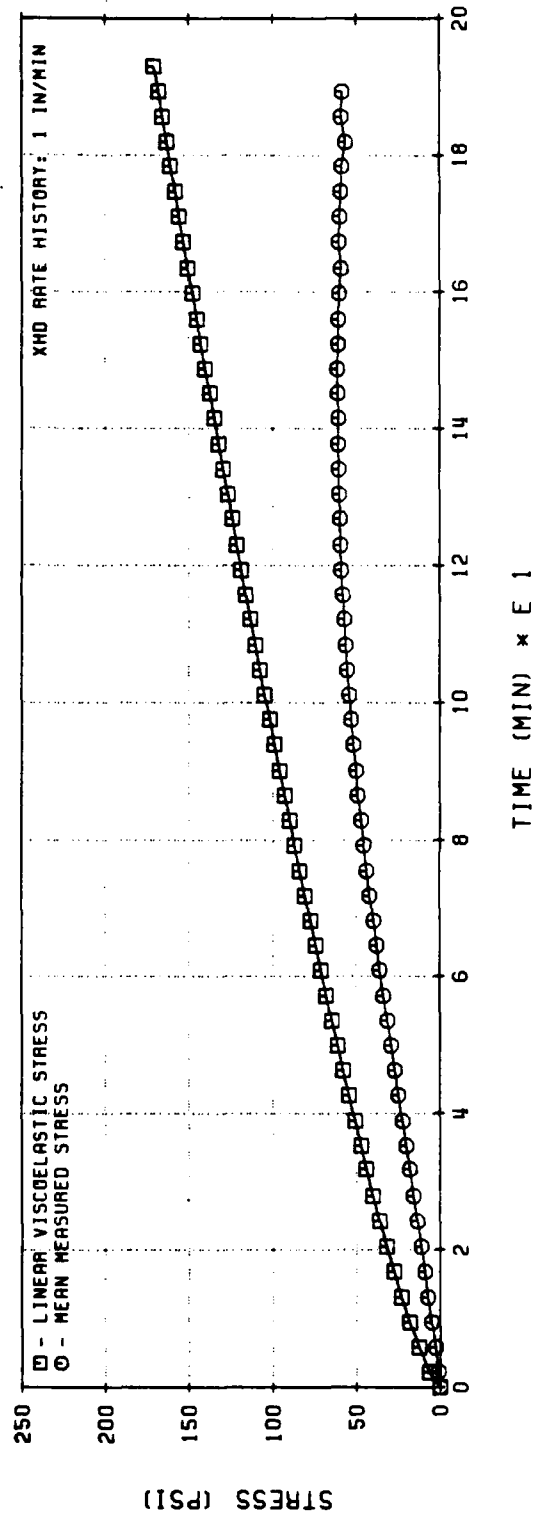
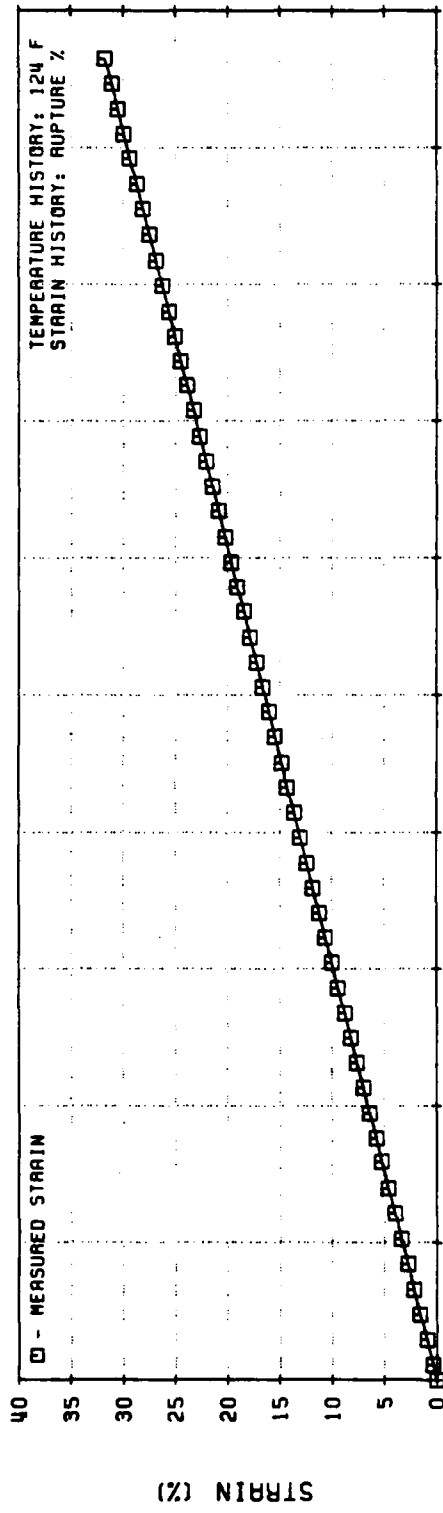


Figure 86. Linear Viscoelastic Stress Prediction for UTP-3001-750/7768
Constant Rate Test History (Code No. 1)

histories that were not included in the set used for material characterization. Although the predictions were generally acceptable for loading histories of the types included in such sets.

The nonlinear theory of Farris was considered in the first phase of the program and it was compared to the other five approaches originally proposed.

Farris postulated a model, based upon previous work on rubber elasticity, to account for the permanent-memory effects exhibited by many solid propellants under constant rate loading. This model presumes the existence of inhomogeneities in the local strain field between filler particles, a distribution of polymer chain lengths between filler particles, and a uniform failure strain for each polymer chain. This model has been successful in predicting the nonlinear permanent memory response of solid propellants before dewetting. The model predicts the same response in compression as in tension. This prediction is in agreement with experimental observations, although the molecular mechanisms contributing to the permanent memory response in compression are clearly different from those in tension.

Once dewetting occurs, the model is modified to account for vacuole formation and different results in compression and tension are expected. Farris presented the constitutive equation as the sum of an essentially time-independent bulk stress σ_B and a time-dependent deviatoric stress σ_{ij}^d , so that in general

$$\sigma_{ij}(t) = \sigma_B \delta_{ij} + \sigma_{ij}^d(t) \quad (8)$$

where δ_{ij} is the Kronecker delta equal to unity if $i = j$ and zero otherwise. The form developed for the deviatoric stress is

$$\sigma_{ij}^d(t) = e^{-BI_d/I_\gamma} \left\{ A_1 \sigma_{ij}^d(t) + A_2 \left(\frac{I_\gamma}{\|I_\gamma\|_{p_2}} \right)^{m_2} \sigma_{ij}^d(t) \right. \\ \left. + \int_0^t A_3(t-\xi) \dot{\sigma}_{ij}^d(\xi) d\xi + \left(\frac{I_\gamma}{\|I_\gamma\|_{p_4}} \right)^{m_4} \int_0^t A_4(t-\xi) \dot{\sigma}_{ij}^d(\xi) d\xi \right\} \quad (9)$$

where

I_d = volume dilatation = $e_{11} + e_{22} + e_{33}$ for small strains

$$I_\gamma = \text{octahedral shear strain} = \frac{1}{3} \left[(e_{11} - e_{22})^2 + (e_{22} - e_{33})^2 + (e_{33} - e_{11})^2 \right]^{1/2} \quad (10)$$

e_{ij}^d = deviatoric strain tensor

$B, A_1, A_2, A_3, A_4, M_2, M_4, P_2, P_4,$ = constants

and

$$\|I_\gamma\|_{p_1} = \left[\int_0^t |I_\gamma(\xi)|^{p_1} d\xi \right]^{1/p_1} \quad (11)$$

Equation (9) has been applied to reasonably complex deformation histories using unpressurized and pressurized uniaxial and biaxial test specimens. The agreement was not as good as would have been desirable, but it was still better than Linear Viscoelasticity. Time-temperature superposition was included in equation (9) by introducing a time-temperature shift factor, a_T , and redefining the L_p norm of equation 140 in the form:

$$\|I_\gamma\|_{p_1} = \left(\int_0^t \frac{|I_\gamma(\xi)|^{p_1}}{a_T(\xi)} d\xi \right)^{1/p_1} \quad (12)$$

Experimental data for simultaneous cooling and straining have been fit using equation (9) with the introduction of a time-temperature shift function a_T through equation (11). The justification for introducing an a_T in the above manner is not immediately obvious or adequately explained in the available literature.

To present the response to interrupted and cyclic constant strain rate tests, equation (9) was modified by setting $P_4 = \infty$ and $A_3 = -A_4$ so that:

$$\sigma_{ij}^d(t) = e^{-BI_d/I_\gamma} \left\{ A_1 e_{ij}^d(t) + A_2 \left(\frac{I_\gamma}{\|I_\gamma\|_{P_2}} \right)^{m_2} e_{ij}^d(t) \right. \\ \left. + \left[1 - \left(\frac{I_\gamma}{\|I_\gamma\|_\infty} \right)^{m_4} \right] \int_0^t A_3(t-\xi) e_{ij}^d(\xi) d\xi \right. \quad (13)$$

where:

$$\|I_\gamma\|_\infty = \max |I_\gamma(\xi)|, \quad 0 < \xi < t$$

The multiplier for the hereditary integral in equation (12) vanishes whenever the current value of I_γ is at its largest, and is non-zero for all other values. This representation allows for viscoelastic (fading memory) response on unloading.

The bulk stress, σ_B , in equation (8) was taken to be essentially time-independent, although there is coupling between distortion and dilatation as indicated in the exponential multiplier in equations (9) and (13).

The first attempt to represent the bulk stress took the form of a series

$$\frac{\sigma_{kk}}{3} = \sum_{i,j=0}^N A_{ij} I_d^i I_\gamma^j ; A_\infty = 0 \quad (14)$$

This equation adequately predicts the bulk stress as long as it does not vary greatly. However, when a hydrostatic pressure is superimposed, very poor results are obtained. In an attempt to overcome this difficulty, Farris modeled the compressibility of the gas voids caused by vacuole dilatation by treating them as spherical voids contained in an elastic medium. Assuming that (1) the voids themselves offer no resistance, (2) that all void dilatation is caused by distortion of the surrounding elastic material, (3) the void content at zero pressure may be represented as a power law in terms of the octahedral shear strain I_γ , and (4) that the bulk behavior varies linearly with hydrostatic pressure (P), the model yields:

$$I_d = C_1 P + C_2 I_\gamma^n e^{\left(\frac{-3P}{4G}\right)} \quad (15)$$

for the dilatation. The C_1 , C_2 and n are constants and G is the shear modulus of the elastic matrix material.

4.2.3 R. Schapery's Nonlinear Stress-Strain Law

4.2.3.1 Original Model

The constitutive theory advanced in References 17 and 18 for viscoelastic materials with microcracking was taken by Dr. R. Schapery as the starting point for predicting the response of solid propellants under general loading conditions. The one-dimensional version of this law takes the following simple form:

$$\sigma = \frac{A_F}{\lambda} \sigma_\ell \quad (16)$$

where σ_ℓ is the linear viscoelastic stress for a thermorheologically simple material:

$$\sigma_\ell = \int_0^t E(\xi - \xi') \frac{d\epsilon_\sigma}{d\tau} d\tau, \quad (17)$$

with

$\epsilon_\sigma \equiv \epsilon - \alpha(T - T_0)$ = strain due to mechanically applied stress

$$\xi = \int_0^t dt' / A_T [T(t')]$$

$$\xi' \equiv \xi(\tau)$$

$E(\xi)$ = linear viscoelastic relaxation modulus

T_0 = temperature at $t = 0$

$A_F = A_F(T)$ = temperature-dependent material function

$\lambda = \lambda(S_\ell)$: softening function in which the damage parameter:

$$S_{\rho} = \int_0^{\hat{\xi}} \left(\frac{\sigma_{\rho} A_F}{f} \right)^q d\hat{\xi} \quad (18)$$

depends only on the strain and temperature histories, and:

$$f = \begin{cases} 1 & \text{for } 0 \leq \epsilon < \epsilon_1 \\ (\epsilon/\epsilon_1)^{\beta} & \text{for } \epsilon_1 \leq \epsilon < \epsilon_2 \\ (\epsilon_2/\epsilon_1)^{\beta} & \text{for } \epsilon \geq \epsilon_2 \end{cases}$$

for constant threshold strains ϵ_1 and ϵ_2 , with $\beta > 0$.

The function $F = F(\epsilon_0)$ and the positive, constant exponent, q , originate with the equation for microcrack speed,

$$\frac{dA}{d\hat{\xi}} = M(K_I/f)^q \quad (19)$$

where M is a positive constant and:

$$d\hat{\xi} = dt/A_c \quad (20)$$

in which $A_c = A_c(T)$ is the shift-factor for microcrack growth rate.

The functional form of the softening function, $\lambda = \lambda(S_{\rho})$, depends on the type of behavior that need be reproduced. The following special case was used:

$$\lambda = [1 + cS_{\rho}]^{p/q}$$

where c and p are positive constants. Note that when $S_{\rho} = 0$, or $c = 0$, a linear viscoelastic stress-strain equation is recovered from Equation (16).

Taking $A_F = 1$, several sets of numerical values for the constitutive parameters corresponding to TP-H1011 were tried without success. This theory was also

used to predict the response of UTP-19,360 and UTP-3001. Having failed to perform better than Linear Viscoelasticity in many cases, it has undergone several changes since.

4.2.3.2 Current Model

The essential form of the modified uniaxial stress-strain relation is given by:

$$\sigma = f(\epsilon^0, \epsilon_m^0, S) \quad (21)$$

where:

σ = engineering stress

ϵ_r^0 = psuedo strain

$$\epsilon_r^0 = \frac{1}{E_R} \int_0^t E(t - \tau) \frac{d\epsilon}{d\tau} d\tau \quad (22)$$

ϵ_m^0 = maximum value of $|\epsilon^0|$ up to the current time

S = damage parameter

$$S = \left(\int_0^t |\epsilon^0|^q dt \right)^{1/q} \quad (23)$$

E_R = arbitrarily selected reference modulus,

$E(t)$ = linear viscoelastic relaxation modulus,

$$= E_e + E_2 t^{-n} \cong E_2 (E_\tau + t^{-n}), \quad (24)$$

$E_\tau = E_e/E_2$,

and

q = positive constant.

The functional form of f in equation (21) depends on the material considered. Studies on solid propellant to date indicate it may be taken as follows for some solid propellants.

$$f = Y_1 Y_2 Y_3 P_{15} \text{ sign } (\epsilon^0) \quad (25)$$

in which

$$\text{sign } (\epsilon^0) = \begin{cases} 1 & \text{if } \epsilon^0 > 0 \\ 0 & \text{if } \epsilon^0 = 0 \\ -1 & \text{if } \epsilon^0 < 0 \end{cases}$$

and P_{15} is used to normalize function Y_3 to unity, at a reference point. The Y_1 's are the following functions of damage and pseudo strain:

$$Y_1 = Y_1 (S) = \begin{cases} 1 + A_1 S + A_2 S^2 + A_3 S^3 & \text{for } S \leq S_0 \\ A_4 S A_5 & \text{for } S > S_0 \end{cases} \quad (26)$$

$$Y_2 = A_2 S^{0.63-Sx} (\epsilon_m^0) (0.463 - M_x - L_x) \left| \epsilon^0 \right|^{L_x} \quad (27)$$

$$Y_3 = C_0 + C_1 x + C_2 x^2 + C_3 x^3 + C_4 x^4 + C_5 x^5 \quad (28)$$

where:

$$x = x_r \left| \frac{\epsilon^0}{\epsilon_m^0} \right|^\lambda \quad (29)$$

in which x_r is the only root of the equation:

$$\max(S_r) = Y_3 (x_r) \quad (30)$$

with $\max (S_r)$ representing the maximum value of S_r up to the current time, and:

$$S_r = \frac{S_x \left| \epsilon_m^0 \right|^{M_x}}{P_{15}} \quad (31)$$

while λ is a factor that accounts for relatively small higher order effects possibly due to rehealing and particle interaction.

The constants entering the definitions of Y_1 , Y_2 , and Y_3 depend on the material. For UTP-19,360B they are:

$$\begin{aligned} S_0 &= 42 \\ S_x &= 0.637 \\ M_x &= -0.387 \\ L_x &= 0.85 \end{aligned} \quad (32)$$

and the factor λ is given by:

$$\lambda = K_x C_{cm}^{-C_x} \quad (33)$$

The resulting form of equation (21) for UTP-19,360B is thus:

$$\sigma = P_{15} A_6 Y_1 Y_3 \left| \epsilon^0 \right|^{L_x} \text{sign}(\epsilon^0) \quad (34)$$

Clearly, if $L_x = 1$, equation (34) may be written as:

$$\sigma = A_F \int_0^t E(t - \tau) \frac{d\epsilon}{d\tau} d\tau \quad (35)$$

in which $a_F = a_F(\epsilon^0, \epsilon_m^0, S)$ plays the role of a softening function, reminiscent of the Mullins-Tobin approach.

4.2.3.3 Stress Predictions

The current version of the nonlinear model developed by R. Schapery may be used to predict the response of solid propellants with a rather remarkable degree of accuracy, as may be seen in Figures 87 to 94, which are sample cases of the isothermal tests considered in the program. The first two plots (Figures 87 and 88) correspond to the highest and lowest constant rate tests

(Text continued on page 216.)

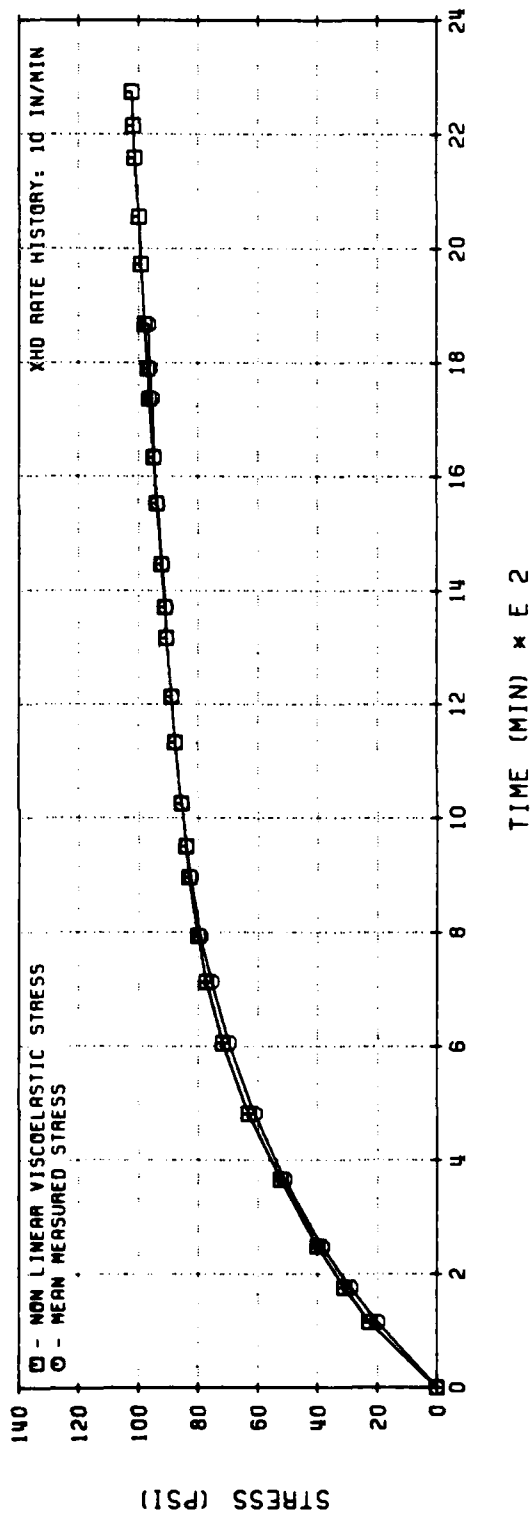
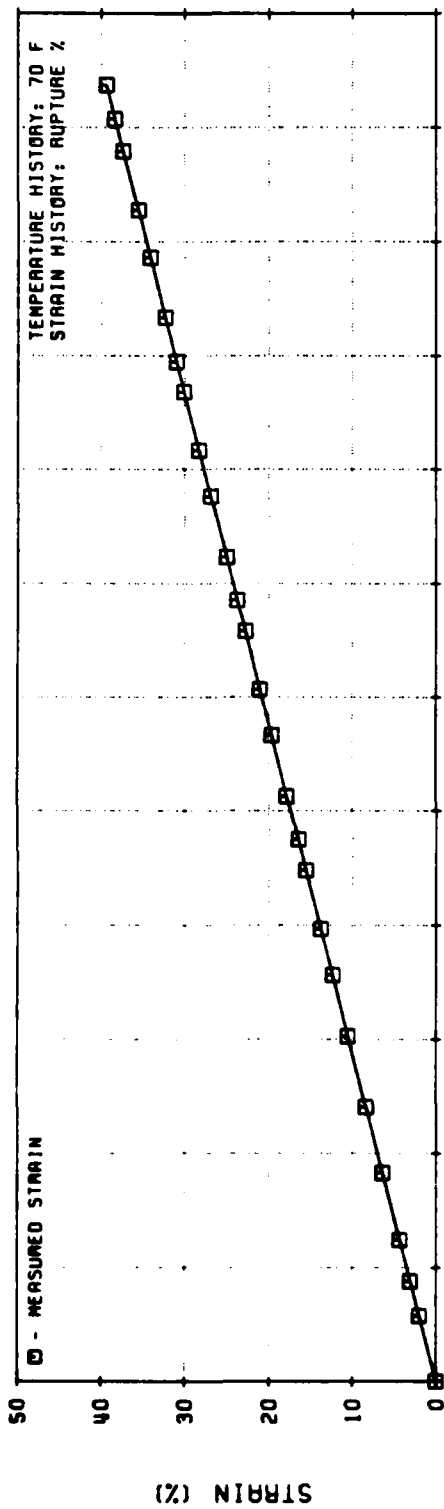


Figure 87. Dr. Schapery's Nonlinear Viscoelastic Stress Predictions for UTP-19,360B 400/1777
Constant Rate Test Data (Code No. 1)

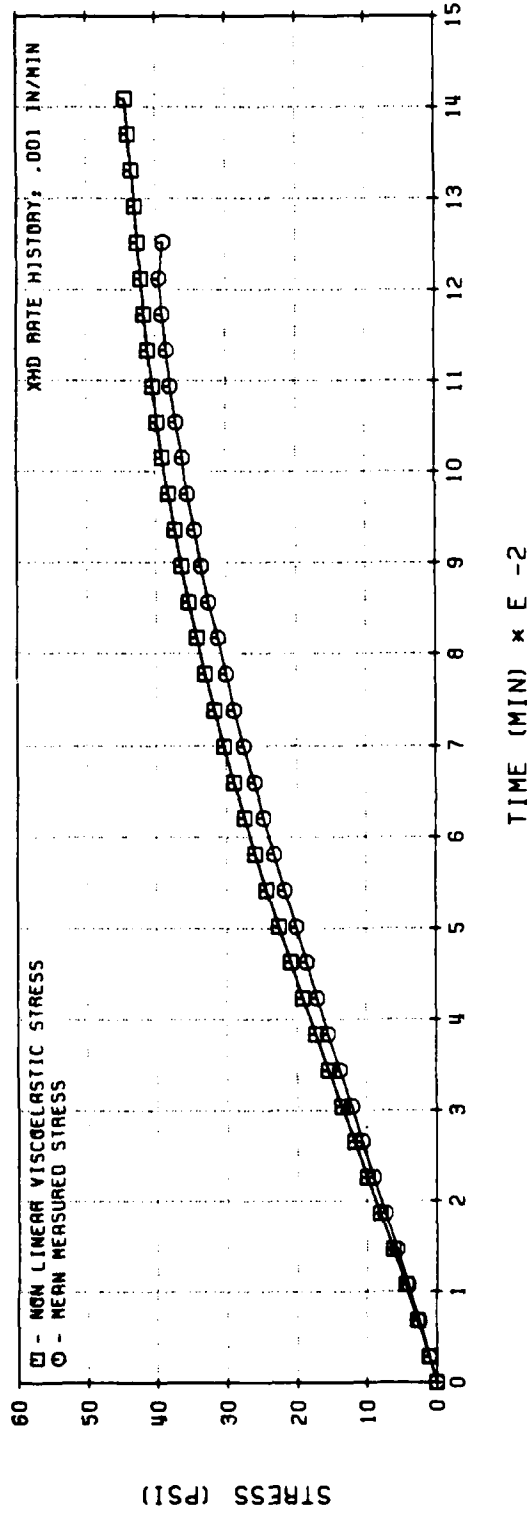
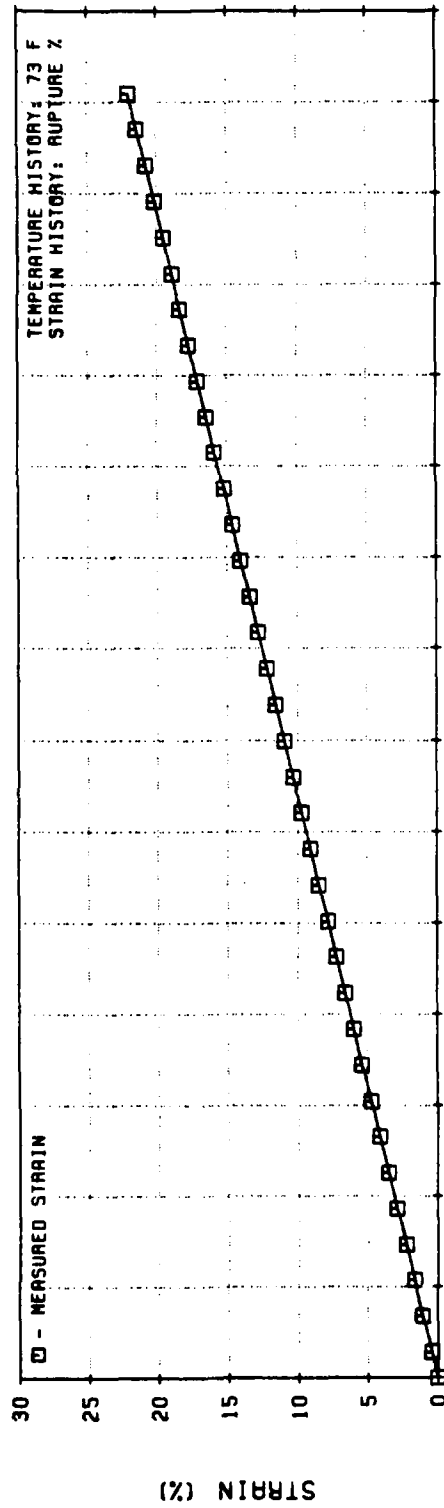


Figure 88. Dr. Schapery's Nonlinear Viscoelastic Stress Predictions for UTP-19,360B 400/1777
Constant Rate Test Data (Code No. 1)

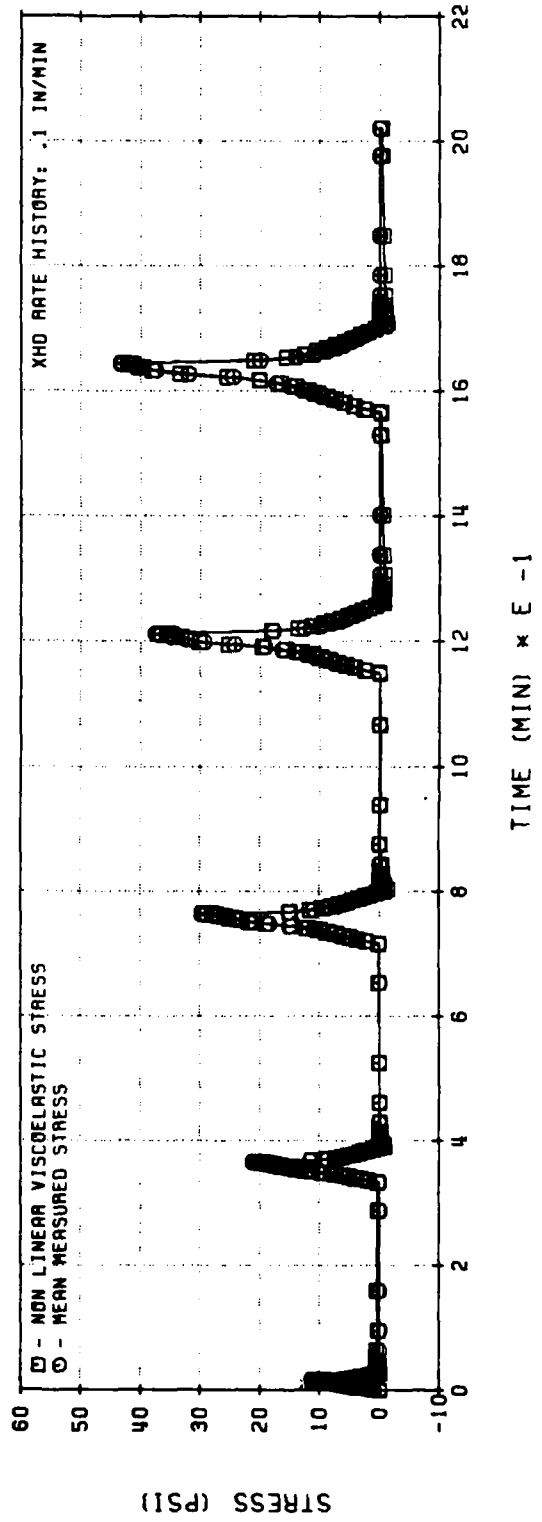
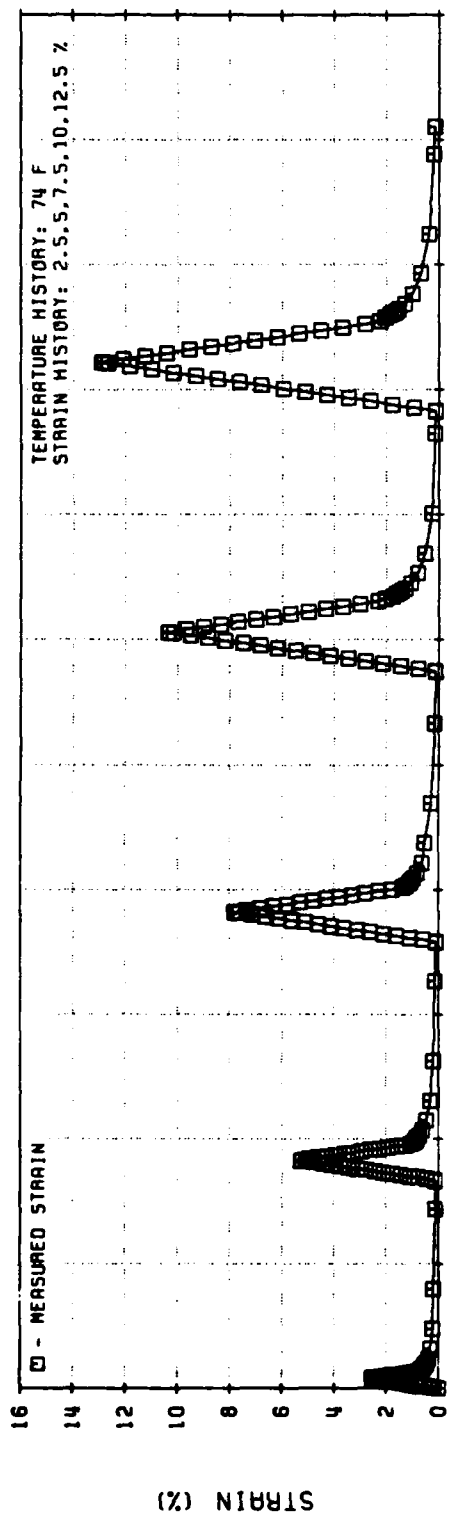


Figure 89. Dr. Schapery's Nonlinear Viscoelastic Stress Predictions for UTP-19,360B 400/1777 Multiple Loading Test History Data (Code No. 5)

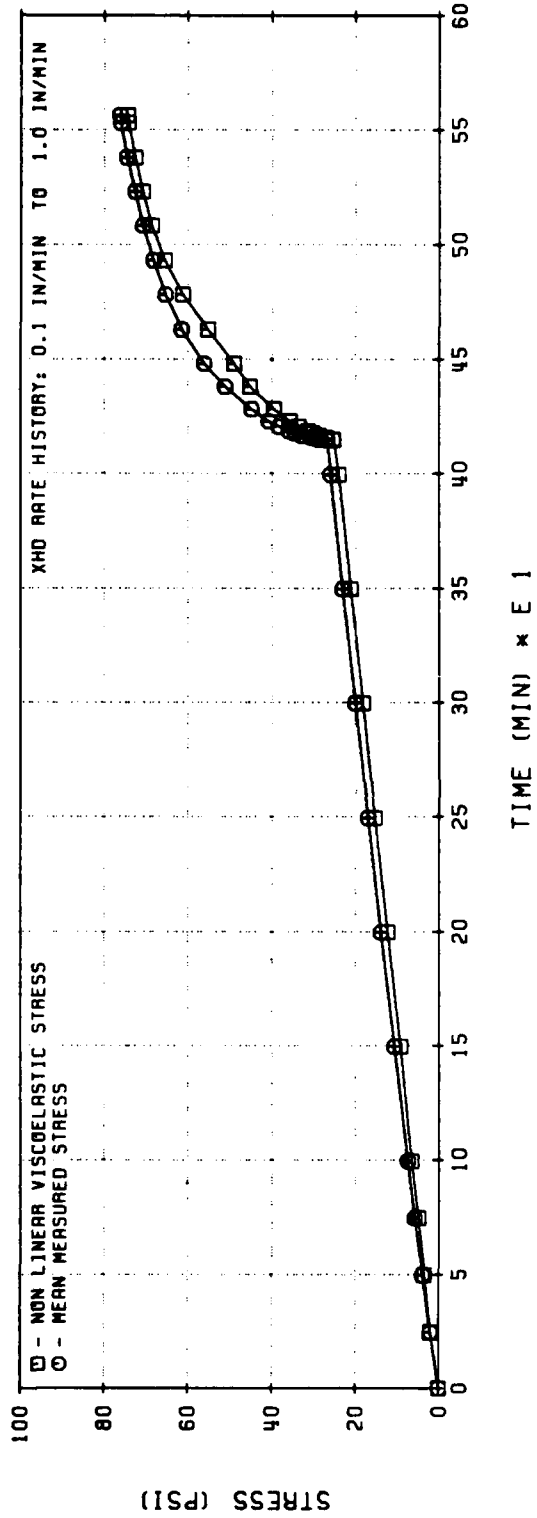
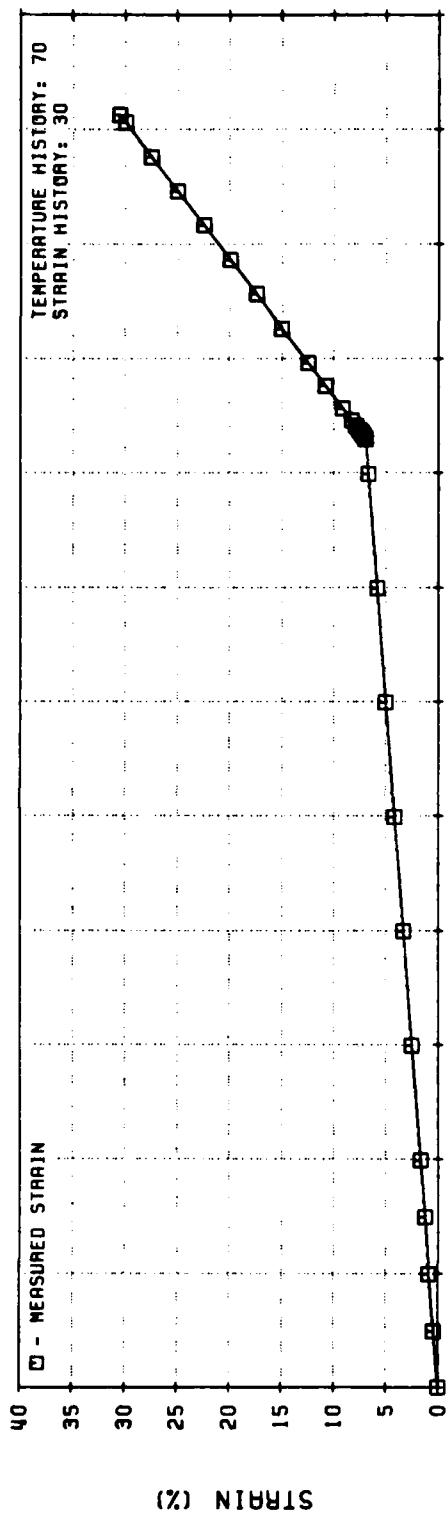


Figure 90. Dr. Schapery's Nonlinear Viscoelastic Stress Predictions for UTP-19,360B 400/1777
Two Rate Test Data (Code No. 3)

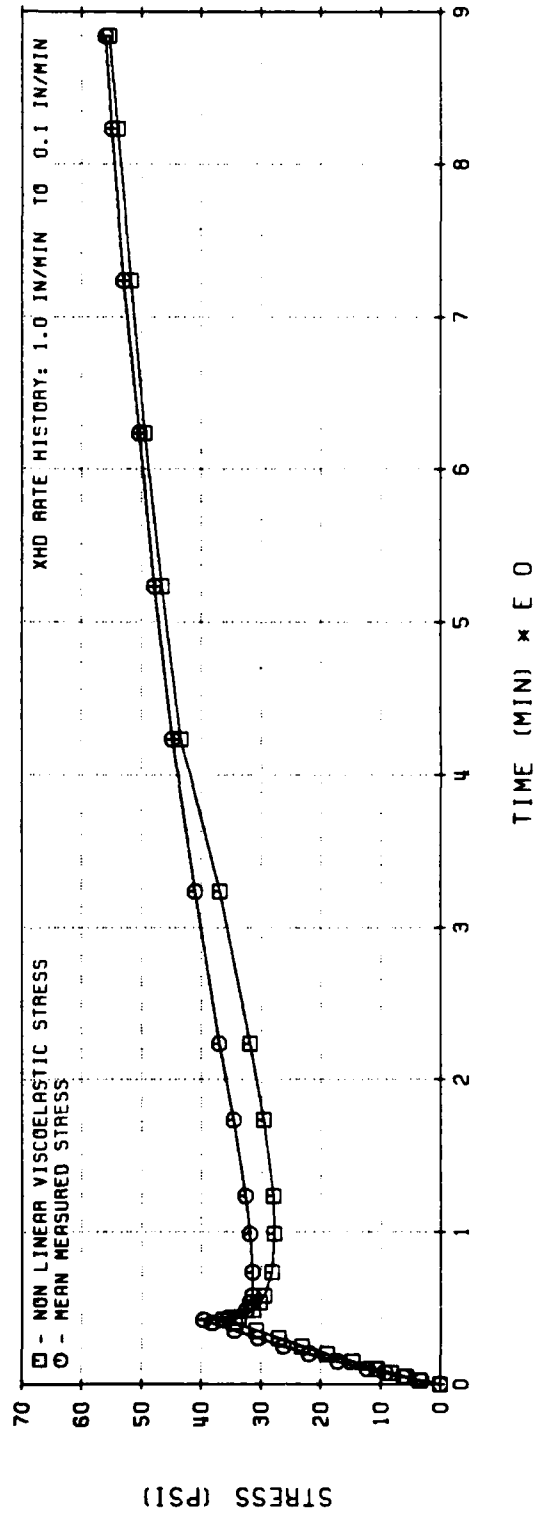
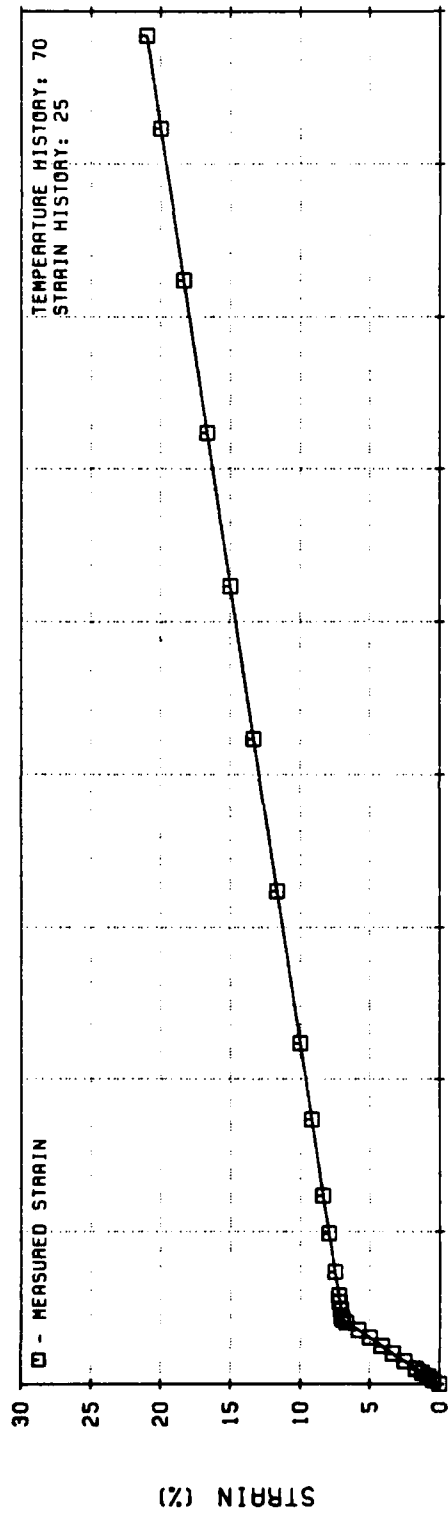


Figure 91. Dr. Schapery's Nonlinear Viscoelastic Stress Predictions for UTP-19,360B 400/1777
Two Rate Test Data (Code No. 3)

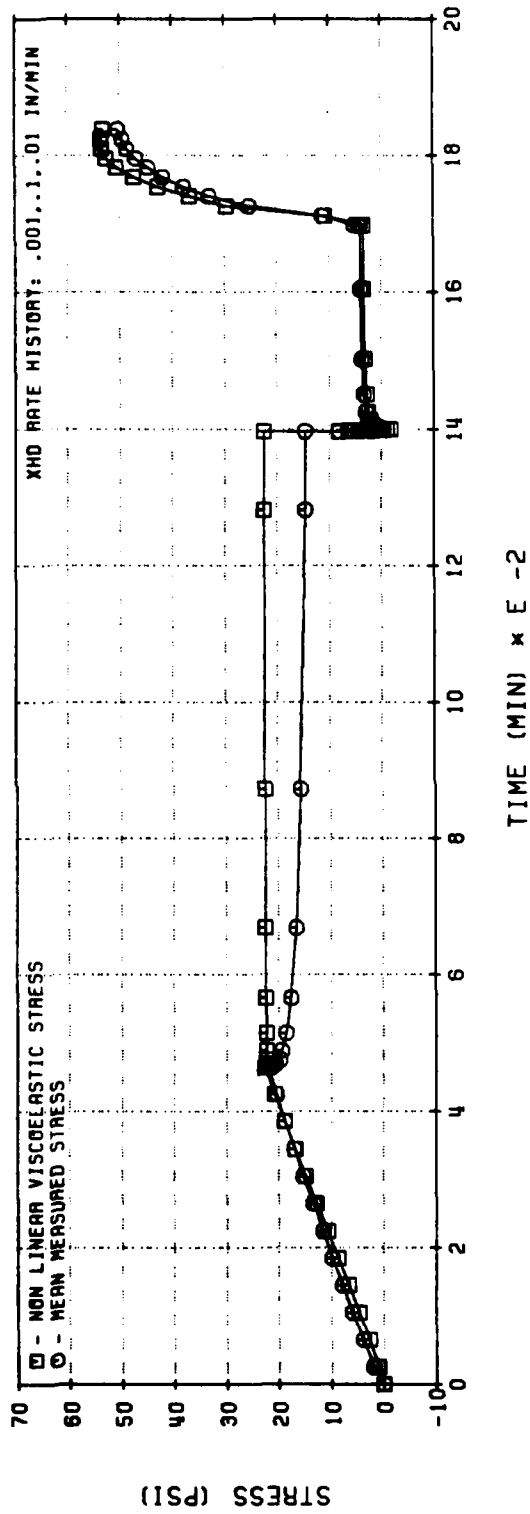
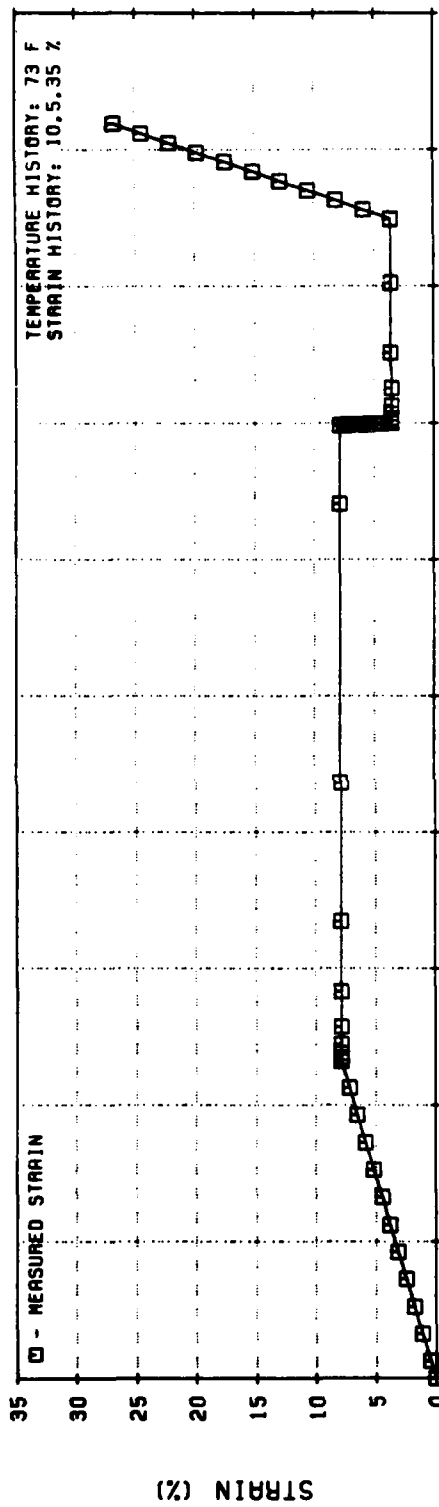


Figure 92. Dr. Schapery's Nonlinear Viscoelastic Stress Predictions for UTP-19,360B 400/1777
Similitude Test History Data (Code No. 12)

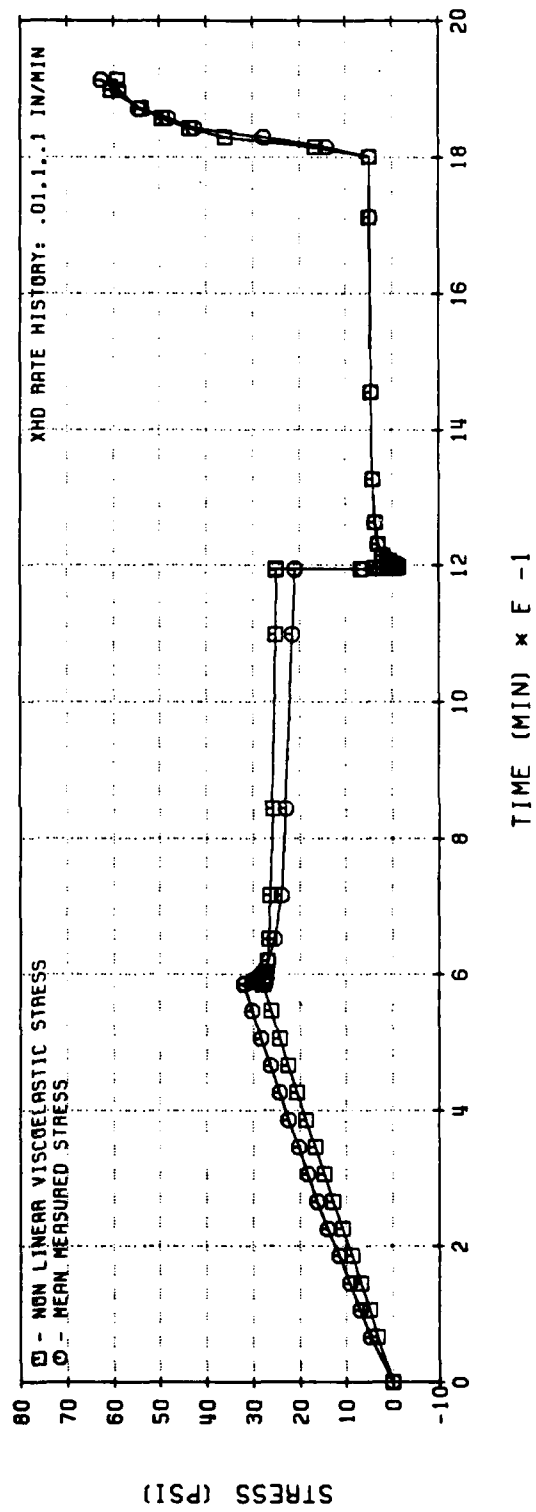
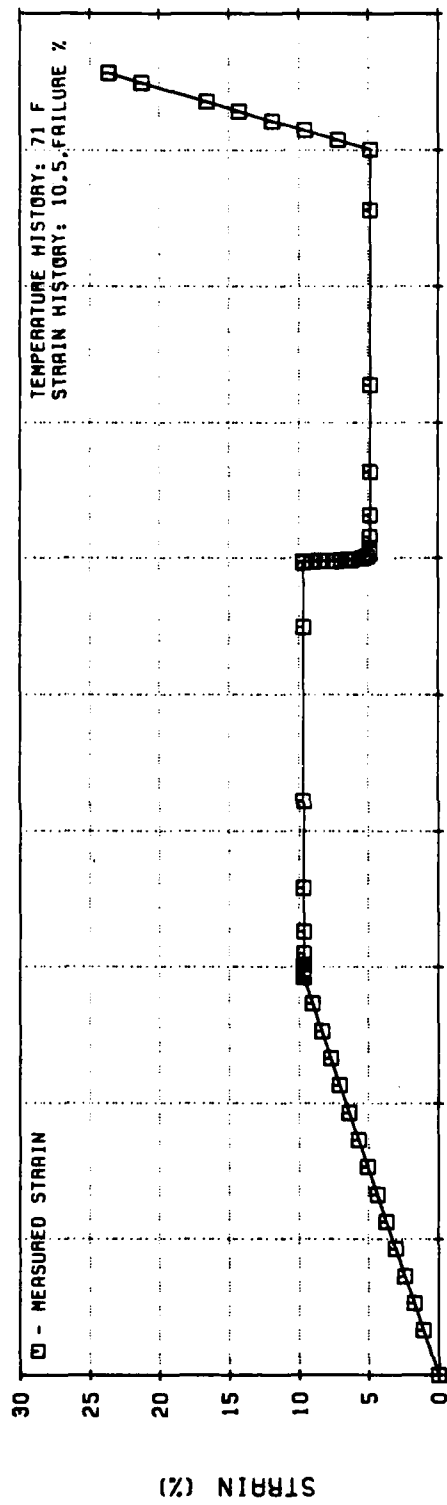


Figure 93. Dr. Schapery's Nonlinear Viscoelastic Stress Predictions for UTP-19,360B 400/1777
Similitude Test History (Code No. 12)

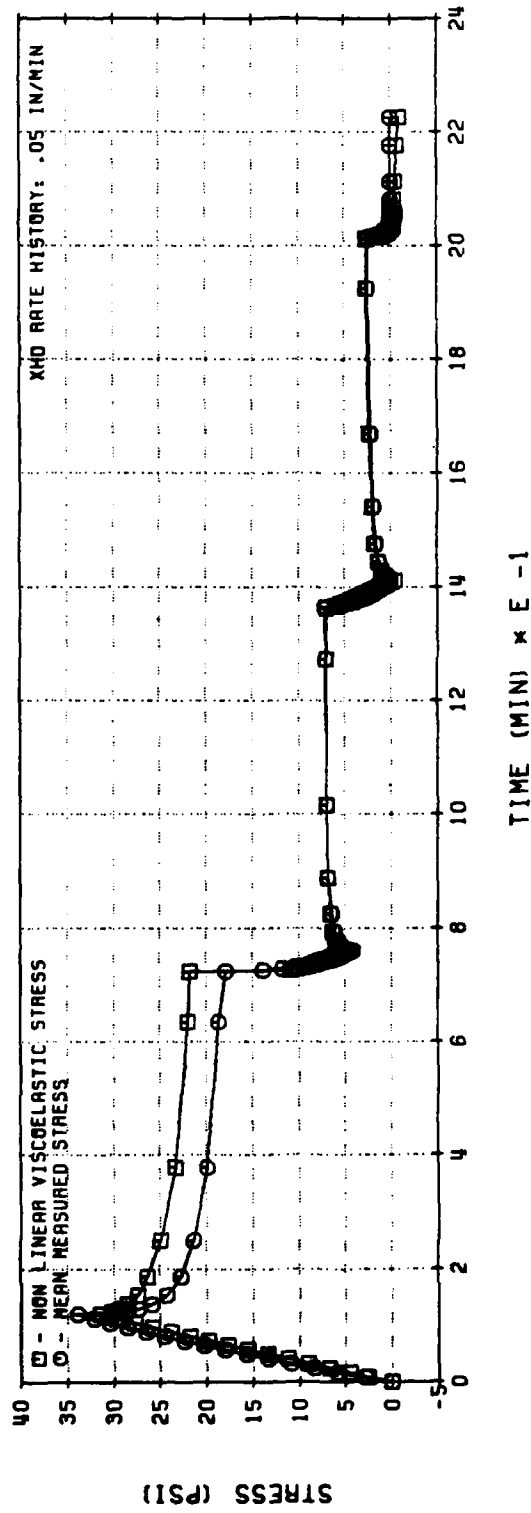
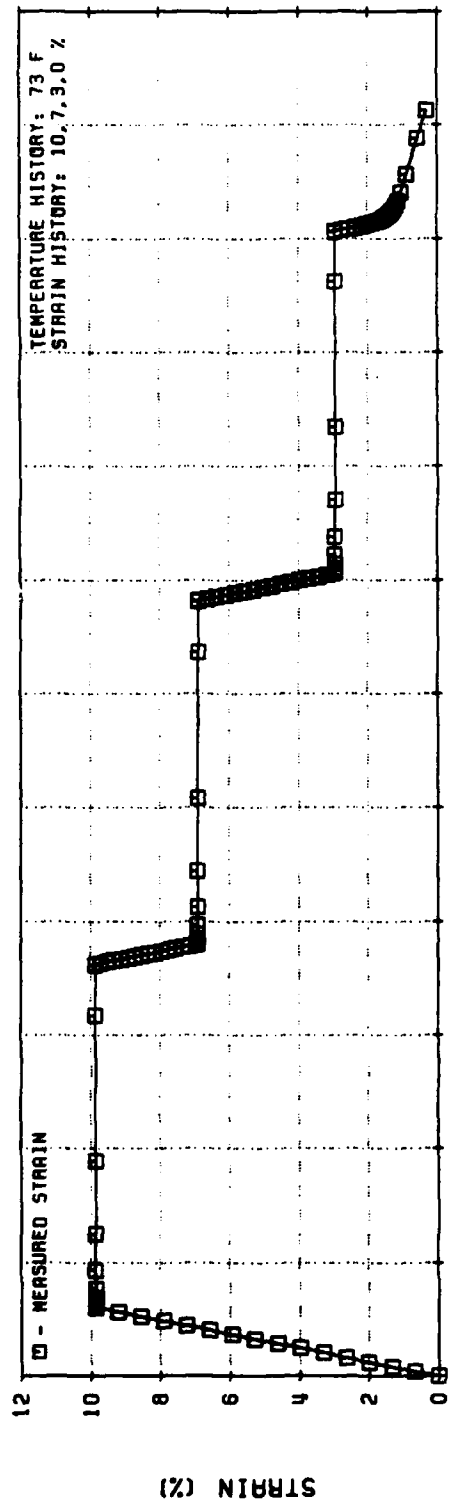


Figure 94. Dr. Schapery's Nonlinear Viscoelastic Stress Predictions for UTP-19,360B 400/1777
Three Step Relaxation Test History (Code No. 13)

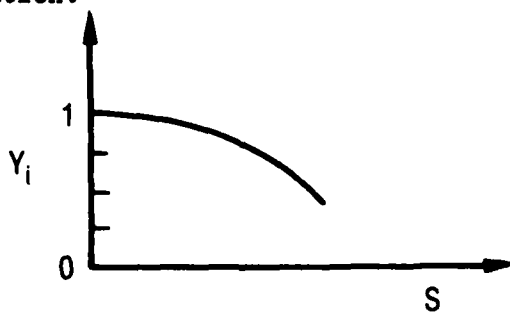
(Test No. 1) available in the data for which the difference between theory and test is greatest. Figure 89 shows the saw tooth test (Test No. 5) at constant rate with increasing strain peaks. Figures 90 and 91 pertain to the dual-rate tests (Test No. 3) Results for the short- and long-duration similitude tests (Test No. 12) are given in Figures 92 and 93, and Figure 94 includes a three-step relaxation test.

Finally, it is important to mention that a complete characterization of UTP-19,360B was also carried out using $L_x = 1$ (the value leading to equation (35)), and the ensuing response predictions were very close to those obtained with $L_x = 0.85$; only the low-to-high dual rate test of Figure 100 was predicted somewhat better with $L_x = 0.85$.

4.2.3.4 Material Characterization

In evaluating the material constants and property functions, the following observations may be valuable:

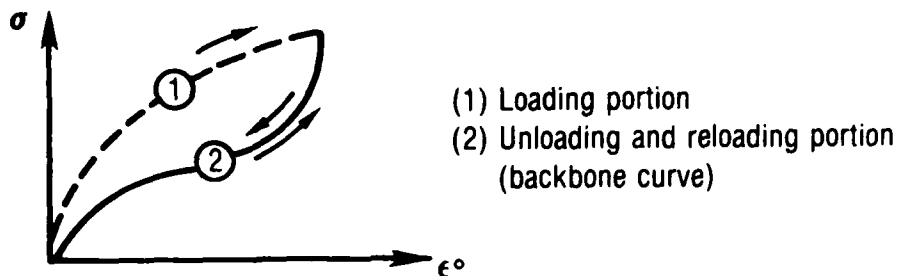
- (1) Y_1 appears to be a decreasing and concave down function of damage, as presented in the following figure, its variation being brought about by vacuole formation.



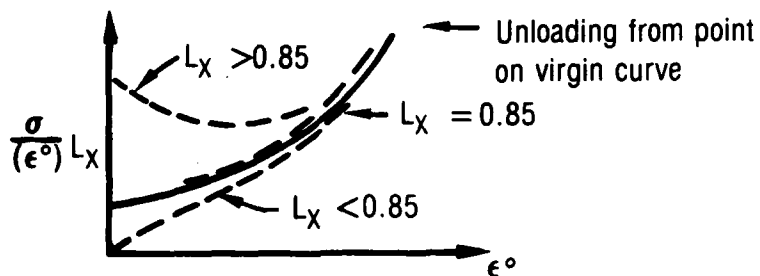
- (2) The function S_r , which provides a certain measure of damage, increases as a direct result of a reduction in the number of polymer chains supporting the internal stresses; the larger S_r , the higher the stress on each chain.
- (3) For UTP-19,360B, the state of damage is essentially constant during unloading and reloading, and the shape of the so-called backbone curve resembles the stress-strain curve for rubber, which is of the form:

$$Y_3 \left| \epsilon^0 \right|^{0.85} \quad (36)$$

as shown in the sketch below, in which the steepness increased with increasing S_r .



- (4) The selection of L_x can be made by plotting unloading data in the form suggested in the following diagram.



Noting that the quantity:

$$\frac{\sigma}{(\epsilon^0) L_x}$$

resembles a secant modulus, and that for most tests of UTP-19,360B $L_x = 0.85$ produced a finite limiting value as ϵ^0 approached zero, it is suggested that L_x be found in this fashion for other propellants.

- (5) For constant-rate tests, one has:

$$\epsilon^0 = \epsilon_m^0$$

$$\lambda = 1$$

and thus, from equation (29):

$$X = X_r$$

Also:

$$S_r = \max (S_r)$$

from which:

$$Y_3 = S_r$$

Equation (34) then reduces to:

$$\sigma = 1.861 Y_1 S^{0.637} (\epsilon_m^0)^{0.463} \quad (37)$$

with $Y_1 = Y_1 (S)$ given by equation (26).

For very small damage:

$$Y_1 (S) = 1$$

so that equation (36) becomes:

$$\sigma \cong 1.861 S^{0.637} (\epsilon_m^0)^{0.463} \quad (38)$$

in which the stress increases with damage, probably because of molecular chain stiffening due to an increase in stress per chain.

With the foregoing observations in mind, determining the material properties can be accomplished as follows:

- (1) The exponent, n , appearing in the relaxation function, is obtained from relaxation-modulus data.
- (2) The normalized coefficient, E_r , entering the relaxation modulus, is determined to make unloading curve 2 in the figure above pass through the origin.

- (3) The exponent, q , present in the definition of the damage parameter, is evaluated using equation (37) and two constant-rate tests at small values of damage.
- (4) The function Y_1 is obtained by curve-fitting equation (36) to constant-rate tests over all strains out to failure.
- (5) Experience to date indicates that the function Y_2 is independent of S and ϵ_m , and therefore equation (30) may be used instead of the more general form of equation (37).
- (6) The backbone curve Y_3 is determined using unloading and reloading data like those available in a cyclic test whose first peak strain is the largest.
- (7) Finally the correction factor, λ , can be ascertained from a relaxation test at a large strain level.

4.2.3.5 Multiaxial Generalization

A micromechanics model has been developed which predicts the form of equation (30), and it is presently being used to develop a multiaxial form of the theory.

4.2.4 M. Gurtin's Theories for Nonlinear Viscoelastic Materials

Four essentially different approaches have been followed by M. Gurtin in trying to predict the response of solid propellants that exhibit damage. The stress-softening theory appears to be the most accurate of the four laws as will be pointed out.

4.2.4.1 Original Model

The one-dimensional stress-strain law for materials undergoing internal damage was based on the hypothesis that the state of damage at any time is completely characterized by the maximum strain, ϵ_m , that the material has experienced.

$$\epsilon_m(t) = \max_{0 \leq s \leq t} \epsilon(s) \quad (39)$$

The stress, σ , is given by a constitutive equation of the form:

$$\sigma(t) = g[\epsilon(t), \epsilon_m(t)] \quad (40)$$

and it depends only on the current values of strain and damage. Such an equation is, of course, rate-independent.

In this theory, if the maximum strain occurs at the present time, then:

$$\epsilon_m(t) = \epsilon(t), \quad (41)$$

and equation (39) reduces to:

$$\sigma = G(\epsilon_m) = g(\epsilon_m, \epsilon_m) \quad (42)$$

The stress-strain curve:

$$\sigma = G(\epsilon_m) \quad (43)$$

is called the virgin curve and is traced out in an experiment with monotonically increasing strain.

Using the virgin curve, equation (39) may be rewritten in the form:

$$\sigma = F(\xi, \epsilon_m) G(\epsilon_m) \quad (44)$$

with:

$$\xi = \frac{\epsilon}{\epsilon_m} \quad (45)$$

the relative strain, and:

$$F(\xi, \epsilon_m) = \frac{g(\epsilon_m, \epsilon_m)}{G(\epsilon_m)} \quad (46)$$

The function $F(\xi, \epsilon_m)$ is called the damage curve at the damage level ϵ_m , and is such that:

$$F(1, \epsilon_m) = 1 \quad (47)$$

In some situations of interest $F(\xi, \epsilon_m)$ is independent of ϵ_m :

$$F(\xi, \epsilon_m) = F(\xi) \quad (48)$$

when this is so, $F(\xi)$ is referred to as the master damage curve, and equation (43) reduces to:

$$\sigma = F(\xi)G(\epsilon_m) \quad (49)$$

As pointed out previously, this is a rate-independent theory, and as such, cannot be used for loading rates that differ much from that used to determine the damage function. This situation was remedied by changing the stress-strain law to the one described next.

4.2.4.2 Nonlinear Model Based on Stress Softening

To develop a simple theory of stress softening which allows for rate effects and which returns to Mullins' original idea of using the past stress maximum as the damage parameter, two fundamental ingredients are considered. The first is the virgin stress, S , which represents the stress the material would experience in the absence of softening. This stress is assumed governed by a constitutive equation of the type encountered in linear viscoelasticity. The second ingredient is a damage function, F , which gives the true stress, σ , when the virgin stress, S , and its past maximum S_m , are known.

The one-dimensional form of the constitutive law for a classical linear viscoelastic material is given by:

$$\sigma(t) = \int_{-\infty}^t G(t - \tau) \dot{\epsilon}(\tau) d\tau \quad (50)$$

in which $\sigma(t)$ is the stress; $\epsilon(t)$, the strain; and $G(t)$, the relaxation function. It is further assumed that $\epsilon(t)=0$, prior to $t = 0$.

The generalization of equation (50) is begun by defining the quantity:

$$S(t) = \int_{-\tau}^t G(t - \tau) \dot{\epsilon}(\tau) d\tau \quad (51)$$

which is called the virgin stress and which represents the stress that would be present in the absence of softening. It is assumed that the extent of softening is governed by a constitutive equation giving the true stress, $\sigma(t)$, when $S(t)$ and its past maximum are known.

$$S_m(t) = \max_{0 < \tau < st} S(\tau) \quad (52)$$

Without loss of generality, this constitutive equation is written in the form:

$$\sigma = S_m F\left(\frac{S}{S_m}, S_m\right) \quad (53)$$

and it is assumed that the damage function, F , satisfies the following conditions:

$$\begin{aligned} F(1, S_m) &= 1 \\ F(x, S_m) &< x \quad \text{for } x < 1 \end{aligned} \quad (54)$$

These restrictions imply that:

$$\sigma(t) < S(t), \quad (55)$$

also that:

$$\sigma_m(t) = S_m(t), \quad (56)$$

and, that the following conditions are equivalent:

$$\begin{aligned}
 & \text{i) } \sigma(t) = S(t) \\
 & \text{ii) } S(t) = S_m(t) \\
 & \text{iii) } \sigma(t) = \sigma_m(t)
 \end{aligned}
 \tag{57}$$

where σ_m is the past stress maximum, defined analogically to S_m . The inequality equation (54) asserts that the material actually softens, while equation (56) indicates that this softening occurs when and only when $S(t) < S_m(t)$ (or equivalently $\sigma(t) < \sigma_m(t)$). The results of equation (55) and (56) show that one may equally well use the true stress, $\sigma(t)$, as the damage parameter.

Equation (54) and the fact that the first relation of equation (57) implies the third are direct consequences of the hypotheses laid down in equation (58). To verify equation (55), note that if the maximum of S on the interval $0 \leq \tau \leq t$, occurs at $\tau = \xi$, then:

$$S_m(t) = S(\xi) \tag{58}$$

thus using equation (57) in (52), and recalling that equation (53):

$$\sigma(\xi) = S(\xi) F(1, S_m) \equiv S(\xi) \tag{59}$$

which, by virtue of (57) and the definition of S_m , implies that:

$$\sigma(\xi) = S(\xi) = S_m(t) \geq S(\lambda) \geq \sigma(\lambda); \quad 0 \leq \lambda \leq t \tag{60}$$

proving equations (54) and (55) and the first two equations of equation (57). To establish the third relation in equation (57), note that if:

$$S_m(t) = S(t)$$

which implies that:

$$S_m(t) = \sigma(t)$$

because of equation (58); then, since

$$S_m = \sigma_m \quad (61)$$

one would have that:

$$\sigma_m(t) = \sigma(t).$$

Conversely, if

$$\sigma(t) = \sigma_m(t),$$

then:

$$S(t) \geq \sigma(t) = \sigma_m(t) = S_m(t)$$

so that:

$$S(t) = S_m(t).$$

Returning to the constitutive equation (52), it is interesting to consider the special case in which the damage function depends only on S/S_m :

$$F\left(\frac{S}{S_m}, S_m\right) \equiv F\left(\frac{S}{S_m}\right); \quad (62)$$

which is a master damage curve of the type considered in the rate-independent model discussed previously.

When the virgin stress obeys an elastic stress-strain relation:

$$S = E \epsilon \quad (63)$$

then:

$$S_m = E \epsilon_m \quad (64)$$

in which ϵ_m is the past strain-maximum, and equation (52) yields:

$$\sigma = E \epsilon_m F\left(\frac{\epsilon}{\epsilon_m}, E \epsilon_m\right) \quad (65)$$

so that, defining:

$$F^* \left(\frac{\epsilon}{\epsilon_m}, \epsilon_m \right) \equiv F\left(\frac{\epsilon}{\epsilon_m}, E \epsilon_m\right) \quad (66)$$

leads to the starting assumption of Gurtin and Francis (Reference 26):

$$\sigma = F^* \left(\frac{\epsilon}{\epsilon_m}, \epsilon_m \right) E \epsilon_m \quad (67)$$

presented earlier as the rate-independent model.

Although implicit in equation (52) is the assumption that the functional form of F would be the same for unloading conditions as for reloading, it was found experimentally that a different damage function is needed for each of these processes. Actually, there is more than one way of obtaining the same damage function. For TP-H1011, for instance, the following procedure was employed.

Considering the strain history shown in Figure 95, on the loading portion we have:

$$S(t) = \dot{\epsilon} \int_0^t G(\tau) d\tau \quad \text{for } t \leq T \quad (68)$$

hence, $S(t)$ increases monotonically and, by equation (55):

$$S_m(t) = S(t) = \sigma(t) \quad (69)$$

and, upon unloading, the past maximum of S is the true stress:

$$\sigma_m = \sigma(T), \quad T \leq t < 2T \quad (70)$$

Further, by equation (50):

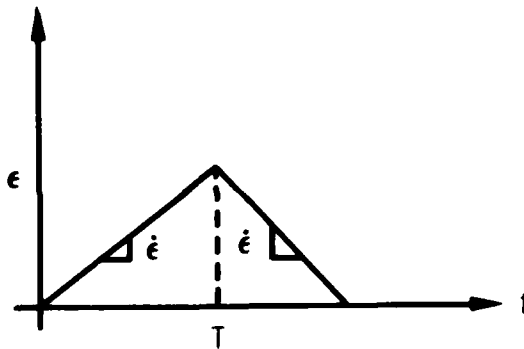
$$S(t) = |\dot{\epsilon}| \left\{ \int_0^T G(t - \tau) d\tau - \int_T^t G(t - \tau) d\tau \right\} \quad (71)$$

or, equivalently:

$$S(T + t) = G(t) - \sigma(t) \quad (72)$$

with:

$$G(t) \equiv |\dot{\epsilon}| \int_t^{t+T} G(\tau) d\tau \quad (73)$$



Letting $\sigma_1(t)$ and $\sigma_2(t)$ denote the true stress during loading and unloading, respectively, with t in $\sigma_2(t)$ measured from the time T at which unloading begins, equations (52) and (67) yield the simple formula:

Figure 95. Strain History Used To Characterize the Damage Function

$$\frac{\sigma_2(t)}{\sigma_m} = F \left[\frac{G(t) - \sigma_1(t)}{\sigma_m}, \sigma_m \right] \quad (74)$$

Thus, summarizing, the stress-softening approach to damage is described through the following constitutive equation:

$$\sigma(t) = S_m F \left(\frac{S}{S_m}, S_m \right) \quad (75)$$

where

$$S(t) = \int_0^t G(t - \tau) \frac{d\epsilon}{d\tau}(\tau) d\tau$$

and in which the damage function, F , may be determined from saw-tooth tests with increasing peak strains and with sufficiently long rest periods between cycles. For conditions of reloading, F is given by:

$$\frac{\sigma_2}{\sigma_m} = F \left[\frac{\sigma_1(t)}{\sigma_m}, \sigma_m \right] \quad (76)$$

while for unloading the following form is employed:

$$\frac{\sigma_2}{\sigma_m} = F \left[\frac{G(t) - \sigma_1(t)}{\sigma_m}, \sigma_m \right] \quad (77)$$

Typical curves for unloading and reloading damage functions of TP-H1011 are included as Figure 96 and 97, respectively.

Finally, we point out that the use of this approach to predict the response of TP-H1011 yielded results that were far more accurate than those obtained with any of the other theories in their original form.

4.2.4.3 Nonlinear Models Based on Maximum Strain.

A series of constitutive relations based on the past maximum strain have been proposed by M. Gurtin. The precursor of these relations took the form:

$$\sigma(t) = \int_0^t G(t - \tau) \frac{de}{d\tau}(\tau) d\tau \quad (78)$$

where G represents the relaxation modulus, and the function e was expressed as a product of the reduced damage function, F , and the virgin-response function, g , in the following way:

$$e = F \left(\frac{\epsilon}{\epsilon_m}, \epsilon_m \right) g(\epsilon_m) \quad (79)$$

with:

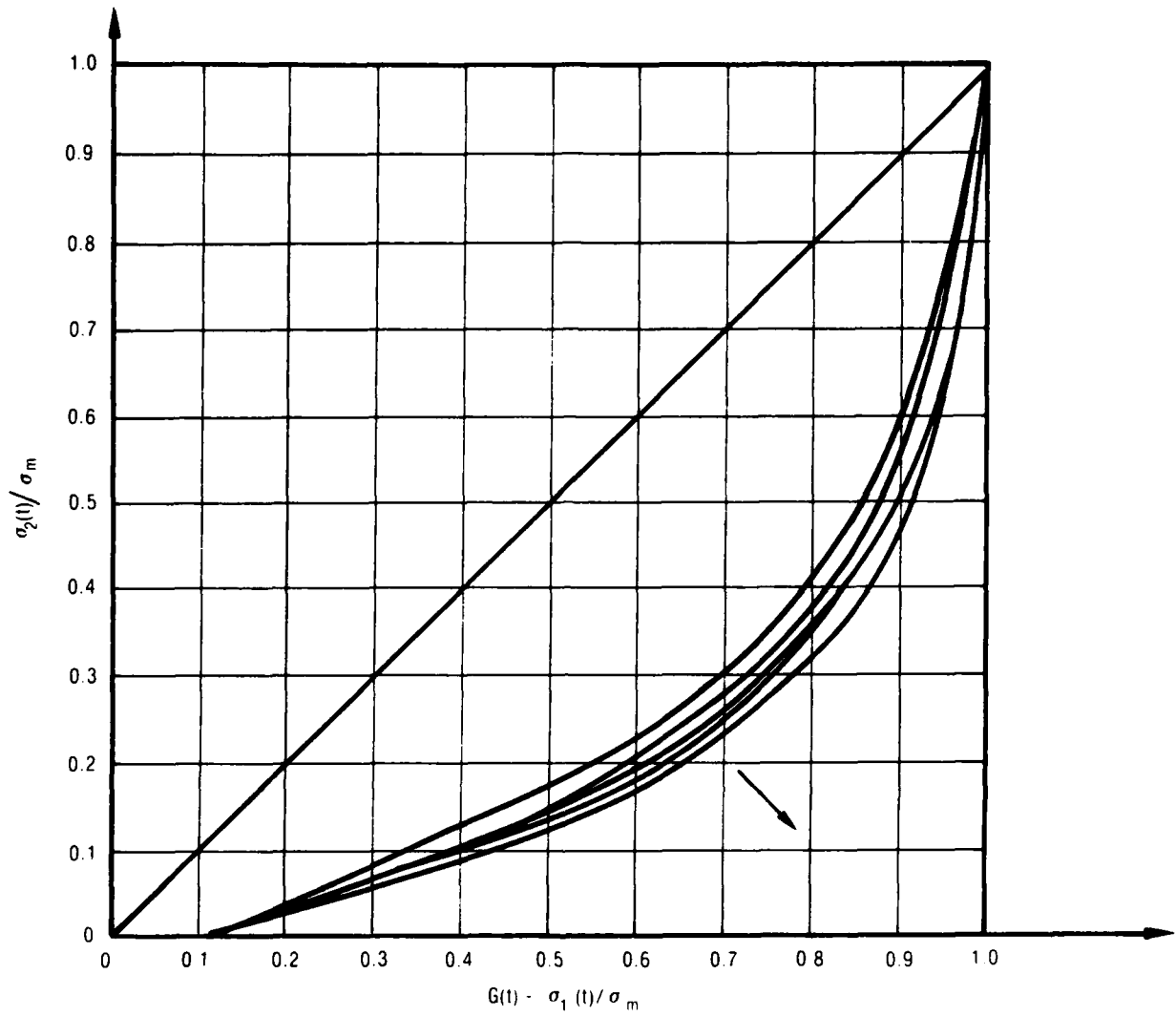


Figure 96. Damage Function for Unloading (TP-H1011)

28896

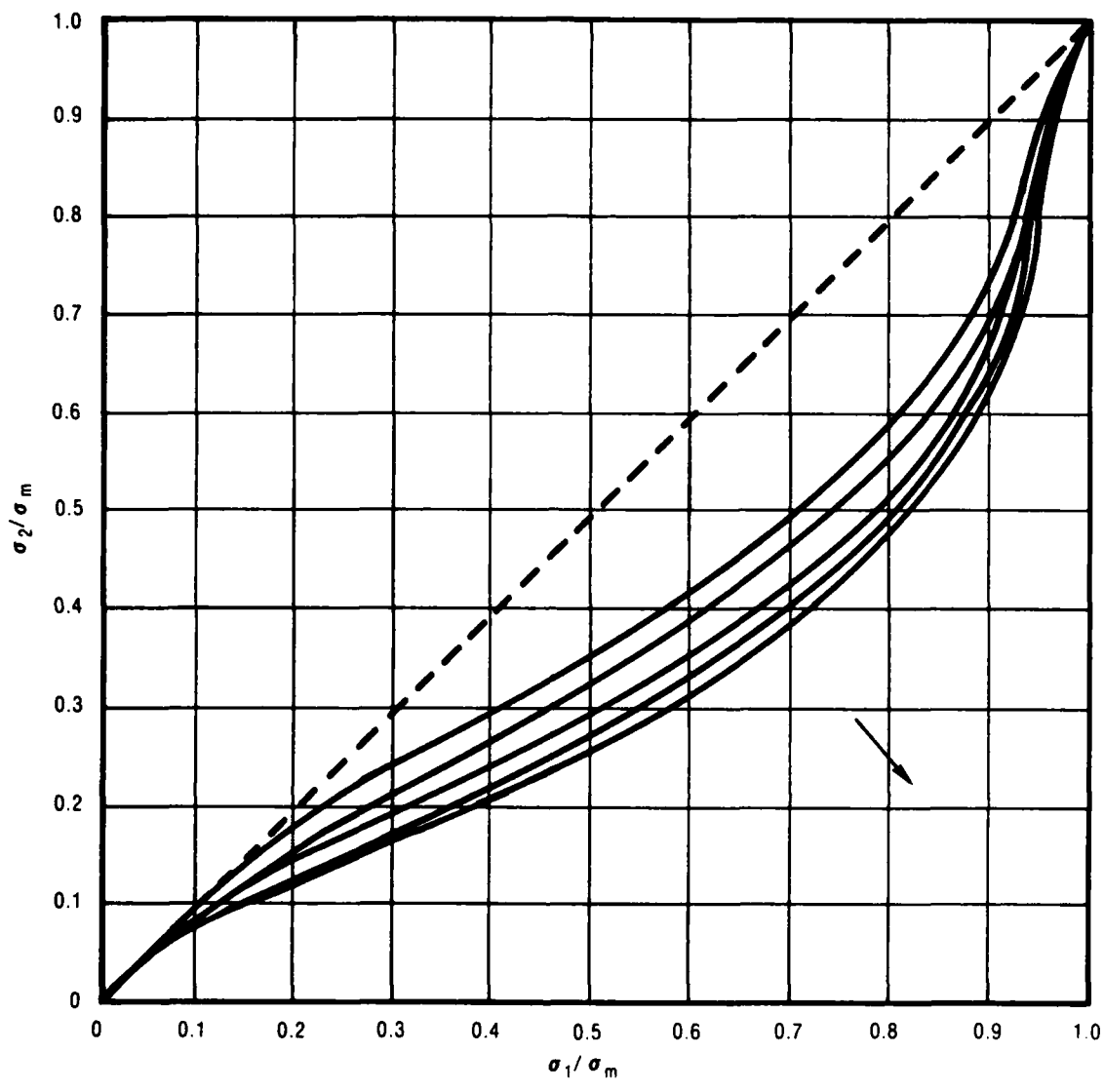


Figure 97. Damage Function for Reloading (TP-H1011)

28892

$$F(1, \epsilon_m) = 1 \quad (80)$$

and

$$\begin{aligned} \epsilon_m &= \max \epsilon(\tau) \\ 0 < \tau < t \end{aligned} \quad (81)$$

so that, during virgin response, since:

$$\epsilon = \epsilon_m \quad (82)$$

one had:

$$\sigma(t) = \int_0^t G(t - \tau) \frac{dg(\epsilon)}{d\epsilon} \frac{d\epsilon(\tau)}{d\tau} d\tau \quad (83)$$

and, by taking:

$$g(\epsilon) = \sum_{k=1}^{k=K} A_k \epsilon^k \quad (84)$$

the best values for the a_k 's could be determined using least squares and the data of all constant-rate tests.

To characterize the reduced damage function, F , involved the determination of a creep function, J , solution of:

$$\int_0^t G(t - \tau) \frac{dJ(\tau)}{d\tau} d\tau = 1 \quad (85)$$

and, such that:

$$e(t) = \int_0^t J(t - \tau) \frac{d\sigma(\tau)}{d\tau} d\tau \quad (86)$$

Thus, taking the reduced damage function, F , in the form:

$$F(x, y) = F_1(x) F_2(x, y) \quad (87)$$

with

$$F_1(x) = x^M + \sum_{m=1}^{M-1} d_m (x^m - x^M) \quad (88)$$

$$F_2(x, y) = 1 + \sum_{p=1}^P b_p y^p \left[x - x^Q + \sum_{q=2}^{Q-1} c_q (x^q - x^Q) \right] \quad (89)$$

and equating equations (71) and (75), the coefficients entering F were to be determined using least squares and all the saw-tooth data with increasing strain peaks.

When this constitutive law was applied to UTP-19,360B data, it was deemed necessary to change the form of the function e , because of the large errors observed in the predicted response.

The last of a sequence of modifications yielded the following stress-strain law:

$$\sigma(t) = \int_0^t G(t - \tau) \left\{ K \left(\epsilon_m, \dot{\epsilon}_m \frac{d}{d\tau} \left[F \left(\frac{\epsilon}{\epsilon_m}, \epsilon_m \right) \epsilon_m \right] \right) \right\} d\tau \quad (90)$$

where, as before, G was the relaxation modulus, and:

$$F(1, \epsilon_m) = 1 \quad (91)$$

with:

$$\begin{aligned} \epsilon_m &= \max \epsilon(\tau) \\ 0 &\leq \tau \leq t \end{aligned} \quad (92)$$

In the present case, the virgin response was given by:

$$\sigma(t) = \int_0^t G(t - \tau) K(\epsilon_m, \dot{\epsilon}_m) \frac{d\epsilon_m}{d\tau} d\tau \quad (93)$$

while, the damage response, for which ϵ_m remains constant, took the form:

$$\sigma(t) = K(\epsilon_m, 0) \int_0^t G(t - \tau) \frac{\partial F}{\partial x}(x, y) d\tau \quad (94)$$

in which:

$$K(\epsilon, \dot{\epsilon}) = 1 + A_1 (\epsilon - \epsilon_0) + A_2 (\epsilon - \epsilon_0)^2 + A_3 (\epsilon - \epsilon_0)^3 + \dot{\epsilon} (B_1 \epsilon + B_2 \epsilon^2 + B_3 \epsilon^3) \quad (95)$$

$$F(x, y) = \alpha(x) \left[1 + (D_5 y + D_7 y^2) \left\{ x - x^3 + D_6 (x^2 - x^3) \right\} \right] \quad (96)$$

$$\alpha(x) \equiv x^5 + \sum_{m=1}^4 D_m (x^m - x^5) \quad (97)$$

with:

$$x \equiv \epsilon / \epsilon_m \quad (98)$$

and:

$$y \equiv \epsilon_m \quad (99)$$

A set of stress predictions obtained for UTP-19,360B, with the resulting version of the theory, is included in Figures 98 through 104. Figure 98 is for the high-to-low dual rate test, Figures 99 through 101 are segments of the long-duration similitude test, and Figure 102 through 104 are segments of the three step relaxation test.

Since the dependence of the function K on the strain rate was felt to be artificial, the treatment of damage was revised in the manner explained next.

4.2.4.4 Current Model

The latest version of M. Gurtin's nonlinear stress-strain law is based on a strain-dependent relaxation function and has the form:

$$\sigma(t) = \int_0^t G[\epsilon(\tau), \tau] \dot{\epsilon}(t - \tau) d\tau \quad (100)$$

where:

$$G(\epsilon, t) = G_r(t) + G_c(\epsilon, t) \quad (101)$$

G = relaxation modulus

G_c = correction modulus, defined as:

$$G_c(\epsilon, t) = \sum_{n=1}^N A_n(\epsilon) (e)^{-t/\tau_n} \quad (102)$$

$$A_n(\epsilon) = \sum_{p=1}^P A_{np} \epsilon^p \quad (103)$$

For this material, the virgin curve ($\epsilon = \epsilon_m = \epsilon$) is:

$$\sigma = \sigma_r + \sigma_c \quad (104)$$

with σ_r , the linear viscoelastic stress:

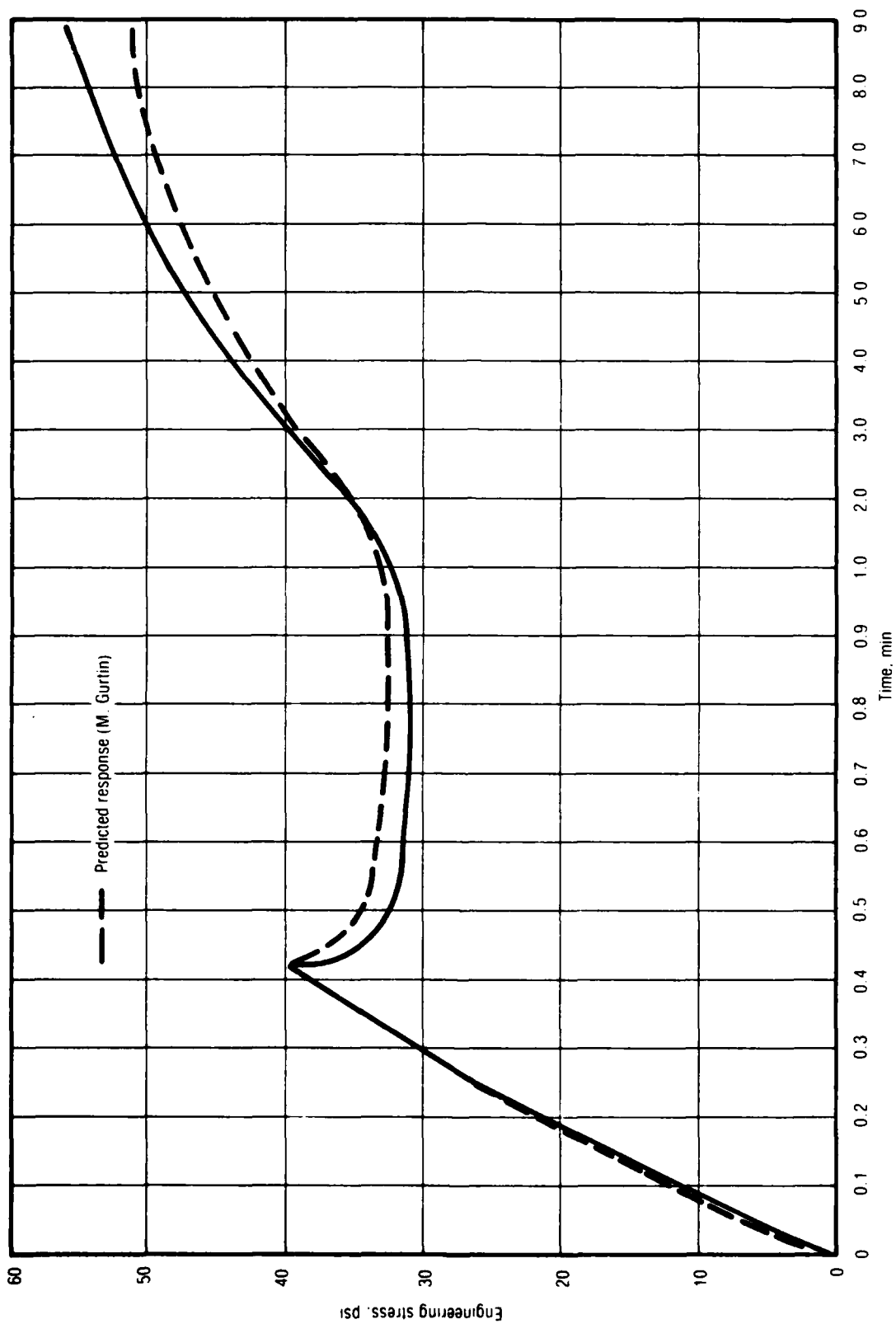


Figure 98. Two-Rate Loading (1 in./min to 0.1 in./min) of UTP-19, 360B-400/1777

28006

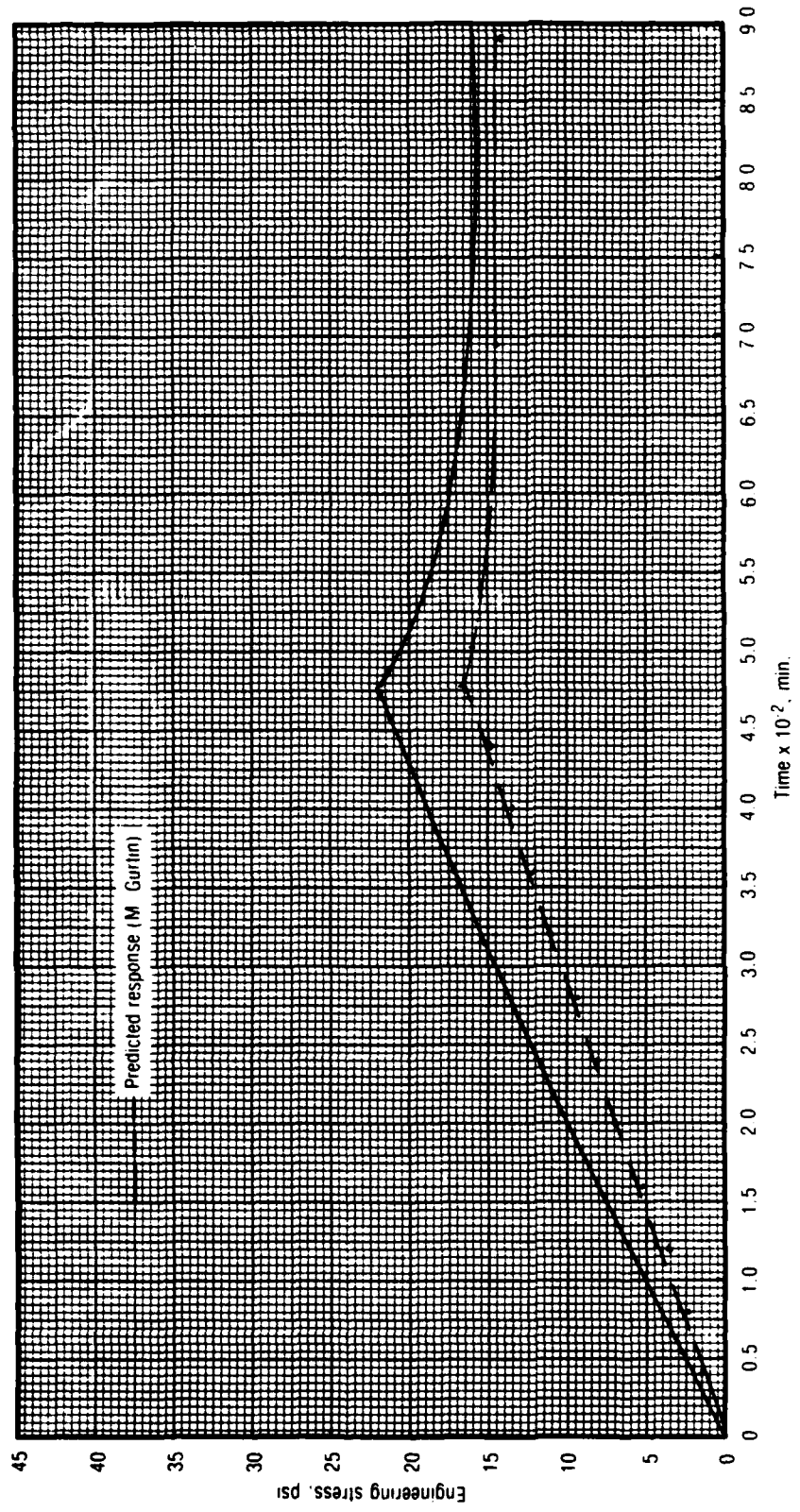


Figure 99. Relaxation-Unload-Reload of 6-in. Bar of UTP-19, 360B-400/1777

28847

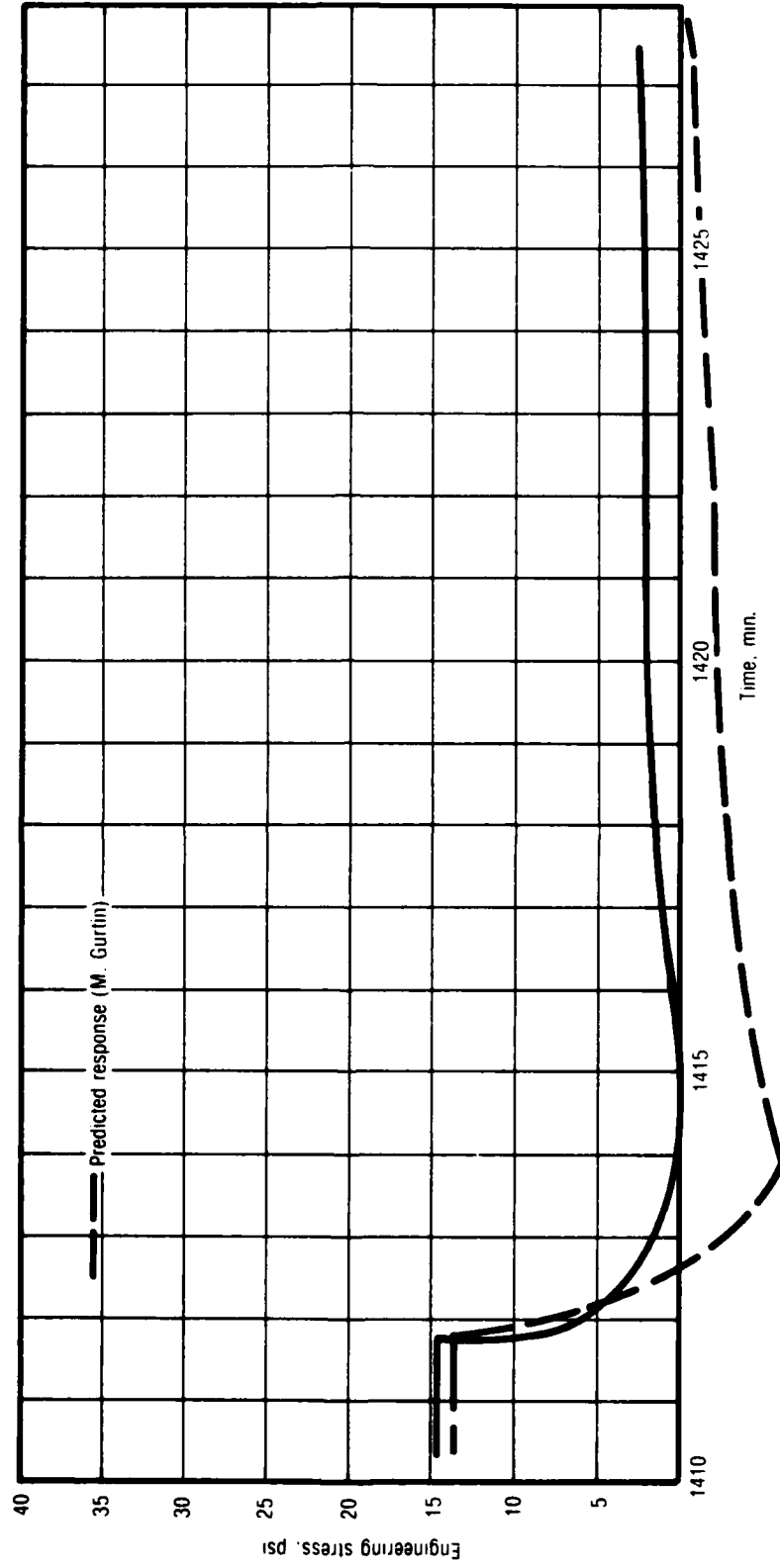


Figure 100. Relaxation-Unload-Reload of 6-in. Bar of UTP-19, 360B-400/1777

28848

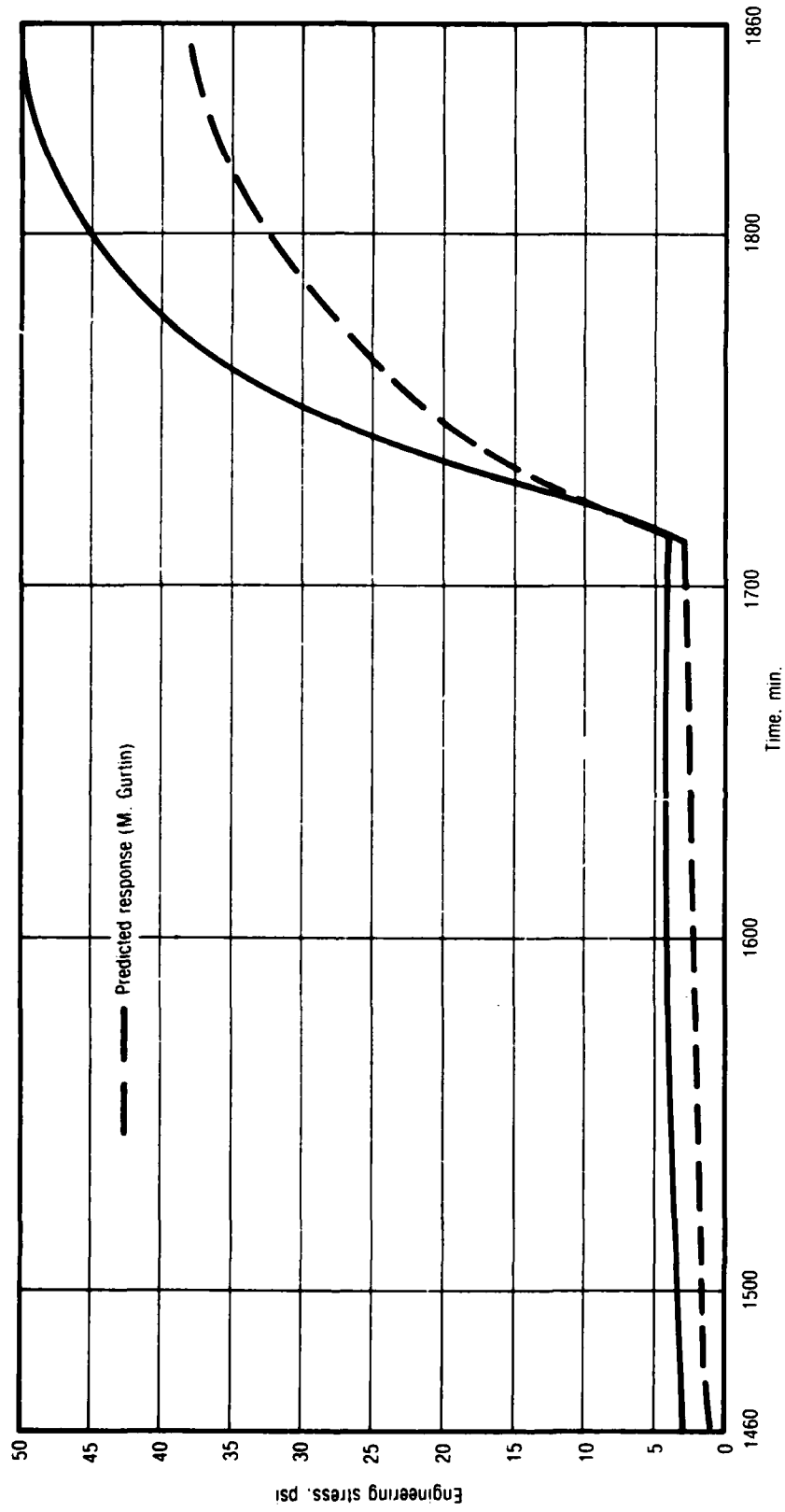


Figure 101. Relaxation-Unload-Reload of 6-in. Bar of UTP-19, 360B-400/1777

28849

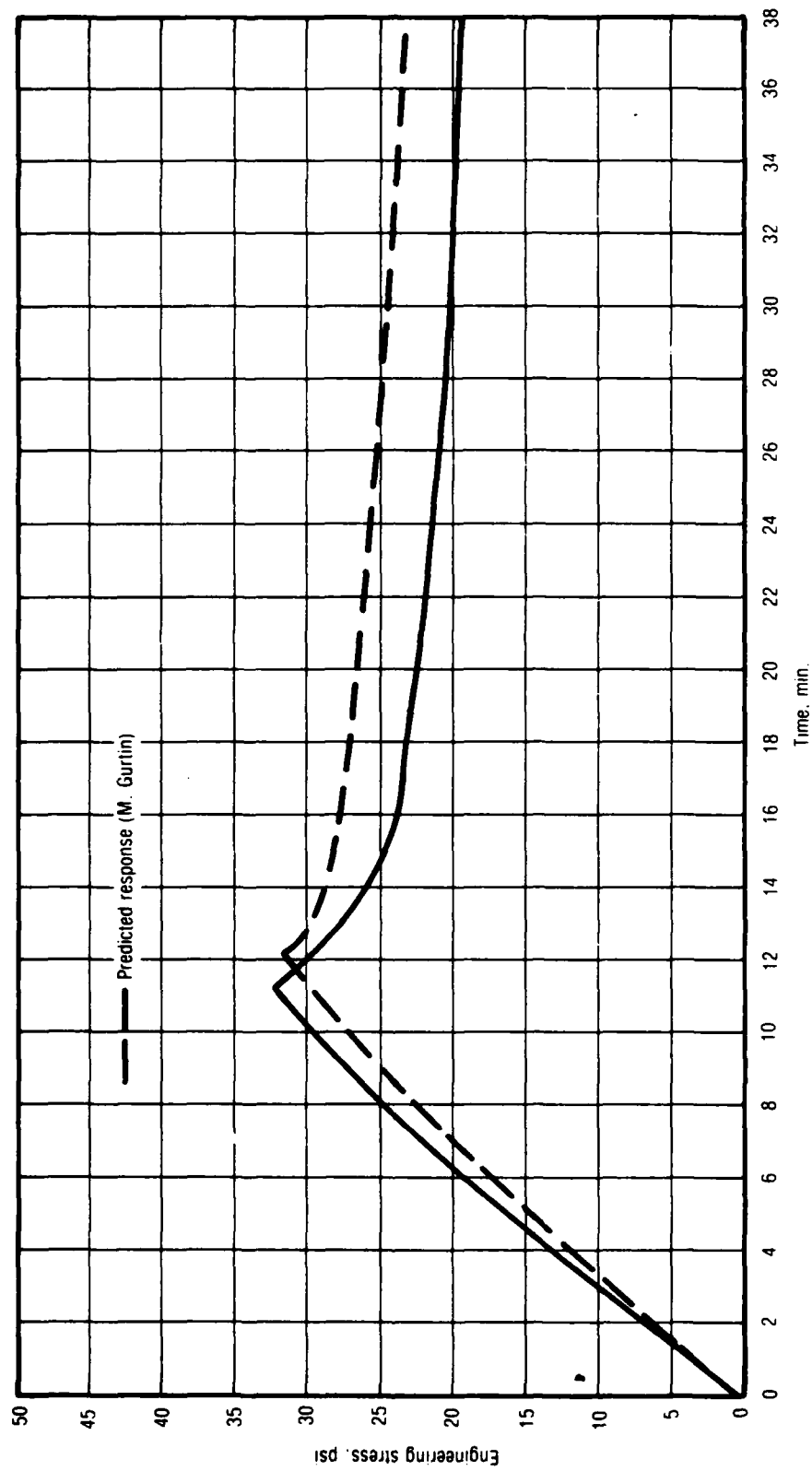


Figure 102. Three-Step Relaxation of 6-in. Bar of UTP-19,360B-400/1777

28850

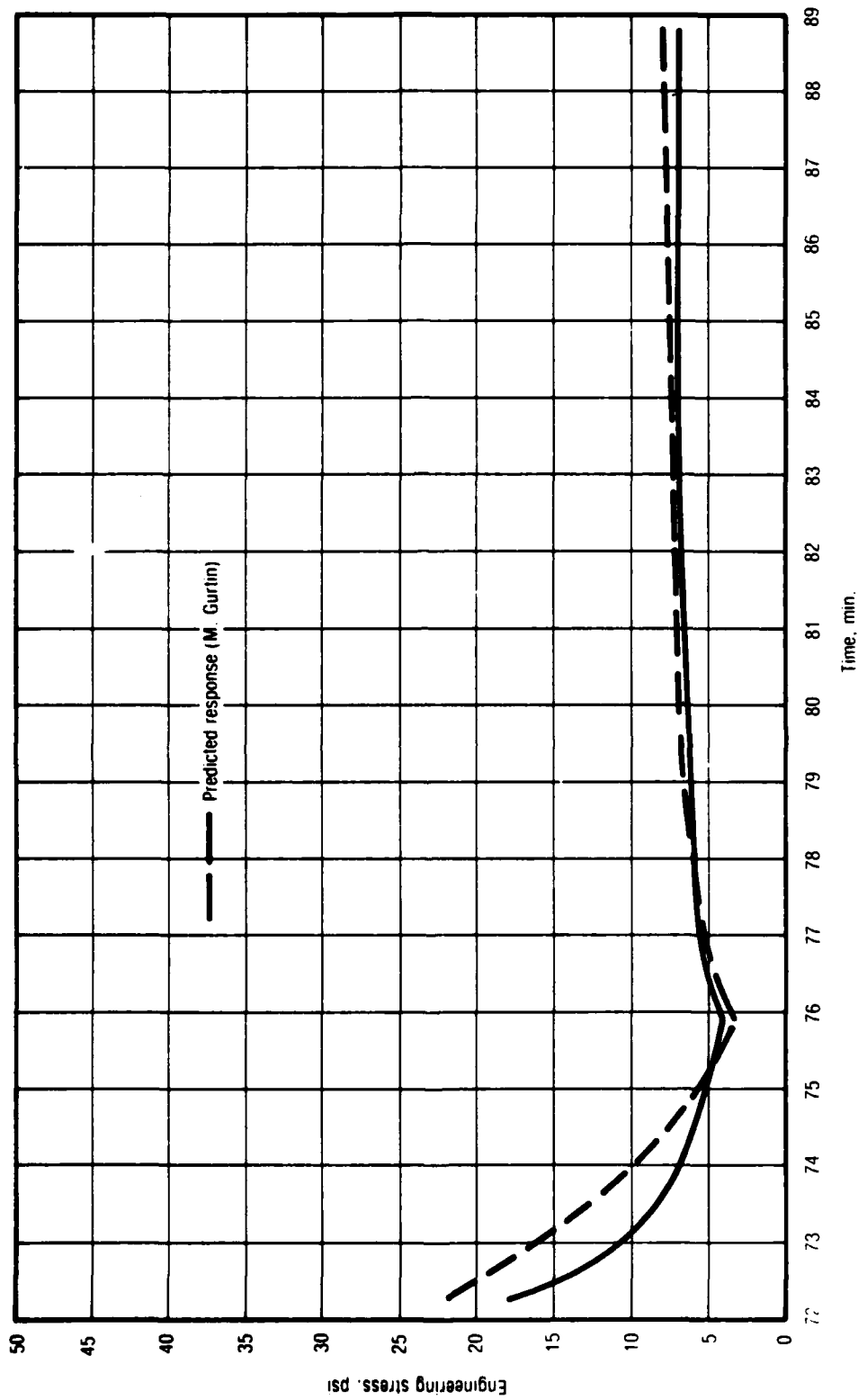


Figure 103. Three-Step Relaxation of 6-in. Bar of UTP-19, 360B-400/1777

28899

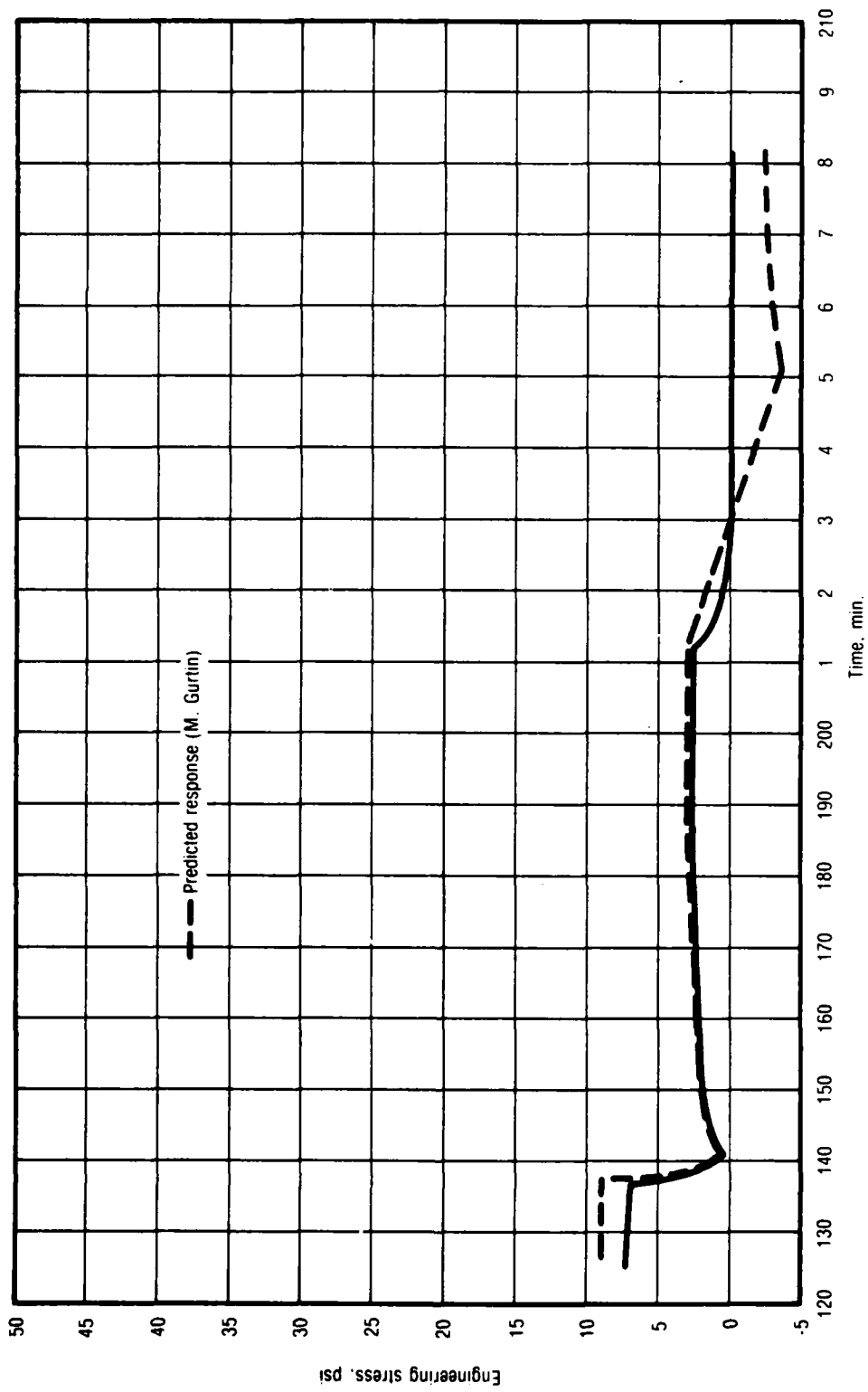


Figure 104. Three-Step Relaxation of 6-in. Bar of UTP-19, 360B-400/1777

28900

$$\sigma_r(t) = \int_0^t G_r(\tau) \dot{\epsilon}(t - \tau) d\tau \quad (105)$$

and the correction stress, σ_c , given by:

$$\sigma_c(t) = \int_0^t G_c[\epsilon(\tau), \tau] \dot{\epsilon}(t - \tau) d\tau \quad (106)$$

Hence, to characterize the virgin response, only constant rate tests need be employed. In this instance, σ and σ_r are known, so that from equation (88), σ_c may be computed, and equated to equation (90) using the fact that $\dot{\epsilon}$ is a constant; i.e.:

$$\sigma(t) - \sigma_r(t) = \sigma_c(t) \equiv \int_0^t G[\epsilon(\lambda), \lambda] d\lambda \quad (107)$$

which, upon recalling equations (91) and (92) becomes:

$$\sigma(t) - \sigma_r(t) = \sum_{n=1}^N \psi_n(t) \quad (108)$$

where:

$$\psi_n(t) = \sum_{p=1}^P A_{np} \dot{\epsilon} \int_0^t \epsilon^p(\lambda) e^{-\lambda/\tau_n} d\lambda \quad (109)$$

Furthermore, since for a constant-rate test:

$$\epsilon(\lambda) = \dot{\epsilon} \lambda \quad (110)$$

it follows that:

$$\psi_n(t) = \sum_{p=1}^P A_{np} \dot{\epsilon}^{p+1} \int_0^t \lambda^p e^{-\lambda/\tau_n} d\lambda \quad (111)$$

and after integrating by parts:

$$\Psi_n(t) = \sum_{p=1}^P A_{np} \dot{\epsilon}_n^{p+1} \tau_n^{p+1} f_p(t/\tau_n) \quad (112)$$

with

$$f_0(x) = 1 - e^{-x} \quad (113)$$

$$f_p(x) = -x^R e^{-x} + p f_{p-1}(x); p = 1, \dots, P$$

Clearly, equations (89) and (92) to (94) may be used to determine the coefficients a_{np} appearing in the definition of the correction modulus. The procedure suggested by M. Gurtin to accomplish this is as follows:

1. Take N tests with constant rates $\dot{\epsilon}_1, \dot{\epsilon}_2, \dots, \dot{\epsilon}_N$; and set:

$$\tau_i = \frac{1}{\dot{\epsilon}_i}; i = 1, \dots, N \quad (114)$$

2. Select the degree, P , of the series expansion of the correction modulus, as it appears in equation (87).
3. Use the $\dot{\epsilon}_1$ test and the approximation:

$$\sigma_c(t) = \Psi_1(\dot{\epsilon}_1, t) \quad (115)$$

to find the a_{1p} .

4. Use the $\dot{\epsilon}_2$ test and the approximation:

$$\sigma_c(t) - \Psi_1(\dot{\epsilon}_2, t) = \Psi_2(\dot{\epsilon}_1, t) \quad (116)$$

to find the a_{2p} .

5. Use the $\dot{\epsilon}_3$ test and the approximation:

$$\sigma_c(t) - \Psi_1(\dot{\epsilon}_3, t) - \Psi_2(\dot{\epsilon}_3, t) = \Psi_3(\dot{\epsilon}_3, t) \quad (117)$$

to find the a_{3p} , and so on for the $a_{4p} \dots a_{np}$.

6. Iterate this procedure if necessary; that is, define:

$$\bar{\Psi}(\dot{\epsilon}, t) = \sum_{n=1}^N \Psi_n(\dot{\epsilon}, t) \quad (118)$$

so that $\bar{\Psi}$ is known. For each ramp test, define:

$$\bar{\sigma}_c = \sigma_c - \bar{\Psi} \quad (119)$$

and repeat the above procedure using $\bar{\sigma}_c$ to find constants \bar{a}_{np} . The new values of the a_{np} are:

$$(A_{np})_{\text{new}} = A_{np} + \bar{A}_{np} \quad (120)$$

7. Repeat the process if necessary.

It is important to point out here that numerical difficulties may be encountered in applying this technique to characterizing the virgin response of solid propellants. In fact, some convergence problems were faced in connection with the UTP-19,360B data. Moreover, characterization of the damaged response calls for a large number of cyclic tests over a wide range of rates. This increases the convergence difficulties. The model was employed with the constant-rate tests only for this reason. Figures 105 to 108 show the results of the stress predictions obtained with the current version of the model. The first two plots correspond, respectively, to the lowest and highest rates available in the data base at ambient temperature.

So far in the program, none of the models developed by Gurtin has taken into account the effects of temperature on propellant response. However, the

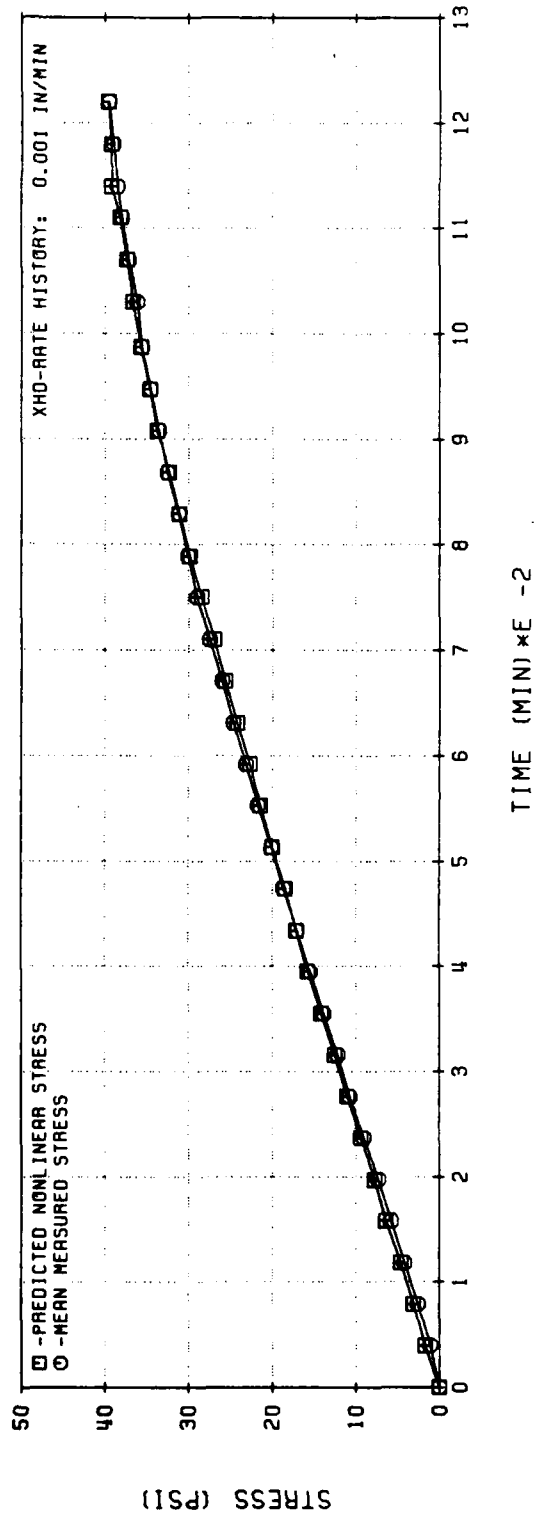
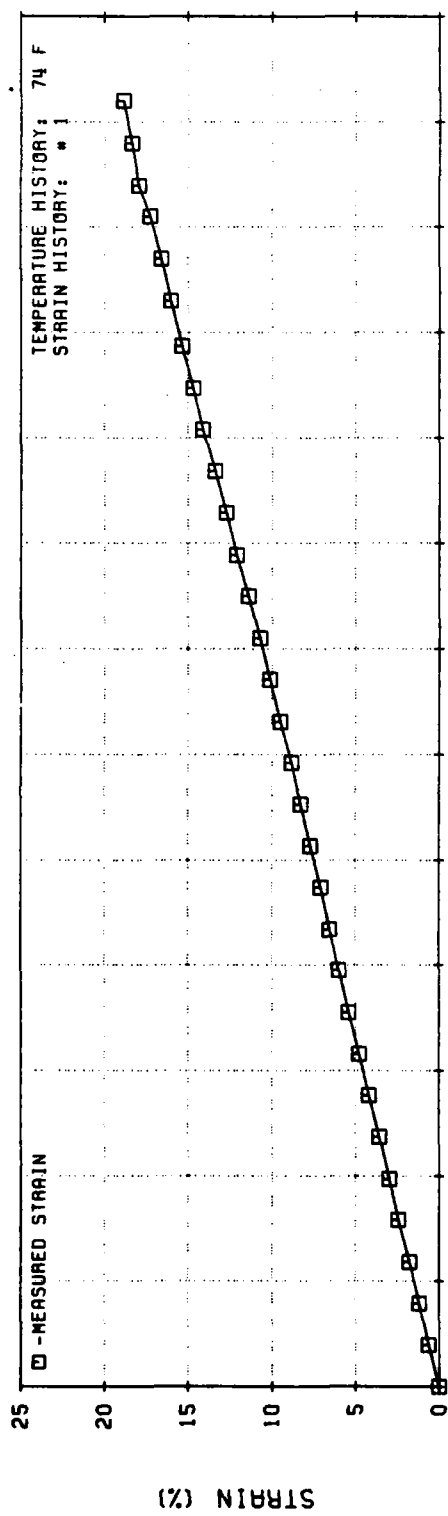


Figure 105. Nonlinear Viscoelastic Stress Predictions for UTP-19,360B-400/1777 at 0.001 in./min and 74 F (M. Gurtin's Theory)

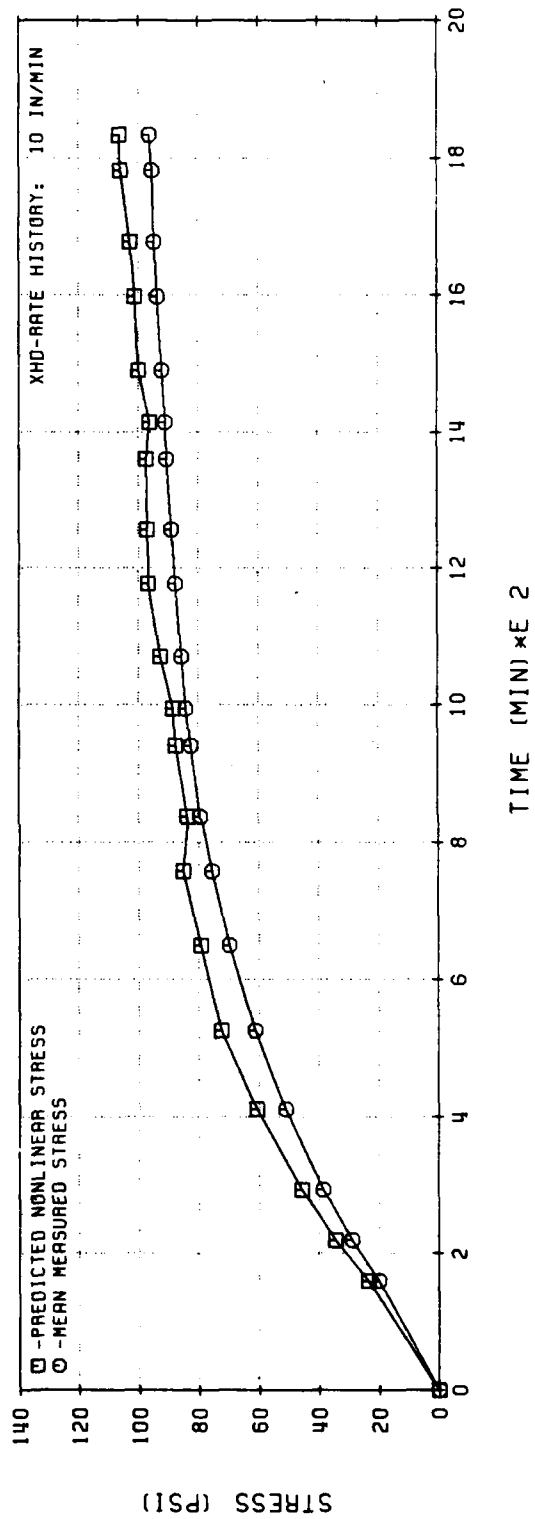
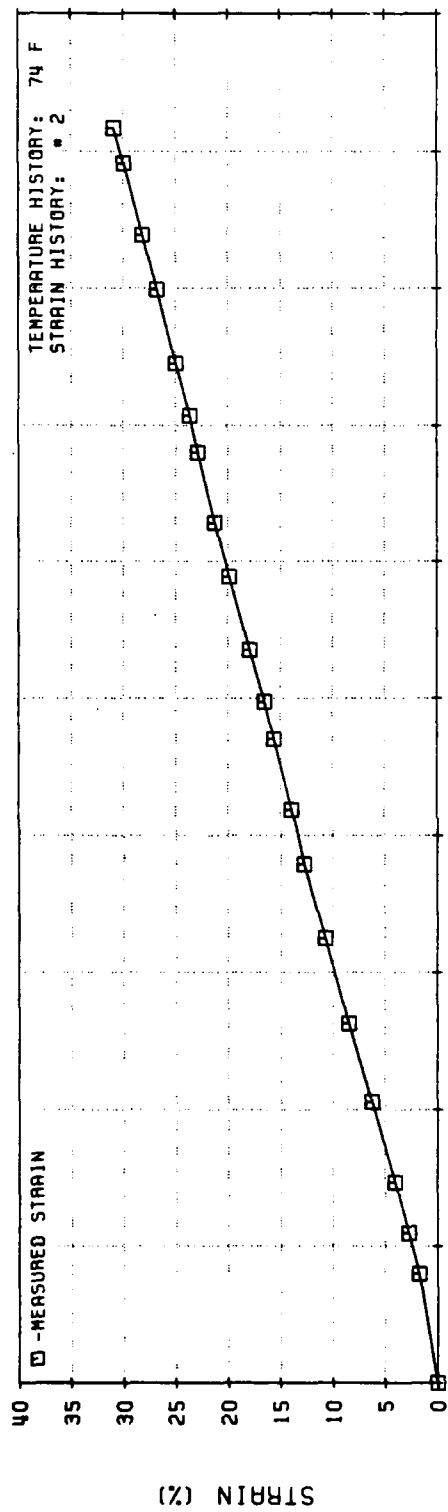


Figure 106. Nonlinear Viscoelastic Stress Predictions for UTP-19,360B-400/1777 at 70 F
(M. Gurtin's Theory)

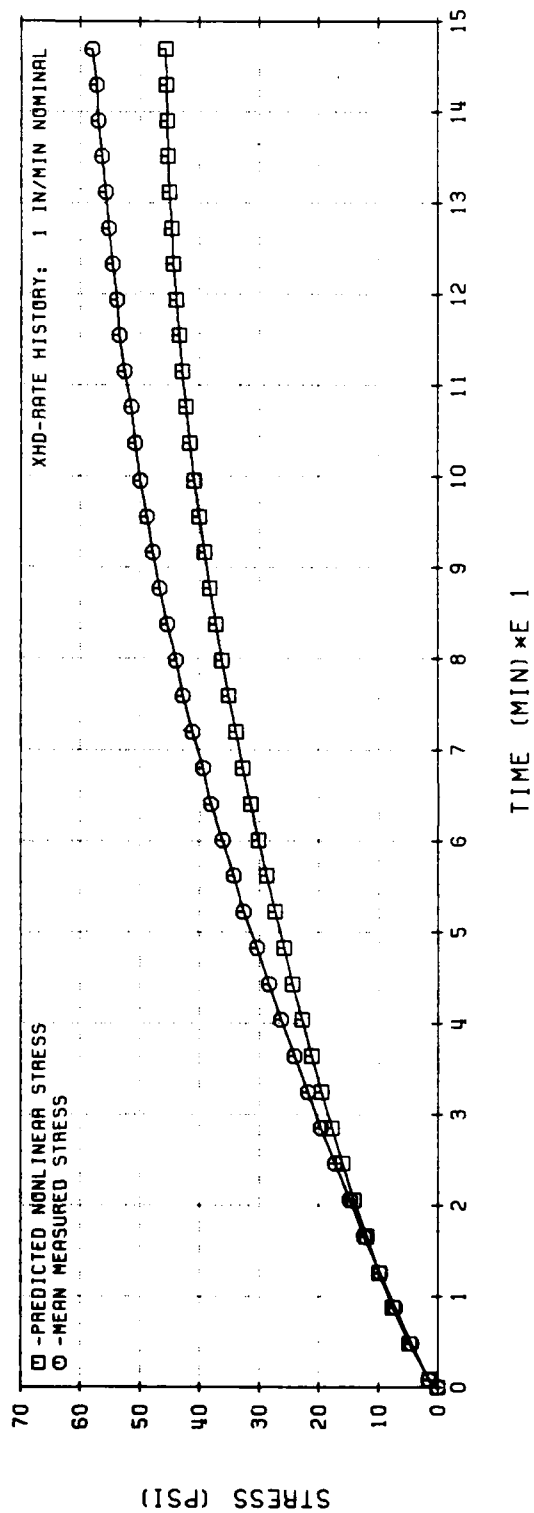
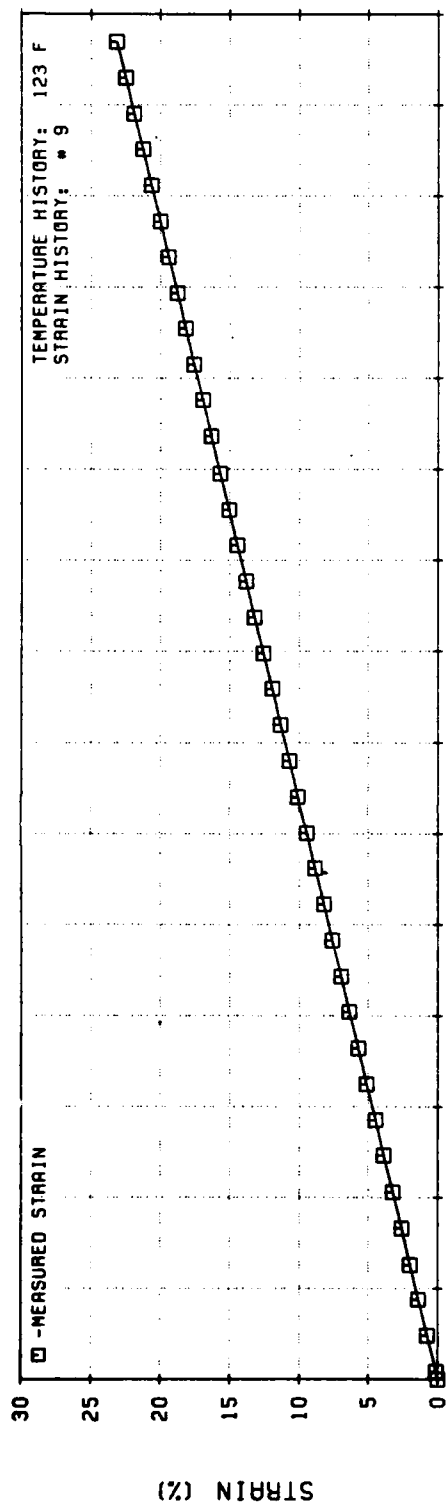


Figure 107. Nonlinear Viscoelastic Stress Predictions for UTP-19, 360B-400/1777 at 123 F
(M. Gurtin's Theory)

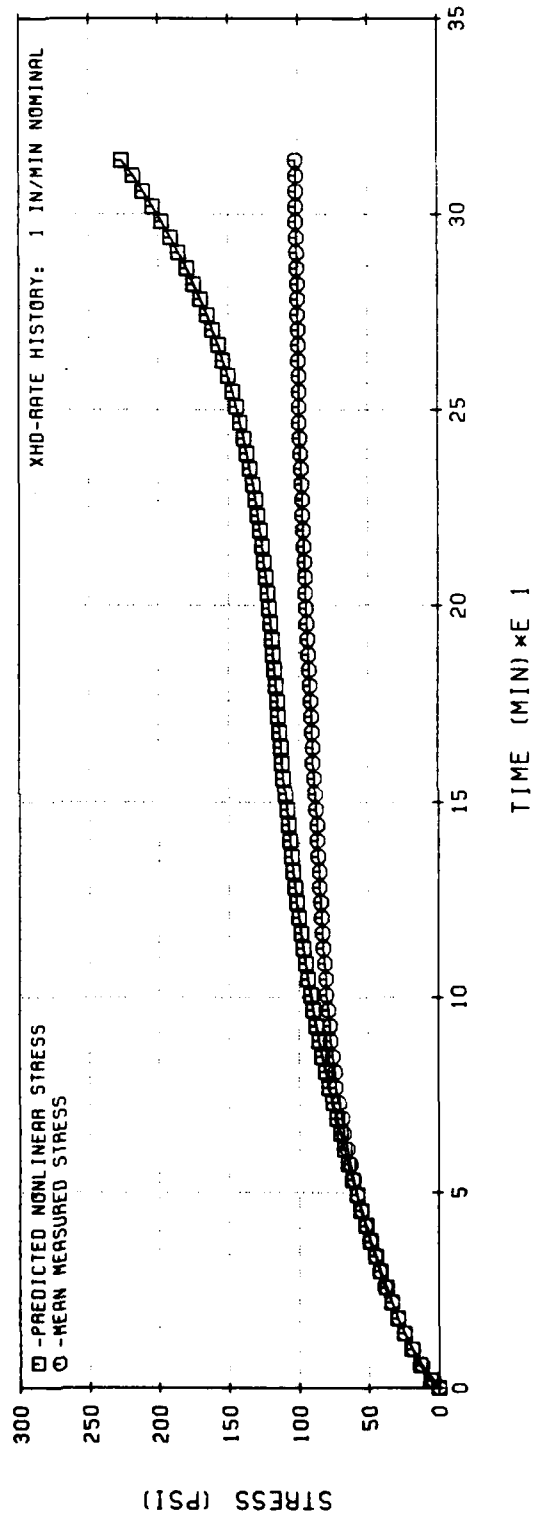
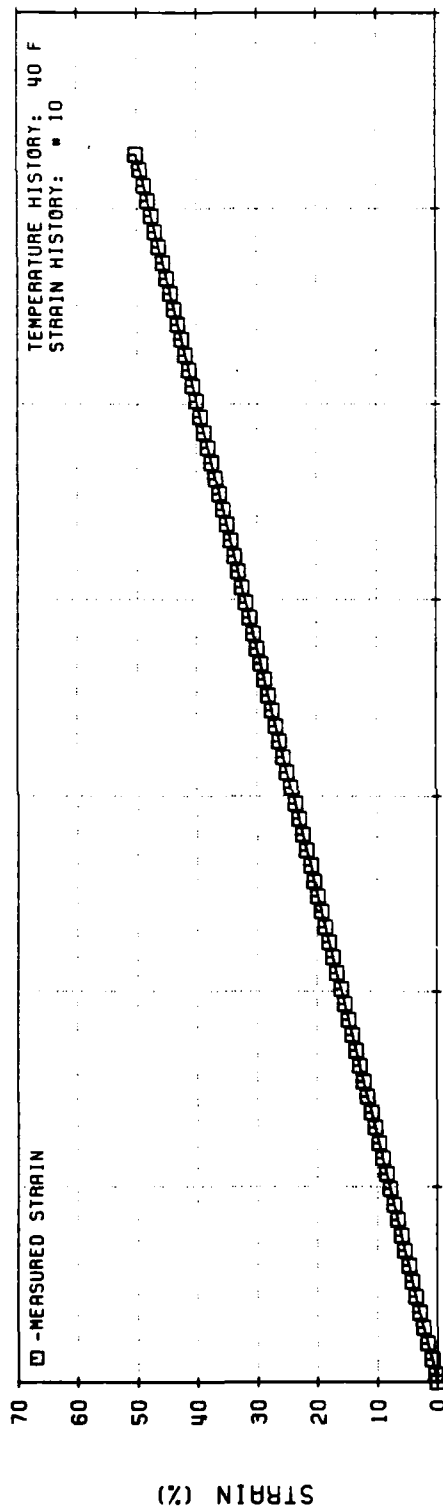


Figure 108. Nonlinear Viscoelastic Stress Predictions for UTP-19, 360B-400/1777 at 40 F
(M. Gurtin's Theory)

time-temperature superposition principle was tested with the current version of the theory. The results appear in Figures 107 and 108 for the thermal tests at 123 and 40°F, respectively. The use of the superposition principle breaks down at a strain of about 39%. This was apparently due to the ambient temperature data base being limited to a low strain level. Also, it might be necessary to allow the relaxation function (G_c) to depend on the glass transition temperature (T_g)

$$G_c = G_c(\epsilon, T_g, t)$$

4.2.5 Russian Approach to Physically Nonlinear Viscoelastic Solids

The Russians have explored two approaches for characterizing damage effects in solid propellants (References 7 and 8). They are a general functional approach, and a kinetic equation of evolution for damage. Both approaches are based on internal-variable concepts, and either approach appears general enough to also incorporate cumulative damage and propellant response under multiaxial stress states. However, the general functional approach may be of little practical engineering value, because a very extensive testing program may be required to evaluate material parameters. This approach requires introduction of damage measures, which should reflect microstructural damage mechanisms, and a damage functional which characterizes the accumulation of damage or defects. The damage functional is then expanded into a series of multiple integrals in an analogous fashion to that followed by Green and Rivlin for nonlinear materials with fading memory. Herein lies the difficulty. Even assuming isotropy, four to six different types of multi-axial tests are required to evaluate the required material property functions for a first-order theory. Although the approach has theoretical merit and may even have some practical application in the future, its pursuit was abandoned in favor of the kinetic approach.

The essential feature of the kinetic approach is to introduce the degree of damage into the constitutive equations as a reduced-time parameter in the same way that temperature is introduced as a reduced-time parameter for the thermorheologically simple materials in linear thermoviscoelasticity. Damage is then defined in terms of some strength parameter of the material, and the degree of

damage is characterized through an equation of evolution for damage, as explained subsequently.

4.2.5.1 Original Model

The one-dimensional constitutive equation taken from the Russian literature by W. L. Hufferd as a means of predicting the response of physically nonlinear viscoelastic materials may be expressed by:

$$\sigma(t) = \int_0^t E(t' - \tau') \frac{d\epsilon}{d\tau}(\tau) d\tau \quad (121)$$

where

σ = stress

ϵ = strain due to mechanically applied stress

$E(t)$ = relaxation modulus

$E(t) = E_e + E_2 t^{-n}$

and

$$t' - \tau' = \int_{\tau}^t \frac{d\epsilon}{a\eta[\eta(\xi)]} \quad (122)$$

represents the damage-reduced time, which is arrived at in the manner described next.

First, a normalized damage function $\omega = \omega(t)$ is introduced through the following kinetic equation of evolution:

$$\frac{d\omega}{dt}(t) = h(\omega) f(t) \quad (123)$$

in which it is further assumed that:

$$f(t) = \int_0^t F(t - \tau) \phi[\sigma_0(\tau)] d\tau \quad (124)$$

together with the conditions:

$$\begin{aligned}\omega(0) &= 0 \\ \omega(t^*) &= 1\end{aligned}\tag{125}$$

indicating that no damage exists at the initial state, and that failure occurs at time t^* .

Next, equation (97) is integrated with $\omega(0) = 0$, leading to:

$$\int_0^{\omega} \frac{d\omega}{h(\omega)} = \int_0^t f(\tau) d\tau\tag{126}$$

Setting $t = t^*$, so that $\omega(t^*) = 1$, and substituting equation (98) for $f(\tau)$, it is obtained that

$$\frac{\int_0^{t^*} d\xi \int_0^{\xi} F(\xi - \tau) \phi[\sigma_0(\tau)] d\tau}{\int_0^1 \frac{d\omega}{h(\omega)}} = 1\tag{127}$$

If now the function $F(t)$ is assumed to have a power-law representation:

$$F(t) = F_0 t^m\tag{128}$$

Equation (101) can be written in the form:

$$\frac{\int_0^{t^*} d\xi \int_0^{\xi} F_0(\xi - \tau)^m \phi[\sigma_0(\tau)] d\tau}{\int_0^1 \frac{d\omega}{h(\omega)}} = 1 \quad (129)$$

and integrating with respect to ξ , assuming that the order of integration may be interchanged, one arrives at:

$$\frac{\frac{F_0}{1+m} \int_0^{t^*} (t^* - \tau)^{1+m} \phi[\sigma_0(\tau)] d\tau}{\int_0^1 \frac{d\omega}{h(\omega)}} = 1 \quad (130)$$

which, for the case where σ_0 and $\phi[\sigma_0] = \phi[\sigma_0]$ are constant, becomes:

$$\frac{F_0 \phi_0(\sigma_0)}{(1+m)(2+m)} \frac{(t_0^*)^{2+m}}{1} = 1 \quad (131)$$

$$\int_0^1 \frac{d\omega}{h(\omega)}$$

where t_0^* is the time to failure under the constant stress σ_0 . Thus equation (104), in this case, may be written as

$$(2+m) \int_0^{t_0^*} (t_0^* - \tau)^{1+m} \frac{d\tau}{(t_0^*)^{2+m}} = 1 \quad (132)$$

If the time to failure under a constant stress, σ_0 , has the power-law representation:

$$\sigma_0^\alpha t_0^* = \text{constant} = \beta \quad (133)$$

then equation (106) can be put in the form:

$$\int_0^{t^*} (t^* - \tau)^{1+m} \sigma_0^{\alpha(2+m)} d\tau = \frac{\beta^{2+m}}{2+m} \quad (134)$$

so that, motivated by equations (106) and (108), the degree of damage accumulation may be introduced through the expression:

$$\eta(t) = (2+m) \int_0^t (t-\tau)^{1+m} \frac{d\tau}{(t_0)^{2+m}} \quad (135)$$

in which, obviously:

$$\begin{aligned} \eta(0) &= 0 \\ \eta(1) &= 1 \end{aligned} \quad (136)$$

The function $\eta(t)$ can be related to the damage function, ω , by:

$$\eta = \frac{\int_0^\omega \frac{d\omega}{h(\omega)}}{\int_0^1 \frac{d\omega}{h(\omega)}} \quad (137)$$

This means that η represents the relative damage in the load history for the power-law representation of t_0^* . From equations (107) and (108), equation (109) may be written as:

$$\eta(t) = \frac{2+m}{\rho^{2+m}} \int_0^t (t-\tau)^{1+m} \sigma_0^{\alpha(2+m)} d\tau \quad (138)$$

and finally, the influence of damage is treated as a reduced variable by introducing the modified time, t' , defined by

$$dt' = \frac{dt}{a_\eta |\eta(t)|} \quad (139)$$

on which equation (96) is based, and where the shift function due to damage, a_η , depends on the material at hand.

Despite its rather appealing physical and mathematical foundations, the original model did not do any better than Linear Viscoelasticity when it was used to predict the response of either TP-H1011 or UTP-19,360B. In those instances, a linear expression:

$$a_\eta = 1 - \eta \quad (140)$$

and an exponential form:

$$a_\eta = e^{-\eta}$$

were used for the damage shift function.

The partial failure of the Russian approach to reproduce solid-propellant behavior made it necessary to change certain aspects of the theory, as explained next.

Current Model. One revised version of the Russian stress-strain law takes the form:

$$\sigma(t) = \int_0^t E \left(\frac{t-\tau}{a_\eta} \right) \frac{d\epsilon}{d\tau}(\tau) d\tau \quad (141)$$

where $a_{\eta}^{\#}$ is a damage-related shift function, assumed to depend only on the current state of strain; specifically:

$$a_{\eta}^{\#} = a_{\eta}^{\#} \left[\epsilon(t), \dot{\epsilon}(t) \right] \quad (142)$$

Clearly, if:

$$E(t) = E_e + E_2 t^{-n} \quad (143)$$

then equation (113) becomes:

$$\sigma(t) = E_e \epsilon(t) + (a_{\eta}^{\#})^n E_2 \int_0^t (t - \tau)^{-n} \frac{d\epsilon}{d\tau}(\tau) d\tau \quad (144)$$

which resembles the classical approach of the softening function used as a stress-correction factor.

Another revised version of the Russian approach consists of retaining most aspects of the original law, but constant strain-rate data are employed to express the time to failure as:

$$t_0^{\#} = \left(\frac{\beta}{\dot{\epsilon}} \right)^{\alpha} \quad (145)$$

and equation (108) is changed to:

$$\eta(t) = \frac{(2 + m)}{\dot{\epsilon} t_0^{\#}} \int_0^t (t - \tau)^{1+m} \phi(\tau) d\tau \quad (146)$$

where:

$$\phi(t) = \epsilon(t) = \dot{\epsilon} t$$

and

$$\eta(t^*) = 1$$

Thus, evaluation of equation (117) at $t = t^*$ yields:

$$\frac{(2 + m)}{\epsilon t_o^*} \int_0^{t^*} (t^* - \tau)^{1+m} \phi(\tau) d\tau = 1 \quad (147)$$

which, through a change of variables and after some algebraic manipulations, may be integrated to:

$$(t_o^*)^{2+m} = 3 + m \quad (148)$$

The solution for m , as a function of strain rate, is easy to obtain using equations (116) and (119) (as presented in Figure 109 for UTP-3001).

In much the same way, integration of equation (117) for the relative damage function, $\eta(t)$, leads to:

$$\eta(t) = \left(\frac{t}{t_o^*} \right)^{3 + m} \quad (149)$$

Hence, using constant strain-rate data to express the time to failure does simplify things, but a major assumption would still be needed regarding the form of the damage shift function as it was in the original set of equations. In this context, it is important to note that the linear expression:

$$a_\eta = 1 - \eta \quad (150)$$

and the exponential form:

$$a_\eta = e^{-\eta} \quad (151)$$

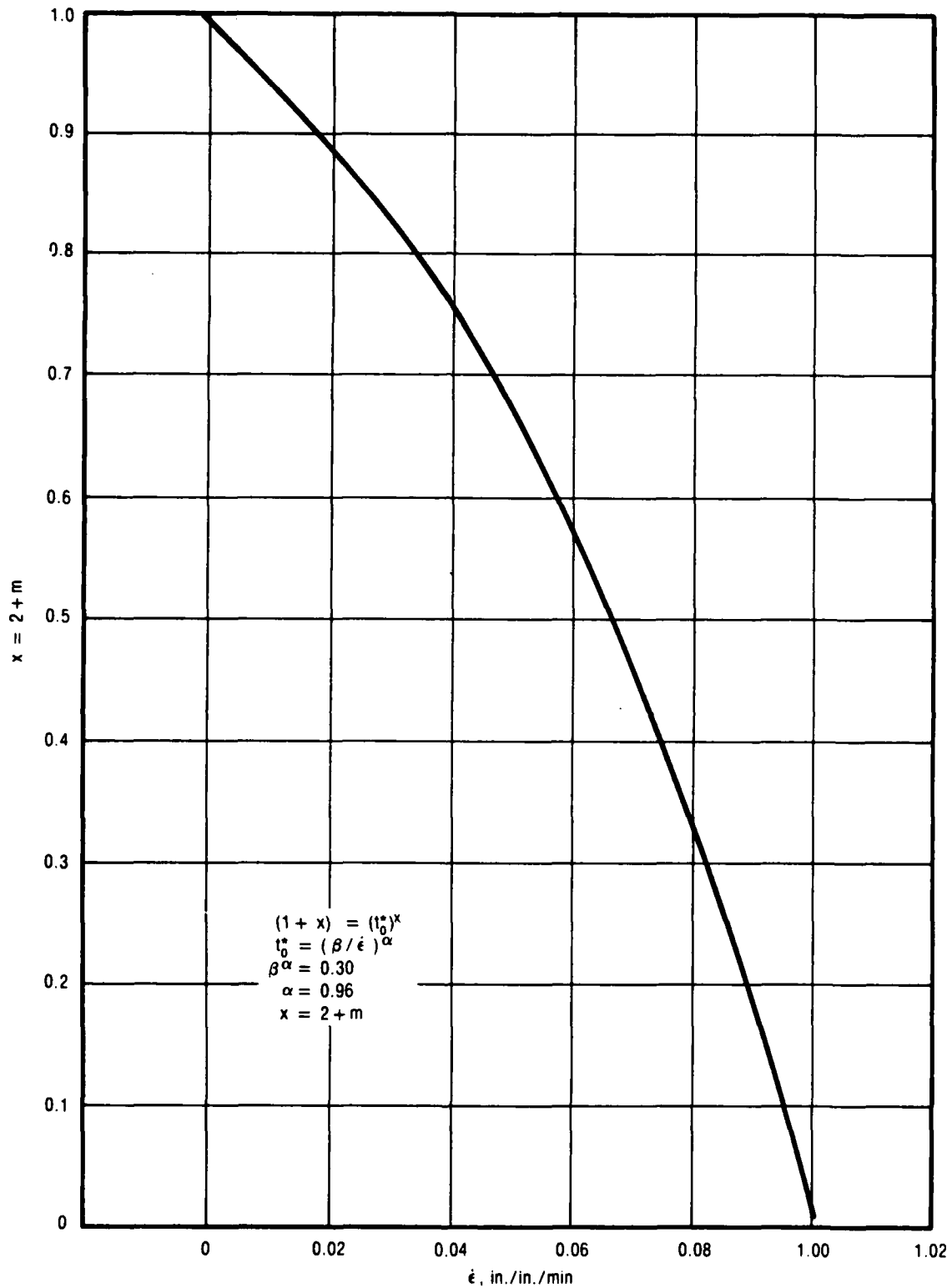


Figure 109. Solution for m as a Function of Strain Rate

28893

were used for the damage shift function without success. For this reason, the modified version used to run the stress predictions included in this report, corresponds to equation (115).

4.2.5.3 Stress Predictions

Figures 110 to 114 show the comparison between the observed response and that calculated using the present theory. As may be seen, the predicted response is quite accurate in all cases considered, which include constant- and dual-rate tests, as well as a short-duration similitude loading.

4.2.5.4 Material Characterization

As may be gathered from equation (115), the simplest version of this theory requires the knowledge of only two material-property functions, to wit:

1. The relaxation modulus, and
2. The damage shift function:

$$(a_{\eta}^*) \stackrel{\text{def}}{=} a_{\eta} = a_{\eta} \left[\epsilon(t), \dot{\epsilon}(t) \right] \quad (152)$$

which is determined in the following ways:

- a. From constant strain-rate tests, to correct the stress response during loading;
- b. From a relaxation test at a large strain level, to account for healing; and
- c. From a constant strain-rate cycle carried out to a large strain level, to more adequately reproduce the hysteretic behavior of the propellant.

The damage shift functions corresponding to UTP-19,360B are shown in Figures 115 to 119. The first three of these plots represent typical curves of a_{η} for low, intermediate and high strain-rate tests, while Figures 118 and 119 give the correction curves for relaxation and unloading, respectively.

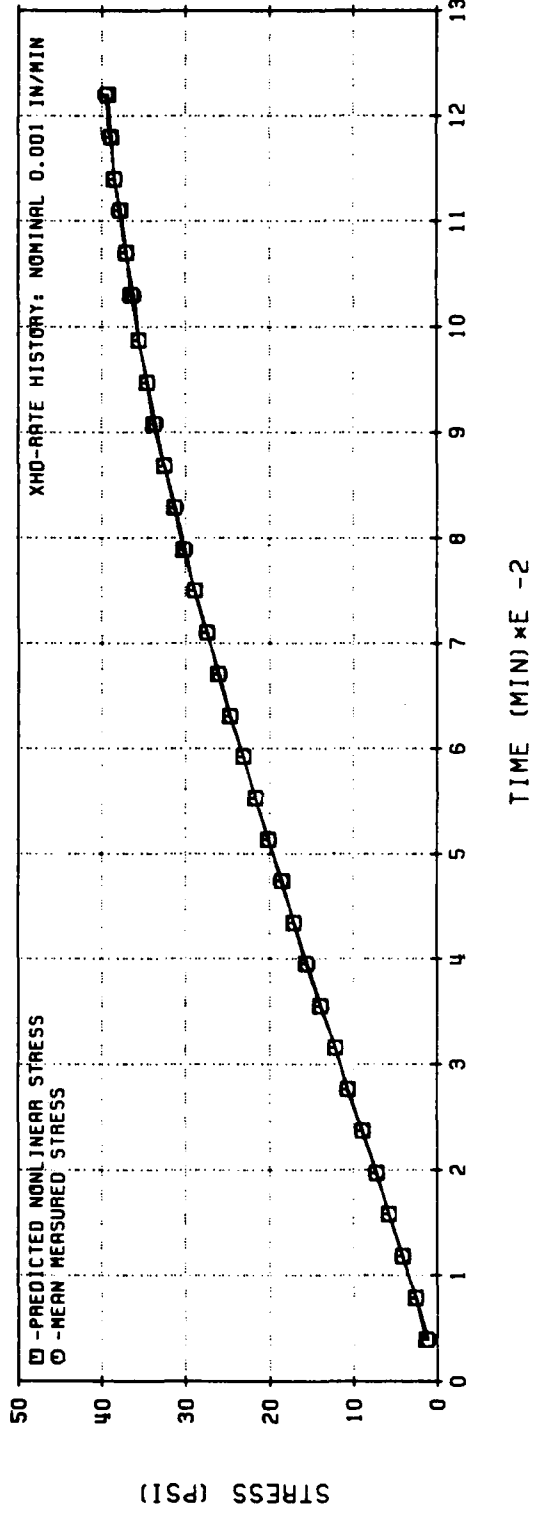
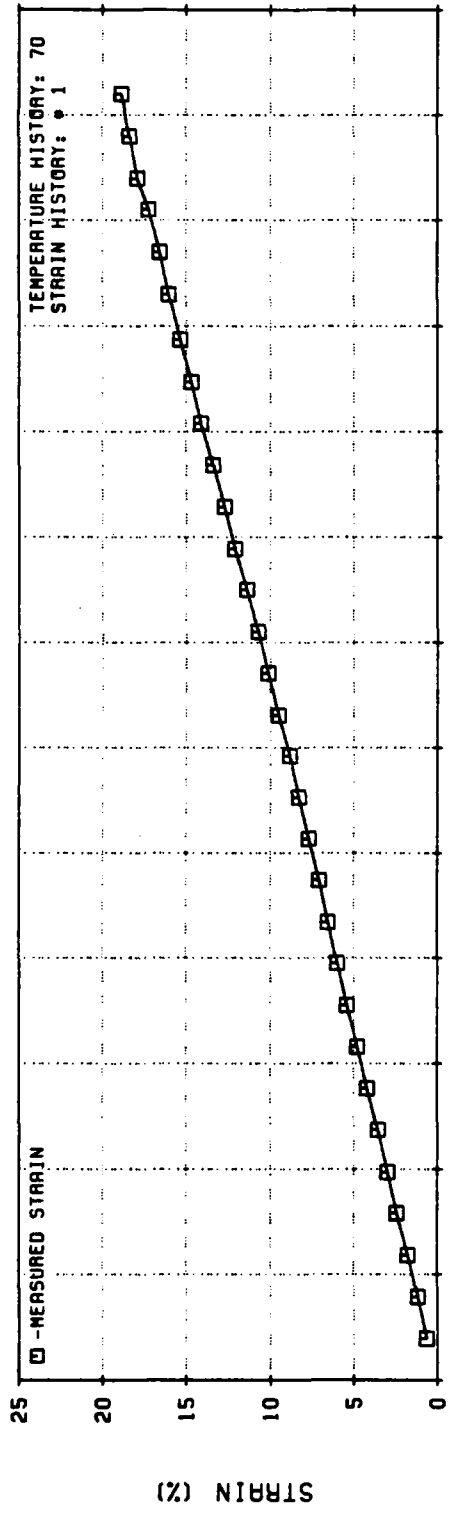


Figure 110. Nonlinear Viscoelastic Stress Predictions for UTP-19,360B-400/1777

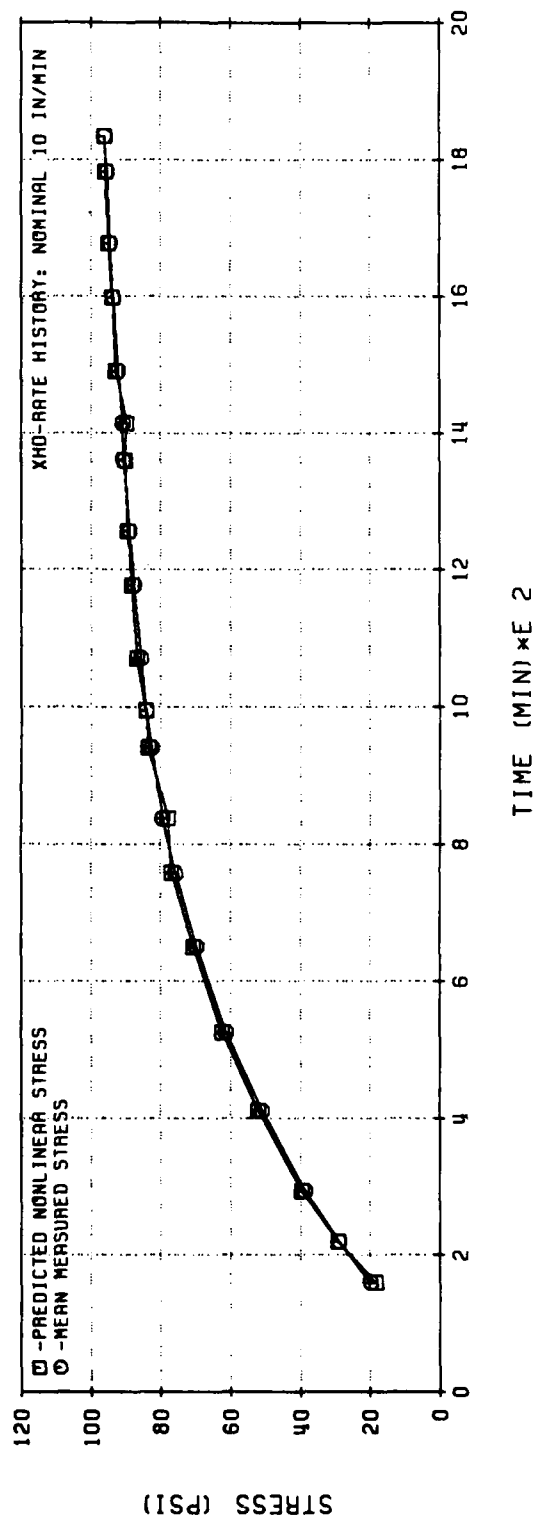
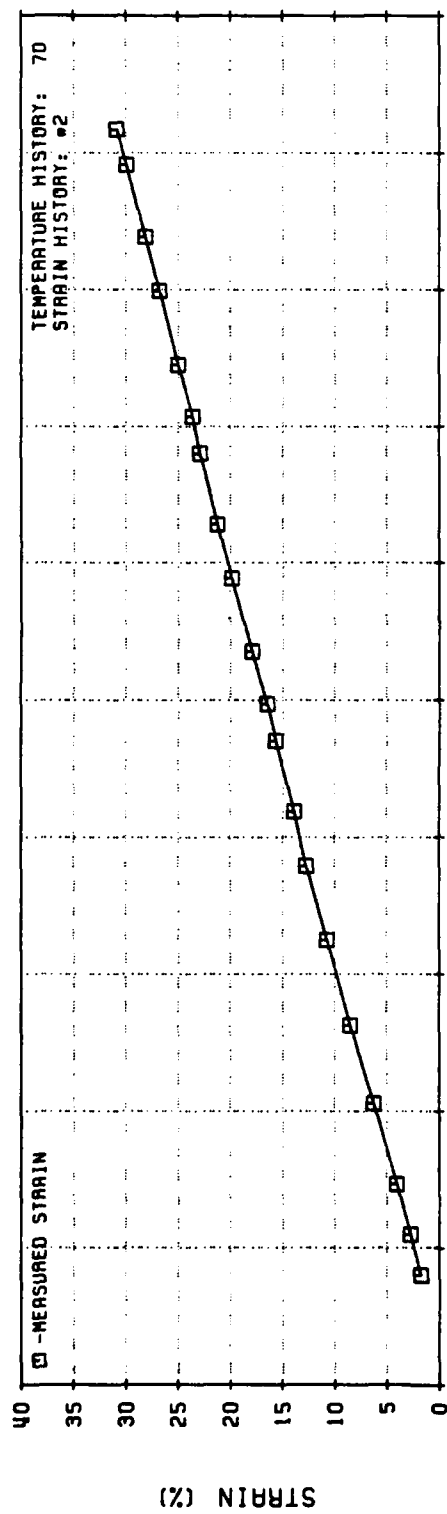


Figure 111. Nonlinear Viscoelastic Stress Predictions for UTP-19,360B-400/1777

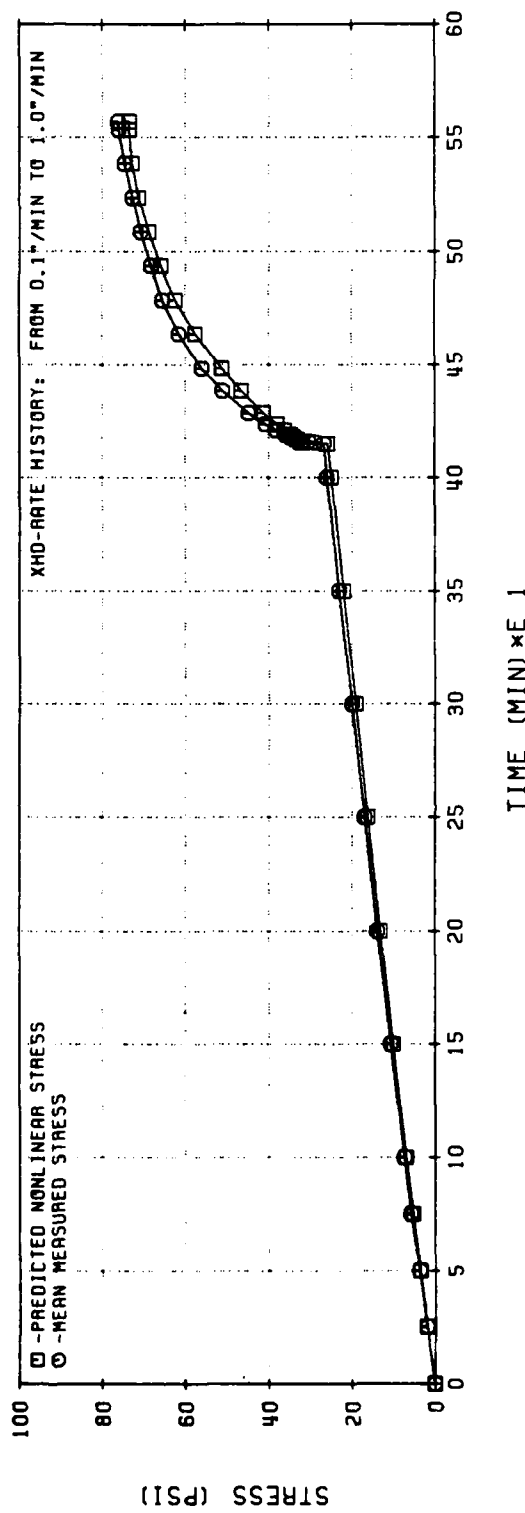
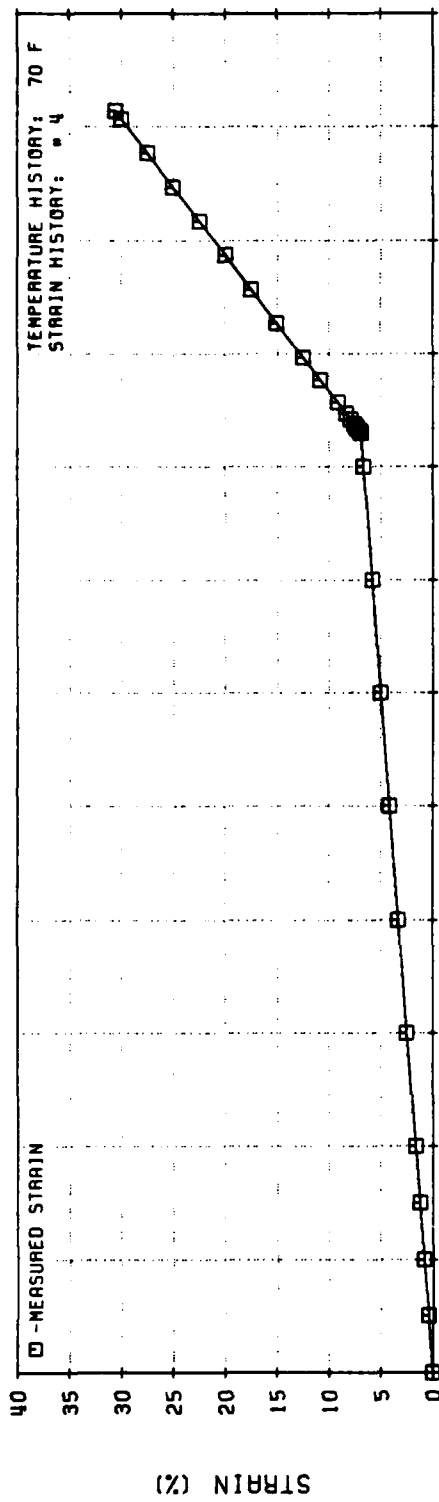


Figure 112. Nonlinear Viscoelastic Stress Predictions for Two-Rate Test (UTP-19,360B-400/1777)

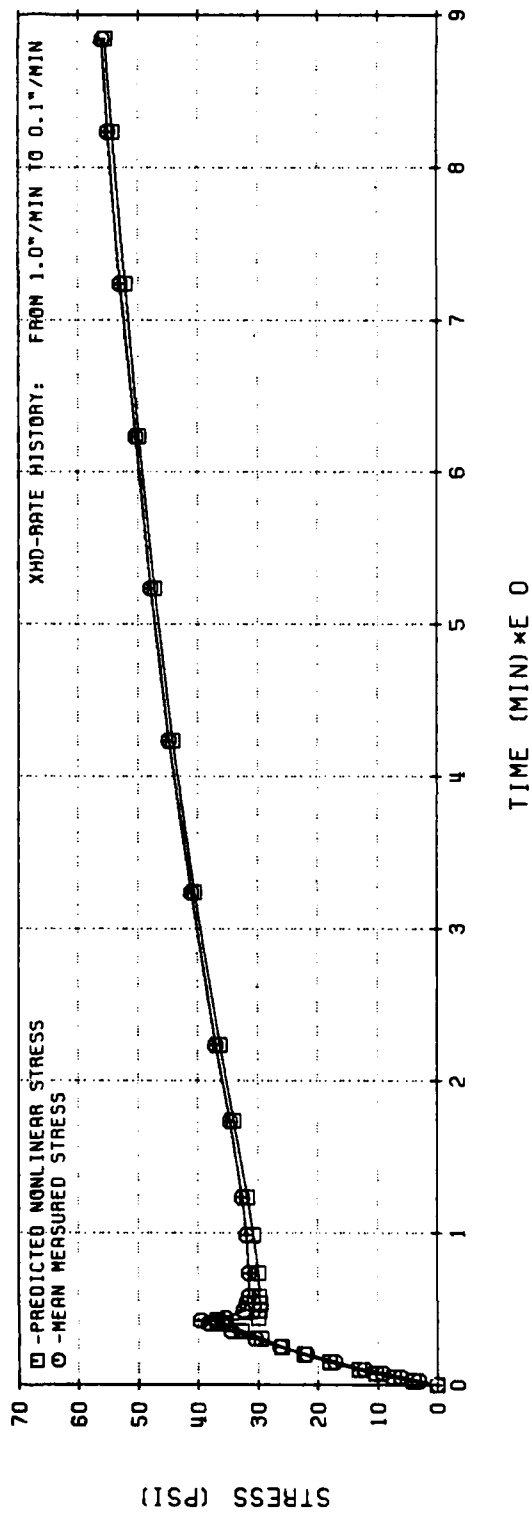
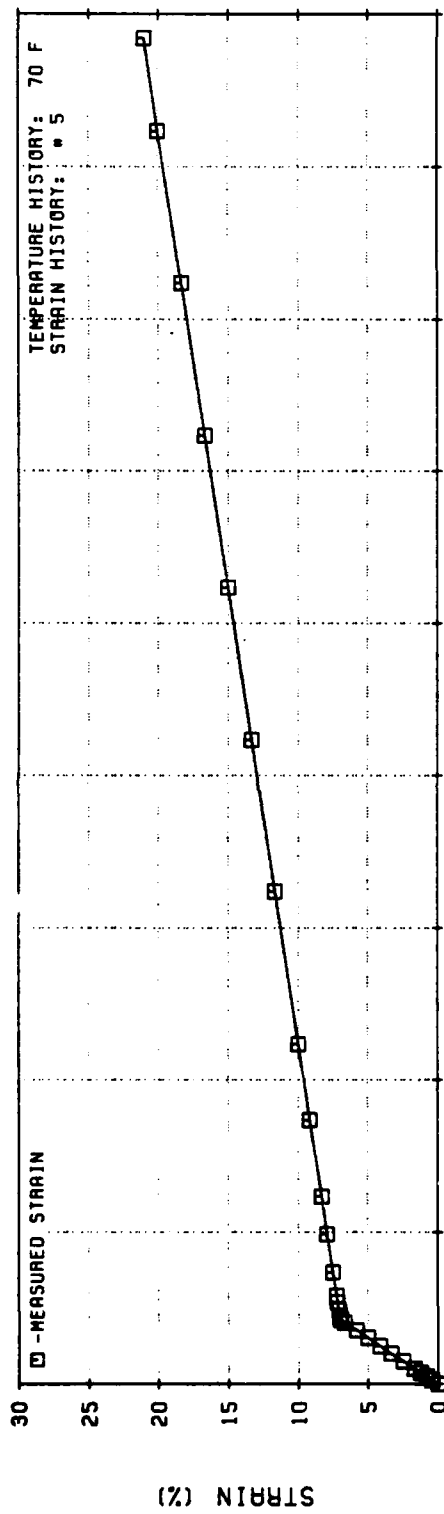


Figure 113. Nonlinear Viscoelastic Stress Predictions for Two-Rate Test (UTP-19,360B-400/1777)

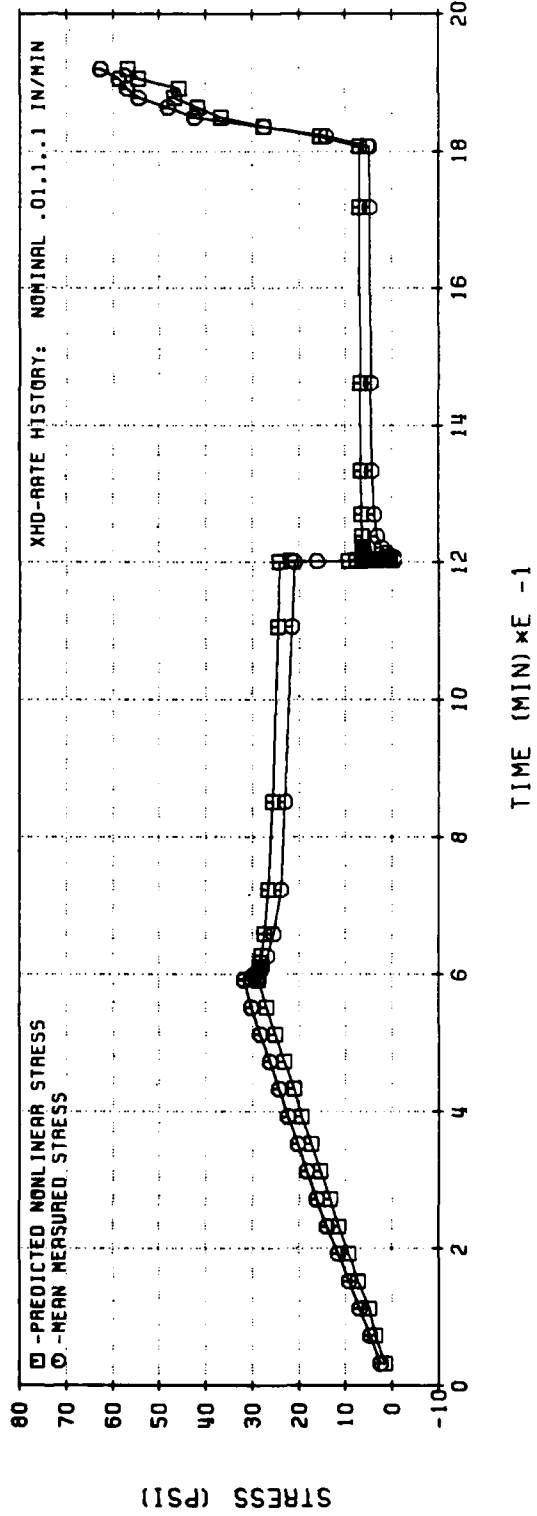
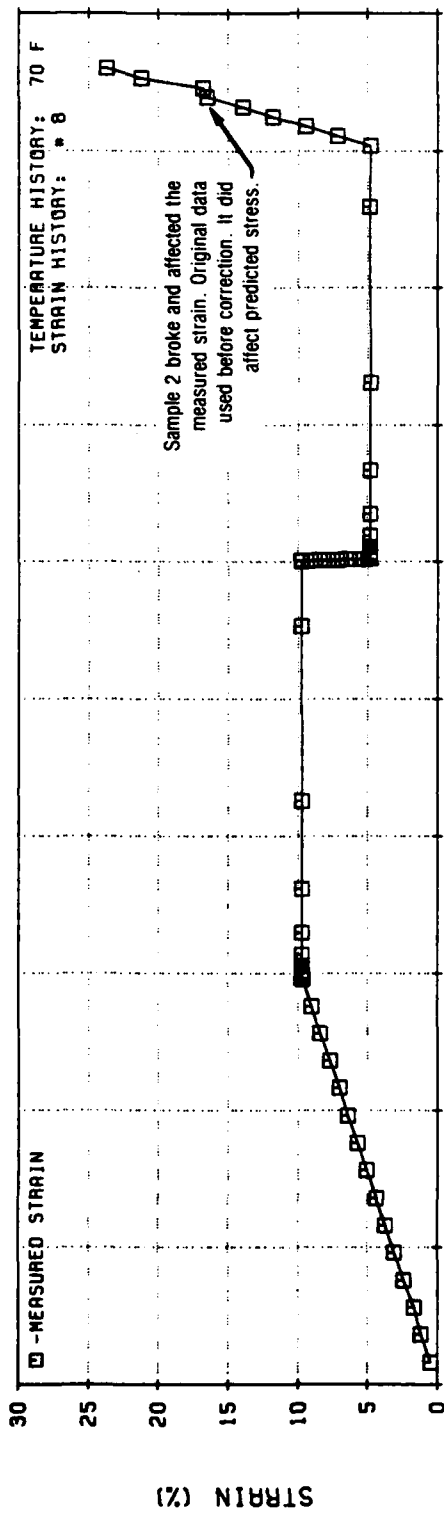


Figure 114. Nonlinear Viscoelastic Stress Predictions for Short Similitude Test (UTP-19, 360B-400/1777) (W. L. Hufford's Theory)

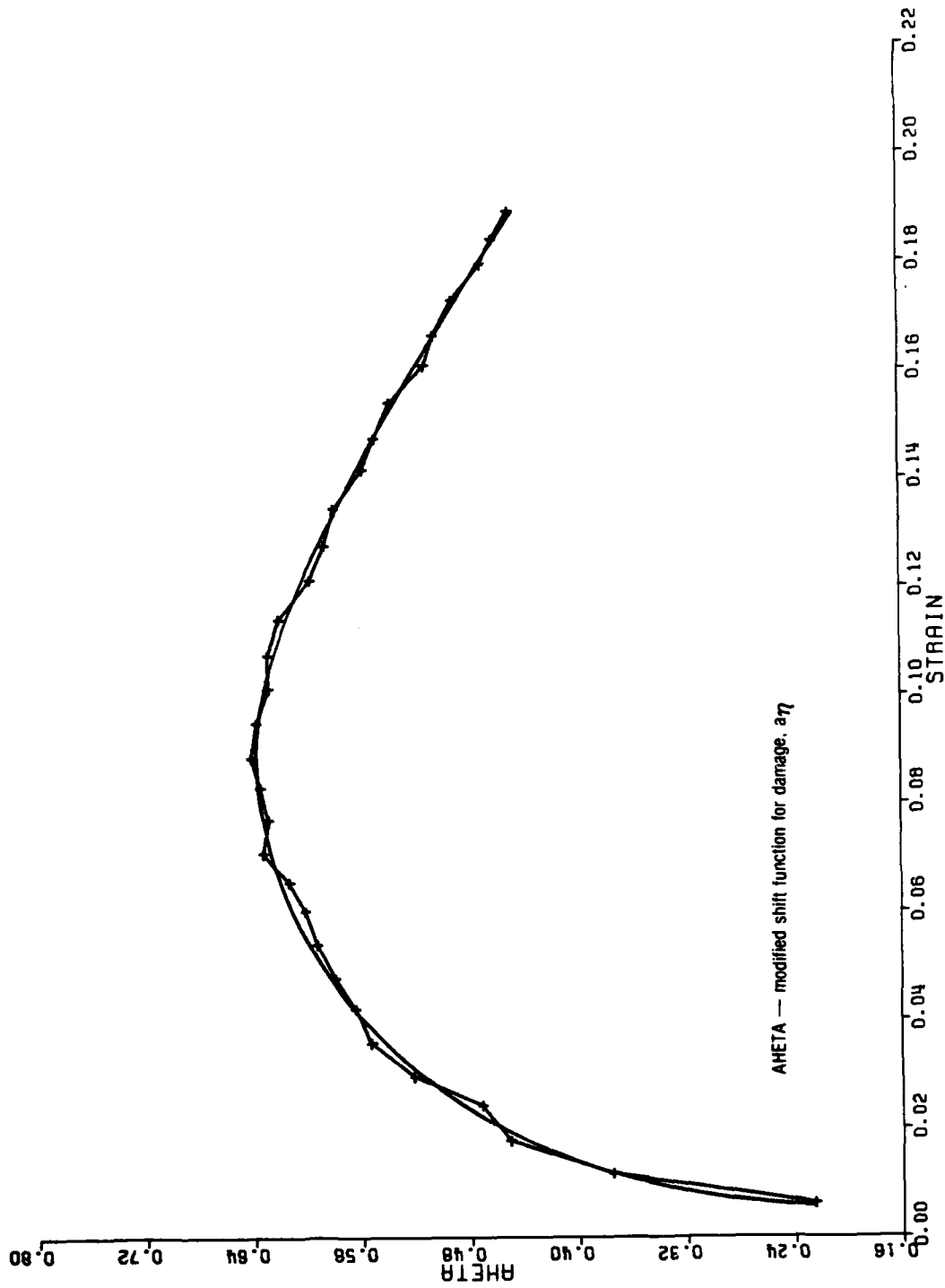


Figure 115. Constant Rate Test (0.001 in./min.)

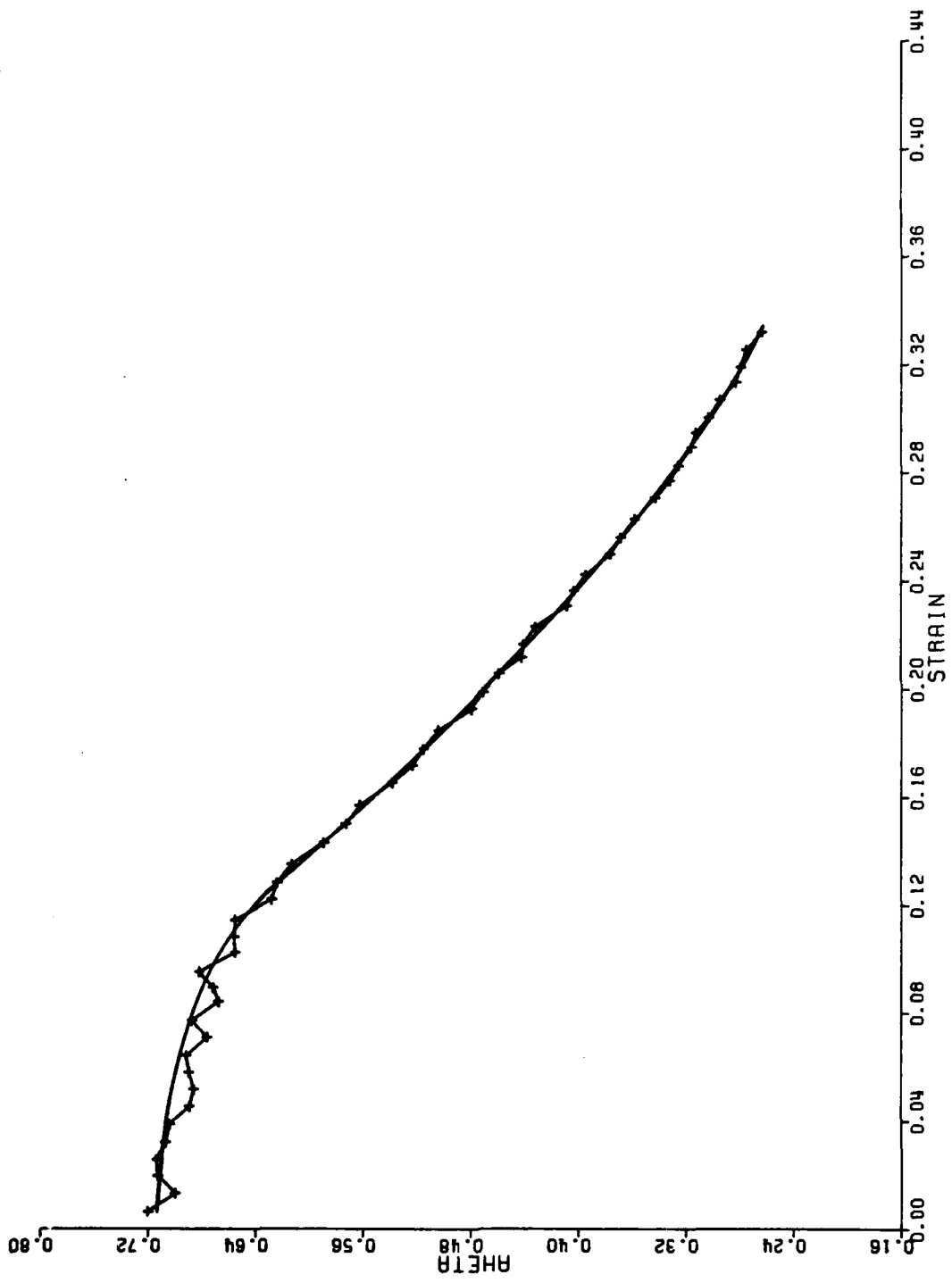


Figure 116. Constant Rate Test (0.1 in./min.)

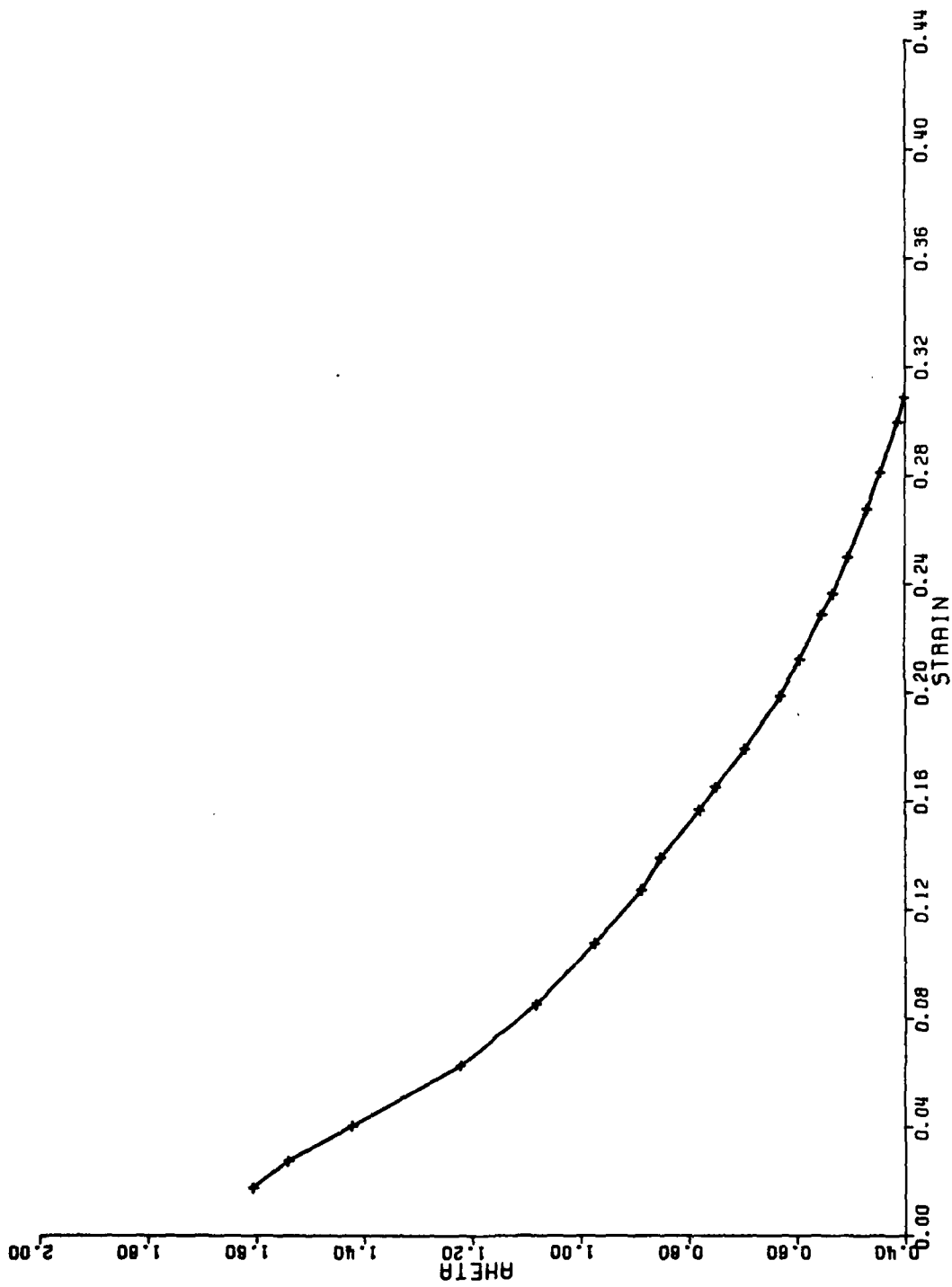


Figure 117. Constant Rate Test (10 in./min.)

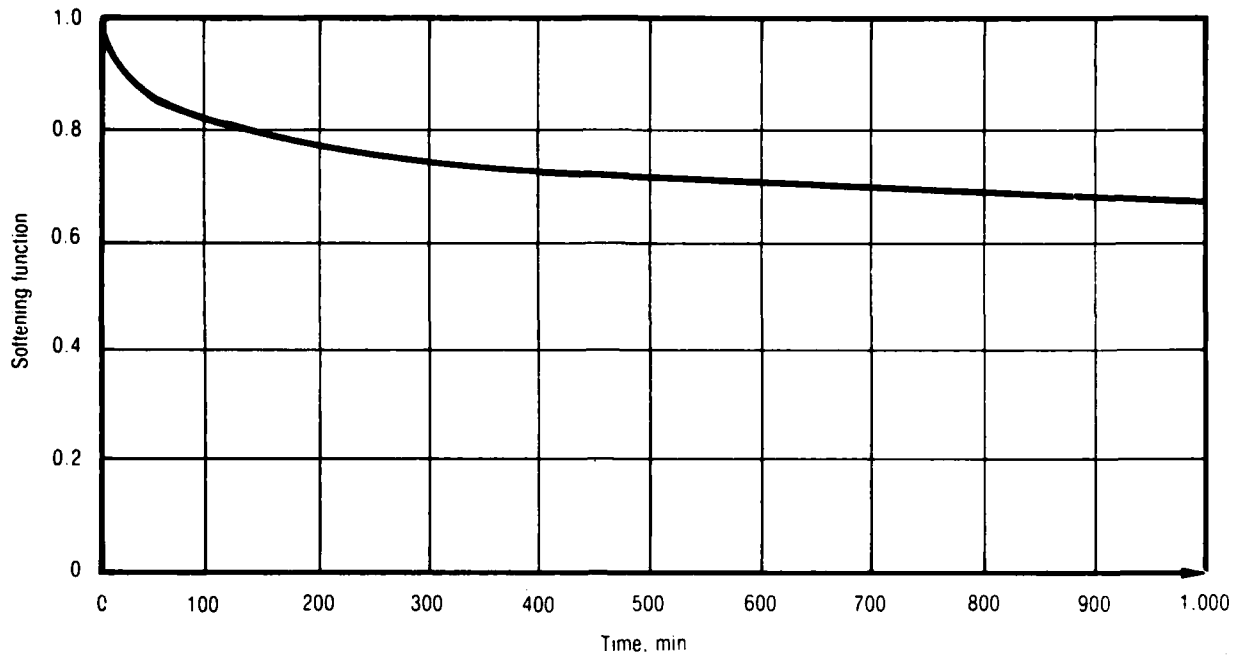


Figure 118. Softening Function During Relaxation

28894

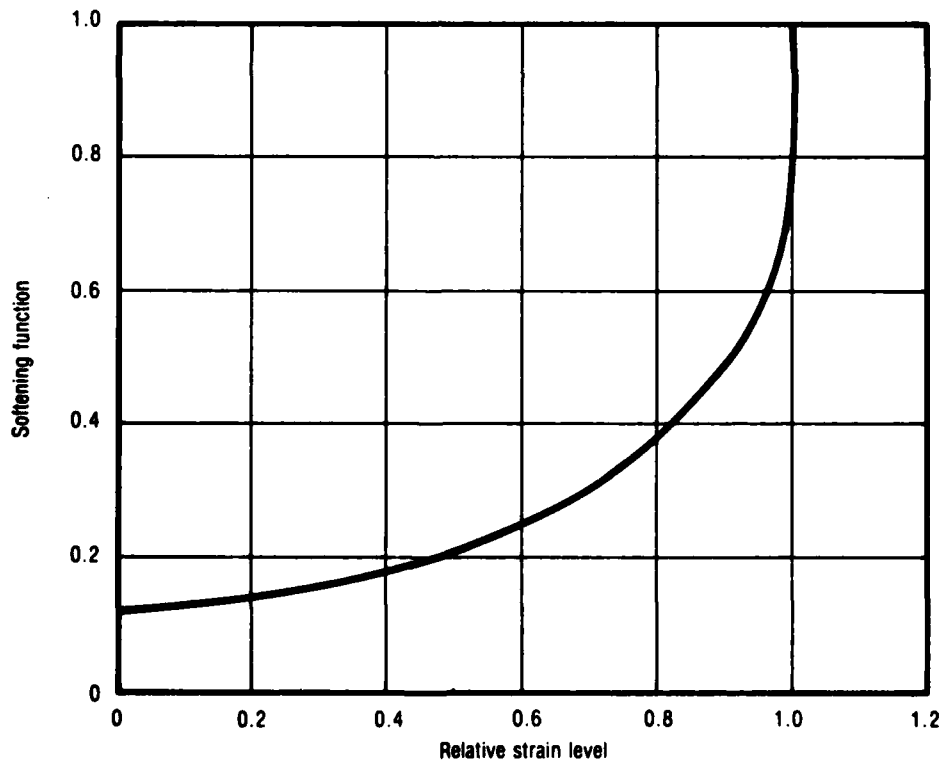


Figure 119. Softening Function During Unloading

28895

4.2.6 The Swanson Nonlinear Constitutive Law

4.2.6.1 Original Model

The framework for this theory was established by taking into account some typical behavior aspects of high-elongation propellants as indicated in Reference 9. The principal features considered were: (1) the usual viscoelastic dependence of the response on the strain rate, (2) the ability of the solid propellant to sustain large strains, (3) the marked deviation of the solid-propellant response from that associated with Linear Viscoelasticity, as evidenced by the large hysteresis exhibited under cyclic loading by many solid propellants, even at small strains, and (4) the dependence of the stress-strain response on superimposed pressure.

Although it is not essential to have done it this way, the capability of handling large strains was incorporated into the constitutive equations by using the cauchy-stress tensor (σ) as a measure of the state of stress at a point. Its conjugate, the left Cauchy-Green deformation tensor (B) was used as the measure of straining. The Cauchy stresses, defined in terms of force per unit deformed area, are also called "true" stresses. In a principal coordinate system, B takes on the diagonal form:

$$B = \begin{bmatrix} \lambda_1^2 & 0 & 0 \\ 0 & \lambda_2^2 & 0 \\ 0 & 0 & \lambda_3^2 \end{bmatrix} \quad (153)$$

in which the λ_1 's are simply the extension ratios in the principal directions.

The remaining aspects of the observed response of solid propellant were modeled through the use of a softening function as a stress correction factor. The major constitutive assumption in this theory relates the second invariants of the deviatoric stress and deformation tensors through the equation:

$$\sqrt{II_{\sigma'}} = (f) (g) \quad (154)$$

This separable form has been used previously (References 11 and 29) and is motivated by the fact that the constant strain rate tensile curves are roughly similar.

In equation (122), f is the following viscoelastic function:

$$f = \int_0^t G(t - \tau) \frac{\partial \sqrt{II_B'}}{\partial \tau} d\tau \quad (155)$$

with G being the relaxation modulus in shear, taken in this theory as one third the tensile relaxation modulus, and:

$$\begin{aligned} g &= \text{softening function} \\ \sigma'_{ij} &= \sigma_{ij} - (\sigma_{kk}/3) \delta_{ij} = \text{deviatoric stress tensor} \\ B'_{ij} &= B_{ij} - (B_{kk}/3) \delta_{ij} = \text{deviatoric deformation tensor} \\ II_\alpha &\equiv \left\{ -[\alpha_{11} \alpha_{22} + \alpha_{22} \alpha_{33} + \alpha_{33} \alpha_{11}] + \alpha_{12}^2 + \alpha_{23}^2 + \alpha_{31}^2 \right\}^{1/2} \end{aligned} \quad (156)$$

Second invariant of tensor $\alpha = \sigma, B$

Now, g is a function of deformation and pressure (mean stress) and can be considered to be primarily a strain-softening function. It is defined as that function of the invariant $\sqrt{II_B'}$ that will force the viscoelastic Cauchy stress to coincide with the experimental results; thus, unloading hysteresis as well as the effects of pressure may be readily incorporated into this theory, simply by obtaining the corresponding forms of the softening function under such conditions.

The softening function corresponding to virgin loading is obtained by fitting the model to uniaxial tensile tests at constant cross-head speed. Under these conditions, the deviatoric stress invariant reduces to:

$$\sqrt{\text{II}_{\sigma'}} = \frac{\sigma_{11}}{\sqrt{3}} \quad (157)$$

where, again σ_{11} is Cauchy stress.

Assuming incompressibility:

$$\lambda_1 \lambda_2 \lambda_3 = 1 \quad (158)$$

and noting that:

$$\lambda_2 = \lambda_3 \quad (159)$$

the deformation invariant becomes

$$\sqrt{\text{II}_{B'}} = \frac{1}{\sqrt{3}} \left(\lambda_1^2 - \frac{1}{\lambda_1} \right) \quad (160)$$

Taking the rate of change of this invariant as being approximately constant results in:

$$\dot{r} = \sqrt{3} \dot{\lambda} \int_0^t G(t - \tau) d\tau \quad (161)$$

so that, from equations (155), (158), and (160), the following is obtained:

$$\frac{\sigma_{11}}{\sqrt{3}} = g \sqrt{3} \dot{\lambda} \int_0^t G(t - \tau) d\tau \quad (162)$$

from which the softening function, g , may be obtained. The assumption leading to equation (160), that the time-rate of change of $\sqrt{\text{II}_{B'}}$ is approximately constant, need be guarded against for conditions of changing strain rate. For example, as in dual-rate tests where viscoelasticity does not predict as fast a response to the rate change as is experimentally observed.

The modification to linear viscoelasticity necessary to accommodate this behavior is as follows. The response of the function f in equation (163) to a constant time rate of change of the deformation invariant is defined as f_c . It can be expressed as:

$$f_c = \sqrt{\dot{II}_{B'}} \int_0^{\xi} G_{rel}(\xi - \tau) d\tau \quad (163)$$

$$\text{where } \xi = \sqrt{II_{B'}} / \sqrt{II_{B'}}$$

The modification to the f function is done in an incremental manner through:

$$\dot{f}_{\text{modified}} = \dot{f} + \beta [f_c - f] \sqrt{\dot{II}_{B'}} \quad (164)$$

and the following incremental relationship is used:

$$f \Big|_{t+dt} = f \Big|_t + \frac{df_{\text{mod}}}{dt} dt \quad (165)$$

The parameter β governs the response of the f function under changing strain rates. As $\beta > 0$, the response is analogous to linear viscoelasticity.

The algorithm developed by Herrman and Peterson (Reference 30) has been used to implement the calculation of the convolution integral for f . In brief, let the shear relaxation modulus be represented by a Prony series as

$$G(t) = \sum_{i=1}^m G_i e^{-\alpha_i t} \quad (166)$$

Then let the f function at time t_n be given by:

$$f(t_n) = \int_0^{t_n} \sum_i G_i e^{-\alpha_i(t_n - \tau)} \frac{\partial \sqrt{II_{B'}}}{\partial \tau} d\tau \quad (167)$$

A recursion relation can be easily developed to compute $f(t_n)$ (Reference 30).

Let

$$f(t_n) = \sum_{i=1}^m I_{n,i} \quad (168)$$

and

$$I_{n,i} \equiv \int_0^{t_n} G_i e^{-\alpha_i(t_n - \tau)} \frac{\partial \sqrt{II B'}}{\partial \tau} d\tau \quad (169)$$

then

$$I_{n,i} = e^{-\alpha_i \Delta t_n} I_{n-1,i} + \sqrt{II B'_n} \frac{G_i}{\alpha_i} \left[1 - e^{-\alpha_i \Delta t_n} \right] \quad (170)$$

giving for the change in these terms

$$\Delta I_{n,i} = \sqrt{II B'_n} \left\{ \frac{G_i}{\alpha_i} \left[1 - e^{-\alpha_i \Delta t_n} \right] + I_{n-1,i} + \left[e^{-\alpha_i t_{n-1}} - 1 \right] \right\} \quad (171)$$

which is directly analogous to linear viscoelasticity. The modification proposed above can then be implemented as

$$(\Delta I_{n,i})_{\text{modified}} = \Delta I_{n,i} + \beta \left[I_{cn,i} - I_{n,i} \right] \Delta \sqrt{II B'} \quad (172)$$

and the I terms can be incremented according to:

$$I_{n,i} = I_{n-1,i} + (\Delta I_{n,i})_{\text{modified}}$$

This has the effect of changing each term of the series so that it approaches the value it would have been if it was always at the new strain rate. Note again that (as discussed in Reference 30) varying temperatures can be incorporated into the time scale as usual.

Unloading tests required a further refinement of the model. For lack of more detailed information, the parameter β may be taken as zero for unloading states (i.e., states in which $\sqrt{II_{B'}}$ is decreasing). The large amount of hysteresis seen in load-unload cycles is then modeled in part by the hysteresis inherent in linear viscoelasticity primarily through the g function. This is accomplished by giving g a different value when the deformation invariant $\sqrt{II_{B'}}$ is less than its maximum previously achieved during the loading history. If $\sqrt{II_{B' \max}}$ is the current maximum value, the function:

$$g = g(\sqrt{II_{B' \max}}) \left\{ 1 - C_1 \left[1 - \sqrt{II_{B'}} / \sqrt{II_{B' \max}} \right] \right\} \quad (174)$$

provides plasticity-like behavior.

The behavior of the g function for unloading and reloading conditions is illustrated in Figure 120 (taken from Reference 9).

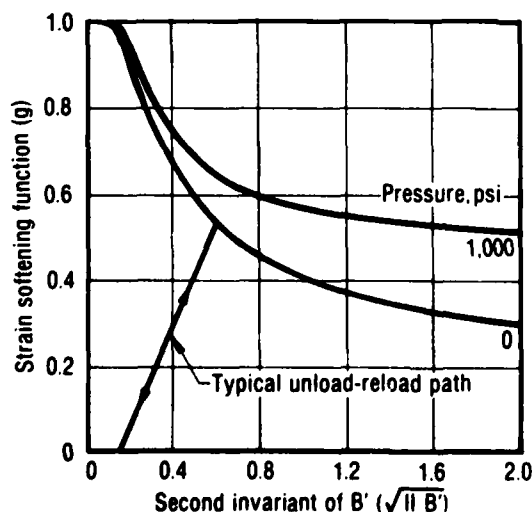


Figure 120. Effect of Deformation and Pressure on the Strain Softening Function 22059

The Swanson approach (Reference 9) was used with an only limited degree of success to predict the stress response of TP-H1011 and UTP-19,360B under several strain histories.

In the case of TP-H1011, the errors in the predictions were believed to be due to uncertainties in the value of the changing-rate coefficient (β). There was no data available to determine β directly for this propellant.

It was possible to characterize UTP-19,360B in a complete fashion. The corresponding predictions were not any better than those obtained for TP-H1011. This led to changing the law as discussed below.

4.2.6.2 Current Model

Analysis of the stress predictions, carried out for UTP-19,360B with the original Swanson theory, revealed the importance of several inadequacies and oversimplifications listed below.

1. The softening function (g) should depend not only on the strain and pressure but also on the strain rate.
2. The softening function, as defined by equations (155) and (163), should be different for unloading than for reloading.
3. The softening function for unloading or for reloading should never become zero for conditions of tensile straining only. A zero value could occur with the softening function defined by equation (174).
4. The healing process observed during relaxation in solid propellants like UTP-19,360B was not taken into consideration by the original Swanson theory.
5. The reverse-recovery observed in solid propellants during relaxation or rest periods that follow an unloading process, only poorly modeled by classical viscoelasticity, is not considered in the approach by Swanson.
6. The changing-rate coefficient (β) is more a mathematical device than it is a material property. If the softening function is made to depend on the strain rate then β need not be used.
7. The use of a softening function as a stress correction factor eliminates the need of using the Cauchy stress (σ) and the nonlinear measure of stretching (B).

All these observations were incorporated into the original stress-strain law but the general form of the corresponding equations remained the same, namely;

AD-A133 364

PROPELLANT NONLINEAR CONSTITUTIVE THEORY EXTENSION:

4/4

PRELIMINARY RESULTS. (U) UNITED TECHNOLOGIES CORP

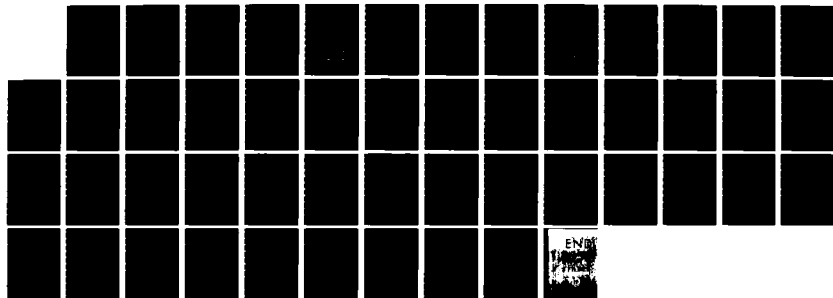
SUNNYVALE CA CHEMICAL SYSTEMS DIV. E C FRANCIS ET AL.

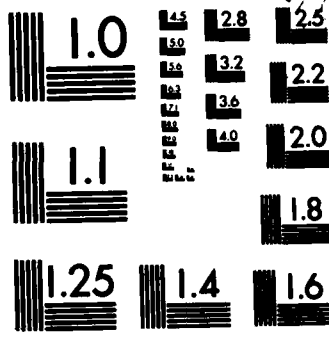
UNCLASSIFIED

AUG 83 UTC/CSD-2742 AFRPL-TR-83-034

F/G 21/9.2

NL





MICROCOPY RESOLUTION TEST CHART
 NATIONAL BUREAU OF STANDARDS-1963-A

$$\sigma_{11} = \sqrt{3} (g) \int_0^t G (s_t - s_\tau) \frac{\partial \sqrt{II_B'}}{\partial \tau} d\tau \quad (175)$$

valid for one-dimensional loading, with:

$$s_t - s_\tau = \int_\tau^t \frac{d\xi}{a_T[\pi(\xi)]} \quad (176)$$

representing temperature-reduced time; and where the time-temperature shift function was taken in the power-law form:

$$a_T = \left(\frac{T_R - T_a}{T - T_a} \right)^m \quad (177)$$

in which T_R is the shift reference temperature, T_a and m are material parameters, and T is the current temperature.

The modified version of the Swanson theory was most successfully used to predict the response of UTP-19,360B, as explained next.

4.2.6.3 Stress Predictions

The degree of accuracy of the predictions made with the current version of the Swanson approach may be realized by examining Figures 121 through 130. The first two figures correspond to the lowest and highest constant-rate tests available. Figure 123 shows the predictions corresponding to a saw-tooth test at constant rate and increasing peak strains. Figures 124 and 125 present the results for the dual-rate tests while Figures 126 and 128 pertain to the long- and short-duration similitude tests, respectively. Figure 127 shows the three-step relaxation test. Finally, Figures 129 and 130 show the results obtained for constant rate tests at 123°F and 40°F.

(Text continued on page 285.)

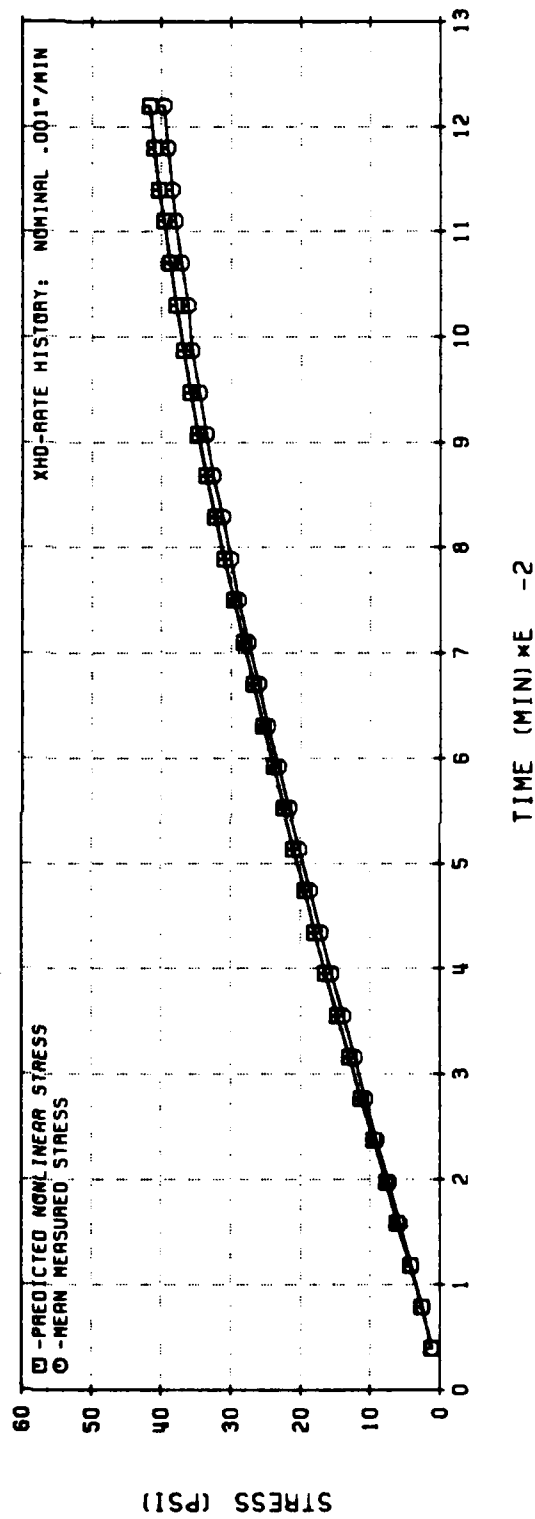
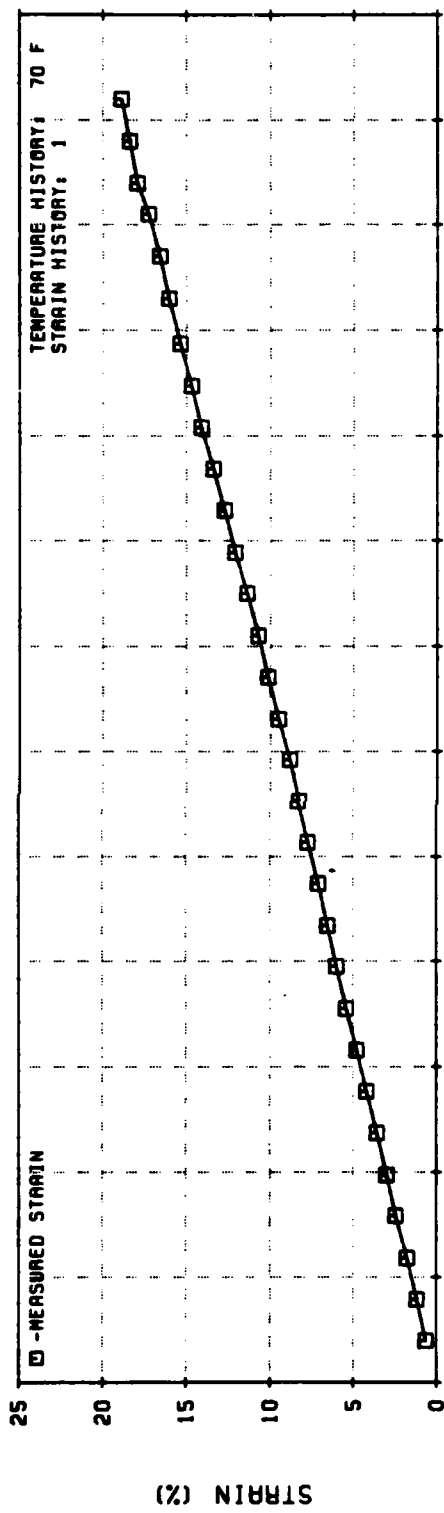


Figure 121. Nonlinear Viscoelastic Stress Predictions for Constant-Rate Test
(UTP-19, 360B-400/1777)

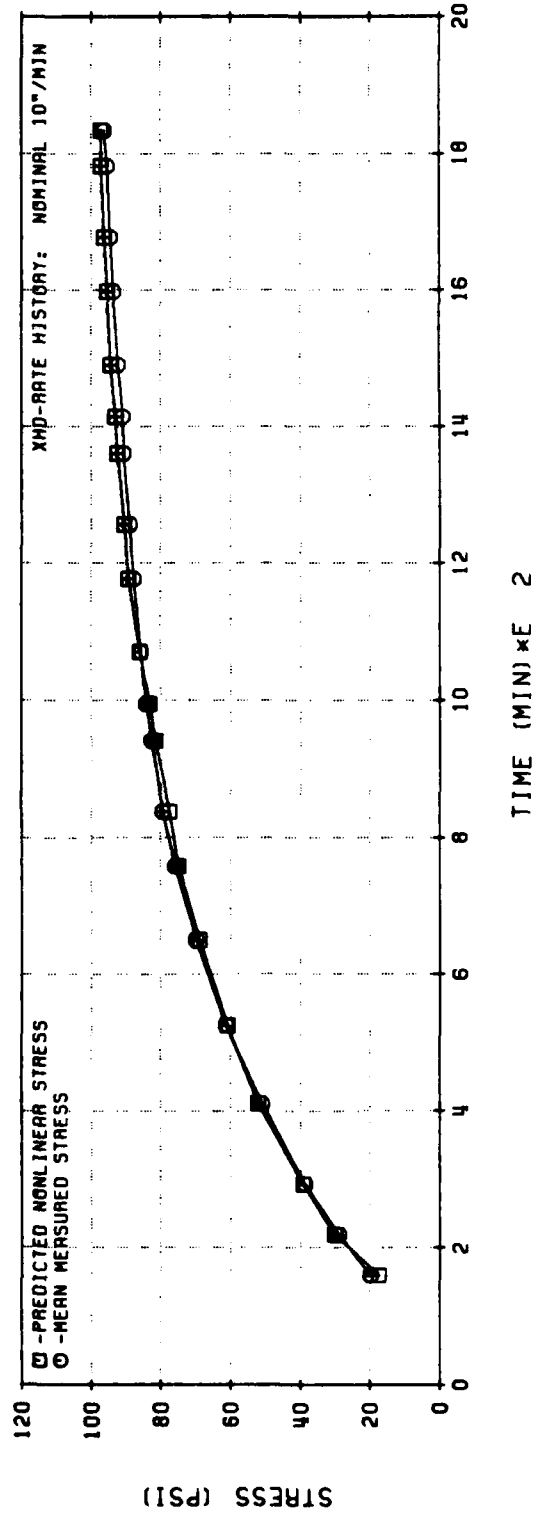
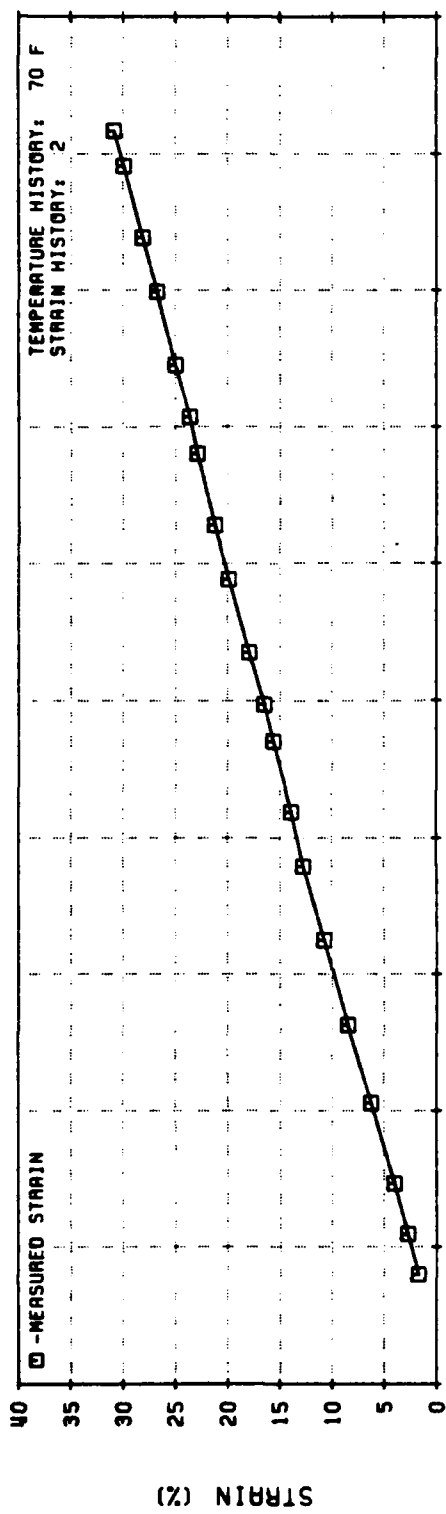


Figure 122. Nonlinear Viscoelastic Stress Predictions for Constant-Rate Test (UTP-19, 360B-400/1777)

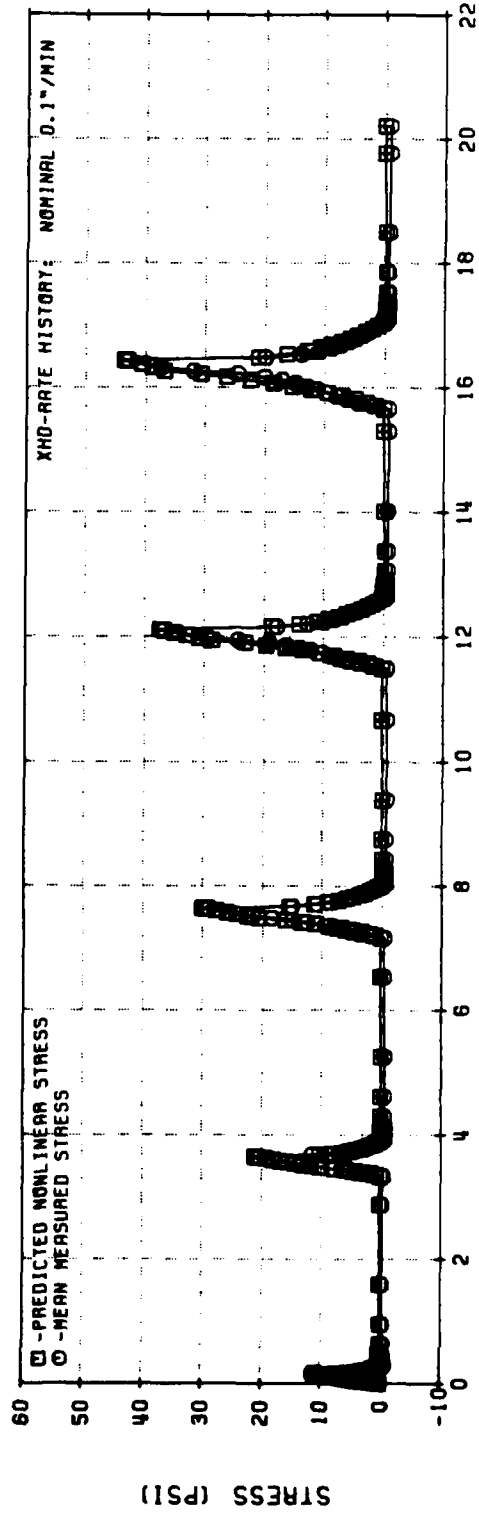
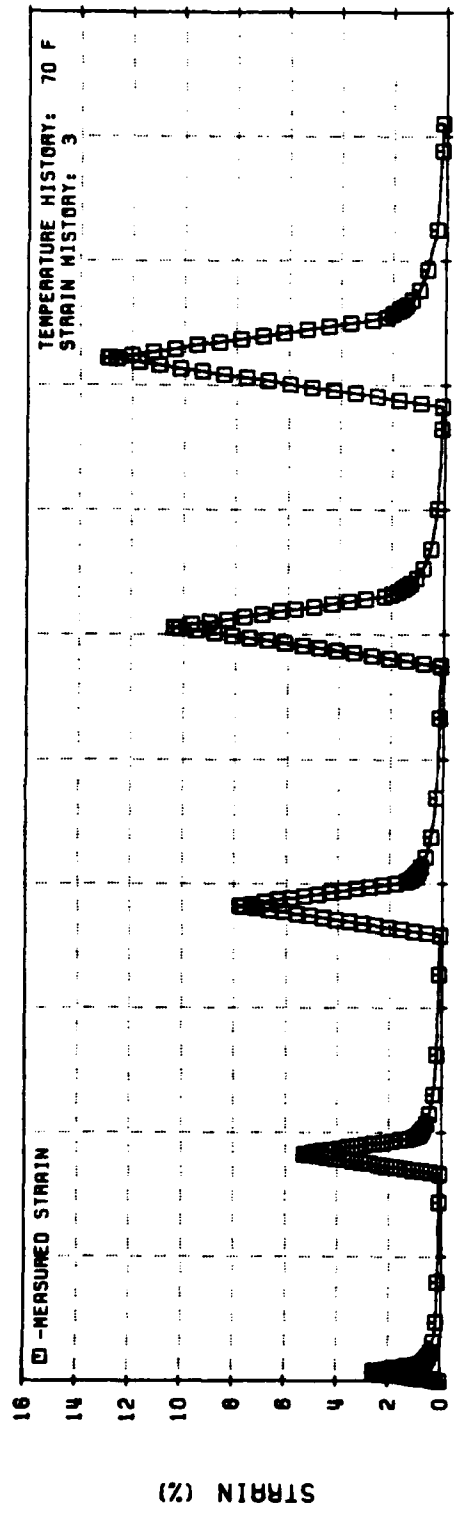


Figure 123. Nonlinear Viscoelastic Stress Predictions for Saw-Tooth Test
(UTP-19,360B-400/1777)

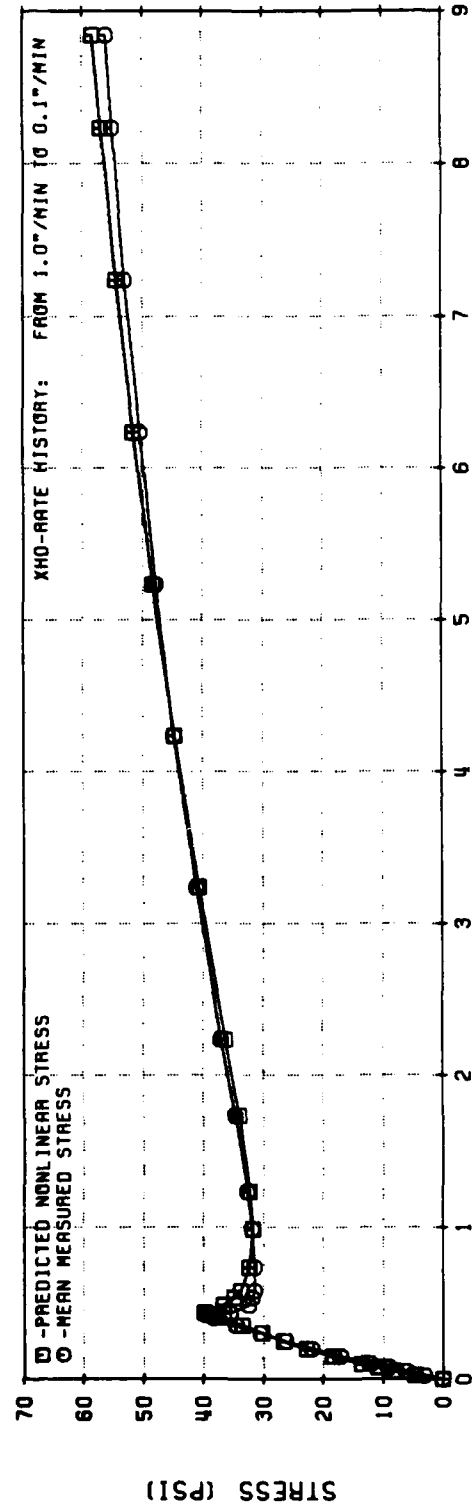
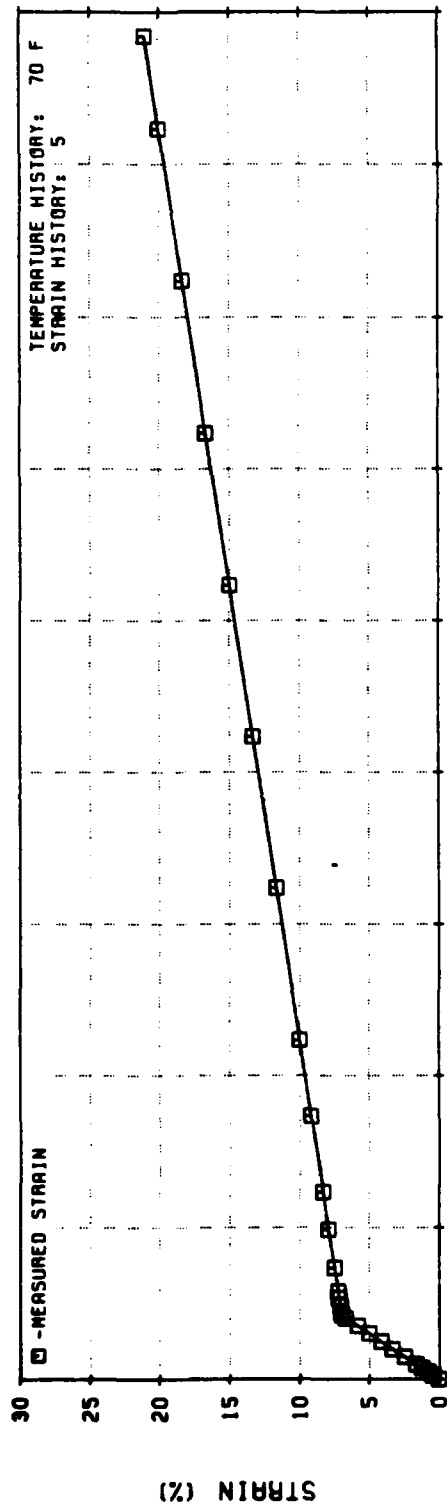


Figure 124. Nonlinear Viscoelastic Stress Predictions for Two-Rate Test
(UTP-19, 360B-400/1777)

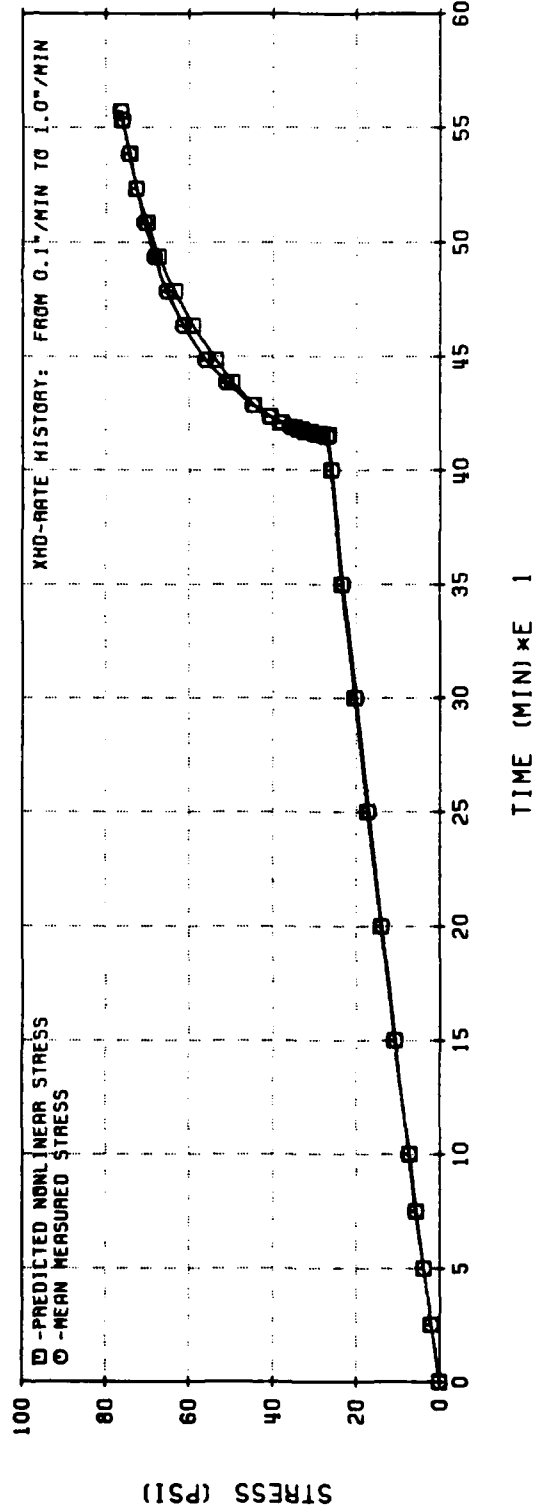
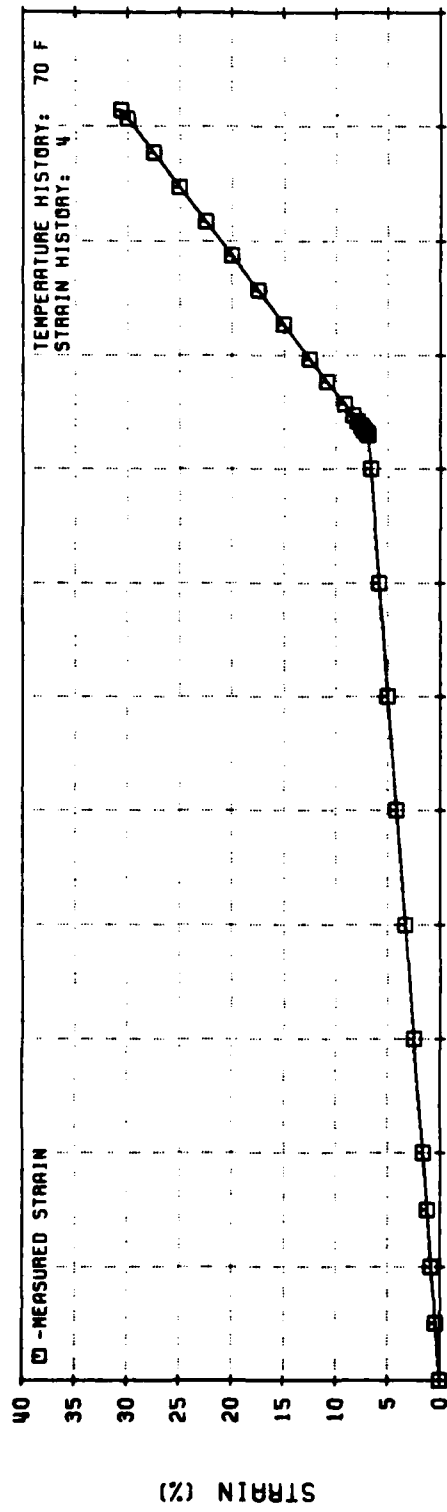


Figure 125. Nonlinear Viscoelastic Stress Predictions for Two-Rate Test
(UTP-19, 360B-400/1777)

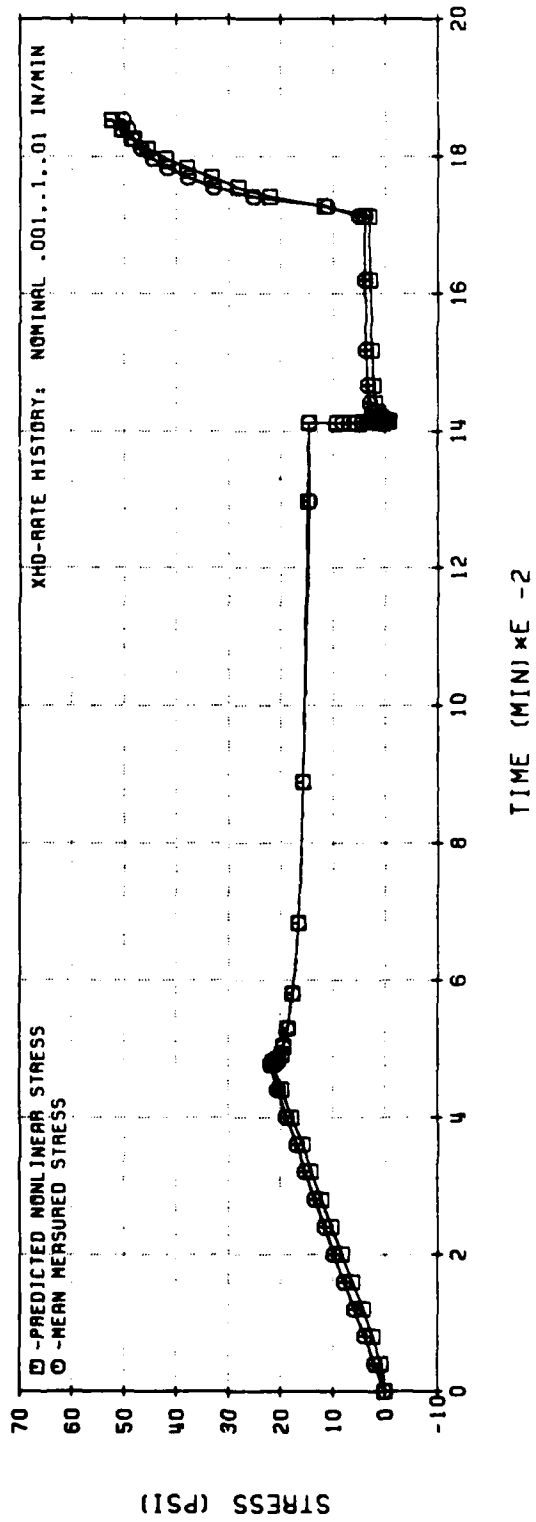
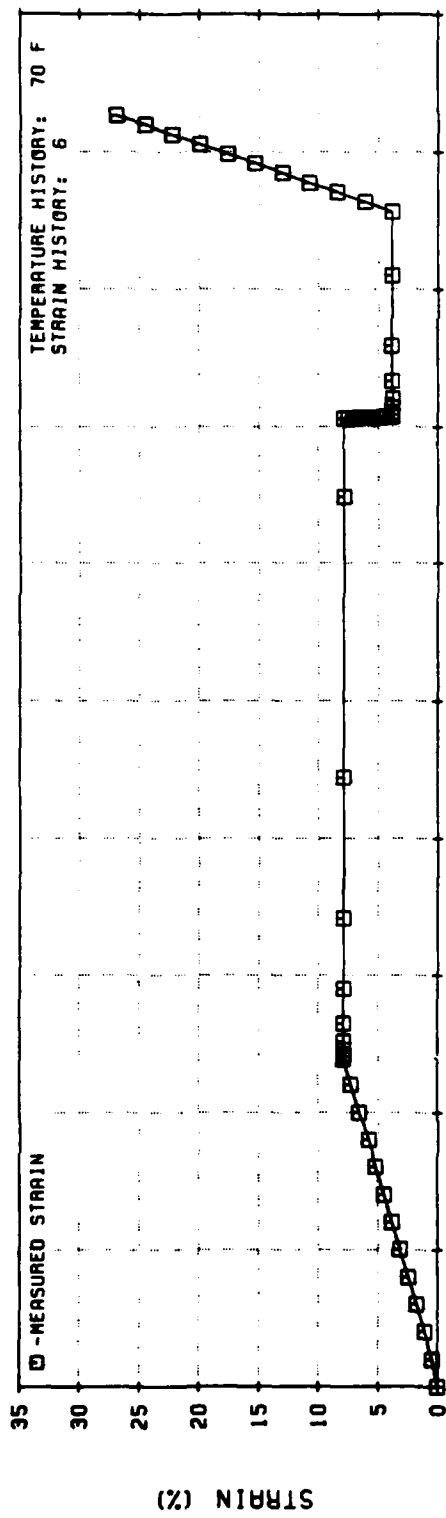


Figure 126. Nonlinear Viscoelastic Stress Predictions for Long Similitude Test (UTP-19, 360B-400/1777)

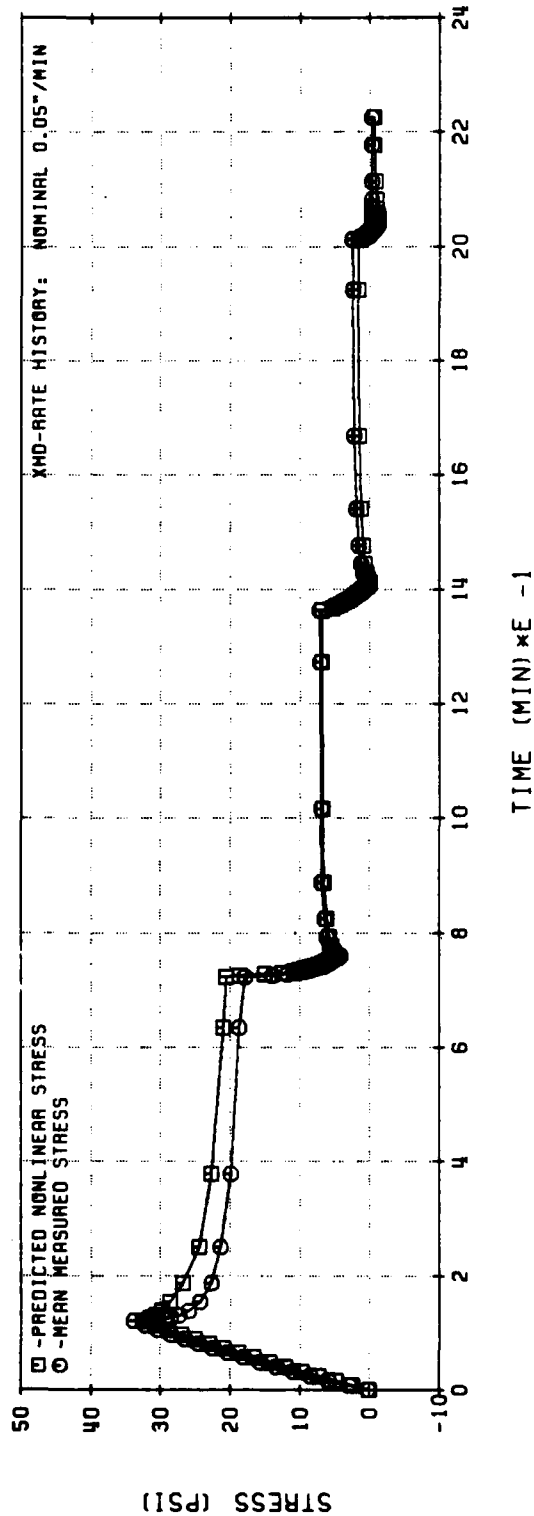
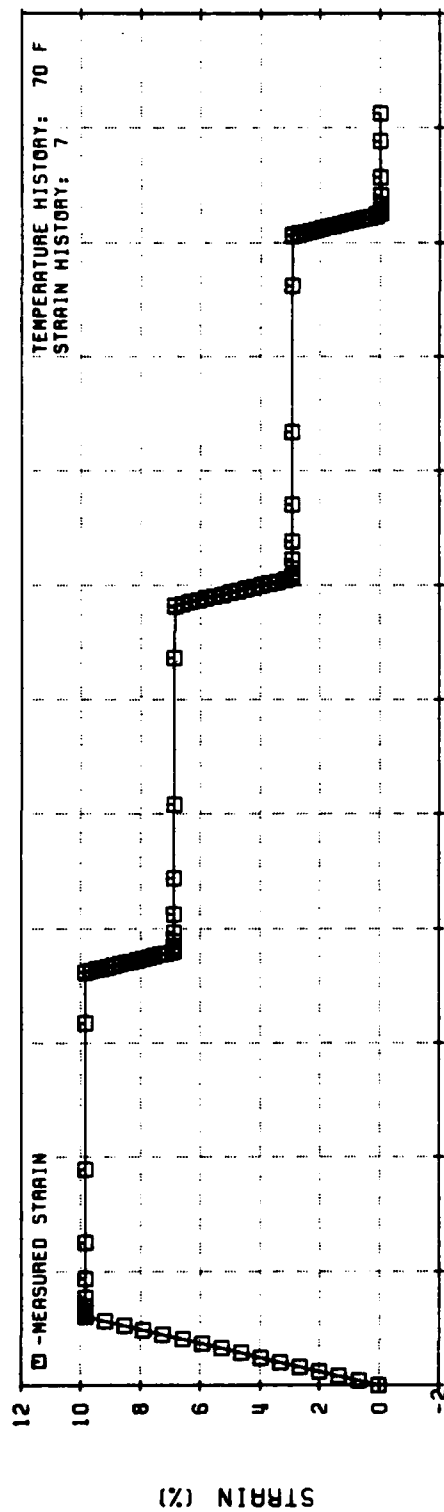


Figure 127. Nonlinear Viscoelastic Stress Predictions for 3-Step Relaxation (UTP-19, 360B-400/1777)

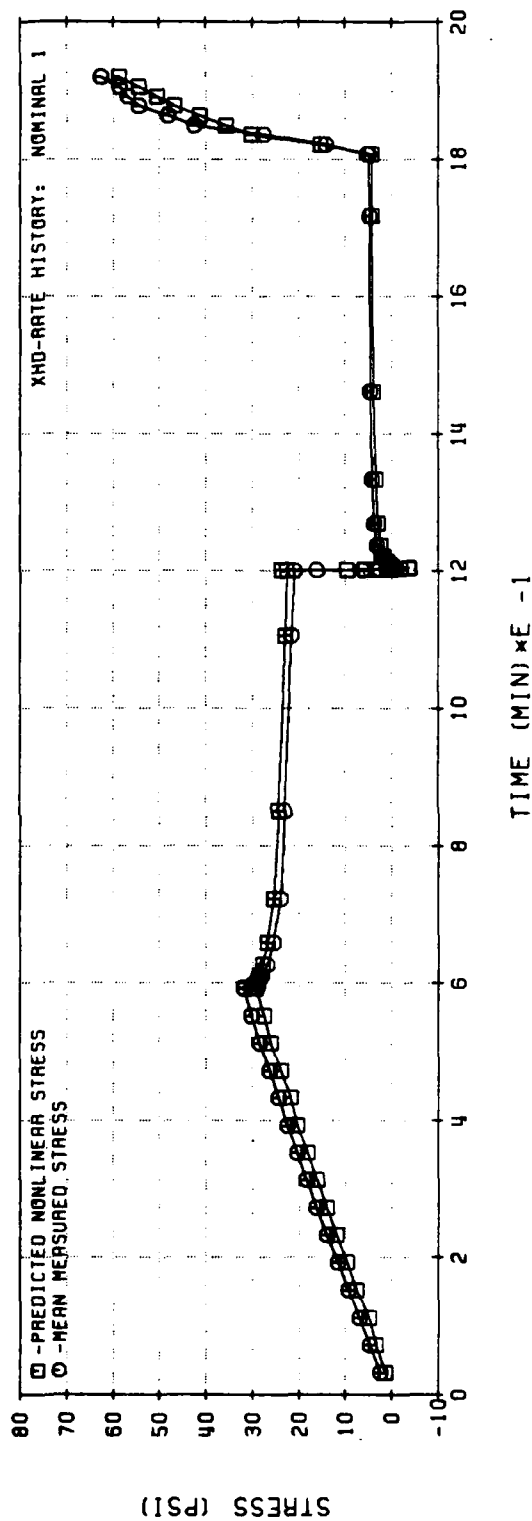
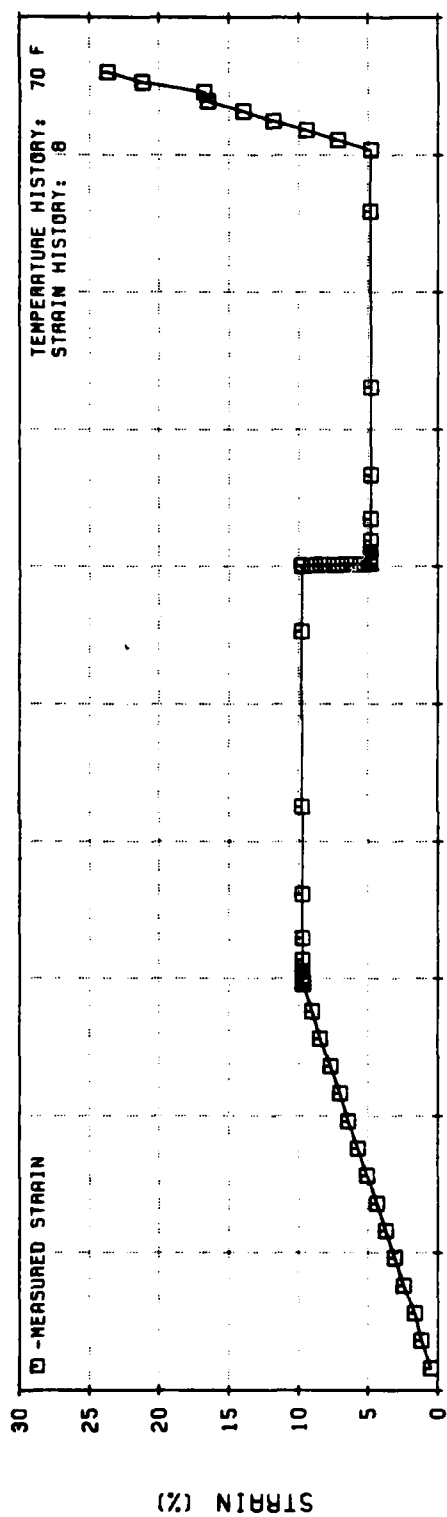


Figure 128. Nonlinear Viscoelastic Stress Predictions for Short Similitude Test
(UTP-19, 360B-400/1777)

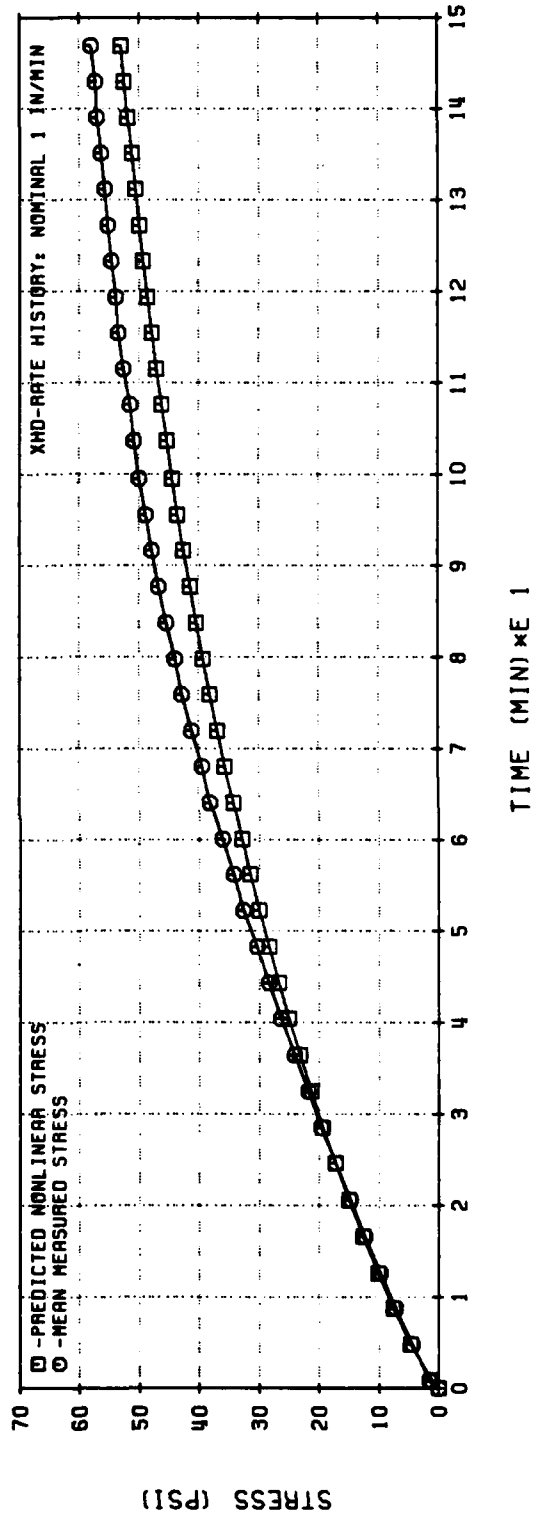
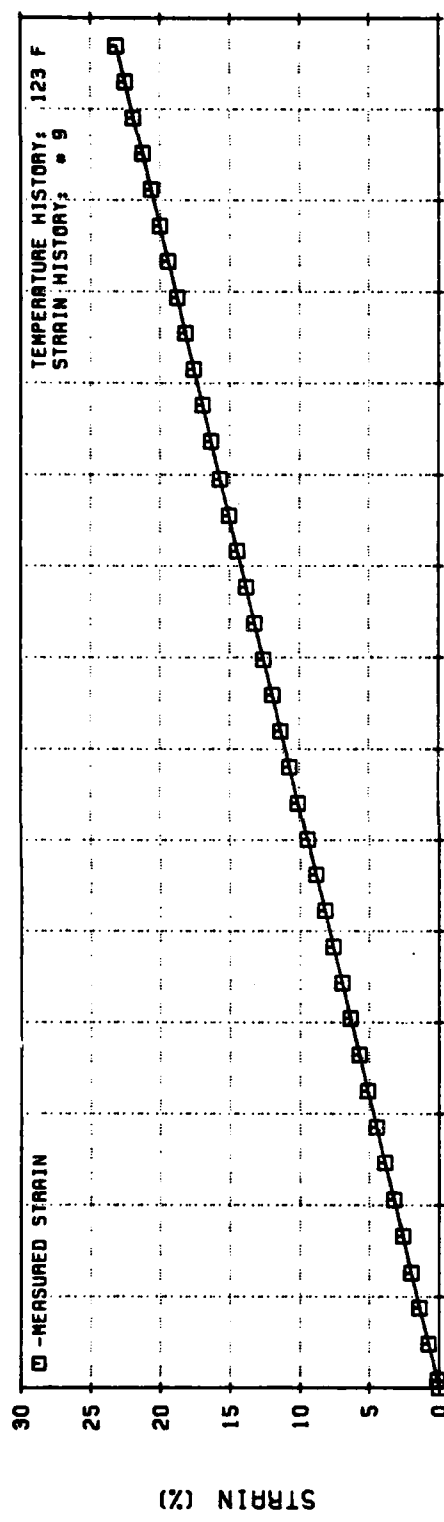


Figure 129. Nonlinear Viscoelastic Stress Predictions for UTP-19,360B-400/1777 at 123 F

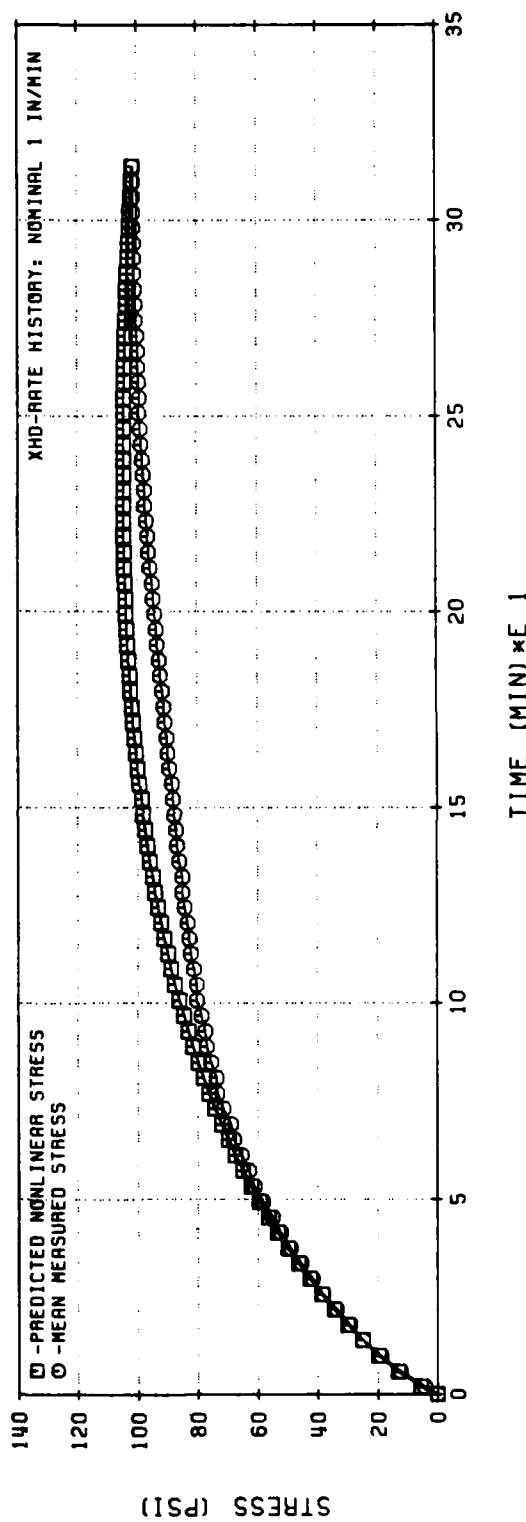
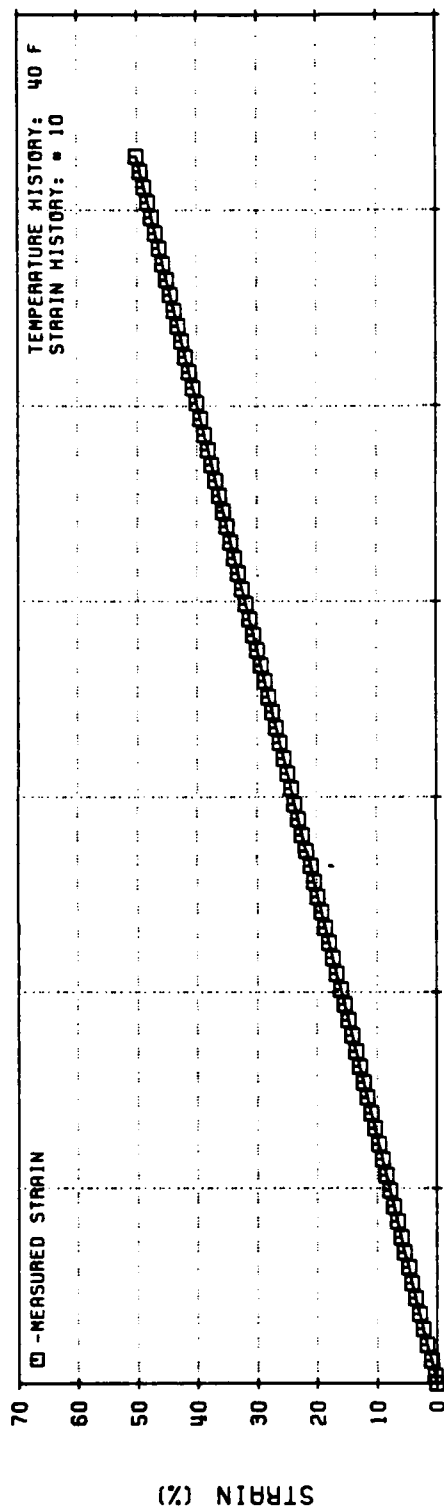


Figure 130. Nonlinear Viscoelastic Stress Predictions for UTP-19, 360B-400/1777 at 40 F

They testify to the fact that the time-temperature superimposition principal may be used without sacrificing more accuracy than is already lost in fitting equation (143) to the very limited time-temperature shift data.

4.2.6.4 Material Characterization

According to this theory, only the following listed properties are needed to characterize a solid propellant completely:

1. The relaxation function, G , defined as:

$$G(t) = \frac{E_{rel}(t)}{3} \quad (178)$$

where $E_{rel}(t)$ is the linear viscoelastic relaxation modulus.

2. The softening function, g , defined and obtained as follows:

- a. For loading conditions:

$$g_L = g(\epsilon, \dot{\epsilon}) \quad (179)$$

and it is obtained from a sequence of constant-rate tests at at least three different rates that span the range expected in the applications.

- b. For unloading conditions:

$$g_u = g(\epsilon/\epsilon_{max}) \quad (180)$$

where ϵ_{max} represents the maximum strain previously achieved during the loading history. The g is determined from the unloading portion of a loading-unloading cycle carried up to an intermediate strain level.

c. For relaxation conditions:

$$\epsilon_r = g_r (t - t_0) \quad (181)$$

in which t_0 is the time at which the relaxation process begins and g is evaluated from a relaxation test at an intermediate strain level.

In addition, for relaxation after partial unloading or during rest periods starting at $t = t_0$:

$$\hat{\epsilon}_r = \frac{1}{g_r (t - t_0)} \quad (182)$$

Also, the stress-correction function for reloading is taken as a linear function of the relative strain. It is a straight line from the point where reloading starts to the point of maximum loading over the past history.

4.2.6.5 Addendum to Swanson Theory

Three-Dimensional Version of the Model

The (general) constitutive assumption used to relate the deviatoric components of the stress and deformation tensors, takes the following form:

$$\frac{\sigma'_{ij}}{\sqrt{II_{\sigma'}}} = \frac{B'_{ij}}{\sqrt{II_{B'}}}; \quad i, j = 1, 2, 3 \quad (183)$$

together with:

$$\sqrt{II_{\sigma'}} = (g) (f) \quad (184)$$

or, equivalently:

$$\sqrt{II_{\sigma}'} = (g) \int_0^t G(t - \tau) \frac{\partial \sqrt{II_B'}}{\partial \tau} d\tau \quad (185)$$

where:

σ'_{ij} = i-j component of the deviatoric Cauchy stress tensor
 B'_{ij} = i-j component of the deviatoric Left Cauchy-Green deformation tensor
 II_{σ}' , II_B' = second invariants of the deviatoric stress and deformation tensors

with:

$$\sigma'_{ij} = \sigma_{ij} + \frac{1}{3} (\sigma_{11} + \sigma_{22} + \sigma_{33}) \delta_{ij}; \quad i, j = 1, 2, 3 \quad (186)$$

$$II_{\sigma}' = \text{def} \left\{ -[\sigma'_{11} \sigma'_{22} + \sigma'_{11} \sigma'_{33} + \sigma'_{22} \sigma'_{33}] + (\sigma'_{12})^2 + (\sigma'_{13})^2 + (\sigma'_{23})^2 \right\} \quad (187)$$

and similarly for B'_{ij} and II_B' ; and in which:

$$\delta_{ij} = \text{def} \begin{cases} 1 & \text{for } i = j \\ 0 & \text{for } i \neq j \end{cases} \quad (188)$$

also:

g = softening function that depends primarily on the strain level, the strain rate, and the applied pressure.

and:

$$G(t) = \text{def} E(t)/3 \quad (189)$$

where $E(t)$ represents the tensile relaxation modulus at a small strain.

According to the constitutive assumptions (183) and (185), the distortional behavior of the material is completely characterized through the softening function, g , and the relaxation function, G , which may be evaluated from one-dimensional tests, as explained in the previous section. Indeed, the stress-strain relations set forth in equation, (183) and (185), reduce, as they should, to those employed in the one-dimensional version of the model.

To complete the theory, an assumption is still needed about volumetric behavior; and although time-dependent bulk response may be important in some applications, the elastic relation:

$$\frac{1}{3} (\sigma_{11} + \sigma_{22} + \sigma_{33}) = K (|\lambda_1 \lambda_2 \lambda_3| - 1) \quad (190)$$

may be employed; in which K is the bulk modulus and the λ_i 's are the stretch ratios.

For an incompressible material (and solid propellants are nearly incompressible):

$$\lambda_1 \lambda_2 \lambda_3 = 1 \quad (191)$$

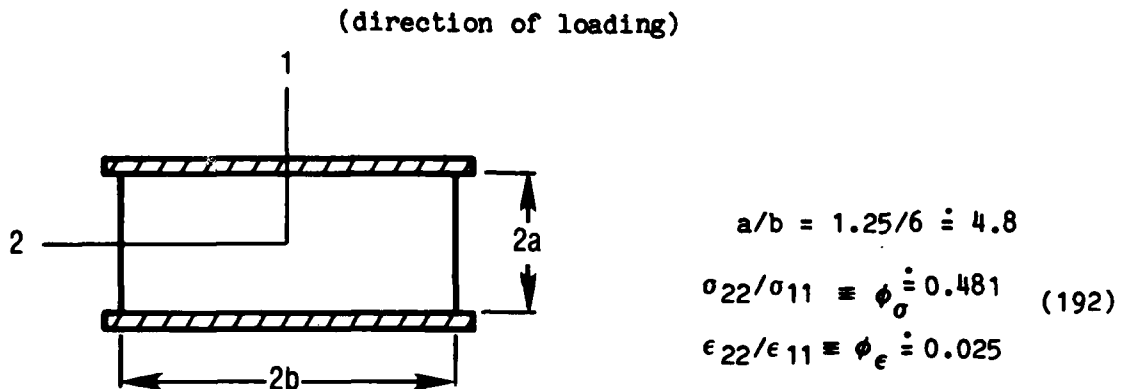
so that equation (190) breaks down, and the stress tensor has to be considered a function of the mean pressure $(\sigma_{11} + \sigma_{22} + \sigma_{33})/3$, as well as of the deformation tensor, leading eventually, to a stress-strain law of the form given in equation (183).

Application of the Model to Two-Dimensional Problems

In order to use the stress-strain law presented in the foregoing section, one must have available the deformation tensor at each point of the continuum where the stresses are desired. This solution in terms of deformation may be arrived at numerically through, say, finite elements, or, analytically.

The accuracy with which the present constitutive theory may predict the two-dimensional response of solid propellants may be seen in Figures 131 to

136, which correspond to constant strain-rate tests of strip-biaxial samples of UTP-19,360B. The first three figures belong to tests performed at a nominal crosshead displacement rate of 0.02 in./min. at 40°F, 70°F, and 120°F, respectively; while Figures 134 to 136 show the results for a crosshead displacement rate of 0.2 in./min. at the same low, intermediate and high temperatures of 40°, 70°, and 120°F. The plotted data refer to the direction of applied loading, which is also the direction of maximum principal stress (and strain). The geometry of the strip-biaxial sample used is as presented in the following sketch.



The stress- and strain-axiality factors, ϕ_{σ} and ϕ_{ϵ} , were taken from Reference (31), and are valid at the center of the sample for small strains only.

The constitutive relations given in (183) and (185) yield:

$$\sigma'_{ij} = (g) \frac{B'_{ij}}{\sqrt{II_{B'}}} \int_0^t G(t - \tau) \frac{\partial \sqrt{II_{B'}}}{\partial \tau} d\tau \quad (193)$$

where:

$$\frac{\partial \sqrt{II_{B'}}}{\partial t} = \frac{\partial \sqrt{II_{B'}}}{\partial B'_{ij}} \frac{\partial B'_{ij}}{\partial t}; \quad i, j = 1, 2, 3 \quad (194)$$

with summation implied over repeated indices.

Now, under conditions of plane stress of an incompressible material, and along the principal directions, one has:

$$[\sigma'_{ij}] = \frac{1}{3} \begin{bmatrix} (2\sigma_1 - \sigma_2) & 0 & 0 \\ 0 & (2\sigma_2 - \sigma_1) & 0 \\ 0 & 0 & -(\sigma_1 + \sigma_2) \end{bmatrix} \quad (195)$$

$$[B'_{ij}] = \frac{1}{3} \begin{bmatrix} (2\lambda_1^2 - \lambda_2^2 - \lambda_3^2) & 0 & 0 \\ 0 & (2\lambda_2^2 - \lambda_3^2 - \lambda_1^2) & 0 \\ 0 & 0 & (2\lambda_3^2 - \lambda_1^2 - \lambda_2^2) \end{bmatrix} \quad (196)$$

$$II B' = -B'_{11} B'_{22} - B'_{11} B'_{33} - B'_{22} B'_{33} \quad (197)$$

To evaluate (194), we first write it in unabridged notation, noting that in this case, if $i \neq j$ then $B'_{ij} = 0$; thus:

$$\frac{\partial \sqrt{II B'}}{\partial t} = \frac{\partial \sqrt{II B'}}{\partial B'_{11}} \frac{\partial B'_{11}}{\partial t} + \frac{\partial \sqrt{II B'}}{\partial B'_{22}} \frac{\partial B'_{22}}{\partial t} + \frac{\partial \sqrt{II B'}}{\partial B'_{33}} \frac{\partial B'_{33}}{\partial t} \quad (198)$$

and using (197):

$$\frac{\partial \sqrt{II B'}}{\partial t} = \frac{1}{2\sqrt{II B'}} \left[(-B'_{22} + B'_{33}) \frac{\partial B'_{11}}{\partial t} + (-B'_{33} - B'_{11}) \frac{\partial B'_{22}}{\partial t} + (-B'_{11} - B'_{22}) \frac{\partial B'_{33}}{\partial t} \right] \quad (199)$$

where, from (196) one has, for instance, that:

$$\frac{\partial B'_{11}}{\partial t} = \frac{2}{3} \left(2\lambda_1 \frac{d\lambda_1}{dt} - \lambda_2 \frac{d\lambda_2}{dt} - \lambda_3 \frac{d\lambda_3}{dt} \right) \quad (200)$$

and similarly for the derivatives of B'_{22} and B'_{33} .

In the previous derivations, the stretch ratios are computed as:

$$\begin{aligned} \lambda_1 &= 1 + \epsilon_1(t) \\ \lambda_2 &= 1 + \epsilon_2(t) \doteq 1 + \phi_e \epsilon_1(t) \\ \lambda_3 &= 1/(\lambda_1 \lambda_2) \end{aligned} \quad (201)$$

in which $\epsilon_1(t)$ is the strain history imposed on the sample along coordinate 1, and the last expression of (201) follows from the incompressibility condition, equation (191).

Hence, the first component-equation of the constitutive relation (193) yields:

$$\sigma'_{11} = \frac{1}{3} (2\sigma_1 - \sigma_2) = (g) \frac{B'_{11}}{\sqrt{II_{B'}}} \int_0^t G(t - \tau) \frac{\partial \sqrt{II_{B'}}}{\partial \tau} d\tau$$

or, in view of (192):

$$\sigma_1 \frac{(2 - \phi_\sigma)}{3} = (g) \frac{B'_{11}}{\sqrt{II_{B'}}} \int_0^t G(t - \tau) \frac{\partial \sqrt{II_{B'}}}{\partial \tau} d\tau$$

and finally:

$$\sigma_1 = \frac{3}{(2 - \phi_\sigma)} (g) \frac{B'_{11}}{\sqrt{II_{B'}}} \int_0^t G(t - \tau) \frac{\partial \sqrt{II_{B'}}}{\partial \tau} d\tau$$

(202)

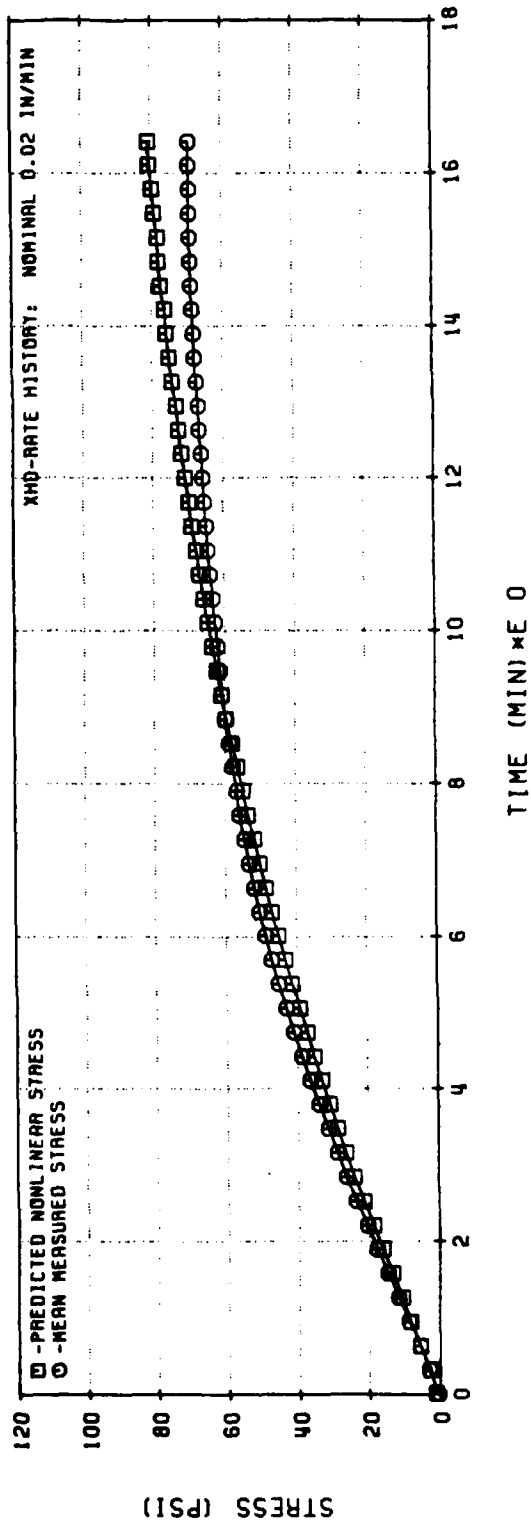
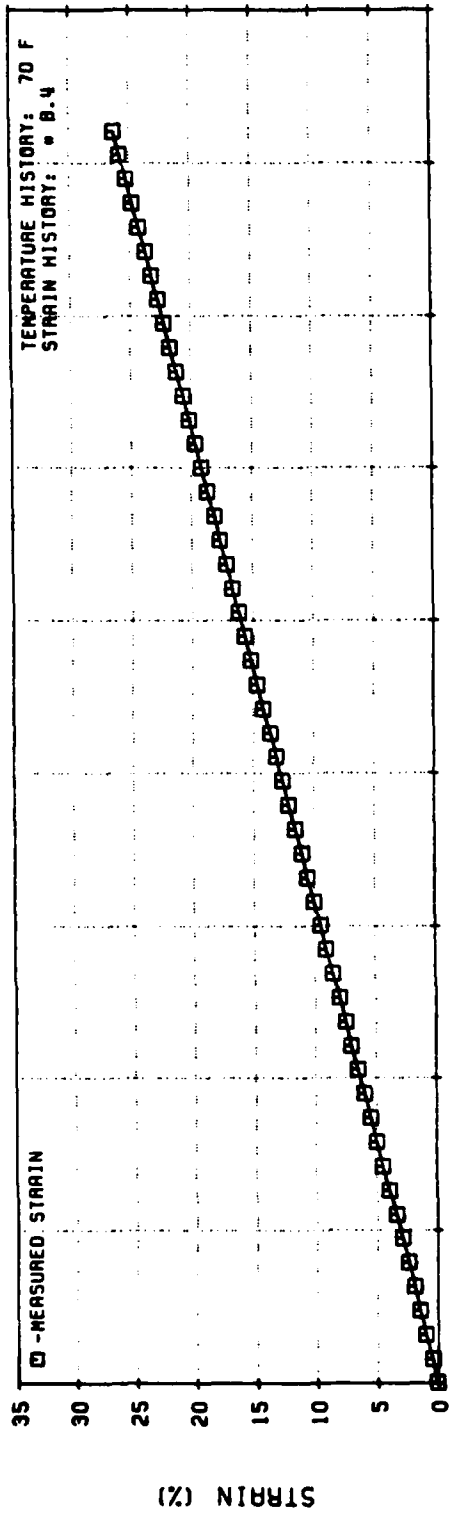


Figure 131. Nonlinear Viscoelastic Stress Predictions for UTP-19, 360B-400/1777 (Biaxial Sample) Hercules Theory

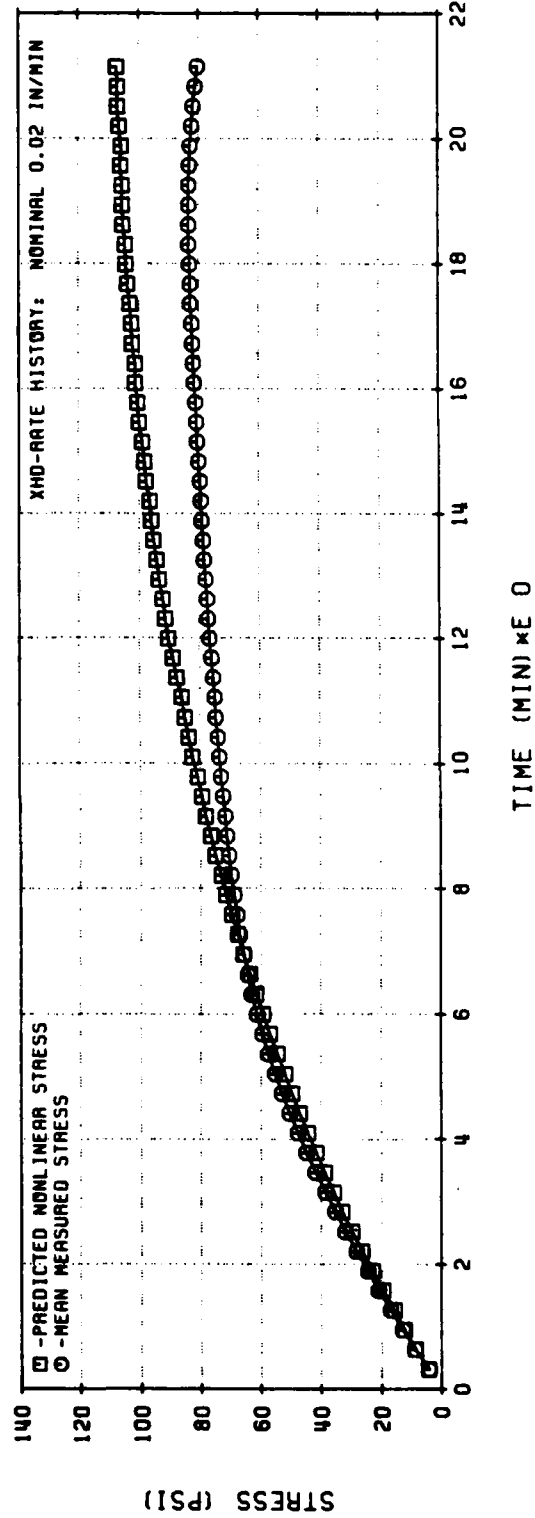
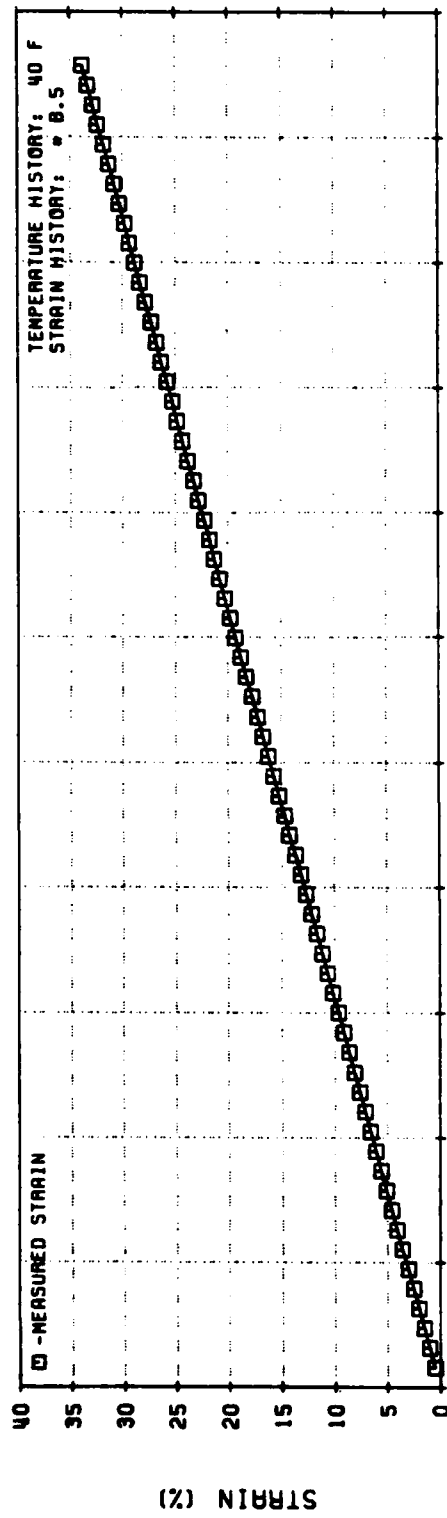


Figure 132. Nonlinear Viscoelastic Stress Predictions for UTP-19, 360B-400/1777 (Biaxial Sample) Hercules Theory

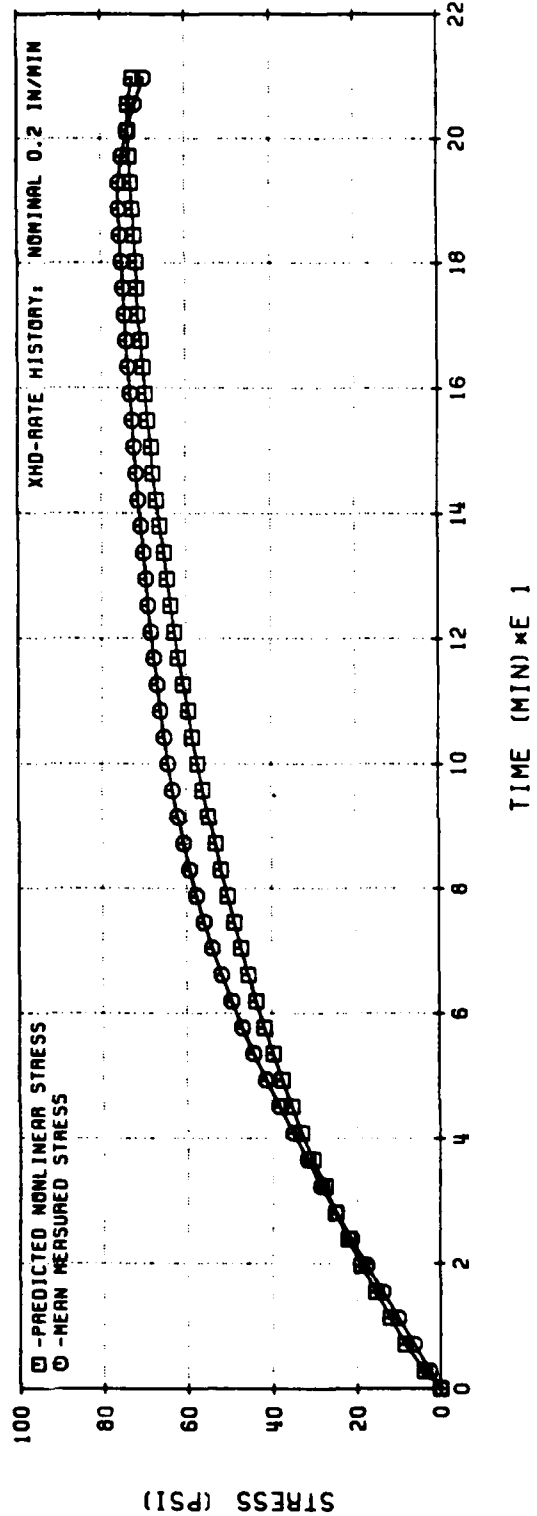
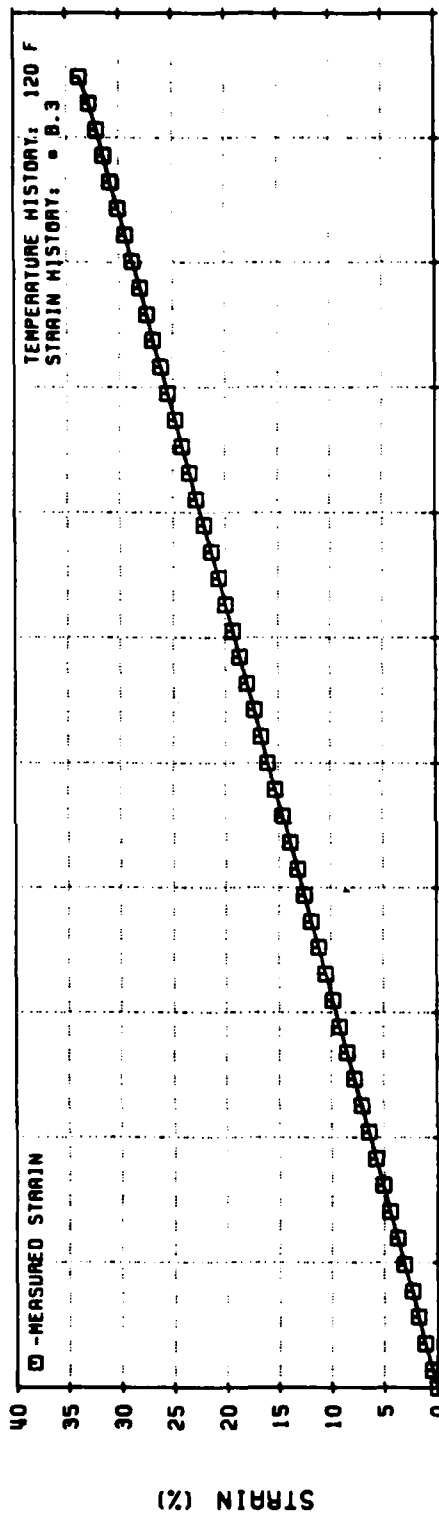


Figure 133. Nonlinear Viscoelastic Stress Predictions for UTP-19, 360B-400/1777 (Biaxial Sample) Hercules Theory

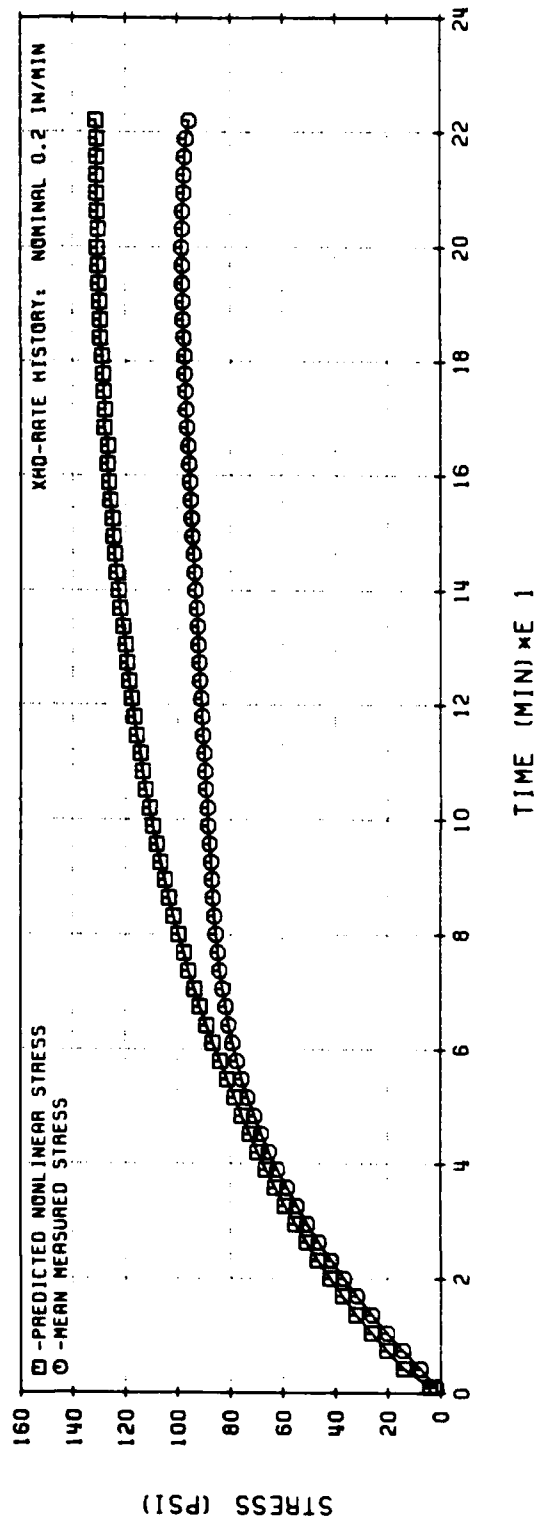
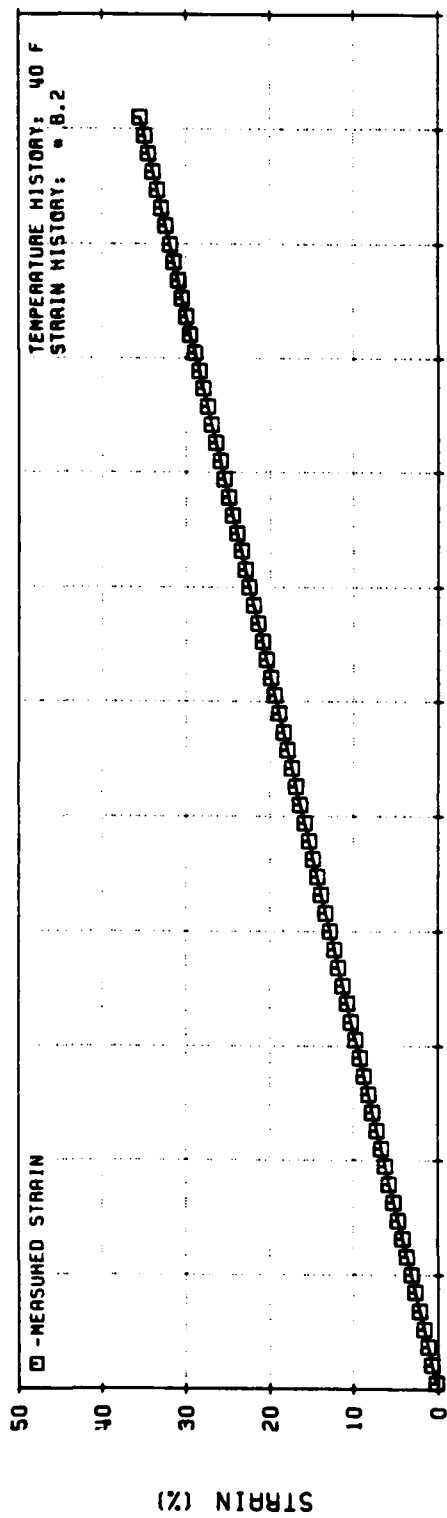


Figure 134. Nonlinear Viscoelastic Stress Predictions for UTP-19,360B-400/1777
(Biaxial Sample) Hercules Theory

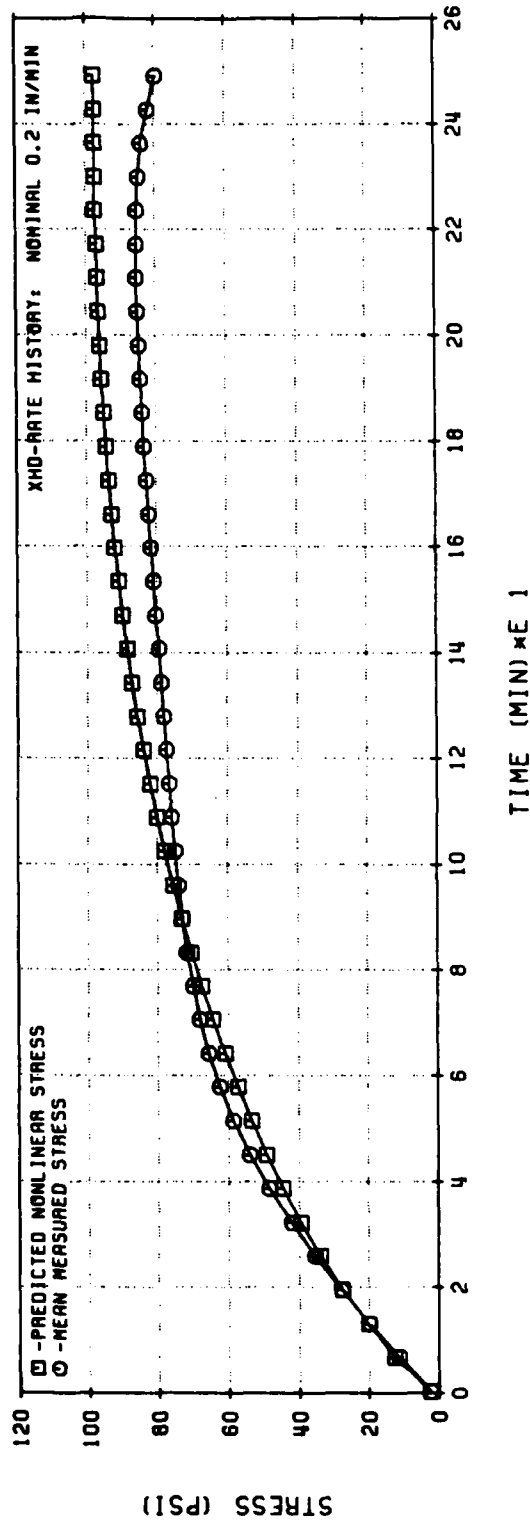
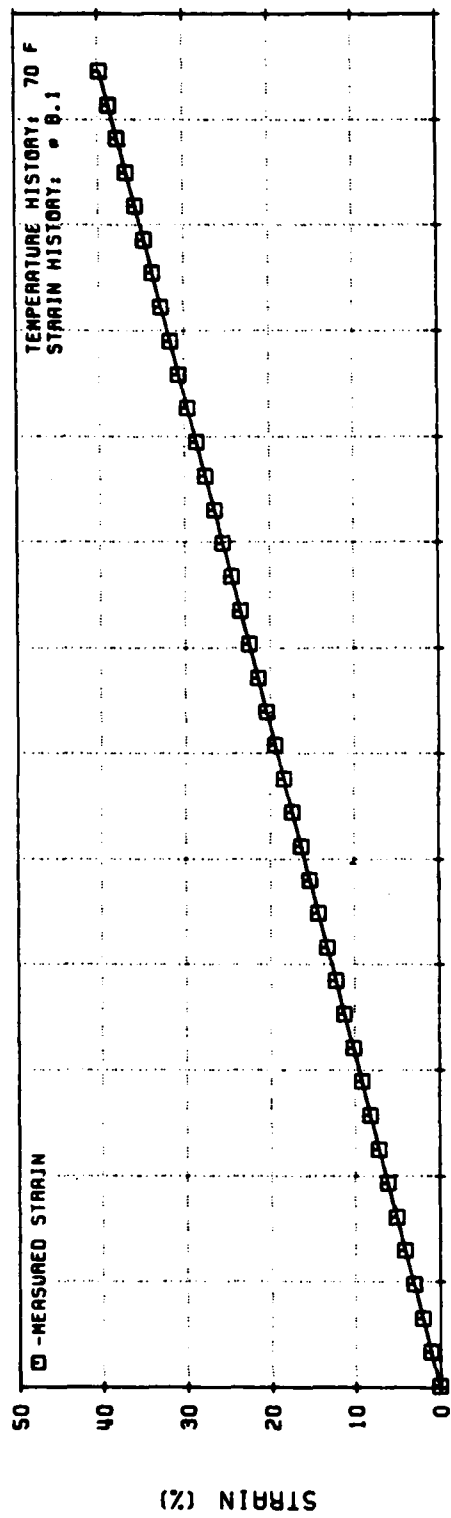


Figure 135. Nonlinear Viscoelastic Stress Predictions for UTP-19,360B-400/1777 (Biaxial Sample) Hercules Theory

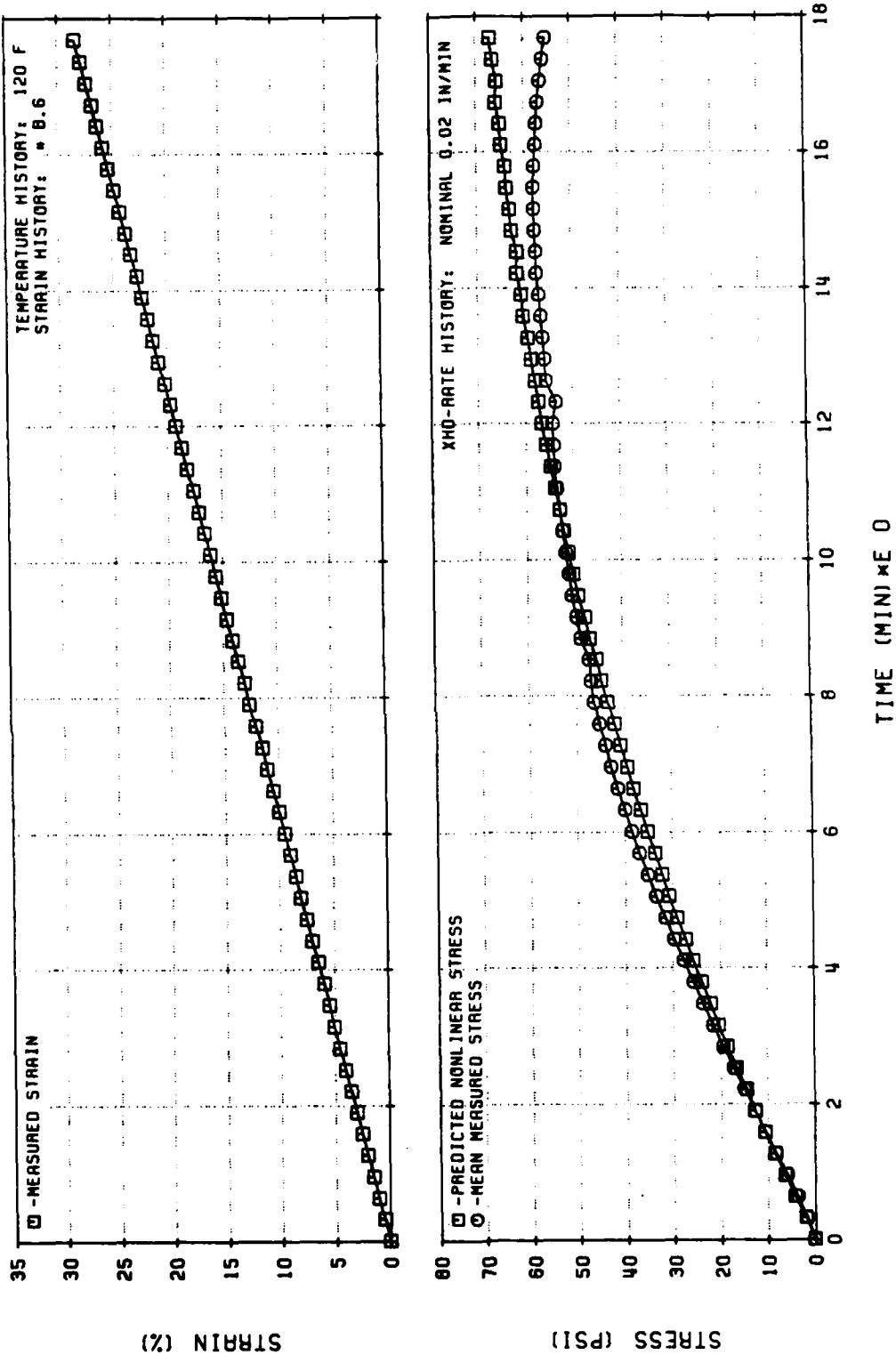


Figure 136. Nonlinear Viscoelastic Stress Predictions for UTP-19, 360B-400/1777 (Biaxial Sample) Hercules Theory

Using equations (192), (196), and (199) to (202), we obtained the response of the biaxial sample in the direction of the applied loading. The plots included in this report, show the engineering stress:

$$\sigma_1 = \sigma_1 / \lambda_1 \quad (203)$$

rather than the Cauchy stress, σ .

4.2.7 M. Quinlan's Theory of Materials with Variable Bonding

4.2.7.1 Original Model

In developing a mathematical framework for his stress-strain law, Quinlan, in Reference 4, reasoned that since propellants consist of minute rigid particles embedded in a polymer matrix, such materials would respond to a deformation process with a change in the amount of species to species bonding. He thus proposed to correct the deficiencies of fading-memory type theories by introducing a correction term that accounted for the changes in the state of bonding that are induced by a deformation process. His constitutive model then took the form:

$$\sigma = \sigma_f + \sigma_b \quad (204)$$

in which:

- σ = current stress
- σ_f = fading-memory type stress
- σ_b = stress correction due to change in the state of bonding

Motivated to some extent by reaction-rate theory, Quinlan modeled the evolution of the bonding state through the following ordinary differential equation:

$$\dot{\pi} = \alpha \left\{ \dot{\phi} - \mu [1 - e^{\nu(\phi - \pi)}] \right\} \quad (205)$$

subject to the initial condition:

$$\pi(0) = 1 \quad (206)$$

in which π represents the state of bonding; α , μ and ν are material parameters, and

$$\phi = 1 + \epsilon \quad (207)$$

is the stretch ratio; with ϵ , the strain.

The unique solution of (204) may be readily obtained for piecewise linear stretch histories, as reported in Reference 4.

Taking a linear viscoelastic relation for σ_f , and considering the stress correction term, σ_b , as proportional to the state of bonding, Quinlan arrived at the following stress-strain law:

$$\sigma(t) = \int_0^t G(t - \tau) \dot{\phi}(\tau) d\tau + B_0 \dot{\pi}(t) \quad (208)$$

with:

$$G(t) = E_0 t^{-n} \quad (209)$$

$$\dot{\pi}(t) = \alpha \left\{ \dot{\phi} - \mu \left[1 - e^{\nu(\phi - \pi)} \right] \right\} \quad (210)$$

and

$$\pi(t = 0) = 1 \quad (211)$$

The six parameters: E_0 , n , B_0 , α , μ and ν , needed in this theory to characterize a propellant, may be obtained by fitting the model to the observed response of the material when subjected to a saw-tooth strain history that has increasing peak strains and sufficiently long rest periods between cycles.

Alternatively, the studies reported in the literature on the effects of employing different data bases for characterization, show that the test history should primarily include the maximum expected strain level, the expected range of strain rates, as well as rest and relaxation periods.

The present model was used to predict the response of TP-H1011 under several loading histories; and it reproduced, somewhat accurately, the general trend of solid propellant behavior.

In an attempt to include healing effects, the underlying assumption for the evolution of damage were revised, as explained next.

4.2.7.2 Current Model

The theory developed by Quinlan has undergone several changes; mainly in the expression defining the evolution of damage. Thus, the form:

$$\sigma(t) = \int_0^t H(t - \tau) \dot{\phi}(\tau) d\tau + C \dot{\pi}(t) \quad (212)$$

has been retained in all versions of this theory, but the rate mechanism underlying damage:

$$\dot{\pi} = P(\pi, \phi, \dot{\phi}) \quad (213)$$

for which:

$$\pi(\dot{\phi} = 1) = 1 \quad (214)$$

was assumed to contain a neutral rate, ζ , at which damage remains constant, i.e.,

$$P(\pi, \phi, \zeta) = 0 \quad (215)$$

This concept then allowed introducing the notion that at rates higher than ζ , bond breakage would take place, while at rates smaller than the neutral rate, bond formation would ensue. The details of the derivations leading to the specific form of equation (213) are presented next.

Equation (215) for the neutral rate, ζ , may be rewritten as:

$$\begin{aligned}\zeta &= Q(\pi, \phi) \\ \zeta &= 0 \text{ if and only if } \pi = \phi\end{aligned}\tag{216}$$

which, upon expansion in Taylor series, becomes:

$$\zeta = Q(\pi, \pi - \phi) \Big|_{\phi=0} + \frac{\partial Q(\pi, \pi - \phi)}{\partial(\pi - \phi)} \Big|_{\phi=0} (\pi - \phi) + Q(|\pi - \phi|^2)$$

The first term on the right-hand side of this equation vanishes by virtue of (216), so that, neglecting the higher order terms, and defining:

$$\mu \stackrel{\text{def}}{=} \frac{\partial Q(\pi, \pi - \phi)}{\partial(\pi - \phi)} \Big|_{\phi=0}\tag{217}$$

leads to the following first-order expression for the neutral rate:

$$\delta = \mu(\pi - \phi)\tag{218}$$

where for bond breakage:

$$\dot{\phi} - \zeta > 0\tag{219}$$

while for bond formation:

$$\dot{\phi} - \zeta < 0\tag{220}$$

In addition, equation (213) may be cast in the following form:

$$\dot{\pi} = P(\pi, \phi, \dot{\phi}) = R(s, u)\tag{221}$$

where:

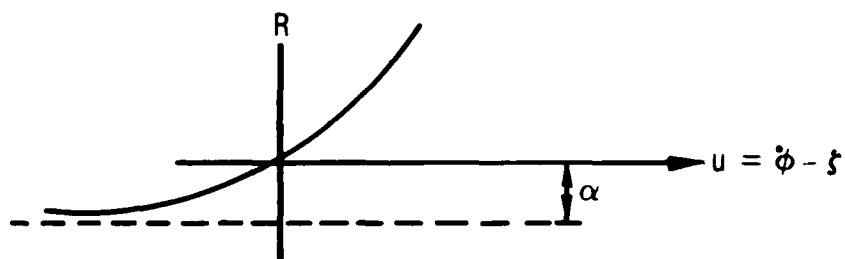
$$s = s(\pi, \phi) \quad (222)$$

and:

$$u = \dot{\phi} - \zeta \quad (223)$$

with ζ given by (218).

Now, under the assumption that the process of bond formation is slower than that of bond breakage, the function R defining the evolution of damage must be of the form shown in the sketch below, in which the parameter α would represent the maximum rate of bond formation.



Hence, R may be defined through the following differential equation:

$$\frac{dR(s, u)}{du} = \nu [R(s, u) - \alpha] \quad (224)$$

where α and ν are positive constants.

Integration of (224) yields:

$$R(s, u) = \alpha(e^{\nu u} - 1) \quad (225)$$

Finally, putting (218), (223), and (225) into (221), results in:

$$\dot{\pi} = \alpha \left\{ \exp \left[\nu \dot{\phi} + \mu \nu (\phi - \pi) \right] - 1 \right\} \quad (226)$$

Equations (212) and (226) subject to (214) were used by Quinlan in several ways to characterize the response of UTP-19,360B. One such stress-strain law took the following form:

$$\sigma(t) = E_0 \epsilon(t) + \left[E_1 + E_2 \epsilon(t) \right] \int_0^t (t - \tau)^{-n} \dot{\epsilon}(\tau) d\tau + C \dot{\pi} \quad (227)$$

in which E_0 , E_1 , E_2 , n and C are constants and ϵ is the strain. Although some aspects of propellant behavior were better modeled than with the original version of the theory, others were not, and further revisions were necessary. In the latest version of his constitutive law, Quinlan used a Prony series to represent the relaxation function and changed strain for stretch in the original equation of evolution for damage, so that, in summary, the current model looks as follows:

$$\begin{aligned} \sigma(t) &= \sigma_v(t) + \sigma_b(t) \\ \sigma_v(t) &= G_e \epsilon(t) + \int_0^t G(t - \tau) \dot{\epsilon}(\tau) d\tau \\ G(t) &= \sum_{i=1}^n G_i e^{-\tau_i t} \\ \sigma_b(t) &= B e^{\gamma(\epsilon - \pi)} \epsilon(t) \\ \dot{\pi}(t) &= \alpha \left\{ e^{\nu(\epsilon - \pi)} - 1 \right\} ; \pi(0) = 0 \end{aligned} \quad (228)$$

This final version of the theory has been employed to characterize UTP-19,360B, but has not been used by Quinlan to predict the response of the propellant under any loading history other than the characterization test.

4.3 CONCLUSIONS

The best nonlinear constitutive theories available for modeling solid propellant response were selected. Each of these theories was able to model some simple constant strain rate test behavior during the early part of the program, but generally gave poor correlation with the long time complex load histories characteristic of rocket motors.

A broad nonlinear data base was developed with two solid propellants. This data was used both at CSD and at some of the University subcontractors facilities. This data base can be used for evaluating any future nonlinear constitutive theories. All data was collected on an HP-9825 computer and is available in a format for a VAX computer system.

This data was used to evaluate and further develop the nonlinear theories for solid propellant response. Each of the theories has been extensively modified and now fits both simple and complex uniaxial load histories.

These theories will be further developed for multiaxial load histories in the last phase of the program.

REFERENCES

1. Solid Propellant Mechanical Behavior Manual, CPIA Publication No. 21, Section 4.3.2.
2. Jones, J., "Solid Propellant Structural Integrity Investigations: Dynamic Response and Failure Mechanisms in Solid Propellants," RPL-TDR-64-32, Vol. I, Lockheed Propulsion Co., February 1964.
3. Francis, E. C. et al., "Predictive Techniques for Failure Mechanisms in Solid Rocket Motors," AFRPL-TR-79-87, Chemical Systems Division, January 1980.
4. Quinlan, M. H., "An Application of the Theory of Materials with Variable Bonding to Solid Propellant," AFRPL-TR-78-37, Air Force Rocket Propulsion Laboratory, June 1979.
5. Farris, R. J., Hermann, L. R., Hutchinson, J. R., and Schapery, R. A., "Development of a Solid Rocket Propellant Nonlinear Viscoelastic Constitutive Theory," AFRPL-TR-75-20, Aerojet Solid Propulsion Co., May 1975.
6. Penny, D. N., "Further Investigations of Permanent Memory Materials," Ph.D. Thesis, University of Utah, June 1975.
7. Ilyushin, A. A., and Pobedrya, B. Ye., "Principles of the Mathematical Theory of Thermoviscoelasticity," FTD Translation FTD-MT-24-9A-71, February 1972.
8. Moskvitin, V. V., "The Strength of Viscoelastic Materials as Applied to Charges of Solid Propellant Rocket Engines," FTD Translation FTD-MT-24-714-73, October 1973.
9. Swanson, S. R., Christensen, L. W., and Christensen, R. J., "A Nonlinear Constitutive Law for High Elongation Propellant," CPIA Publication 331, December 1980, pp. 149-161.
10. Schapery, R. A., "Recent Developments in the Nonlinear Viscoelastic Characterization of Solid Propellant," Lead Article, Solid Rocket Structural Integrity Abstracts, Vol. 8, No. 2, University of Utah, April 1971
11. Quinlan, M. H., "Materials with Variable Bonding," Arch. Rational Mechanics and Analysis, 1978, Vol. 67, pp. 165-181.
12. Farris, R. J. and Fitzgerald, J. E., "Deficiencies of Viscoelastic Theories as Applied to Solid Propellants," Bulletin of the 8th JANNAF Mechanical Behavior Working Group Meeting, CPIA Publication No. 193, Vol. 1, The Johns Hopkins University, March 1970, pp. 163-192.

13. Lindsey, G. H. and Murch, S. A., "On the Mechanical Behavior of Dewettable Solids," Bulletin of the 8th JANNAF Mechanical Behavior Working Group Meeting, CPIA Publication No. 193, Vol. I, The Johns Hopkins University, March 1970, pp. 139-151.
14. Farris, R. J., "Homogeneous Constitutive Equations for Materials with Permanent Memory," Project Thesis Report AFOSR 70-1962TR, University of Utah, June 1970.
15. Fitzgerald, J. E. and Farris, R. J., "Characterization and Analysis Methods for Nonlinear Viscoelastic Materials," Project Thesis Report UTEC TH 70-204, University of Utah, November 1970.
16. Schapery, R. A., "On the Mechanical Behavior of Solid Propellant under Transient Temperatures," section in Texas A & M Report No. MM 3064-783, August 1978.
17. Schapery, R. A., "Application of Viscoelastic Fracture Mechanics to Nonlinear Behavior and Fracture of Solid Propellant," Report No. MM 2995-74-5, Texas A & M University, July 1974.
18. Schapery, R. A., "A Nonlinear Constitutive Theory for Particulate Composites Based on Viscoelastic Fracture Mechanics," Proc. 1974 Combined JANNAF Structures and Mechanical Behavior and Operational Serviceability Working Groups, CPIA Publication No. 253, The Johns Hopkins University, July 1974, pp. 345-355
19. Schapery, R. A., "Studies on the Nonlinear Viscoelastic Behavior of Solid Propellant," Report No. MM 2803-73-2, Texas A & M University, May 1973.
20. Farris, R. J., "The Stress Strain Behavior of Mechanically Degradable Polymers," in Polymer Networks: Structural and Mechanical Properties, edited by A. J. Chompft and S. Newman, Plenum Publishing Co., New York 1971, pp. 341-394.
21. Quinlan, M. H., "On the Theory of Materials with Permanent Memory," Ph.D. Thesis, University of Utah, June 1974.
22. Lee, T. Y., "Permanent Memory and Coupled Thermomechanical Effects in Filled Polymers," Ph.D. Thesis, University of Utah, June 1975.
23. Hufferd, W. L., Fitzgerald, J. E., and Sulijoadikusumo, A. U., "Permanent Memory Effects in Solid Propellants," UTEC CE 73-217, Proc. 1974 Combined JANNAF Structures and Mechanical Behavior and Operational Serviceability Working Groups, CPIA Publication, No. 253, The Johns Hopkins University, July 1974, pp. 371-384.
24. Lepie, A. H. and Adicoff, A., "Energy Balances and Internal Damage of Solid Propellants," Proc. 1974 Combined JANNAF Structures and Mechanical Behavior and Operational Serviceability Working Groups, CPIA Publication No. 253, The Johns Hopkins University, July 1974, pp. 371-384.

25. Blatz, P. J., "A New Theory of Solid Propellant Mechanical Behavior," Proc. 1974 Combined JANNAF Structures and Mechanical Behavior and Operational Serviceability Working Groups, CPIA Publication No. 253, July 1974, pp. 403-426.
26. Gurtin, M., and Francis, E. C., "On a Simple Rate-Independent Model for Damage", Preliminary Report, in CPIA Publication 331, Dec. 1980. pp. 127-133.
27. Mullins, L., "Softening of Rubber by Deformation," Rubber Chem. Technol., 1969, Vol. 31, pp. 333-362.
28. Oberth, A. E., and Brenner, R. S., "Tear Phenomena Around Solid Inclusions In Castable Elastomers," Transaction of the Society of Rheology 912, pp. 165-185 (1965).
29. Farris, R. J., and R. A. Schapery, "Development of a Solid Rocket Propellant Nonlinear Viscoelastic Constitutive Theory," AFRPL-TR-73-50, June 1973.
30. Hermann, L. R., and Peterson, F. E., "A Numerical Procedure for Viscoelastic Stress Analysis," Proc. 7th Mtg. of ICRPG Mech. Beh. Working Group, CPIA Pub No. 177 (1968).
31. Cost, T. L. and Parr, C. H., "Analysis of the Biaxial Strip Test for Polymeric Materials," J. Materials J MLSA, Vol. 4, pp. 312-323, 1969.

Appendix A

MULTISTATION AUTOMATED DATA REDUCTION

INTRODUCTION

Automated handling of multistation tester data is accomplished with a system of interactive programs on the HP 9825 desk top computer (Figure A-137). These programs include data acquisition, stress relaxation-master modulus, straining while cooling or heating, straining to failure, and complex histories. The acquisition of data and test control are functions of the data acquisition program which supplies data to the data reduction programs. The reduction programs reduce and output data for a particular type of test history. In addition, terminal emulating software for the HP 9825 provide a data link for the transfer of data to the VAX-11 mainframe computer. This makes the data directly available to the nonlinear constitutive theory programs.

SYSTEM INSTRUMENT CONFIGURATION

The multistation data acquisition instruments are configured to provide load, crosshead position, temperature and elapsed time data to the data acquisition program. The system consists of a Hewlett Packard 9825 desk top computer, 3455 digital voltmeter, 3495 scanner, 98035 programmable clock and 9885 flexible disk drive (Figure A-138).

The HP 9825 and data acquisition program act as the system controller. The controller processes incoming test data and crosshead information and responds by sending instructions to other instruments in the system over an HP-IB interface. Output signals from the tester's load transducers, linear potentiometer, and analog thermometers are input into the scanner's programmable relay cards. The scanner's relays under command of the controller can be opened independently to route output data signals individually to the digital voltmeter where they are digitized and read by the program. Crosshead control information from output lines connected to the tester's motor-clutch assembly, is supplied to the program through the scanner in the same way as the data output signals. These

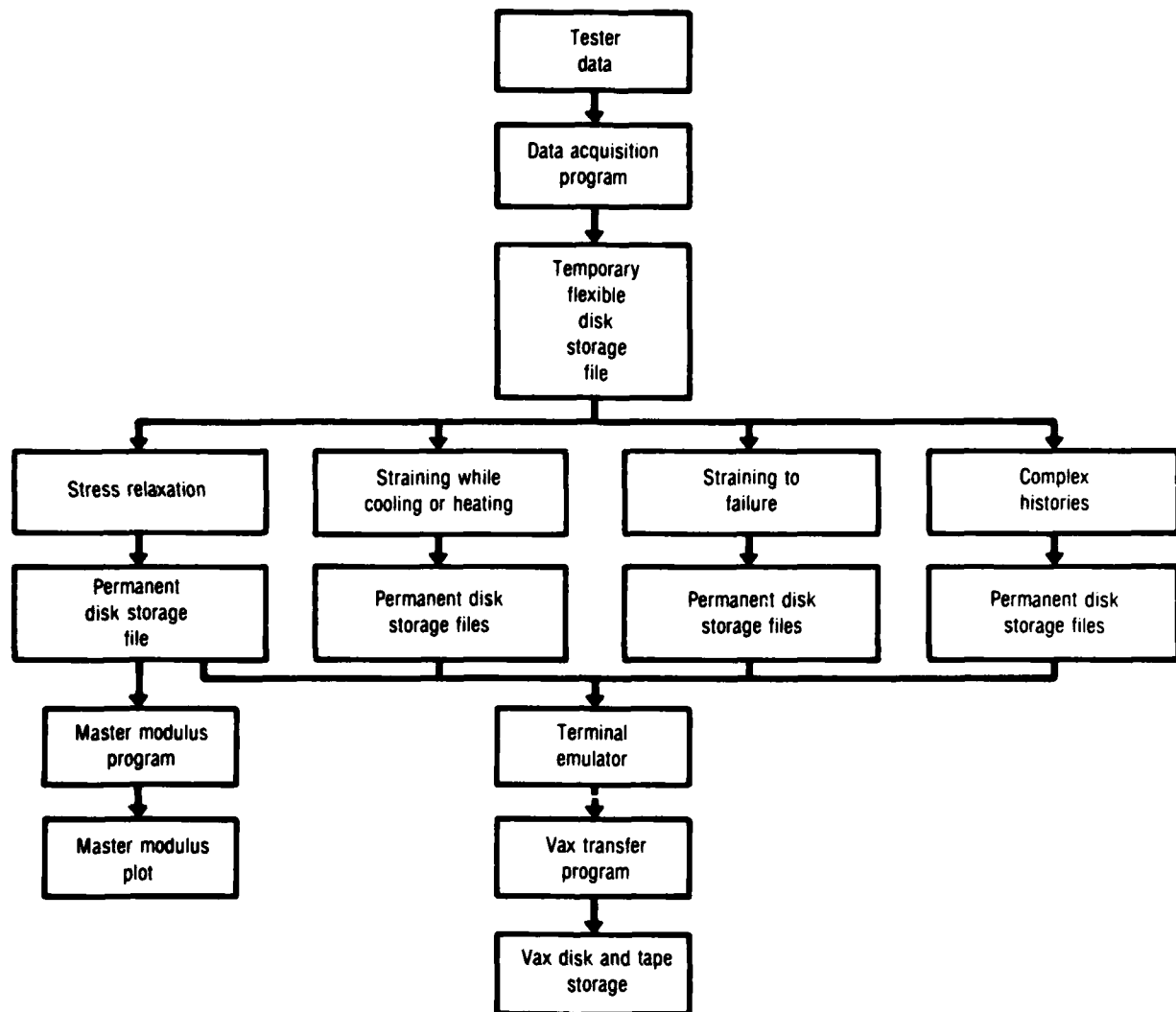


Figure A-137.

28842

signals enable the controller to react to changes in crosshead movement and direction without relying on operator intervention. The programmable clock connects directly to one of the computer's I/O ports. It provides the program with elapsed time data and a program interrupt capability for controlling the rate at which data is taken. The flexible disk drive provides a mass storage medium where data is stored during testing for later access by one of the data reduction programs.

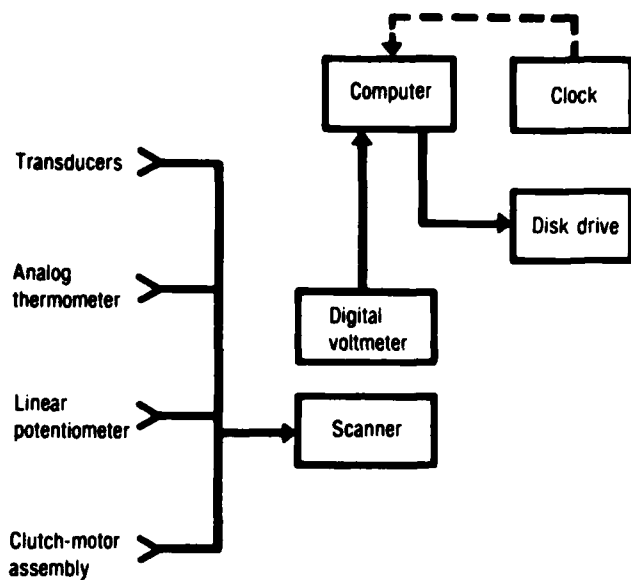


Figure A-138.

PROGRAMS

Data Acquisition:

As previously stated, the data acquisition program is used to collect data from the multistation tester. Operation of the program involves steps to initialize the program, calibrate the system, and collect and store test data.

Initialization of the program is accomplished by operator entered information used to identify the particular test and define samples

being tested. In response to prompts from the computer display, the operator inputs descriptions on test material, crosshead rates, strain levels, and temperature levels of the test history. Data input on the test samples include their number, gage length, and individual cross sectional areas, along with their channel locations. In addition, the operator enters pairs of crosshead rates and delta strains for each test interval used to compute sampling rates. The operator also determines how data is taken during relaxation cycles by specifying whether sampling is to be done in a fixed or log time interval.

Calibration of the system is done by an operator-interactive procedure to determine the tester's transducers and potentiometer sensitivities. This involves the operator queuing the program to take readings from the transducers at differing load conditions. By comparing the change in output signals for a known change in load, the lb/volt sensitivity of each transducer may be determined. Similarly, by moving the linear potentiometer probe a known distance its in./volt sensitivity is determined. The analog thermometers are not calibrated at the time of testing. These units output a 10 mv/°F representation of the test chamber and internal sample temperature. Calibration on them is done periodically by the CSD electronics laboratory. For short time and isothermal tests, calibration is done once before testing begins. For tests

lasting over a long time period, a second calibration is done when testing is complete to enable compensation for drift in the tester's electronics. Since the load transducers are temperature sensitive, for thermal tests two calibrations must be performed at differing temperatures to determine the change in sensitivity per degree change in temperature.

When calibration is complete, the program stops operation until testing is ready to begin. On a cue from the operator, zero load and position data is taken and the system's instruments programmed to their initial conditions. The clock interrupt period is set for a sampling rate determined from the initial crosshead rate and delta strain information. Scanner relays are also arranged to monitor the tester's break input voltage.

The program monitors the brake voltage until detecting the brake has disengaged which signifies crosshead motion. The clock's counter and interrupt units are then started. Interrupt signals are output by the clock at the set sampling rate until changed by the program at the end of the straining interval.

When interrupt instructions are received from the clock, program operation branches to a data collection subroutine. The voltmeter and scanner are set to read output signals from each of the transducer, potentiometer and thermometer channels. Fifty milliseconds are required to read each channel. Elapsed time, read from the clock counter, is taken as the mean time over which the data set was read. The test data is retained in a memory buffer until transferred to a disk storage file.

The program continues to monitor the crosshead break and clock information channels throughout the test. When a change in crosshead motion is detected, the clock interrupt is stopped. From the test description data corresponding to the test interval, a sampling rate is determined and the clock reset. For log time interval samplings, the clock interrupt unit is stopped after each reading and the time doubled.

Up to 600 data sets may be retained in the computer's memory at one time. Data is transferred to the disk either between data set samplings, if time allows, or when testing is complete.

Data Reduction Programs:

The reduction programs reduce and output multistation data pertinent to particular types of test histories. The programs are stress relaxation-master modulus, straining while cooling or heating, straining to failure and complex histories. A description of the strain and temperature histories relevant to each is listed in Table A-35.

Test identification, calibration, load, sample extension, thermal, and time data are supplied to the programs from the acquisition data files or entered directly by the operator. In addition, relaxation cathetometer strain measurements and the thermal expansion coefficient may be optionally entered.

Each program reduces stress, strain, modulus, temperature and elapsed time data when applicable. The method by which each is determined depends on the test history and amount of information available to the program.


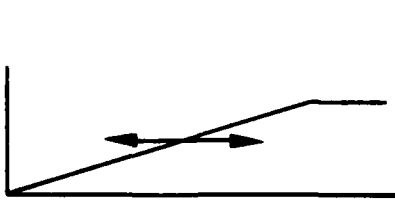
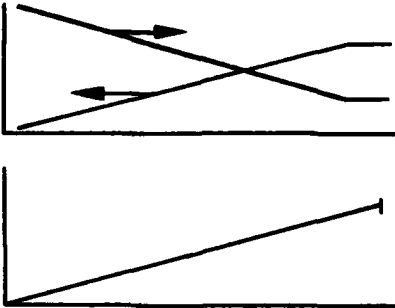
Calibration sensitivity (S) of the transducer and potentiometer are determined in general by

$$S = \text{load}/(\text{load output}-\text{zero load output})$$

where load is the transducer calibration weight or potentiometer probe displacement. For tests where multiple calibrations were performed, the sensitivities at time t are corrected for electrical drift and thermal variations with the linear relationships

$$S(t) = S_{\text{initial}} + \frac{(S_{\text{final}} - S_{\text{initial}})}{X_{\text{final}} - X_{\text{initial}}} X(t)$$

TABLE A-35

Program	Test Strain History	Output
1. Stress relaxation		Tabular - time, modulus Graphic - modulus vs time
2. Straining while cooling or heating		Tabular - time, strain, temperature, stress Graphic - stress vs time and temperature
3. Straining to failure		Test History - Tabular - time, strain and stress Graphic - stress vs time and straining Mech Properties Tabular - initial modulus, maximum stress and strain - corrected stress and strain - rupture strain
4. Complex histories	Combination of straining, relaxation and temperature intervals	Tabular - time, strain temperature and stress Graphic - stress vs time and strain and temperature vs time

where X is time for isothermal and temperature for nonisothermal tests.

Temperature corrections are not made on the potentiometer sensitivity since it is located outside the environmental test chamber.

Zero load outputs (ZO) for the transducers are also corrected for electrical drift and thermal variation by the same method as the sensitivities.

Corrections on the zero position output of the potentiometer cannot be made since the crosshead can't be accurately returned to its initial position.

Sample stresses (σ) at time t are calculated by

$$\sigma(t) = \left[\text{transducer output} - Z_0(t) \right] S(t) / \text{cross-sectional area}$$

Sample strain (ϵ) at time t is determined by

$$\epsilon(t) = \left[\text{pot output} - Z_0 \right] S(t) / \text{gage length}$$

For nonisothermal tests a strain correction may be applied using the thermal expansion coefficient (α). In this case, the total sample strain becomes

$$\epsilon(t) = \text{mechanical strain} + \left[T(t) - T_{\text{initial}} \right] \alpha / \text{gage length}$$

An additional correction for effective gage length may be made using cathetometer measurements of actual sample strains. The correction factor is determined as the ratio of the mean intervals in the test history. For histories where multiple cathetometer measurements were made, the correction factors are linearized to measured strain between them.

Relaxation and secant modulus (E) at time t is determined by

$$E(t) = \sigma(t) \left[1 + \epsilon(t) / \epsilon(t) \right]$$

where $\epsilon(t)$ is held constant over relaxation test intervals.

Temperature is reduced from analog thermometer readings by converting the millivolt output to volts.

Elapsed time is calculated as the difference between when the data was taken and when initial loading occurred (t_0) since loading times may vary from sample to sample, t_0 is approximated by the time of initial straining.

Once data is reduced, a tabular and graphic summary of the test is output by each program. A description of the outputs is listed in Table A-35. To

retain data for future reference and reuse, identification, calibration and raw test data are stored on permanent diskette data files.

Terminal Emulator

The program is used to transfer data between the HP 9825 and VAX-11, desktop and mainframe computers.

A link is created between the computer types utilizing the VAX-11's dial-in lines and an RS-232 interface which connects the 9825 to an acoustic coupler. The emulator software then supplies the capability of using the 9825 as an intelligent terminal through which data may be read from the flexible disks and sent over phone lines to the VAX.

Data transfer is accomplished with a VAX program which reads data sent from the terminal and retains it in storage files for access by the nonlinear theory programs.

SYMBOLS

A_c	microcrack growth rate shift factor
A_F	temperature dependent material function
A_{ij}	expansion coefficients of bulk stress in terms of octahedral strains
A_n	constant
A_o	initial area
A_T	temperature shift factor (a_T)
a_η	(AHETA) damage related shift function
a	half sample width
a_F	softening function
a_k	constant
a_{np}	expansion coefficients of correction modulus
$A_1, A_2, A_3, A_4, A_6, A_i$	constants
$2a$	biaxial sample width
B	Cauchy-green deformation tensor
B	bulk modulus and a constant
B'	deviatoric deformation tensor
$2b$	biaxial sample height (gage length)
C	softening function
CSD	Chemical Systems Division
C_x	rehealing parameter
c	constant
C, C_1, C_2, C_i	constants

d	constant
D_m, D_5, D_6, D_7	constants
E	modulus
E_e	equilibrium modulus
E_R	reference modulus and normalized coefficient for modulus
E_R	relaxation modulus
$E(t), E_{rel}(t)$	linear viscoelastic relaxation modulus
e	product of F and virgin response function g
e_{ij}	deviatoric strain tensor
$E(\xi)$	linear viscoelastic modulus
F	force
$F(t)$	constant rate modulus
$F(\xi, \epsilon_m)$	damage curve at ϵ_m damage level
f	material parameter
(f)	deformation function
f_c	constant time rate of change of deformation invariant
$f(t)$	viscoelastic type function
$^{\circ}F$	degrees Fahrenheit
F	damage function or softening function
F	strain magnification factor
G	shear modulus
$G. L.$	gage length
G_c	corrected modulus
G_r	relaxation modulus

G_{rel}	shear relaxation modulus
$G(t)$	shear relaxation modulus
g	virgin response function
$g()$	function of
(g)	strain softening function
h	function of damage in kinetic equation of evolution
HTPB	Hydroxy Terminated Polybutadiene
I_d	volume dilatation
I_n	contribution to stress at time t_n
I_γ	octahedral shear strain
$\ I_\gamma \ _{pi}$	L_p norm
J	creep function
JANNAF	Joint Army Navy NASA Air Force
K	constant
K_I	stress intensity factor
K_x	rehealing parameter
k	constant
L_x	constant
M	constant
M_x, M_2, M_4	constants
n	constant
mV	millivolts
n, n_2, n_4	material parameters

N	number of cycles
n	constant
P	terms of equation under summation
P	hydrostatic pressure
PBAN	Polybutadiene Acrylonitrile
p	constant
P_2, P_4	constants
P_{15}	used to normalize Y_3 to 1
Q	terms of equation under summation
q	constant
RH	relative humidity
S	virgin stress and damage parameter constant
S_d	damage parameter
S_0	constant
S_r	certain measure of damage
$S_t - S_r$	temperature shifted time
S_x	constant
\int	damage parameter
T	temperature
T	peak stress time
T_a	material property and shift temperature
T_0	temperature at $t = 0$
T_R	reference temperature

t	time
t_n	time
t_0^*	time to failure under constant load
UTP	United Technologies Propellant
x	$\equiv \epsilon/\epsilon_m$
X	width position from center of biaxial sheet
X_r	root of Y_3
y	$\equiv e_{10}$
Y_1, Y_1, Y_2, Y_3	functions related to damage
α	coefficient of thermal expansion
α	constant
β	constant
β	parameter
γ	shear strain
ΔL	change in length
δ_{ij}	Kronecker delta
ϵ	strain
ϵ_1	principal strain
ϵ_2	lateral strain
$\epsilon_{11}, \epsilon_{22}, \epsilon_{33}$	principal strains
ϵ_0	pseudo strain
$\epsilon_m, \epsilon_{max}$	maximum strain
$\epsilon(t)$	strain at time t
ϵ_u	strain of unfilled polymer
ϵ_σ	strain due to mechanical stress

η	compressibility ($\eta = 0$ is incompressibility)
$\eta(t)$	related to damage function,
λ	extension ratio ($1 + \epsilon$)
λ	healing correction factor
λ	softening function
λ	width to height ratio
ξ	reduced time
ξ	ratio of position to half sample
ξ	width (x/a)
π_{α}	second invariant of tension ($\alpha = \sigma, B$)
\sum	summation
σ	engineering stress or stress
σ	Cauchy-stress tensor
σ_B	bulk stress
σ_c	stress correction
σ_{ij}^d	deviatoric stress
σ'	deviatoric stress
σ_l	linear viscoelastic stress
σ_o	constant stress
σ_{kk}	bulk stress
σ_r	linear viscoelastic stress
$\sigma(t)$	stress at time t
$\sigma_f(t)$	fading memory stress
τ	reduced time
τ	shear stress

τ	shifted time
ϕ	function of loading
ψ_n	nth component of stress correction
ω	normalized damage function
II_α	second invariant of tensor ($\alpha = \sigma, B$)
$\sqrt{II_B'}$	second invariant of deformation tensor
$\sqrt{II_\sigma'}$	second invariant of deviatoric stress
$ \cdot $	denotes absolute value

